DESIGNING BIO-FORMULATIONS BASED ON ORGANIC AMENDMENTS, BENEFICIAL MICROBES AND THEIR METABOLITES

EDITED BY: Francesco Vinale, Giuliano Bonanomi, Sheridan Lois Woo, Roberta Marra and Santiago Gutierrez

PUBLISHED IN: Frontiers in Microbiology and Frontiers in Plant Science

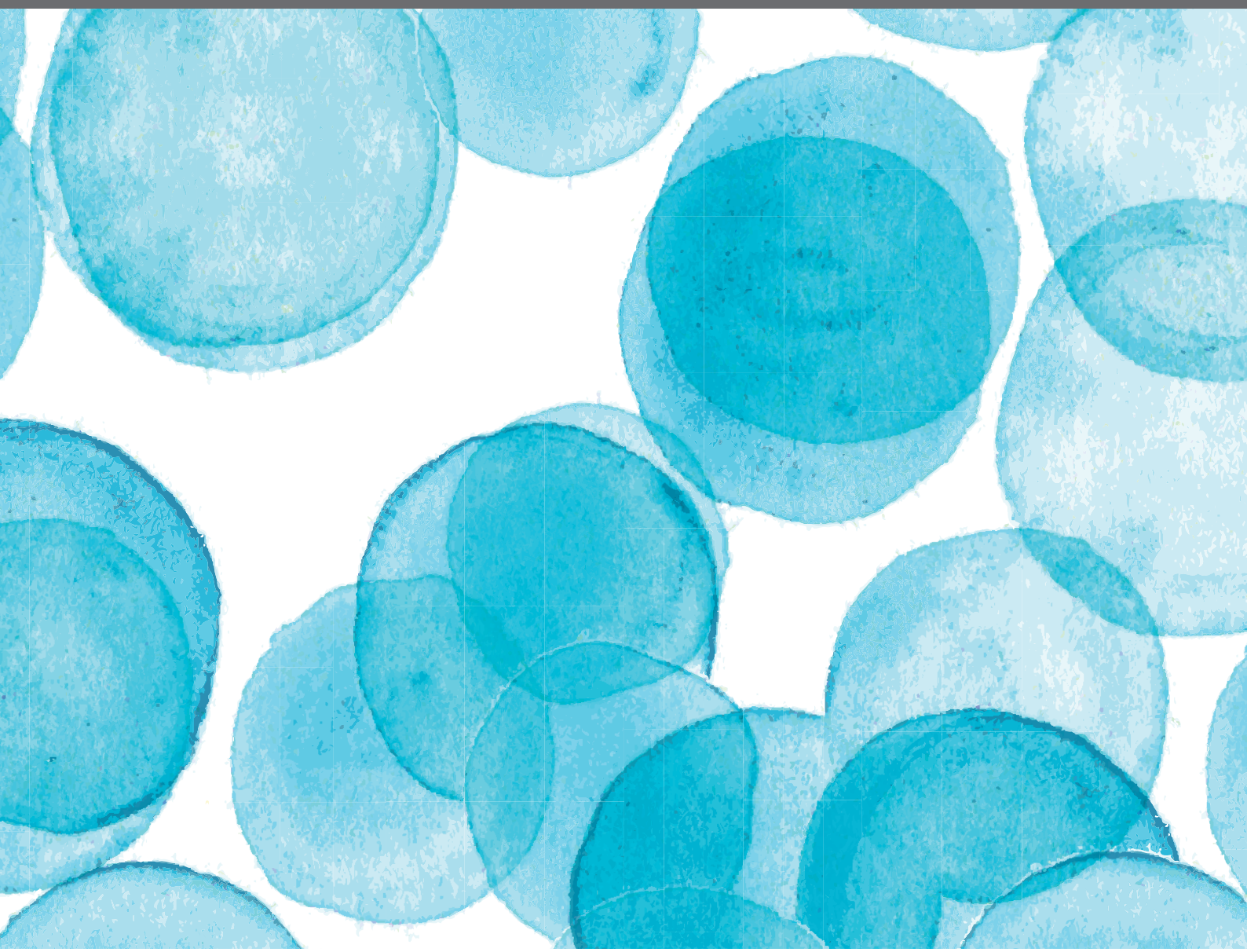

frontiers Research Topics

frontiers

ISSN 1664-8714
ISBN 978-2-88974-468-8
DOI 10.3389/978-2-88974-468-8

About Frontiers

Frontiers is more than just an open-access publisher of scholarly articles: it is a pioneering approach to the world of academia, radically improving the way scholarly research is managed. The grand vision of Frontiers is a world where all people have an equal opportunity to seek, share and generate knowledge. Frontiers provides immediate and permanent online open access to all its publications, but this alone is not enough to realize our grand goals.

Frontiers Journal Series

The Frontiers Journal Series is a multi-tier and interdisciplinary set of open-access, online journals, promising a paradigm shift from the current review, selection and dissemination processes in academic publishing. All Frontiers journals are driven by researchers for researchers; therefore, they constitute a service to the scholarly community. At the same time, the Frontiers Journal Series operates on a revolutionary invention, the tiered publishing system, initially addressing specific communities of scholars, and gradually climbing up to broader public understanding, thus serving the interests of the lay society, too.

Dedication to Quality

Each Frontiers article is a landmark of the highest quality, thanks to genuinely collaborative interactions between authors and review editors, who include some of the world's best academicians. Research must be certified by peers before entering a stream of knowledge that may eventually reach the public - and shape society; therefore, Frontiers only applies the most rigorous and unbiased reviews.
Frontiers revolutionizes research publishing by freely delivering the most outstanding research, evaluated with no bias from both the academic and social point of view. By applying the most advanced information technologies, Frontiers is catapulting scholarly publishing into a new generation.

What are Frontiers Research Topics?

Frontiers Research Topics are very popular trademarks of the Frontiers Journals Series: they are collections of at least ten articles, all centered on a particular subject. With their unique mix of varied contributions from Original Research to Review Articles, Frontiers Research Topics unify the most influential researchers, the latest key findings and historical advances in a hot research area! Find out more on how to host your own Frontiers Research Topic or contribute to one as an author by contacting the Frontiers Editorial Office: frontiersin.org/about/contact

DESIGNING BIO-FORMULATIONS BASED ON ORGANIC AMENDMENTS, BENEFICIAL MICROBES AND THEIR METABOLITES

Topic Editors:
Francesco Vinale, University of Naples Federico II, Italy
Giuliano Bonanomi, University of Naples Federico II, Italy
Sheridan Lois Woo, University of Naples Federico II, Italy
Roberta Marra, University of Naples Federico II, Italy
Santiago Gutierrez, Universidad de León, Spain

Citation: Vinale, F., Bonanomi, G., Woo, S. L., Marra, R., Gutierrez, S., eds. (2022). Designing Bio-Formulations Based On Organic Amendments, Beneficial Microbes And Their Metabolites. Lausanne: Frontiers Media SA.
doi: 10.3389/978-2-88974-468-8

Table of Contents

frontiers in Microbiology

EDITORIAL
published: 18 January 2022
doi: 10.3389/fmicb.2021.832149

Editorial: Designing Bio-Formulations Based on Organic Amendments, Beneficial Microbes and Their Metabolites

Roberta Marra[1,2*], *Santiago Gutiérrez*[3], *Sheridan Lois Woo*[2,4,5], *Giuliano Bonanomi*[1,2,5] *and Francesco Vinale*[2,6,7]

[1] *Department of Agricultural Sciences, University of Naples Federico II, Naples, Italy,* [2] *Center for Studies on Bioinspired Agro-Environmental Technology (BAT Center), University of Naples Federico II, Naples, Italy,* [3] *Area of Microbiology, University of León, Ponferrada, Spain,* [4] *Department of Pharmacy, University of Naples Federico II, Naples, Italy,* [5] *Task Force on Microbiome Studies, University of Naples Federico II, Naples, Italy,* [6] *Institute for Sustainable Plant Protection, National Research Council, Naples, Italy,* [7] *Department of Veterinary Medicine and Animal Productions, University of Naples Federico II, Naples, Italy*

Keywords: microbial community, microbiomes, plant protection products, plant-microbe interactions, volatilome, proteome, metabolome, transcriptome

Edited and reviewed by:
Takema Fukatsu, National Institute of Advanced Industrial Science and Technology (AIST), Japan

***Correspondence:**
Roberta Marra
robmarra@unina.it

Specialty section:
This article was submitted to Microbial Symbioses, a section of the journal Frontiers in Microbiology

Received: *09 December 2021*
Accepted: *24 December 2021*
Published: *18 January 2022*

Citation:
Marra R, Gutiérrez S, Woo SL, Bonanomi G and Vinale F (2022) Editorial: Designing Bio-Formulations Based on Organic Amendments, Beneficial Microbes and Their Metabolites. Front. Microbiol. 12:832149. doi: 10.3389/fmicb.2021.832149

Editorial on the Research Topic

Designing Bio-Formulations Based on Organic Amendments, Beneficial Microbes and Their Metabolites

The future scenario in the agricultural sector, challenged by regulatory pressure, public concern and environmental issues, continues to motivate the development of alternative methods to chemicals for applications as fertilizers and pesticides (Martin, 2003). Among these, the use of organic amendments and microbial biocontrol agents represents the most promising soil management strategy, that may contribute both directly and indirectly to crop production and plant health (Bargaz et al., 2018).

The aim of this Research Topic was to provide insight in recent advances and challenges of plant-microbiomes studies focused on novel bio-formulations useful for the development of sustainable and eco-efficient approaches for plant disease control. The Topic includes 19 original research and review articles, which have been grouped in four categories.

MODULATION OF PLANT RESPONSE BY BENEFICIAL MICROBES

The interactions between plant and microbes have attracted great attention in the last decades. Biotechnological applications of beneficial microbes (BMs) in different areas, e.g., stimulation of plant-growth, biocontrol, bioremediation of contaminated sites and production of bioactive compounds with pharmaceutical and industrial relevance have been evaluated (Wu et al., 2009). Several studies have investigated the molecular changes occurring in the host plant and the interacting microbe aiming to improve our understanding about how plants respond to microbial

colonization or attack and how microbes affect plant cellular processes (Cheng et al., 2019; Adeniji et al., 2020; Jain et al., 2021). In their work, Bonini et al. showed that the metabolic profile in pepper leaves was modulated in response to microbial treatments consisting of arbuscular mycorrhizal fungi (AMF: *Rhizoglomus irregularis* and *Funneliformis mosseae*), and *Trichoderma koningii*. Root colonization by BMs increased total fruit yield, modified gibberellin, auxin, and cytokinin plant hormone patterns, as well as other secondary metabolism processes, determining the accumulation of carotenoids, saponins, and phenolic compounds. Similarly, Lombardi et al. found that selected *Trichoderma* strains stimulated the growth of strawberry plants and improved crop yield. Moreover, proteomic analysis of the produced fruits revealed a complex reprogramming of physiological processes e.g., stress response, nutrient uptake, protein metabolism, etc., that improved the health properties.

The application of microbial (e.g., AMF, *Trichoderma koningii* and rhizobacteria) or non-microbial (e.g., a protein hydrolyzate) biostimulants elicited biomass increase in maize plants and affected the metabolomic response in leaves and roots (Rouphael et al.). Interestingly, most of the differential metabolites consisting mainly of phenylpropanoids and terpenes were accumulated more in plant tissues following the application of the protein hydrolyzate in comparison to the treatments with microorganisms alone. The treatments also induced a reprogramming of the entire phytohormone profile, particularly in the roots, thus supporting the hypothesis that some biostimulants may have a hormone-like activity.

Conventional farming relies highly on N-fertilizers to improve crop yield, but this practice can lead to severe environmental pollution, hence the urgent need to find sustainable alternatives to inorganic fertilizers. Rubio et al. analyzed the transcriptomic response of wheat seedling roots inoculated with *Trichoderma harzianum* under different inorganic N supplies using wheat genome 61K microarrays. Forty-eight hours after inoculation, *Trichoderma* induced a greater expression of defense-related genes than the calcium nitrate application, that also down-regulated expression of genes involved in plant growth and development processes. Moreover, genes involved in the flavonoid biosynthetic pathway were differentially expressed in treated plants, thus reinforcing the hypothesis that *Trichoderma* is capable of inducing plant defense through the modulation of secondary metabolism.

EFFECTS OF MICROBIAL METABOLITES ON PLANT-MICROBE INTERACTIONS

Greater understanding about the effects induced by microbial metabolites on the host plant or by the host plant on the metabolism of the associated microbes could ultimately lead to the development of new crop protection bio-formulations for improving crop quality and yields. In their review, Tilocca et al. discussed the potential exploitation of volatile organic compounds (VOCs) produced by bacterial and fungal biocontrol agents (BCAs) in the control of many important phytopathogens. The authors underline the importance of the ecosystem in shaping the microbial VOCs composition. The adoption of holistic approaches, such as -omics and bioinformatics prediction tools, may help scientists to unravel the dynamic network of molecular cross-talk occurring between microbial partners and their plant hosts.

Members of the genus *Bacillus* are examples of well-known producers of antifungal compounds (Chaurasia et al., 2005). Zhang et al. analyzed the antifungal effects of twenty-nine VOCs produced by a novel strain of *B. subtilis* (ZD01) against the airborne plant pathogen *Alternaria solani*. VOCs produced by ZD01 caused a strong decrease in hyphae penetration, inhibition of conidia germination, and reduced virulence of the fungus on potato leaves. Moreover, the expression of two virulence-associated genes (*sod* and *slt2*) in *A. solani* was strongly down-regulated after exposure to ZD01 VOCs.

Marine-derived fungi are considered good producers of valuable compounds with original structures and interesting biochemical properties that can be exploited for new drug discovery (Silber et al., 2016; Nicoletti and Vinale, 2018; Vinale et al., 2020). Zhao et al. isolated two novel fusarisetins, namely fusarisetins C and D, and four known compounds produced by the fungus *Fusarium equiseti* D39. These 3-decalinoyltetramic acid (3DTA) derivatives showed potent phytotoxicological and antimicrobial activities. Moreover, the optimization of fermentation conditions favoring equisetin production was conducted by using the "one strain many compounds" (OSMAC) approach.

A new method to rhizosphere engineering proposes the inoculation of microbial consortia to emulate the complex biological networks in natural soils, thus recruiting beneficial microbes and establishing optimized plant microbiomes (Syed Ab Rahman et al., 2018; Woo and Pepe, 2018). Inoculation with endophytes was found to stimulate the biosynthesis of secondary metabolites (SMs) in medicinal plants (Pandey et al., 2016a,b, 2018). The inoculation of an endopyhytic-consortium, consisting of *Acinetobacter* sp. and *Marmoricola* sp., significantly increased the biosynthesis of benzylisoquinoline alkaloids including morphine and thebaine in poppy plants, as well as improvement in plant growth and yield (Ray et al.). Interestingly, the increment in metabolite content was related to the modulation of the biosynthetic pathway due to the complementary activities of the consortium member endophytes. Lin et al. observed that the production of plant alkaloids by the association between the fungal endophyte *Epichloë* and the perennial grass *Festuca sinensis* depended mainly on the environmental growth conditions. In field and greenhouse tests, the seasonal variation more than the plant ecotype significantly affected the concentrations of alkaloids (peramine, lolitrem B, and ergot) produced by *F. sinensis*.

Plant–microbe interactions can be exploited to enhance the production of important SMs having multiple roles (Singh et al., 2017). As an alternative approach to the application of phytohormones and plant growth regulators, Luziatelli et al. investigated the biostimulant properties of compounds secreted by *Pantoea agglomerans* strain C1, known to produce indole-3-acetic acid (IAA) and siderophores (Luziatelli et al., 2019). The *P. agglomerans* C1 metabolites effectively

stimulated root formation and plant development of woody fruit crops, thus offering novel opportunities in designing innovative biostimulants.

Microbial metabolites have been proposed as alternatives to the use of living BCAs, because the efficacy of the latter is often limited by their low persistence in the environment, inconsistent performance under diverse field conditions and slower mode of action against pathogens, in comparison to chemical counterparts (Zaidi and Singh, 2013). Berini et al. investigated the activity of two metagenome-sourced microbial chitinases (Chi18H8 and 53D1) as potential insecticidal proteins against *Bombyx mori*, a model system among Lepidoptera. Although both proteins gave similar results *in vitro*, only 53D1 orally administered to *B. mori* larvae induced mortality and dramatically affected insect development. This study confirms that novel insecticidal formulations based on microbial bioactive proteins may be used in the progressive reduction of synthesized chemical compound applications, thus reducing the environmental impact of single active substances and the risk of resistance selection (Chandler et al., 2011; Hardy, 2014).

New microbial species or antimicrobial metabolites can be found by exploring environments having a high microbial biodiversity. Xu et al. observed that among insect symbionts, fungi isolated from the termite species *Odontotermes formosanus* demonstrated a great diversity and revealed the association with different bacterial symbionts. Moreover, the fungal metabolites exhibited antimicrobial activities when used in combination both as crude extracts and when applied as purified compounds. These results demonstrated that insect symbionts may represent a powerful source of novel species useful in agriculture or for drug discovery.

NOVEL BIOFORMULATIONS FOR APPLICATIONS IN AGRICULTURE

Trichoderma spp. are well-known examples of BCAs used as active ingredients of many plant protection products for agriculture and are also known for their ability to promote plant growth and/or induce disease resistance (Woo et al., 2014; Woo and Pepe, 2018). Besides the continuous search for novel effective natural strains, numerous efforts have been carried out to obtain modified microbial isolates with improved abilities compared to wild type strains, produced by using processes including UV radiation or chemical mutagenesis (Papavizas et al., 1982). Mukherjee et al. developed a novel seed dressing formulation based on a *T. virens* mutant (named G2) obtained by gamma-ray-induced mutagenesis. In comparison to the wild-type strain, *T. virens* G2 revealed a superior ability to contrast pathogens, both *in vitro* and in greenhouse or field trials. Transcriptome analysis revealed an up-regulation of genes involved in the synthesis of SMs. The proposed formulation consisted of the *T. virens* G2, tamarind seeds as a fermentation medium and talcum powder as a carrier and demonstrated a better efficacy in controlling *Sclerotium rolfsii* in chickpea and lentil production. In addition, it exerted multiple beneficial effects on plant, but it did not have toxic effects on mammals, birds or fish. Commercial formulations of *Trichoderma* spp. have been also tested as systemic resistance inducers of plants attacked by the parasitic nematode *Meloidogyne incognita*. Pocurull et al., in agreement with previous studies (de Medeiros et al., 2017; Martínez-Medina et al., 2017), showed that *T. asperellum* T34 and *T. harzianum* T22 induced resistance in tomato plants against *M. incognita*. Interestingly, the resistance was also induced in tomato bearing the *Mi-1.2* root-knot nematode resistance gene, and this protective effect was additive to that observed in T34-inoculated plants. In the review by Poveda et al., *Trichoderma*, mycorrhizal and endophytic fungi were indicated as the main filamentous fungi used as BCAs or resistance inducers against plant-parasitic nematodes. Different mechanisms of action were discussed that were differentiated according to each group of fungi, including those employing the production of SMs and lytic enzymes, the competition for space and nutrients, or direct parasitism; and those relying on the activation of plant defense mechanisms, such as the activation of SAR and ISR, modification of root exudates composition, or production of strigolactones. The wide diversity of mechanisms used by this consortium of microorganisms may represent a valid durable strategy for the control of plant-parasitic nematodes, but several issues (e.g., the influence of local environment and the results in field experiments) require further investigations before BCA applications may be used effectively in nematode-control of a particular crop.

Romano et al. isolated and characterized plant growth-promoting bacteria (PGPB) from the rhizosphere of wheat plants cultivated under abiotic stresses as plant probiotics. Two isolates of *Kosakonia pseudosacchari* TL8 and TL13 were identified that showed multiple plant growth promotion activities as well as antimicrobial activity and stress tolerance. TL13, the best PGP performer, was selected to develop a novel microbial-based formulation obtained using agro-industrial by-products as carbon source. This permits a reduction of costs and the development of an eco-sustainable inoculant, resulting in an eco-friendly, easy and economically advantageous approach to manage by-products.

ECOLOGY AND FUNCTIONALITY OF PLANT-SOIL MICROBIAL COMMUNITY

Complex interactions are established in the soil microbial community with plant roots and soil components, that significantly influence plant growth and resistance toward multiple stresses (Vishwakarma et al., 2020). Understanding the processes in the rhizosphere, as well as unraveling the composition and biological functions of the plant-root microbiome becomes essential, since recent evidence has confirmed that host plants and their associated microbes function as metaorganisms or holobionts (Hacquard, 2016).

Rhizosphere microbial community structures is continuously adapting to the environment, particularly to the agronomic practices. Bacterial and fungal community structures were strongly affected by soil and soilless cultivation systems of tomato plants subjected to different fertilization strategies (Grunert et al.). In both cultivation systems, similar plant performance was observed, but multivariate analysis showed

that physicochemical characteristics (e.g., plant length, pH, phosphorous, ammonium, potassium, etc.) changed and altered mainly the bacterial community composition. These results may offer novel opportunities for designing tailored fertilizers applicable to sustainable agriculture.

The development of novel bio-formulations also requires an in-depth study of the molecular factors regulating plant-microbe interactions and to possibly unravel the interactive mechanisms occurring in the rhizosphere (Vishwakarma et al., 2020). In the study by Pachauri et al. the characterization of the mutant M7 of *Trichoderma virens*, previously obtained by gamma-ray induced mutagenesis, showing morphological and metabolic deficiencies compared to the wild-type strain (Mukherjee et al., 2006), was completed. Transcriptome analysis showed that several genes involved in secondary metabolism, carbohydrate metabolism, hydrophobicity, and transportation were down-regulated in M7. In addition, a genetic deletion comprising a total of 250 kb, including 71 predicted ORFs, was found by whole genome sequencing. This approach could help in the identification of novel regulators resulting in the beneficial traits of *Trichoderma* fungi.

Despite the importance of plant-fungus interactions, the molecular factors involved in the regulation of these systems are not fully understood. By using the filamentous fungus *Neurospora crassa* as a model organism to study plant-fungal relationships, Martins et al. demonstrated that the deletion of the gene encoding the zinc finger transcription factor PAC-3, regulated by ambient pH, affected numerous physiological functions, including adaptation to nutritional conditions, regulation of virulence, or regulating the expression of genes associated with structural and metabolic features. These findings highlighted the pivotal role of PAC-3 as regulatory mediator involved in fungal pathogenesis.

CONCLUSION

Currently, the most active research field of investigating integrated pest management strategies is the development of sustainable and eco-efficient approaches for plant disease control. The commercial development of a microbial formulation requires several steps including: isolation, identification and characterization of selected microbes and their biological activity; the optimization of fermentation processes, storage conditions, and the development of the formulation; the registration through opportune patenting, and commercialization (Montesinos, 2003). The articles included in this Research Topic cover different aspects of the interactions occurring in agroecosystems between plants and microbes that will facilitate the implementation of novel sustainable strategies for plant defense.

AUTHOR CONTRIBUTIONS

The authors defined the subject of this Research Topic and joined in the editing procedure. RM wrote the first draft of the manuscript. SW, GB, FV, and SG revised and improved the manuscript. All authors approved this editorial for publication.

FUNDING

This work was supported by MISE CRESO (Grant number **PROTECTION** n. F/050421/01-03/X32); PRIN 2017 (Grant number **PROSPECT** 2017JLN833); MISE Sportello Agrifood DM 5/3/2018 (Grant **VIABIO**); European Union Horizon 2020 Research and Innovation Program, **ECOSTACK** (Grant agreement number 773554); MUR, PNR 2015-2020. ARS01_00985 **BIOFEEDSTOCK** - Sviluppo di Piattaforme Tecnologiche Integrate per la Valorizzazione di Biomasse Residuali; PSR Veneto 16.1.1 (Grant number **DIVINE** n. 3589659); PSR Campania 2014/2020 Misura 16.1 Azione 2 Progetto **DI.O.N.IS.O.** (C.U.P. B98H19005010009).

ACKNOWLEDGMENTS

The editors would like to thank all authors who chose this Topic to publish their work and all reviewers who evaluated the manuscripts.

REFERENCES

Adeniji, A. A., Babalola, O. O., and Loots, D. T. (2020). Metabolomic applications for understanding complex tripartite plant-microbes interactions: Strategies and perspectives. *Biotechnol. Rep*. 25:e00425. doi: 10.1016/j.btre.2020.e00425

Bargaz, A., Lyamlouli, K., Chtouki, M., Zeroual, Y., and Dhiba, D. (2018). Soil microbial resources for improving fertilizers efficiency in an integrated plant nutrient management system. *Front. Microbiol*. 9:1606. doi: 10.3389/fmicb.2018.01606

Chandler, D., Bailey, A. S., Tatchell, G. M., Davidson, G., Greaves, J., and Grant, W. P. (2011). The development, regulation and use of biopesticides for integrated pest management. *Philos. Trans. R. Soc. Lond. Ser. B Biol. Sci*. 366, 1987–1998. doi: 10.1098/rstb.2010.0390

Chaurasia, B., Pandey, A., Palni, L. M. S., Trivedi, P., Kumar, B., and Colvin, N. (2005). Diffusible and volatile compounds produced by an antagonistic *Bacillus subtilis* strain cause structural deformations in pathogenic fungi *in vitro*. *Microbiol. Res*. 160, 75–81. doi: 10.1016/j.micres.2004.09.013

Cheng, Y. T., Li, Z., and Sheng, Y. H. (2019). Plant-microbe interactions facing environmental challenge. *Cell Host Microbe*. 26, 183–192. doi: 10.1016/j.chom.2019.07.009

de Medeiros, H. A., de Araújo Filho, J. V., de Freitas, L. G., Castillo, P., Rubio, M. B., Hermosa, R., et al. (2017). Tomato progeny inherit resistance to the nematode *Meloidogyne javanica* linked to plant growth induced by the biocontrol fungus *Trichoderma atroviride*. *Sci. Reps*. 7:40216. doi: 10.1038/srep40216

Hacquard, S. (2016). Disentangling the factors shaping microbiota composition across the plant holobiont. *New Phytol*. 209, 454–457. doi: 10.1111/nph.13760

Hardy, M. C. (2014). Resistance is not futile: it shapes insecticide discovery. *Insects* 5, 227–242. doi: 10.3390/insects5010227

Jain, A., Singh, H. B., and Das, S. (2021). Deciphering plant-microbe crosstalk through proteomics studies. *Microbiol Res*. 242:126590. doi: 10.1016/j.micres.2020.126590

Luziatelli, F., Ficca, A. G., Melini, F., and Ruzzi, M. (2019). Genome sequence of the plant growth-promoting rhizobacterium (PGPR) *Pantoea agglomerans* C1. *Microbiol. Resour. Announc*. 8:e00828–e00819. doi: 10.1128/MRA.00828-19

Martin, F. N. (2003). Development of alternative strategies for management of soilborne pathogens currently controlled with methyl bromide. *Annu. Rev. Phytopathol*. 41, 325–350. doi: 10.1146/annurev.phyto.41.052002.095514

Martínez-Medina, A., Fernandez, I., Lok, G. B., Pozo, M. J., Pieterse, C. M., and Van Wees, S. C. (2017). Shifting from priming of salicylic acid- to jasmonic acid-regulated defences by *Trichoderma* protects tomato against the root knot nematode Meloidogyne incognita. *New Phytol*. 213, 1363–1377. doi: 10.1111/nph.14251

Montesinos, E. (2003). Development, registration and commercialization of microbial pesticides for plant protection. *Int. Microbiol*. 6:, 245–252. doi: 10.1007/s10123-003-0144-x

Mukherjee, M., Horwitz, B. A., Sherkhane, P. D., Hadar, R., and Mukherjee, P. K. (2006). A secondary metabolite biosynthesis cluster in *Trichoderma virens*: evidence from analysis of genes under expressed in a mutant defective in morphogenesis and antibiotic production. *Curr. Genet*. 50, 193–202. doi: 10.1007/s00294-006-0075-0

Nicoletti, R., and Vinale, F. (2018). Bioactive compounds from marine-derived *Aspergillus, Penicillium, Talaromyces and Trichoderma* species. *Mar. Drugs*. 16:408. doi: 10.3390/md16110408

Pandey, S. S., Singh, S., Babu, C. V., Shanker, K., Srivastava, N. K., and Kalra, A. (2016a). Endophytes of opium poppy differentially modulate host plant productivity and genes for the biosynthetic pathway of benzylisoquinoline alkaloids. *Planta* 243, 1097–1114. doi: 10.1007/s00425-016-2467-9

Pandey, S. S., Singh, S., Babu, C. V., Shanker, K., Srivastava, N. K., Shukla, A. K., et al. (2016b). Fungal endophytes of *Catharanthus roseus* enhance vindoline content by modulating structural and regulatory genes related to terpenoid indole alkaloid biosynthesis. *Sci. Rep*. 6:26583. doi: 10.1038/srep26583

Pandey, S. S., Singh, S., Pandey, H., Srivastava, M., Ray, T., Soni, S., et al. (2018). Endophytes of *Withania somnifera* modulate in planta content and the site of withanolide biosynthesis. *Sci. Rep*. 8:5450. doi: 10.1038/s41598-018-23716-5

Papavizas, G. C., Lewis, J. A., and Moity, T. H. A. E. (1982). Evaluation of new biotypes of *Trichoderma harzianum* for tolerance to benomyl and enhanced biocontrol capabilities. *Phytopathologia* 72, 126–132. doi: 10.1094/Phyto-72-126

Silber, J., Kramer, A., Labes, A., and Tasdemir, D. (2016). From discovery to production: Biotechnology of marine fungi for the production of new antibiotics. *Mar Drugs* 14, 137. doi: 10.3390/md14070137

Singh, R., Kumar, M., Mittal, A., and Mehta, P. K. (2017). Microbial metabolites in nutrition, healthcare and agriculture. *3 Biotech*. 7:15. doi: 10.1007/s13205-016-0586-4

Syed Ab Rahman, S. F., Singh, E., Pieterse, C. M. J., and Schenk, P. M. (2018). Emerging microbial biocontrol strategies for plant pathogens. *Plant Sci*. 267, 102–111. doi: 10.1016/j.plantsci.2017.11.012

Vinale, F., Salvatore, M. M., Nicoletti, R., Staropoli, A., Manganiello, G., Venneri, T., et al. (2020). Identification of the main metabolites of a marine-derived strain of *Penicillium brevicompactum* using LC and GC MS techniques. *Metabolites* 10:55. doi: 10.3390/metabo10020055

Vishwakarma, K., Kumar, N., Shandilya, C., Mohapatra, S., Bhayana, S., and Varma, A. (2020). Revisiting plant-microbe interactions and microbial consortia application for enhancing sustainable agriculture: a review. *Front. Microbiol*. 11:560406. doi: 10.3389/fmicb.2020.560406

Woo, S. L., and Pepe, O. (2018). Microbial consortia: promising probiotics as plant biostimulants for sustainable agriculture. *Front. Plant Sci*. 9:1801. doi: 10.3389/fpls.2018.01801

Woo, S. L., Ruocco, M., Vinale, F., Nigro, M., Marra, R., Lombardi, N., et al. (2014). *Trichoderma*-based products and their widespread use in agriculture. *Open Mycol. J*. 8, 71–126. doi: 10.2174/1874437001408010071

Wu, C. H., Bernard, S. M., Andersen, G. L., and Chen, W. (2009). Developing microbe-plant interactions for applications in plant-growth promotion and disease control, production of useful compounds, remediation and carbon sequestration. *Microb Biotech* 2, 428–440. doi: 10.1111/j.1751-7915.2009.00109.x

Zaidi, N. W., and Singh, U. S. (2013). "*Trichoderma* in plant health management," in *Trichoderma: Biology and Applications,* eds P. K. Mukherjee, B. A. Horwitz, U. S. Singh, M. Mukherjee, and M. Schmoll (CABI Publishing). doi: 10.1079/9781780642475.0230

Conflict of Interest: The authors declare that the research was conducted in the absence of any commercial or financial relationships that could be construed as a potential conflict of interest.

Publisher's Note: All claims expressed in this article are solely those of the authors and do not necessarily represent those of their affiliated organizations, or those of the publisher, the editors and the reviewers. Any product that may be evaluated in this article, or claim that may be made by its manufacturer, is not guaranteed or endorsed by the publisher.

frontiers in Microbiology

ORIGINAL RESEARCH
published: 30 April 2019
doi: 10.3389/fmicb.2019.00925

Endophytic Consortium With Diverse Gene-Regulating Capabilities of Benzylisoquinoline Alkaloids Biosynthetic Pathway Can Enhance Endogenous Morphine Biosynthesis in *Papaver somniferum*

Tania Ray[1†], Shiv S. Pandey[1†], Alok Pandey[2], Madhumita Srivastava[3], Karuna Shanker[3] and Alok Kalra[1]*

[1] *Microbial Technology Department, CSIR-Central Institute of Medicinal and Aromatic Plants, Lucknow, India,* [2] *Biotechnology Division, CSIR-Central Institute of Medicinal and Aromatic Plants, Lucknow, India,* [3] *Analytical Chemistry Department, CSIR-Central Institute of Medicinal and Aromatic Plants, Lucknow, India*

OPEN ACCESS

Edited by:
Sheridan Lois Woo,
University of Naples Federico II, Italy

Reviewed by:
Roberta Fulthorpe,
University of Toronto Scarborough, Canada
Piippa Riitta Wäli,
University of Oulu, Finland

****Correspondence:***
Alok Kalra
alok.kalra@yahoo.com

† These authors have contributed equally to this work

Specialty section:
This article was submitted to Microbial Symbioses, a section of the journal Frontiers in Microbiology

Received: *08 January 2019*
Accepted: *11 April 2019*
Published: *30 April 2019*

Citation:
Ray T, Pandey SS, Pandey A, Srivastava M, Shanker K and Kalra A (2019) Endophytic Consortium With Diverse Gene-Regulating Capabilities of Benzylisoquinoline Alkaloids Biosynthetic Pathway Can Enhance Endogenous Morphine Biosynthesis in Papaver somniferum. Front. Microbiol. 10:925. doi: 10.3389/fmicb.2019.00925

Secondary metabolite biosynthesis in medicinal plants is multi-step cascade known to be modulated by associated endophytes. While a single endophyte is not able to upregulate all biosynthetic steps, limiting maximum yield achievement. Therefore to compliment the deficient characteristics in an endophyte we tried consortium of endophytes to achieve maximum yield. Here, efforts were made to maximize the *in planta* morphine yield, using consortium of two endophytes; SM1B (*Acinetobacter* sp.) upregulating most of the genes of morphine biosynthesis except *T6ODM* and *CODM*, and SM3B (*Marmoricola* sp.) upregulating *T6ODM* and *CODM* in alkaloid-less *Papaver somniferum* cv. Sujata. Consortium-inoculation significantly increased morphine and thebaine content, and also increased the photosynthetic efficiency of poppy plants resulted in increased biomass, capsule weight, and seed yields compared to single-inoculation. The increment in morphine content was due to the modulation of metabolic-flow of key intermediates including reticuline and thebaine, via upregulating pertinent biosynthetic genes and enhanced expression of *COR*, key gene for morphine biosynthesis. This is the first report demonstrating the endophytic-consortium complimenting the functional deficiency of one endophyte by another for upregulating multiple genes of a metabolic pathway similar to transgenics (overexpressing multiple genes) for obtaining enhanced yield of pharmaceutically important metabolites.

Keywords: endophytes, consortium, benzylisoquinoline alkaloids, morphine, *Papaver somniferum*, opium

INTRODUCTION

Increasing populations have threatened food security due to the availability of limited land for cultivation. Moreover, changing environmental conditions are also causing a considerable reduction in the crop productivity. It is estimated that by the year 2050, the world population may reach nine billion. Therefore, to satisfy the needs of the growing population diverse approaches have been tried to increase the food production at the same or even higher rates. Developing transgenics

has so far received foremost attention by introducing desired traits to produce the desired product and improving the productivity in normal as well as changing environmental conditions including cultivation under biotic and abiotic stresses. Plant yield and tolerance to different environmental stresses are polygenic traits and regulated by multiple genes (Bohnert et al., 2006). Therefore, integration/expression/genetic manipulation of more than one genes in a plant became the preferred choice for improvement of plant yield and performance under stressful environmental conditions. However, these practices have limitations related to production cost, social acceptability, and sustainability (Halpin, 2005). Therefore, besides developing transgenic plants, alternate sustainable approaches need to be explored for achieving maximum plant yield.

Endophytes have emerged as a promising candidate for sustainable agriculture. Endophytes are plant-associated microbes residing within the plant without harming or causing any disease symptoms. They promote plant growth, protect plants from environmental stresses and are the promising source of therapeutic secondary metabolites (Kuklinsky-Sobral et al., 2004; Strobel et al., 2004; Waller et al., 2005; Rodriguez et al., 2008; Staniek et al., 2008; Kusari et al., 2012; Quecine et al., 2012; Otieno et al., 2015; Egamberdieva et al., 2017). Involvement of endophytes in the modulation of secondary metabolite biosynthesis of the host plant has also been established (Pandey et al., 2016a,b, 2018). Bacterial endophyte interaction with *E. purpurea* enhances its secondary metabolites which contributes to therapeutic properties of this medicinal plant (Maggini et al., 2017). An *Artemisia annua* endophytic actinobacterium *Pseudonocardia* strain YIM 63111 has been able to induce artemisinin production by upregulating the genes of artemisinin biosynthetic pathway, i.e., cytochrome P450 monooxygenase and cytochrome P450 oxidoreductase (Li et al., 2012). Also role of microbial community present in the cortical parenchymatous tissue of *Vetiver* in essential oil biosynthesis has been reported (Del Giudice et al., 2008). Inoculation with bacterial endophytes increases biomass and in planta content of terpenoid indole alkaloids like vindoline in *Catharanthus roseus* (Tiwari et al., 2013). *Paenibacillus strain* has been found to strongly influence the plant metabolites of *in-vitro* grown poplar plants (Scherling et al., 2009). Interestingly, endophytes are also able to produce secondary metabolites analogous to their host plants, e.g., camptothecin and analogs (Shweta et al., 2010), taxol (Soliman et al., 2011), vincristine, and vinblastine (Kumar et al., 2013). Fungal endophytes as symbiotically modified organism (SMO) have also been used to improve grass yield, provide resistance against pests, weeds and herbivores by accumulation of alkaloids and antioxidants (Gundel et al., 2013, 2018). It has been demonstrated in our laboratory that endophytes are involved in the improvement of the content of vindoline (intermediate for the biosynthesis of anticancerous vinblastine and vincristine) in *Catharanthus roseus* (Pandey et al., 2016a), withanolides in *Withania somnifera* (Pandey et al., 2018), and benzylisoquinoline alkaloids (BIAs) in *Papaver somniferum* (Pandey et al., 2016b). Previous studies have also demonstrated the diverse role of endophytes in a host plant (Di Fiore and Del Gallo, 1995; Saikkonen et al., 1998; Singh et al., 2011; Hardoim et al., 2015; Pandey et al., 2016a,b, 2018). Every endophyte has a specific characteristic, up/down-regulating certain specific genes responsible for plant growth, yield, and modulation of secondary metabolite biosynthesis. Although reports signifying the role of a particular endophyte modulating a single functional characteristic like growth promotion or disease resistance, stress tolerance or enhance secondary metabolite production are available, but the information on the possibility of strengthening multiple functional characteristics through the use of consortium is scarce. Therefore, the use of consortium of endophytes having different functional characteristics should be explored to maximize the yields and desired products.

Here, we demonstrated the use of consortium of selected endophytes associated with the capsule of opium poppy plant which is the site for BIA biosynthesis to maximize the yield of pharmaceutically important metabolite morphine. Opium poppy is an important medicinal plant and sole source of therapeutically important BIAs such as morphine, codeine, thebaine, papaverine, noscapine, and sanguinarine. Morphine belongs to the group "opioids" which are key drugs for the alleviation of moderate-to-severe acute pain associated with cancer and other diseases or after any surgery or physical trauma (Rosenblum et al., 2008; Whittle et al., 2011).

Previously we have established that the opium poppy has potential endophytes which can enhance *in planta* BIA biosynthesis. We demonstrated that different endophytes are associated with different parts of poppy plants performing an important role in a tissue-specific manner. In general, endophytes related with leaf were involved in modulating photosynthetic efficiency and endophytes associated with the capsule were drawn in modulating the BIA-biosynthesis of the poppy plant. It was observed that endophytes SM1B and SM3B isolated from capsule of alkaloid rich Sampada were unable to enhance the BIA production in *P. somniferum* cv. Sampada plants. However, these capsule-associated endophytes were able to increase the production of BIAs in alkaloid-less cv. Sujata. The cv. Sujata was developed from alkaloid-rich cv. Sampada with the aim to convert a narcotic "opium poppy" (i.e., cv. Sampada) into non-narcotic seed poppy (i.e., cv. Sujata) using gamma rays and EMS (ethyl methane sulphonate) (Sharma et al., 1999). The cv. Sujata is considered to be having the potential for commercial cultivation of seeds due to high nutritive value of 24% protein, >58% oil with high unsaturated fatty acids makes it a safe and potential food crop having protein rich seeds (Sharma et al., 2002). Previously we have established that the individual inoculation with endophytes SM1B and SM3B increased biomass upto 44% in cv. Sujata. SM1B inoculation in cv. Sujata plants increased content of Morphine by 1044%, Papaverine by 349% and Noscapine by 936%, and SM3B inoculation increased Morphine by 37%, Papaverine by 66%, Noscapine by 72%, and Thebiane by 154% (Pandey et al., 2016b). It was observed that endophyte SM1B could upregulate most of the genes of BIA biosynthesis except thebaine 6-O-demethylase (*T6ODM*) and codeine O-demethylase (*CODM*) (Pandey et al., 2016b). However, we could also identify another endophyte SM3B that was able to upregulate *T6ODM* and *CODM* expression. We, therefore, expected that the consortium of SM1B and SM3B will

lead to the overexpression of all BIA biosynthetic pathway genes simultaneously and will produce more morphine than single inoculation. Here, efforts were made to maximize morphine yield using the consortium of two capsule-associated endophytes SM1B (*Acinetobacter* sp.) and SM3B (*Marmoricola* sp.) in the poppy plant by upregulating different genes of BIA biosynthesis.

MATERIALS AND METHODS

Plant Materials and Growth Conditions

Seeds of *Papaver somniferum* cv. Sujata was obtained from the National Gene Bank for Medicinal and Aromatic Plants at CSIR-CIMAP, Lucknow. Poppy plants were grown in pots filled with 3.5 kg of autoclaved soil and vermicompost mixture (2:1, v/v) having dimension (17 cm height × 22 cm top diameter × 12 cm bottom diameter and 3.7 l volume) and irrigated with sterile water with an ordinary photoperiod in a greenhouse under natural light intensity at 20°C ± 2°C.

Antagonistic Activity of Endophytes

Antagonistic activity of both the selected endophytes was tested by *in vitro* antimicrobial assay. For this, the disc diffusion method of Bhunia et al. (1988) was followed with some modifications. SM1B and SM3B both were grown in nutrient broth for 24 h at 28°C. The final concentration of each bacterium was adjusted to 10^6 CFU/ml. 100 μl 10^6 CFU/ml cell suspension was spread on nutrient agar media and leave the plates to get dried on room temperature (Tajehmiri et al., 2014). The sterile paper disc (6 mm) were placed over nutrient agar media plates, seeded with indicator strains. Hundred microliter of culture was added to the sterile paper disc and incubated at 28°C for 48 h. After incubation, antagonistic activity was observed around the paper disc. As there was no zone of inhibition around the paper disc and both the bacteria were growing with each other which confers that there is no antagonistic activity between the two bacterial strains and they synergistically performed their function.

Endophyte Inoculation

For consortium development individual suspension (1×10^8 CFU ml^{-1}) of the two endophytes (SM1B and SM3B) was prepared in PBS and were mixed at a CFU of 1×10^8 ml^{-1} microbes each in 5 ml culture prepared in PBS. Endophyte-free seeds were treated by putting them in consortium suspension for 2 h and then used for sowing in pots. Pots were kept in the controlled condition in greenhouse. For each treatment the experiment was conducted in triplicates. Initially, there were 25 seeds sown in each pot, and when the seeds grown for 2 weeks. Only five healthy seedlings were kept in each pot. In order to boost up the soil with sufficient inoculum of endophyte, to ensure their presence in the soil. The pots were again inoculated with 10 ml pot^{-1} of the endophyte suspension (1×10^8 CFU ml^{-1}). To make certain the presence of adequate numbers of endophyte in the soil, pots were inoculated for a second time after 2 weeks of germination of seeds. PBS was used in place of endophyte suspension in case of the control plants (uninoculated). To confirm the presence of specific endophytes, re-isolation of endophyte has been done from various parts of poppy plants at 60 days stage. No endophytes were found to be present at any stage from the uninoculated endophyte-free control plants. SM1B and SM3B inoculated plants (individual inoculation) were grown simultaneously with the consortium-inoculated (SM1B and SM3B) plants.

Colonization of Endophytes

Endophyte colonization was inspected in the capsule of poppy plants in triplicates after 90 days of growth. Tissues were surface sterilized and sterility check was performed as illustrated previously (Pandey et al., 2016b). Under sterile conditions, the surface sterilized tissues were thoroughly macerated, and serial dilutions were plated on nutrient agar with three replications each. The plates were then incubated at 28°C for 24–72 h and then the CFU were estimated. The obtained colonies were confirmed by the morphological characteristics followed by 16S rRNA sequencing.

Photosynthetic Pigment Content, Photosynthetic Rate, Stomatal Conductance, Transpiration Rate

Photosynthetic pigment (Chlorophyll) content and photosynthetic efficiency of fully expanded leaves (third from the top) of 60 days poppy plants (n = 6) were measured. Chlorophyll extraction was performed in chilled methanol, and the content was estimated (Lichtenthaler and Buschmann, 2001). Photosynthetic efficiency (net CO_2 assimilation, transpiration rate and stomatal conductance) was measured in the attached leaves (third from the top) using the Portable Photosynthesis System (CIRAS-3, PP System, United States) attached with the Chlorophyll fluorescence module (CFM-3). For photosynthesis measurement, CO_2 concentration in leaf cuvette was maintained at ambient CO_2 (400 ppm), temperature (25°C) and 400 μmol photons m^{-2} s^{-1} light.

Biomass, Capsule Weight, and Seed Yield

Biomass of 60 days old poppy plant (n = 6) was measured by harvesting the entire shoots and dried at 70°C for 5 days, and their dry weights were measured. Capsule weight and seed yield were measured from 120 days mature poppy plants.

Benzylisoquinoline Alkaloids

BIAs analysis was performed from the capsules of 120 days old poppy plants. Capsules were completely dried and ground to fine powder. Powdered samples (1 g) were extracted three times in 100% methanol (30 ml) with 20 min sonication at 42°C. Extract was filtered through Whatman Number 1 filter paper and then the filtrates were concentrated in Rotavapour, dried, and re-dissolved in methanol. BIAs (morphine, codeine, thebaine, papaverine, noscapine and reticuline) were analyzed by isocratic reverse-phase HPLC using phosphate buffer (0.1 M $NaH_2PO_4.2H_2O$, pH 3.5, 77%, v/v) and acetonitrile (23%, v/v), sample injection volume of 20 μl, at flow rate of 1.0 ml min^{-1} on Phenomenex, Luna C_{18} column®, Waters (4.6 × 250 mm, 5 μm).

The analysis was performed with Empower Pro software (Waters, United States). Photodiode array data acquisition was in the range of 200–400 nm and the quantitation was done at 240 nm. Peaks of analyzed alkaloids were identified by comparing their retention times with commercially available authentic standards. Noscapine and reticuline were purchased from Sigma-Aldrich, St. Louis, United States. Morphine, codeine, thebaine and papaverine were gifted from CSIR-National Botanical Research Institute, Lucknow. The data was an average of two independent quantifications repeated in three biological replicates ($n = 6$).

qRT-PCR Analysis

Total RNA was isolated from the green capsule of un-inoculated endophyte-free control and endophytes-inoculated 90 days old poppy plants by using TRI-reagent (Sigma-Aldrich). RNA quantification was done using NanoDrop 1000 spectrophotometer (Thermo Fisher Scientific). Genomic-DNA contamination in the total RNA preparation was eliminated using RNase-free DNase I enzyme (Thermo Scientific). First-strand cDNA synthesis was performed with ∼5 μg of total RNA using the RevertAid First Strand cDNA Synthesis Kit with oligo$(dT)_{18}$ primer (Thermo Scientific) following the manufacturer's instructions. Previously described gene-specific primers were used for the analysis of relative quantification of 16 biosynthetic gene transcripts involved in BIA biosynthetic pathway (Pandey et al., 2016b). qRT-PCR was performed using SYBR-Green I detection on triplicate technical replicates of triplicate biological samples ($n = 3$) on an Applied Biosystems StepOnePlus™ Real-Time PCR System as described previously (Pandey et al., 2016b). PCR mixture contains 1 μl of 10 times diluted cDNA synthesis reaction, 300 nM each forward and reverse primers and 5 μl Power SYBR Green PCR Master Mix (Applied Biosystems), in a 10 μl reaction volume. PCR conditions were maintained at 95°C for 10 min, followed by 40 cycles of denaturation at 95°C for 15 s each and annealing at 60°C for 1 min each. The intensities of fluorescent signal were recorded on an Applied Biosystems StepOnePlusTM Real Time PCR System and analysis were carried out using StepOne software (Applied Biosystems). Specificity of RT-qPCR was evaluated by using the dissociation method (Applied Biosystems) subjecting all amplicons to a melt-curve analysis. The threshold cycle (Ct) for each gene was normalized against the Ct for β-actin (EB740770) of opium poppy, which was used as the endogenous reference transcript. Further, Mean Ct values were calculated from technical triplicates, and the relative levels of transcripts of different genes. BIAs biosynthetic genes in endophyte-inoculated plants were compared with the calibrator (non-inoculated control plant) using the relative quantification $2^{-\Delta\Delta Ct}$ method and efficiency of PCR was also determined by the method of Livak and Schmittgen (2001) and Schmittgen and Livak (2008). For amplification serially diluted cDNA was used as template for different target genes and reference gene. To determine ΔCt (Ct target – Ct reference) the average Ct was calculated for both target gene and reference gene. A plot of the log cDNA dilution versus ΔCt was drawn, and the absolute value of the slope were found to be near zero for all the target genes that showed that the efficiencies of the target and reference genes were quite similar. Therefore, relative quantification $2^{-\Delta\Delta Ct}$ method was applied to analyze the data (Livak and Schmittgen, 2001).

Statistical Analysis

Statistical analysis of data was carried out following ANOVA analysis of variance, suitable to completely randomized design (CRD), using SPSS (IBM, Chicago, IL, United States). Comparisons between means were carried out using Duncan's multiple range tests at a significance level of $P \leq 0.05$.

RESULTS

Antagonistic Activity of Endophytes and Their Colonization in the Capsule of Poppy Plants

Antagonistic activity of SM1B and SM3B was tested. It was observed that both endophytes grew well together and did not inhibit the growth of each other (**Supplementary Figure S1**). Colonization of SM1B and SM3B endophytes was determined in the capsule of poppy plant inoculated with SM1B and SM3B individually as well as a consortium of SM1B and SM3B. It was observed that both endophytes could successfully colonize the capsule of *P. somniferum* plant (**Figure 1**). Colonization of SM1B was reduced in the poppy plants inoculated with a consortium of SM1B and SM3B compared to individual inoculation of SM1B. However, the colonization of SM3B was found to be similar

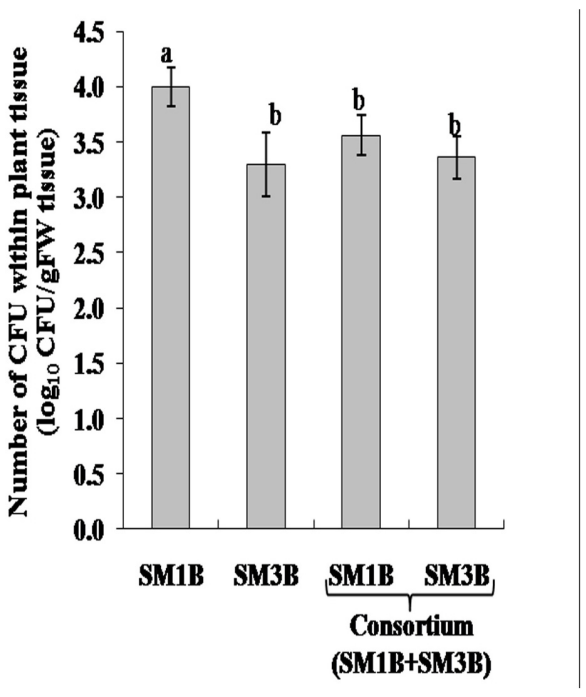

FIGURE 1 | Colonization of endophytes in the capsule of *Papaver somniferum* plants. CFU- colony forming unit. Values are the mean ± SE of three replicates ($n = 3$). Different letters (a–b) indicate statistically significant differences between treatments (Duncan's multiple range test $P < 0.05$).

TABLE 1 | Effect of inoculation of consortium of endophytes on different physiological parameters of *Papaver somniferum* plant.

Physiological parameters	Control	SM1B	SM3B	Consortium (SM1B+SM3B)
Chlorophyll (mg gFW^{-1})	0.70 ± 0.03^{b}	0.85 ± 0.06^{ab}	0.82 ± 0.03^{ab}	0.89 ± 0.04^{a}
Net CO_2 assimilation (μMole CO_2 $m^{-2}s^{-1}$)	7.87 ± 0.16^{c}	9.10 ± 0.12^{b}	7.90 ± 0.24^{c}	9.90 ± 0.11^{a}
Stomatal conductance (mMole $m^{-2}s^{-1}$)	321.67 ± 2.86^{c}	419.33 ± 1.22^{b}	325.67 ± 7.35^{c}	448.00 ± 6.12^{a}
Transpiration rate (mMole $m^{-2}s^{-1}$)	3.53 ± 0.20^{c}	4.30 ± 0.10^{b}	3.56 ± 0.06^{c}	5.17 ± 0.06^{a}
Biomass (g $Plant^{-1}$)	0.60 ± 0.04^{c}	0.79 ± 0.03^{b}	0.68 ± 0.02^{c}	1.05 ± 0.01^{a}
Capsule weight (g $Plant^{-1}$)	1.22 ± 0.12^{c}	1.59 ± 0.02^{b}	1.18 ± 0.09^{c}	2.03 ± 0.11^{a}
Seed yield (g $Plant^{-1}$)	0.52 ± 0.06^{b}	0.66 ± 0.02^{b}	0.57 ± 0.04^{b}	0.93 ± 0.09^{a}

Different letters (a–c) indicate statistically significant differences between treatments (Duncan's multiple range test $P < 0.05$). Data are means ± SD ($n = 6$).

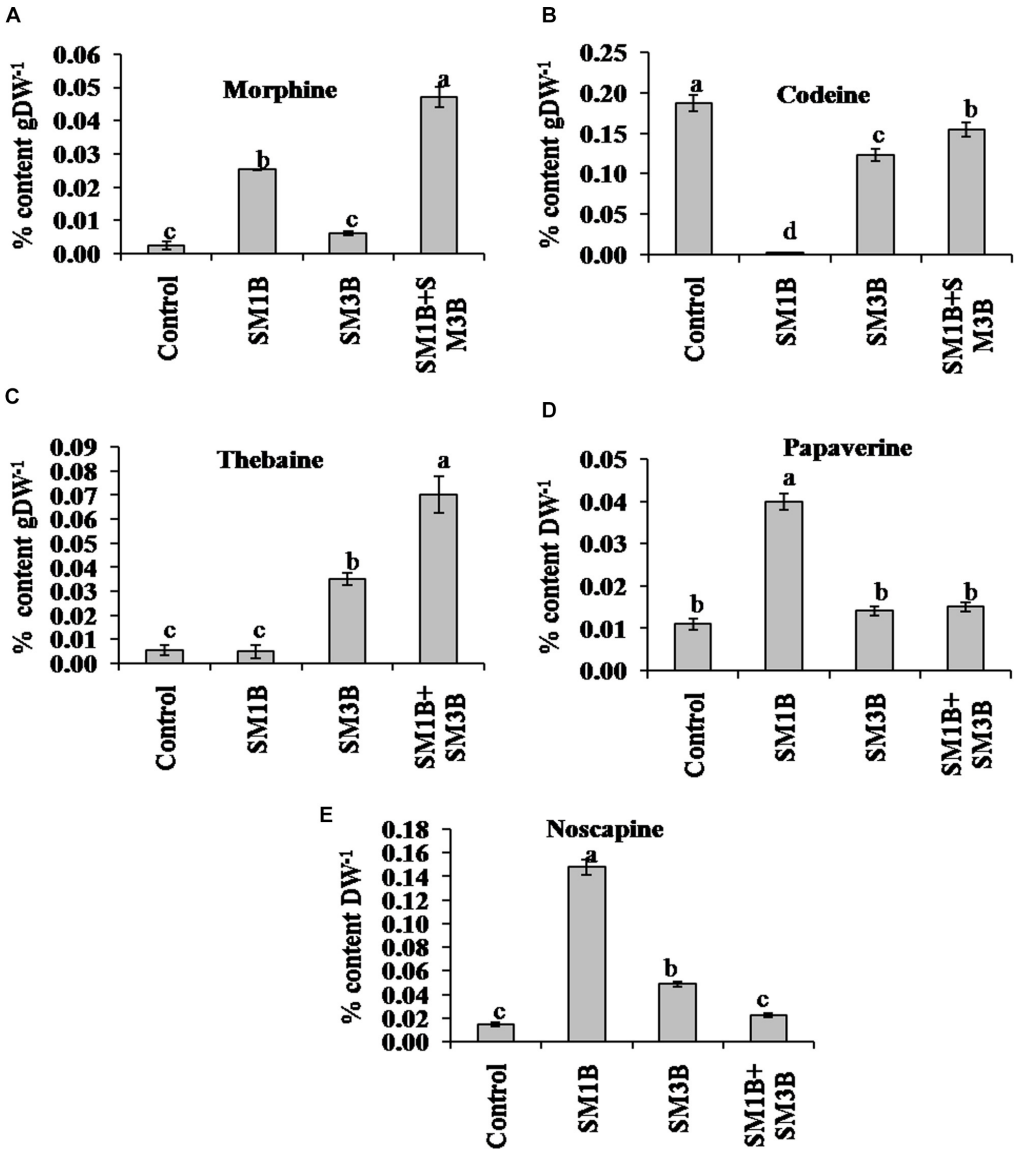

FIGURE 2 | Effect of endophytes inoculation on the alkaloid content of *Papaver somniferum*. Morphine **(A)**, codeine **(B)**, thebaine **(C)**, papaverine **(D),** and noscapine **(E)** content was measured from the dried capsule of 120 days old *P. somniferum* plants inoculated with endophytes SM1B and SM3B individually, and in the form of consortium (SM1B+SM3B). Non-inoculated endophyte free plants were used as a control. The data was an average of two independent quantifications repeated in three biological replicates ($n = 6$) and represented in % content/gram of dry weight (DW). Error bars represent standard errors. Different letters (a–d) indicate statistically significant differences between treatments (Duncan's multiple range test $P < 0.05$).

in both individual (SM3B), and consortium inoculated plants (**Supplementary Table S1**).

Effect of a Consortium of Endophytes on Photosynthetic Efficiency of the Plant

Photosynthetic efficiency of plants was studied by measuring the chlorophyll content, net CO_2 assimilation rate, stomatal conductance, and transpiration rate. Application of endophytic consortium improved the measured parameters. Inoculation with the consortium of SM1B and SM3B in *P. somniferum* plants increased chlorophyll content, net CO_2 assimilation rate, stomatal conductance, and transpiration rate by 27.1, 25.8, 39.3, and 46.5%, respectively, compared to endophyte-free control plants (**Table 1**). Individual inoculation of SM1B could increase the chlorophyll (21.43%), net CO_2 assimilation rate (15.63%), stomatal conductance (30.36%), and transpiration rate (21.81%), however, SM3B inoculation could only increase the chlorophyll content (17.14%).

Effect of a Consortium of Endophytes on Biomass, Capsule Weight, and Seed Yield

Application of consortium of endophytes significantly enhanced the biomass, capsule weight and seed yield of *P. somniferum* plants. Inoculation with a consortium of SM1B and SM3B increased the biomass of *P. somniferum* plant by 75% compared to endophyte-free control plants (**Table 1**). Consortium inoculated plants also had 66.4% higher capsule weight than that of endophyte-free control plants. More importantly, the consortium of endophytes could enhance the yield of seeds, another economic part of the plant, by 78.8% over control (**Table 1**). Individual inoculation (SM1B) could only increase the biomass by 31.7%, capsule weight by 30.3% and seed yield by 26.9% which was considerably lower than the consortium inoculated plants. However, SM3B inoculation could only increase the biomass (13.3%) (**Table 1**).

Effect of a Consortium of Endophytes on Alkaloid Content

To study the impact of a consortium of endophytes on BIA production, the content of morphine, codeine, thebaine, papaverine, and noscapine was estimated in the capsule of individual, consortium inoculated and non-inoculated endophyte-free control poppy plants (**Figure 2**). Consortium inoculation increased the content of morphine content (2250%) than that of endophyte-free control plants. Consortium inoculation also increased papaverine and noscapine content by 36.4 and 53.3%, respectively.

Individual inoculation of SM1B and SM3B could increase the morphine (200–1150%) which was considerably lower than consortium inoculated plants; also an increase in the content of papaverine (27.3–263.6%) and noscapine (226.7–886.7%) was noticed over non-inoculated plants. Although consortium inoculated plants, had 1067% higher thebaine than that of endophyte-free control plants, inoculation of SM3B could enhance thebaine content only by 483% whereas inoculation SM1B did not affect the thebaine content. Individual inoculation of both the endophytes as well as consortium, on the other hand, decreased the content of codeine (17.6–98.9%).

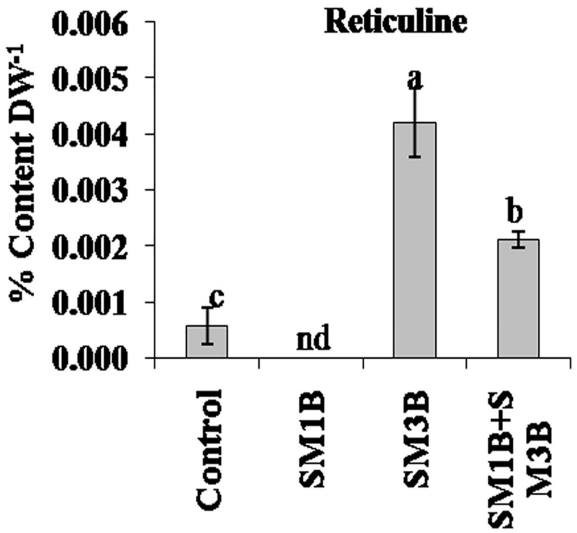

FIGURE 3 | Effect of endophytes inoculation on the reticuline content of *Papaver somniferum*. Reticuline was measured from the dried capsule of 120 days old *P. somniferum* plants inoculated with endophytes SM1B and SM3B individually, and in the form of consortium (SM1B+SM3B). Non-inoculated endophyte free plants were used as a control. The data was an average of two independent quantifications repeated in three biological replicates ($n = 6$) and represented in % content/gram of dry weight (DW). Error bars represent standard errors. Different letters (a–c) indicate statistically significant differences between treatments (Duncan's multiple range test $P < 0.05$). nd, not detected.

Reticuline content was also found to be affected with the endophyte inoculations. Reticuline was not detected in SM1B-inoculated plants. However, SM3B-inoculated plants had a higher accumulation of reticuline compared to endophyte-free control plants (**Figure 3**). Consortium-inoculated plants had lower reticuline accumulation than that of SM3B, however, content was higher than that of endophyte-free control plants (**Supplementary Table S2**).

Expression of Genes of BIA Biosynthesis

To understand the mechanism of endophytes consortium-mediated increase in morphine content the expression of different genes of BIA biosynthesis was quantified using qRT-PCR. Transcript of a total of 16 genes was quantified. Results were normalized to endogenous gene of opium poppy reference transcript (β-actin) and are presented relative to the level in non-inoculated endophyte-free control plants (calibrator). RQ was calculated using the equation; $RQ = 2^{-\Delta\Delta Ct}$. Expression of *TyrAT* was not affected significantly due to the individual as well as consortium inoculations. The expression of *TYDC, NCS,* and *6OMT* in the consortium-inoculated plants was 4.4-, 5.3-, and 7.6-fold higher compared to non-inoculated endophyte-free control plants, respectively (**Figure 4**). Contrary, SM1B alone inoculated plants had only 2.5- and 3.2-fold

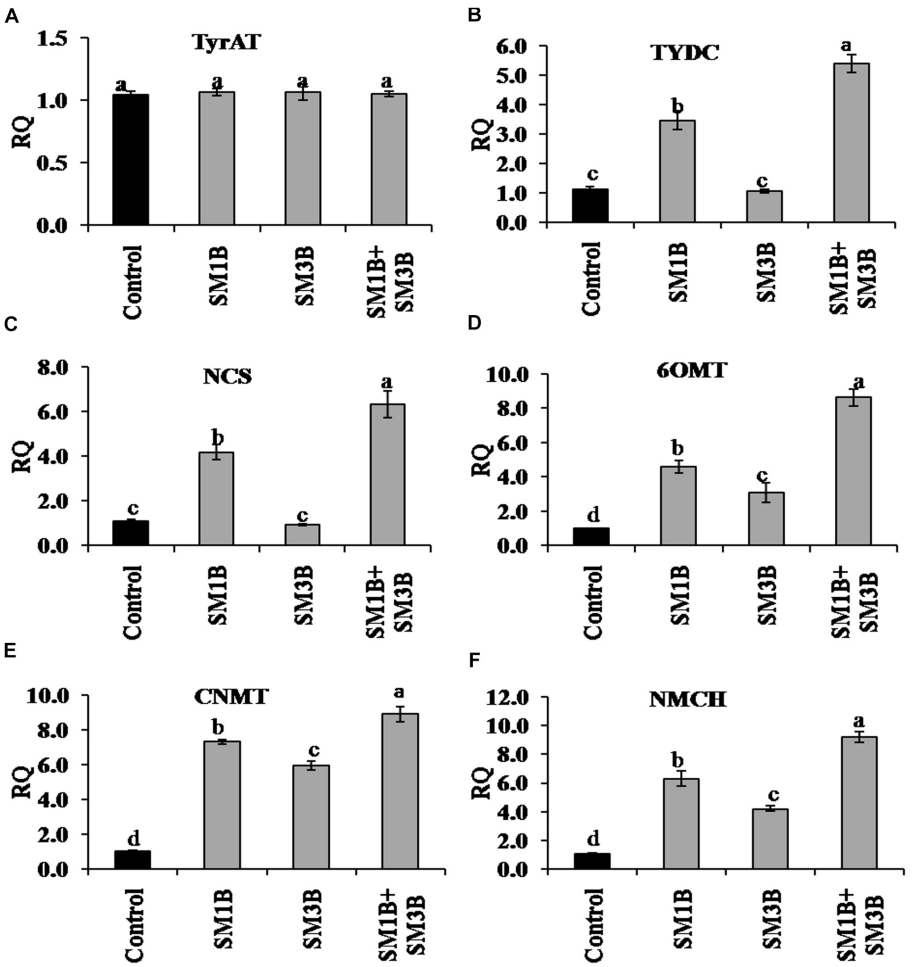

FIGURE 4 | Effect of endophytes inoculation on the expression of genes involved in reticuline biosynthesis. Total RNA was isolated from the green capsule of 90 days old *P. somniferum* plants inoculated with endophytes SM1B and SM3B individually, and in the form of consortium (SM1B+SM3B), reverse transcribed and used as a template for RT-qPCR with SYBR Green detection. The capsules of non-inoculated endophyte free plants were used as a control. Expression of *TyrAT* **(A)**, *TYDC* **(B)**, *NCS* **(C)**, *6OMT* **(D)**, *CNMT* **(E)**, *NMCH* **(F)** was analyzed. Results were normalized to actin (reference transcript) and are shown relative to the level in non-inoculated endophyte free control plants (calibrator). qRT-PCR was performed on triplicate technical replicates of triplicate biological samples ($n = 3$). Data are means ± SE ($n = 3$ biological replicates) and *Y*-axis represents relative quantity (RQ). RQ was calculated using the equation; RQ = $2^{-\Delta\Delta Ct}$. Different letters (a–d) indicate statistically significant differences between treatments (Duncan's multiple range test $P < 0.05$).

higher expression of *TYDC* and *NCS*, respectively, while SM3B inoculation did not affect their expression significantly. *6OMT* expression was lower in individual inoculated plants compared to consortium inoculated plants. Expression of *CNMT* and *NMCH* in consortium-inoculated plants was 8.9- and 9.2-fold higher than that of endophyte-free control plants, respectively (**Figure 4**). Individual inoculation of SM1B and SM3B could also increase the expression of *CNMT* (5.9–7.3-fold) and *NMCH* (4.2–6.3-fold), but the increment was lower compared to consortium inoculation.

Expression of genes involved in papaverine biosynthesis, i.e., *N7OMT* and *7OMT* was increased by 7.2- and 2.6-fold, in consortium-inoculated plants, respectively (**Figure 5**). Individual inoculation could also upregulate *N7OMT* and *7OMT* expression but were lower than that of consortium inoculated plants. In consortium-inoculated plants expression of genes involved in noscapine biosynthesis, i.e., *BBE* and *TNMT* was increased by 5.3- and 7.3-fold, respectively (**Figure 5**) whereas individual-inoculation could also increase *BBE* (5.5–11.8-fold) and *TNMT* (4.5–8-fold) expression.

The increment in the expression of *SalSyn*, *SalR,* and *SalAT* mediated by consortium inoculation was higher than the individual endophyte inoculation (**Figure 6**). Consortium-inoculated plants had 7.0-, 5.9-, and 6.4-fold higher *SalSyn*, *SalR,* and *SalAT* expression compared to non-inoculated endophyte-free control plants. Individual inoculation of SM1B and SM3B could increase the expression of *SalSyn* (2.8–5.8-fold), *SalR* (2.7–2.8-fold) and *SalAT* (3.6-fold) to lower levels only. The consortium-inoculated plants and SM1B inoculated plants had reduced expression of *T6ODM*, however, SM3B inoculated plants had 2.4-fold higher *T6ODM* expression compare to endophyte-free control plants (**Figure 6**).

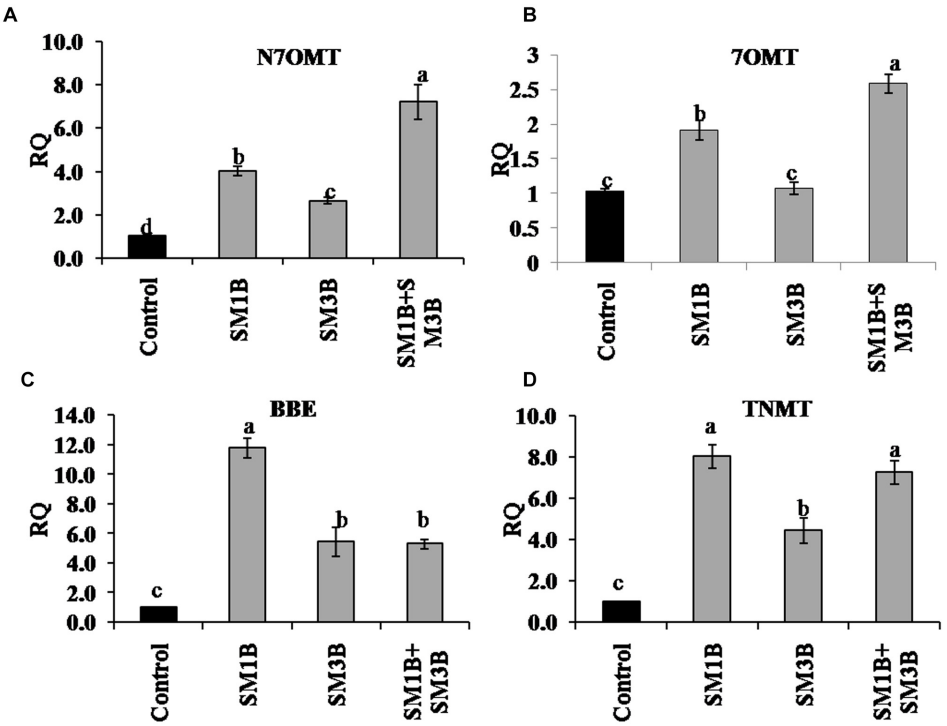

FIGURE 5 | Effect of endophytes inoculation on the expression of genes involved in papaverine and noscapine biosynthesis. Total RNA was isolated from the green capsule of 90 days old *P. somniferum* plants inoculated with endophytes SM1B and SM3B individually, and in the form of consortium (SM1B+SM3B), reverse transcribed and used as a template for RT-qPCR with SYBR Green detection. The capsules of non-inoculated endophyte free plants were used as a control. Expression of genes involved in papaverine biosynthesis *N7OMT* **(A)**, *7OMT* **(B)** and noscapine biosynthesis *BBE* **(C)**, *TNMT* **(D)** was analyzed. Results were normalized to actin (reference transcript) and are shown relative to the level in non-inoculated endophyte free control plants (calibrator). qRT-PCR was performed on triplicate technical replicates of triplicate biological samples ($n = 3$). Data are means ± SE ($n = 3$ biological replicates) and *Y*-axis represents relative quantity (RQ). RQ was calculated using the equation; RQ = $2^{-\Delta\Delta Ct}$. Different letters (a–d) indicate statistically significant differences between treatments (Duncan's multiple range test $P < 0.05$).

Expression of *CODM* was not affected significantly due to the consortium- and SM1B-inoculation. However, SM3B inoculated plants had almost twofold higher *CODM* expression than the endophyte-free control plants, SM1B and consortium inoculated plants (**Figure 6**). Expression of *COR,* considered to be the most critical regulatory gene, was 2.3-fold higher in the consortium- inoculated plants whereas SM1B alone could increase it to the level of 0.9-folds only and SM3B inoculation reduced *COR* expression compare to endophyte-free control (**Figure 6**). Upregulation of multiple genes involved in morphine biosynthesis due to inoculation of a consortium of endophytes is represented in **Figure 7** (**Supplementary Table S3**).

DISCUSSION

Due to limitations related to social acceptability and cost-effectiveness in genetic manipulation approaches such as the development of transgenics by overexpressing single or multiple genes simultaneously, there is a need of an alternate sustainable approach for improvement of crop production and a healthier environment. Microbes associated with plants such as plant growth promoting rhizobacteria (PGPRs) and endophytes have been used as promising candidates for sustainable agriculture. They are found to be involved in improving plant growth and protection from environmental stresses. We have demonstrated that PGPRs and endophytes can protect the plant from environmental stresses by modulating the phytohormone status of plants and by modulating the expression of stress-responsive genes (Bharti et al., 2016; Barnawal et al., 2016, 2017). Also, endophytes residing in most of the parts of the plant including root, stem, leaves, seeds, fruits, flower, and found to perform the tissue-specific function may also modulate primary and secondary metabolism of a plant (Pandey et al., 2016a). Endophytes are considered better candidates than PGPR because they function residing inside the plant and therefore, they do not face any competition with the resident soil microorganisms and also escape from the surrounding harsh environmental conditions. Diverse endophytes are available with specific characteristics related to growth promotion ability and stress tolerance such as an ability of nutrient acquisition, nitrogen fixation, phosphate solubilization, ACC-deaminase production, phytohormone production and suppression of plant pathogens that make them useful for improvement of plant growth and for providing tolerance to environmental stresses. A single endophyte may not be able to carry said multiple

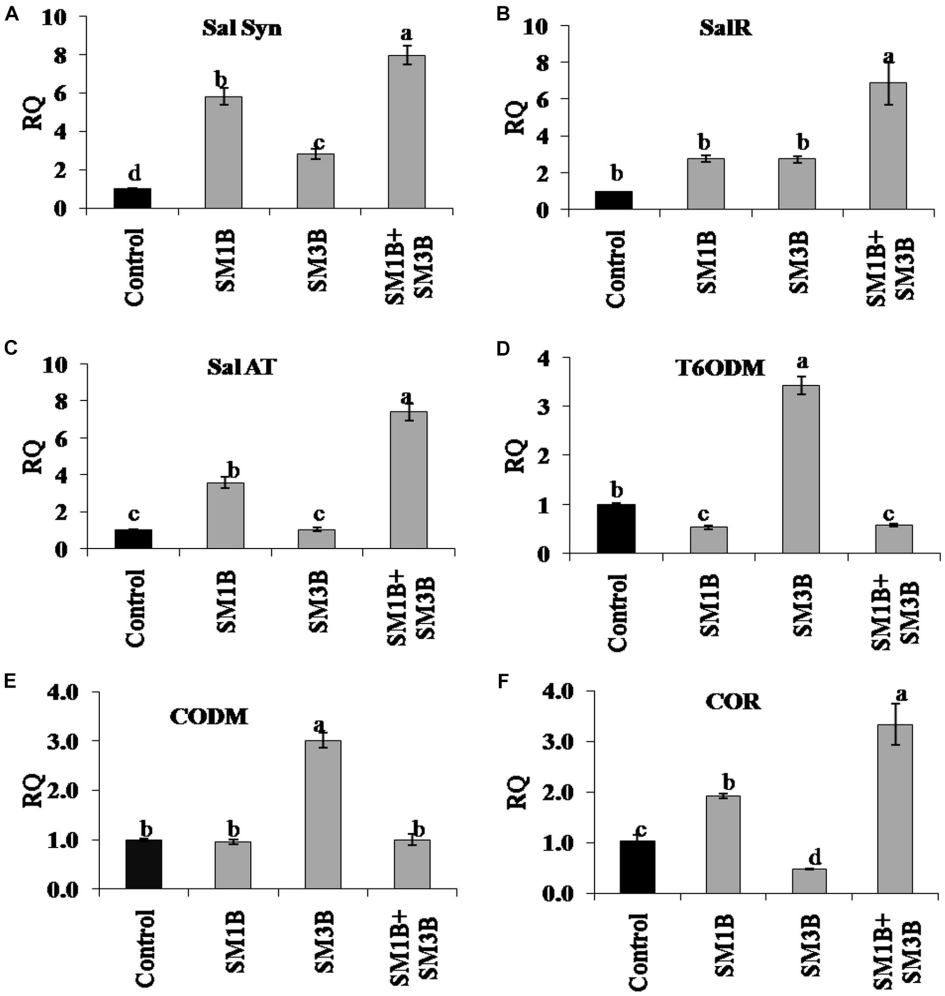

FIGURE 6 | Effect of endophytes inoculation on the expression of genes involved in morphine biosynthesis. Total RNA was isolated from the green capsule of 90 days old *P. somniferum* plants inoculated with endophytes SM1B and SM3B individually, and in the form of consortium (SM1B+SM3B), reverse transcribed and used as a template for RT-qPCR with SYBR Green detection. The capsules of non-inoculated endophyte free plants were used as a control. Expression of *SalSyn* **(A)**, *SalR* **(B)**, *SalAT* **(C)**, *T6ODM* **(D)**, *CODM* **(E)**, *COR* **(F)** was analyzed. Results were normalized to actin (reference transcript) and are shown relative to the level in non-inoculated endophyte free control plants (calibrator). qRT-PCR was performed on triplicate technical replicates of triplicate biological samples ($n = 3$). Data are means ± SE ($n = 3$ biological replicates) and *Y*-axis represents relative quantity (RQ). RQ was calculated using the equation; RQ = $2^{-\Delta\Delta Ct}$. Different letters (a–d) indicate statistically significant differences between treatments (Duncan's multiple range test $P < 0.05$).

growth promotion activities. Therefore, to obtain maximum growth and crop yield consortium of endophytes having different characteristics will be a better approach than single-endophyte inoculation.

Previously, we have demonstrated that inoculation of an endophyte of opium poppy SM1B (*Acinetobacter* sp.) which was isolated from the capsule of an alkaloid-rich cultivar of *P. somniferum* (cv. Sampada) enhanced morphine content substantially in alkaloid-less cv. Sujata. However, the accumulation of intermediates of morphine synthesis; thebaine and codeine was very low in SM1B-inoculated plants (Pandey et al., 2016b). Also, another endophyte SM3B (*Marmoricola* sp.) inoculation could not increase the morphine content significantly, but substantially increased the thebaine (another important alkaloid) accumulation compared to endophyte-free control plants. Gene expression study of these endophytes (SM1B and SM3B) inoculated plants showed that most of the genes (except *T6ODM* and *CODM*) of BIA biosynthesis were upregulated in SM1B-inoculated plants. On the other hand, *T6ODM* and *CODM* could be upregulated by SM3B-inoculation. The present study therefore aimed at upregulation of all the genes involved in morphine biosynthesis by inoculating these two endophytes through complementarity. Single-inoculation of these endophytes enhanced the morphine content in a morphine-less cultivar of *P. somniferum* (cv. Sujata), however, this could not increase up to the level of an alkaloid-rich cultivar of *P. somniferum* (cv. Sampada) from where these endophytes were isolated. Therefore, the efficacy of combined inoculation of both the endophytes (SM1B and SM3B) in maximizing the production of morphine, was tested

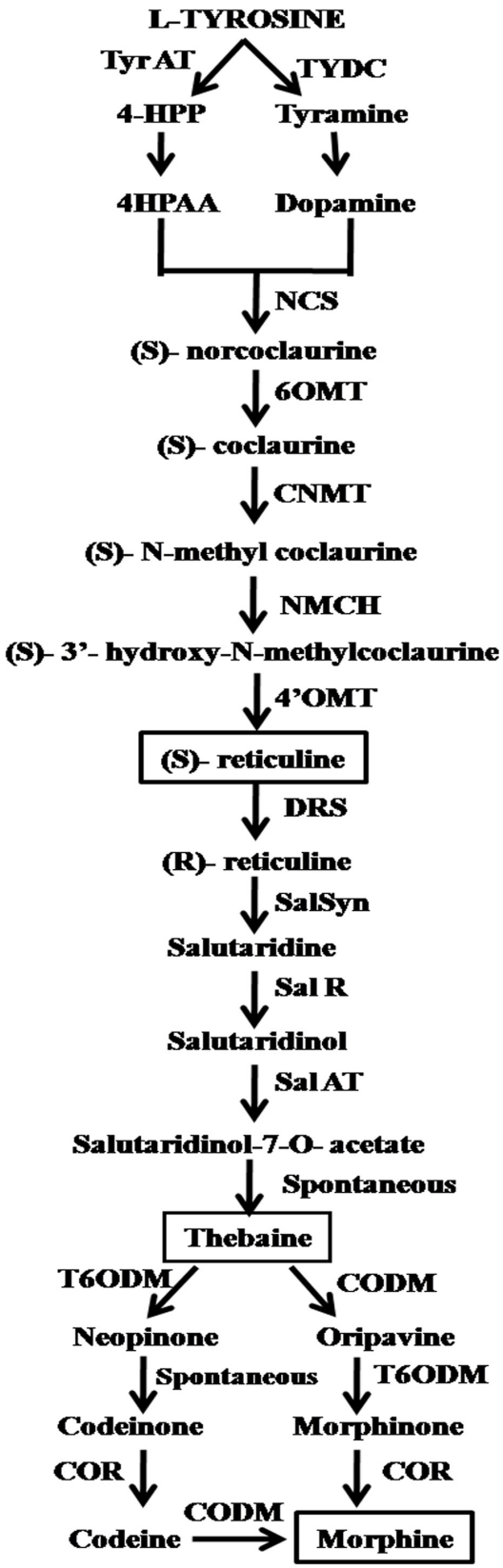

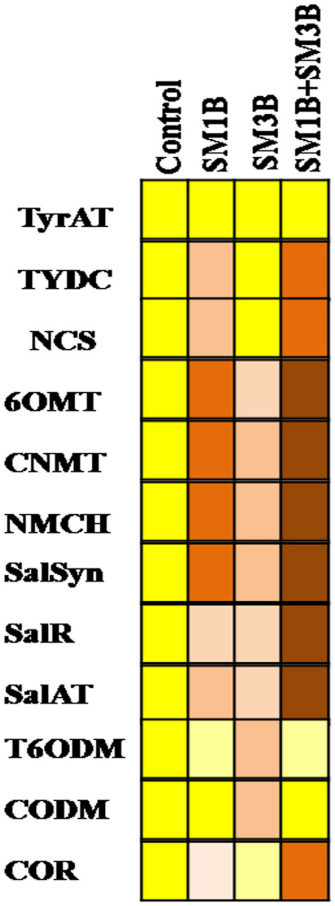

FIGURE 7 | Continued

FIGURE 7 | Upregulation of multiple genes involved in morphine biosynthesis due to inoculation of a consortium of endophytes. SM1B (*Acinetobacter*) endophytes upregulated the expression of most of the genes of BIAs pathway except *T6ODM* and *CODM* whereas SM3B (*Marmoricola* sp.) inoculation upregulated the *T6ODM* and *CODM*. Consortium-inoculation (SM1B+SM3B) could enhance the morphine production by upregulating, the expression of most of the BIA biosynthetic genes (*TYDC*, *NCS*, *6OMT*, *CNMT*, *NMCH*, *SalSyn*, *SalR*, *SalAT*, *COR*) involved in morphine biosynthesis to a greater extent, than that of single-inoculations. Expression of different genes was presented in square boxes. Red color of boxes indicate upregulated expression (intensity of red color shows the level of expression, i.e., more red more expression and vice versa), yellow color shows the level of expression in non-inoculated endophyte free control plants and light yellow color shows downregulated expression. *Enzyme abbreviations:* TyrAT, tyrosine aminotransferase; TYDC, tyrosine/ dopa decarboxylase; NCS, norcoclaurine synthase; 6OMT, (S)-norcoclaurine 6-O-methyltransferase; CNMT, (S)- coclaurine N-methyltransferase; NMCH, (S)-N-methylcoclaurine 3-hydroxylase; 4-OMT, (S)-30-hydroxy-N-methylcoclaurine 4-O-methyltransferase; DRS, 1,2-dehydroreticuline synthase; SalSyn, salutaridine synthase; SalR, salutaridine reductase; SalAT, salutaridinol 7-O-acetyltransferase; T6ODM, thebaine 6-O-demethylase; COR, codeinone reductase; CODM, codeine O-demethylase.

in *P. somniferum* cv. Sujata which is otherwise morphine-less variety.

Both the endophytes (SM1B and SM3B) were able to survive and perpetuate in combination and could colonize successfully in the capsule of the poppy plant when applied as a consortium. However, consortium inoculation slightly reduced the colonization of SM1B compared to individual SM1B inoculation. Consortium inoculation could enhance the growth of *P. somniferum* cv. Sujata plants compared to individual inoculations by increasing the content of photosynthetic pigments, photosynthetic rate, transpiration rate and stomatal conductance. The increased photosynthetic efficiency of the consortium-inoculated poppy plant could enhance the biomass (73.3%), capsule weight (66%), and seed yield (79%) which was substantially higher than single-inoculation.

Combined-inoculation of SM1B and SM3B could generate higher increments in morphine content compared to individual-inoculations by modulating the utilization of the key intermediates (reticuline and thebaine) of morphine biosynthesis. Enhanced morphine content was due to more thebaine production in consortium inoculated plants (0.07% content gDW^{-1}) compared to individual-inoculation (0.005% content gDW^{-1} in case of SM1B and 0.035% content gDW^{-1} in case of SM3B). Higher thebaine production could result in lower accumulation of reticuline (upstream intermediate) in consortium inoculated plants compare to single inoculation of SM3B. However, very low accumulation of reticuline and thebaine indicates complete utilization of these intermediates for morphine biosynthesis in the case of SM1B-inoculated plants.

Consortium-inoculation could enhance the morphine production by upregulating, the expression of most of the BIA biosynthetic genes (*TYDC*, *NCS*, *6OMT*, *CNMT*, *NMCH*, *SalSyn*, *SalR*, *SalAT*, *COR*) involved in morphine biosynthesis to a greater extent, than that of single-inoculations (**Figure 7**). Expression of *TYDC*, *NCS*, *6OMT*, *CNMT*, *NMCH* which are the genes upstream to reticuline biosynthesis was higher in consortium inoculated plants, clearly indicating greater flux of BIA biosynthesis toward central intermediate, i.e., reticuline. However, due to the increased expression of *SalSyn*, *SalR,* and *SalAT* (which was higher in consortium-inoculated plants than that of single-inoculation); reticuline accumulation was found to be low than that of SM3B-inoculated plants. Due to higher expression of *SalSyn*, *SalR*, and *SalAT* than that of single inoculation; conversion of reticuline to thebaine was higher, and that could have resulted in more thebaine accumulation in consortium-inoculated plants compared to single-inoculated plants.

Here, we probably for the first time demonstrated that endophytes affecting the host metabolism at gene expression level having different modes/targets of action could be combined to compliment the inability of one endophyte to upregulate certain genes thus improving the biosynthesis of secondary metabolites. Also, by using the consortium of different endophytes with diverse functional growth attributes, we can compliment the functional deficiency of one by another. These endophytes would be a better alternative in place of transgenic plants and also could be explored for the development of designer plants. Here, in the present study, we also established that consortium of selected endophytes could be applied to overexpress multiple genes to increase the plant yield/desired product. The present study was conducted in morphine-less genotype Sujata to establish the role of combined inoculation of endophytes in enhancing morphine, and therefore the magnitude of enhancement was quite high considering very low concentrations inherently present in genotype Sujata. These enhancements, however, might not be possible in morphine/alkaloid rich variety(ies). It is, however, essential to understand the detailed mechanism of action of promising endophytes, and then a combined approach can be applied to attain maximum yields.

AUTHOR CONTRIBUTIONS

AK, TR, and SP conceived and designed the experiments and wrote the manuscript. TR and MS performed the experiments. AK, KS, TR, SP, and AP analyzed the data. All authors read and approved the manuscript.

FUNDING

This work was supported by grant NWP BSC0117 (XII Five Year Plan Network Project) from the Council of Scientific and Industrial Research (CSIR), India.

ACKNOWLEDGMENTS

The authors are thankful to Director, CSIR-CIMAP, Lucknow, India for providing laboratory facilities and Director, CSIR-NBRI,

Lucknow, India for providing BIA standards. SP greatly acknowledge CSIR for financial assistance in the form of Senior Research Associateship. TR is thankful to Department of Science and Technology, India for INSPIRE fellowship. AP is grateful to DST for INSPIRE Faculty award (IFA13-LSPA-20).

SUPPLEMENTARY MATERIAL

The Supplementary Material for this article can be found online at: https://www.frontiersin.org/articles/10.3389/fmicb.2019.00925/full#supplementary-material

REFERENCES

Barnawal, D., Bharti, N., Tripathi, A., Pandey, S. S., Chanotiya, C. S., and Kalra, A. (2016). ACC-deaminase-producing endophyte *Brachybacterium paraconglomeratum* strain SMR20 ameliorates Chlorophytum salinity stress via altering phytohormone generation. *J. Plant Growth Regul.* 35, 553–564.

Barnawal, D., Pandey, S. S., Bharti, N., Pandey, A., Ray, T., Singh, S., et al. (2017). ACC deaminase-containing plant growth-promoting rhizobacteria protect *Papaver somniferum* from downy mildew. *J. Appl. Microbiol.* 122, 1286–1298. doi: 10.1111/jam.13417

Bharti, N., Pandey, S. S., Barnawal, D., Patel, V. K., and Kalra, A. (2016). Plant growth promoting rhizobacteria *Dietzia natronolimnaea* modulates the expression of stress responsive genes providing protection of wheat from salinity stress. *Sci. Rep.* 6:34768. doi: 10.1038/srep34768

Bhunia, A. K., Johnson, M. C., and Ray, B. (1988). Purification, characterization and antimicrobial spectrum of a bacteriocin produced by *Pediococcus acidilactici*. *J. Appl. Bacteriol.* 65, 261–268.

Bohnert, H. J., Gong, Q., Li, P., and Ma, S. (2006). Unraveling abiotic stress tolerance mechanisms–getting genomics going. *Curr. Opin. Plant Biol.* 9, 180–188. doi: 10.1016/j.pbi.2006.01.003

Del Giudice, L., Massardo, D. R., Pontieri, P., Bertea, C. M., Mombello, D., Carata, E., et al. (2008). The microbial community of Vetiver root and its involvement into essential oil biogenesis. *Environ. Microbiol.* 10, 2824–2841. doi: 10.1111/j.1462-2920.2008.01703.x

Di Fiore, S., and Del Gallo, M. (1995). "Endophytic bacteria: their possible role in the host plant," in *Azospirillum VI and Related Microorganisms*, eds I. Fendrik, M. del Gallo, J. Vanderleyden, and M. de Zamaroczy (Heidelberg: Springer), 169–187.

Egamberdieva, D., Wirth, S. J., Shurigin, V. V., Hashem, A., and Abd Allah, E. F. (2017). Endophytic bacteria improve plant growth, symbiotic performance of chickpea (Cicer arietinum L.) and induce suppression of root rot caused by *Fusarium solani* under salt stress. *Front. Microbiol.* 8:1887. doi: 10.3389/fmicb.2017.01887

Gundel, P. E., Pérez, L. I., Helander, M., and Saikkonen, K. (2013). Symbiotically modified organisms: nontoxic fungal endophytes in grasses. *Trends Plant Sci.* 18, 420–427. doi: 10.1016/j.tplants.2013.03.003

Gundel, P. E., Seal, C., Biganzoli, F., Molina Montenegro, M., Vazquez-de-Aldana, B., Zabalgogeazcoa, I., et al. (2018). Occurrence of alkaloids in grass seeds symbiotic with vertically-transmitted epichloë fungal endophytes and its relationship with antioxidants. *Front. Ecol. Evol.* 6:211. doi: 10.3389/fevo.2018.00211

Halpin, C. (2005). Gene stacking in transgenic plants–the challenge for 21st century plant biotechnology. *Plant Biotechnol. J.* 3, 141–155. doi: 10.1111/j.1467-7652.2004.00113.x

Hardoim, P. R., Van Overbeek, L. S., Berg, G., Pirttilä, A. M., Compant, S., Campisano, A., et al. (2015). The hidden world within plants: ecological and evolutionary considerations for defining functioning of microbial endophytes. *Microbiol. Mol. Biol. Rev.* 79, 293–320. doi: 10.1128/MMBR.00050-14

Kuklinsky-Sobral, J., Araújo, W. L., Mendes, R., Geraldi, I. O., Pizzirani-Kleiner, A. A., and Azevedo, J. L. (2004). Isolation and characterization of soybean-associated bacteria and their potential for plant growth promotion. *Environ. Microbiol.* 6, 1244–1251.

Kumar, A., Patil, D., Rajamohanan, P. R., and Ahmad, A. (2013). Isolation, purification and characterization of vinblastine and vincristine from endophytic fungus *Fusarium oxysporum* isolated from *Catharanthus roseus*. *PLoS One* 8:e71805. doi: 10.1371/journal.pone.0071805

Kusari, S., Verma, V. C., Lamshoeft, M., and Spiteller, M. (2012). An endophytic fungus from *Azadirachta indica* A. Juss. that produces azadirachtin. *World J. Microbiol. Biotechnol.* 28, 1287–1294. doi: 10.1007/s11274-011-0876-2

Li, J., Zhao, G. Z., Varma, A., Qin, S., Xiong, Z., Huang, H. Y., et al. (2012). An endophytic pseudonocardia species induces the production of artemisinin in *Artemisia annua*. *PLoS One* 7:e51410. doi: 10.1371/journal.pone.0051410

Lichtenthaler, H. K., and Buschmann, C. (2001). "Chlorophylls and carotenoids: Measurement and characterization by UV-VIS spectroscopy," in *Current Protocols in Food Analytical Chemistry (CPFA)*, eds R. E. Wrolstad, T. E. Acree, H. An, E. A. Decker, M. H. Penner, D. S. Reid, et al. (New York, NY: Wiley).

Livak, K. J., and Schmittgen, T. D. (2001). Analysis of relative gene expression data using real-time quantitative PCR and the 2_ΔΔCt method. *Methods* 25, 402–408.

Maggini, V., De Leo, M., Mengoni, A., Gallo, E. R., Miceli, E., Reidel, R. V. B., et al. (2017). Plant-endophytes interaction influences the secondary metabolism in *Echinacea purpurea* (L.) Moench: an in vitro model. *Sci. Rep.* 7:16924. doi: 10.1038/s41598-017-17110-w

Otieno, N., Lally, R. D., Kiwanuka, S., Lloyd, A., Ryan, D., Germaine, K. J., et al. (2015). Plant growth promotion induced by phosphate solubilizing endophytic *Pseudomonas* isolates. *Front. Microbiol.* 6:745. doi: 10.3389/fmicb.2015.00745

Pandey, S. S., Singh, S., Babu, C. V., Shanker, K., Srivastava, N. K., and Kalra, A. (2016a). Endophytes of opium poppy differentially modulate host plant productivity and genes for the biosynthetic pathway of benzylisoquinoline alkaloids. *Planta* 243, 1097–1114. doi: 10.1007/s00425-016-2467-9

Pandey, S. S., Singh, S., Babu, C. V., Shanker, K., Srivastava, N. K., Shukla, A. K., et al. (2016b). Fungal endophytes of Catharanthus roseus enhance vindoline content by modulating structural and regulatory genes related to terpenoid indole alkaloid biosynthesis. *Sci. Rep.* 6:26583. doi: 10.1038/srep26583

Pandey, S. S., Singh, S., Pandey, H., Srivastava, M., Ray, T., Soni, S., et al. (2018). Endophytes of *Withania somnifera* modulate in planta content and the site of withanolide biosynthesis. *Sci. Rep.* 8:5450. doi: 10.1038/s41598-018-23716-5

Quecine, M. C., Araújo, W. L., Rossetto, P. B., Ferreira, A., Tsui, S., Lacava, P. T., et al. (2012). Sugarcane growth promotion by the endophytic bacterium *Pantoea agglomerans* 33.1. *Appl. Environ. Microbiol.* 78, 7511–7518. doi: 10.1128/AEM.00836-12

Rodriguez, R. J., Henson, J., Van Volkenburgh, E., Hoy, M., Wright, L., Beckwith, F., et al. (2008). Stress tolerance in plants via habitat-adapted symbiosis. *ISME J.* 2, 404–416. doi: 10.1038/ismej.2007.106

Rosenblum, A., Marsch, L. A., Joseph, H., and Portenoy, R. K. (2008). Opioids and the treatment of chronic pain: controversies, current status, and future directions. *Exp. Clin. Psychopharmacol.* 16, 405–416. doi: 10.1037/a0013628

Saikkonen, K., Faeth, S. H., Helander, M., and Sullivan, T. J. (1998). Fungal endophytes: a continuum of interactions with host plants. *Annu. Rev. Ecol. Syst.* 29, 319–343.

Scherling, C., Ulrich, K., Ewald, D., and Weckwerth, W. (2009). A metabolic signature of the beneficial interaction of the endophyte Paenibacillus sp. Isolate and in vitro–grown poplar plants revealed by metabolomics. *Mol. Plant Microbe Interact.* 22, 1032–1037. doi: 10.1094/MPMI-22-8-1032

Schmittgen, T. D., and Livak, K. J. (2008). Analyzing real-time PCR data by the comparative C_T method. *Nat. Protoc.* 3, 1101–1108. doi: 10.1038/nprot.2008.73

Sharma, J. R., Lal, R. K., Gupta, A. P., Misra, H. O., Pant, V., Singh, N. K., et al. (1999). Development of non-narcotic (opiumless and alkaloid-free) opium poppy, Papaver somniferum. *Plant Breed.* 118, 449–452.

Sharma, J. R., Lal, R. K., Gupta, M. M., Verma, R. K., and Misra, H. O. (2002). A novel non-narcotic seed variety sujata of opium poppy (*Papaver somniferum*). *J. Med. Arom. Plant Sci.* 24, 481–485.

Shweta, S., Zuehlke, S., Ramesha, B. T., Priti, V., Mohana Kumar, P., Ravikanth, G., et al. (2010). Endophytic fungal strains of *Fusarium solani*, from *Apodytes dimidiata* E. *Mey. ex Arn (Icacinaceae)* produce camptothecin,

10- hydroxycamptothecin and 9-methoxycamptothecin. *Phytochemistry* 71, 117–122.

Singh, S. K., Strobel, G. A., Knighton, B., Geary, B., Sears, J., and Ezra, D. (2011). An endophytic phomopsis sp. Possessing bioactivity and fuel potential with its volatile organic compounds. *Microb. Ecol.* 61, 729–739. doi: 10.1007/s00248-011-9818-7

Soliman, S. S., Tsao, R., and Raizada, M. N. (2011). Chemical inhibitors suggest endophytic fungal paclitaxel is derived from both mevalonate and non-mevalonate-like pathways. *J. Nat. Prod.* 74, 2497–2504. doi: 10.1021/np200303v

Staniek, A., Woerdenbag, H. J., and Kayser, O. (2008). Endophytes: exploiting biodiversity for the improvement of natural product-based drug discovery. *J. Plant Interact.* 3, 75–93.

Strobel, G., Daisy, B., Castillo, U., and Harper, J. (2004). Natural products from endophytic microorganisms. *J. Nat. Prod.* 67, 257–268.

Tajehmiri, A., Darsanaki, R. K., Moslem, M. N., Lozoumi, Z., Kolavani, M. H., and Aliabadi, M. A. (2014). antimicrobial activity of lactobacillus spp. Isolated from commercial yoghurts against pathogenic bacteria. *J. Pure Appl. Microbiol.* 8, 2211–2215.

Tiwari, R., Awasthi, A., Mall, M., Shukla, A. K., Srinivas, K. S., Syamasundar, K. V., et al. (2013). Bacterial endophyte-mediated enhancement of in planta content of key terpenoid indole alkaloids and growth parameters of *Catharanthus roseus*. *Ind. Crops Prod.* 43, 306–310.

Waller, F., Achatz, B., Baltruschat, H., Fodor, J., Becker, K., Fischer, M., et al. (2005). The endophytic fungus Piriformospora indica reprograms barley to salt-stress tolerance, disease resistance, and higher yield. *Proc. Natl. Acad. Sci. U.S.A.* 102, 13386–13391.

Whittle, S. L., Richards, B. L., Husni, E., and Buchbinder, R. (2011). Opioid therapy for treating rheumatoid arthritis pain. *Cochrane Database Syst. Rev.* 11:CD003113. doi: 10.1002/14651858.CD003113.pub3

Conflict of Interest Statement: The authors declare that the research was conducted in the absence of any commercial or financial relationships that could be construed as a potential conflict of interest.

frontiers in Microbiology

ORIGINAL RESEARCH
published: 07 June 2019
doi: 10.3389/fmicb.2019.01285

Bioactive 3-Decalinoyltetramic Acids Derivatives From a Marine-Derived Strain of the Fungus *Fusarium equiseti* D39

Donglin Zhao[1†], Xiaobin Han[2†], Dan Wang[1], Minghong Liu[2], Jianyu Gou[2], Yulong Peng[2], Jing Liu[2], Yiqiang Li[1], Fei Cao[3] and Chengsheng Zhang[1]**

[1] Marine Agriculture Research Center, Tobacco Research Institute of Chinese Academy of Agricultural Sciences, Qingdao, China, [2] Zunyi Branch, Guizhou Tobacco Company, Zunyi, China, [3] College of Pharmaceutical Sciences, Hebei University, Baoding, China

Two novel 3-decalinoyltetramic acid (3DTA) derivatives, namely fusarisetins C and D (**1** and **2**), and four known derivatives (**3–6**) were isolated from the marine-derived fungus *Fusarium equiseti* D39. Their structures were determined by spectroscopic data, vibrational circular dichroism (VCD) calculations, and X-ray crystallography. Compound **2** was identified as the first fusarisetin to possess an unprecedented carbon skeleton with a tetracyclic ring system comprised of a decalin moiety (6/6) and a tetramic acid moiety. A plausible biosynthetic pathway for the isolated compounds was proposed. All 3DTAs derivatives exhibited a potent phytotoxicity, and **5** also displayed a remarkable anti-phytopathogenic activity superior to the positive control resulting in damage of the cell membrane of *Pseudomonas syringae* and ensuing leakage of the intracellular components. Here, the phytotoxicity of fusarisetins has been reported for the first time. The OSMAC fermentation optimization approach to give **5** was performed by varying the culture media and salinities. The results showed that potato liquid medium with 1% salinity is the most favorable condition for the production of **5**.

Keywords: 3-decalinoyltetramic acid, fusarisetin, phytotoxicity, anti-phytopathogenic activity, OSMAC fermentation

OPEN ACCESS

Edited by:
Roberta Marra,
University of Naples Federico II, Italy

Reviewed by:
Rosario Nicoletti,
Council for Agricultural and Economics Research, Italy
Anna Andolfi,
University of Naples Federico II, Italy

****Correspondence:***
Fei Cao
caofei542927001@163.com
Chengsheng Zhang
zhchengsheng@126.com

† These authors have contributed equally to this work

Specialty section:
This article was submitted to Microbial Symbioses, a section of the journal Frontiers in Microbiology

Received: *08 March 2019*
Accepted: *23 May 2019*
Published: *07 June 2019*

Citation:
Zhao D, Han X, Wang D, Liu M, Gou J, Peng Y, Liu J, Li Y, Cao F and Zhang C (2019) Bioactive 3-Decalinoyltetramic Acids Derivatives From a Marine-Derived Strain of the Fungus Fusarium equiseti D39. Front. Microbiol. 10:1285. doi: 10.3389/fmicb.2019.01285

INTRODUCTION

3-Decalinoyltetramic acids (3DTAs) are natural products that contain the tetramic acid structure (pyrrolidine-2,4-dione) featuring substituted decalin ring systems (Schobert and Schlenk, 2008; Mo et al., 2014). The most representative compound is equisetin, which was the first member of this family to be identified (Royles, 1995). 3-Decalinoyltetramic acids have been isolated from various terrestrial and marine microorganisms, but mainly from fungi (Mo et al., 2014). These compounds exhibited various notable biological activities, such as antimicrobial, antiviral, cytotoxic, and phytotoxic activities (Schobert and Schlenk, 2008; Mo et al., 2014). In 2011, the biogenetically related compound fusarisetin A, that possesses both an unprecedented carbon skeleton and a new pentacyclic ring system with acinar morphogenesis inhibitory activity, was identified, thereby enriching the structural and biological diversity of 3DTAs (Jang et al., 2012). Thus, due to their intriguing structures and associated biological activities, 3DTAs are gaining growing attention from the communities of biologists and chemists.

Marine fungi are a hotspot for the study of various natural products, as they produce secondary metabolites with novel structures and interesting bioactivities endowed by the unique marine environment (Carroll et al., 2019). However, each microbial strain has the potential to produce multiple compounds, and only subsets of these compounds are produced under specific growth conditions. Based on this, the "one strain many compounds" (OSMAC) culture strategy was conceptualized to increase the chemical diversity and improve the yields of new microbial bioactive compounds by varying the nutrient content, temperature, salinity, aeration, etc. (Romano et al., 2018).

During our ongoing search for novel secondary metabolites with agricultural bioactivities from marine-derived fungi (Huang et al., 2018; Zhao et al., 2018), the fungus *Fusarium equiseti* D39 (previously numbered as GLY27 and P18), collected from the intertidal zones of the Yellow Sea in Qingdao, China, attracted our attention because the extract of the fungal culture exhibited a strong anti-phytopathogenic activity. Using the bioassay-LCMS-^{1}H NMR screening technology, the HPLC profile and ^{1}H NMR spectrum of the extract of the fungal culture were obtained and found to exhibit distinctive UV-absorption peaks and proton signals corresponding to 3DTAs, while the MS spectrum indicated the presence of some novel 3DTAs. However, only two anthraquinone derivatives were isolated from the fungal cultures (Zhao et al., 2018), thereby prompting further investigations into the metabolome of this fungus to isolate the 3DTAs. Further chemical investigation of the ethyl acetate (EtOAc) extracts led to the isolation of six 3DTAs (**Figure 1**), including two novel fusarisetins, namely fusarisetins C and D (**1** and **2**), and the four known compounds fusarisetin B (**3**), fusarisetin A (**4**), equisetin (**5**), and epi-equisetin (**6**). To the best of our knowledge, only two fusarisetins have been reported as natural products to date (Ahn et al., 2012; Jang et al., 2012). Thus, we herein report the isolation, structural elucidation, and biological activities of these compounds. In addition, to improve the yield of compound **5**, fermentation optimization was carried out using the OSMAC approach.

MATERIALS AND METHODS

General Experimental Procedures

Optical rotations were measured on a JASCO P-1020 digital polarimeter with a 1 dm cell (Jasco, Inc., Easton, MD, United States). UV spectra were recorded on a Techcomp UV2310II spectrophotometer (Techcomp, Ltd., Shanghai, China). IR and vibrational circular dichroism (VCD) spectra were acquired using a BioTools ChiralIR-2X spectrophotometer (BioTools Inc., Olathe, KS, United States). NMR spectra were acquired on an Agilent DD2 500 MHz NMR spectrometer (500 MHz for ^{1}H and 125 MHz for ^{13}C; Agilent Technologies, Santa Clara, CA, United States), using tetramethylsilane (TMS) as an internal standard. Electrospray ionization mass spectrometry (ESIMS) and high resolution ESIMS (HRESIMS) were carried out using a Micromass Q-TOF spectrometer (Waters, Milford, MA, United States) and a Thermo Scientific LTQ Orbitrap XL spectrometer (Thermo Fisher Scientific, Waltham, MA, United States). Single-crystal data were collected on an Aglient Technologies Gemini E Ultra system (Cu Kα radiation) (Agilent Technologies). Semi-preparative HPLC was performed on a C_{18} (Waters, 5 μm, 10 × 250 mm) column using a Waters e2695 separation module equipped with a Waters 2998 detector (Waters). Silica gel (200–300 mesh; Qing Dao Hai Yang Chemical Group Co., Qingdao, China), octadecylsilyl silica gel (ODS) (RP18, 40–63 μm; Merck, Billerica, MA, United States), and Sephadex LH-20 (GE Healthcare, Pittsburgh, PA, United States) were used for column chromatography. Compounds were monitored by thin layer chromatography (TLC) (G60, F-254; Yan Tai Zi Fu Chemical Group Co., Yantai, China), and spots were visualized by heating the silica gel plates sprayed with 12% H_2SO_4 in H_2O containing saturated vanillins. All the solvents for extraction and isolation were of analytical and HPLC grade.

Fungal Material

The fungal strain *F. equiseti* D39 was isolated from a piece of fresh tissue obtained from the inner part of an unidentified plant, which was collected from the intertidal zone of the Yellow Sea, Qingdao, China, in July 2016. The fungus was identified according to its morphological characteristics and a molecular protocol by amplification and sequencing of the DNA sequences of the ITS region of the rDNA gene (Zhao et al., 2018). The strain was deposited in the Marine Agriculture Research Center, Tobacco Research Institute of Chinese Academy of Agricultural Sciences, Qingdao, China, with the GenBank (NCBI) accession number KY945342.

Extraction and Isolation

The fungal strain *F. equiseti* D39 was fermented by solid-state fermentation (SSF) on rice medium in 100 Erlenmeyer flasks (each containing 80 g of rice and 120 mL of H_2O) at 28° C for 30 days. The culture medium was extracted three times repeatedly with EtOAc, and the solvent was concentrated under reduced pressure to yield the EtOAc extract (25.8 g). This EtOAc extract was then subjected to vacuum liquid chromatography (VLC) on silica gel using a step gradient elution of EtOAc–petroleum ether (0–100%) and subsequently EtOAc–MeOH (0–100%) to provide six fractions (Fr.1–Fr.6). Fraction 3 was initially fractionated using an ODS gel column with a step gradient elution of MeOH–H_2O (30–90%), followed by separation on Sephadex LH-20 CC (CH_2Cl_2/MeOH, v/v, 1/1) to afford Fr. 3-1–Fr. 3-8. Fraction 3-6 was then purified by reversed phase (RP)-HPLC eluting with 55% MeOH–H_2O to obtain compound **1** (5.0 mg). Fraction 4 was separated on silica gel CC (EtOAc/petroleum ether = 20/80 to 100/0) to obtain Fr. 4-1–Fr. 4-5. Fraction 4-2 was applied to an ODS column eluting with 30–90% MeOH–H_2O, followed by purification on Sephadex LH-20 CC (CH_2Cl_2/MeOH, v/v, 1/1) to obtain Fr. 4-2-1–Fr. 4-2-9. Fraction 4-2-6 was further separated by HPLC using 40% MeCN–(H_2O + 0.1% TFA) to yield compounds **3** (61.2 mg) and **4** (28.5 mg). Fraction 4-2-7 was purified by HPLC using 55% MeCN–H_2O (containing 0.1% TFA) to give compounds **5** (238.2 mg) and **6** (126.5 mg). Fraction 5 was subjected to ODS column chromatography using a gradient elution of 30–80% MeOH–H_2O to afford subfractions Fr.5-1–Fr.5-8. Fraction 5-7 was then subjected to

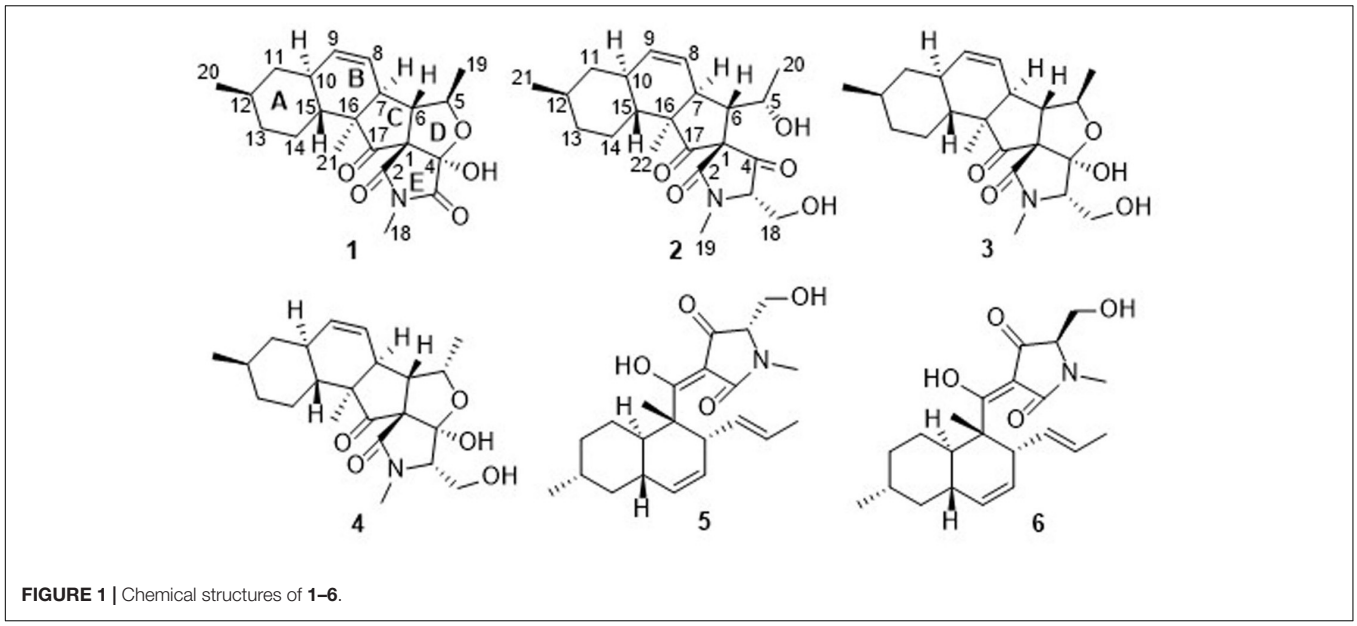

FIGURE 1 | Chemical structures of **1–6**.

chromatography on Sephadex LH-20 (CH_2Cl_2–MeOH, v/v, 1/1) and finally purified by semipreparative HPLC eluting with 60% MeOH–H_2O to give compound **2** (4.0 mg).

Fusarisetin C (**1**): Colorless crystals; $[\alpha]^{20}_D$ +15.0 (*c* 0.25, MeOH); UV (MeOH) λ_{max} (log ε) 202 (3.42) nm; ^1H and ^{13}C NMR data, **Tables 1**, **2**; HRESIMS *m/z* 372.1825 $[M - H]^-$ (calcd for $C_{21}H_{27}NO_5$, 372.1816).

Fusarisetin D (**2**): Colorless oil; $[\alpha]^{20}_D$ -9.2 (*c* 0.13, MeOH); UV (MeOH) λ_{max} (log ε) 200 (3.19) nm; ^1H and ^{13}C NMR data, **Tables 1**, **2**; HRESIMS *m/z* 390.2278 $[M + H]^+$ (calcd for $C_{22}H_{32}NO_5$, 390.2275).

X-ray crystallographic analysis of **1** and **3**. Colorless crystals of **1** and **3** were obtained upon evaporation of the CH_2Cl_2–MeOH (2:1, v/v) solvent mixture by maintaining the sample at 25°C for 3 days. Single-crystal X-ray diffraction data were recorded on a Xcalibur, Eos, Gemini ultra diffractometer at 298 K. The structures were solved by direct methods (SHELXS-2018) and refined using full-matrix least-squares difference Fourier techniques. All non-hydrogen atoms were refined anisotropically, and all hydrogen atoms were placed in idealized positions and refined relatively isotropically with a riding model. Crystallographic data for **1** and **3** were deposited in the Cambridge Crystallographic Data Centre with the deposition numbers 1893702 and 1895292, respectively. Copies of the data can be obtained, free of charge, on application to the Director, CCDC, 12 Union Road, Cambridge CB21EZ, United Kingdom (fax: +44 (0)-1233-336033 or e-mail: deposit@ccdc.cam.ac.uk).

Crystal data for **1**: $C_{21}H_{27}NO_5$, M_r = 373.44, monoclinic, *a* = 12.5780 (12) Å, *b* = 7.4893 (8) Å, *c* = 22.119 (2) Å, α = 90.00°, β = 95.281 (10)°, γ = 90.00°, *V* = 2074.7 (4) $Å^3$, space group *C*2, *Z* = 4, D_x = 1.196 mg/m^3, μ = 0.694 mm^{-1}, and *F*(000) = 800. Crystal size: 0.08 mm × 0.07 mm × 0.07 mm. Reflections collected/unique: 6383/2896 [*R*(int) = 0.0556]. The final indices were R_1 = 0.0607, wR_2 = 0.1313 [$I > 2\sigma(I)$]. Flack parameter = 0.0 (5).

Crystal data for **3**: $C_{22}H_{31}NO_5$, M_r = 389.22, monoclinic, *a* = 10.1548 (5) Å, *b* = 17.3448 (9) Å, *c* = 11.9203 (6) Å, α = 90.00°, β = 94.435 (4)°, γ = 90.00°, *V* = 2093.27 (19) $Å^3$, space group $P2_1$, *Z* = 4, D_x = 1.236 mg/m^3, μ = 0.705 mm^{-1}, and *F*(000) = 840. Crystal size: 0.12 mm × 0.11 mm × 0.11 mm. Reflections collected/unique: 8355/5693 [*R*(int) = 0.0199]. The final indices were R_1 = 0.0459, wR_2 = 0.1026 [$I > 2\sigma(I)$]. Flack parameter = 0.0 (2).

Phytotoxicity Bioassays

The phytotoxicities of the isolated compounds against the seedling growth of amaranth (*Amaranthus retroflexus*) and lettuce (*Lactuca sativa*) were tested using a previously reported method (Zhang et al., 2013; Huang et al., 2018). Glyphosate was used as a positive control with concentrations of 200 and 50 μg/mL, respectively.

Antibacterial and Antifungal Assays

The antibacterial and antifungal activities were evaluated using the conventional broth dilution assay (Appendino et al., 2008; Wang et al., 2016). Five phytopathogenic bacterial strains, including *Acidovorax avenae*, *Clavibacter michiganensis*, *Pseudomonas syringae*, *Ralstonia solanacearum*, and *Xanthomonas campestris*, and 12 phytopathogenic fungal strains, including *Alternaria alternata*, *Alternaria brassicicola*, *Aspergillus niger*, *Botrytis cinerea*, *Botryosphaeria dothidea*, *Colletotrichum* sp., *Fusarium graminearum*, *Fusarium oxysporum*, *Magnaporthe grisea*, *Pseudopestalotiopsis theae*, *Rhizoctonia cerealis*, and *Valsa mali* were used. Streptomycin sulfate, carbendazim, and prochloraz were used as positive controls for the bacteria and fungi, respectively.

TEM was performed to evaluate the effects of **5** (MIC and 4 × MIC) on *P. syringae* according to previously described methods (Liu et al., 2018; Zhao et al., 2018).

TABLE 1 | ^{1}H NMR Data (500 MHz, δ in ppm, *J* in Hz) and ^{13}C NMR Data (125 MHz, δ in ppm) for **1**.

	1 (CD_3OD)		1 (DMSO-d_6)	
Position	**δ_C, type**	**δ_H (*J* in Hz)**	**δ_C, type**	**δ_H (*J* in Hz)**
1	75.3		73.3	
2	174.0		172.6	
3	174.6		172.9	
4	106.9		105.5	
5	85.4	4.74 (dq, *J* = 6.5, 2.0 Hz)	82.8	4.74 (dq, *J* = 6.5, 1.5 Hz)
6	58.8	2.73 (dd, *J* = 10.5, 2.0 Hz)	56.8	2.63 (dd, *J* = 10.5, 1.5 Hz)
7	50.6	2.48 (dd, *J* = 10.5, 4.5 Hz)	48.3	2.42 (dd, *J* = 10.5, 4.5 Hz)
8	125.3	5.84 (ddd, *J* = 10.0, 4.5, 2.5 Hz)	124.5	5.86 (ddd, *J* = 10.0, 4.5, 2.0 Hz)
9	133.5	5.59 (d, *J* = 10.0 Hz)	131.8	5.54 (d, *J* = 10.0 Hz)
10	37.9	1.91-1.93 (m)	35.9	1.86-1.88 (m)
11	43.1	1.88-1.90 (m)	41.3	1.84-1.86 (m)
		0.84 (q, *J* = 12.5 Hz)		0.74–0.78 (m)
12	34.1	1.44-1.53 (m)	32.2	1.46 (m)
13	36.4	1.76 (m)	34.8	1.71 (brd, *J* = 12.0 Hz)
		0.91-0.98 (m)		0.81-0.85 (m)
14	26.3	1.44-1.53 (m)	24.7	1.36-1.39 (m)
		1.09-1.16 (m)		1.01-1.09 (m)
15	39.1	1.44-1.53 (m)	37.4	1.32-1.34 (m)
16	55.2		53.2	
17	210.8		209.0	
18	25.4	3.02 (s)	25.0	2.96 (s)
19	23.2	1.15 (d, *J* = 6.5 Hz)	22.6	1.06 (d, *J* = 6.5 Hz)
20	22.7	0.94 (d, *J* = 6.5 Hz)	22.2	0.88 (d, *J* = 5.5 Hz)
21	14.3	0.98 (s)	13.8	0.88 (s)
4-OH				8.17 (s)

TABLE 2 | ^{1}H NMR Data (500 MHz, δ in ppm, *J* in Hz) and ^{13}C NMR Data (125 MHz, δ in ppm) for **2**.

	2 (CD_3OD)		2 (DMSO-d_6)	
Position	**δ_C, type**	**δ_H (*J* in Hz)**	**δ_C, type**	**δ_H (*J* in Hz)**
1	73.9		71.7	
2	171.7		168.3	
3	71.2	4.12 (dd, *J* = 5.0, 3.0 Hz)	69.7	4.06 (dd, *J* = 6.0, 3.0 Hz)
4	204.2		203.8	
5	68.1	4.08 (m)	65.8	3.94 (m)
6	58.5	2.64 (brd, *J* = 11.5 Hz)	57.3	2.45 (dd, *J* = 11.5, 9.5 Hz)
7	47.1	2.67 (brd, *J* = 11.5 Hz)	45.2	2.59 (dd, *J* = 11.5, 5.0 Hz)
8	126.4	5.87 (m)	125.5	5.82 (m)
9	133.6	5.58 (d, *J* = 10.0 Hz)	131.8	5.53 (brd, *J* = 10.0 Hz)
10	38.2	1.86 (brd, *J* = 12.0 Hz)	36.2	1.80 (brd, *J* = 11.0 Hz)
11	42.9	1.89 (brd, *J* = 12.0 Hz)	41.2	1.85 (brd, *J* = 11.0 Hz)
		0.83 (m)		0.74 (m)
12	34.1	1.48 (m)	32.1	1.46 (m)
13	36.4	1.74 (m)	34.8	1.72 (brd, *J* = 12.5 Hz)
		0.90 (m)		0.79 (m)
14	26.5	1.32 (m)	24.8	1.24 (m)
		1.11 (m)		1.03 (m)
15	39.0	1.52 (dt, *J* = 10.5, 2.0 Hz)	37.2	1.39 (dt, *J* = 12.0, 2.0 Hz)
16	55.6		53.5	
17	210.6		210.1	
18	61.5	3.93 (dd, *J* = 12.0, 3.5 Hz)	61.3	3.75 (m)
		3.83 (dd, *J* = 12.0, 4.5 Hz)		3.61 (m)
19	28.6	3.11 (s)	23.8	1.15 (d, *J* = 6.5 Hz)
20	24.1	1.26 (d, *J* = 6.5 Hz)	28.1	2.99 (s)
21	22.7	0.93 (d, *J* = 6.5 Hz)	22.2	0.87 (d, *J* = 9.0 Hz)
22	15.4	0.98 (s)	14.8	0.86 (s)
5-OH				4.98 (d, *J* = 5.0 Hz)
18-OH				4.94 (m)

Fermentation Optimization

The fungal strain *F. equiseti* D39 was cultured according to the OSMAC approach (Wang et al., 2017). To prepare the seed culture, a portion of fresh fungal mycelium was inoculated in potato dextrose water (PDW, 200 mL) culture medium with shaking (180 rpm) at 28°C for 3 days. For medium optimization, 500 mL baffled Erlenmeyer flasks, each containing a different medium (250 mL), were inoculated using the seed culture (5 mL) and grown at 28°C for 9 days with shaking (180 rpm). The seven media contained different crops, including carrots, maize kernels, malt, tuberous root of pachyrhizus, peanuts, potatoes, and soybean seeds, and were labeled as crops A–G. A portion of each product (200 g) was then boiled in water for 60 min, and the broth obtained was filtered through gauze. The infusion volume was subsequently adjusted to 1 L by adding distilled water, followed by the addition of glucose (20 g) to obtain the culture media. *F. equiseti* D39 was fermented in three 500-mL Erlenmeyer flasks each containing 250 mL crops A–G liquid medium and was shaken for 9 days at 28°C and 180 rpm. The culture media (750 mL) were then filtered to separate the broth from the mycelia, the broth samples were extracted three times with equal volumes of EtOAc. The mycelia were extracted twice with CH_2Cl_2–MeOH (v/v, 1/1), and then extracted three times with EtOAc after concentration. The organic extracts were combined and concentrated under vacuum, in order to get a total extract. The extracts were dissolved in MeCN to a final concentration of 10.0 mg/mL for HPLC analysis.

The production of **5** was estimated by establishing the standard curve between the HPLC peak areas and the concentrations of **5**. The standard curve was established using standard solutions of 0.05, 0.1, 0.2, 0.4, 0.6, and 1.0 mg/mL (sample size 10.0 μL) with a flow rate of 1.0 mL/min (MeCN/[H_2O + 0.1% TFA], v/v, 60/40) on a C_{18} (Waters, 5 μm, 4.6 × 250 mm) column using a Waters e2695 separation module equipped with a Waters 2998 photodiode array detector. The linear curve and its fitting equation were established, and the production of **5** was calculated according to the fitting equation.

The optimal culture medium for production of **5** selected among crops A–G was further optimized with reference to salt concentration. In this respect, cultures were prepared in this medium after adjusting salinity at the levels of 1, 3, 5, 7, and 9% by adding natural sea salt. The procedure for determining the optimal fermentation salinity was as that described above.

RESULTS AND DISCUSSION

Chemical Identification of the 3-Decalinoyltetramic Acids

Fusarisetin C (**1**) was obtained as colorless crystals and assigned the molecular formula $C_{21}H_{27}NO_5$ by HRESIMS, indicating nine degrees of unsaturation (**Supplementary Figure S13**). The ^{1}H NMR spectrum in CD_3OD (**Table 1**) displayed signals corresponding to two mutually coupled olefinic protons at δ_H 5.84 (ddd, J = 10.0, 4.5, 2.5 Hz) and 5.59 (d, J = 10.0 Hz), one oxymethine at δ_H 4.74 (dq, J = 6.5, 2.0 Hz), one *N*-methyl proton at δ_H 3.02 (s), two doublet methyl protons at 1.15 (d, J = 6.5 Hz) and 0.94 (d, J = 6.5 Hz), together with one singlet methyl proton at δ_H 0.98. Additionally, one exchangeable proton signal was observed in DMSO-d_6 at δ 8.17 (s), and assigned as a hydroxyl proton (**Table 1**). The ^{13}C NMR (**Table 1**) and DEPT spectra in DMSO showed resonances corresponding to three carbonyl groups including one ketone (δ_C 209.0) and two acylamides (δ_C 172.9, 172.6), eight methine carbons (δ_C 131.8, 124.5, 82.8, 56.8, 48.3, 37.4, 35.9, and 32.2), three quaternary carbons (δ_C 105.5, 73.3, and 53.2), three methylene carbons (δ_C 41.3, 34.8, and 24.7), one *N*-methyl carbon (δ_C 25.0), and three methyl carbons (δ_C 22.6, 22.2, and 13.8). These spectroscopic features suggested that **1** is a type of fusarisetin, possessing a carbon skeleton with a pentacyclic ring system comprising a decalin moiety (6/6) and a tricyclic moiety (5/5/5) (**Supplementary Figures S3–S7, S9–S11**). This structure is similar to fusarisetin B, which was isolated from the soil fungus, *Fusarium* sp. FN080326 (Jang et al., 2012). Compared to fusarisetin B, the disappearance of signals corresponding to oxymethylene and methine moieties, in addition to the appearance of an acylamide peak indicated that the -CHCH$_2$OH group in the ring E of fusarisetin B was replaced by an acylamide carbonyl group in fusarisetin C. Indeed, the HMBC correlations from H-18 to C-2 and C-3, and from 4-OH to C-1 and C-3 confirmed the above conclusion (**Figure 2**). Detailed analysis of the HMQC, COSY, and HMBC spectra allowed the assignment of all carbon and proton resonances of **1**, and the planar structure of **1** was elucidated. In the NOESY spectrum, the correlations of H-21 with H-7 and H-10, and of H-10 with H-12, as well as of H-5 with H-7 and 4-OH indicated that these groups are positioned on the same face (**Figure 2**). These NOESY data and the relevant coupling constants confirmed the *trans* junction of the decalin ring system and the *cis* junction between the tricyclic and decalin ring systems (**Supplementary Figures S8, S12**). Thus, the relative configuration of **1** was thereby established as 1*R*′,4*R*′,5*R*′,6*S*′,7*S*′,10*S*′,12*R*′,15*R*′,16*S*′ since the 1*S*,4*R*′,5*R*′,6*S*′,7*S*′,10*S*′,12*R*′,15*R*′,16*S*′ combination does not lead to a reasonable model according to 3D simulations.

Recently, the VCD approach has become a robust and reliable alternative for the stereochemical characterizations of natural products (Sadlej et al., 2010; Keiderling and Lakhani, 2018). Thus, the experimental IR and VCD spectra of **1** (5.0 mg) were measured in DMSO-d_6 (120 μL) using a BioTools dual PEM Chiral*IR*-2X spectrophotometer. The IR and VCD frequencies of (1*R*,4*R*,5*R*,6*S*,7*S*,10*S*,12*R*,15*R*,16*S*)-**1** were calculated at the MPW1PW91/6-311+G(d)//B3LYP/6-311+G(d) level of theory in the gas phase and the spectra were compared with the experimental IR and VCD spectra of **1** (**Supplementary Table S1**). As shown in **Figure 3**, all calculated IR and VCD signals of (1*R*,4*R*,5*R*,6*S*,7*S*,10*S*,12*R*,15*R*,16*S*)-**1** agreed with the experimental IR and VCD signals of **1**, thereby confirming the (1*R*,4*R*,5*R*,6*S*,7*S*,10*S*,12*R*,15*R*,16*S*) configuration

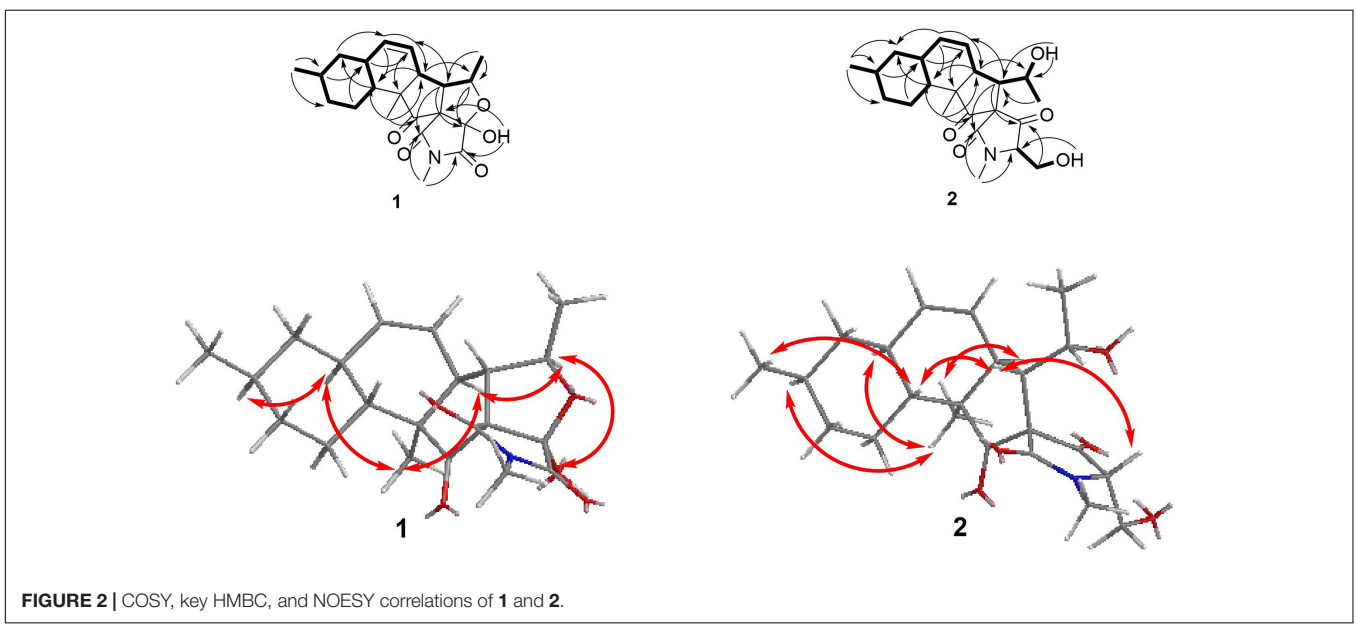

FIGURE 2 | COSY, key HMBC, and NOESY correlations of **1** and **2**.

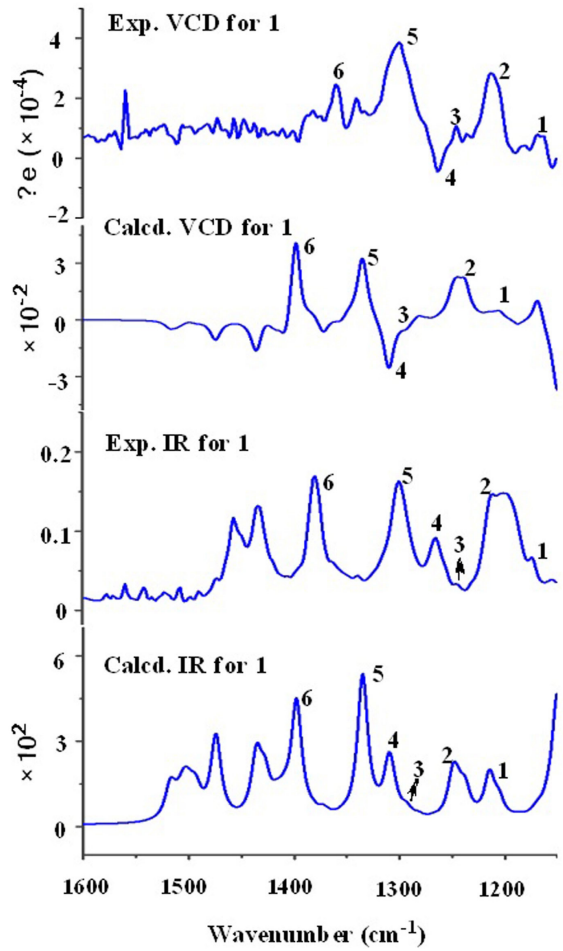

FIGURE 3 | Comparison of the calculated VCD/IR spectra of (1*R*,4*R*,5*R*,6*S*,7*S*,10*S*,12*R*,15*R*,16*S*)-**1** and the experimental VCD/IR spectra of **1**.

for **1**. Fortunately, **1** was recrystallized from a mixture of dichloromethane/methanol (2:1) to yield crystals that were suitable for single-crystal X-ray diffraction. This confirmed the unambiguous assignment of the absolute configuration as 1*R*,4*R*,5*R*,6*S*,7*S*,10*S*,12*R*,15*R*,16*S* (**Figure 4**).

Fusarisetin D (**2**) was isolated as colorless oil possessing the molecular formula $C_{22}H_{31}NO_5$ with eight degrees of unsaturation (**Supplementary Figure S25**). The general features of its ^{1}H and ^{13}C NMR spectra (**Table 2**) suggested that **2** is also a 3-decalinoyltetramic acid, and belongs to the family of fusarisetins. Analysis of the 1D and 2D NMR spectra indicated that the main differences between **2** and fusarisetin B could be found in the C, D, and E rings (**Supplementary Figures S14–S18, S20–S22**). The additional keto carbonyl signal and the disappearance of the C-4 oxymethine signal indicated that ring D was not present in **2**. In addition, the COSY cross-peaks of H-7/H-6/H-5/H-20, together with the HMBC correlations from H-6 to C-1, C-2, C-4, and C-8, and from H-20 to C-6 (**Figure 2**) reavealed that there was a $-CH(OH)CH_3$ group anchored to C-6. The HMBC correlations from H-3 and H-18 to C-4 suggested that the C-O bond at C-4 in fusarisetin B was fractured in **2**. Thus, the planar structure of **2** was confirmed. Indeed, compound **2** represents the first 3-decalinoyltetramic acid, possessing an unprecedented carbon skeleton with a tetracyclic ring system comprising a decalin moiety (6/6) and a bicyclic moiety (5/5).

The relative configuration of **2** (with the exception of C-1 and C-5) was then deduced on the basis of NOESY spectroscopic data (**Figure 2** and **Supplementary Figures S19, S23**). The correlations of H-22 with H-7, H-10, and H-12 indicated that these groups are positioned on the same face. The correlations of H-6 with H-3 and H-15, and of H-15 with H-21 reaveled a *cis*-relationship. Furthermore, the relative configuration between C-5 and C-6 was determined by *J*-based configuration analysis (including $^{2}J_{C,H}$ and $^{3}J_{C,H}$ carbon-proton spin coupling constants, and proton-proton spin coupling constants $^{3}J_{H,H}$) (Matsumori et al., 1999; Halecker et al., 2014)

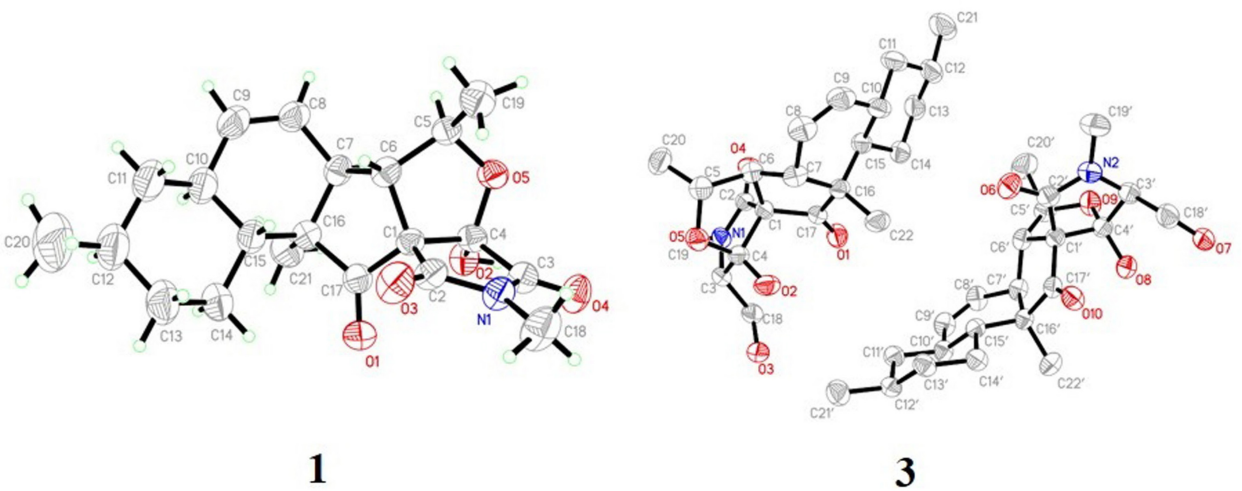

FIGURE 4 | X-ray structure of **1** and **3**.

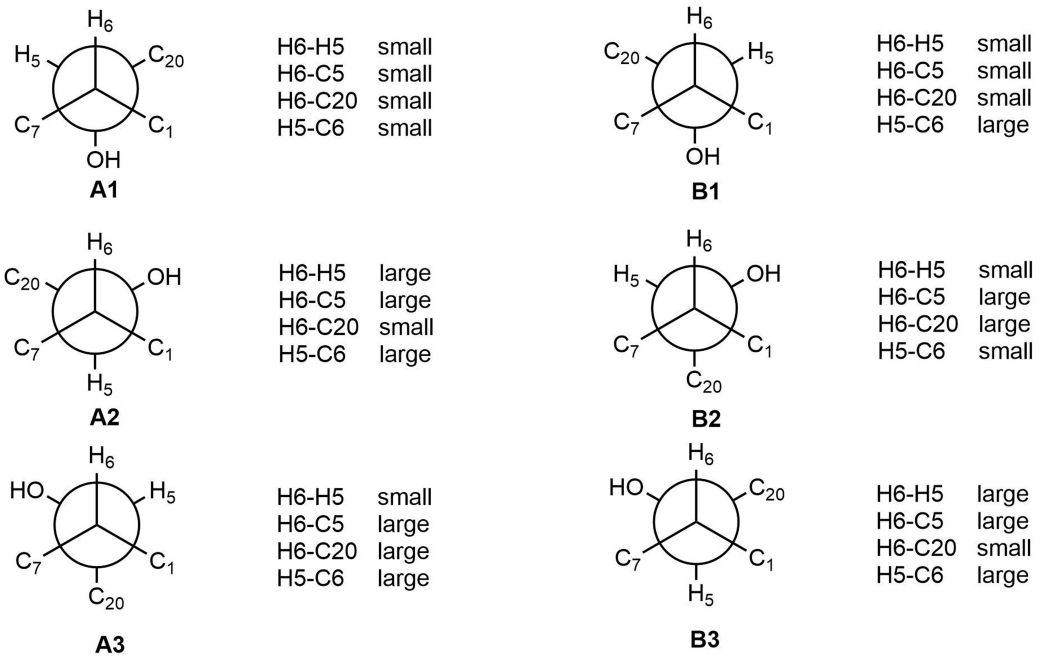

FIGURE 5 | *J*-Based analysis of six hypothetical rotamers with 5*R*,6*S* **(A1–A3)** and 5*S*,6*S* **(B1–B3)** configuration to determine the stereochemistry of **2**.

(**Supplementary Figure S24**). In acyclic systems such as the side chain of **2**, the configuration of adjacent asymmetric centers can be represented by staggered rotamers (**Figure 5**). Among the various configurations, four conformers, namely A-1, A-3, B-1, and B-2, could be identified using the $^{3}J_{H,H}$, $^{2}J_{C,H}$, and $^{3}J_{C,H}$ values, while rotamers A-2 and B-3 could not be distinguished. The small coupling constants of ^{3}J (H_5,H_6) = 1.5 Hz, ^{2}J (H_5, C_6) = 1.8 Hz, and the large coupling constant of ^{3}J (H_6, C_5) = 6.0 Hz, indicated an *anti*-like configuration between the proton and hydroxyl functions corresponding to B2 in **Figure 4**, thereby confirming the relative configuration of **2**.

Attempts were then made to determine the absolute configuration of **2** at the C-5 position using the modified Mosher's method (Kusumi et al., 1991); however, neither the reactants nor the corresponding acylation products were detected, possibly because **2** was not stable under the alkaline conditions required for this technique. As the various natural fusarisetins included in the present study (i.e., **1**, **3**–**4**) have the same configuration in the A, B, and C rings, based on the biogenetic consideration, the absolute configuration of **2** should be 1*R*,3*S*,5*S*,6*S*,7*S*,10*S*,12*R*,15*R*,16*S*.

Known compounds **3**–**6** were identified as fusarisetin B (Ahn et al., 2012), fusarisetin A (Jang et al., 2012), equisetin (Singh et al., 1998), and *epi*-equisetin (Singh et al., 1998), by comparison of their spectroscopic data with the literature. Compound **3** was previously reported as its enantiomer in a patent, but was cited in another article as fusarisetin B, which corresponds with the structure determined herein (Ahn et al., 2012; Caro-Diaz et al., 2014). Although the structure of **4** was revised in 2012, that of **3** was not, and the determination of its absolute configuration was also not discussed. Fortunately, **3** was crystallized herein by evaporation from a solution of 20:1 MeOH/H_2O over the course of 1 w, and the absolute configuration was determined to be 1*R*,3*S*,4*R*,5*R*,6*S*,7*S*,10*S*,12*R*,15*R*,16*S* (**Figure 4**).

Plausible Biosynthetic Pathway Toward Compounds 1–4

To the best of our knowledge, only two fusarisetins have been previously isolated from nature. Inspection of the fusarisetin and equisetin frameworks revealed that fusarisetins A–D may derive biogenetically from the oxidation of equisetin upon exposure to reactive oxygen species (ROS) (**Figure 6**; Xu et al., 2012; Yin et al., 2012). This biosynthetic scenario could account for the formation of a stabilized radical that, upon cyclization at the pendant alkene followed by trapping by ROS, could produce fusarisetins through single-electron oxidation and hemiketalization. Thus, the absolute configurations of the chiral centers in rings A, B, and C of fusarisetins A and D should be the same as those of fusarisetins B and C, which were confirmed by their X-ray structures (**Figure 4**).

Bioactivities of Compounds 1–6

3-Decalinoyltetramic acids and their derivatives have been found to exhibit a broad range of biological activities, including antiviral, antimicrobial, cytotoxic, and phytotoxic activities (Schobert and Schlenk, 2008; Mo et al., 2014). In the present study, all isolated compounds were subjected to a panel of bioassays to evaluate their potential activities. These included evaluation of their anti-phytopathogenic bacterial activities against *A. avenae, C. michiganensis*, *P. syringae*, *R. solanacearum*, and *X. campestris*, anti-phytopathogenic fungal

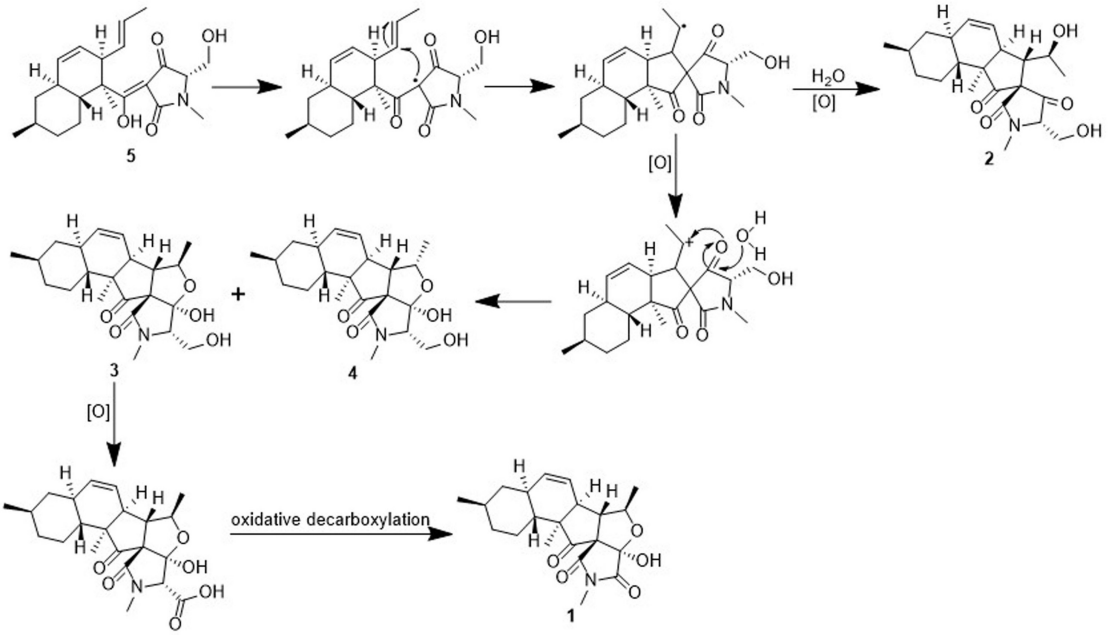

FIGURE 6 | Proposed biosynthetic pathway of compounds **1**-**4**.

TABLE 3 | Anti-phytopathogenic bacterial and fungal activities of **5** and **6**.

Compunds	MIC (μM)				
	C. michiganensis	***P. syringae***	***A. brassicicola***	***F. graminearum***	***R. cerealis***
5	4.2	1.1	8.4	133.9	8.4
6	4.2	4.2	16.7	133.9	–
Streptomycin sulfate[a]	0.9	3.4	No test	No test	No test
Carbendazim[b]	No test	No test	–	8.2	16.3
Prochloraz[b]	No test	No test	0.4	No test	No test

[a]Streptomycin sulfate was used as a positive control for antibacterial assays. [b]Carbendazim and prochloraz were used as positive controls for antifungal assays. "–" means no antifungal activity.

activities against *A. alternata*, *A. brassicicola*, *A. niger*, *B. cinerea*, *B. dothidea*, *Colletotrichum* sp., *F. graminearum*, *F. oxysporum*, *M. grisea*, *P. theae*, *R. cerealis*, and *V. mali*, and phytotoxicities toward the seedling growth of amaranth (*A. retroflexus*) and lettuce (*L. sativa*). The corresponding results are outlined in **Tables 3–5**. As indicated, compounds **1–6** displayed obvious phytotoxicities, while compounds **5** and **6** also exhibited potent anti-phytopathogenic bacterial and fungal activities. Notably, compounds **5** and **6** showed remarkable antimicrobial activities against *P. syringae* and *R. cerealis*, with minimum inhibitory concentration (MIC) values of 1.1 and 8.4 μM, respectively, compared to 3.4 μM for streptomycin sulfate, and 16.3 μM for carbendazim. Interestingly, the equisetins have been widely reported for their antibacterial activities against Gram-positive bacteria (Schobert and Schlenk, 2008; Mo et al., 2014), and in this study, their remakable anti-Gram negative bacterial activity was also found. Moreover, compounds **4–6** exhibited a prominent phytotoxicity against growth of amaranth and lettuce seedlings at 200 μg/mL, and this strong phytotoxicity was still evident at lower concentrations (50 μg/mL). In addition, the fusarisetins were quoted as exhibiting acinar morphogenesis inhibitory activities (Ahn et al., 2012; Jang et al., 2012), and were reported to be phytotoxic for the first time in the present paper.

The effect of **5** on the cell membrane of *P. syringae* was then examined by TEM. The untreated cells appeared to be intact with the typical cellular organization (**Supplementary Figure S1**), while cells treated with **5** (1 × MIC and 4 × MIC) disintegrated, with this effect being more pronounced at higher concentration (**Supplementary Figure S1**). Indeed, compound **5** completely lysed the cell walls of the majority of cells, which were misshapen and disproportionate (**Supplementary Figure S1**). Hence, **5** treatment was confirmed to damage the cell membrane of *P. syringae* resulting in leakage of the intracellular components.

Fermentation Optimization of 5

Due to the prominent bioactivities exhibited by compound **5**, the fermentation optimization was performed based on the OSMAC approach to improve its yield. Strain D39 was initially cultivated

TABLE 4 | Phytotoxicity of compounds **1–6** (200 μg/mL) toward seedling growth of amaranth and lettuce.

Strains	Root length (mm)		Hypocotyl length (mm)	
	Amaranth	Lettuce	Amaranth	Lettuce
1	4.60 ± 0.00	–	–	–
2	13.03 ± 0.32	–	–	–
3	7.65 ± 2.90	–	–	–
4	0	–	0	–
5	0	0	0	6.36 ± 0.59
6	0	0	0	4.90 ± 1.43
Glyphosate	0	0	0	3.75 ± 0.25
H_2O	16.43 ± 1.55	20.94 ± 2.15	7.40 ± 0.77	8.40 ± 0.59

The concentration of glyphosate was 200 μg/mL. A length <2.0 mm was regarded as no germination. "–" means no obvious effect on seedling growth.

TABLE 5 | Phytotoxicity of compounds **4–6** (50 μg/mL) toward seedling growth of amaranth.

Strains	Amaranth	
	Root length (mm)	Hypocotyl length (mm)
4	6.77 ± 1.93	6.30 ± 1.01
5	0	4.47 ± 1.29
6	0	5.20 ± 0.87
Glyphosate	0	0
H_2O	16.43 ± 1.55	7.40 ± 0.77

The concentration of glyphosate was 50 μg/mL. A length <2.0 mm was regarded as no germination.

by SSF on rice medium, as it was reported that SSF is an efficient fermentation process in terms of producing complex metabolites due to its longer metabolic circle. In addition, SSF offers potential benefits for microbial cultivation for bioprocesses and product development (Dong et al., 2016). However, many fatty acids and other components from the solid culture medium could be mixed with those from the fungus during the extraction process, which can significantly affect the bioassays and chemical fingerprint assays. The long fermentation time of SSF is also a disadvantage, and so submerged flask fermentation (SmF) using seven different crop media was applied for the purpose of this study.

The standard curve of **5** was established by means of HPLC-UV measurements. Thus, the linear regression equation for **5** was determined to be y = 8.34 × 10^6 × −3.54 × 10^4 (R^2 = 0.99) (**Supplementary Figure S2**) (R^2 = 0.99), where x is the concentration of **5** (mg/mL), and y is the peak area. All curves showed good linear relationships that could be used to estimate the production of **5** from the corresponding HPLC peak areas. The crude extracts were then subjected to HPLC analysis to determine the yields of **5**, which varied significantly (**Supplementary Table S2**). The results showed that the highest production of **5** was obtained using the crop F medium, yielding 21.61 mg/L.

Thus, the productivity of **5** was further optimized in the crop F medium by investigating the effects of salinity (i.e., 0, 1, 3, 5, 7, and 9%). It was found that the highest production of **5** was obtained under 1% salinity with a yield of 59.85 mg/L (**Supplementary Table S2**), and the production decreased upon increasing the salinity. Thus, crop F medium with a salinity of 1% was found to be the most favorable condition for the production of **5** from *F. equiseti* D39.

CONCLUSION

In conclusion, we herein reported the isolation and identification of two novel fusarisetins (**1** and **2**), along with four known antimicrobial and phytotoxic analogs (**3–6**) from the marine-derived fungus *F. equiseti* D39. The absolute configuration of **1**, which was difficult to be determined by common means, such as ECD calculations and chemical conversions, due to the lack of chromophores and low yields, was determined by VCD method and verified by X-ray diffraction, suggesting a new horizon to define the absolute configurations of fusarisetins. The phytotoxicity of fusarisetins was reported for the first time in the present study. Furthermore, as the need for subsequent field trials, the OSMAC fermentation optimization approach toward the most bioactive compound **5** was employed, and the potato dextrose liquid medium with a salinity of 1% was found to be the most favorable, with a high yield of 59.85 mg/L. Due to the neglect on the study of agricultural biological activities of marine-derived fungi worldwide, the present study revealed that searching for new biopesticides from secondary metabolites of marine-derived fungi has a very broad prospect.

DATA AVAILABILITY

The raw data supporting the conclusions of this manuscript will be made available by the authors, without undue reservation, to any qualified researcher.

AUTHOR CONTRIBUTIONS

DZ and CZ conceived and designed the experiments. XH, DW, ML, and JG performed the experiments. FC performed the VCD calculations. YP, JL, and YL analyzed the data. DZ wrote the manuscript. All authors reviewed the manuscript.

FUNDING

This work was supported by the National Natural Science Foundation of China (41806194), the Fundamental Research Funds for Central Non-profit Scientific Institution and (1610232017013), the Agricultural Science and Technology Innovation Program of China (ASTIP-TRIC07), and the Science Foundation for Young Scholars of Tobacco Research Institute of Chinese Academy of Agricultural Sciences (2017B08).

SUPPLEMENTARY MATERIAL

The Supplementary Material for this article can be found online at: https://www.frontiersin.org/articles/10.3389/fmicb.2019.01285/full#supplementary-material

REFERENCES

Ahn, J. S., Jang, J. H., Kim, B. Y., Jang, J., Asami, Y., and Oh, H. (2012). *Novel Fusarisetin Compounds and use Thereof*. U.S. Patent No 2013/0116297A1: Wasington, DC: U.S. Patent and Trademark Office.

Appendino, G., Gibbons, S., Giana, A., Pagani, A., Grassi, G., Stavri, M., et al. (2008). Antibacterial cannabinoids from *Cannabis sativa*: a structure-activity study. *J. Nat. Prod.* 71, 1427–1430. doi: 10.1021/np8002673

Caro-Diaz, E. J., Aung, A., Xu, J., Varghese, S., and Theodorakis, E. A. (2014). Fusarisetins: structure-function studies on a novel class of cell migration inhibitors. *Org. Chem. Front.* 1, 135–139. doi: 10.1039/c3qo00067b

Carroll, A. R., Copp, B. R., Davis, R. A., Keyzers, R. A., and Prinsep, M. R. (2019). Marine natural products. *Nat. Prod. Rep.* 36, 122–173. doi: 10.1039/c8np00092a

Dong, J. W., Cai, L., Li, X. J., Duan, R. T., Shu, Y., Chen, F. Y., et al. (2016). Production of a new tetracyclic triterpene sulfate metabolite sambacide by solid-state cultivated *Fusarium sambucinum* B10.2 using potato as substrate. *Bioresour. Technol.* 218, 1266–1270. doi: 10.1016/j.biortech.2016.07.014

Halecker, S., Surup, F., Kuhnert, E., Mohr, K. I., Brock, N. L., Dickschat, J. S., et al. (2014). Hymenosetin, a 3-decalinoyltetramic acid antibiotic from cultures of the ash dieback pathogen. *Hymenoscyphus* pseudoalbidus. *Phytochemistry* 100, 86–91. doi: 10.1016/j.phytochem.2014.01.018

Huang, R. H., Gou, J. Y., Zhao, D. L., Wang, D., Liu, J., Ma, G. Y., et al. (2018). Phytotoxicity and anti-phytopathogenic activities of marine-derived fungi and their secondary metabolites. *Rsc Adv.* 8, 37573–37580. doi: 10.1039/c8ra08047j

Jang, J. H., Asami, Y., Jang, J. P., Kim, S. O., Moon, D. O., Shin, K. S., et al. (2012). Fusarisetin A, an acinar morphogenesis inhibitor from a soil fungus, *Fusarium* sp. FN080326. *J. Am. Chem. Soc.* 134, 7194–7194. doi: 10.1021/ja302285e

Keiderling, T. A., and Lakhani, A. (2018). Mini review: instrumentation for vibrational circular dichroism spectroscopy, still a role for dispersive instruments. *Chirality* 30, 238–253. doi: 10.1002/chir.22799

Kusumi, T., Fujita, Y., Ohtani, I., and Kakisawa, H. (1991). Anomaly in the modified Mosher's method: absolute configurations of some marine cembranolides. *Tetrahedron Lett.* 32, 2923–2926. doi: 10.1016/0040-4039(91)80650-U

Liu, F., Wang, F., Du, L., Zhao, T., Doyle, M. P., Wang, D., et al. (2018). Antibacterial and antibiofilm activity of phenyllactic acid against *Enterobacter cloacae*. *Food Control* 84, 442–448. doi: 10.1016/j.foodcont.2017.09.004

Matsumori, N., Kaneno, D., Murata, M., Nakamura, H., and Tachibana, K. (1999). Stereochemical determination of acyclic structures based on carbon-proton spin-coupling constants. a method of configuration analysis for natural products. *J. Org. Chem.* 64, 866–876. doi: 10.1021/jo981810k

Mo, X., Li, Q., and Ju, J. (2014). Naturally occurring tetramic acid products: isolation, structure elucidation and biological activity. *Rsc Adv.* 4, 50566–50593. doi: 10.1039/c4ra09047k

Romano, S., Jackson, S. A., Patry, S., and Dobson, A. D. W. (2018). Extending the "one strain many compounds" (OSMAC) principle to marine microorganisms. *Mar. Drugs* 16:244. doi: 10.3390/md16070244

Royles, B. J. L. (1995). Naturally-occurring tetramic acids—Structure, isolation, and synthesis. *Chem. Rev.* 95, 1981–2001. doi: 10.1021/cr00038a009

Sadlej, J., Dobrowolski, J. C., and Rode, J. E. (2010). VCD spectroscopy as a novel probe for chirality transfer in molecular interactions. *Chem. Soc. Rev.* 39, 1478–1488. doi: 10.1039/b915178h

Schobert, R., and Schlenk, A. (2008). Tetramic and tetronic acids: an update on new derivatives and biological aspects. *Bioorgan. Med. Chem.* 16, 4203–4221. doi: 10.1016/j.bmc.2008.02.069

Singh, S. B., Zink, D. L., Goetz, M. A., Dombrowski, A. W., Polishook, J. D., and Hazuda, D. J. (1998). Equisetin and a novel opposite stereochemical homolog phomasetin, two fungal metabolites as inhibitors of HIV-1 integrase. *Tetrahedron Lett.* 39, 2243–2246. doi: 10.1016/s0040-4039(98)00269-x

Wang, D., Wang, C., Gui, P., Liu, H., Khalaf, S. M. H., Elsayed, E. A., et al. (2017). Identification, bioactivity, and productivity of actinomycins from the marine-derived *Streptomyces heliomycini*. *Front. Microbiol.* 8:1147. doi: 10.3389/fmicb.2017.01147

Wang, J., He, W., Huang, X., Tian, X., Liao, S., Yang, B., et al. (2016). Antifungal new oxepine-containing alkaloids and xanthones from the deep-sea-derived fungus *Aspergillus versicolor* SCSIO 05879. *J. Agric. Food Chem.* 64, 2910–2916. doi: 10.1021/acs.jafc.6b00527

Xu, J., Caro-Diaz, E. J. E., Lacoske, M. H., Hung, C. I., Jamora, C., and Theodorakis, E. A. (2012). Fusarisetin A: scalable total synthesis and related studies. *Chem. Sci.* 3, 3378–3386. doi: 10.1039/c2sc21308g

Yin, J., Wang, C., Kong, L., Cai, S., and Gao, S. (2012). Asymmetric synthesis and biosynthetic implications of (+)-fusarisetin A. *Angew. Chem. Int. Edit.* 51, 7786–7789. doi: 10.1002/anie.201202455

Zhang, Q., Wang, S. Q., Tang, H. Y., Li, X. J., Zhang, L., Xiao, J., et al. (2013). Potential allelopathic indole diketopiperazines produced by the plant endophytic Aspergillus fumigatus using the one strain-many compounds method. *J. Agric. Food Chem.* 61, 11447–11452. doi: 10.1021/jf403200g

Zhao, D. L., Wang, D., Tian, X. Y., Cao, F., Li, Y. Q., and Zhang, C. S. (2018). Anti-phytopathogenic and cytotoxic activities of crude extracts and secondary metabolites of marine-derived fungi. *Mar. Drugs* 16:36. doi: 10.3390/md16010036

Conflict of Interest Statement: XH, ML, JG, YP, and JL were employed by Zunyi Branch, Guizhou Tobacco Company.

The remaining authors declare that the research was conducted in the absence of any commercial or financial relationships that could be construed as a potential conflict of interest.

frontiers in Microbiology

ORIGINAL RESEARCH
published: 18 June 2019
doi: 10.3389/fmicb.2019.01358

Metagenome-Sourced Microbial Chitinases as Potential Insecticide Proteins

Francesca Berini[1†], Morena Casartelli[2†], Aurora Montali[3], Marcella Reguzzoni[4], Gianluca Tettamanti[3] and Flavia Marinelli[1*]*

[1] Laboratory of Microbial Biotechnology, Department of Biotechnology and Life Sciences, University of Insubria, Varese, Italy, [2] Laboratory of Insect Physiology and Biotechnology, Department of Biosciences, University of Milan, Milan, Italy, [3] Laboratory of Invertebrate Biology, Department of Biotechnology and Life Sciences, University of Insubria, Varese, Italy, [4] Laboratory of Human Morphology, Department of Medicine and Surgery, University of Insubria, Varese, Italy

Microbial chitinases are gaining interest as promising candidates for controlling plant pests. These enzymes can be used directly as biocontrol agents as well as in combination with chemical pesticides or other biopesticides, reducing their environmental impact and/or enhancing their efficacy. Chitinolytic enzymes can target two different structures in insects: the cuticle and the peritrophic matrix (PM). PM, formed by chitin fibrils connected to glycoproteins and proteoglycans, represents a physical barrier that plays an essential role in midgut physiology and insect digestion, and protects the absorptive midgut epithelium from food abrasion or pathogen infections. In this paper, we investigate how two recently discovered metagenome-sourced chitinases (Chi18H8 and 53D1) affect, *in vitro* and *in vivo*, the PM integrity of *Bombyx mori*, a model system among Lepidoptera. The two chitinases were produced in *Escherichia coli* or, alternatively, in the unconventional – but more environmentally acceptable – *Streptomyces coelicolor*. Although both the proteins dramatically altered the structure of *B. mori* PM *in vitro*, when administered orally only 53D1 caused adverse and marked effects on larval growth and development, inducing mortality and reducing pupal weight. These *in vivo* results demonstrate that 53D1 is a promising candidate as insecticide protein.

Keywords: insecticidal proteins, chitinase, metagenomics, heterologous expression, *Streptomyces*, insect control, *Bombyx mori*, peritrophic matrix

OPEN ACCESS

Edited by:
Roberta Marra,
University of Naples Federico II, Italy

Reviewed by:
Umut Toprak,
Ankara University, Turkey
Andrea Battisti,
University of Padua, Italy

***Correspondence:**
Gianluca Tettamanti
gianluca.tettamanti@uninsubria.it
Flavia Marinelli
flavia.marinelli@uninsubria.it

† These authors have contributed equally to this work

Specialty section:
This article was submitted to Microbial Symbioses, a section of the journal Frontiers in Microbiology

Received: *07 April 2019*
Accepted: *31 May 2019*
Published: *18 June 2019*

Citation:
Berini F, Casartelli M, Montali A, Reguzzoni M, Tettamanti G and Marinelli F (2019) Metagenome-Sourced Microbial Chitinases as Potential Insecticide Proteins. Front. Microbiol. 10:1358. doi: 10.3389/fmicb.2019.01358

INTRODUCTION

Pesticides derived from chemical synthesis are massively used to control different pests that constantly threaten crop production (Atwood and Paisley-Jones, 2017). The main drawbacks of chemically synthesized pesticides are their broad toxicity and accumulation into ecosystems and food chains (Kumar et al., 2019). Alternatively, biocontrol or biological control, i.e., the use of organisms or their products (biopesticides), is favored by the better selectivity of these agents toward the target pests, their biodegradability, and reduced toxicity (Czaja et al., 2015; Bonanomi et al., 2018; Damalas and Koutroubas, 2018). In contrast, the successful use of biocontrol agents is often limited by their instability and scarce persistence into environment, as well as by their slower mode of action and reduced efficacy in comparison to chemical pesticides. Bacteria and fungi exhibiting

fungicidal, insecticidal, and/or nematicidal action are commonly used as biocontrol agents. They produce antibiotics and secrete a variety of hydrolytic enzymes (chitinases, proteases, lipases, and glucanases), which concur in disrupting essential structures for pathogen life. A compelling alternative is formulating cocktails of (semi)purified antibiotics and enzymes, which mimic living biocontrol agents, without presenting the limitations inherent to their use and storage. Such biopesticides can be used alone or in combination with other controlling agents to enhance their efficacy (Regev et al., 1996; Karasuda et al., 2003; Liu et al., 2010). If added to chemically synthesized pesticides, biopesticides might allow the reduction of their dosage, alleviating their negative impact on the ecosystem (Karasuda et al., 2003). To this purpose, chitinases represent promising biopesticides, since they hydrolyze chitin, which is present in different plant pests, i.e., insects, fungi, and nematodes (Mavromatis et al., 2003; Neeraja et al., 2010; Hjort et al., 2014; Soares et al., 2015; Berini et al., 2016, 2017b, 2018). Additionally, they are harmless for plants and vertebrates, which do not possess chitin in their tissues. Chitin is a linear homopolymer of *N*-acetylglucosamine (GlcNAc) and exerts fundamental roles in the vital structures of pests. It is a structural component of cell wall in fungi, of eggshell in nematodes, and of both cuticle and peritrophic matrix (PM) in insects. PM is a thin acellular sheath formed by chitin, glycoproteins, and proteoglycans, which lines the midgut epithelium of most insects (Hegedus et al., 2009; Berini et al., 2018). Chitinases belong to the family of glycosyl hydrolases. Based on their mode of action on chitin, they are classified as endochitinases, which split chitin randomly at internal sites, or as exochitinases that remove monomers (β-*N*-acetyl glucosaminidases) or dimers (chitobiosidases) of GlcNAc from the non-reducing end of chitin chains (Adrangi and Faramarzi, 2013; Berini et al., 2018).

In the recent years, we applied function- and/or sequence-based screening approaches to different metagenomes for discovering novel bioactive chitinases of microbial source, which differ from those already known that have been discovered by classical microbiological methods (Hjort et al., 2014; Cretoiu et al., 2015; Berini et al., 2017b). Since the vast majority of microorganisms present in natural samples (up to 99–99.9%) are recalcitrant to cultivation, metagenomics, being culture-independent, facilitates the task of encrypting novel chitinases (Berini et al., 2017a). Thanks to this approach, two of the first metagenomics-sourced chitinases were recently discovered: Chi18H8 was identified in 2014 from a naturally phytopathogen-suppressive soil in Sweden (Hjort et al., 2014; Berini et al., 2017b), whereas 53D1 was identified in 2015 in a chitin-supplemented agricultural soil from an experimental farm in the Netherlands (Cretoiu et al., 2015). Few milligrams of both chitinases were initially produced in *Escherichia coli* as heterologous host and partially biochemically/functionally characterized. Interestingly, Chi18H8 showed antifungal activity toward the phytopathogen fungi *Fusarium graminearum* and *Rhizoctonia solani* (Hjort et al., 2014; Berini et al., 2017b), whereas 53D1 looked interesting since it was markedly stable in a wide range of conditions, including in the presence of high salt concentrations (Cretoiu et al., 2015). We recently described the development to a 30-L bioreactor pilot scale of an effective process to produce Chi18H8 by mild solubilization of inclusion bodies (IBs) in *E. coli* (Berini et al., 2017b). Herein, we describe the optimization of 53D1 production by using an alternative heterologous host – the Gram-positive bacterium *Streptomyces coelicolor* A3(2) – and report on producing and testing both Chi18H8 and 53D1 as insecticidal proteins in *Bombyx mori*, a reference model among Lepidoptera. To our knowledge, this is the first investigation on the insecticidal activity of metagenome-sourced chitinases, which might represent promising candidates as biocontrol agents.

MATERIALS AND METHODS

53D1 Gene Cloning

The nucleotide sequence of the metagenomic fosmid insert that includes *53D1* chitinase gene was deposited in the GenBank database (accession number LN824156.1) (Cretoiu et al., 2015). The chitinase-encoding cDNA was sub-cloned into the multi-copy expression vector pIJ86 (Binda et al., 2013) (kindly gifted by M. J. Bibb, John Innes Centre, Norwich, United Kingdom) under the control of the constitutive *ermE** promoter, by using the fosmid DNA as template. Primers used for amplification were pIJ86_53D1_FW (5′ ATATGGATCCGTATGAAGGAGGTCA TTCATGAGTCACGGTTCGGTC 3′) and pIJ86_53D1_RV (5′ ATTAAAGCTTCTAGTGGTGGTGGTGGTGGTGCGGTCTCA GCCGGGA 3′), including the restriction sites (underlined) for *Bam*HI and *Hin*dIII, respectively, and introducing a C-terminal His_6-Tag in the recombinant protein. All cloning procedures were carried out in *E. coli* DH5α (Invitrogen-Life Technology, Carlsbad, CA, United States). The construct was checked by DNA sequencing (BMR Genomics, Padua, Italy) and transformed into the non-methylating *E. coli* ET12567/pUZ8002 cells (Marcone et al., 2010b). Luria-Bertani (LB, Sigma-Aldrich, St. Louis, MO, United States) agar plates were used for propagating *E. coli* strains.

Intergeneric conjugation between the *E. coli* donor and the recipients *S. coelicolor* A3(2), *S. venezuelae* ATCC 10595, and *S. lividans* TK24 was conducted following the protocol reported in Binda et al. (2013). Transformation of the recombinant *Streptomyces* spp. was checked by colony PCR (Binda et al., 2013). pIJ86_53D1_FW and pIJ86_53D1_RV primers were used to verify ex-conjugants carrying pIJ86::*53D1* plasmid. Primers pIJ86_FW (5′ TGCACGCGGTCGATCTTGAC 3′) and pIJ86_RV (5′ TCATGGTCGGTCTCCTGGTG 3′), annealing to regions of the vector around the multiple cloning site, were used to check transformation with the empty pIJ86 vector.

53D1 Heterologous Production

Reagents were purchased from Sigma-Aldrich, St. Louis, MO, United States, unless otherwise indicated. Mannitol soya flour (MS) agar medium (Kieser et al., 2000) was used for propagating *Streptomyces* spp. Streptomycetes were stored for long-term preservation as spores in 10% (v/v) glycerol. For cultivating the recombinant strains, agar plates and liquid media were always supplemented with 50 μg/mL apramycin. Strains were

reactivated by growing them for 72 h into 100-mL Erlenmeyer flasks containing 20 mL AurM medium (in g/L: 20 maltose, 10 dextrin, 15 soybean meal, 4 casein enzymatic hydrolysate, 4 bacteriological peptone, 2 yeast extract, 2 $CaCO_3$, pH 7.0) (Marcone et al., 2010b). Three hundred milliliters baffled flasks containing 50 mL YEME (yeast extract – malt extract, in g/L: 3 yeast extract, 5 bacteriological peptone, 3 malt extract, 20 glucose, pH 7.0) (Binda et al., 2013) were then inoculated at 10% (v/v) and further shaken at 200 revolutions per minute (rpm) at 28°C for 72 h. Finally, 500-mL baffled flasks containing 100 mL of five different production media (commonly used for streptomycetes) were inoculated at 10% (v/v), incubated at 200 rpm and 28°C for 240 h. Liquid production media used were YEME, MV (medium V) (Marcone et al., 2010a), R5 medium (Kieser et al., 2000), TSB (tryptone soya broth) (Kieser et al., 2000), and Bennett's medium (Dalmastri et al., 2016). All media were supplemented with 20 g/L glucose, if not already included, in order to repress the endogenous chitinolytic system of streptomycetes (Berini et al., 2018).

Every 24 h, 10 mL of culture broth were centrifuged at 1900 × *g* for 10 min at 4°C. Cell-free culture broths were collected and pH and residual glucose were measured by pH Test Strips 4.5–10.0 and Diastix strips (Bayer, Leverkusen, Germany). Secreted 53D1 production was estimated in cell-free culture broths by western blot analysis [after protein concentration by 10% (v/v) trichloracetic acid precipitation] and fluorimetric enzyme activity assay (see below). In parallel, cell pellets were recovered and biomass production was measured as wet weight. Then, pellets were sonicated on ice with 10–15 cycles of 30 s each (interposed with 30-s intervals), using a Branson Sonifier 250 (Dansbury, CT, United States) in 20 mM sodium acetate pH 5.0 supplemented with 10 μg/mL deoxyribonuclease (DNase) and 0.19 mg/mL phenylmethylsulfonylfluoride (PMSF). To remove insoluble material, centrifugation at 20,000 × *g* for 40 min at 4°C followed. Production of intracellular 53D1 was checked in the soluble fractions by western blot analysis and fluorimetric enzyme activity assay (see below).

53D1 Purification

For 53D1 purification, *S. coelicolor*/pIJ86::*53D1* was grown for 192–240 h in YEME medium. Proteins secreted in the cell-free culture broth were precipitated by slowly adding 80% (w/v) ammonium sulfate. After 2 h incubation at 4°C, centrifugation at 12,000 × *g* at 4°C for 40 min followed. The pellet was re-suspended in 1/5 (v/v) of 20 mM Tris–HCl pH 8.0 and dialyzed against the same buffer. The recombinant protein was purified onto a 5-mL Ni^{2+}-Hitrap chelating affinity column (1.6 cm × 2.5 cm; GE Healthcare Sciences, Little Chalfont, United Kingdom), according to manufacturer's instructions. The column was equilibrated with 20 mM Tris–HCl pH 8.0, 500 mM NaCl, and 20 mM imidazole. After extensive washing, the recombinant protein was eluted with 20 mM Tris–HCl pH 8.0, 500 mM NaCl, and 250 mM imidazole, followed by dialysis for 3 h against 20 mM sodium acetate pH 5.0. The purified protein was finally concentrated with 30 K Amicon Ultra-2 centrifugal filter devices (Merck KGaA, Darmstadt, Germany).

Chi18H8 Production and Purification

Chi18H8 production in *E. coli* BL21 Star™ (DE3), carrying the pET24b(+)::*chi18H8* expression plasmid, and its solubilization from IBs were accomplished as previously described (Berini et al., 2017b). In brief, to prepare the protein used in this work, *E. coli* BL21 Star™ (DE3)/pET24b(+)::*chi18H8* cells were grown in 300-mL baffled Erlenmeyer flasks containing 80 mL LB medium supplemented with 50 μg/mL kanamycin, incubated overnight at 37°C and 200 rpm. Two liters flasks with 750 mL selective LB medium were inoculated with the pre-cultures (initial $OD_{600\ nm}$ = 0.1), and incubated at 37°C and 200 rpm until $OD_{600\ nm}$ reached 0.6. Protein production was induced by adding 0.4 mM isopropyl β-D-1-thiogalactopyranoside (IPTG) and cultivation was prolonged at 20°C for further 24 h.

Cells were harvested by centrifugation and re-suspended in 50 mM Tris–HCl pH 8.0, 25% (w/v) sucrose, and 1 mM ethylenediaminetetraacetic acid (EDTA). After incubation for 30 min at room temperature and vigorous shaking, samples were sonicated (six cycles of 30 s each). A total of 0.2 M NaCl, 1% (w/v) sodium deoxycholate (DOC), and 1% (v/v) Nonidet P-40 were added; the samples were further incubated as above and centrifuged (20,000 × *g* at 4°C for 30 min). The pellet was washed with 1% (v/v) Triton X-100 and 1 mM EDTA and centrifuged (12,000 × *g* at 4°C for 10 min). IB washing with this buffer was repeated twice, followed by washing with deionized water. After overnight storage at −20°C, the frozen pellet was resuspended in 10 mM lactic acid (10 mL/g cell) and incubated at 37°C and 200 rpm for 5 h. Centrifugation at 1900 × *g* at 4°C for 5 min was employed for removing insoluble material. Finally, solubilized Chi18H8 was dialyzed overnight against 20 mM sodium acetate pH 5.0.

SDS-PAGE Electrophoresis and Western Blot

Protein fractions were analyzed by sodium dodecyl sulfate polyacrylamide (12% w/v) gel electrophoresis (SDS-PAGE), using a Tris-glycine system and Coomassie brilliant blue R-250 straining. For western blot analysis, anti His-Tag Antibody HRP conjugate (Novagen Inc., Madison, WI, United States) and chemiluminescence (ECL Western Blotting Detection System, GE Healthcare Sciences, Little Chalfont, United Kingdom) were used for protein identification.

Chitinase Activity Assays

Chitinase activities were assayed by using the fluorimetric chitooligosaccharide analogs 4-methylumbelliferyl *N*-acetyl-β-D-glucosaminide (4-MU-GlcNAc), 4-methylumbelliferyl *N,N′*-diacetyl-β-D-chitobioside [4-MU-$(GlcNAc)_2$], and 4-methylumbelliferyl *N,N′,N″*-triacetyl-β-D-chitotrioside [4-MU-$(GlcNAc)_3$] (Cretoiu et al., 2015). Activity on these synthetic compounds was assayed in 100 mM sodium acetate pH 5.0, at 37°C. Chitinolytic activity was also determined on colloidal chitin as described in Berini et al. (2016). In this case, activity was measured at pH 3.0, 5.0, 7.0, or 9.0, by adjusting colloidal chitin's pH with 0.1 M NaOH. One unit (U) of chitinase activity was defined as the amount of enzyme required for the

release of 1 μmol of 4-MU or of GlcNAc per min at 37°C. The control of protease or lipase activities in purified 53D1 and Chi18H8 preparations was conducted as described in Berini et al. (2016).

Experimental Insects

Larvae of *B. mori* [polyhybrid strain (126 × 57) (70 × 90)] were provided by CREA – Honeybee and Silkworm Research Unit (Padua, Italy). Insects were reared on artificial diet (Cappellozza et al., 2005) at 25 ± 0.5°C, under a 12:12 light-dark photoperiod, with 70 ± 5% relative humidity. Once insects had reached the last larval instar, they were staged and synchronized (see Franzetti et al., 2012 for details).

Ultrastructural Analysis of the PM

Isolation of the PM and *in vitro* Incubation With Chi18H8 or 53D1 Chitinases

On second day of the fifth instar, larvae were anaesthetized with CO_2. Midgut was isolated by cutting the insect dorsally and the PM was carefully separated from the midgut epithelium. The lumen content was removed from the PM by rinsing the matrix with PBS (phosphate-buffered saline, 137 mM NaCl, 2.7 mM KCl, 4.3 mM Na_2HPO_4, 1.4 mM KH_2PO_4, pH 7.0). Each sample was divided into four pieces and transferred into a 24-multiwell plate: two pieces were treated with Chi18H8 or 53D1 (40.5 U_{tot} per well, calculated as the sum of chitobiosidase and endochitinase activities on 4-MU-$(GlcNAc)_2$ and 4-MU-$(GlcNAc)_3$, respectively, in 100 mM sodium acetate buffer pH 5.0, while the other two were incubated in the same buffer in the absence of chitinases (controls). All the samples were processed for electron microscopy analysis.

Scanning Electron Microscopy (SEM)

After incubation with 53D1 or Chi18H8, PM was fixed with 4% (v/v) glutaraldehyde in 0.1 M sodium cacodylate buffer pH 7.4, overnight at 4°C. After post-fixation with 1% (w/v) osmium tetroxide and 1.25% (w/v) potassium ferrocyanide for 1 h, samples were dehydrated in an ethanol series and then incubated in hexamethyldisilazane (two steps of 10 min each). Samples were mounted on stubs, carbon coated with a Sputter K250 coater, and finally observed with a SEM-FEG XL-30 microscope (Philips, Eindhoven, Netherlands).

Transmission Electron Microscopy (TEM)

To analyze the samples at TEM, PM was fixed with 4% (v/v) glutaraldehyde in 0.1 M sodium cacodylate buffer pH 7.4, overnight at 4°C and then post-fixed with 1% (w/v) osmium tetroxide for 1 h. After dehydration in an ethanol series, specimens were embedded in an Epon/Araldite 812 mixture. Ultra-thin sections were obtained with Leica Reichert Ultracut S (Leica, Nußloch, Germany), then stained with lead citrate and uranyl acetate, and finally observed with a JEM-1010 transmission electron microscope (Jeol, Tokyo, Japan). Images were acquired with a Morada digital camera (Olympus, Münster, Germany).

Bioassays With Chi18H8 and 53D1 Chitinases

After hatching, larvae were reared as reported in the Section "Experimental Insects," and fed *ad libitum* with small pieces of artificial diet (1 cm × 1 cm × 1 mm), each overlaid with an equal volume (65 μL) of Chi18H8 or 53D1 (6 U_{tot}/cm^2 diet) dissolved in 100 mM sodium acetate, pH 5.0. Control larvae were grown on small pieces of artificial diet overlaid with the same volume of sodium acetate buffer. The diet was replaced every day. Different parameters were recorded: larval mortality (reported as percentage of the initial number of larvae), length of the larval stage (from hatching to the occurrence of wandering behavior), and weight of the pupae (evaluated on the eighth day of the pupal stage). For bioassays with 53D1, maximal larval weight before pupation and cocoon weight (measured on the eighth day of the pupal stage) were registered, too. Developmental stages of *B. mori* were defined according to Franzetti et al. (2012). Bioassays were performed in triplicate, by using at least 11 larvae for each experimental group. PM samples from larvae at the second day of the fifth instar reared on diet overlaid with 53D1 and relative controls were collected and processed for the analysis at SEM and TEM, as reported in the Section "Ultrastructural Analysis of the PM."

In vitro Incubation of Chitinases With Midgut Juice

Midgut juice was extracted from larvae at the second day of the fifth instar. Insects were anaesthetized with CO_2, whole midguts were dissected and their luminal content was collected into a centrifuge tube. Centrifugation at 15,000 × *g* for 10 min was performed to remove insoluble material. Supernatants were aliquoted, stored at −80°C, and used within 2 weeks. Six U_{tot} of Chi18H8 or 53D1 were incubated at 25°C in 100 mM Tris–HCl pH 8.0 (control) or in the presence of different dilutions of the midgut juice (undiluted, or diluted 1:10 or 1:100 in 100 mM Tris–HCl pH 8.0). Aliquots were withdrawn at regular intervals up to 8 h and the residual chitobiosidase activity was measured using 4-MU-$(GlcNAc)_2$ as substrate, according to the standard protocol described in the Section "Chitinase Activity Assays."

RESULTS

Production and Characterization of Chi18H8

Chi18H8 is a protein of 424 amino acids with a predicted molecular mass of 45.96 kDa and a theoretical isoelectric point of 7.75. To assay its insecticidal activity, Chi18H8 was produced in 2-L flasks and recovered from *E. coli* BL21 Star™ (DE3)/pET24b(+)::*chi18H8* cells (**Table 1**) by using a newly developed process based on the mild solubilization of IBs, as recently described in Berini et al. (2017b). Following purification, Chi18H8 migrated in SDS-PAGE gels as a single band of ca. 47 kDa (46.77 kDa is the expected molecular mass for the recombinant His_6-tagged protein). Protein purity was estimated to be >85% (**Figure 1**).

TABLE 1 | Purification of Chi18H8 (A) from *E. coli* BL21 Star™ (DE3)/pET24b(+)::*chi18H8* IBs and 53D1 (B) from *S. coelicolor*/pIJ86::*53D1* culture broth.

Purification step	Volume (mL)	Total proteins (mg)	Total activity (U)	Specific activity (U/mg protein)	Purification (-fold)	Yield (%)
(A)						
IBs	10.6	123.0	33.4	0.27	1.0	100.0
Soluble fraction from IBs	53.0	71.8	2623.0	36.7	78.5	84.0
(B)						
Crude broth	1000.0	1125.0	1080.0	0.96	1.0	100.0
Ammonium sulfate precipitation	200.0	1090.0	1067.1	0.98	1.0	98.8
Affinity chromatography	114.1	34.9	956.6	27.4	28.5	88.5

For both proteins, data are relative to cells (Chi18H8) or cell-free culture broth (53D1) from 1 L of culture. Activity was assayed on 4-MU-$(GlcNAc)_2$ as substrate, in 100 mM sodium acetate pH 5.0.

Fluorimetric enzyme assay using standard synthetic oligosaccharides confirmed the Chi18H8 prevalent chitobiosidase activity on 4-MU-$(GlcNAc)_2$ (37.92 ± 1.17 U/mg protein), its weaker endochitinase activity on 4-MU-$(GlcNAc)_3$ (8.91 ± 1.72 U/mg protein), and none β-*N*-acetyl-glucosaminidase activity on 4-MU-GlcNAc. As reported in **Table 2**, pure Chi18H8 was able to hydrolyze colloidal chitin – a substrate that, although soluble, resembles the chemical structure of the naturally occurring insoluble chitin – with a maximum activity of about 1.47 ± 0.25 U/mg protein at pH 5.0. At pH 3.0, 7.0, and 9.0, ca. 22, 83, and 72% of the maximum activity were maintained, respectively (**Table 2**). None protease or lipase activity (lipases and proteases are enzymes usually secreted by streptomycetes that could interfere with the following insecticide assays) was detected in the enzyme preparation (data not shown).

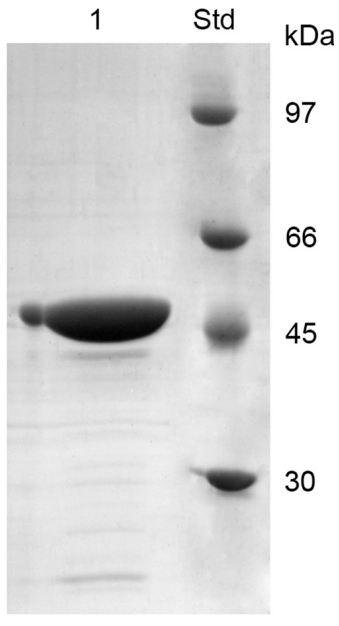

FIGURE 1 | SDS-PAGE of Chi18H8 solubilization from *E. coli* BL21 Star™ (DE3)/pET24b(+)::*chi18H8* IBs. 1, solubilized Chi18H8; Std, standard reference proteins.

Heterologous Expression of 53D1 in *Streptomyces* spp.

53D1 gene (63.03% G+C) consists of 1191 nucleotides coding for a protein of 396 amino acids with a predicted molecular mass of 43.60 kDa and a theoretical isoelectric point of 4.83. When cloned and expressed in *E. coli*, >80% of the recombinant protein accumulated as inactive form in insoluble fractions. Despite many efforts, we could not develop a protocol for solubilizing 53D1 in a biologically active form from IBs, as we did for Chi18H8. In addition, as reported in Cretoiu et al. (2015), the recovery yield of the soluble active form of 53D1 from *E. coli* cytoplasmic fraction was too low (no more than 0.60 mg/L culture and 0.12 mg/g cell) to support its further trials as insecticide protein. Thus, in this paper we report an alternative expression platform using soil Gram-positive actinomycetes belonging to the genus *Streptomyces* as heterologous hosts for 53D1 production.

53D1 coding gene was thus cloned into the multicopy plasmid pIJ86 and introduced by intergeneric conjugation into *S. lividans* TK24, *S. venezuelae* ATCC 10595, and *S. coelicolor* A3(2). For selecting the best expression system, the three recombinant streptomycetes (and their control strains carrying empty vectors) were cultivated in five different media (see section "53D1 Heterologous Production"). Recombinant *S. lividans*/pIJ86::*53D1* did not produce the heterologous chitinase -neither inside nor outside the cells – in any of the cultivation media used (data not shown). 53D1 was instead secreted by the recombinant *S. venezuelae*/pIJ86::*53D1* growing in YEME medium (data not shown) and, to a major extent, by *S. coelicolor*/pIJ86::*53D1* cultivated in the same condition (**Figure 2**). Western blot analysis indicated that *S. venezuelae*/pIJ86::*53D1* produced a maximum of 8.75 mg/L of extracellular 53D1 (corresponding to 0.27 mg/g cell) (data

TABLE 2 | Chi18H8 and 53D1 activity on colloidal chitin at different pHs (mean ± standard error from at least three independent experiments).

pH	Chi18H8 (U/mg protein)	53D1 (U/mg protein)
3.0	0.32 ± 0.07	2.75 ± 0.35
5.0	1.47 ± 0.25	10.15 ± 1.40
7.0	1.22 ± 0.01	7.10 ± 0.20
9.0	1.06 ± 0.04	7.00 ± 0.10

not shown), whereas *S. coelicolor*/pIJ86::*53D1* secreted up to 45 mg/L (0.83 mg/g cell) of 53D1 (**Figure 2B**). No traces of 53D1 were detected into cytoplasmic soluble fractions of both the recombinant strains (data not shown).

Comparison of *S. coelicolor*/pIJ86::*53D1* (**Figure 2B**) growth curve with the one of its control strain carrying the empty vector (**Figure 2A**) indicated that *S. coelicolor*/pIJ86::*53D1* grew faster and consumed glucose more efficiently. This better performance of *S. coelicolor*/pIJ86::*53D1* was quite unexpected since the expression of heterologous genes usually causes a metabolic burden to the producing bacterial host, which slows down its growth rate (Binda et al., 2013). When observed at the optical microscope, the mycelium of *S. coelicolor*/pIJ86::*53D1* was less clumpy than in the control strain; this phenotype might be due to a putative lysozyme-like activity of 53D1. It has been demonstrated that lysozyme, producing a more disperse mycelium, facilitates streptomycetes growth in liquid media (Hobbs et al., 1989). A lysozyme activity of several chitinases was indeed previously reported by other authors (Bokma et al., 1997; Wohlkönig et al., 2010).

Cells of *S. coelicolor*/pIJ86::*53D1* started to secrete 53D1 after approximately the first 24 h of growth and continued to produce the heterologous protein during the stationary growth phase: the maximum specific productivity was reached after 240 h (**Figure 2B**). Consistently, in the same period of time, the chitinase enzyme activity measured in cell-free culture broths of *S. coelicolor*/pIJ86::*53D1* progressively increased and reached a maximum of ca. 18.5 U/g cell after 240 h (**Figure 2D**). As expected, no 53D1 was detectable by western blot analysis in the cell-free culture broths of *S. coelicolor*/pIJ86 (**Figure 2A**). The traces of chitinase activity detectable in the cell-free culture broths of the control strain (never exceeding the level 0.1 U/g cell; **Figure 2C**) were due to the endogenous streptomycetes chitinolytic system, opportunely

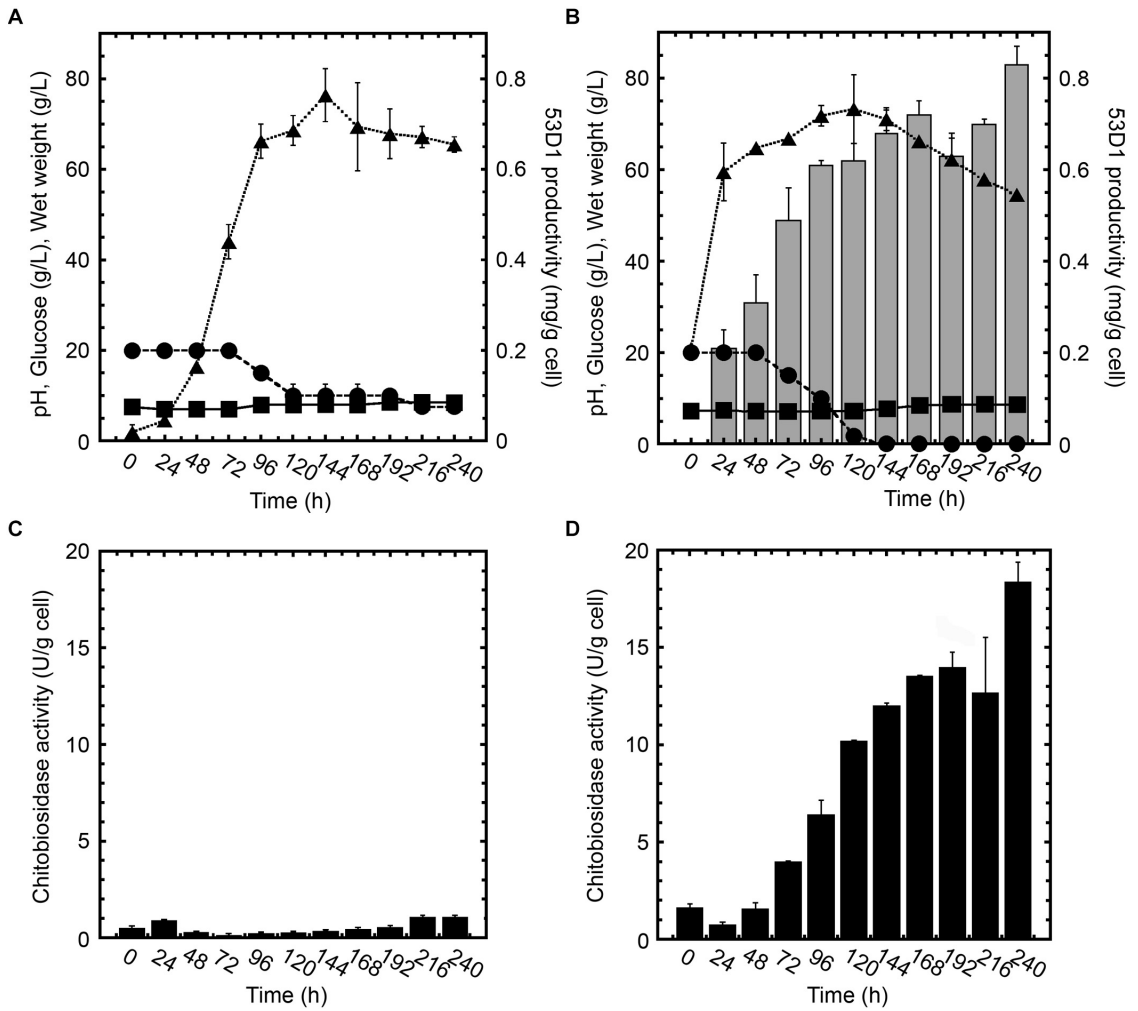

FIGURE 2 | Growth curves, 53D1 production **(A,B)**, and chitinase activities **(C,D)** in *S. coelicolor*/pIJ86 (left panels) and *S. coelicolor*/pIJ86::*53D1* (right panels), grown in YEME medium. In panels **(A,B)**, wet weight (▲, dotted line), pH (■, solid line), glucose consumption (●, dashed line), and 53D1 production determined by western blot analysis of cell-free culture broths (gray bars). In panels **(C,D)**, chitinase activity of cell-free culture broths measured by fluorimetric activity assay on 4-MU-$(GlcNAc)_2$ as substrate (black bars).

repressed by the addition of glucose to the cultivation medium (Berini et al., 2018).

53D1 Purification and Characterization

53D1 was recovered from the culture broth of *S. coelicolor*/pIJ86::*53D1*, harvested after 192–240 h of growth in YEME medium, as described in the Sections "53D1 Heterologous Production" and "53D1 Purification." His_6-53D1 was then purified as a single band of ca. 44 kDa (44.40 kDa is the expected molecular mass for the recombinant His_6-tagged protein) by means of HiTrap-chelating affinity chromatography, with a purity of ca. 90% (**Figure 3**). Purification yield was 34.9 mg/L (**Table 1**), corresponding to ca. 0.64 mg/g cell. Fluorimetric enzyme assay using standard synthetic oligosaccharides confirmed that 53D1 has a prevalent chitobiosidase activity on 4-MU-$(GlcNAc)_2$ (31.60 ± 2.90 U/mg protein), a weaker endochitinase activity on 4-MU-$(GlcNAc)_3$ (16.42 ± 1.85 U/mg protein), and none β-*N*-acetyl-glucosaminidase activity on 4-MU-GlcNAc. On colloidal chitin, the maximum activity of 53D1 was measured at pH 5.0, although the protein conserved ca. 70% of its maximum activity also at neutral and basic pH. It conserved ca. 27% of its initial activity at pH 3.0 (**Table 2**). None protease or lipase activity was detected in the enzyme preparation (data not shown).

In vitro Effects of 53D1 and Chi18H8 on the PM of *B. mori* Larvae

To evaluate the potential insecticidal effects of 53D1 and Chi18H8, both chitinases were first tested *in vitro* by exposing the PM isolated from last instar larvae to a concentrated preparation of pure enzymes (40.5 U_{tot}). SEM and TEM analyses of untreated PM (control) highlighted the well-organized and compact structure of *B. mori* PM: chitin fibrils were properly aligned and PM showed a continuous surface (**Figures 4A,D**). On the contrary, the analysis of the PM treated with Chi18H8 revealed a marked effect induced by the chitinase (**Figures 4B,E**). In particular, ruptures of the superficial layers (**Figure 4B**) and alteration of the integrity of the chitin network (**Figures 4B,E**) were clearly visible. The morphological analysis revealed a significant alteration of the structural organization of PM also when treated with 53D1 (**Figures 4C,F**). As for the PM treated with Chi18H8, the superficial layers of 53D1-treated PM were damaged (**Figure 4C**) and the disruption of the fibril network was visible (**Figure 4F**).

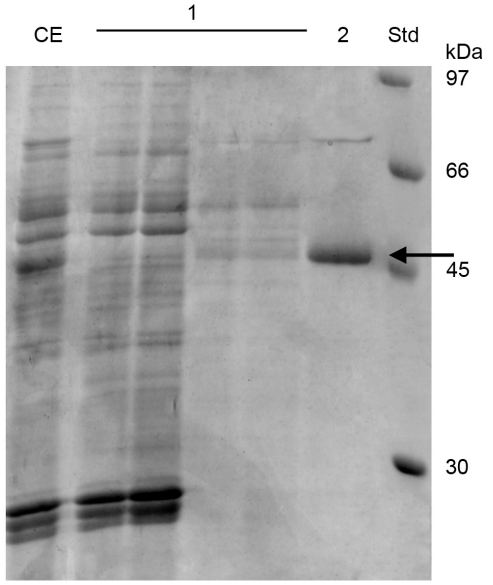

FIGURE 3 | SDS-PAGE of 53D1 purification. CE, crude extract, i.e., *S. coelicolor*/pIJ86::*53D1* concentrated culture broth, loaded onto HiTrap-Chelating affinity column; 1, fractions collected from the initial washing of the column; 2, purified 53D1; Std, standard reference proteins. 53D1 protein band is indicated with an arrow.

In vivo Effects of 53D1 and Chi18H8 on *B. mori* Larvae

To evaluate the *in vivo* effects of 53D1 and Chi18H8, bioassays exposing the larvae of *B. mori* to chitinase-containing diet were conducted. The larval mortality, the length of the larval stage, and the weight of the pupae were not significantly different between untreated (control) and Chi18H8-treated larvae (**Table 3**). In contrast, the developmental parameters recorded for larvae fed with 53D1-containing diet indicated a clear detrimental effect of the chitinase (**Table 4**). In fact, the mortality of 53D1-treated larvae was significantly higher than in control larvae, the duration of the larval stage of the survived larvae was 25% longer, and their maximal larval weight before pupation was markedly reduced. As shown in **Figure 5**, the effect on larval development was visible from early instars onward. Moreover, pupal and cocoon weight was significantly lower in 53D1-treated larvae than in controls (**Table 4**). Finally, the PM isolated from survived last instar larvae reared on 53D1 chitinase-containing diet showed a compromised structure both at SEM and TEM (**Figure 6**). These effects on PM caused by 53D1 were comparable to those previously observed in *in vitro* experiments (see **Figure 4**), indicating that the alterations of the larval growth and development observed in the bioassay were due to the direct effect of 53D1 chitinase on PM.

53D1 and Chi18H8 Residual Activity in *B. mori* Midgut Juice

To explain the different *in vivo* activity of the two chitinases, the residual enzyme activity of Chi18H8 and 53D1 was measured following their incubation for different time intervals in the absence or presence of midgut juice (at different dilutions) isolated from *B. mori* larvae. Indeed, the midgut juice from lepidopteran larvae has an alkaline pH and contains enzymes responsible for macromolecule digestion, including proteases (Terra and Ferreira, 1994). 53D1 activity was stable in the control buffer at alkaline pH 8 for at least 8 h (**Figure 7A**). In the presence of midgut juice, its residual activity was dependent on midgut juice dilution: anyhow, after 8 h of incubation with undiluted midgut juice the enzyme still retained ca. the 40% of its initial activity (**Figure 7A**). In contrast, the activity of Chi18H8 was much more drastically reduced by incubating the enzyme in the

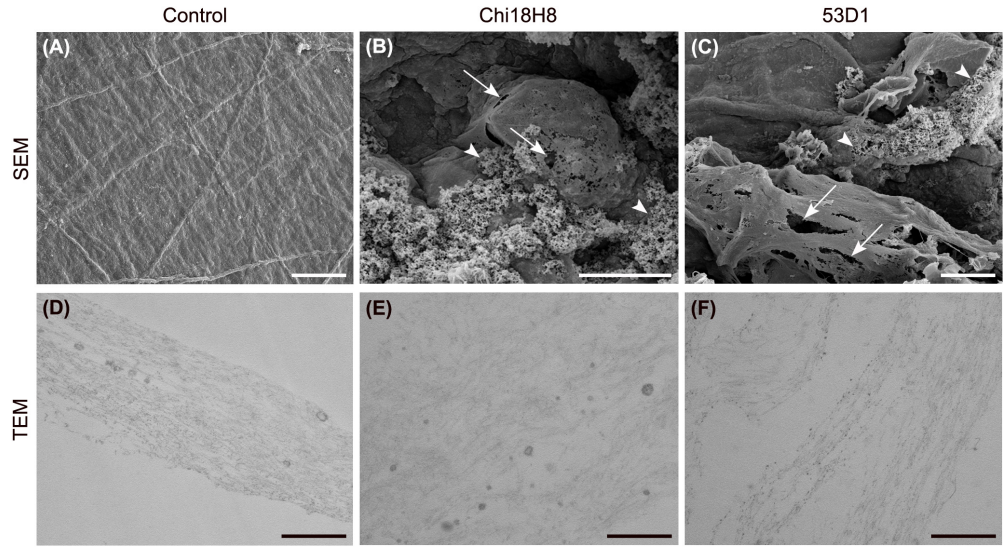

FIGURE 4 | Morphology of the peritrophic matrix treated with chitinases. SEM **(A–C)** and TEM **(D–F)**. **(A,D)** Control samples; **(B,E)** in PM treated with Chi18H8, ruptures of the superficial layers (arrows) and alteration of the fibril network (arrowheads) are visible, as confirmed by TEM analysis; **(C,F)** similar effects can be observed in PM treated with 53D1. Bars: **(A–C)** 10 μm; **(D–F)** 0.5 μm.

control buffer at alkaline pH and in the presence of midgut juice (**Figure 7B**). After 8 h in the control buffer, the residual activity was reduced to less than 40%. When incubated with 10- and 100-fold diluted midgut juice, the residual activity after 8 h was ca. 3 and 23% of the initial activity, respectively. In the presence of undiluted midgut juice, Chi18H8 completely lost its enzymatic activity within 1 h of incubation. These results indicated that the lack of *in vivo* effects of Chi18H8 in *B. mori* larvae was due to the loss of enzyme activity in the alkaline midgut juice environment, coupled with a probable proteolytic damage caused by the proteases present in the midgut lumen.

DISCUSSION

In the present work, we tested the insecticidal activity of two recently discovered soil metagenome-sourced chitinases on the larvae of *B. mori*, by using a combined *in vivo* and *in vitro* approach. *B. mori* is a model organism among Lepidoptera, which represent the second largest order of insects, including damaging phytophagous species that are still mainly controlled with chemicals. The two chitinases used in this study (Chi18H8 and 53D1) are diverse from all those described previously, possessing specific structural and functional features. Previous results both from sequence and substrate specificity analyses indicated that Chi18H8 belongs to family 18 of glycosyl hydrolases (GH18), showing less than 45% amino acid sequence identity to any known chitinase (Hjort et al., 2014). Additionally, Chi18H8 possesses an antifungal activity which is uncommon among GH18 chitinases (Hjort et al., 2014; Berini et al., 2017b). This protein seems enough stable to be used in semi-field or field applications, since its range of activity appears adequate for inhibiting fungal phytopathogens growing in acidic and mesophilic environments (Hjort et al., 2014; Berini et al., 2017b). Also 53D1 belongs to GH18 chitinases, showing less than 46% amino acid sequence identity to any known chitinase. It probably derives from an uncultivable bacterium related to the *Chloroflexus* species *Nitrolancetus hollandicus* and *Ktedonobacter racemifer* (Cretoiu et al., 2015). Although a more complete characterization of 53D1 was hampered by the poor production yield of its recombinant form in *E. coli* (see below), previous studies showed that this protein tolerates elevated levels of NaCl: since its activity increases at higher salt levels, 53D1 is considered an uncommon halophilic (rather than halotolerant) chitinase (Cretoiu et al., 2015).

Initially, the major bottleneck to testing insecticidal activity of the two metagenome-sourced chitinases was providing the milligrams needed to perform *in vitro* and *in vivo* assay in *B. mori*. Unfortunately, there is not a highly predictable, all-purpose, and rational protocol to succeed in metagenome-sourced protein expression. Each protein requires the development of its own tailored production process and the selection of the more adequate expression host (Davy et al., 2017). *E. coli* still remains the first-choice host for protein production, but intrinsic limits of this bacterium are its poor secretory machinery and its tendency

TABLE 3 | Effects of Chi18H8 on *B. mori* growth and development.

Doses of Chi18H8 (U_{tot}/cm^2 diet)	Larval mortality (%)	Duration of larval stage (days)	Pupal weight at day 8 (g)
0 (control)	0.00 ± 0.00	27.21 ± 0.27	1.32 ± 0.04
6	6.06 ± 3.03	27.58 ± 0.32	1.31 ± 0.05

Each value represents the mean ± standard error of three independent experiments. Each experimental group was composed of 11 larvae. Larvae mortality is reported as the percentage of the initial number of larvae.

TABLE 4 | Effects of 53D1 on *B. mori* growth and development.

Doses of 53D1 (U_{tot}/cm^2 diet)	Larval mortality (%)	Duration of larval stage (days)	Maximal larval weight before pupation (g)	Pupal weight at day 8 (g)	Cocoon weight at day 8 (g)
0 (control)	2.78 ± 2.78	24.83 ± 0.21	3.32 ± 0.09	1.06 ± 0.04	0.24 ± 0.01
6	61.11 ± 2.78*	31.69 ± 1.37*	2.14 ± 0.15*	0.80 ± 0.06*	0.13 ± 0.01*

*Each value represents the mean ± standard error of three independent experiments. Each experimental group was composed of 12 larvae. Larvae mortality is reported as the percentage of the initial number of larvae. *$p < 0.001$ versus control, Student's t-test.*

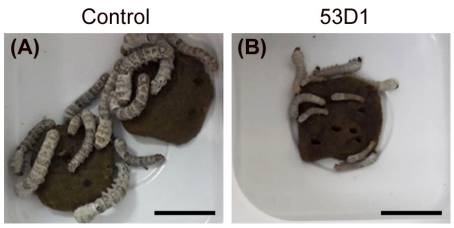

FIGURE 5 | Pictures of *B. mori* larvae, on the 11th day after hatching, reared on artificial diet overlaid with 100 mM sodium acetate, pH 5 (**A**, control) or 6 U_{tot}/cm^2 of 53D1 dissolved in the same buffer **(B)**. All the control larvae are alive and the majority of them have reached the third instar **(A)**; a few larvae treated with the chitinase are already dead, and the majority of the survived larvae are still in the second instar **(B)**. Bars: 1 cm.

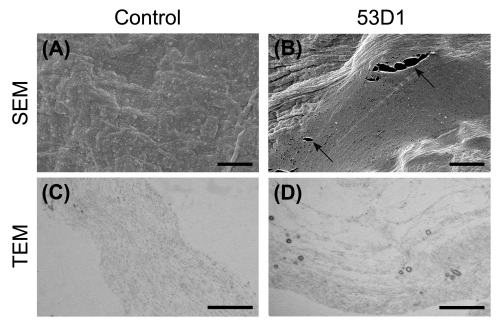

FIGURE 6 | Morphology of the peritrophic matrix isolated from larvae treated with 53D1. SEM **(A,B)** and TEM **(C,D)**. **(A,C)** Control samples; **(B,D)** the treatment with 53D1 determines ruptures of the PM (arrows) and the disruption of the fibril network as confirmed by TEM analysis. Bars: **(A,B)** 5 μm; **(C,D)** 0.5 μm.

to accumulate heterologous proteins into IBs, mostly in inactive form. In the case of Chi18H8, we could recover hundreds of milligrams of pure and active chitinase from processing IBs, following a previously developed and scaled-up process (Berini et al., 2017b), but this approach was not transferable to 53D1 production. In fact, it is widely recognized that the outcome of IB processing is unpredictable and has to be empirically determined for each protein (de Marco et al., 2019; Slouka et al., 2019). After some unsuccessful attempts, 53D1 was finally successfully expressed in *S. coelicolor* A3(2), although its codon usage was slightly different from the one of streptomycetes [63% G+C content for *53D1* gene vs. ca. 72% for *S. coelicolor* A3(2) genome] (Kieser et al., 2000). The production level in *S. coelicolor* A3(2) was satisfactory (around 45 mg/L) and the heterologous protein was entirely secreted into the culture broth, thus markedly facilitating its recovery and purification. A single step of affinity chromatography allowed us to recover ca. 35 mg/L of highly pure protein, with a 60-fold improvement in volumetric yield when compared to *E. coli*. Streptomycetes, although still relatively poorly explored for the expression of heterologous chitinases, have important advantages versus *E. coli*. They are non-pathogenic microorganisms, commonly inhabiting soil, where they establish beneficial interactions with plants, by modulating plant defense mechanisms or facilitating symbioses between plant roots and beneficial microbes (Schrey and Tarkka, 2008). Additionally, streptomycetes are already commonly used as components of commercial soil amendments for bioremediation (Sharma et al., 2016; Cuozzo et al., 2018) or biocontrol (González-García et al., 2019; Olanrewaju and Babalola, 2019) and they are generally considered safe for agricultural use. Using this environment-friendly expression system for producing chitinases might represent a further advantage to support their sustainable development as promising insecticide proteins.

Once the supply issue of both proteins was overcome, we decided to test the insecticidal activity of the two pure preparations of Chi18H8 or 53D1 using the PM of *B. mori* as *in vitro* and *in vivo* target. Insects offer two potential targets for chitinases: cuticle, which consists of a pluristratified structure mainly formed by proteins and chitin chains, and PM, where chitin fibrils act as a scaffold for binding glycoproteins and proteoglycans. Both structures exert fundamental roles for the insect survival. Cuticle protects insects from parasites, pathogens, and dangerous chemicals, while allowing muscle attachment and preventing water loss from the body (Moussian, 2010). PM helps in the compartmentalization of digestive processes, protecting the midgut epithelium against abrasive food particles and defending the insect from ingested pathogens (Hegedus et al., 2009). Previous works recently reviewed in Berini et al. (2018) reported that entomopathogenicity of microbial strains is mediated by a cocktail of cuticle-hydrolyzing enzymes, which include chitinases. Indeed, the topical insecticide potential of these enzyme combinations is often limited due to the long time required for their action, the need of high local concentrations, and their poor stability and persistence in changing environmental conditions. A more promising perspective seems to be using chitinases for targeting PM via oral ingestion (Berini et al., 2016, 2018). An advantage of this approach is that chitinases might be formulated with other insecticidal molecules,

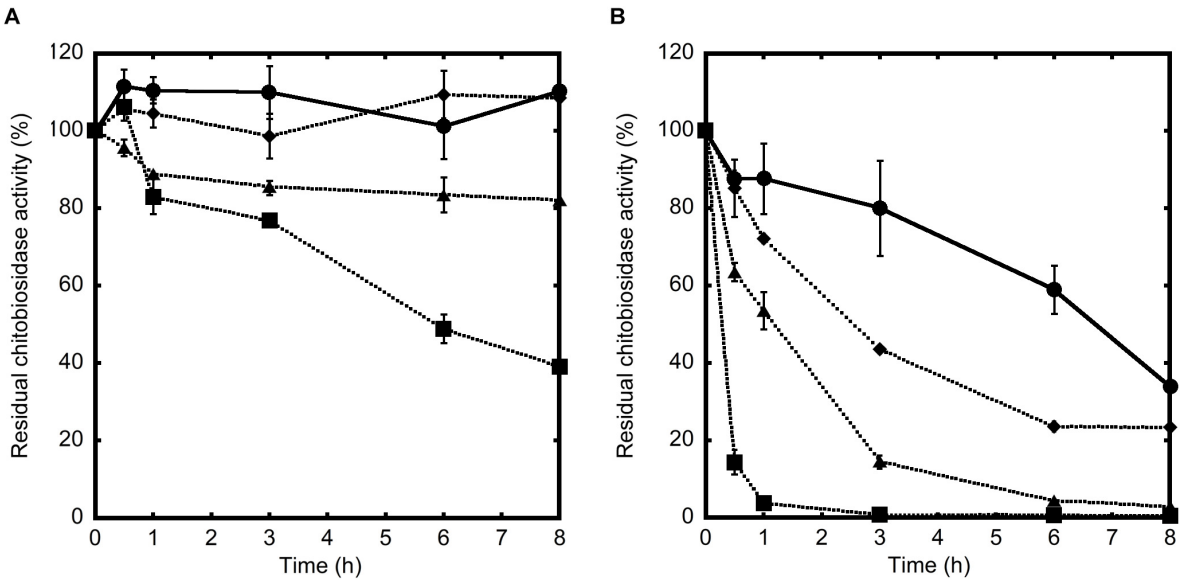

FIGURE 7 | Residual chitinolytic activities of 53D1 **(A)** and Chi18H8 **(B)**, incubated at 25°C in Tris–HCl pH 8.0 (control, ●, solid line) or in the presence of undiluted (■, dotted line), 10-fold diluted (▲, dotted line), or 100-fold diluted (◆, dotted line) midgut juice from *B. mori* larvae. Enzyme aliquots were collected at increasing time intervals and the residual activity was measured on 4-MU-$(GlcNAc)_2$ as substrate.

facilitating their adsorption/penetration into the midgut epithelium and thus increasing their activity. For instance, the combined oral administration of chitinases with *Bacillus thuringiensis* δ-endotoxin crystal proteins was reported to dramatically enhance the toxic effect of the latter (Regev et al., 1996; Liu et al., 2010). Additionally, the insecticide activity of TMOF, a peptide that inhibits trypsin synthesis, was increased by combined administration with a viral chitinase (Fiandra et al., 2010).

Our results demonstrated that when the PM of the silkworm was exposed *in vitro* to chitinases, the combination of endo- and exo-activities possessed by both enzymes significantly altered the structure of PM, disrupting the organization of chitin fibrils. Peeling of the superficial layers, ruptures, separation of the fibril networks, and a general weakening of the PM were observed. The effects of the two enzymes were similar, although 53D1 appeared to cause a more marked damage to PM structure. This result was consistent with the demonstrated 53D1 greater activity on colloidal chitin, which mimics the complex insoluble-chitin-containing natural structures. Once orally administered to *B. mori* larvae, 53D1 induced mortality, enhanced dramatically the duration of the larval stage, and reduced both the maximal larval weight before pupation and pupal and cocoon weight, whereas Chi18H8 did not provoke any consequences on insect development. Ultrastructural analysis of PMs isolated from larvae reared on 53D1-containing diet, showed significant alterations, confirming that the structural damage of this matrix dramatically affected insect development probably due to a reduced nutrient digestion capability. The different *in vivo* activity between Chi18H8 and 53D1, which might appear puzzling considering that both the enzymes disrupted (although at a different extent) the PM integrity *in vitro*, became understandable once the poor residual activity of Chi18H8 in the alkaline and proteolytic environment of Lepidoptera midgut lumen was demonstrated. Apparently, the intrinsic properties of 53D1 made this enzyme less susceptible to degradation in the above-mentioned conditions. Although the administration of both chitinases to other insects, especially to those having a midgut lumen with neutral or acidic pH, is worthy to be investigated, this work demonstrates that actually 53D1 can be considered a more promising candidate than Chi18H8 as insecticide protein for oral administration. Fortunately, 53D1 further *in vivo* and in-field trials will be possible due to the development of a reliable and sustainable production process using as expression platform the unconventional -but more environmentally acceptable-*S. coelicolor*.

In conclusion, this work shed light on (i) the efficacy of metagenomic investigations for discovering novel enzymes to be implemented as part of integrated pest management programs; (ii) the potential of metagenome-sourced microbial chitinases as promising insecticide proteins; and (iii) the need to develop unconventional heterologous expression platforms to support insecticide protein development and use. Although insecticide formulations based on chemically synthesized compounds still represent a relevant part of crop protection, it is undeniable that insecticide proteins will contribute in future to the progressive reduction of chemicals, introducing novel strategies for managing insect pests. Formulation of chitinases with other biopesticides or chemically synthesized pesticides might allow the reduction of the environmental impact of single toxic compounds and reduce the risk of resistance selection (Chandler et al., 2011; Hardy, 2014). Microbial biotechnology will be crucial to support the development and sustainable production of novel insecticide proteins.

DATA AVAILABILITY

All datasets generated for this study are included in the manuscript and/or the supplementary files.

AUTHOR CONTRIBUTIONS

FB, MC, GT, and FM conceived the experiments, interpreted the results, and wrote the manuscript. FB cloned the metagenome-sourced genes and produced the metagenome-sourced chitinases. AM and GT tested the insecticide proteins *in vitro*. MC tested the insecticide proteins *in vivo*. MR performed the microscopical observations. FM and GT managed the project. All authors reviewed and approved the final manuscript.

FUNDING

This research was supported by the MAECI (Ministero degli Affari Esteri e della Cooperazione Internazionale) for the CHITOBIOCONTROL project (Israel-Italy Joint Innovation Program for Industrial, Scientific and Technological Cooperation in R&D, Industrial Track, call 2016). FB received contributions from the Consorzio Italiano per le Biotecnologie (CIB) and Fermentation Journal (MDPI, Basel, Switzerland) for congress participations.

ACKNOWLEDGMENTS

The authors thank Silvia Cappellozza and Alessio Saviane (CREA-AA, Sericulture Laboratory of Padua, Padua, Italy) for providing *Bombyx mori* larvae. The authors also acknowledge Sara Sjöling (Södertörn University, Huddinge, Sweden), Jan Dirk Van Elsas (University of Groningen, Groningen, Netherlands), Ilaria Presti (Chemo Biosynthesis, Corana, Pavia, Italy), and Silvia Cretoiu (University of Groningen, Groningen, Netherlands) – previous partners in MetaExplore EU-funded project (grant agreement 222625) – for the discovery of the metagenome-sourced chitinases. Israeli CHITOBIOCONTROL partners Chen Katz and Uri Marchaim are also acknowledged for collaboration and useful discussions. AM is a Ph.D. student of the "Life Science and Biotechnology" course at the University of Insubria.

REFERENCES

Adrangi, S., and Faramarzi, M. A. (2013). From bacteria to human: a journey into the world of chitinases. *Biotechnol. Adv.* 31, 1786–1795. doi: 10.1016/j.biotechadv.2013.09.012

Atwood, D., and Paisley-Jones, C. (2017). *Pesticide Industry Sales and Usage. 2008-2012 Market Estimates*. Washington, DC: United States Environmental Protection Agency.

Berini, F., Caccia, S., Franzetti, E., Congiu, T., Marinelli, F., Casartelli, M., et al. (2016). Effects of *Trichoderma viride* chitinases on the peritrophic matrix of Lepidoptera. *Pest Manag. Sci.* 72, 980–989. doi: 10.1002/ps.4078

Berini, F., Katz, C., Gruzdev, N., Casartelli, M., Tettamanti, G., and Marinelli, F. (2018). Microbial and viral chitinases: attractive biopesticides for integrated pest management. *Biotechnol. Adv.* 36, 818–838. doi: 10.1016/j.biotechadv.2018.01.002

Berini, F., Casciello, C., Marcone, G. L., and Marinelli, F. (2017a). Metagenomics: novel enzymes from non-culturable microbes. *FEMS Microbiol. Lett.* 364:fnx211. doi: 10.1093/femsle/fnx211

Berini, F., Presti, I., Beltrametti, F., Pedroli, M., Vårum, K. M., Pollegioni, L., et al. (2017b). Production and characterization of a novel antifungal chitinase identified by functional screening of a suppressive-soil metagenome. *Microb. Cell Fact.* 16:16. doi: 10.1186/s12934-017-0634-8

Binda, E., Marcone, G. L., Berini, F., Pollegioni, L., and Marinelli, F. (2013). Streptomyces spp. as efficient expression system for a D,D-peptidase/D,D-carboxypeptidase involved in glycopeptide antibiotic resistance. *BMC Biotechnol.* 13:24. doi: 10.1186/1472-6750-13-24

Bokma, E., van Koningsveld, G. A., Jerominus-Stratingh, M., and Beintema, J. J. (1997). Hevamine, a chitinase from the rubber tree *Hevea brasiliensis*, cleaves peptidoglycan between the C-1 of N-acetylglucosamine and C-4 of N-acetylmuramic acid and therefore is not a lysozyme. *FEBS Lett.* 411, 161–163. doi: 10.1016/S0014-5793(97)00682-0

Bonanomi, G., Lorito, M., Vinale, F., and Woo, S. L. (2018). Organic amendments, beneficial microbes, and soil microbiota: toward a unified framework for disease suppression. *Annu. Rev. Phytopathol.* 56, 1–20. doi: 10.1146/annurev-phyto-080615-100046

Cappellozza, L., Cappellozza, S., Saviane, A., and Sbrenna, G. (2005). Artificial diet rearing system for the silkworm *Bombyx mori* (Lepidoptera: Bombycidae): effect of vitamin C deprivation on larval growth and cocoon production. *Appl. Entomol. Zool.* 40, 405–412. doi: 10.1303/aez.2005.405

Chandler, D., Bailey, A. S., Tatchell, G. M., Davidson, G., Greaves, J., and Grant, W. P. (2011). The development, regulation and use of biopesticides for integrated pest management. *Philos. Trans. R. Soc. Lond. Ser. B Biol. Sci.* 366, 1987–1998. doi: 10.1098/rstb.2010.0390

Cretoiu, M. S., Berini, F., Kielak, A. M., Marinelli, F., and van Elsas, J. D. (2015). A novel salt-tolerant chitobiosidase discovered by genetic screening of a metagenomic library derived from chitin-amended agricultural soil. *Appl. Microbiol. Biotechnol.* 99, 8199–8215. doi: 10.1007/s00253-015-6639-5

Cuozzo, S. A., Sineli, P. E., Davila Costa, J., and Tortella, G. (2018). Streptomyces sp. is a powerful biotechnological tool for the biodegradation of HCH isomers: biochemical and molecular basis. *Crit. Rev. Biotechnol.* 38, 719–728. doi: 10.1080/07388551.2017

Czaja, K., Góralczyk, K., Struciński, P., Hernik, A., Korcz, W., Minorczyk, M., et al. (2015). Biopesticides – towards increased consumer safety in the European Union. *Pest Manag. Sci.* 71, 3–6. doi: 10.1002/ps.3829

Dalmastri, C., Gastaldo, L., Marcone, G. L., Binda, E., Congiu, T., and Marinelli, F. (2016). Classification of *Nonomuraea* sp. ATCC 39727, an actinomycete that produces the glycopeptide antibiotic A40926, as *Nonomuraea gerenzanensis* sp. nov. *Int. J. Syst. Evol. Microbiol.* 66, 912–921. doi: 10.1099/ijsem.0.000810

Damalas, C. A., and Koutroubas, S. D. (2018). Current status and recent developments in biopesticide use. *Agriculture* 8:13. doi: 10.3390/agriculture8010013

Davy, A. M., Kildegaard, H. F., and Andersen, M. R. (2017). Cell factory engineering. *Cell Syst.* 4, 262–275. doi: 10.1016/j.cels.2017.02.010

de Marco, A., Ferrer-Miralles, N., Garcia-Fruitós, E., Mitraki, A., Peternel, S., Rinas, U., et al. (2019). Bacterial inclusion bodies are industrially exploitable amyloids. *FEMS Microbiol. Rev.* 43, 53–72. doi: 10.1093/femsre/fuy038

Fiandra, L., Terracciano, I., Fanti, P., Garonna, A., Ferracane, L., Fogliano, V., et al. (2010). A viral chitinase enhances oral activity of TMOF. *Insect Biochem. Mol. Biol.* 40, 533–540. doi: 10.1016/j.ibmb.2010.05.001

Franzetti, E., Huang, Z. J., Shi, Y. X., Xie, K., Deng, X. J., Li, J. P., et al. (2012). Autophagy precedes apoptosis during the remodeling of silkworm larval midgut. *Apoptosis* 17, 305–324. doi: 10.1007/s10495-011-0675-0

González-García, S., Alvarez-Pérez, J. M., Sáenz de Miera, L. E., Cobos, R., Ibañez, A., Díez-Galán, et al. (2019). Developing tools for evaluating inoculation methods of biocontrol *Streptomyces* sp. strains into grapevine plants. *PLoS One* 14:e0211225. doi: 10.1371/journal.pone.0211225

Hardy, M. C. (2014). Resistance is not futile: it shapes insecticide discovery. *Insects* 5, 227–242. doi: 10.3390/insects5010227

Hegedus, D., Erlandson, M., Gillott, C., and Toprak, U. (2009). New insights into peritrophic matrix synthesis, architecture and function. *Annu. Rev. Entomol.* 54, 285–302. doi: 10.1146/annurev.ento.54.110807.090559

Hjort, K., Presti, I., Elväng, A., Marinelli, F., and Sjöling, S. (2014). Bacterial chitinase with phytopathogen control capacity from suppressive soil revealed by functional metagenomics. *Appl. Microbiol. Biotechnol.* 98, 2819–2828. doi: 10.1007/s00253-013-5287-x

Hobbs, G., Frazer, C. M., Gardner, D. C. J., Cullum, J. A., and Oliver, S. G. (1989). Dispersed growth of *Streptomyces* in liquid culture. *Appl. Microbiol. Biotechnol.* 31, 272–277. doi: 10.1007/BF00258408

Karasuda, S., Tanaka, S., Kajihara, H., Yamamoto, Y., and Koga, D. (2003). Plant chitinase as a possible biocontrol agent for use instead of chemical fungicides. *Biosci. Biotechnol. Biochem.* 67, 221–224. doi: 10.1271/bbb.67.221

Kieser, T., Bibb, M. J., Buttner, M. J., Chater, K. F., and Hopwood, D. A. (2000). *Practical Streptomyces Genetics*. Norwich: John Innes Foundation.

Kumar, S., Nehra, M., Dilbaghi, N., Marrazza, G., Hassan, A. A., and Kim, K. H. (2019). Nano-based smart pesticide formulations: emerging opportunities for agriculture. *J. Control Release* 294, 131–153. doi: 10.1016/j.jconrel.2018.12.012

Liu, D., Cai, J., Xie, C. C., Lium, C., and Chen, Y. H. (2010). Purification and partial characterization of a 36-kDa chitinase from *Bacillus thuringiensis* subsp. colmeri and its biocontrol potential. *Enzym. Microb. Technol.* 46, 252–256. doi: 10.1016/j.enzmictec.2009.10.007

Marcone, G. L., Carrano, L., Marinelli, F., and Beltrametti, F. (2010a). Protoplast preparation and reversion to the normal filamentous growth in antibiotic-producing uncommon actinomycetes. *J. Antibiot.* 63, 83–88. doi: 10.1038/ja.2009.127

Marcone, G. L., Foulston, L., Binda, E., Marinelli, F., Bibb, M. J., and Beltrametti, F. (2010b). Methods for the genetic manipulation of *Nonomuraea* sp. ATCC 39727. *J. Ind. Microbiol. Biotechnol.* 37, 1097–1103. doi: 10.1007/s10295-010-0807-805

Mavromatis, K., Lorito, M., Woo, S. L., and Bouriotis, V. (2003). Mode of action and antifungal properties of two cold-adapted chitinases. *Extremophiles* 7, 385–390. doi: 10.1007/s00792-003-0338-3

Moussian, B. (2010). Recent advances in understanding mechanisms of insect cuticle differentiation. *Insect Biochem. Mol. Biol.* 40, 363–375. doi: 10.1016/j.ibmb.2010.03.003

Neeraja, C., Anil, K., Purushotham, P., Suma, K., Sarma, P., Moerschbacher, B. M., et al. (2010). Biotechnological approaches to develop bacterial chitinases as a bioshield against fungal diseases of plants. *Crit. Rev. Biotechnol.* 30, 231–241. doi: 10.3109/07388551.2010.487258

Olanrewaju, O. S., and Babalola, O. O. (2019). *Streptomyces*: implications and interactions in plant growth promotion. *Appl. Microbiol. Biotechnol.* 103, 1179–1188. doi: 10.1007/s00253-018-09577-y

Regev, A., Keller, M., Strizhov, N., Sneh, B., Prudovsky, E., Chet, I., et al. (1996). Synergistic activity of a *Bacillus thuringiensis* delta-endotoxin and a bacterial endochitinase against *Spodoptera littoralis* larvae. *Appl. Environ. Microbiol.* 62, 3581–3586.

Schrey, S. D., and Tarkka, M. T. (2008). Friend and foes: streptomycetes as modulators of plant disease and symbiosis. *Antonie Van Leeuwenhoek* 94, 11–19. doi: 10.1007/s10482-008-9241-3

Sharma, A., Singh, S. B., Sharma, R., Chadhary, P., Pandey, A. K., Ansari, R., et al. (2016). Enhanced biodegradation of PAHs by microbial consortium with different amendment and their fate in in-situ condition. *J. Environ. Manage.* 181, 728–736. doi: 10.1016/j.jenvman.2016.08.024

Slouka, C., Kopp, J., Spadiut, O., and Herwig, C. (2019). Perspectives of inclusion bodies for bio-based products: curse or blessing? *Appl. Microbiol. Biotechnol.* 103, 1143–1153. doi: 10.007/s00253-018-9569-1

Soares, F. E. D. F., Queiroz, J. H. D., Araújo, J. V. D., Queiroz, P. V., Gouveia, A. D. S., Hiura, E., et al. (2015). Nematicidal action of chitinases produced by the fungus *Monacrosporium thaumasium* under laboratorial conditions. *Biocontrol Sci. Techn.* 25, 1–17. doi: 10.1080/09583157.2014.979133

Terra, W. R., and Ferreira, C. (1994). Insect digestive enzymes: properties, compartmentalization and function. *Comp. Biochem. Physiol.* 109, 1–62. doi: 10.1016/0305-0491(94)90141-4

Wohlkönig, A., Huet, J., Looze, Y., and Wintjens, R. (2010). Structural relationship in the lysozyme superfamily: significant evidence for glycoside hydrolase signature motifs. *PLoS One* 5:e15388. doi: 10.1371/journal.pone.0015388

Conflict of Interest Statement: The authors declare that the research was conducted in the absence of any commercial or financial relationships that could be construed as a potential conflict of interest.

frontiers in Microbiology

ORIGINAL RESEARCH
published: 25 July 2019
doi: 10.3389/fmicb.2019.01695

Effects of Seasonal Variation on the Alkaloids of Different Ecotypes of *Epichloë* Endophyte-*Festuca sinensis* Associations

Weihu Lin[1], Yu Kuang[2], Jianjun Wang[1], Dongdong Duan[1], Wenbo Xu[1], Pei Tian[1], Clement Nzabanita[1], Meining Wang[1], Miaomiao Li[1] and Bihua Ma[1]*

[1]State Key Laboratory of Grassland Agro-ecosystems, Key Laboratory of Grassland Livestock Industry Innovation, Ministry of Agriculture and Rural Affairs, College of Pastoral Agriculture Science and Technology, Lanzhou University, Lanzhou, China, [2]Agricultural and Rural Bureau of Liling City, Liling, China

The *Epichloë* endophyte-*Festuca sinensis* association produces alkaloids which can protect the host plant from biotic and abiotic stresses. Alkaloid concentrations depend on the genetic predisposition of grass and endophyte, and are affected by the environment. Endophyte infected *F. sinensis* of six ecotypes were grown in experimental field and greenhouse for 2 years. Their aboveground plant tissues were collected each season to test for peramine, lolitrem B, and ergot concentrations. The results showed that seasonal changes affected the peramine, lolitrem B and ergot concentrations of *Epichloë* endophyte-*F. sinensis* associations; and these three different alkaloids responded differently to seasonal variation. The peramine concentration of six ecotypes of *F. sinensis* decreased significantly ($p < 0.05$) from spring to autumn. The lolitrem B concentration of *F. sinensis* was higher in autumn than in other seasons. Ergot concentrations of five ecotypes (41, 57, 84, 99, and 141) of *F. sinensis* peaked in the summer, and lowered in spring and autumn. In addition, the ecotype has insignificant effect ($p > 0.05$) on the peramine and lolitrem B concentrations of *F. sinensis*, but it has a significant impact ($p < 0.05$) on the ergot concentrations. We concluded that the seasonal variation and ecotypes can influence the alkaloids produced by the *F. sinensis*-endophyte associations, but the effects of seasonal conditions on the alkaloid concentrations are more pronounced than ecotypes.

Keywords: alkaloids, *Festuca sinensis*, *Epichloë* endophyte, ecotype, season

OPEN ACCESS

Edited by:
Giuliano Bonanomi,
University of Naples Federico II, Italy

Reviewed by:
Tapan Kumar Adhya,
KIIT University, India
Mohamed Idbella,
University of Naples Federico II, Italy

****Correspondence:***
Pei Tian
tianp@lzu.edu.cn

Specialty section:
This article was submitted to Microbial Symbioses, a section of the journal Frontiers in Microbiology

Received: *19 December 2018*
Accepted: *09 July 2019*
Published: *25 July 2019*

Citation:
Lin W, Kuang Y, Wang J, Duan D, Xu W, Tian P, Nzabanita C, Wang M, Li M and Ma B (2019) Effects of Seasonal Variation on the Alkaloids of Different Ecotypes of Epichloë Endophyte-Festuca sinensis Associations. Front. Microbiol. 10:1695. doi: 10.3389/fmicb.2019.01695

INTRODUCTION

In grassland ecosystems, most grasses are infected by endophytic fungi and produce alkaloids in their tissues (Nan, 1996a,b; Gao and Nan, 2007). Many grass species are symbiotic with systemic, vertically transmitted, asymptomatic *Epichloë* endophytic fungi. These fungi often generate alkaloids in order to defend the host against herbivores (Helander et al., 2016). Alkaloids increase the capacity of host plants to resist the biotic and abiotic stresses (Charles, 1993; Malinowski and Belesky, 2000). In the past few decades, scholars have explored the categories, mechanism of synthesis, and factors driving the synthesis of alkaloids. The alkaloids are the products of complex biochemical pathways which are becoming well understood (Schardl et al., 2012, 2013a). Until recently, four alkaloid categories have been identified, i.e., indole diterpenes, ergot alkaloids, peramine, and loline (Johnson et al., 2013).

Alkaloid concentrations depend on the genetic predisposition of grass and endophyte, and are influenced by the environmental conditions, e.g., seasonal variation, plant age, ecotypes, plant nutrition, temperature change, and drought occurrence (Helander et al., 2016; Fuchs et al., 2017).

Endophytes are microorganisms that reside within sturdy plant tissues intercellularly and/or intracellularly but usually remain asymptomatic and do not show any noticeable damage to the host (Siegel et al., 1987; Nazir and Rahman, 2018). They are an important component that colonizes in healthy tissues of living plants and can be readily isolated from any microbial or plant growth medium. Endophytic fungal associations with grasses are very common, and the most intensively studied are those between ascomycete fungi and temperate grasses, in particular those involving asexual endophytes of the genus *Epichloë* (Schardl et al., 2004; Li et al., 2017). Negative impact on herbivores is attributed to secondary metabolites alkaloids, which are produced by the endophytic fungus-grass symbiosis (Schardl et al., 2004). Animal toxicity due to the accumulation of nitrogenous compounds, e.g., endophyte-derived alkaloids, particularly in areas and periods under abiotic stress, still prevents widespread application of endophyte-infected grasses in agroecosystems (Hume et al., 2016). Over 30 years of study on the benefits of symbiotic *Epichloë* fungal endophytes for host grasses, investigations have focused on the major agricultural species, tall fescue and perennial ryegrass. However, many other grass species remain to be evaluated for the effects of *Epichloë* endophytes.

Festuca sinensis is a key native cool-season perennial grass species that is widely distributed across the cold and semi-arid regions. It plays an important role in the meadow ecosystem of the Qinghai-Tibetan Plateau in China (Lin et al., 2018). This grass species often hosts the systemic endophytic fungus, *Epichloë* endophyte (Zhou et al., 2015b; Song et al., 2016). Recent studies have detected three different alkaloids (i.e., peramine, lolitrem B, and ergot) in *F. sinensis* due to the infection of *Epichloë* endophyte tissue (Zhou et al., 2015a; Tian et al., 2018). An earlier study found that the presence of *Epichloë* endophyte could promote the growth of *F. sinensis* (Nan and Li, 2004). Some recent studies reported that *Epichloë* endophyte could also enhance host plant resistance to drought and waterlogged conditions (Wang et al., 2017) and promote its seeds' germination and growth (Peng et al., 2013). On top of the direct defense (in the form of alkaloids), the *Epichloë* endophyte enhances the host plant defense through improving the plant odor, which in turn attracts more olfactory foraging aphid predators (Fuchs and Krauss, 2018). Cold shock also induces ergot alkaloid changes in *F. sinensis* symbionts, and the degree of these changes differs between ecotypes and temperatures (Zhou et al., 2015a). Previous studies found that ecotypes can affect the concentrations of alkaloids in *Lolium perenne* and *Festuca pratensis* (Cagas et al., 1999). In addition, higher alkaloid levels were detected in *Achnatherum inebrians* plants under salt or drought stress and the concentrations of alkaloids increased over the plant growing period (Zhang et al., 2011). Interestingly, despite the infection of *Epichloë* endophyte on *F. sinensis*, there were no reports of intoxicated grazing animals on consuming *F. sinensis*-endophyte associations. This might indicate the existence of "mammalian-safe" nontoxic endophytes. Nonetheless, it remains unclear whether seasonal variation and ecotypes affect the alkaloid concentration of *Epichloë* endophyte-*F. sinensis* associations.

By performing a series of experiments under field and greenhouse conditions, we determine the alkaloid concentration of six ecotypes of *Epichloë* endophyte-*F. sinensis* associations under different seasonal conditions. We also explore the effects of seasonal variation, ecotypes, and their interactions on the alkaloids (peramine, lolitrem B, and ergot) produced by the *Epichloë* endophyte-*F. sinensis* associations.

MATERIALS AND METHODS

Plant Materials and Growing Conditions

The seeds of six *F. sinensis* ecotypes were obtained from the Institute of Grassland, Qinghai Academy of Animal Husbandry and Veterinary Sciences and the Sichuan Academy of Grassland Science. These seeds of six locations were collected in summer 2013 (**Table 1**), regarded as six ecotypes, and 100 g seed of per ecotype was dispatched to Lanzhou University in February 2014. The storage temperature was maintained at 4°C to retain seed viability (Tian et al., 2018).

Here, the first set (consisted of six different plant shoots) of ecotypes of *F. sinensis* were obtained from the field of the College of Pastoral Agriculture Science and Technology, Yuzhong campus of Lanzhou University (latitude: 35°89′ N, longitude: 104°39′ E; altitude: 1,653 m). These plants were grown for about 2 years (from June 2014 to December 2016). The second set (also consisted of six different plant shoots) were acquired from the greenhouse of Lanzhou University, and were grown for about 2 years (from April 2014 to December 2016). Note that the seed sources of these growing conditions (field and greenhouse) are identical.

TABLE 1 | Collection location of six *Epichloë* endophyte-*F. sinensis* association ecotypes.

Location	Ecotype	Latitude	Longitude	Altitude (m)
Bazanggou, Pingan, Qinghai, China	41	36°20′ N	102°06′ E	3,129 m
Bazanggou, Pingan, Qinghai, China	57	36°20′ N	102°06′ E	2,994 m
Shagou, Pingan, Qinghai, China	84	36°17′ N	102°05′ E	3,032 m
Guchengzhen, Pingan, Qinghai, China	99	36°17′ N	101°58′ E	3,060 m
Hongyuan, Sichuan, China	111	32°48′ N	102°33′ E	3,491 m
Shihuiyao, Pingan, Qinghai, China	141	36°19′ N	101°51′ E	2,922 m

Experimental Design

The seeds of six *F. sinensis* ecotypes were planted in the two sets, to explore the effects of seasonal variation on the alkaloids of different ecotypes of *Epichloë* endophyte-*F. sinensis* associations in the same growing location (Lanzhou University).

In June 2014, the six different ecotypes of *F. sinensis* were planted under field conditions. There were five field pots for each ecotype. Each experimental field pot was 4 m long and 3.2 m wide, and the seedlings were planted at 40-cm intervals. Each pot contained five plants of each ecotype, which were randomly arranged. The E+ and E− plants of these six ecotypes of *Festuca sinensis* were set up in May 2014 after aniline blue microscopic examination (Li et al., 2004) in greenhouse and transplanted in field block with random design (Kuang, 2016; Tian et al., 2018).

In March 2014, healthy and well-filled seeds were planted into a 72-hole plastic seedling tray containing sterilized vermiculite under greenhouse conditions. One month after sowing, the presence of endophyte in the seedlings was determined by performing the microscopic examination of host leaf-sheath samples after staining with aniline blue. The selected plants E+ (infected by endophyte) were transported to the pots and were randomly placed in the greenhouse. They were maintained at a constant temperature (temperature: 24°C, moisture: 50%) and a 12:12-h light-dark cycle. Each ecotype of *F. sinensis* was transplanted into pot and the process was repeated 40 times.

Plant samples were obtained in March (spring), June (summer), September (autumn), and November (winter), respectively, in 2016. The sampling conducted four times a year, collected a total of 1 year. The plant shoots of six *F. sinensis* ecotypes were harvested by cutting them at 2 cm above the soil surface. For each ecotype under field conditions, we randomly sampled five E+ plants from five field pots. All plant samples were freeze-dried (PowerDry LL 3000; Thermo Fisher Scientific, Waltham, MA, USA). Subsequently, the plant samples were ground into powder in a mixer mill (MM 400; Retsch, Haan, Germany) for 2 min at 30 Hz for analyzing the endophyte-derived alkaloid content.

Determination of Alkaloids

The ground shoot powder was weighed for measuring the concentrations of peramine, lolitrem B, and ergot *via* high-performance liquid chromatography (HPLC) (Gallagher et al., 1985; Barker et al., 1993; Ball et al., 1995; Tian et al., 2013, 2018). The "ergot" is total ergot alkaloid. Five biological replicates per ecotype and three technical replicates per biological replicate were tested (Tian et al., 2018).

Peramine Analysis

The 100-mg freeze-dried shoot powder was extracted in a solution of 3 ml of methanol and 3 ml of trichloromethane for 30 min under ultrasonic cleaner. The mixture material was centrifuged for 10 min at 1000 rpm, where 3 ml of *n*-hexane and 3 ml of ultra-pure water were added respectively, then extracted for 30 min and centrifuged for 12 min at 1000 rpm. Peramine was removed from shoot powder extracts by passing 1-ml portions through preconditioned 1-ml Agilent Bond Elut carboxylic acid (CBA) columns packed with 100 mg of adsorbent. The peramine was then eluted with 1 ml of a 5% formic acid-40% methanol solution. Peramine was measured by HPLC with an Agilent (Agilent 1100, America) liquid chromatograph fitted with a C18 column (Eclipse XDB-C18, 250 mm × 4.6 mm, 5 μm). Detection was performed with an ultraviolet (UV) wavelength spectrophotometric detector set at 280 nm. Mobile phase "A" was 1.8 g L^{-1} guanidine carbonate, and phase "B" was acetonitrile. The quantity of peramine in 25-μl injection samples was determined, based on pre-established standard curve peak area values. All reagents were chromatographically pure.

Lolitrem B Analysis

The 200-mg freeze-dried shoot powder was extracted in a solution of 4 ml of dichloromethane for 5 min under ultrasonic cleaner. The mixture material was centrifuged for 10 min at 1000 rpm. Lolitrem B was removed from shoot powder extracts by passing 2.5-ml portions through preconditioned Sep-Pak (Agilent Bont Elut SI, 500 mg, 3 ml) columns. The lolitrem B was then eluted with 0.7 ml of a 20% methanol-80% dichloromethane solution. Lolitrem B was measured by HPLC with an Agilent (Agilent 1100, America) liquid chromatograph fitted with a Zorbax-RX column (Zorbax RX-SIL, 250 mm × 4.6 mm, 5 μm). Detection was performed with a fluorescence detector, the excitation wavelength was set at 268 nm and the emission wavelength was 440 nm. Mobile phase "A" was acetonitrile, and phase "B" was dichloromethane. The quantity of lolitrem B in 20-μl injection samples was determined, based on pre-established standard curve peak area values. All reagents were chromatographically pure.

Ergot Analysis

The 200-mg freeze-dried shoot powder was extracted in a solution of 4-ml 20% glacial acetic acid for 5 min under ultrasonic cleaner. The mixture material was centrifuged for 5 min at 1700 rpm. Ergot was removed from shoot powder extracts by passing 2-ml portions through preconditioned PCX (Agilent Bond Elute, 60 mg, 3 ml) columns. The ergot was then eluted with l ml of a 95% methanol-5% ammonium hydroxide solution. Ergot was measured by HPLC with an Agilent (Agilent 1100, America) liquid chromatograph fitted with a C18 column (Eclipse XDB-C18, 250 mm × 4.6 mm, 5 μm). Detection was performed with a fluorescence detector, the excitation wavelength was set at 312 nm, and the emission wavelength was 427 nm. Mobile phase "A" was 7.708 g L^{-1} ammonium acetate, and phase "B" was acetonitrile. The quantity of lolitrem B in 20-μl injection samples was determined, based on pre-established standard curve peak area values. All reagents were chromatographically pure.

Data Analysis

Statistical data analysis was performed with the SPSS Inc. (Released 2009. PASW Statistics for Windows, Version 18.0. Chicago: SPSS Inc). The effects of seasonal variation and ecotypes on the peramine, lolitrem B, and ergot concentrations were evaluated using one-way and two-way ANOVA, respectively. A repeated-measure ANOVA with Fisher's least significant difference (LSD) test was applied to determine whether the differences between the means were statistically significant or not. Statistical significance was defined at the 95% confidence level. The means were expressed together with their standard errors.

RESULTS

Peramine

The two-way ANOVA revealed that seasonal variation significantly affected the peramine concentration of *F. sinensis* ($p < 0.05$), but the role of ecotype appeared statistically insignificant (**Tables 2, 3**). However, the interactions between ecotypes and seasonal variation had a significant impact on the peramine concentration of *F. sinensis* ($p < 0.05$; **Table 3**). The peramine concentrations of six ecotypes of *F. sinensis* decreased significantly ($p < 0.05$) from spring to autumn (**Figures 1, 2**), but they increased in winter only under field conditions (**Figure 1**). The peramine concentrations of six ecotypes of *F. sinensis* bottomed in autumn, and the differences between the ecotypes were insignificant (**Figures 1, 2**). The peramine concentrations of ecotype 41 and 141 reached the peak and trough during the trial period, respectively (**Figures 1, 2**).

Lolitrem B

The results showed that seasonal variation significantly affected the lolitrem B concentration of *F. sinensis* ($p < 0.05$). Although the ecotype did not significantly affect it, the interactions between ecotype and seasonal variation were obvious ($p < 0.05$) on the lolitrem B concentration of *F. sinensis* (**Tables 2, 3**). Under field conditions, the lolitrem B concentration of ecotype 41 of *F. sinensis* was significantly higher in spring-winter ($p < 0.05$) than in summer-autumn (**Figure 3**). Under greenhouse conditions, the lolitrem B concentration of ecotype 41 of *F. sinensis* was significantly higher in autumn-winter than in spring-summer (**Figure 4**). While the lolitrem B concentration of ecotype 57 of *F. sinensis* was significantly higher in autumn ($p < 0.05$) than other seasons under field conditions (**Figure 3**), its concentration hit the lowest in spring with little difference among other seasons under greenhouse conditions (**Figure 4**). The lolitrem B concentrations of ecotype 84, 99, 111, and 141 of *F. sinensis* were significantly higher in autumn ($p < 0.05$) than in spring under both field and greenhouse conditions (**Figures 3, 4**). Overall, the lolitrem B concentration of *F. sinensis* was higher in autumn than in other seasons.

Ergot

The interactions between seasonal variation and ecotypes significantly influenced the ergot concentrations of six *F. sinensis* ecotypes ($p < 0.05$); and the seasonal variation significantly ($p < 0.05$) affected the ergot concentration of six ecotypes of *F. sinensis* (**Tables 2, 3**). Ecotype had a significant ($p < 0.05$) impact on the ergot concentration only under greenhouse conditions (**Table 3**). For five ecotypes (41, 57, 84, 99, and 141) of *F. sinensis*, the ergot concentrations peaked in the summer, but lowered in spring and autumn (**Figures 5, 6**). The ergot concentrations of ecotype 99 and 111 were significantly higher in summer ($p < 0.05$) relative to other four ecotypes (**Figure 5**). Note that ecotype has no significant effect on the ergot concentration (**Figure 6**).

DISCUSSION

We demonstrated that the concentrations of alkaloids produced by the *Epichloë* endophyte-*F. sinensis* associations changed with seasonal variation. There were differences in the trends of the three alkaloids (peramine, lolitrem B, and ergot). We revealed that ecotypes significantly affect some alkaloids under the same seasonal conditions. The concentrations of similar alkaloids were quite different under field and greenhouse conditions.

Many previous studies have shown that grasses without endophyte did not produce alkaloids. It is concluded that the alkaloids tested in our manuscript were only produced by endophyte rather than host plants (Young et al., 2009; Schardl et al., 2013a,b). This study did not detect the three alkoids in the E-*F. siensis* plants through HPLC. Seasonal variation can influence the peramine concentrations produced by the endophyte of *F. sinensis*. A previous study on grazing grassland showed that the peramine concentrations of *L. perenne* displayed a seasonal rhythm with peak concentrations in summer and minimal

TABLE 2 | Results of two-way ANOVA for the effects of season and ecotype on peramine, lolitrem B, and ergot concentration of *Epichloë* endophyte-*F. sinensis* under field conditions.

Treatment (field)	df	Peramine		Lolitrem B		Ergot	
		F	*p*	*F*	*p*	*F*	*p*
Ecotype	5	0.8810	0.4540	0.4470	0.7200	0.2830	0.8380
Season	3	3.8900	0.0030	3.7900	0.0040	6.9410	<0.001
Ecotype × Season	15	1.6990	0.0640	1.8620	0.0370	4.2810	<0.001

TABLE 3 | Results of two-way ANOVA for the effects of season and ecotype on peramine, lolitrem B, and ergot concentration of *Epichloë* endophyte-*F. sinensis* under greenhouse conditions.

Treatment (greenhouse)	df	Peramine		Lolitrem B		Ergot	
		F	*p*	*F*	*p*	*F*	*p*
Ecotype	5	1.8785	0.1157	0.9566	0.4537	5.0900	0.0010
Season	3	384.1653	<0.001	19.4855	<0.001	22.4080	<0.001
Ecotype × Season	15	2.1973	0.0200	2.9501	0.0023	2.9070	0.0030

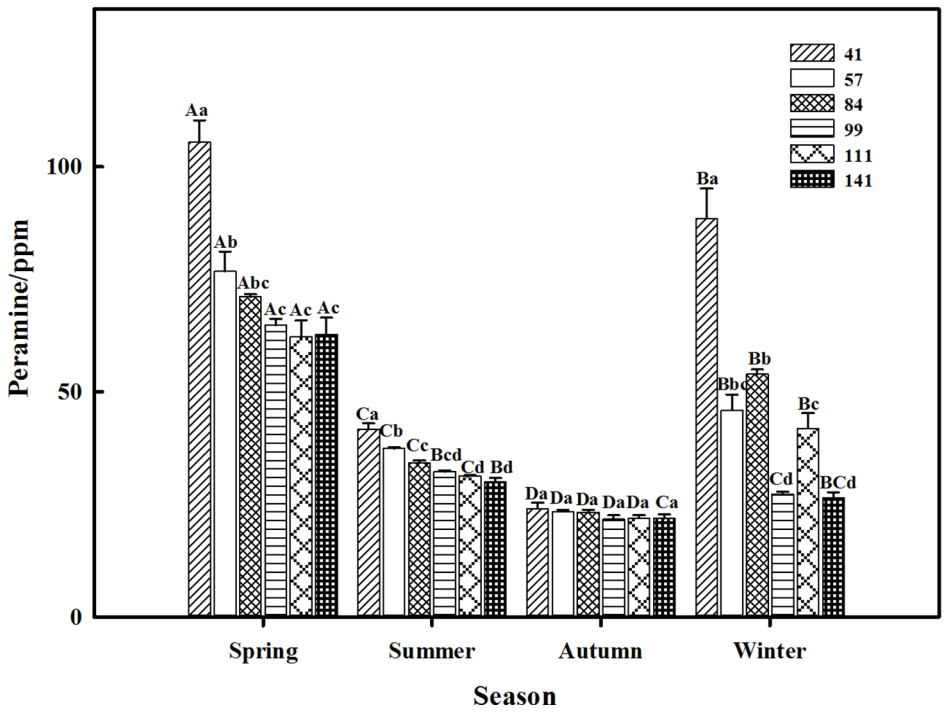

FIGURE 1 | Effects of season and ecotype on the peramine concentration of *Epichloë* endophyte-*F. sinensis* under field conditions. Values are the mean ± standard error (SE). Different uppercase letters indicate significant differences among the same ecotype under different seasonal conditions at $p < 0.05$, different lowercase letters indicate significant differences among the different ecotypes under the same seasonal conditions at $p < 0.05$.

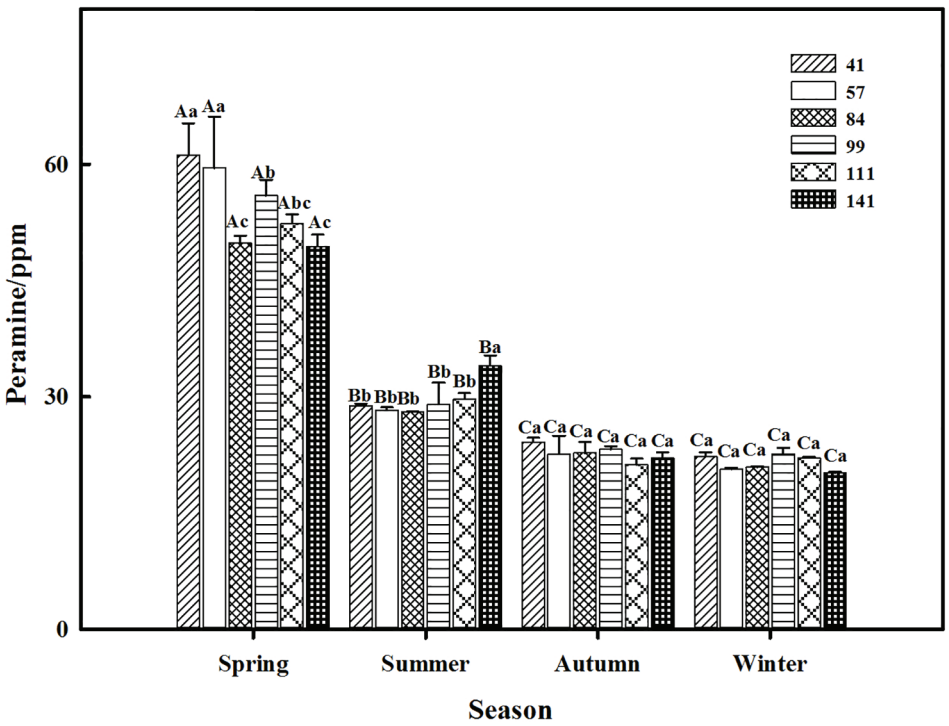

FIGURE 2 | Effects of season and ecotype on the peramine concentration of *Epichloë* endophyte-*F. sinensis* under greenhouse conditions. Values are the mean ± standard error (SE). Different uppercase letters indicate significant differences among the same ecotype under different seasonal conditions at $p < 0.05$, different lowercase letters indicate significant differences among the different ecotypes under the same seasonal conditions at $p < 0.05$.

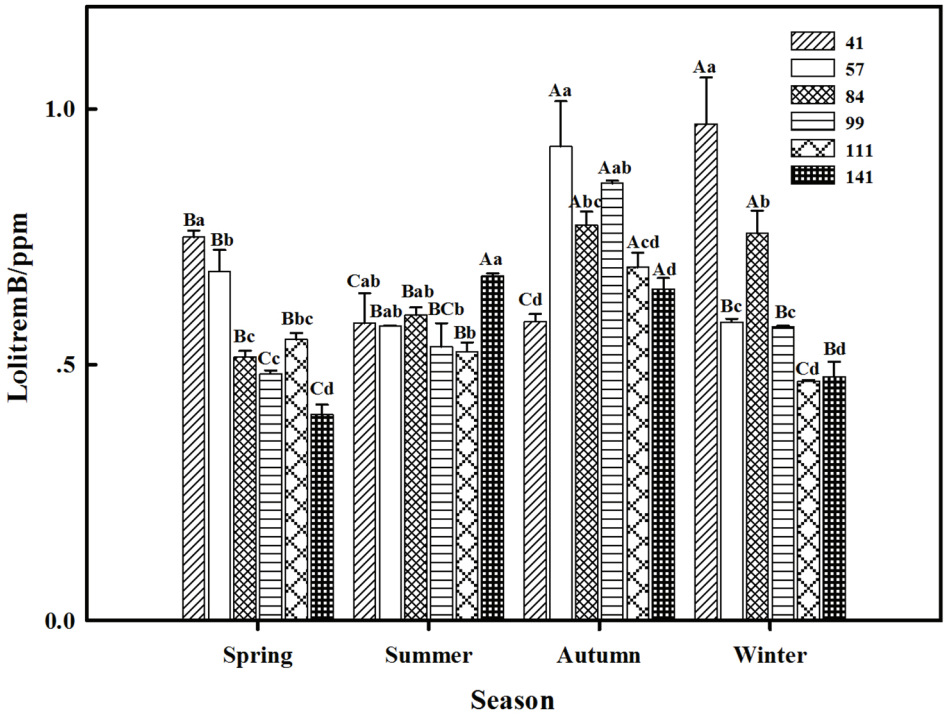

FIGURE 3 | Effects of season and ecotype on the lolitrem B concentration of *Epichloë* endophyte-*F. sinensis* under field conditions. Values are the mean ± standard error (SE). Different uppercase letters indicate significant differences among the same ecotype under different seasonal conditions at $p < 0.05$, and different lowercase letters indicate significant differences among the different ecotypes under the same seasonal conditions at $p < 0.05$.

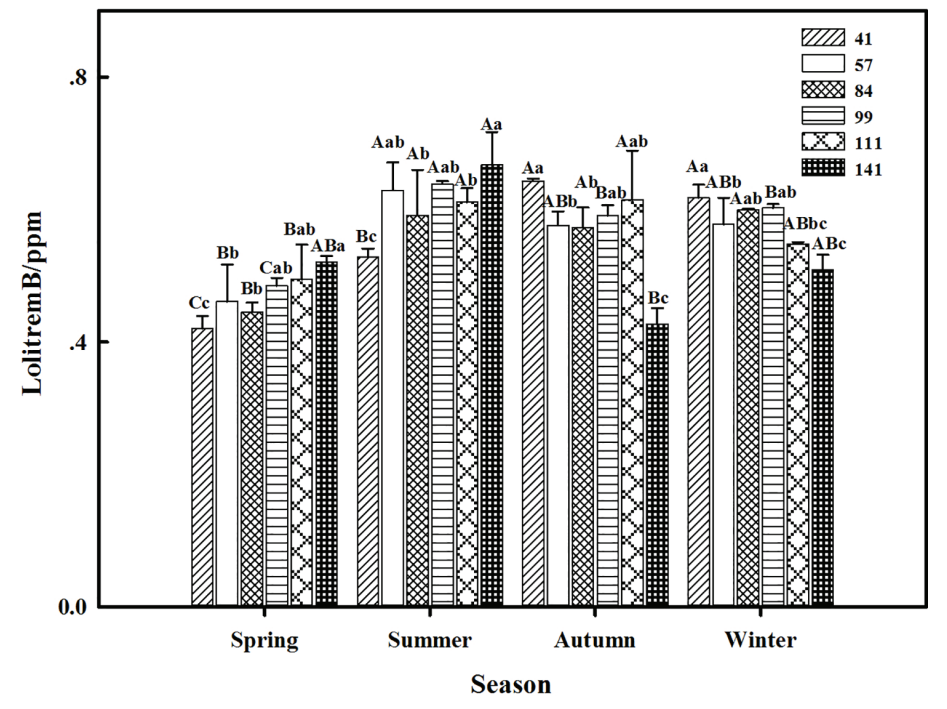

FIGURE 4 | Effects of season and ecotype on the lolitrem B concentration of *Epichloë* endophyte-*F. sinensis* under greenhouse conditions. Values are the mean ± standard error (SE). Different uppercase letters indicate significant differences among the same ecotype under different seasonal conditions at $p < 0.05$, and different lowercase letters indicate significant differences among the different ecotypes under the same seasonal conditions at $p < 0.05$.

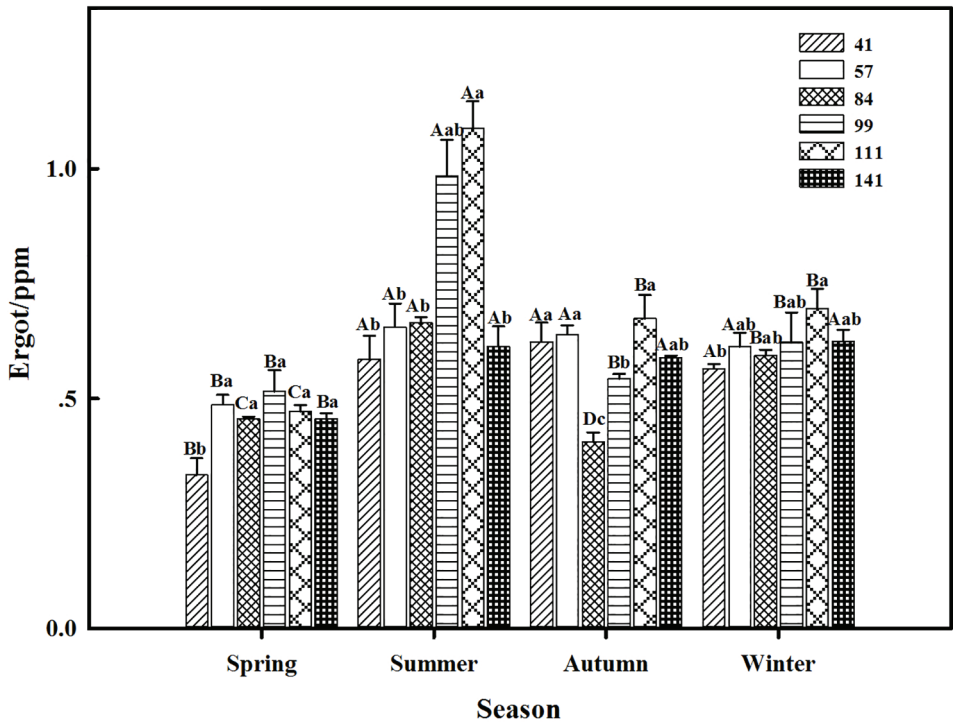

FIGURE 5 | Effects of season and ecotype on the ergot concentration of *Epichloë* endophyte-*F. sinensis* under field conditions. Values are the mean ± standard error (SE). Different uppercase letters indicate significant differences among the same ecotype under different seasonal conditions at $p < 0.05$, and different lowercase letters indicate significant differences among the different ecotypes under the same seasonal conditions at $p < 0.05$.

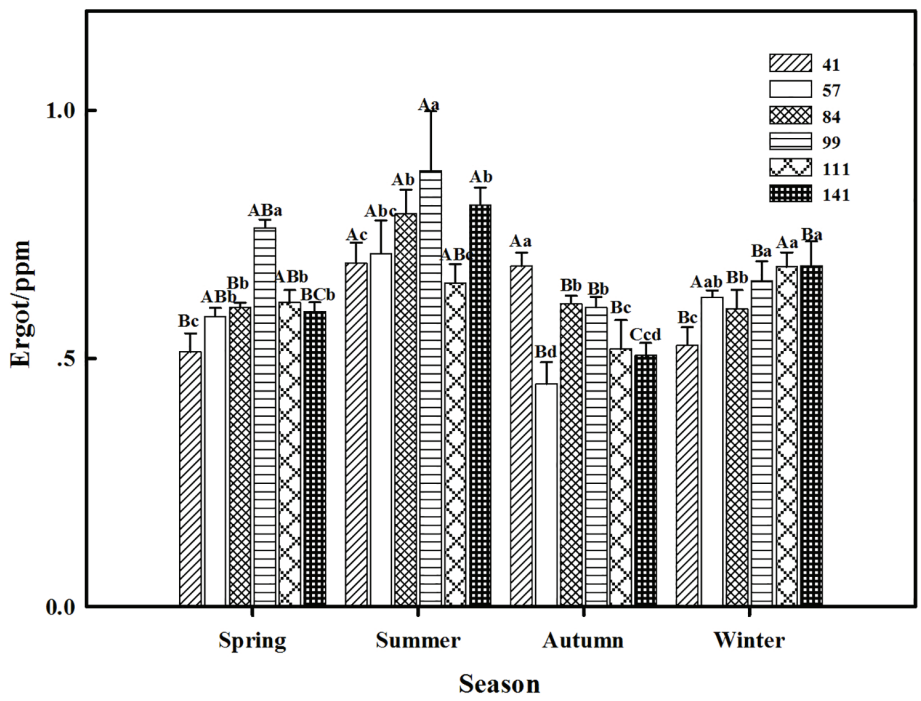

FIGURE 6 | Effects of season and ecotype on the ergot concentration of *Epichloë* endophyte-*F. sinensis* under greenhouse conditions. Values are the mean ± standard error (SE). Different uppercase letters indicate significant differences among the same ecotype under different seasonal conditions at $p < 0.05$, and different lowercase letters indicate significant differences among the different ecotypes under the same seasonal conditions at $p < 0.05$.

concentrations in winter (Fuchs et al., 2017). However, our study indicated that the peramine concentrations of six ecotypes of *F. sinensis* decreased from spring to autumn. The *F. sinensis* prefers cooler growth conditions, with a tendency to grow rapidly in spring and autumn but achieves slower growth in summer and winter. The *Epichloë* endophytes rely on their host plants to acquire the desired growth nutrients (Nan and Li, 2004). The growth of *Epichloë* endophyte slows down as the host plants grow slowly. This explains why the concentration of peramine produced by endophyte reduced in summer. In addition, the peramine concentration produced by the host plant is affected by the genotype (Faeth et al., 2002). Peramine is a natural insecticide. High levels of peramine (ranges 54–80 ppm) produced by the *F. sinensis*-endophyte associations would have strong resistance to insect feeding (Tian et al., 2018). The present study showed that the peramine concentrations of six ecotypes of *F. sinensis* bottomed in autumn. This implied that the insect resistance of *F. sinensis*-endophyte associations weakened in autumn. In addition, our results revealed that the ecotype had no significant effect on the peramine concentration produced by *F. sinensis*-endophyte associations under field and greenhouse conditions. We speculated that there were effects of the seasonal conditions instead of ecotypes on the peramine concentration.

Early studies found that ryegrass staggers was caused largely by the presence of lolitrem B (Gallagher et al., 1981; Ball et al., 1995). Endophytic fungal has long been assumed to grow only at the hyphal tip. However, Christensen et al. (2008) showed an intercalary division and extension of fungal tissue, which is connected to enlarging host plant cells, enables the fungal extension at the same rate as the host growth. This study showed that the lolitrem B concentration of *F. sinensis* was higher in autumn than in other seasons corresponding to the plant phenotype, indicating that endophyte grows concurrently with the grass through intercalary division, as postulated by Christensen et al. (2008). Low alkaloid concentrations in young plants indicate alkaloid biosynthesis to be costly (Fuchs et al., 2017). Spring and summer are the growth periods for the *F. sinensis* seedlings. In younger plants, nutrient resources are mainly used for primary metabolism such as plant and endophyte growth, rather than secondary metabolite synthesis (Faeth and Fagan, 2002). The present study also found that the endophytic fungi of the *F. sinensis* produced peramine instead of lolitrem B. This could be caused by chemical complexity and biosynthetic cost difference, which is similar to the plant secondary metabolite synthesis (Nishida, 2002). In addition, temperature rise might increase the alkaloid concentrations (Hennessy et al., 2016).

The present study showed that the interactions between seasonal variation and ecotypes significantly affected the ergot concentrations of six *F. sinensis* ecotypes; and the seasonal variation significantly impacted the ergot concentration of six ecotypes of *F. sinensis*. For five ecotypes (41, 57, 84, 99, and 141) of *F. sinensis*, the ergot concentrations peaked in summer, and declined in spring and autumn. Previous studies suggested that phosphorus had an effect on the ergot alkaloid concentration of *Neotyphodium coenophialum*-infected *Festuca arundinacea* (Malinowski et al., 1998). Our research supported that seasonal change affected the alkaloid concentrations produced by the endophytes of *L. perenne*; the alkaloid concentrations showed a seasonal rhythm with peak concentrations in summer and minimal concentrations in winter across all 3 years (2013–2015) (Fuchs et al., 2017). The short-term cold stress could also affect the ergot alkaloids of *F. sinensis* (Zhou et al., 2015a). Moreover, there were host genotype or endophyte genotype effects on the quantitative differences in the alkaloid concentration of *F. sinensis*. This has been reported by previous studies on different species (Easton et al., 2002; Tian et al., 2013).

CONCLUSION

In conclusion, both seasonal variation and ecotypes can affect the alkaloids produced by the *F. sinensis*-endophyte associations (especially true for seasonal variation). Different categories of alkaloids vary differently over a seasonal cycle. In autumn, the peramine concentration of *F. sinensis*-endophyte associations was at the lowest level, but the lolitrem B hit the highest level. The ergot concentration was at the lowest level in summer. Hence, the presence of endophyte is beneficial to *F. sinensis* in natural grasslands.

AUTHOR CONTRIBUTIONS

PT, WL, and YK designed experiments. WL, DD, and JW carried out the experiments. CN, MW, ML, and BM analyzed experimental results. WL and WX wrote the manuscript.

FUNDING

This research was supported by the National Nature Science Foundation of China (31502001), the National Basic Research Program of China (2014CB138702), China Agriculture Research System (CARS-22 Green Manue), and the 111 project (B12002).

REFERENCES

Ball, O. J. P., Prestidge, R. A., and Sprosen, J. M. (1995). Interrelationships between acremonium lolii, peramine, and lolitrem B in perennial ryegrass. *Appl. Environ. Microbiol.* 61, 1527–1533.

Barker, D., Davies, E., Lane, G., Latch, G., Heather, M., and Tapper, B. (1993). "Effect of water deficit on alkaloid concentrations in perennial ryegrass endophyte associations" in *Proceedings of the second international symposium on Acremonium/grass interactions*. eds. D. E. Hume, G. C. M. Latch, and H. S. Easton (New Zealand: At Palmerston North), 67–71.

Cagas, B., Flieger, M., and Olsovska, J. (1999). Concentration of ergot alkaloids in czech ecotypes of *Lolium perenne* and *Festuca pratensis*. *Grass Forage Sci.* 54, 365–370. doi: 10.1046/j.1365-2494.1999.00183.x

Charles, W. B. (1993). Abiotic stress tolerances (moisture, nutrients) and photosynthesis in endophyte-infected tall fescue. *Agric. Ecosyst. Environ.* 44, 123–141. doi: 10.1016/0167-8809(93)90042-N

Christensen, M. J., Bennett, R. J., Ansari, H. A., Koga, H., Johnson, R. D., Bryan, G. T., et al. (2008). *Epichloë* endophytes grow by intercalary hyphal extension in elongating grass leaves. *Fungal Genet. Biol.* 45, 84–93. doi: 10.1016/j.fgb.2007.07.013

Easton, H. S., Latch, G. C. M., Tapper, B. A., and Ball, O. J. P. (2002). Ryegrass host genetic control of concentrations of endophyte-derived alkaloids. *Crop Sci.* 42, 51–57. doi: 10.2135/cropsci2002.5100

Faeth, S. H., Bush, L. P., and Sullivan, T. J. (2002). Peramine alkaloid variation in *Neotyphodium*-infected *Arizona fescue*: effects of endophyte and host genotype and environment. *J. Chem. Ecol.* 28, 1511–1526. doi: 10.1023/A:1019916227153

Faeth, S. H., and Fagan, W. F. (2002). Fungal endophytes: common host plant symbionts but uncommon mutualists. *Integr. Comp. Biol.* 42, 360–368. doi: 10.1093/icb/42.2.360

Fuchs, B., and Krauss, J. (2018). Can *Epichloë* endophytes enhance direct and indirect plant defence? *Fungal Ecol.* 38, 98–103. doi: 10.1016/j.funeco.2018.07.002

Fuchs, B., Krischke, M., Mueller, M. J., and Krauss, J. (2017). Plant age and seasonal timing determine endophyte growth and alkaloid biosynthesis. *Fungal Ecol.* 29, 52–58. doi: 10.1016/j.funeco.2017.06.003

Gallagher, R. T., Hawkes, A. D., and Stewart, J. (1985). Rapid determination of the neurotoxin lolitrem B in perennial ryegrass by high-performance liquid chromatography with fluorescence detection. *J. Chromatogr. A* 321, 217–226. doi: 10.1016/S0021-9673(01)90438-8

Gallagher, R. T., White, E. P., and Mortimer, P. H. (1981). Ryegrass staggers: isolation of potent neurotoxins lolitrem A and lolitrem B from staggers-producing pastures. *N. Z. Vet. J.* 29, 189–190. doi: 10.1080/00480169.1981.34843

Gao, J., and Nan, Z. (2007). A review of bioprotective alkaloids of grass-fungal endophyte symbioses. *Acta Ecol. Sin.* 27, 2531–2546. doi: 10.3321/j.issn:1000-0933.2007.06.048

Helander, M., Phillips, T., Faeth, S. H., Bush, L. P., Mcculley, R., Saloniemi, I., et al. (2016). Alkaloid quantities in endophyte-infected tall fescue are affected by the plant-fungus combination and environment. *J. Chem. Ecol.* 42, 118–126. doi: 10.1007/s10886-016-0667-1

Hennessy, L. M., Popay, A. J., Finch, S. C., Clearwater, M. J., and Cave, V. M. (2016). Temperature and plant genotype alter alkaloid concentrations in ryegrass infected with an *Epichloë* endophyte and this affects an insect herbivore. *Front. Plant Sci.* 7, 1–10. doi: 10.3389/fpls.2016.01097

Hume, D. E., Ryan, G. D., Gibert, A., Helander, M., Mirlohi, A., and Sabzalian, M. R. (2016). "*Epichloë* fungal endophytes for grassland ecosystems" in *Book: Sustainable agriculture reviews*. E. Lichtfouse (Cham: Springer), 233–305.

Johnson, L. J., De Bonth, A. C. M., Briggs, L. R., Caradus, J. R., Finch, S. C., Fleetwood, D. J., et al. (2013). The exploitation of *Epichloae* endophytes for agricultural benefit. *Fungal Divers.* 60, 171–188. doi: 10.1007/s13225-013-0239-4

Kuang, Y. (2016). Characteristics of *Epichloë* endophyte–*Festuca sinensis* symbiote. Lanzhou, Gansu, China: thesis. Lanzhou University.

Li, C., Nan, Z., Volker, H., Peter, D., and Liu, Y. (2004). A new *Neotyphodium* species symbiotic with drunken horse grass (*Achnatherum inebrians*) in China. *Mycotaxon* 91, 141–147.

Li, X. Z., Song, M. L., Yao, X., Chai, Q., Simpson, W. R., Li, C. J., et al. (2017). The effect of seed-borne fungi and *Epichloë* endophyte on seed germination and biomass of *Elymus sibiricus*. *Front. Microbiol.* 8, 1–8. doi: 10.3389/fmicb.2017.02488

Lin, W. H., Wang, X. X., Wang, J. J., Nzabanita, C., Xu, W. B., Yang, L., et al. (2018). Intra- and interspecific competition of *Elymus nutans* griseb. and *Festuca sinensis* Keng. Ex eb alexeev. Infected by *Epichloë* endophyte. *Bangl. J. Bot.* 47, 699–709.

Malinowski, D. P., and Belesky, D. P. (2000). Adaptations of endophyte-infected cool-season grasses to environmental stresses. *Crop Sci.* 40, 923–940. doi: 10.2135/cropsci2000.404923x

Malinowski, D. P., Belesky, D. P., Hill, N. S., Baligar, V. C., and Fedders, J. M. (1998). Influence of phosphorus on the growth and ergot alkaloid content of *Neotyphodium coenophialum*-infected tall fescue (*Festuca arundinacea* schreb.). *Plant Soil* 198, 53–61. doi: 10.1023/A:1004279401196

Nan, Z. B. (1996a). Incidence and distribution of endophytic fungi in seedlings and plants of some native and introduced grasses in China. *Acta Pratacul. Sin.* 5, 13–17.

Nan, Z. B. (1996b). Incidence and distribution of endophytic fungi in seeds of some native and introduced grasses in China. *Acta Pratacul. Sin.* 5, 1–8.

Nan, Z. B., and Li, C. J. (2004). Roles of the grass-*Neotyphodium* association in pastoral agriculture systems. *Acta Ecol. Sin.* 24, 605–616. doi: 10.3321/j.issn:1000-0933.2004.03.031

Nazir, A., and Rahman, H. A. (2018). Secrets of plants: endophytes. *Int. J. Plant Biol.* 9, 1–17. doi: 10.4081/pb.2018.7810

Nishida, R. (2002). Sequestration of defensive substances from plants by lepidoptera. *Annu. Rev. Entomol.* 47, 57–92. doi: 10.1146/annurev.ento.47.091201.145121

Peng, Q. Q., Li, C. J., Song, M. L., and Nan, Z. B. (2013). Effects of seed hydropriming on growth of *Festuca sinensis* infected with *Neotyphodium* endophyte. *Fungal Ecol.* 6, 83–91. doi: 10.1016/j.funeco.2012.08.001

Schardl, C. L., Leuchtmann, A., and Spiering, M. J. (2004). Symbioses of grasses with seedborne fungal endophytes. *Annu. Rev. Plant Biol.* 55, 315–340. doi: 10.1146/annurev.arplant.55.031903.141735

Schardl, C. L., Young, C. A., Faulkner, J. R., Florea, S., and Pan, J. (2012). Chemotypic diversity of *Epichloae*, fungal symbionts of grasses. *Fungal Ecol.* 5, 331–344. doi: 10.1016/j.funeco.2011.04.005

Schardl, C. L., Young, C. A., Hesse, U., Amyotte, S. G., Andreeva, K., Calie, P. J., et al. (2013a). Plantsymbiotic fungi as chemical engineers: multi-genome analysis of the *Clavicipitaceae* reveals dynamics of alkaloid loci. PLOS Genetics 9:e1003323. doi: 10.1371/journal.pgen.1003323

Schardl, C. L., Young, C. A., Pan, J., Florea, S., Takach, J. E., Panaccione, D. G., et al. (2013b). Currencies of mutualisms: sources of alkaloid genes in vertically transmitted epichloae. *Toxins* 5, 1064–1088. doi: 10.3390/toxins5061064

Siegel, M. R., Latch, G. C. M., and Johnson, M. C. (1987). Fungal endophytes of grasses. *Annu. Rev. Phytopathol.* 25, 293–315. doi: 10.1146/annurev.py.25.090187.001453

Song, H., Nan, Z., Song, Q., Xia, C., Li, X., Yao, X., et al. (2016). Advances in research on *Epichloë* endophytes in Chinese native grasses. *Front. Microbiol.* 7:1399. doi: 10.3389/fmicb.2016.01399

Tian, P., Kuang, Y., Lin, W., Wang, J., and Nan, Z. (2018). Shoot morphology and alkaloid content of *Epichloë* endophyte–*Festuca sinensis* associations. *Crop Pasture Sci.* 69, 430–438. doi: 10.1071/CP17231

Tian, P., Le, T. N., Ludlow, E. J., Smith, K. F., Forster, J. W., Guthridge, K. M., et al. (2013). Characterisation of novel perennial ryegrass host–*Neotyphodium* endophyte associations. *Crop Pasture Sci.* 64, 716–725. doi: 10.1071/CP13067

Wang, J., Zhou, Y., Lin, W., Li, M., Wang, M., Wang, Z., et al. (2017). Effect of an *Epichloë* endophyte on adaptability to water stress in *Festuca sinensis*. *Fungal Ecol.* 30, 39–47. doi: 10.1016/j.funeco.2017.08.005

Young, C. A., Tapper, B. A., May, K., Moon, C. D., Schardl, C. L., and Scott, B. (2009). Indole-diterpene biosynthetic capability of *Epichloë* endophytes as predicted by *ltm* gene analysis. *Appl. Environ. Microbiol.* 75, 2200–2211. doi: 10.1128/AEM.00953-08

Zhang, X., Li, C., and Nan, Z. (2011). Effects of salt and drought stress on alkaloid production in endophyte-infected drunken horse grass (*Achnatherum inebrians*). *Biochem. Syst. Ecol.* 39, 471–476. doi: 10.1016/j.bse.2011.06.016

Zhou, L., Li, C., Zhang, X., Johnson, R., Bao, G., Yao, X., et al. (2015a). Effects of cold shocked *Epichloë* infected *Festuca sinensis* on ergot alkaloid accumulation. *Fungal Ecol.* 14, 99–104. doi: 10.1016/j.funeco.2014.12.006

Zhou, L. Y., Zhang, X. X., Li, C. J., Christensen, M. J., and Nan, Z. B. (2015b). Antifungal activity and phytochemical investigation of the asexual endophyte of *Epichloë sp*. from *Festuca sinensis*. *Sci. China Life Sci.* 58, 821–826. doi: 10.1007/s11427-015-4845-0

Conflict of Interest Statement: The authors declare that the research was conducted in the absence of any commercial or financial relationships that could be construed as a potential conflict of interest.

frontiers in Microbiology

ORIGINAL RESEARCH
published: 30 August 2019
doi: 10.3389/fmicb.2019.01910

A Novel Seed-Dressing Formulation Based on an Improved Mutant Strain of *Trichoderma virens*, and Its Field Evaluation

Prasun K. Mukherjee[1], Sayaji T. Mehetre[1†], P. D. Sherkhane[1†], Gopi Muthukathan[1], Ananya Ghosh[2], A. S. Kotasthane[3], N. Khare[3], Parshuram Rathod[3], Kishan Kumar Sharma[3], Rajib Nath[2], Anand K. Tewari[4], Somnath Bhattacharyya[2‡], Meenakshi Arya[5], D. Pathak[6], A. R. Wasnikar[7], R. K. S. Tiwari[3‡] and D. R. Saxena[8]*

[1] Nuclear Agriculture and Biotechnology Division, Bhabha Atomic Research Centre, Mumbai, India, [2] Department of Agronomy, Bidhan Chandra Krishi Viswavidyalaya, Mohanpur, India, [3] Department of Plant Pathology, Indira Gandhi Krishi Vishwavidyalaya, Raipur, India, [4] Department of Plant Pathology, G. B. Pant University of Agriculture and Technology, Pantnagar, India, [5] Department of Plant Pathology, Rani Lakshmi Bai Central Agricultural University, Jhansi, India, [6] Regional Agricultural Research Station, Assam Agricultural University, Shillongani, India, [7] Department of Plant Pathology, Jawaharlal Nehru Krishi Vishwa Vidyalaya, Jabalpur, India, [8] R.A.K. College of Agriculture, Rajmata Vijayaraje Scindia Krishi Vishwa Vidyalaya, Sehore, India

Using gamma-ray-induced mutagenesis, we have developed a mutant (named G2) of *Trichoderma virens* that produced two- to three-fold excesses of secondary metabolites, including viridin, viridiol, and some yet-to-be identified compounds. Consequently, this mutant had improved antibiosis against the oomycete test pathogen *Pythium aphanidermatum*. A transcriptome analysis of the mutant vis-à-vis the wild-type strain showed upregulation of several secondary-metabolism-related genes. In addition, many genes predicted to be involved in mycoparasitism and plant interactions were also upregulated. We used tamarind seeds as a mass multiplication medium in solid-state fermentation and, using talcum powder as a carrier, developed a novel seed dressing formulation. A comparative evaluation of the wild type and the mutant in greenhouse under high disease pressure (using the test pathogen *Sclerotium rolfsii*) revealed superiority of the mutant over wild type in protecting chickpea (*Cicer arietinum*) seeds and seedlings from infection. We then undertook extensive field evaluation (replicated micro-plot trials, on-farm demonstration trials, and large-scale trials in farmers' fields) of our mutant-based formulation (named TrichoBARC) for management of collar rot (*S. rolfsii*) in chickpea and lentil (*Lens culinaris*) over multiple locations in India. In certain experiments, other available formulations were included for comparison. This formulation consistently, over multiple locations and years, improved seed germination, reduced seedling mortality, and improved plant growth and yield. We also noticed growth promotion, improved pod bearing, and early flowering (7–10 days) in TrichoBARC-treated chickpea and lentil plants under field conditions. In toxicological studies in animal models, this formulation exhibited no toxicity to mammals, birds, or fish.

Keywords: *Trichoderma*, mutant, tamarind seeds, formulation, chickpea, lentil, farmers' fields

OPEN ACCESS

Edited by:
Santiago Gutierrez, Universidad de León, Spain

Reviewed by:
Birinchi Kumar Sarma, Banaras Hindu University, India
Akanksha Singh, Central Institute of Medicinal and Aromatic Plants (CIMAP), India

****Correspondence:***
Prasun K. Mukherjee
prasunm@barc.gov.in; prasunmukherjee1@gmail.com

[†] These authors have contributed equally to this work

[‡] Present address:
Somnath Bhattacharyya, Department of Genetics and Plant Breeding, Bidhan Chandra Krishi Viswavidyalaya, Mohanpur, India
R. K. S. Tiwari, B.T.C. College of Agriculture, Indira Gandhi Krishi Vishwavidyalaya, Bilaspur, India

Specialty section:
This article was submitted to Microbial Symbioses, a section of the journal Frontiers in Microbiology

Received: *30 May 2019*
Accepted: *05 August 2019*
Published: *30 August 2019*

Citation:
Mukherjee PK, Mehetre ST, Sherkhane PD, Muthukathan G, Ghosh A, Kotasthane AS, Khare N, Rathod P, Sharma KK, Nath R, Tewari AK, Bhattacharyya S, Arya M, Pathak D, Wasnikar AR, Tiwari RKS and Saxena DR (2019) A Novel Seed-Dressing Formulation Based on an Improved Mutant Strain of Trichoderma virens, and Its Field Evaluation. Front. Microbiol. 10:1910. doi: 10.3389/fmicb.2019.01910

INTRODUCTION

Trichoderma spp. are among the most widely used bioagents in today's agriculture throughout the world (Mukherjee et al., 2013). The popularity of these fungi stems from their ability to kill other fungi (mycoparasitism), produce several hundred secondary metabolites (some are antimicrobial), induce local and systemic resistance in plants against invading pests and pathogens, improve nutrient (especially nitrogen) use efficiency, promote plant growth, and impart tolerance to abiotic stresses (Lorito et al., 2010). Even though there are more than 200 well-defined species reported in literature, the formulations that are in use are based on only a handful of species like *T. harzianum*, *T. afroharzianum*, *T. viride*, *T. asperellum*, *T. koningiopsis*, and *T. virens* (Atanasova et al., 2013; Mukherjee et al., 2013). The main constraint in using these bioagents has been their inconsistent performance under field conditions, compared to their chemical counterparts that are not much influenced by environmental factors (Zaidi and Singh, 2013). There have been earlier reports to develop novel *Trichoderma* strains using mutagenesis (Papavizas et al., 1982; Ahmad and Baker, 1988; Mukherjee et al., 1997, 1999; Szekeres et al., 2007; Olejníková et al., 2010). However, to the best of our knowledge, these have not been formulated, field-tested, and developed as commercial products. Among the formulations that are commercially available and are successful is one based on a protoplast fusant strain of *T. afroharzianum* (Shoresh et al., 2010; Chaverri et al., 2015; Harman and Uphoff, 2019). We report here improvement of a strain of *Trichoderma virens* that has been widely studied for biocontrol properties (Mukhopadhyay et al., 1992; Mukherjee et al., 2013; Sherkhane et al., 2017), using gamma-ray-induced mutagenesis. In addition to strain improvement, we also report here a novel mass multiplication protocol and a formulation strategy for *Trichoderma*, and report on the non-toxic nature of the *T. virens* mutant formulation in mammals, birds, and fish.

MATERIALS AND METHODS

Strains and Culture Conditions

Trichoderma virens IMI 304061 and the plant pathogens *Pythium aphanidermatum* and *Sclerotium rolfsii* were taken from our previous studies (Mukherjee et al., 2007). Fungal cultures were routinely grown in potato dextrose medium and stored in −80°C as glycerol stock for maintaining genetic purity.

Mutagenesis of *T. virens* and Isolation of a Secondary Metabolite Overproducing Mutant

Sporulated culture (grown in potato dextrose agar slants) of wild-type strain of *T. virens* was irradiated with gamma ray at 1,250 Gy, as described previously (Mukherjee and Mukhopadhyay, 1993). The spores were harvested in sterile distilled water and dilution-plated on PDA amended with rose bengal (100 mg/L) to restrict colony growth. Morphologically different colonies were transferred to fresh PDA plates. One colony having brown color conidia and secreting dark pigments in the medium was purified by repeated single-spore isolation and selected for further studies. Stability of the mutant was tested for 20 generations by repeated subculturing. For antibiosis assay, the strains were grown in PDB for 3 days with continuous shaking, and the filtrate was harvested, passed through 0.22-μm syringe filters, and added to PDA at 3% (v/v). Control was amended with 3% water. The indicator plant pathogen *P. aphanidermatum* was inoculated centrally on filtrate-amended plates and observation was recorded on the growth after 24 h of incubation. The ability of wild type and G2 to overgrow colonies of the plant pathogen *S. rolfsii* was assessed using confrontation assay (Mukherjee et al., 2013). The ability of the strains to colonize and kill sclerotia of *S. rolfsii* was assessed by spreading conidial suspension (100 μl of 10^6/ml) on 1% water agar plates and then seeding the sclerotia on it. Parasitization of the sclerotia was recorded daily and sclerotial viability was determined by plating on PDA amended with 10 mg/L benomyl (to selectively inhibit the growth of *T. virens*). For HPLC, the filtrates were extracted with ethyl acetate, concentrated (10-fold) using nitrogen flush, and subjected to HPLC analysis as described earlier (Mukherjee et al., 2006).

Transcriptome Analysis

For RNA extraction, *T. virens* WT and G2 were grown on PDA plates lined with a dialysis membrane (MWCO 12,000–14,000) for 3 days and the tissue (containing both mycelia and conidia) were harvested by scraping with a sterile spatula, ground in liquid nitrogen, and RNA extracted with TriReagent (MRC). A paired-end library was prepared, and *de novo* transcriptome sequencing and assembly were performed on Illumina HiSeq 2500 platform at M/S Scigenom, Cochin, Kerala, India. Adaptor trimming, quality filtering, and end trimming were performed and the cleaned reads were assembled using Trinity software with default settings. All assembled transcripts were found to be of length of more than 200 bp. The trimmed reads were aligned to the assembled transcriptome using the Bowtie2 program. Of all filtered reads, about 95% of reads from each sample were properly aligned back to the assembled transcriptome. Differential gene expression analysis was performed using DESeq program. The assembled transcript was annotated using an in-house pipeline (CANoPI – Contig AnnotatorPipeline) at M/S Scigenome Labs., Cochin, Kerala, India, for *de novo* transcriptome assembly using the following steps: Comparison with NCBI database using BLASTX program, organism annotation, gene and protein annotation to the matched transcript, and domain search by using NCBI-CDD search database. Fold change was calculated based on the FPKM values, and genes having $\log_2$ fold change $\geq$1.5 was considered for comparison.

Mass Multiplication, Formulation, and Seed Treatment

For mass multiplication of *T. virens*, we used a novel medium, i.e., tamarind seeds in solid-state fermentation. Tamarind seed is a cheap by-product of tamarind pulp industry and is available locally in all parts of India. The seeds were cut in four pieces,

and 100 g was soaked overnight in 180-ml tap water in a 500-ml conical flask. Even though whole tamarind seeds support profuse growth of *T. virens*, cut seeds were used to increase substrate surface area, resulting in higher fungal biomass production. After autoclaving for 15 min at 15 psi, seeds were inoculated with *Trichoderma* and incubated for 7–10 days. The growth was mixed thoroughly with 400 g of autoclaved talcum powder and sieved through a stainless steel sieve (8 mesh). The powder was air dried and kept refrigerated for further use. The formulation was stable for at least 6 months at 4–6°C, without any significant loss of viability. Colony-forming units were counted by dilution plating on rose bengal agar plates. For seed treatment, 5 to 10 g of the formulation was suspended in 25 ml of water to make a slurry, and seeds were treated with this slurry by shaking in a polybag. Seeds were air dried before sowing.

Greenhouse Assay for Control of *S. rolfsii*

In order to have a comparative assessment of wild type and G2, we checked for the ability to protect chickpea seeds and seedlings from *S. rolfsii*, a serious pathogen of chickpea (and of more than 500 plant species), in a greenhouse pot experiment. Two kilograms of non-sterile soil was taken in plastic pots. For inoculum, *S. rolfsii* was grown in sorghum grains for 10 days. Four grams (determined experimentally to create high disease pressure, i.e., about 100% mortality) of *S. rolfsii* culture was mixed with top 3 cm soil. The pots were covered for 3 days to help the pathogen get established in soil. Twenty treated (wild type or G2 @ 2.5 and 5 g/kg seeds, treated in slurry form as described above) chickpea seeds were sown per pot in pathogen-infested soil or pathogen-free soil, in three replicates. Observation on seed germination was recorded after 3 days and healthy plant stand was recorded after 7 days.

Replicated Field Trials for Control of Chickpea Collar Rot

Experiment at Crop Research Centre, G.B. Pant University of Agriculture and Technology, Pantnagar, Uttarakhand, India

A replicated trial was conducted at Pantnagar in a field naturally infested with root rot and wilt pathogens (*S. rolfsii*, *Rhizoctonia solani*, and *Fusarium oxysporum* f.sp. *ciceris*) in the 2017–2018 crop season. Individual plot size was 3 m × 2 m, and the experiment was laid out in randomized block design (RBD) with three replicates. Several biocontrol formulations of *Trichoderma* isolates/spp. and *Pseudomonas fluorescens* were compared with our formulation. Chickpea seeds were treated with 5 g/kg seeds (TrichoBARC) or 10 g/kg seeds (other bioagents) formulation, and 240 seeds were sown per plot. Moist seeds were treated with dry talcum-based formulations of the bioagents. Seedling and plant mortality was recorded between 30 and 120 days and mature plant wilt 120 days after sowing (DAS).

Trials Under All-India Coordinated Research Project on Chickpea at Four Locations

Multi-location replicated field trials were conducted at Raipur (Chhattisgarh State), Jhansi (Uttar Pradesh), Jabalpur (Madhya Pradesh), and Shillongani (Assam) in the 2017–2018 and 2018–2019 crop seasons. Plot size was 4 m × 3 m and the experiments were laid out in RBD with three replicates. Seeds of chickpea were treated with 1% of the *T. virens* G2 formulation grown in tamarind seeds. Three other strains of *Trichoderma* spp. and chemical seed treatment were included for comparison. Observations of seedling emergence, seedling mortality, and yield were recorded.

On-Farm Demonstration Trials

On-farm demonstration trials for control of chickpea collar rot was conducted in the 2015–2016 and 2016–2017 crop seasons at Indira Gandhi Krishi Vishwavidyalaya, Raipur, Chhattisgarh. In Raipur in 2015–2016, experiment was taken in a plot of 16 m × 7 m. Chickpea seeds treated with 0.5% TrichoBARC formulation was sown and observation on seed yield and biomass production was recorded. In 2016–2017, 63 m × 24 m plots were used to demonstrate the effect of TrichoBARC seed treatment on chickpea yield.

Trials in Farmers' Field

In 2017–2018, trials were conducted in the field of 30 lentil farmers in four villages (Jahirapara, Kurumbelia, Bizra, and Panpur) in Nadia district of West Bengal province, India. Experimental plot size was 0.3 acres. Seeds were treated @ 5 g/kg seeds of Moitri variety, and observations on seedling mortality and grain yield were recorded, and compared with non-treated plots. Trials in farmers' field were repeated the same way in the 2018–2019 crop season.

Toxicological Studies

A toxicological study with TrichoBARC formulation was conducted at the Department of Toxicology, IIBAT, Padappai, Tamil Nadu, India. The study was performed in accordance with the US-EPA, OPPTS microbial pesticide test guidelines and Committee for Control and Supervision of Experiments on Animals (CPCSEA) Prevention of Cruelty to Animals Act 1960 (formed in 1964 and revived in 1998). Animals were fasted for 3 h before the treatment and 0.3 ml (twice) containing

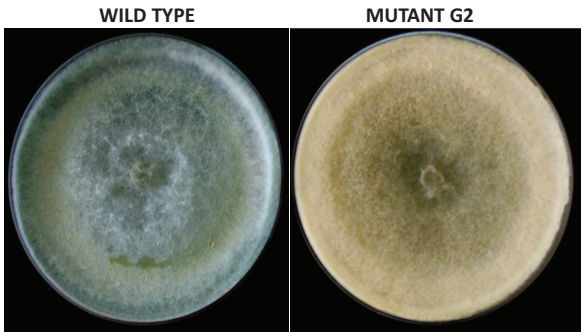

FIGURE 1 | Colony morphology of wild-type and mutant strain of *Trichoderma virens*, after growth on potato dextrose agar for 5 days.

approximately 10^8 colony-forming units of the formulation was administered in split dose orally to each animal in the treatment groups (rat, mice, and rabbit). Untreated animals were used as controls. Food was withdrawn for 1 h post-administration. The treated and control animals were sacrificed at various points during the study on days 3, 7, 14, and 21. All animals were observed daily for clinical signs, mortality, and morbidity until the day of their scheduled sacrifice. Body weights of individual animals were recorded shortly before the administration, weekly thereafter, at interim and final sacrifice. For toxicity studies in chicken (*Gallus gallus domesticus*), the desired quantity (20 g) of the test item was weighed and made up to 100 ml using distilled water and thereafter administered to the birds by oral intubation to five female chickens (bird nos. 6–10) at the dose level of 2,000 mg/kg body weight. Five control female chickens (bird nos. 1–5) were similarly treated but with distilled water alone. All birds were observed individually for toxicity signs and mortality thrice on day 0

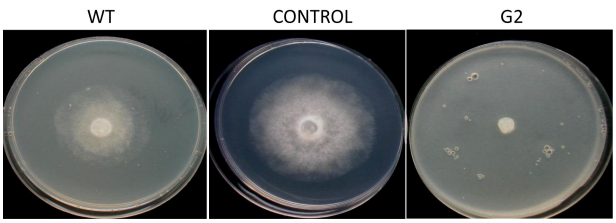

FIGURE 2 | Inhibition of *Pythium aphanidermatum* by culture filtrate of WT and G2.

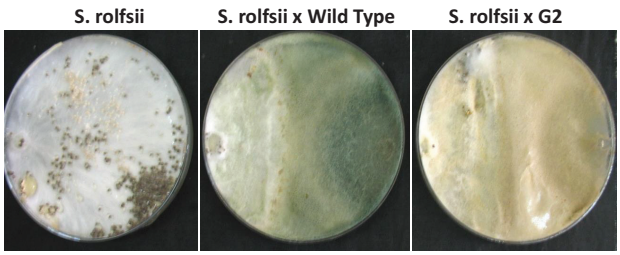

FIGURE 3 | Confrontation assay between *Sclerotium rolfsii* and *Trichoderma virens* mutant/wild-type strain.

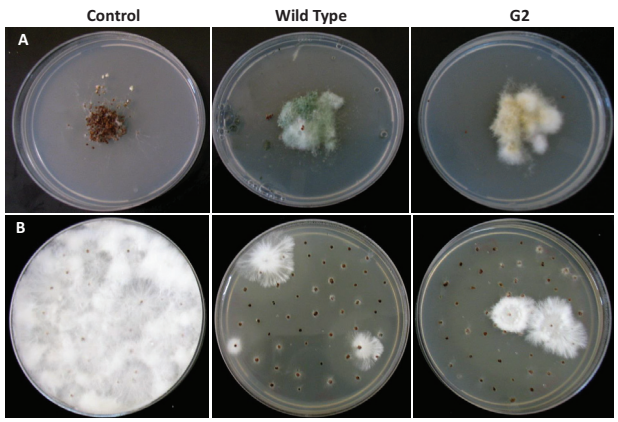

FIGURE 4 | Parasitism of sclerotia of *Sclerotium rolfsii* by wild type and mutant of *Trichoderma virens*. **(A)** Sclerotia colonized after 5 days of co-incubation of *Trichoderma* and sclerotia of *S. rolfsii*. **(B)** Growth of *S. rolfsii* from sclerotia after 3 days of incubation on benomyl-amended PDA medium.

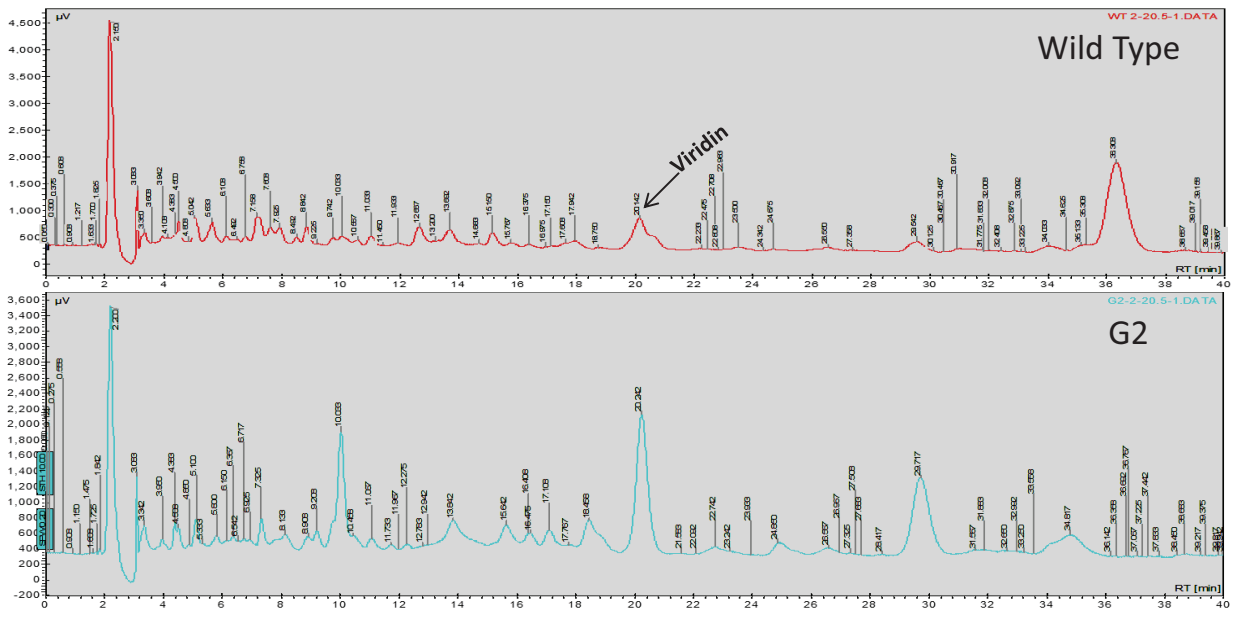

FIGURE 5 | HPLC analysis of culture filtrate of WT and G2.

and thereafter daily for 14 days. The body weight of each bird was recorded just prior to administration of dose (0 day) and on days 3, 7, and 14 after administration. Food consumption was measured daily. Water consumption data were collected on days 3, 7, and 14. At the end of the test, all surviving birds were humanely euthanized by carbon dioxide asphyxiation and gross pathology was conducted on all birds from the treatment group and control. Samples of liver, lungs, kidney, brain, spleen, and blood were collected aseptically and homogenized in cold phosphate buffered saline for microbial evaluation from the treated and control birds at the end of the experimental period. Similar studies were conducted in Pigeon (*Columba livia*). A study was also conducted to evaluate the acute toxicity of the formulation to freshwater fish, *Danio rerio*. In a range-finding experiment, groups of seven fish each in two replicates were exposed to control and test material concentrations of 25.0, 50.0, and 100.0 mg/L TrichoBARC formulation corresponding to 0, 3.9×10^5, 7.8×10^5, and 1.56×10^6 CFU/ml, respectively, for 96 h. The fish were observed for mortality and abnormal behavior twice on the day (3 and 6 h) of exposure and, thereafter, at the end of every 24 h throughout the experimental period. Based on the results of the range-finding experiment, the limit test was conducted with control and test material concentration of 100 mg/L in two replicates at 7 fish/replicate for 96 h. The fish were observed for mortality and abnormal behavior as described above. All the data were analyzed statistically.

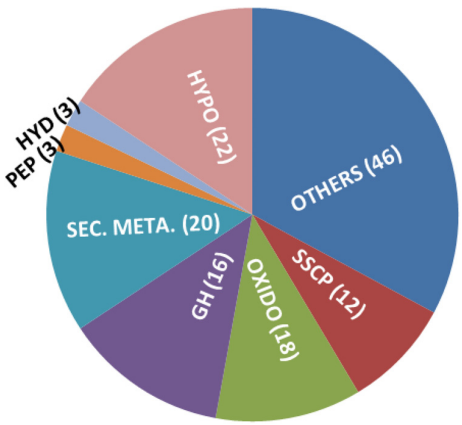

FIGURE 6 | Genes upregulated in *T. virens* mutant G2, over wild type, when grown on PDA for 3 days. Hypo: hypothetical/unknown proteins; SSCP: small, cysteine-rich secreted proteins; OXIDO: oxidoreductases; GH: glycosyl hydrolases; SEC. META.: gene predicted to be involved in secondary metabolism (includes PKS, P450, NRPS-like, OMT-B, and MFS transporters); HYD: hydrophobins; PEP: peptidases.

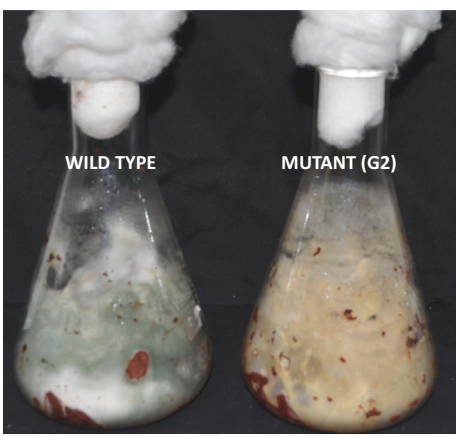

FIGURE 7 | Growth of *Trichoderma virens* wild type and mutant on tamarind seeds, 7 days after inoculation.

RESULTS AND DISCUSSION

G2 Is a Secondary Metabolite Overproducing Mutant

Exposure to 1,250 Gy of gamma ray followed by selection for varied colony morphology and hyperpigmentation of culture

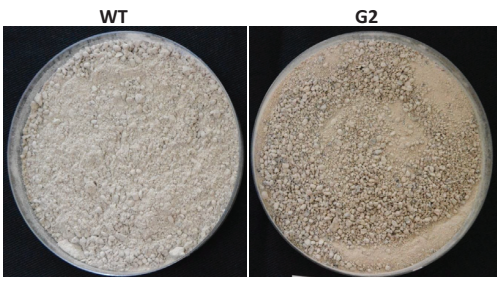

FIGURE 8 | Formulated product of *Trichoderma virens* wild type and mutant.

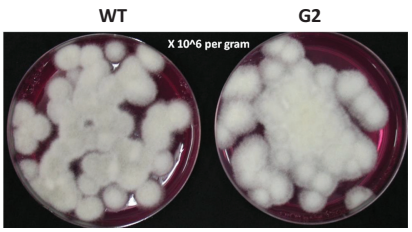

FIGURE 9 | Colony-forming units of *Trichoderma virens* on PDA-rose bengal medium.

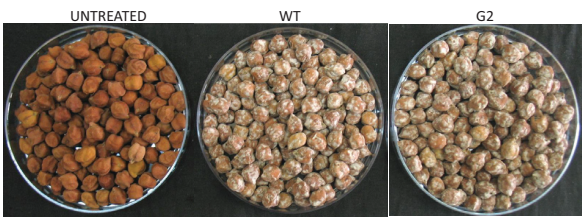

FIGURE 10 | Seeds treated with wild type and G2 formulations.

medium (by examining the reverse side of the culture plate) led to the isolation of a stable mutant (designated as G2) that has yellow-brown conidia, dark coloration of the medium, and normal growth and conidiation like the wild-type strain (**Figure 1**). The mutant, when grown in potato dextrose broth for 3 days in shake culture, produced dark pigment(s) in liquid medium and the filtrate was more inhibitory than the wild type on growth of the test plant pathogen *P. aphanidermatum* (**Figure 2**). In a confrontation assay, the mutant was as effective as the wild type in overgrowing the plant pathogen *S. rolfsii* (**Figure 3**). The mutant was also as effective as the wild type in parasitism of the sclerotia of *S. rolfsii* (**Figure 4**). In HPLC analysis, the mutant produced about 3-fold more of secondary metabolites, including the known metabolites viridin and viridiol, and many yet-to-be identified compounds (**Figure 5**). These data indicate that the mutant is a hyper-producer of several secondary metabolites, and as effective as the wild type in mycoparasitism. The mutant has been deposited with the Microbial Type Culture Collection, Chandigarh, India (Acc. No. MTCC 11567).

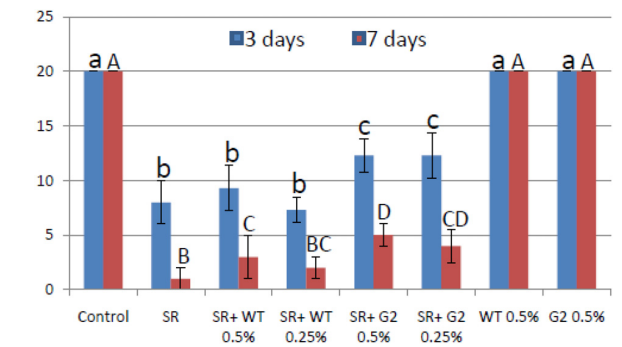

FIGURE 11 | Pot assay for biocontrol of *Sclerotium rolfsii* in chickpea treated with wild type or mutant, in the presence and absence of the pathogen. Treatments with same letters (case-sensitive) are not significantly different ($P < 0.05$).

Several Genes Related to Secondary Metabolism, Mycoparasitism, and Plant Interactions Are Upregulated in G2

In order to understand the genomic basis of enhanced secondary metabolite biosynthesis, we did a transcriptome analysis of the mutant vis-à-vis the wild-type strain, grown on potato dextrose agar medium for 3 days. Indeed, several secondary metabolism biosynthesis and transport-related genes like polyketide synthases (6), *O*-methyl transferases (4, including one involved in viridin biosynthesis – Bansal et al., 2018), cytochrome P450s (4), and MFS transporters (4) were upregulated in the mutant, compared to wild type (**Figure 6** and **Supplementary Table S1**). This excludes 16 oxidoreductases that are upregulated in the mutant; oxidoreductases are also known to be part of several secondary metabolism gene clusters and some of these might also be involved in secondary metabolite biosynthesis (Zeilinger et al., 2016). Interestingly, in addition to genes for secondary metabolism, 18 glycosyl hydrolases (GHs) are also upregulated in the mutant. This is surprising because most of the GHs are under catabolite repression in glucose-rich medium (like PDA).

TABLE 1 | Efficacy of bio-agents against seed and plant mortality of chickpea in field at Crop Research Centre, Pantnagar (2017–2018).

Treatment	Plant stand (30 DAS) ± SE (*N*)	Germination (30 DAS) (%)	Plant stand (30–120 DAS) ± SE (*N*)	Plant mortality (30–120 DAS) (%)	Plant stand (120 DAS) ± SE (*N*)	Mature plant wilt (120 DAS) (%)	Plant mortality including wilted plants (30–120 DAS)(%)
TCMS-36	157.0 ± 3.2	65.4	144.3 ± 0.9	8.0	130.0 ± 4.6	9.9	17.9
PBAT-3(Ta + Pf)	165.0 ± 2.1	68.7	146.3 ± 4.3	11.3	139.3 ± 3.8	4.7	15.8
Th-14	155.3 ± 4.4	64.7	147.6 ± 4.7	4.9	138.6 ± 6.1	6.0	10.9
Th-17	163.0 ± 4.7	67.9	143.9 ± 2.0	11.7	134.6 ± 4.7	6.4	18.1
Th-39	165.3 ± 7.3	68.8	135.6 ± 5.6	17.9	129.0 ± 7.0	4.8	22.7
Th-19	150.6 ± 3.7	62.7	126.2 ± 4.8	16.2	114.6 ± 6.4	9.1	25.3
Psf-173	155.6 ± 3.2	64.8	128.2 ± 3.4	17.6	121.6 ± 4.3	5.1	22.7
Psf-2	162.6 ± 5.5	67.7	138.3 ± 4.3	14.9	131.0 ± 5.5	5.2	20.1
NBAIR1-Th	167.6 ± 5.5	69.8	142.2 ± 3.3	15.1	129.6 ± 6.5	8.8	23.9
NBAIR2-Ta	153.6 ± 8.0	64.0	124.6 ± 8.2	18.8	112.0 ± 6.5	10.1	28.9
TrichoBARC	158.3 ± 3.8	65.9	147.3 ± 4.1	6.9	140.3 ± 6.4	4.7	11.6
Sanjeevni TV	158.0 ± 5.2	65.8	130.9 ± 1.2	17.1	121.3 ± 5.6	7.3	24.4
Carbendazim	167.6 ± 4.6	69.8	125.2 ± 6.2	25.2	114.6 ± 5.2	8.4	33.6
Control	156.0 ± 3.2	65.0	114.6 + 3.9	26.5	102.6 ± 7.2	10.4	36.9
CD (0.05)	11.1				12.98		
CV (%)	4.1	–	–		130.0	–	–

Seeds were treated with the following bioagents: TCMS-36: Trichoderma asperellum; PBAT-3: T. asperellum strain; Th14 + : Pseudomonas fluorescens strain Psf 173; Th-14: T. asperellum; Th-17: T. asperellum; Th-39: T. harzianum; Th-19: T. harzianum; Psf-173: P. fluorescens; Psf-2: P. fluorescens; NBAIR1-Th: T. harzianum; NBAIR2-Ta: T. asperellum; Sanjeevni TV: T. viride each @10 g/kg seeds; TrichoBARC: T. virens mutant G2 @ 5 g/kg seeds. Other Trichoderma and Pseudomonas strains were isolated from the Uttarakhand state of India, grown in sorghum grains (Trichoderma) or nutrient broth (Pseudomonas), and applied as talcum-based non-commercial formulations.

TABLE 2A | Evaluation of new stains of *Trichoderma* along with fungicides for the management of collar rot of chickpea (2017–2018) – Seedling emergence.

S. No.	Treatment Details	Raipur ± SE	Jhansi ± SE	Shillongani ± SE	Jabalpur ± SE	Mean
T_1	*Trichoderma harzianum* T-6 (@10 g/kg seed)	196 ± 28.5	225 ± 5.8	313 ± 19.2	177 ± 9.1	227.75
T_2	*Trichoderma harzianum* T-28 (@10 g/kg seed)	263 ± 50.5	209 ± 8.7	286 ± 12.0	181 ± 3.1	234.75
T_3	*Trichoderma viride* T-18 (@10 g/kg seed)	292 ± 8.7	168 ± 19.2	297 ± 9.4	185 ± 8.7	235.50
T_4	TrichoBARC (@10 g/kg seed)	291 ± 4.7	186 ± 6.6	288 ± 15.8	185 ± 9.3	237.50
T_5	Propineb (Antracol) @3 g/kg seed	238 ± 66.7	203 ± 4.0	287 ± 12.6	178 ± 4.8	226.50
T_6	Hexaconazol + Zineb (Avtar) @3 g/kg seed	301 ± 10.8	204 ± 17.1	286 ± 20.0	182 ± 5.8	243.25
T_7	*Trichoderma harzianum* T-6 + Propineb (@10 g + 1.5 g/kg seed)	182 ± 2.6	273 ± 12.9	309 ± 5.7	182 ± 2.3	236.50
T_8	Control	181 ± 13.9	140 ± 8.9	277 ± 15.1	175 ± 7.5	193.25
	C.D. at 5%	69.60	25.90	7.91	1.40	
	C.V. (%)	19.54	8.80	13.02–	1.368	

TABLE 2B | Evaluation of new stains of *Trichoderma* along with fungicides for the management of collar rot of chickpea (2017–2018) – Disease incidence (%).

S. No.	Treatment Details	Raipur ± SE	Jhansi ± SE	Shillongani ± SE	Jabalpur ± SE	Mean
T_1	*Trichoderma harzianum* T-6 (@10 g/kg seed)	196 ± 28.5	225 ± 5.8	313 ± 19.2	177 ± 9.1	227.75
T_2	*Trichoderma harzianum* T-28 (@10 g/kg seed)	263 ± 50.5	209 ± 8.7	286 ± 12.0	181 ± 3.1	234.75
T_3	*Trichoderma viride* T-18 (@10 g/kg seed)	292 ± 8.7	168 ± 19.2	297 ± 9.4	185 ± 8.7	235.50
T_4	TrichoBARC (@10 g/kg seed)	291 ± 4.7	186 ± 6.6	288 ± 15.8	185 ± 9.3	237.50
T_5	Propineb (Antracol) @3 g/kg seed	238 ± 66.7	203 ± 4.0	287 ± 12.6	178 ± 4.8	226.50
T_6	Hexaconazol + Zineb (Avtar) @3 g/kg seed	301 ± 10.8	204 ± 17.1	286 ± 20.0	182 ± 5.8	243.25
T_7	*Trichoderma harzianum* T-6 + Propineb (@10 g + 1.5 g/kg seed)	182 ± 2.6	273 ± 12.9	309 ± 5.7	182 ± 2.3	236.50
T_8	Control	181 ± 13.9	140 ± 8.9	277 ± 15.1	175 ± 7.5	193.25
	C.D. at 5%	69.60	25.90	7.91	1.40	
	C.V. (%)	19.54	8.80	13.02	1.368	

TABLE 2C | Evaluation of new stains of *Trichoderma* along with fungicides for the management of collar rot of chickpea (2017–2018) – Yield (kg/ha).

S. No.	Treatment Details	Raipur ± SE	Jhansi ± SE	Shillongani ± SE	Jabalpur ± SE	Mean
T_1	*Trichoderma harzianum* T-6 (@10 g/kg seed)	676 ± 96.6	564 ± 22.5	733 ± 7.3	520 ± 23.1	623.25
T_2	*Trichoderma harzianum* T-28 (@10 g/kg seed)	902 ± 160.1	410 ± 40.0	848 ± 7.3	497 ± 3.8	664.25
T_3	*Trichoderma viride* T-18 (@10 g/kg seed)	952 ± 44.6	226 ± 25.5	825 ± 8.7	603 ± 6.0	651.50
T_4	TrichoBARC (@10 g/kg seed)	925 ± 61.2	282 ± 24.4	878 ± 6.0	647 ± 11.6	683.00
T_5	Propineb (Antracol) @3 g/kg seed	995 ± 162.1	387 ± 28.3	800 ± 11.5	436 ± 6.6	654.50
T_6	Hexaconazol + Zineb (Avtar) @3 g/kg seed	980 ± 8.3	324 ± 29.5	927 ± 10.1	494 ± 13.0	681.25
T_7	*Trichoderma harzianum* T-6 + Propineb (@10 g + 1.5 g/kg seed)	796 ± 74.5	674 ± 31.3	977 ± 10.1	500 ± 15.5	736.75
T_8	Control	584 ± 76.5	194 ± 3.7	624 ± 9.2	383 ± 64.2	446.25
	C.D. at 5%	223	62	7	75	
	C.V. (%)	17.82	10.99	0.58	8.32	

TABLE 3A | Evaluation of new stains of *Trichoderma* along with fungicides for the management of collar rot of chickpea (2018–2019) – Seedling emergence.

S. No.	Treatment Details	Raipur ± SE	Jhansi ± SE	Shillongani ± SE	Jabalpur ± SE	Mean
T_1	*Trichoderma harzianum* T-6 (@10 g/kg seed)	219 ± 17.8	231 ± 5.3	330 ± 1.8	180 ± 3.1	240.00
T_2	*Trichoderma harzianum* T-28 (@10 g/kg seed)	211 ± 25.9	204 ± 7.5	345 ± 2.3	184 ± 4.2	236.00
T_3	*Trichoderma viride* T-18 (@10 g/kg seed)	173 ± 13.6	143 ± 6	344 ± 3.0	182 ± 2.9	210.50
T_4	TrichoBARC (@10 g/kg seed)	286 ± 11.9	179 ± 1.2	349 ± 2.9	186 ± 0.3	250.00
T_5	Propineb (Antracol) @3 g/kg seed	209 ± 17.9	207 ± 13.3	330 ± 2.9	186 ± 1.2	233.00
T_6	Hexaconazol + Zineb (Avtar) @3 g/kg seed	232 ± 13.2	203 ± 4.5	353 ± 2.4	178 ± 1.2	241.50
T_7	*Trichoderma harzianum* T-6 + Propineb (@10 g + 1.5 g/kg seed)	260 ± 14.4	288 ± 3.2	366 ± 3.1	180 ± 0.9	273.50
T_8	Control	143 ± 10.7	130 ± 9.6	284 ± 2.9	170 ± 1.5	240.00
	C.D. at 5%	50.130	23.078	5.690	7.274	
	C.V. (%)	13.068	6.588	0.952	2.271	

Several GHs like chitinases, chitosanases, and beta-glucanases that are upregulated in the mutant are known to be involved in mycoparasitism and biocontrol (Inbar and Chet, 1995; Haran et al., 1996; Carsolio et al., 1999; Djonović et al., 2006b, 2007b). Certain GHs like pectinases are induced during root colonization by *Trichoderma* and are known to be involved in penetration of roots (Morán-Diez et al., 2009, 2015). Small cysteine-rich secreted proteins (SSCPs) are a broadly defined group of proteins that are secreted, small (300 amino acids or less), and have at least four cysteine residues (Mendoza-Mendoza et al., 2018). Many of the proteins involved in plant–microbe interactions (as elicitors and effectors) are SSCPs, for example, Sm1 and Sm2 of *T. virens* as elicitors and four SSCPs as effectors that presumably facilitate root internalization (Djonović et al., 2006a, 2007a; Gaderer et al., 2015; Lamdan et al., 2015; Mendoza-Mendoza et al., 2018). In this study, as many as 12 SSCPs are upregulated in mutant G2 over wild type, even when it was grown on PDA, and not in association with roots. In addition, an ortholog of *hce2*, gene encoding a pathogen effector and a putative necrosis-inducing factor (Ecp2 is a member of this family), is also induced in G2. *Trichoderma* hydrophobins are known to be involved in attachment of hyphae to roots – deletion of *hyd2* resulted in compromising cucumber root colonization by *T. asperellum* (Viterbo and Chet, 2006). *Trichoderma* hydrophobins are also reported to be involved in mycoparasitism, plant growth promotion, and induced resistance (Ruocco et al., 2015; Guzmán-Guzmán et al., 2017; Przylucka et al., 2017; Yu et al., 2019; Zhang et al., 2019). Three hydrophobins are upregulated in G2, compared to wild type. In short, many genes that can have a positive effect on plants are induced in G2 even when grown on a nutrient-rich medium not under induction by its host fungi or plants.

Tamarind Seeds Support Profuse Growth of *T. virens*

Tamarind seeds are a by-product of tamarind pulp industry and are cheap and locally available. In order to replace widely used food grains as a medium for growth of *Trichoderma*, we tested the ability of tamarind seeds to support growth and conidiation of *T. virens* in solid-state fermentation. Broken tamarind seeds supported profuse growth and conidiation of both wild type and the mutant (**Figure 7**). The final formulation with talcum powder (80%, W/W) appeared darker for the mutant, because of hyperpigmentation (**Figure 8**). The colony-forming units

TABLE 3B | Evaluation of new stains of *Trichoderma* along with fungicides for the management of collar rot of chickpea (2018–2019) – Disease incidence (%).

S. No.	Treatment Details	Raipur ± SE	Jhansi ± SE	Shillongani ± SE	Jabalpur ± SE	Mean
T_1	*Trichoderma harzianum* T-6 (@10 g/kg seed)	22.82 ± 9.8 (28.459)	22.33 ± 2.2 (28.155)	31.80 ± 1.3 (34.30)	15.333 ± 2.73 (22.866)	23.07
T_2	*Trichoderma harzianum* T-28 (@10 g/kg seed)	30.57 ± 11.8 (33.495)	32.00 ± 3.2 (34.402)	22.20 ± 0.7 (28.10)	18.867 ± 3.1 (25.578)	25.91
T_3	*Trichoderma viride* T-18 (@10 g/kg seed)	34.04 ± 5.5 (35.536)	52.00 ± 5.2 (46.129)	24.20 ± 0.9 (29.50)	14.917 ± 0.7 (22.701)	31.29
T_4	TrichoBARC (@10 g/kg seed)	14.39 ± 7.3 (22.199)	40.00 ± 4.0 (39.215)	16.80 ± 1.2 (24.20)	20.48 ± 2.5 (26.811)	22.92
T_5	Propineb (Antracol) @3 g/kg seed	23.37 ± 8.7 (28.839)	30.67 ± 3.1 (33.486)	28.40 ± 1.6 (32.2)	20.333 ± 3.2 (26.644)	25.69
T_6	Hexaconazol + Zineb (Avtar) @3 g/kg seed	25.00 ± 8.8 (29.938)	32.00 ± 3.2 (34.425)	12.90 ± 1.8 (20.90)	17.847 ± 3.5 (24.777)	21.94
T_7	*Trichoderma harzianum* T-6 + Propineb (@10 g + 1.5 g/kg seed)	9.18 ± 4.6 (17.376)	4.00 ± 0.4 (11.277)	7.30 ± 0.4 (15.70)	31.667 ± 2.0 (34.209)	13.04
T_8	Control	38.14 ± 9.5 (38.038)	56.67 ± 5.7 (48.830)	58.10 ± 1.7 (49.60)	29.667 ± 0.9 (32.984)	45.64
	C.D. at 5%	6.911	5.020	2.150	3.619	
	C.V. (%)	13.369	8.232	4.150	7.561	

TABLE 3C | Evaluation of new stains of *Trichoderma* along with fungicides for the management of collar rot of chickpea (2018–2019) – Yield (kg/ha).

S. No.	Treatment Details	Raipur ± SE	Jhansi ± SE	Shillongani ± SE	Jabalpur ± SE	Mean
T_1	*Trichoderma harzianum* T-6 (@10 g/kg seed)	570.00 ± 26.5	567 ± 13.8	765 ± 2.08	481 ± 12.1	595.75
T_2	*Trichoderma harzianum* T-28 (@10 g/kg seed)	693.33 ± 30.9	426 ± 12.6	890 ± 30.6	525 ± 46.7	633.58
T_3	*Trichoderma viride* T-18 (@10 g/kg seed)	673.33 ± 23.1	222 ± 11.3	860 ± 23.1	581 ± 42.2	584.08
T_4	TrichoBARC (@10 g/kg seed)	836.67 ± 28.4	262 ± 15.4	935 ± 15.3	500 ± 12.0	633.42
T_5	Propineb (Antracol) @3 g/kg seed	616.33 ± 23.6	409 ± 5.2	830 ± 20.8	596 ± 52.3	612.83
T_6	Hexaconazol + Zineb (Avtar) @3 g/kg seed	735.00 ± 17.3	314 ± 5.2	980 ± 20.8	530 ± 45.0	639.75
T_7	*Trichoderma harzianum* T-6 + Propineb (@10 g + 1.5 g/kg seed)	773.33 ± 20.3	671 ± 17.4	1030 ± 20.8	442 ± 29.8	729.08
T_8	Control	438.33 ± 28.9	196 ± 9.3	650 ± 36.1	360 ± 6.4	411.08
	C.D. at 5%	71.861	29.246	78.3	70.87	
	C.V. (%)	6.097	4.308	5.1	7.978	

were determined to be 10^8/g for both the wild type and the mutant formulations (**Figure 9**). The formulation was free of any bacterial or mold contamination.

G2-Based Formulation Is Superior to Wild Type in Greenhouse Assays

Most *Trichoderma* formulations available in the market have added amendments like carboxy-methyl cellulose and/or a detergent that acts as a spreader/sticker. Hence, *sensu stricto*, these formulations are not organic. Tamarind seeds have intrinsic sticking properties as it is rich in xylo-glucan (Mishra and Malhotra, 2009). Seeds could be easily coated with this formulation without adding any sticker (**Figure 10**). When coated chickpea seeds were sown in pot soil heavily infested with the pathogen *S. rolfsii*, the mutant-based formulation showed improved disease control potential compared to wild type (**Figure 11**). This experiment was repeated several times and the superiority of the mutant to reduce seedling mortality was reproducible. We therefore proceeded to field trials with the mutant-based formulation (named TrichoBARC) at multiple locations over several years.

The Formulation Is Effective in Reducing Seedling Mortality and Improving Yield of Chickpea Under Field Conditions

In a replicated filed trial at Pantnagar conducted during the 2017–2018 crop season in soil naturally infested with collar rot, root rot, and wilt pathogens, TrichoBARC formulation significantly reduced chickpea plant mortality (11.6% wilted plants, as against 36.9% in control plot) and was superior to other *Trichoderma* or *P. fluorescens*-based formulations (**Table 1**). In multi-location trials on collar-rot control, TrichoBARC was evaluated and compared with a few other *Trichoderma* strains, fungicides, and combination treatment, at four locations/states of India over 2 years. TrichoBARC treatment of seeds significantly improved seedling emergence, reduced disease incidence, and improved yield in all four locations over both years (**Tables 2A–C**, **3A–C**).

The Formulation Enhanced Chickpea Yield in "On-Farm" Demonstration Trials

We demonstrated the potential of the formulation to enhance chickpea yield at Raipur, Chhattisgarh (for chickpea) over 2 years. In the 2015–2016 demonstration trial in Raipur, TrichoBARC-treated chickpea plot (112 m^2) recorded 54.2 kg bundle weight (biomass production) and 14 kg grain yield, compared to 29.16 and 8.8 kg, respectively, in the control plot; the TrichoBARC-treated plot had lower incidence of seedling mortality (**Figure 12**). In 2016–2017, in a bigger plot size (1512 m^2), the grain yield was 161 kg in the TrichoBARC-treated plot, compared to 142 kg in control, and bundle weight was 386 and 271 kg per plot, respectively.

TrichoBARC Seed Treatment Improved Lentil Yield in Farmers' Field

In 2017–2018, trials were taken up in 30 lentil farmers' field in West Bengal. On average, yield per hectare was 1,533 kg, compared to 1,269 in the non-treated field, with the maximum yield recorded in the TrichoBARC-treated field being 1,800 kg/ha and the minimum being 1,275 kg/ha, compared to 1425 and 1125 kg/ha in control fields, and the

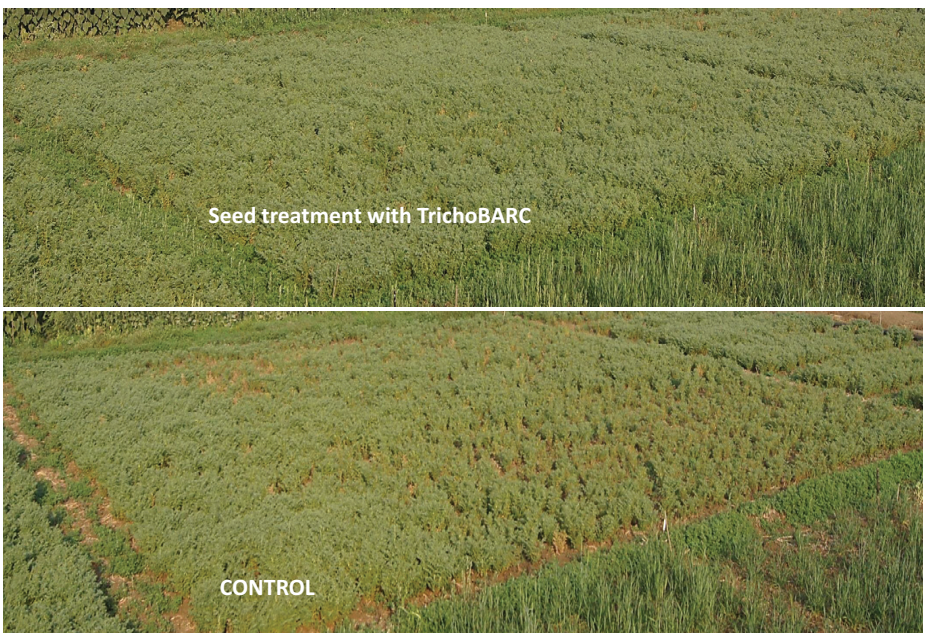

FIGURE 12 | Demonstration trial on control of collar rot of chickpea in experimental field at Raipur (2015–2016).

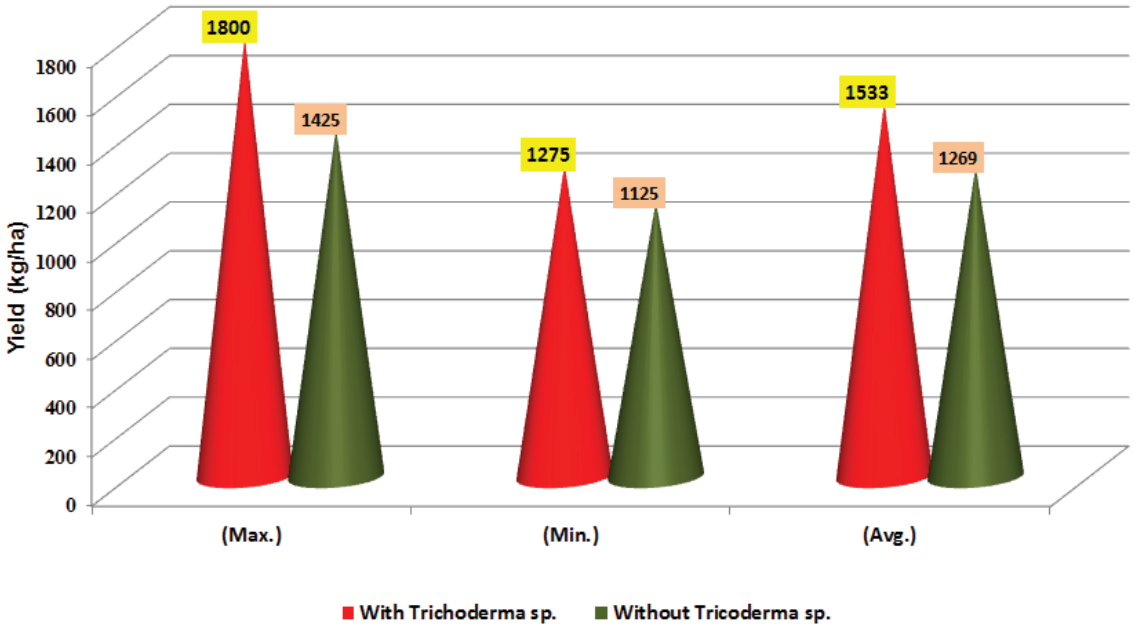

Lentil	Yield (kg/ha)			Comparison of Yield (t-test)		
	Max.	Min.	Avg.	$t_{cal(0.05)}$	$t_{tab(0.05)}$	Significance
With *Trichoderma*	1800	1275	1533	2.87	2.16	Sig.
Without *Trichoderma*	1425	1125	1269			

FIGURE 13 | Yield data of farmers' field trials taken at 30 farmers' fields in Nadia district of West Bengal (2017–2018).

yield gain was statistically significant (**Figure 13**). In 2018–2019 too, average yield gain in 30 farmers' fields across four villages in Nadia district of West Bengal was more than 200 kg/ha (**Figure 14**).

The Formulation Developed Is Non-toxic to Mammals, Birds, and Fish

The toxicological studies of TrichoBARC formulation on rat, mice, rabbit, chicken, pigeon, and a freshwater fish *D. rerio* revealed that the formulation is non-toxic to these test animals (**Table 4**).

SUMMARY AND CONCLUSION

Trichoderma spp. are widely used in agriculture, several formulations being available as biofungicides and plant growth promoters. *T. virens* is also commercially sold as a biofungicide[1] and plant growth promoter (in combination with *Bacillus amyloliquefaciens*[2]) in the United States. Even though natural strains of *Trichoderma* are effective, there is always a scope for strain improvement. Induced mutation is a powerful tool for genetic enhancement of microbes. For example, the industrial strain RutC 30 of *Trichoderma reesei* (used for enzyme production) is derived from a natural strain QM6A through repeated mutagenesis resulting in 15- to 20-fold improvement in cellulase biosynthesis (Peterson and Nevalainen, 2012). Another example is the enhancement of penicillin biosynthesis – it has been possible to enhance the titer by 85-fold through mutation (Ziemons et al., 2017). There are several such examples in industry, but only a few in microbes of agricultural importance. Even though attempts were made to "improve" biocontrol potential of *Trichoderma* strains through mutagenesis, seldom they have been commercialized. Biocontrol potential of *Trichoderma* spp. can also be enhanced by improving formulation strategy. In the present study, we have demonstrated that it is possible to improve the antagonistic and biocontrol potential of a strain of *T. virens* that has widely been studied

[1]http://certisusa.com/pest_management_products/biofungicides/soilgard_12g_microbial_fungicide.htm

[2]https://www.aganytime.com/dekalb/protection/Pages/Monsanto-BioAg.aspx

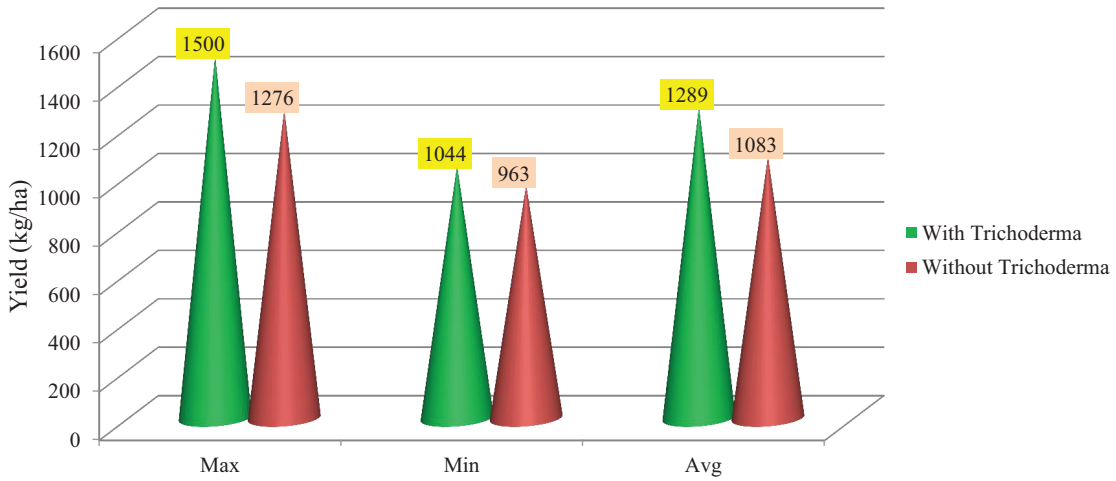

Lentil	Yield (kg/ha)			Comparison of Yield (t-test)		
	Max	Min	Avg	$t_{cal(0.05)}$	$t_{tab(0.05)}$	Significance
With *Trichoderma*	1500	1044	1289	2.30	2.16	Sig.
Without *Trichoderma*	1276	963	1083			

FIGURE 14 | Yield data of farmers' field trials taken at 30 farmers' fields in Nadia district of West Bengal (2018–2019).

TABLE 4 | Toxicity of TrichoBARC formulation on mammals, birds, and fish.

S. No.	Study Title	Results
1	Acute Oral Toxicity/Pathogenicity in Wistar Rat	No toxicity, infectivity, or pathogenicity
2	Acute Oral Toxicity/Pathogenicity in CD 1 Mice	No toxicity, infectivity, or pathogenicity
3	Acute Pulmonary Toxicity/Pathogenicity Study in Wistar Rat	No toxicity, infectivity, or pathogenicity
4	Acute Dermal Toxicity/Pathogenicity Study in New Zealand White Rabbits	No treatment-related toxicity, pathogenicity, or skin irritation
5	Acute Intraperitoneal Toxicity/Pathogenicity Study in Wistar Rats	No treatment-related toxicity, infectivity, or pathological effects
6	Acute Dermal Irritation in New Zealand White Rabbits	Non-irritating
7	Acute Eye Irritation in New Zealand White Rabbits	Non-irritating
8	Acute Oral Toxicity Study in Chicken	Non-toxic and non-virulent
9	Acute Oral Toxicity Study in Pigeon	Non-toxic and non-virulent
10	Acute Toxicity Study to Freshwater Fish, *Danio rerio*	>100 mg/L (non-toxic and non-virulent)

for biocontrol properties as well as genetics. We have combined genetic enhancement with novel formulation strategy, and through extensive evaluation over many years in several locations, we demonstrate the commercial potential of such a novel formulation. The use of tamarind seeds as a mass multiplication medium has unique advantages. In developing countries, including India, food grains like sorghum are extensively used for growing *Trichoderma* at industry scale, while tamarind seeds are by-products of tamarind pulp that are very popular as a culinary ingredient throughout India. This technology thus replaces expensive food grains with cheap tamarind seeds. Moreover, tamarind seed-based formulations, being sticky in nature, do not require addition of stickers/spreaders like carboxy-methyl cellulose and detergents that are routinely used in *Trichoderma* formulations. This formulation described here is thus an organic formulation *sensu stricto*. The extensive field testing data (including farmers' field) that we present here clearly establish our formulation as an excellent technology for crop production, especially pulses. The formulation has been proven to not only be effective in controlling collar rot, a serious problem in more than 500 crop species, but also cause robust plant growth (**Supplementary Figures S1, S2**). We also noticed early flowering (by 7–10 days) in TrichoBARC-treated chickpea and lentil under field conditions at multiple locations. We are yet to study the mechanism of improved biocontrol and growth enhancement, which could be due to the overproduction of secondary metabolites, and constitutive overexpression of many genes known to be involved in mycoparasitism (like chitinases, chitosanases, and glucanases), root colonization (like pectinases), and SSCPs (known to play role as

elicitors and effectors). The formulation developed by us using a novel mutant combined with a novel formulation strategy thus holds promise for commercial success as a novel plant bio-inoculant. Additionally, through toxicology studies, we also provide evidence that this formulation is safe, which adds to the commercial prospect of this technology described here.

DATA AVAILABILITY

The datasets generated for this study can be found in the RNAseq data included as **Supplementary File**.

ETHICS STATEMENT

This study was performed in accordance with the USEPA, OPPTS microbial pesticide test guidelines, and Committee for the Purpose of Control and Supervision of Experiments on Animals (CPCSEA), Animal Welfare Division of Ministry of Environment, Forest and Climate Change, Government of India guidelines under the Prevention of Cruelty to Animals Act 1960 (formed in 1964 and revived in 1998). The experiments were approved and monitored by the Institutional Animal Ethics Committee (IAEC), IIBAT.

AUTHOR CONTRIBUTIONS

PM, SM, PS, and GM performed the laboratory and greenhouse experiments. PM and PS prepared the formulations for field studies. AG, AK, NK, PR, KS, RN, AT, SB, MA, DP, AW, RT, and DS performed the field trials. PM conceptualized, designed, and coordinated the studies, and wrote the manuscript.

ACKNOWLEDGMENTS

PM would like to thank Dr. P. Suprasanna, Head, NA&BT Division, and Dr. V. P. Venugopalan, Associate Director, Bioscience Group, BARC, for encouragement and support and Mr. A. D. Chavan for excellent technical assistance. The authors would like to thank Directors of Research, BCKVV, IGKV, and GBPUA&T, and Dr. B. P. Tripathi, KVK, Kawardha, for support. The authors are grateful to ICAR for including our formulation in All-India Coordinated trials. The work was carried out as part of an MoU between BARC and IGKV/BCKVV/GBPUA&T.

SUPPLEMENTARY MATERIAL

The Supplementary Material for this article can be found online at: https://www.frontiersin.org/articles/10.3389/fmicb.2019.01910/full#supplementary-material

REFERENCES

Ahmad, J. S., and Baker, R. (1988). Rhizosphere competence of benomyl-tolerant mutants of *Trichoderma* spp. *Can. J. Microbiol.* 34, 694–696. doi: 10.1139/m88-116

Atanasova, L., Druzhinina, I. S., and Jaklitsch, W. M. (2013). "Two hundred *Trichoderma* species recognized based on molecular phylogeny," in *Trichoderma: Biology and Application*, eds P. K. Mukherjee, B. A. Horwitz, U. S. Singh, M. Mukherjee, and M. Schmoll (Wallingford: CABI).

Bansal, R., Sherkhane, P. D., Oulkar, D., Khan, Z., Banerjee, K., and Mukherjee, P. K. (2018). The viridin biosynthesis gene cluster of *Trichoderma virens* and its conservancy in the bat white-nose fungus *Pseudogymnoascus destructans*. *ChemistrySelect* 3, 1289–1293. doi: 10.1002/slct.201703035

Carsolio, C., Benhamou, N., Haran, S., Cortés, C., Gutierrez, A., Chet, I., et al. (1999). Role of the *Trichoderma harzianum* endochitinase gene, ech42, in mycoparasitism. *Appl. Environ. Microbiol.* 65, 929–935.

Chaverri, P., Branco-Rocha, F., Jaklitsch, W., Gazis, R., Degenkolb, T., Samuels, G. J., et al. (2015). Systematics of the *Trichoderma harzianum* species complex and the re-identification of commercial biocontrol strains. *Mycologia* 10, 558–590. doi: 10.3852/14-147

Djonović, S., Pozo, M. J., Dangott, L. J., Howell, C. R., and Kenerley, C. M. (2006a). Sm1, a proteinaceous elicitor secreted by the bio control fungus *Trichoderma virens* induces plant defense responses and systemic resistance. *Mol. Plant Microbe Interact.* 19, 838–853. doi: 10.1094/mpmi-19-0838

Djonović, S., Pozo, M. J., and Kenerley, C. M. (2006b). Tvbgn3, a β-1, 6-glucanase from the biocontrol fungus *Trichoderma virens*, is involved in mycoparasitism and control of *Pythium ultimum*. *Appl. Environ. Microbiol.* 72, 7661–7670. doi: 10.1128/aem.01607-06

Djonović, S., Vargas, W. A., Kolomiets, M. V., Horndeski, M., Wiest, A., and Kenerley, C. M. (2007a). A proteinaceous elicitor Sm1 from the beneficial fungus *Trichoderma virens* is required for induced systemic resistance in maize. *Plant Physiol.* 145, 875–889. doi: 10.1104/pp.107.103689

Djonović, S., Vittone, G., Mendoza-Herrera, A., and Kenerley, C. M. (2007b). Enhanced biocontrol activity of *Trichoderma virens* transformants constitutively coexpressing β-1,3- and β-1,6-glucanase genes. *Mol. Plant Pathol.* 8, 469–480. doi: 10.1111/j.1364-3703.2007.00407.x

Gaderer, R., Lamdan, N. L., Frischmann, A., Sulyok, M., Krska, R., Horwitz, B. A., et al. (2015). Sm2, a paralog of the *Trichoderma* cerato-platanin elicitor Sm1, is also highly important for plant protection conferred by the fungal–root interaction of *Trichoderma* with maize. *BMC Microbiol.* 15:2. doi: 10.1186/s12866-014-0333-0

Guzmán-Guzmán, P., Alemán-Duarte, M. I., Delaye, L., Herrera-Estrella, A., and Olmedo-Monfil, V. (2017). Identification of effector-like proteins in *Trichoderma* spp. and role of a hydrophobin in the plant–fungus interaction and mycoparasitism. *BMC Genet.* 18:16. doi: 10.1186/s12863-017-0481-y

Haran, S., Schickler, H., and Chet, I. (1996). Molecular mechanisms of lytic enzymes involved in the biocontrol activity of *Trichoderma harzianum*. *Microbiology* 142, 2321–2331. doi: 10.1099/00221287-142-9-2321

Harman, G. E., and Uphoff, N. (2019). Symbiotic root-endophytic soil microbes improve crop productivity and provide environmental benefits. *Scientifica* 2019:9106395. doi: 10.1155/2019/9106395

Inbar, J., and Chet, I. (1995). The role of recognition in the induction of specific chitinases during mycoparasitism by *Trichoderma harzianum*. *Microbiology* 141, 2823–2829. doi: 10.1099/13500872-141-11-2823

Lamdan, N. L., Shalaby, S., Ziv, T., Kenerley, C. M., and Horwitz, B. A. (2015). Secretome of *Trichoderma* interacting with maize roots: role in induced systemic resistance. *Mol. Cell Proteom.* 14, 1054–1063. doi: 10.1074/mcp.M114.046607

Lorito, M., Woo, S. L., Harman, G. E., and Monte, E. (2010). Translational research on *Trichoderma*: from 'omics to the field. *Annu. Rev. Phytopathol.* 48, 395–417. doi: 10.1146/annurev-phyto-073009-114314

Mendoza-Mendoza, A., Zaid, R., Lawry, R., Hermosa, R., Monte, E., Horwitz, B. A., et al. (2018). Molecular dialogues between *Trichoderma* and roots: role of the fungal secretome. *Fun. Biol. Rev.* 32, 62–85. doi: 10.1016/j.fbr.2017.12.001

Mishra, A., and Malhotra, A. V. (2009). Tamarind xyloglucan: a polysaccharide with versatile application potential. *J. Mat. Chem.* 19, 8528–8536.

Morán-Diez, E., Hermosa, R., Ambrosino, P., Cardoza, R. E., Gutiérrez, S., Lorito, M., et al. (2009). The ThPG1 endopolygalacturonase is required for

the *Trichoderma harzianum*–plant beneficial interaction. *Mol. Plant Microbe Interact.* 22, 1021–1031. doi: 10.1094/MPMI-22-8-1021

Morán-Diez, M. E., Trushina, N., Lamdan, N. L., Rosenfelder, L., Mukherjee, P. K., Kenerley, C. M., et al. (2015). Host-specific transcriptomic pattern of *Trichoderma virens* during interaction with maize or tomato roots. *BMC Genom.* 16:8. doi: 10.1186/s12864-014-1208-3

Mukherjee, M., Horwitz, B. A., Sherkhane, P. D., Hadar, R., and Mukherjee, P. K. (2006). A secondary metabolite biosynthesis cluster in *Trichoderma virens*: evidence from analysis of genes under expressed in a mutant defective in morphogenesis and antibiotic production. *Curr. Genet.* 50, 193–202. doi: 10.1007/s00294-006-0075-0

Mukherjee, M., Mukherjee, P. K., and Kale, S. P. (2007). Camp signalling is involved in growth, germination, mycoparasitism and secondary metabolism in *Trichoderma virens*. *Microbiology* 153, 1734–1742. doi: 10.1099/mic.0.2007/005702-0

Mukherjee, P. K., Haware, M. P., and Raghu, K. (1997). Induction and evaluation of benomyl-tolerant mutants of *Trichoderma viride* for biological control of botrytis gray mold of chickpea. *Indian Phytopath.* 50, 107–111.

Mukherjee, P. K., Horwitz, B. A., Herrera-Estrella, A., Schmoll, M., and Kenerley, C. M. (2013). *Trichoderma* research in the genome era. *Ann. Rev. Phytopath.* 51, 105–129.

Mukherjee, P. K., and Mukhopadhyay, A. N. (1993). Induction of stable mutants of *Gliocladium virens* by gamma-irradiation. *Indian Phytopath.* 46, 393–397.

Mukherjee, P. K., Sherkhane, P. D., and Murthy, N. B. K. (1999). Induction of stable benomyl-tolerant phenotypic mutants of *Trichoderma pseudokoningii* MTCC 3011, and their evaluation for antagonistic and biocontrol potential. *Indian. J. Exp. Biol.* 37, 710–712.

Mukhopadhyay, A. N., Shrestha, S. M., and Mukherjee, P. K. (1992). Biological seed treatment for control of soil-borne plant pathogens. *FAO Plant Prot. Bull.* 40, 21–30.

Olejníková, P., Ondrusová, Z., Krystofová, S., and Hudecová, D. (2010). Benomyl-resistant mutant strain of *Trichoderma* sp. with increased mycoparasitic activity. *Folia Microbiol.* 55, 102–104. doi: 10.1007/s12223-010-0016-7

Papavizas, G. C., Lewis, J. A., and Moity, T. H. A. E. (1982). Evaluation of new biotypes of *Trichoderma harzianum* for tolerance to benomyl and enhanced biocontrol capabilities. *Phytopathologia* 72, 126–132.

Peterson, R., and Nevalainen, H. (2012). *Trichoderma reesei* RUT-C30—Thirty years of strain improvement. *Microbiology* 158, 58–68. doi: 10.1099/mic.0.054031-0

Przylucka, A., Akcapinar, G. B., Chenthamara, K., Cai, F., Grujic, M., Karpenko, J., et al. (2017). HFB7—A novel orphan hydrophobin of the harzianum and virens clades of *Trichoderma*, is involved in response to biotic and abiotic stresses. *Fungal Genet. Biol.* 102, 63–76. doi: 10.1016/j.fgb.2017.01.002

Ruocco, M., Lanzuise, S., Lombardi, N., Woo, S. L., Vinale, F., Marra, R., et al. (2015). Multiple roles and effects of a novel *Trichoderma* hydrophobin. *Mol. Plant. Microbe. Interact.* 28, 167–179. doi: 10.1094/MPMI-07-14-0194-R

Sherkhane, P. D., Bansal, R., Banerjee, K., Chatterjee, S., Oulkar, D., Jain, P., et al. (2017). Genomics-driven discovery of the gliovirin biosynthesis gene cluster in the plant beneficial fungus *Trichoderma Virens*. *ChemistrySelect.* 2, 3347–3352. doi: 10.1002/slct.201700262

Shoresh, M., Harman, G. E., and Mastouri, F. (2010). Induced systemic resistance and plant responses to fungal biocontrol agents. *Annu. Rev.Phytopathol.* 48, 21–43. doi: 10.1146/annurev-phyto-073009-114450

Szekeres, A., Hatvani, L., and Leitgeb, B. (2007). Colony morphology mutants of *Trichoderma harzianum* with increased beta-1,4-N-acetyl-glucosaminidase production. *Acta Microbiol. Immunol. Hung.* 54, 23–34. doi: 10.1556/amicr.54.2007.1.3

Viterbo, A. D. A., and Chet, I. (2006). TasHyd1, a new hydrophobin gene from the biocontrol agent *Trichoderma asperellum*, is involved in plant root colonization. *Mol. Plant. Pathol.* 7, 249–258. doi: 10.1111/j.1364-3703.2006.00335.x

Yu, C., Dou, K., Wang, S., Wu, Q., Ni, M., Zhang, T., et al. (2019). Elicitor hydrophobin Hyd1 interacts with ubiquilin1-like to induce maize systemic resistance. *Integr. Plant. Biol.* doi: 10.1111/jipb.12796 [Epub ahead of print].

Zaidi, N. W., and Singh, U. S. (2013). "*Trichoderma* in plant health management," in *Trichoderma: Biology and Applications*, eds P. K. Mukherjee, B. A. Horwitz, U. S. Singh, M. Mukherjee, and M. Schmoll (Wallingford: CABI).

Zeilinger, S., Gruber, S., Bansal, R., and Mukherjee, P. K. (2016). Secondary metabolism in *Trichoderma*–chemistry meets genomics. *Fungal Biol. Rev.* 30, 74–90. doi: 10.1016/j.fbr.2016.05.001

Zhang, H., Ji, S., Guo, R., Zhou, C., Wang, Y., Fan, H., et al. (2019). Hydrophobin HFBII-4 from *Trichoderma asperellum* induces antifungal resistance in poplar. *Braz. J. Microbiol.* 50, 603–612. doi: 10.1007/s42770-019-00083-5

Ziemons, S., Koutsantas, K., Becker, K., Dahlmann, T., and Kück, U. (2017). Penicillin production in industrial strain *Penicillium chrysogenum* P2niaD18 is not dependent on the copy number of biosynthesis genes. *BMC Biotechnol.* 17:16. doi: 10.1186/s12896-017-0335-8

Conflict of Interest Statement: The authors declare that the research was conducted in the absence of any commercial or financial relationships that could be construed as a potential conflict of interest.

frontiers in Microbiology

ORIGINAL RESEARCH
published: 04 September 2019
doi: 10.3389/fmicb.2019.02076

The pH Signaling Transcription Factor PAC-3 Regulates Metabolic and Developmental Processes in Pathogenic Fungi

Maíra Pompeu Martins[1], Nilce M. Martinez-Rossi[1], Pablo R. Sanches[1], Eriston Vieira Gomes[2], Maria Célia Bertolini[3], Wellington R. Pedersoli[1], Roberto Nascimento Silva[4] and Antonio Rossi[1]*

[1] Department of Genetics, Ribeirão Preto Medical School, University of São Paulo, Ribeirão Preto, Brazil, [2] Department of Biofunctional, Morgana Potrich College, Mineiros, Brazil, [3] Department of Biochemistry and Technological Chemistry, São Paulo State University, UNESP, Institute of Chemistry, Araraquara, Brazil, [4] Department of Biochemistry and Immunology, Ribeirão Preto Medical School, University of São Paulo, Ribeirão Preto, Brazil

The zinc finger transcription factor PAC-3/RIM101/PacC has a defined role in the secretion of enzymes and proteins in response to ambient pH, and also contributes to the virulence of species. Herein we evaluated the role of PAC-3 in the regulation of *Neurospora crassa* genes, in a model that examined the plant-fungi interactions. *N. crassa* is a model fungal species capable of exhibiting dynamic responses to its environment by employing endophytic or phytopathogenic behavior according to a given circumstance. Since plant growth and productivity are highly affected by pH and phosphorus (P) acquisition, we sought to verify the impact that induction of a Δ*pac-3* mutation would have under limited and sufficient Pi availability, while ensuring that the targeted physiological adjustments mimicked ambient pH and nutritional conditions required for efficient fungal growth and development. Our results suggest direct regulatory functions for PAC-3 in cell wall biosynthesis, homeostasis, oxidation-reduction processes, hydrolase activity, transmembrane transport, and modulation of genes associated with fungal virulence. Pi-dependent modulation was observed mainly in genes encoding for transporter proteins or related to cell wall development, thereby advancing the current understanding regarding colonization and adaptation processes in response to challenging environments. We have also provided comprehensive evidence that suggests a role for PAC-3 as a global regulator in plant pathogenic fungi, thus presenting results that have the potential to be applied to various types of microbes, with diverse survival mechanisms.

Keywords: ***Neurospora crassa*, mycorrhizal association, phytopathogen, inorganic orthophosphate, RNA-sequencing**

OPEN ACCESS

Edited by:
Santiago Gutierrez, Universidad de León, Spain

Reviewed by:
Pedro A. Casquero, Universidad de León, Spain
Rolf A. Prade, Oklahoma State University, United States
Arnaldo Videira, University of Porto, Portugal

****Correspondence:***
Nilce M. Martinez-Rossi
nmmrossi@usp.br

Specialty section:
This article was submitted to Plant Microbe Interactions, a section of the journal Frontiers in Microbiology

Received: *21 June 2019*
Accepted: *22 August 2019*
Published: *04 September 2019*

Citation:
Martins MP, Martinez-Rossi NM, Sanches PR, Gomes EV, Bertolini MC, Pedersoli WR, Silva RN and Rossi A (2019) The pH Signaling Transcription Factor PAC-3 Regulates Metabolic and Developmental Processes in Pathogenic Fungi. Front. Microbiol. 10:2076. doi: 10.3389/fmicb.2019.02076

INTRODUCTION

Soil nutrient cycling is primarily performed by microorganisms and serves to support plant development through the uptake of soil minerals and by facilitating the decomposition of organic matter. Phosphorus (P) acquisition and soil pH are two of the most influential factors affecting plant growth and productivity and are regulated primarily by the indigenous microbial

community. Moreover, studies have suggested that changes in the composition of the soil fungal community are strongly correlated with changes in soil pH, which subsequently controls the availability of carbon (C), nitrogen (N) and phosphorus (P) (Hinsinger, 2001; Kemmitt et al., 2006; Rousk et al., 2009; Zhang et al., 2016).

In the soil, P exists as inorganic orthophosphate (Pi), either as $H_2PO_4^-$ or HPO_4^{2-}, depending on the soil pH, or less commonly, as organic Pi (phytates). Uptake of P occurs via two distinct routes. The first is direct and occurs through plant roots. The second route is indirect and occurs via mycorrhizal symbiosis. Briefly, the host plant obtains P primarily from soil fungal partners supported by chemotropism, which is the ability of fungi to sense and grow toward a chemical gradient. The association with specialized soil fungi, and subsequent formation of mycorrhizal roots, serves to improve and increase the P content in plants. However, the beneficial effect afforded by the development of mycorrhizal symbiosis varies according to the fungal species involved (Hinsinger, 2001; Plassard et al., 2011; Johri et al., 2015; Turrà and Di Pietro, 2015).

Despite the importance of fungus-plant interactions, our current knowledge regarding the molecular regulation of these systems is rudimentary. However, recent advances have been made in the genomics of fungal model systems, which have contributed to our understanding of the cellular machinery responsible for regulating the chemoattraction of filamentous hyphae by plant roots, thereby enabling plants to forage for essential nutrients (Turrà and Di Pietro, 2015).

An example of a model for the study of plant-fungi interactions is the filamentous fungus *Neurospora crassa,* which has contributed significantly to the development of modern genomic studies. *N. crassa* grows on decaying plant material, and is capable of exhibiting endophytic or phytopathogenic behavior depending on the specific environmental circumstances (Kuo et al., 2014). Further, this fungal species has been shown to express defense- and pathogenicity-related genes including oxidoreductases and necrosis-inducing proteins (Leal et al., 2009; Kuo et al., 2014). It has also exhibited the ability to synthesize and secrete cellulases and hemicellulases, which function in the degradation of lignocellulosic material (Kuo et al., 2014; Kourist et al., 2015; Antonieto et al., 2017). Thus, *N. crassa* serves as a model organism for the investigation of a wide range of plant-fungal relationships.

The availability of P and the modulation of soil pH are important limiting factors in plant health and development, and thus, the ability to rapidly adapt to the environment via modulation of specific genes, is critical for efficient utilization of the available nutrients and overall survival. The transcription factor PAC-3, a new designation for *N. crassa* PacC (Virgilio et al., 2016), has a well-defined role in the pH-signaling pathway, and has also been shown to be required for virulence in specific plant pathogens, namely, *Penicillium digitatum* (Zhang et al., 2013), *Fusarium oxysporum* (Caracuel et al., 2003b), *Sclerotinia sclerotiorum* (Rollins, 2003), *Colletotrichum gloeosporioides* (Miyara et al., 2008), and *Colletotrichum acutatum* (You and Chung, 2007), thus suggesting a critical role for this protein in host-pathogen interactions.

Herein we present an overview of the effect induced following deletion of *pac-3* in *N. crassa* when cultivated in media containing low and high concentrations of Pi. Results from the Gene Ontology (GO) enrichment analysis indicated that the most highly modulated gene groups were integral to the membrane, or with associated with oxidation-reduction processes, hydrolase activity, and transmembrane transport.

Our results suggest potential regulatory mechanisms employed by *pac-3* in a ubiquitous filamentous fungus, thereby providing a comprehensive overview of genetic modulation in a model organism that is proficient in deconstruction of plant cell walls (Antonieto et al., 2017). These results, therefore, contribute to the understanding of possible mechanisms associated with plant-pathogen interactions.

MATERIALS AND METHODS

Neurospora crassa Strains and Culturing Conditions

The *N. crassa* Δ*pac-3* knockout strain (*pac-3*^{KO}) was generated by replacing the *pacC* open reading frame (ORF; NCU00090) with the bar gene from a *mus-52*^{KO} background strain. Gene knockout in the mutant strain was confirmed via polymerase chain reaction (PCR) using specific oligonucleotides (Cupertino et al., 2012). All strains were maintained on solid Vogel's Minimal (VM) medium supplemented with 2% sucrose at 30°C and pH 5.8 (Vogel, 1956).

Following 5 days (Δ*mus-52*) or 10 days (Δ*pac-3*) of culturing consisting of 3 days at 30°C in the dark and 2 (Δ*mus-52*) or 7 (Δ*pac-3*) days at room temperature in ambient light, conidia (approximately 10^7 cells/mL^{-1}) were germinated in an orbital shaker for 5 h at 30°C (200 rpm) in low- and high-Pi media (final concentrations, 10 μM or 10 mM Pi, respectively). Media was supplemented with 44 mM sucrose as the carbon source, and 50 mM of sodium citrate was used to adjust the pH to 5.4, as previously described (Nyc et al., 1966; Nahas et al., 1982; Gras et al., 2007). The mycelium was then harvested, frozen in liquid nitrogen, and stored at −80°C until RNA isolation was performed. All experiments were performed in three biological replicates.

RNA Extraction

Total RNA was isolated using TRIzol™ Reagent (Invitrogen, United States) according to manufacturer's instructions and treated with DNAse I, RNAse-free (Thermo Fisher, United States). The RNA concentration was quantified using a NanoDrop ND-1000 spectrophotometer (Thermo Fisher). RNA integrity was determined via agarose electrophoresis and by employing the Agilent Bioanalyzer platform 2100 (Agilent, United States).

RNA-Seq Data Analysis

Four cDNA libraries were sequenced (Δ*mus-52* and Δ*pac-3* strains, cultivated in media with high- or low-Pi concentration), with their respective biological triplicates to generate 100 bp

paired-end reads using an Illumina HiSeq 2000 sequencer (Illumina, United States). To assess the library quality prior to and after trimming, we used the FastQC software. To remove the sequencing bases from the end of the reads, we applied a minimum Phred score of 20. The genome of *N. crassa*[1] and the Bowtie2 software (Langmead and Salzberg, 2012) were then employed to map the filtered reads. The coverage and alignments of the transcripts were visually inspected using Integrative Genomics Viewer software (IGV) (Robinson et al., 2011; Thorvaldsdottir et al., 2012). After performing library alignment and quality filtering steps, read count values were obtained. Once the read count table was generated, differential expression and statistical analysis were performed using the DESeq2 Bioconductor package (Love et al., 2014).

We adjusted the *p*-value threshold set to 0.05 with a $\log_2$ fold change ±1.5 using the Benjamini-Hochberg procedure (Benjamini and Hochberg, 1995) to denote statistical significance in changes for a given gene's expression levels. Functional annotation was performed according to GO (Blake and Harris, 2008), using the Bast2GO software (Gotz et al., 2008). The BayGO algorithm was then applied to perform GO term enrichment (Vencio et al., 2006).

Validation of RNA-Seq by RT-qPCR

One microgram of total RNA, extracted from the fungal mycelia, was reverse transcribed into complementary DNA (cDNA) using the High Capacity cDNA Reverse Transcription Kit (Applied Biosystems, United States) according to manufacturer's instructions. The expression pattern for the selected genes was quantified via real-time quantitative reverse transcription polymerase chain reaction (qRT-PCR) using Power SYBR Green PCR Master Mix (Applied Biosystems) with the StepOnePlus Real-Time PCR System (Applied Biosystems) for 40 cycles. The initial denaturation step was performed at 50°C for 2 min and at 95°C for 10 min, followed by 40 cycles at 95°C for 15 s and 60°C for 1 min. Specific primer sequences used as well as the concentration in each reaction, and reaction efficiencies are presented in **Supplementary Table S1**. Two reference genes, namely, actin (NCU04173), and β-tubulin (NCU04054) were used as controls. Each gene had its relative expression level quantified using the Livak ($2^{-\Delta\Delta Ct}$) method (Livak and Schmittgen, 2001). We performed statistical analysis using Student *t*-tests with GraphPad Prism v. 5.1 software.

The Analysis of Putative PAC-3 Binding Sites *in silico*

The complete genome sequence of *N. crassa* OR74A was used to obtain the 5′upstream regions (1 kb) for each gene. The occurrence of the PAC-3 motif, 5′-GCCARG-3′, was determined using an *ad hoc* perl script.

[1]ftp://ftp.broadinstitute.org/pub/annotation/fungi/neurospora_crassa/assembly/NC12/

RESULTS

The Transcriptional Response of the *N. crassa* Δ*pac*-3-Mutant

Results from Bowtie2 analysis revealed that approximately 84–86% of the total high-quality reads were found to align with the reference genome of *N. crassa* (Langmead and Salzberg, 2012; **Supplementary Table S2**). Furthermore, we identified 145 DEGs that were modulated regardless of the Pi concentration, however, were responsive to deletion of *pac-3*; while 171 DEGs were found to be modulated concomitantly with the deletion of *pac-3* and with low-Pi availability. An additional 111 DEGs were found to be responsive to *pac-3* deletion and high-Pi concentration (**Figure 1**). For each condition analyzed, a list of all DEGs was generated and is presented in **Supplementary Table S3**.

An analysis of the relevant biological processes associated with the DEGs was conducted to increase the understanding of the functional categories affected by the deletion of *pac-3*. The most representative gene group in both Pi conditions was identified as being integral to membranes, followed by those that are related to oxidation-reduction processes. Genes related to hydrolase activity, transmembrane transport, cytoplasm, and nucleus were also significantly represented in both analyzed Pi conditions (**Figure 2**). Further, the most significantly affected DEGs in both nutritional conditions were plotted in a volcano plot, highlighting those genes with $\log_2$ fold change ≥ or ≤5.0 (**Supplementary Figure S1**).

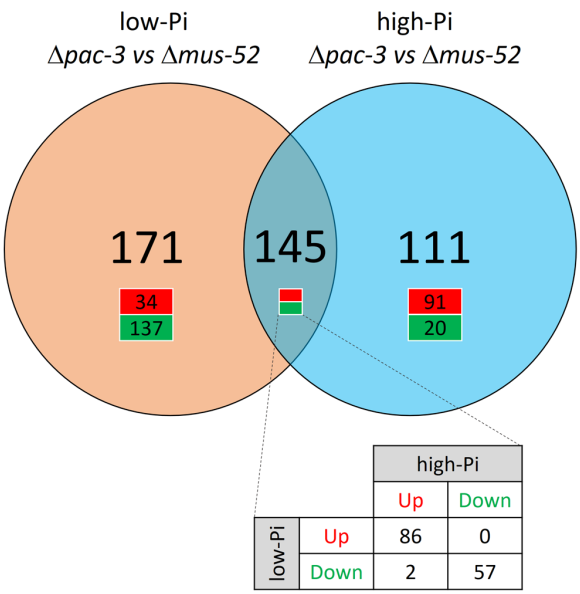

FIGURE 1 | Venn diagram indicating the number of DEGs identified in the mutant Δ*pac-3* strain (test) compared to the control (Δ*mus-52* strain) in media containing low-Pi (orange) and high-Pi (blue). The green color indicates down-regulated genes and the red color indicates up-regulated genes. Thresholds for the classification of DEGs were ($P < 0.05$), up-regulated: $\log_2$ (Fold Change) ≥1.5 or down-regulated: $\log_2$ (Fold Change) ≤−1.5.

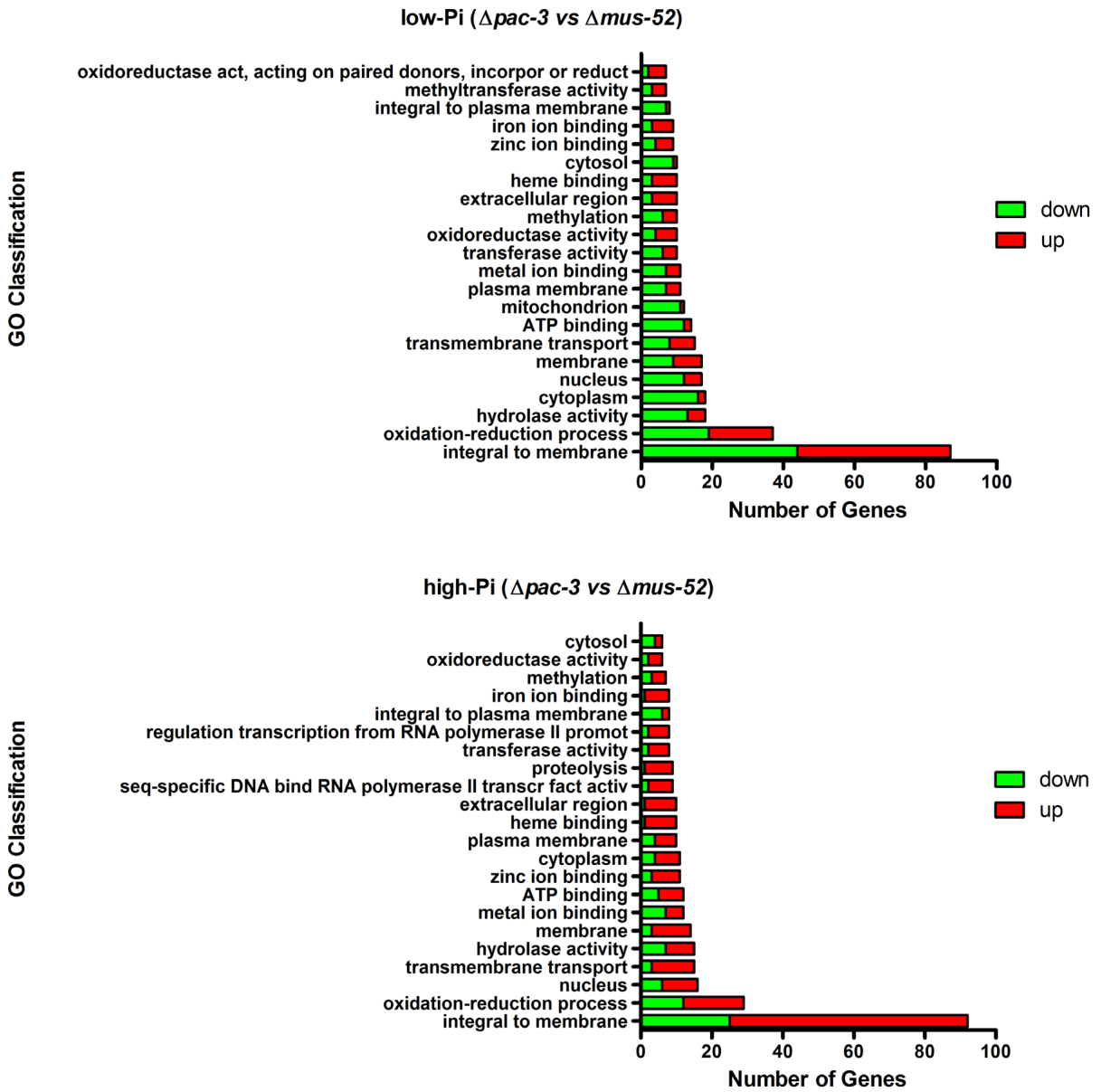

FIGURE 2 | Gene Ontology-based functional categorization of the most representative differentially expressed genes ($P < 0.05$). The red and green bars indicate the number of up- and down-regulated genes, respectively.

Modulation of Genes Identified as Integral to Membrane and Transmembrane Transport

A large high number of genes were identified as being modulated in response to both high- and low-Pi concentrations, thereby revealing a transcriptional response that was exclusive to the deletion of *pac-3*. Among these genes, the most highly up-regulated was the amino-acid permease INDA1 (NCU07129), which was modulated by approximately 200-fold ($\log_2$ = 7.82 in high- and 7.16 in low-Pi). Moreover, a high-affinity potassium transporter-1 (NCU00790), three hypothetical proteins (NCU06328, NCU08490, and NCU03240) and a sugar transporter (NCU07607) were also up-regulated in both Pi conditions.

Further, we assessed the repressive effects caused by deletion of *pac-3* in both Pi conditions. Most notably, different ATPase coding-genes, including the plasma membrane proton pump H^+-ATPase (E1-E2 ATPase-1; NCU05046), a P-type ATPase (NCU08147), and a calcium-transporting ATPase 3 (NCU07966), all of which have central roles in fungal physiology, were found to be down-regulated. Furthermore, *pac-3* deletion was seen to induce the repression of transporters for zinc/iron (NCU02879 and NCU06132), phosphorus (NCU08325 and NCU09564), and ammonium (NCU01065).

Influence of *pac*-3 in the Oxidation-Reduction Process

We determined that the catalase-3 (NCU00355) gene, along with other essential genes, including l-amino acid oxidase (NCU01066), a flavoprotein oxidoreductase (NCU06061), and an ornithine-N5-oxygenase (NCU07117), were repressed in both Pi conditions.

Among the genes that were up-regulated in response to *pac-3* deletion were an oxidoreductase (NCU00260), a polyketide synthase-3 (NCU04865), a norsolorinic acid reductase (NCU07723), a glutathione S-transferase-1 (NCU05780), the P-450-related genes (NCU05185, NCU09185, and NCU06327) and a dyp-type peroxidase (NCU09210).

Differentially Expressed Genes Associated With Hydrolase Activity

Our results revealed the down-regulation of a β-(1,3)-glucanosyltransferase gene (*gel1*; NCU07253), that codes for the GEL/GAS/PHR protein, in both low- and high-Pi conditions. The lipase (NCU03639) was also down-regulated in response to *pac-3* deletion. Alternatively, one metalloprotease (NCU07200) as well as members of the glycosyl hydrolase family (NCU07355, NCU08127, NCU04395, and NCU00130) were identified as up-regulated in both Pi conditions, along with.

Gene Modulation in Response to Pi Variation

NCU06351, which codes for a phytase-1 gene, was found to be down-regulated in conditions with high-Pi concentration. Alternatively, an alternate phytase gene, NCU03255, exhibited opposing modulation and was up-regulated. However, only phytase-1 possesses a binding motif for PAC-3 in its promoter region.

Among the several proteins modulated in response to low Pi concentration and *pac-3* deletion a large portion were identified as down-regulated while only a few were up-regulated. Specifically, we identified many genes encoding for proteins related to cell wall that were down-regulated, including a chitinase-1 protein (NCU02184), a GNAT family N-acetyltransferase (NCU04039), two non-anchored cell wall proteins, -3 and -6 (NCU07817 and NCU00586), and the glycosylhydrolase family 61-5 (NCU08760). Further, the hypothetical protein NCU01311 was determined to also be repressed, which gene is associated with pathogenesis, according to GO functional annotation. The asparagine synthetase 2 (NCU04303) was also found to be down-regulated in these experimental conditions. The genes that were identified as up-regulated in response to low Pi concentration were determined to be also be associated with the deletion of *pac*-3.

In conditions containing high Pi concentrations, a large proportion of the DEGs were identified as genes that encode for transporter proteins, specifically the ABC drug exporter AtrF (NCU08056), the multidrug resistance protein MDR (NCU07546), a major facilitator superfamily transporter (NCU06847), the MFS monocarboxylate transporter (NCU05089), and the MFS multidrug transporter (NCU06860). In high Pi conditions we observed significantly more induced genes than repressed, in response to *pac-3* deletion.

Modulated Genes Contained the Consensus Binding Motif for PAC-3

To determine which DEGs were directly or indirectly affected by the deletion of *pac-3*, we examined which DEGs contained PAC-3 binding motifs within their 1 kb promoter region. Of the total 427 identified DEGs, 231 contained potential motifs for PAC-3 binding, 85 of which (36.8%) were found within the low Pi conditions and 62 (26.84%) in high Pi conditions. Furthermore, 84 (36.36%) DEGs with the PAC-3 putative consensus-binding site (5′-GCCARG-3′) had their expression modulated in both low and high Pi concentrations. Conversely, 196 DEGs were modulated in response to the absence of the PAC-3 even without the binding motif in their promoter region, which suggests that either indirect regulation by PAC-3 occurred or there was a PAC-3 binding motif located outside the promoter region that was analyzed (1 kb). Among these DEGs, 86 (43.88%) and 49 (25%) were determined to be modulated in low and high Pi environments, respectively; while 61 DEGs (31.12%) were identified in both culture conditions simultaneously.

Validation of Gene Expression

Expression analysis by qRT-PCR for the 15 selected genes using independent RNA samples was employed to validate the RNA-seq data. The results from both experiments were compared to the $\log_2$ ratio between the Δ*pac-3* mutant and control strains (**Table 1** and **Figure 3**). The correlation between RNA-seq and qRT-PCR results, obtained from biological replicates, was determined to be strong and statistically significant (Pearson's correlation, $r = 0.953$, $P < 0.001$).

DISCUSSION

The transcription factor PAC-3 is critical component in the regulation of pH-responsive genes in fungi. As observed in various pathogenic fungi species, deletion of this transcription factor affects many cellular and molecular pathways thereby serving to interfere in the appropriate control of physiological processes essential for induction of pathogenesis (Rollins, 2003). *N. crassa* Δ*pac-3*-mutation negatively impacts on aerial hyphae growth, conidiation, and raises the production of dark pigment (Virgilio et al., 2016). These phenotypical disturbances suggest an important role for PAC-3/PacC in fungal infective success, as observed in a dermatophyte fungus (Ferreira-Nozawa et al., 2006). In *Aspergillus nidulans*, nutrient changes have been shown to modulate the transcription of the *pac-3* homolog gene, indicating the presence of interconnections between ambient pH, carbon availability, and Pi variance in a complex metabolic network (Trevisan et al., 2011; Rossi et al., 2013). Through the assessment of transcriptional changes arising from the deletion of *pac-3*, we evaluated the relevance of this transcription factor in the model fungal species *N. crassa*.

TABLE 1 | Validation of differentially expressed genes by real-time PCR (qPCR).

ID	Gene product name	GO classification	Low-Pi		High-Pi	
			RNA-seq	qPCR	RNA-seq	qPCR
NCU00282	Hypothetical protein	Seq-specific DNA binding RNA polymerase II transcr fact activity	3.89	2.69	4.34	4.91
NCU01386	Hypothetical protein	Zinc ion binding	–	0.53	1.50	0.97
NCU02879	Zinc/iron transporter	Zinc ion transmembrane transporter activity	−4.61	−3.52	−4.32	−3.63
NCU03107	MFS transporter		−1.79	−2.06	–	−0.51
NCU03921	Mitochondrial chaperone bcs1	ATP binding	−2.12	−4.14	2.15	1.74
NCU04197	CipC protein	Molecular function	6.62	6.64	8.44	6.52
NCU04912	HET domain-containing protein		1.94	1.50	2.21	0.94
NCU05308	Zn(II)2Cys6 transcription factor	Seq-specific DNA binding RNA polymerase II transcr fact activity	1.94	0.34	1.79	1.93
NCU06132	Siderophore iron transporter	Integral to plasma membrane	−2.98	−2.64	−2.09	−2.72
NCU06328	Hypothetical protein	Integral to membrane	4.12	3.52	4.43	4.67
NCU07253	1.3-beta-glucanosyltransferase gel1	Integral to membrane	−3.56	−0.69	−3.26	−3.33
NCU08325	Phosphorus-5	Integral to plasma membrane	−5.04	−5.75	−3.86	−5.34
NCU08726	Fluffy	Zinc ion binding	–	2.61	1.94	1.55
NCU09210	Dyp-type peroxidase	Heme binding	3.96	5.61	4.78	2.84
NCU09629	Hypothetical protein		−1.81	−3.41	2.12	1.77

(–) not modulated at the time point.

The Import and Export of Essential Substrates Requires PAC-3

The repression of specific genes that encode proteins related to membrane transport in both high and low Pi conditions revealed a regulatory role for PAC-3 in transmembrane transport activity. Specifically, the E1-E2 ATPase-1 (ENA1), the P-type ATPase, and the calcium-transporting ATPase 3 are P-type ATPases that are involved in the active transport of cations across cellular membranes (Moller et al., 1996). As was observed in *F. oxysporum,* a functional link exists between pH signaling and the expression of the gene encoding a P-type Na^+-ATPase. Moreover, at ambient alkaline pH, PacC serves to activate the P-Type Na^+-ATPase *ena1* gene. This is achieved through binding of the activated form of PacC to its cognate binding sites in the promoter of *ena1*, which results in the control of ion homeostasis, a determinant for Na^+ detoxification (Caracuel et al., 2003a).

We also determined that the ammonium transporter MEP2 was down-regulated in response to *pac-3* deletion. Since phytopathogenic fungi secrete ammonia to alkalinize the host tissue, reduced expression of MEP genes would function to directly impact fungal pathogenicity (Miyara et al., 2010).

Our results have also revealed that PAC-3 is involved in the effective transport of ions and in the homeostasis of fungal virulence. Specifically, we also observed down-regulation in the expression of a zinc/iron transporter, which is important in trafficking of metal ion substrates and in fungal homeostasis, and a siderophore-iron transporter, which functions in iron acquisition and is essential in both virulence and modulation of the plant immune system (Greenshields et al., 2007; Bailão et al., 2012; Albarouki et al., 2014). Further, expression of the H^+-coupled *pho84/pho-5* gene, which encodes a high affinity inorganic phosphate transporter that transports manganese, zinc, cobalt, and copper ions (Jensen et al., 2003), was found to be down-regulated following the deletion of *pac-3*.

The transport-regulatory activity associated with PAC-3 seems to impact the fungal-pathogen relationship, and also symbiotic fungal associations. ATPases are thought to contribute to the uptake of Pi and other nutrients from the symbiotic interface via proton symport (Johri et al., 2015). Moreover, the acquisition of N from the soil is dependent on ammonium transporters; while the internal concentration of ions such as calcium, are responsible for the regulation of rhizobial symbiosis (Hazledine et al., 2009; Bonfante and Genre, 2010). PAC-3 serves to regulate all of these transmembrane flux processes. Furthermore, all of the genes analyzed in our study contained the PAC-3 binding motif in their promoter regions, save for the P-type ATPase (NCU08147) and the siderophore-iron transporter (NCU06132) (**Supplementary Table S4**).

The high-affinity transporters pho84/pho-5 and pho89/pho-4, which have been described as having Na + /Pi symporter activity (Versaw, 1995), were found to be strongly down-regulated in our study. These results suggest that PAC-3 regulates the phosphate traffic in the cell. Similarly, the *PiPT* gene, which is a *pho84* phosphate transporter homolog, from the root of the endophytic fungus *Piriformospora indica*, was reported to actively transport phosphate to the hosting plant. Further, *PiPT* knockdown mutants resulted in detrimental effects to both fungal and host, indicating that these transporters function to ameliorate the nutritional status of the host plant (Yadav et al., 2010).

Among the DEGs that were identified as being up-regulated in response to the deletion of *pac-3*, one of the strongest modulations was observed in the amino-acid permease INDA1,

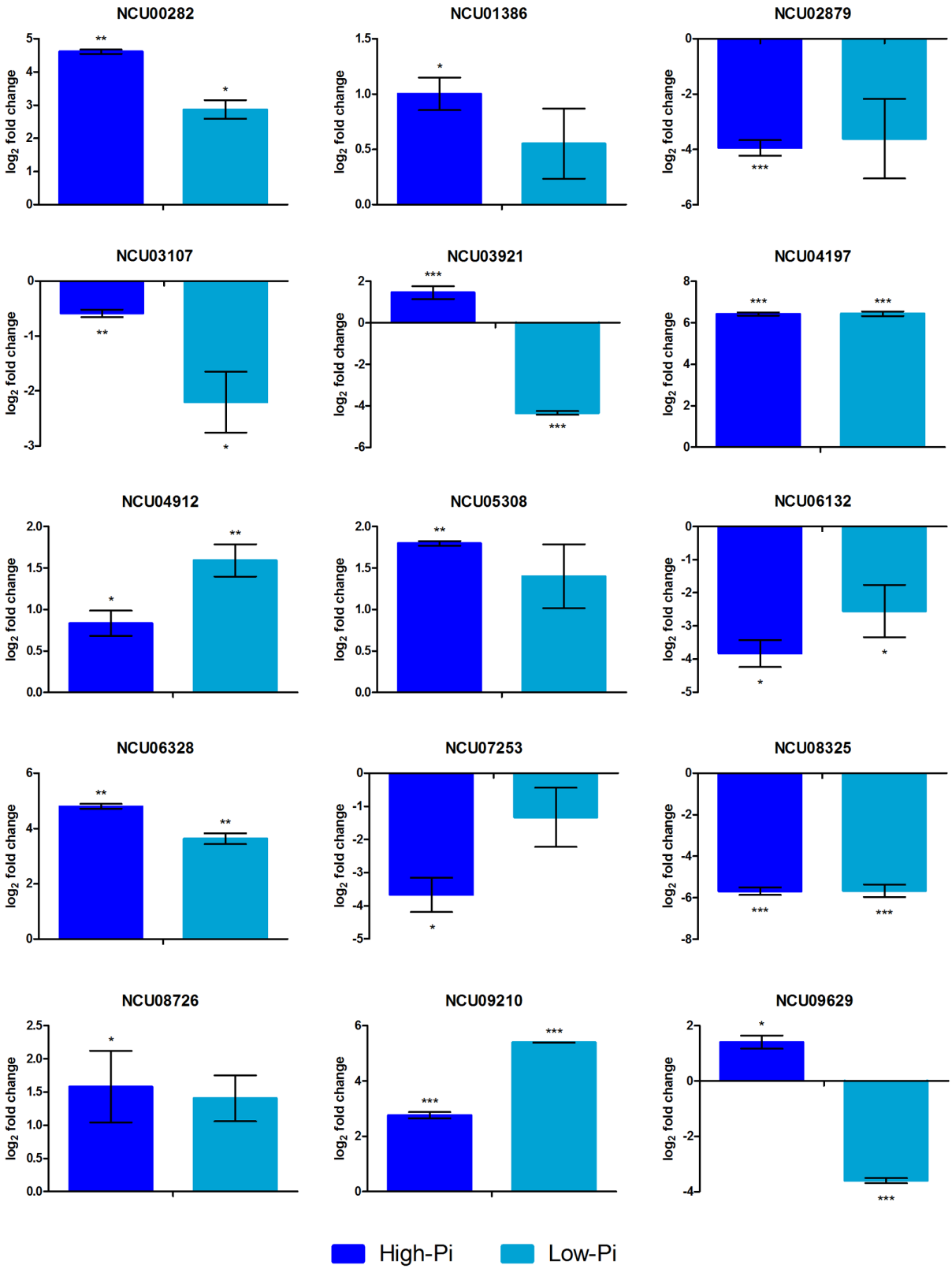

FIGURE 3 | Gene expression levels represented as $\log_2$-fold change comparing the mutant strain Δ*pac-3* (test) to the control (Δ*mus-52* strain) in media containing low and high Pi concentrations. Asterisks indicate statistical significance determined by Student's *t*-tests comparing treatment and control conditions at each time point (*$P < 0.05$; **$P < 0.01$; ***$P < 0.001$).

which has three PAC-3 binding sites within its promoter region (**Supplementary Table S4**). The transporter activity of INDA1, previously reported in *Trichoderma harzianum*, and expressed during development of *Rhizoctonia solani* cell walls, is thus an important factor in the mycoparasitic activity (Vasseur et al., 1995). Additionally, the expression of the high affinity potassium transporter-1, the hypothetical proteins NCU08490, with proposed Ca^{2+}/Cation antiporter activity, NCU06328, identified as the integral membrane protein *pth11* (Pare et al., 2012), and NCU03240, identified as a member of the glycosyltransferase family group 2 (Wang et al., 2015), as well as a sugar transporter were all identified as being up-regulated following deletion of *pac*-3, suggesting that PAC-3 serves to coordinate the efficient acquisition of nutrients and efflux of toxic compounds.

PAC-3 Is Involved in Secondary Metabolism, Detoxification, and Virulence

Sequencing of the *Neurospora* genome revealed several putative genes that encode proteins associated with secondary metabolite catabolism, including proteins from the polyketide synthase (PKS), non-ribosomal peptide-synthetase (NRPS) and terpenoid families (Galagan et al., 2003). Moreover, we identified DEGs whose putative products are strictly associated with fungal pathogenesis. We observed the up-regulation of the polyketide synthase-3, similar to the type I PKS from *Cochliobolus heterostrophus* (Bohnert et al., 2004), of a norsolorinic acid reductase, as well as the induction of an oxidoreductase gene, which are associated with the biosynthesis of aflatoxins, highly toxic and carcinogenic substances produced by specific fungi, including *Aspergillus flavus* and *Aspergillus parasiticus* (Yabe and Nakajima, 2004). These results suggest a role for PAC-3 in the regulation of secondary metabolism-related genes.

We also observed an up-regulation in the expression of glutathione S-transferase-1 (GST), which is associated with tolerance to oxidative stress and detoxification of a wide range of endogenous and environmental chemicals, thereby functioning to protect fungal species from plant-derived toxic metabolites. Thus, suggesting that there is an apparent regulatory effect exhibited by PAC-3 in fungal protection. GSTs are also essential for full aggressiveness of *Alternaria brassicicola* on the host plant, evidencing a role for PAC-3 in the regulation of fungal virulence (Calmes et al., 2015).

Genes that encode for the hypothetical protein NCU09185, which has potential pisatin demethylase cytochrome P450 activity, together with genes for benzoate 4-monooxygenase cytochrome P450, and a bifunctional P-450:NADPH-P450 reductase were found to be up-regulated in the absence of PAC-3. Moreover, the fungal cytochrome P450 systems are critical components in the primary and secondary metabolic pathways, and in the detoxification of xenobiotics in plant pathogenic fungi (Podobnik et al., 2008). Thus, the observed regulation via PAC-3 in *N. crassa* suggests a role for this transcription factor in plant-pathogen interactions.

A previous study has reported extracellular peroxidase activity in *Thanatephorus cucumeris*, capable of degrading lignin through the dyp-type peroxidase activity (Sugano, 2009). In our results, the up-regulation of a similar peroxidase that has been shown to be active in cellular oxidant detoxification, and to also be associated with enzymatic functions including hydrolase activity, demonstrates a potential role for PAC-3 in regulating the decomposition of extracellular compounds.

Deletion of *pac*-3 also resulted in the down-regulation of *cat3* gene, which encodes an enzyme essential for detoxification of reactive oxygen species (ROS) such as hydrogen peroxide (H_2O_2). Plants produce hydrogen peroxide as a mechanism of defense during pathogen interactions; thus, the observed repression in the expression of this catalase enzyme would affect the success of the pathogenic process (Tondo et al., 2010).

Furthermore, the down-regulation in the expression of L-amino acid oxidase, a flavoprotein that catalyzes the oxidative deamination of the L-amino acid α-amino group resulting in subsequent release of H_2O_2 and ammonia (Nuutinen and Timonen, 2008), suggests a perturbation in the fungal infection progress, since release of ammonia and H_2O_2 serves to propagate fungal spread.

Differential Hydrolase Activity Affects Virulence and Activates Compensatory Enzymes

Fungal pathogens secrete a myriad of extracellular enzymes, which are assumed to be involved propagating in host infection. Specifically, in *Fusarium graminearum,* a destructive pathogen of cereals, reduced extracellular lipolytic activity was seen to reduce virulence (Voigt et al., 2005). Herein, we revealed that repression of the hydrolytic-related encoding enzyme lipase, also suggests a role for PAC-3 in fungal virulence, thereby affecting host-fungal interactions.

The β-(1,3)-glucanosyltransferase gene (*gel1*), of the glycosyl hydrolase family GH72, was identified as significantly down-regulated in the Δ*pac-3* mutant in both low and high Pi cultures. This enzyme is related to cell wall biogenesis through the incorporation of nascent β−1,3−glucan molecules into the existing β−glucan network (Kamei et al., 2013). In *F. oxysporum,* the β-1,3-glucanosyltransferase (*gas1*) is required for virulence in tomato plants, and in *Candida albicans*, the orthologue gene (*PHR1*) was reported to be pH-regulated. These enzymes have crucial roles in cell wall assembly, thus serving to maintain hyphal growth and the maintenance of the morphological state, which is imperative for its adhesive and invasive pathogenic properties (Calderon et al., 2010). Our data, therefore, highlights the direct regulatory activity that PAC-3 has on cell wall integrity, which was supported by the presence of a PAC-3 consensus sequence in the *gel1* promoter region (**Supplementary Table S3**). As previously observed, Rim101/PacC is required for fungal virulence and functions to positively control cell wall functions in *C. albicans* (Nobile et al., 2008). Conversely, a different beta-1,3-glucanosyltransferase was found to be up-regulated in response to *pac-3* deletion. However, since *gel1* contains a PAC-3 motif in its promoter region,

and the other modulated glucanosyltransferase does not, we hypothesize that the up-regulation of this alternate enzyme is a means by which the fungus is compensating for the loss of PAC-3 function.

Among the up-regulated genes, we also identified an extracellular metalloprotease. In *Fusarium oxysporum f.* sp. *lycopersici,* a metalloprotease acts synergistically with a serine protease to cleave host chitinases thereby preventing their activity in the degradation of fungal cell wall (Jashni et al., 2015). Moreover, the hydrolytic activity of secreted proteases serves to promote the colonization and growth of the pathogen. Therefore, the induction of the metalloprotease gene suggests a protective function, acting to enhance fungal virulence thereby compensating for *pac-3* deletion.

Genes that code for glycosyl hydrolases were also found to be up-regulated as a consequence of *pac-3* deletion. Rim101/PacC have been previously shown to differentially regulate the expression of genes involved in the synthesis of specific cell wall components, including glycosyl hydrolases (Franco-Frias et al., 2014). The hydrolase-related genes found to be up-regulated in our study, may therefore, suggest the occurrence of noticeable changes in cell wall structure to compensate for the absence of PAC-3.

Deletion of *pac*-3 Modulates Genes According to Pi Availability

The predominant form of organic phosphorus present in soils is phytate, which must be dephosphorylated via phytase and phosphatase activity before being utilized by the plants. Plants naturally produce phytases (*myo*-inositol hexakisphosphate phosphohydrolases), however, the lack of adequate levels of extracellular phytases compromises the acquisition of phosphorous. Microorganisms, principally fungi, are capable of favoring phytate-phosphorus acquisition by plants (Wyss et al., 1999; Singh and Satyanarayana, 2011). Our results revealed down-regulation of the phytase-1 gene in environments with high-Pi, thereby confirming its phosphatase activity, which is unnecessary in the presence of free Pi. Moreover, the 3-phytase A gene was found to be up-regulated in high Pi conditions. However, only the phytase-1 protein was found to contain a PAC-3 binding motif in its promoter region and thus, the induction of a 3-phytase A gene, was not regulated by the presence of PAC-3 motif.

Further, the expression of the asparagine synthetase 2 (*asn−2*), which is a notoriously non-Pi−repressible gene, was found to be down-regulated in low Pi conditions in response to deletion of *pac-3*. This enzyme is involved in *de novo* biosynthesis of nucleotides and amino acids. Within an alternate study, similar patterns of repressiveness were observed in the Δ*mak−2* strain, irrespective of the supply of Pi (Gras et al., 2013; Mendes et al., 2016). Therefore, Pi-repressiveness is potentially affected by both *pac-3* and *mak−2* deletions in *N. crassa*.

Many of the DEGs found to be down-regulated in response to *pac*-3 deletion and low-Pi were those that encode proteins related to cell wall development, including chitinase-1, a member of the GNAT N-acetyltransferase family, the non-anchored cell wall proteins -3 and -6, and the glycosylhydrolase family 61-5. As demonstrated in various fungi, fungal development, cell wall-degradation, and virulence genes are regulated by PacC/Rim101 (Caracuel et al., 2003b; Rollins, 2003; Zhang et al., 2013; Franco-Frias et al., 2014). The Δ*pac-3* mutant revealed that PAC-3 also serves to mediate adaptations in *N. crassa* within Pi-restrictive conditions through changes in cell wall biosynthesis.

Conversely, in high Pi environments, we observed many up-regulated genes in response to both the Pi condition and the absence of PAC-3. Several up-regulated genes encoding for transporter proteins were identified as being associated with drug export, multidrug resistance, and monocarboxylate transport. *Neurospora* contains a notably high number of transporter systems, which function in the secretion of secondary metabolites, the regulation of resistance to plant-produced secondary metabolites or other toxic compounds, or in the flow of signaling molecules (Borkovich et al., 2004). Here, we identified a relationship between Pi active transport and *pac-3* deletion, thereby associating PAC-3 with Pi homeostasis.

CONCLUSION

We have generated a robust dataset, which advances our knowledge on regulatory mechanisms of PAC-3 within a fungus-host system. We found that in a mutually beneficial, symbiotic fungus-plant relationship (as occurs during interactions in mycorrhizal symbiosis) or during a pathogenic interaction, PAC-3 functions to regulate ambient pH while also affecting myriad of physiological functions, including adaptation to nutritional conditions, regulation of virulence, or regulating the transcription of genes associated with structural and metabolic features. Herein, we highlight the role of PAC-3 in Pi adaptation, acting as a critical regulator of environmental challenges. We hypothesize that the widespread regulatory activity of PAC-3 in fungal physiology indicates its role in the propagation of successful infections within hosts.

DATA AVAILABILITY

The RNA-seq data are available at the GEO database with accession number GSE132373.

AUTHOR CONTRIBUTIONS

MM performed the experimental procedures and drafted the manuscript. PS performed all computational and statistical analyses. EG supported the drafting of the manuscript. WP performed some experimental procedures. RS revised the manuscript. MB revised the manuscript and provided fungal lineages. AR and NM-R designed the project, supervised the research, and prepared the manuscript. All authors participated in data analysis and interpretation, read, critically revised the manuscript, and approved the final version.

FUNDING

The work was supported by grants from the Brazilian Funding Agencies: Research Support Foundation of São Paulo State (FAPESP; Grant No. 2014/03847-7, and Postdoctoral Fellowships No.2018/11319-1, and No. 2016/04274-6), the National Council for Scientific and Technological Development – CNPq (Grant Nos. 305252/2013-5 and 304222/2013-5), Coordination for the Improvement of Higher Education Personnel – CAPES (Finance Code 001), and Foundation for Support to Teaching, Research and Assistance – FAEPA of the HCFMRP-USP.

ACKNOWLEDGMENTS

We thank C. A. Vieira and S. H. Castrechini for technical assistance.

SUPPLEMENTARY MATERIAL

The Supplementary Material for this article can be found online at: https://www.frontiersin.org/articles/10.3389/fmicb.2019.02076/full#supplementary-material

REFERENCES

Albarouki, E., Schafferer, L., Ye, F., Von Wiren, N., Haas, H., and Deising, H. B. (2014). Biotrophy-specific downregulation of siderophore biosynthesis in *Colletotrichum graminicola* is required for modulation of immune responses of maize. *Mol. Microbiol.* 92, 338–355. doi: 10.1111/mmi.12561

Antonieto, A. C. C., Pedersoli, W. R., Dos Santos Castro, L., Da Silva Santos, R., Cruz, A. H., Nogueira, K. M., et al. (2017). Deletion of pH regulator pac-3 affects cellulase and xylanase activity during sugarcane bagasse degradation by *Neurospora crassa*. *PLoS One* 12:e0169796. doi: 10.1371/journal.pone.0169796

Bailão, E. F. L. C., Parente, A. F. A., Parente, J. A., Silva-Bailão, M. G., De Castro, K. P., Kmetzsch, L., et al. (2012). Metal acquisition and homeostasis in fungi. *Curr. Fungal Infect. Rep*. 6, 257–266.

Benjamini, Y., and Hochberg, Y. (1995). Controlling the false discovery rate: a practical and powerful approach to multiple testing. *J. R. Stat. Soc. Ser. B* 57, 289–300.

Blake, J. A., and Harris, M. A. (2008). The gene ontology (GO) project: structured vocabularies for molecular biology and their application to genome and expression analysis. *Curr. Protoc. Bioinformatics* Chapter 7, Unit7.2. doi: 10.1002/0471250953.bi0702s23

Bohnert, H. U., Fudal, I., Dioh, W., Tharreau, D., Notteghem, J. L., and Lebrun, M. H. (2004). A putative polyketide synthase/peptide synthetase from *Magnaporthe grisea* signals pathogen attack to resistant rice. *Plant Cell* 16, 2499–2513.

Bonfante, P., and Genre, A. (2010). Mechanisms underlying beneficial plant-fungus interactions in mycorrhizal symbiosis. *Nat. Commun.* 1:48. doi: 10.1038/ncomms1046

Borkovich, K. A., Alex, L. A., Yarden, O., Freitag, M., Turner, G. E., Read, N. D., et al. (2004). Lessons from the genome sequence of *Neurospora crassa*: tracing the path from genomic blueprint to multicellular organism. *Microbiol. Mol. Biol. Rev.* 68, 1–108.

Calderon, J., Zavrel, M., Ragni, E., Fonzi, W. A., Rupp, S., and Popolo, L. (2010). PHR1, a pH-regulated gene of *Candida albicans* encoding a glucan-remodelling enzyme, is required for adhesion and invasion. *Microbiology* 156, 2484–2494. doi: 10.1099/mic.0.038000-0

Calmes, B., Morel-Rouhier, M., Bataille-Simoneau, N., Gelhaye, E., Guillemette, T., and Simoneau, P. (2015). Characterization of glutathione transferases involved in the pathogenicity of *Alternaria brassicicola*. *BMC Microbiol.* 15:123. doi: 10.1186/s12866-015-0462-0

Caracuel, Z., Casanova, C., Roncero, M. I., Di Pietro, A., and Ramos, J. (2003a). pH response transcription factor PacC controls salt stress tolerance and expression of the P-Type Na+ -ATPase Ena1 in *Fusarium oxysporum*. *Eukaryot Cell* 2, 1246–1252.

Caracuel, Z., Roncero, M. I. G., Espeso, E. A., González-Verdejo, C. I., García-Maceira, F. I., and Di Pietro, A. (2003b). The pH signalling transcription factor PacC controls virulence in the plant pathogen *Fusarium oxysporum*. *Mol. Microbiol.* 48, 765–779.

Cupertino, F. B., Freitas, F. Z., De Paula, R. M., and Bertolini, M. C. (2012). Ambient pH controls glycogen levels by regulating glycogen synthase gene expression in *Neurospora crassa*. New insights into the pH signaling pathway. *PLoS One* 7:e44258. doi: 10.1371/journal.pone.0044258

Ferreira-Nozawa, M. S., Silveira, H. C., Ono, C. J., Fachin, A. L., Rossi, A., and Martinez-Rossi, N. M. (2006). The pH signaling transcription factor PacC mediates the growth of *Trichophyton rubrum* on human nail *in vitro*. *Med. Mycol.* 44, 641–645.

Franco-Frias, E., Ruiz-Herrera, J., and Arechiga-Carvajal, E. T. (2014). Transcriptomic analysis of the role of Rim101/PacC in the adaptation of *Ustilago maydis* to an alkaline environment. *Microbiology* 160, 1985–1998. doi: 10.1099/mic.0.076216-0

Galagan, J. E., Calvo, S. E., Borkovich, K. A., Selker, E. U., Read, N. D., Jaffe, D., et al. (2003). The genome sequence of the filamentous fungus *Neurospora crassa*. *Nature* 422, 859–868.

Gotz, S., Garcia-Gomez, J. M., Terol, J., Williams, T. D., Nagaraj, S. H., Nueda, M. J., et al. (2008). High-throughput functional annotation and data mining with the Blast2GO suite. *Nucleic Acids Res.* 36, 3420–3435. doi: 10.1093/nar/gkn176

Gras, D. E., Persinoti, G. F., Peres, N. T., Martinez-Rossi, N. M., Tahira, A. C., Reis, E. M., et al. (2013). Transcriptional profiling of *Neurospora crassa* Δ*mak-2* reveals that mitogen-activated protein kinase MAK-2 participates in the phosphate signaling pathway. *Fungal Genet. Biol.* 60, 140–149.

Gras, D. E., Silveira, H. C., Martinez-Rossi, N. M., and Rossi, A. (2007). Identification of genes displaying differential expression in the nuc-2 mutant strain of the mold *Neurospora crassa* grown under phosphate starvation. *FEMS Microbiol. Lett.* 269, 196–200.

Greenshields, D. L., Liu, G., and Wei, Y. (2007). Roles of iron in plant defence and fungal virulence. *Plant Signal. Behav.* 2, 300–302.

Hazledine, S., Sun, J., Wysham, D., Downie, J. A., Oldroyd, G. E., and Morris, R. J. (2009). Nonlinear time series analysis of nodulation factor induced calcium oscillations: evidence for deterministic chaos? *PLoS One* 4:e6637. doi: 10.1371/journal.pone.0006637

Hinsinger, P. (2001). Bioavailability of soil inorganic P in the rhizosphere as affected by root-induced chemical changes: a review. *Plant Soil* 237, 173–195.

Jashni, M. K., Dols, I. H., Iida, Y., Boeren, S., Beenen, H. G., Mehrabi, R., et al. (2015). Synergistic action of a metalloprotease and a serine protease from *Fusarium oxysporum* f. *sp. lycopersici* cleaves chitin-binding tomato chitinases, reduces their antifungal activity, and enhances fungal virulence. *Mol. Plant Microbe Interact.* 28, 996–1008. doi: 10.1094/MPMI-04-15-0074-R

Jensen, L. T., Ajua-Alemanji, M., and Culotta, V. C. (2003). The *Saccharomyces cerevisiae* high affinity phosphate transporter encoded by PHO84 also functions in manganese homeostasis. *J. Biol. Chem.* 278, 42036–42040.

Johri, A. K., Oelmuller, R., Dua, M., Yadav, V., Kumar, M., Tuteja, N., et al. (2015). Fungal association and utilization of phosphate by plants: success, limitations, and future prospects. *Front. Microbiol.* 6:984. doi: 10.3389/fmicb.2015.00984

Kamei, M., Yamashita, K., Takahashi, M., Fukumori, F., Ichiishi, A., and Fujimura, M. (2013). Deletion and expression analysis of beta-(1,3)-glucanosyltransferase genes in *Neurospora crassa*. *Fungal Genet. Biol.* 52, 65–72. doi: 10.1016/j.fgb.2012.12.001

Kemmitt, S. J., Wright, D., Goulding, K. W. T., and Jones, D. L. (2006). pH regulation of carbon and nitrogen dynamics in two agricultural soils. *Soil Biol. Biochem.* 38, 898–911.

Kourist, R., Bracharz, F., Lorenzen, J., Kracht, O. N., Chovatia, M., Daum, C., et al. (2015). Genomics and transcriptomics analyses of the oil-accumulating basidiomycete yeast *Trichosporon oleaginosus*: insights into substrate utilization and alternative evolutionary trajectories of fungal mating systems. *mBio* 6:e00918. doi: 10.1128/mBio.00918-15

Kuo, H. C., Hui, S., Choi, J., Asiegbu, F. O., Valkonen, J. P., and Lee, Y. H. (2014). Secret lifestyles of *Neurospora crassa*. *Sci. Rep.* 4:5135. doi: 10.1038/srep05135

Langmead, B., and Salzberg, S. L. (2012). Fast gapped-read alignment with Bowtie 2. *Nat Methods* 9, 357–359. doi: 10.1038/nmeth.1923

Leal, J., Squina, F. M., Freitas, J. S., Silva, E. M., Ono, C. J., Martinez-Rossi, N. M., et al. (2009). A splice variant of the *Neurospora crassa* hex-1 transcript, which encodes the major protein of the Woronin body, is modulated by extracellular phosphate and pH changes. *FEBS Lett.* 583, 180–184. doi: 10.1016/j.febslet.2008.11.050

Livak, K. J., and Schmittgen, T. D. (2001). Analysis of relative gene expression data using real-time quantitative PCR and the 2-ΔΔCT Method. *Methods* 25, 402–408.

Love, M. I., Huber, W., and Anders, S. (2014). Moderated estimation of fold change and dispersion for RNA-seq data with DESeq2. *Genome Biol.* 15:550.

Mendes, N. S., Silva, P. M., Silva-Rocha, R., Martinez-Rossi, N. M., and Rossi, A. (2016). Pre-mRNA splicing is modulated by antifungal drugs in the filamentous fungus *Neurospora crassa*. *FEBS Open Bio* 6, 358–368. doi: 10.1002/2211-5463.12047

Miyara, I., Shafran, H., Davidzon, M., Sherman, A., and Prusky, D. (2010). pH Regulation of ammonia secretion by *Colletotrichum gloeosporioides* and its effect on appressorium formation and pathogenicity. *Mol. Plant Microbe Interact.* 23, 304–316. doi: 10.1094/MPMI-23-3-0304

Miyara, I., Shafran, H., Kramer Haimovich, H., Rollins, J., Sherman, A., and Prusky, D. (2008). Multi-factor regulation of pectate lyase secretion by *Colletotrichum gloeosporioides* pathogenic on avocado fruits. *Mol. Plant Pathol.* 9, 281–291. doi: 10.1111/j.1364-3703.2007.00462.x

Moller, J. V., Juul, B., and Le Maire, M. (1996). Structural organization, ion transport, and energy transduction of P-type ATPases. *Biochim. Biophys. Acta* 1286, 1–51.

Nahas, E., Terenzi, H. F., and Rossi, A. (1982). Effect of carbon source and pH on the production and secretion of acid-phosphatase (EC3.1.3.2) and alkaline-phosphatase (EC3.1.3.1) in *Neurospora crassa*. *J. Gen. Microbiol.* 128, 2017–2021.

Nobile, C. J., Solis, N., Myers, C. L., Fay, A. J., Deneault, J. S., Nantel, A., et al. (2008). *Candida albicans* transcription factor Rim101 mediates pathogenic interactions through cell wall functions. *Cell Microbiol.* 10, 2180–2196. doi: 10.1111/j.1462-5822.2008.01198.x

Nuutinen, J. T., and Timonen, S. (2008). Identification of nitrogen mineralization enzymes, L-amino acid oxidases, from the ectomycorrhizal fungi *Hebeloma* spp. *and Laccaria bicolor*. *Mycol. Res.* 112, 1453–1464. doi: 10.1016/j.mycres.2008.06.023

Nyc, J. F., Kadner, R. J., and Crocken, B. J. (1966). A repressible alkaline phosphatase in *Neurospora crassa*. *J. Biol. Chem.* 241, 1468–1472.

Pare, A., Kim, M., Juarez, M. T., Brody, S., and Mcginnis, W. (2012). The functions of grainy head-like proteins in animals and fungi and the evolution of apical extracellular barriers. *PLoS One* 7:e36254. doi: 10.1371/journal.pone.0036254

Plassard, C., Louche, J., Ali, M. A., Duchemin, M., Legname, E., and Cloutier-Hurteau, B. (2011). Diversity in phosphorus mobilisation and uptake in ectomycorrhizal fungi. *Ann. For. Sci.* 68, 33–43.

Podobnik, B., Stojan, J., Lah, L., Krasevec, N., Seliskar, M., Rizner, T. L., et al. (2008). CYP53A15 of *Cochliobolus lunatus*, a target for natural antifungal compounds. *J. Med. Chem.* 51, 3480–3486. doi: 10.1021/jm800030e

Robinson, J. T., Thorvaldsdottir, H., Winckler, W., Guttman, M., Lander, E. S., Getz, G., et al. (2011). Integrative genomics viewer. *Nat. Biotechnol.* 29, 24–26.

Rollins, J. A. (2003). The *Sclerotinia sclerotiorum pac1* gene is required for sclerotial development and virulence. *Mol. Plant Microbe Interact.* 16, 785–795.

Rossi, A., Cruz, A. H., Santos, R. S., Silva, P. M., Silva, E. M., Mendes, N. S., et al. (2013). Ambient pH sensing in filamentous fungi: pitfalls in elucidating regulatory hierarchical signaling networks. *IUBMB Life* 65, 930–935. doi: 10.1002/iub.1217

Rousk, J., Brookes, P. C., and Baath, E. (2009). Contrasting soil pH effects on fungal and bacterial growth suggest functional redundancy in carbon mineralization. *Appl. Environ. Microbiol.* 75, 1589–1596. doi: 10.1128/AEM.02775-08

Singh, B., and Satyanarayana, T. (2011). Microbial phytases in phosphorus acquisition and plant growth promotion. *Physiol. Mol. Biol. Plants* 17, 93–103. doi: 10.1007/s12298-011-0062-x

Sugano, Y. (2009). DyP-type peroxidases comprise a novel heme peroxidase family. *Cell Mol. Life Sci.* 66, 1387–1403. doi: 10.1007/s00018-008-8651-8

Thorvaldsdottir, H., Robinson, J. T., and Mesirov, J. P. (2012). Integrative genomics viewer (IGV): high-performance genomics data visualization and exploration. *Brief Bioinformatics* 14, 178–192. doi: 10.1093/bib/bbs017

Tondo, M. L., Petrocelli, S., Ottado, J., and Orellano, E. G. (2010). The monofunctional catalase KatE of *Xanthomonas axonopodis* pv. *citri* is required for full virulence in citrus plants. *PLoS One* 5:e10803. doi: 10.1371/journal.pone.0010803

Trevisan, G. L., Oliveira, E. H., Peres, N. T., Cruz, A. H., Martinez-Rossi, N. M., and Rossi, A. (2011). Transcription of *Aspergillus nidulans* pacC is modulated by alternative RNA splicing of palB. *FEBS Lett.* 585, 3442–3445. doi: 10.1016/j.febslet.2011.09.037

Turrà, D., and Di Pietro, A. (2015). Chemotropic sensing in fungus–plant interactions. *Curr. Opin. Plant Biol.* 26, 135–140.

Vasseur, V., Van Montagu, M., and Goldman, G. H. (1995). *Trichoderma harzianum* genes induced during growth on *Rhizoctonia solani* cell walls. *Microbiology* 141(Pt 4), 767–774.

Vencio, R. Z., Koide, T., Gomes, S. L., and Pereira, C. A. (2006). BayGO: bayesian analysis of ontology term enrichment in microarray data. *BMC Bioinformatics* 7:86.

Versaw, W. K. (1995). A phosphate-repressible, high-affinity phosphate permease is encoded by the pho-5+ gene of *Neurospora crassa*. *Gene* 153, 135–139.

Virgilio, S., Cupertino, F. B., Bernardes, N. E., Freitas, F. Z., Takeda, A. A., Fontes, M. R., et al. (2016). Molecular components of the *Neurospora crassa* pH signaling pathway and their regulation by pH and the PAC-3 transcription factor. *PLoS One* 11:e0161659. doi: 10.1371/journal.pone.0161659

Vogel, H. J. (1956). A convenient growth medium for *Neurospora crassa* (medium N). *Microb. Genet. Bull.* 13, 42–43.

Voigt, C. A., Schafer, W., and Salomon, S. (2005). A secreted lipase of *Fusarium graminearum* is a virulence factor required for infection of cereals. *Plant J.* 42, 364–375.

Wang, K., Zhang, Z., Chen, X., Sun, X., Jin, C., Liu, H., et al. (2015). Transcription factor ADS-4 regulates adaptive responses and resistance to antifungal azole stress. *Antimicrob. Agents Chemother.* 59, 5396–5404. doi: 10.1128/AAC.00542-15

Wyss, M., Pasamontes, L., Friedlein, A., Remy, R., Tessier, M., Kronenberger, A., et al. (1999). Biophysical characterization of fungal phytases (*myo*-inositol hexakisphosphate phosphohydrolases): molecular size, glycosylation pattern, and engineering of proteolytic resistance. *Appl. Environ. Microbiol.* 65, 359–366.

Yabe, K., and Nakajima, H. (2004). Enzyme reactions and genes in aflatoxin biosynthesis. *Appl. Microbiol. Biotechnol.* 64, 745–755.

Yadav, V., Kumar, M., Deep, D. K., Kumar, H., Sharma, R., Tripathi, T., et al. (2010). A phosphate transporter from the root endophytic fungus *Piriformospora indica* plays a role in phosphate transport to the host plant. *J. Biol. Chem.* 285, 26532–26544. doi: 10.1074/jbc.M110.111021

You, B.-J., and Chung, K.-R. (2007). Phenotypic characterization of mutants of the citrus pathogen *Colletotrichum acutatum* defective in a PacC-mediated pH regulatory pathway. *FEMS Microbiol. Lett.* 277, 107–114.

Zhang, T., Sun, X., Xu, Q., Candelas, L. G. L., and Li, H. (2013). The pH signaling transcription factor PacC is required for full virulence in *Penicillium digitatum*. *Appl. Microbiol. Biotechnol.* 97, 9087–9098. doi: 10.1007/s00253-013-5129-x

Zhang, T., Wang, N.-F., Liu, H.-Y., Zhang, Y.-Q., and Yu, L.-Y. (2016). Soil pH is a key determinant of soil fungal community composition in the Ny-Ålesund region, svalbard (High Arctic). *Front. Microbiol.* 7:227. doi: 10.3389/fmicb.2016.00227

Conflict of Interest Statement: The authors declare that the research was conducted in the absence of any commercial or financial relationships that could be construed as a potential conflict of interest.

frontiers in Microbiology

ORIGINAL RESEARCH
published: 25 October 2019
doi: 10.3389/fmicb.2019.02444

Early Root Transcriptomic Changes in Wheat Seedlings Colonized by *Trichoderma harzianum* Under Different Inorganic Nitrogen Supplies

*M. Belén Rubio[1], A. Emilio Martínez de Alba[1], Carlos Nicolás[2], Enrique Monte[1] and Rosa Hermosa[1]**

[1] Department of Microbiology and Genetics, Spanish-Portuguese Institute for Agricultural Research (CIALE), University of Salamanca, Salamanca, Spain, [2] Department of Botany and Plant Pathology, Spanish-Portuguese Institute for Agricultural Research (CIALE), University of Salamanca, Salamanca, Spain

Wheat is one of the most important crops worldwide. The use of plant growth promoting microorganisms, such as those of the genus *Trichoderma,* constitutes an alternative to chemical fertilizers, since they are cheaper and are not detrimental to the environment. However, the interaction between *Trichoderma* and wheat plants has been scarcely studied, at least at a molecular level. In the present work, a microarray approach was used to study the early transcriptomic changes induced in wheat roots by *Trichoderma harzianum,* applied alone or in combination with different concentrations of calcium nitrate [$Ca(NO_3)_2$], which was last used as nitrogen (N) source. Our results show that *T. harzianum* causes larger transcriptomic changes than $Ca(NO_3)_2$ in wheat roots, and such changes are different when plants are challenged with *Trichoderma* alone or treated with a combination of *T. harzianum* and $Ca(NO_3)_2$. Overall, *T. harzianum* activates the expression of defense-related genes at early stages of the interaction with the roots, while this fungus reduces the expression of genes related to plant growth and development. Moreover, the current study in wheat roots, subjected to the different *T. harzianum* and $Ca(NO_3)_2$ combinations, reveals that the number of transcriptomic changes was higher when compared against those caused by the different $Ca(NO_3)_2$ concentrations than when it was compared against those caused by *T. harzianum*. N metabolism gene expression changes were in agreement with the levels of nitrate reductase activity measured in plants from *Trichoderma* plus $Ca(NO_3)_2$ conditions. Results were also concordant with plant phenotypes, which showed reduced growth at early interaction stages when inoculated with *T. harzianum* or with its combination with $Ca(NO_3)_2$ at the lowest dosage. These results were in a good agreement with the recognized role of *Trichoderma* as an inducer of plant defense.

Keywords: Wheat Genome Array, plant defense, plant growth, *Trichoderma*, chemical fertilization, nitrogen use

OPEN ACCESS

Edited by:
Francesco Vinale, University of Naples Federico II, Italy

Reviewed by:
Walter Alberto Vargas, National Scientific and Technical Research Council (CONICET), Argentina
Artemio Mendoza-Mendoza, Lincoln University, New Zealand

****Correspondence:***
Rosa Hermosa
rhp@usal.es

Specialty section:
This article was submitted to Microbial Symbioses, a section of the journal Frontiers in Microbiology

Received: *31 July 2019*
Accepted: *10 October 2019*
Published: *25 October 2019*

Citation:
Rubio MB, Martínez de Alba AE, Nicolás C, Monte E and Hermosa R (2019) Early Root Transcriptomic Changes in Wheat Seedlings Colonized by Trichoderma harzianum Under Different Inorganic Nitrogen Supplies. Front. Microbiol. 10:2444. doi: 10.3389/fmicb.2019.02444

INTRODUCTION

Wheat (*Triticum aestivum* L.) is one of the most important crops on Earth, with an area harvested of 220 million ha and a global production of 770 million tons, China and India being the major producers followed by Russia and United States (FAOSTAT, 2018). It is considered to be the most important food grain source for humans, providing about a 19% of the total calories consumed

by humans, as well as representing a 20% of proteins in the human diet (Botha et al., 2017; International Wheat Genome Sequencing Consortium [IWGSC], 2018). Wheat flour is used for the production of bread, pasta, biscuits and other bakery and industrial products.

Nitrogen (N) is the most important nutrient for plants and, after water, is the major limiting factor for their growth and development. Thus, in modern extensive agriculture, the application of N fertilizer is a common practice, aiming to increase production and achieve maximum yields in many crops (Rockström et al., 2009). There is an absolute requirement of N for wheat growth, and crop yield and quality depend upon substantial N inputs (Vicente et al., 2016; Zörb et al., 2018). However, it is well known that the most diffused cereal crops, like wheat, rice and maize, use only 30–40% of the applied N fertilizers, while the rest remains unused causing severe environmental pollution (Curci et al., 2017). It has been reported that the human processes -primarily the manufacture of fertilizer for food production- have converted around 120 million tons of N_2 from the atmosphere per year into reactive forms, and most of them end up polluting the environment. Thus, this value has overcame by four times the capacity of recycling that our planet possesses (Rockström et al., 2009). The H2020 program of the EU has suggested a reduction of N fertilization to reach a limit of 170 kg/ha/year. However, currently in Spain, 2.4 million ha are devoted to wheat crops employing 200 kg/ha/year. This drastic situation is a suitable scenario for developing novel strategies to increase crop yields. This need has led to the search for biostimulants for plant nutrition as biological and environmentally friendly alternatives to reduce or substitute the use of inorganic fertilizers, while ensuring the yield and high quality of crops (Vita et al., 2018).

Despite the fact that wheat is economically one of the most important crops, until quite recently, there have not been many tools available for analyzing the molecular mechanisms of gene expression. Most probably due to the vast size of the wheat genome (about five times larger than the human genome or 40 times than the rice genome) and its high content of repetitive highly sequences, as a consequence of being a hybrid of three highly similar subgenomes (International Wheat Genome Sequencing Consortium [IWGSC], 2018). Early transcriptomic studies used 8K wheat microarrays derived from expressed sequence tag (EST) clones. These initial tools allowed to partially study the response of the wheat plant to pathogens, such as *Fusarium graminearum* (Golkari et al., 2007, 2009), or to abiotic stresses such as low temperature (Laudencia-Chingcuanco et al., 2011). The availability of 61K commercial microarrays enabled analysis of around a half of the wheat genome, which represented a seven-fold increase when compared with previous microarray versions (Brenchley et al., 2012). For instance, wheat plant responses to a herbicide have been analyzed using that tool (Pilcher et al., 2017). Nowadays, up to 94% of wheat genome has been covered and 107,891 gene models proposed (Brenchley et al., 2012; International Wheat Genome Sequencing Consortium [IWGSC], 2018), facilitating genome-wide studies. In fact, a recent study has employed RNA-seq technology to analyze the transcriptomic response of wheat plants to N starvation (Curci et al., 2017). RNA-seq is currently the most advantageous and economical tool for exploring genomes, as it does not suffer from hybridization-based limitations and has demonstrated a broader dynamic range than microarrays. Although, when using the same set of samples, both platforms have shown a high correlation between gene expression profiles (Zhao et al., 2014). In any case, RNA-seq data storage is particularly challenging and analysis is more complex when it comes to analyzing wheat genes belonging to what is likely the most complicated genome. The limited number of wheat studies based on RNA-seq is likely a consequence of its polyploidy, which complicates the step of sequence assembly and annotation, generating a bottleneck for data interpretation.

Trichoderma is a genus of filamentous fungi that includes strains that are able to colonize the rhizosphere and promote plant growth (Shoresh et al., 2010; Hermosa et al., 2012), and can help plants to overcome biotic and abiotic stress conditions (Rubio et al., 2014, 2017). The growth-promoting activity of *Trichoderma* isolates was already described in horticultural plants during the 80's decade (Chang et al., 1986) and their beneficial effects have been attributed to different mechanisms including solubilization of several plant nutrients, root colonization and secretion of siderophores, phytohormones, vitamins and enzymes (Altomare et al., 1999; Viterbo et al., 2010; Li et al., 2015). However, the *Trichoderma*-plant cross-talk is a dynamic process that depends on the *Trichoderma* strain, the concentration used, the plant material, the developmental stage of the plant and the interaction time (Harman, 2006; Hermosa et al., 2012). Actually, the EU legislation allows the registration and commercialization of *Trichoderma* strains as biostimulants with the limitation of those strains already registered as biocontrol agents and included in the EU list of approved active substances (Annex I of Directive 98/8/EC).

Little is known about *Trichoderma*-wheat interactions, and transcriptional responses of wheat plants to strains belonging to this fungal genus. Here, we have studied the early global transcriptomic responses of wheat seedling roots to *Trichoderma harzianum* T34 under different N supplies, using wheat genome 61K microarrays. The former results indicate that under our experimental conditions, after 48 h interaction, strain T34 causes transcriptional changes to a larger extent than the N source, these being majorly related to an increase of defenses accompanied by reduced growth of wheat seedlings.

MATERIALS AND METHODS

Microorganisms and Wheat Seeds

Trichoderma harzianum CECT 2413 (Spanish Type Culture Collection, Valencia, Spain), also referred to as strain T34, was grown on potato dextrose agar medium (PDA, Difco Laboratories, Detroit, MI, United States) and spores were harvested as previously described by Rubio et al. (2017).

Wheat seeds (*Triticum durum* "Dorondon") were surface-sterilized by gentle sequential shaking in 2% (v/v) sodium

hypochlorite for 20 min and 0.1N HCl for 2 min, and then rinsed four times with sterile distilled water. Stratification of the seeds was conducted for 2 days at 4°C.

Plant Material and Total RNA Extraction

Wheat seeds were placed inside Phytatray II boxes (Sigma-Aldrich, Madrid, Spain) containing Murashige & Skoog medium (MS, Duchefa Biochemie BV, Haarlem, Netherlands), as previously described in Rubio et al. (2014), and boxes were kept at 25°C under gentle stirring for 72 h. Spores of T34 were used to inoculate flasks containing 100 mL of potato dextrose broth medium (PDB, Difco Laboratories) at a concentration of 10^6 spores/mL. T34 cultures were then maintained at 25°C and 180 rpm for 16 h. Then, fungal germlings were harvested by centrifugation at 4000 × *g* for 10 min, washed, resuspended in sterile distilled water and used to inoculate, at a concentration of 10^5 germlings/mL, Phytatray II boxes that contained 72-h-old wheat seedlings. Phytatray II boxes containing wheat seedlings without inoculation of fungus were grown in parallel as a control. After 24 h incubation at 25°C and gentle shaking, the lids were removed in sterile conditions and the MS medium was replaced with a minimal medium (Lullien et al., 1987) containing 0, 0.1, 0.5, or 1 mM $Ca(NO_3)_2$ as N source. The eight culture conditions assayed were coded as follows: T0N0 [without T34 strain and 0 mM $Ca(NO_3)_2$], T0N0.1 [without T34 strain and 0.1 mM $Ca(NO_3)_2$], T0N0.5 [without T34 strain and 0.5 mM $Ca(NO_3)_2$], T0N1 [without T34 strain and 1 mM $Ca(NO_3)_2$], T1N0 [T34 strain and without $Ca(NO_3)_2$], T1N0.1 [T34 strain and 0.1 mM $Ca(NO_3)_2$], T1N0.5 [T34 strain and 0.5 mM $Ca(NO_3)_2$] and T1N1 [T34 strain and 1 mM $Ca(NO_3)_2$]. These culture conditions were chosen after evaluating the growth of 72-h-old wheat seedlings for 48 h in the above described Phytatray boxes in minimal medium containing 0, 0.1, 0.5, 1, 2, 5, 7, or 10 mM $Ca(NO_3)_2$ (**Supplementary Figure S1**).

Roots from 10 wheat seedlings were pooled and homogeneized under liquid nitrogen. A fraction of 0.1 g of roots was taken and used for analyzing nitrate reductase activity, and the rest was kept at −80°C until total RNA extraction. At the same time, ten wheat seedlings from each 48 h-Phytatray culture were taken to measure length of aerial part, fresh weight and dry weight, after maintaining wheat seedlings at 65°C for 2 days. 48-h Phytatray cultures were performed in duplicate for each tested condition.

RNA from roots was extracted using TRIZOL reagent (Invitrogen, Gaithersburg, MD, United States), following manufacturer's instructions. For microarray hybridizations, RNA was purified using the RNeasy MinElute Cleanup kit (Qiagen, Hilden, Germany). Purified total RNA samples were quantified with a NanoDrop® ND-1000 (NanoDrop, Wilmington, DE, United States) spectrophotometer, and satisfactory purity was indicated by A260:280 ratios of 1.9–2.1. Integrity of total RNA samples was assessed by denaturing formaldehyde gel electrophoresis, where the presence of sharp 28S and 18S ribosomal RNA bands at an intensity ratio of ∼2:1 (28S:18S) indicated good integrity.

Wheat Genome Array Hybridization and Data Analysis

cDNA was synthesized from 100 ng of purified RNA and used for production of labeled probes, which were used to hybridize the Affymetrix GeneChip Wheat Genome Array (Affymetrix, Santa Clara, CA, United States), employing the GeneChip Fluidics Station 450. The GeneChip Wheat Genome Array contains 61,127 probe sets representing 55,052 transcripts for all 42 chromosomes (21 in duplicate) in the wheat genome. 59,356 probe sets represent a modern hexaploid bread wheat (*Triticum aestivum*) and 1,759 probe sets derive from ESTs, 1,215 being from a diploid wheat (*T. monococcum*), 539 from a tetraploid macaroni wheat (*T. turgidum*), and five from a diploid known as *Aegilops tauschii*.

A total of 16 GeneChips were used in this study, two for each one of the eight assayed growth conditions. Purified RNA from roots of 10 wheat seedlings was labeled and used for hybridizing each GeneChip. All steps were done according to protocols described in the Gene Expression Analysis Technical Manual[1]. Briefly, following chips hybridization, the fluorescent signals emitted were scanned in a calibrated Affymetrix GeneChip Scanner 3000, and images analyzed in an Affymetrix GeneChip Operating Software (GCOS 1.2) for calculating the mean signal and for normalizing with the on-chip control genes using the Model Based Expression (dChip) Index (Li and Wong, 2001). The probe sets, showing differential expression [fold-change (FC) ≥ 2 and corrected - value < 0.015] in both biological replicates, were associated to wheat transcripts through a search in the IWGSC v0.4 genome and manually annotated using Gene Ontology (GO) terms (Ashburner et al., 2000), which were based on the BLAST definitions, applying an *E*-value < 10^{-20} level.

Validation of Differential Expression by Quantitative Real-Time PCR

Seven genes, which showed significant differential expression from the microarray data, were selected for quantitative real-time PCR (qPCR) analysis. cDNA was synthesized from 1 μg total RNA using the Transcriptor First Strand cDNA Synthesis kit (Takara, Inc., Tokyo, Japan) with an oligo (dT) primer, following the manufacturer's protocol. Then, 1 μL of cDNA was used in the subsequent PCR. All PCRs were performed in triplicate on a StepOne PlusTM device (Applied Biosystems, Foster City, CA, United States). Reaction mixtures and PCR amplification conditions were carried out as previously described (Rubio et al., 2017). Primers used are listed in **Supplementary Table S1**, and were designed using PerlPrimer software. The relative expression levels were calculated applying the $2^{-\Delta\Delta Ct}$ method (Livak and Schmittgen, 2001) and using the actin transcript as an internal reference.

Nitrate Reductase Assay

Protein extract was obtained from root material (0.1 g) that was grounded under liquid nitrogen. Extraction buffer (0.5 mL) containing 50 mM Tris (pH 8.5), 10 mM DTT, 0.02 mM

[1]http://www.affymetrix.com

Leupeptin, 0.01 mM FAD and 10 mM $MgCl_2$ was added to the vegetal tissue, homogenized by vortexing, and supernatant containing proteins were recovered by centrifugation at 12,000 rpm for 10 min at 4°C. Nitrate reductase activity was determined following a previously described method (Abenavoli et al., 2016). Non-phosphorilated nitrate reductase activity was defined as μmol of nitrite produced in 1 min, and specific activity was such activity expressed per mg of protein. A standard curve was prepared using buffer, without NADH, with a final concentration of KNO_2 ranging from 0 to 0.015 mM. The protein concentration was measured by Bradford assay using the Dye Reagent Concentrate (Bio-Rad Laboratories GmbH, München, Germany) and bovine serum albumin as a protein standard.

Statistical Analyses

Data used for statistical analyses were obtained from at least three independent replicates, and expressed as the mean values. Statistical comparisons were evaluated by one-way ANOVA, followed by a *post hoc* Tukey's test using the Statview 5.0 software. Confidence intervals of 95% were set.

RESULTS AND DISCUSSION

Overview of the Wheat Gene Expression Data From Microarray Analysis

A microarray-based transcriptome analysis was done using roots of wheat seedlings after 48 h culture under different N supplies, and colonized or not by *Trichoderma* with the aim of identifying genes that are differently regulated due to the presence of the fungus, the concentration of the N source or a combination of both parameters. In the present study, we have used wheat microarrays because this technology has become more available to us (Morán-Diez et al., 2012; Rubio et al., 2014), with well-established protocols and capacity to analyze data. Out of a total of 61,127 probe sets deposited on the microarray, only 226 genes showed at least a twofold significant change in expression using a P-value < 0.015 in at least one of the eight assayed conditions (**Supplementary Table S2**). No GO categories were significantly over-represented after comparing the expression changes detected in the eight considered growth conditions. For this reason, all the differentially expressed genes were analyzed independently and then manually grouped into physiological processes (**Supplementary Table S2**). The vast majority of the differentially expressed genes (50.9%) corresponded to hypothetical proteins with unknown function, without matches in databases, or to probes to which no transcript was found associated, despite having a hit in the wheat genome (**Figure 1**). A plausible explanation for this fact could be that the durum wheat is a polyploid plant, thus, obtaining a suitable sequence assembly and annotation is very complex due to occurrence of multiple copies of gene sequences (homologous or paralogous genes) (Singh et al., 2014). The largest number of the genes with a putative function were classified into "metabolism" (21.7%), most of them being involved in "carbohydrate metabolism" (6.6%), and a second gene set was grouped in "cellular processes and signaling" (19.5%), the majority of them corresponding to transport processes (6.2%) (**Figure 1**). The expression changes observed affecting such biological processes could be an indication of the active adaptation process of wheat seedlings to new growth conditions. Most of the genes exhibited expression changes only in one of the eight tested conditions and only 19 genes showed transcriptional changes in two or more conditions (**Supplementary Table S2**). Six out of the 19 genes encoded hypothetical proteins with unknown function or had no matches in databases. The other 13 were related to metabolism (five genes), cellular processes and signaling (six genes), response to stimulus (one gene) and information storage and processing (one gene).

To validate microarray results, qPCR assays were performed for seven genes within the set of 111 genes with putative function, that were differentially expressed in wheat roots under at least one of the eight growth conditions assayed (**Figure 2**). Non-specific lipid transfer protein gene represents those genes for which expression is dependent on $Ca(NO_3)_2$ concentration in the absence of *T. harzianum* T34, two genes coding for an expansin and an ABC transporter represent those differentially expressed in response to T34 strain in the absence of N source, and five genes are representative of those differentially expressed in growth conditions where T34 strain and $Ca(NO_3)_2$ combinations were applied. qPCR results correlated well with the data from the microarray experiment.

Wheat Genes Differentially Expressed in Response to $Ca(NO_3)_2$ or *T. harzianum*

It has been recently described that $Ca(NO_3)_2$ concentrations higher than 5 mM suppressed cucumber seedlings growth (Fan et al., 2017). Thus, the N concentration effect on the growth of 72-h-old wheat seedlings was firstly evaluated, employing a $Ca(NO_3)_2$ concentration ranging from 0 to 10 mM. In terms of plant size after 48 h growth, the best result matched with 1 mM since 95% of plants had a size of 13 cm or larger, while a detrimental effect was observed when N concentration was increased (**Supplementary Figure S1**). It is noteworthy to mention that concentrations of 5, 7, or 10 mM $Ca(NO_3)_2$ gave rise to percentages lower than 35% plants belonging to the larger size group. Results obtained for wheat seedlings growth under the described experimental conditions are in a good agreement with those reported for cucumber (Fan et al., 2017). Therefore, in the current study, plant culture media containing a $Ca(NO_3)_2$ concentration ranging from 0 to 1 mM were used for exploring the effect of the N dosage on wheat seedling roots at a transcriptomic level. No differences in gene expression were detected between T0N0.1 and T0N0 conditions, thus indicating that, at least after 48 h $Ca(NO_3)_2$ application, a 0.1 mM concentration was not sufficient to cause transcriptomic changes in wheat seedling roots, in comparison with those that occurred in the absence of a N source. Four and ten genes, respectively, differed significantly in expression by at least twofold in T0N0.5 and T0N1 conditions when compared to the T0N0 condition (**Supplementary Table S3**). Most of them being down-regulated. Among them, three genes were common for both conditions (T0N0.5 and T0N1), encoding a putative

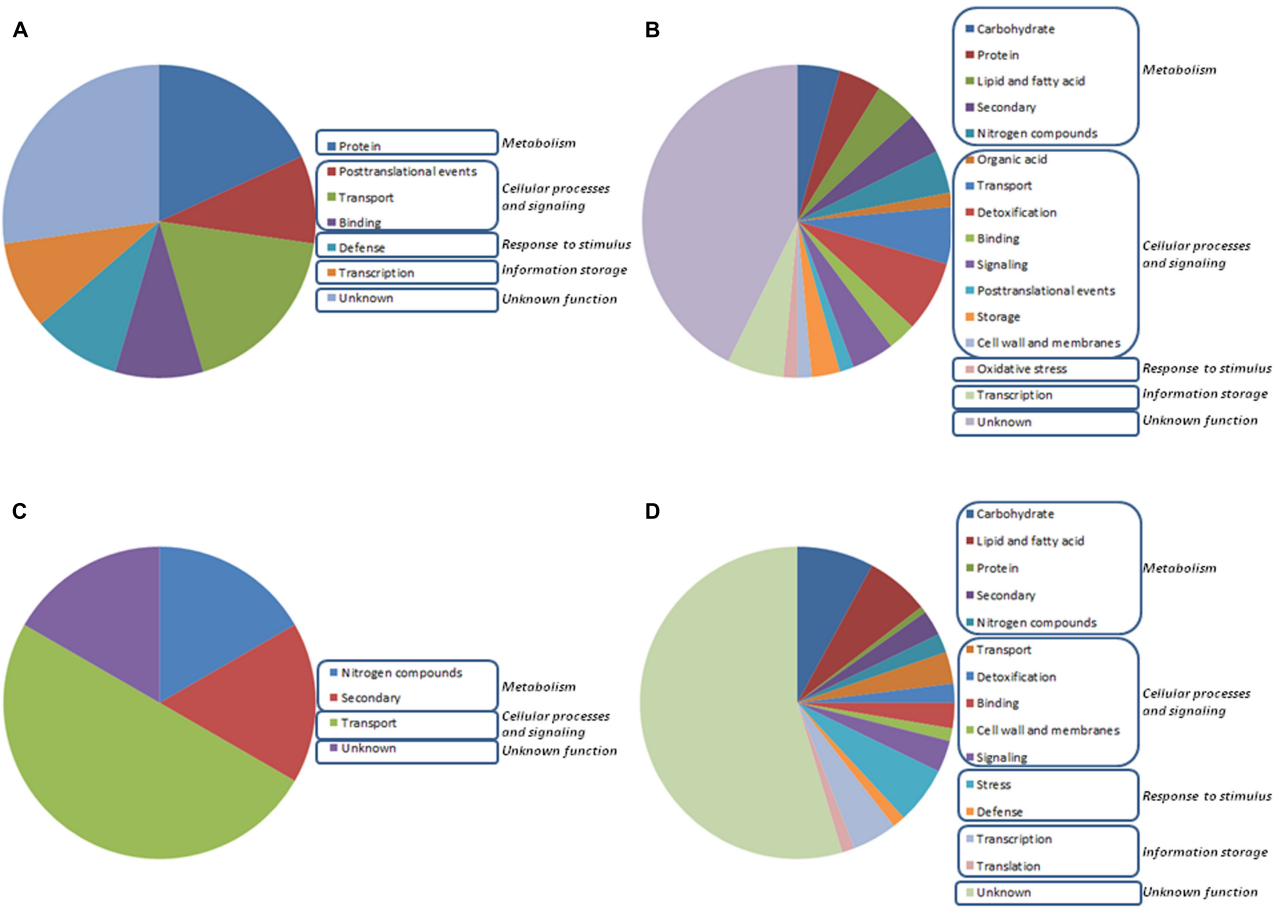

FIGURE 1 | Distribution within physiological processes of the 226 differentially expressed genes at early stage (48 h growth) in wheat seedling roots resulting from the GeneChip Wheat Genome Array analysis is depicted for eight different growth conditions with (T1) or without (T0) *Trichoderma harzianum* T34 and 0 (N0), 0.1 (N0.1), 0.5 (N0.5) or 1 (N1) mM calcium nitrate. Gene significance was assigned to at least twofold change (*P*: 0.15). Comparisons were performed between **(A)** T0N0 and T0N0.5 or T0N1, **(B)** T0N0 and T1N0, **(C)** T1N0 and T1N0.5 or T1N1, and **(D)** T0N0.1, T0N0.5 or T0N1 and T1N0.1, T1N0.5 or T1N1.

ripening-related protein, a cysteine peptidase and a non-specific lipid transfer protein, respectively (**Table 1**). It has been reported that cysteine proteases are strongly expressed in wheat upon exposure to abiotic stresses, such as drought, heat or salinity conditions, which can also cause premature senescence (Botha et al., 2017). On the other hand, non-specific lipid transfer proteins are able to transfer lipids between membranes and it has been reported that they play several roles in plants, including defense against pathogens (Boutrot et al., 2005), as well as tolerance to salinity, cold and drought (Pitzschke et al., 2014). Similarly, a gene coding for an F-box protein was differentially down-regulated in the T0N1 condition, and it has been described that it is involved in wheat tolerance to abiotic stresses (Li et al., 2018). Thus, the down-regulation of these genes could be indicative of an absence of stress in wheat seedlings after 48 h growing under T0N0.5 or T0N1 conditions.

Regarding *Trichoderma* application, a total of 67 genes differed significantly in their expression in root by at least twofold when T0N0 and T1N0 conditions were compared. They would be associated with the effect of the T34 strain in the absence of a N source (**Supplementary Table S4**): 55 genes were up-regulated, whereas 12 were down-regulated. "Metabolism" and "cellular processes and signaling" were the two most affected physiological processes. Interestingly, in spite of being grouped in different biological processes, several of the up-regulated genes were related to plant defense responses and tolerance to stress conditions. In this sense, numerous studies have shown that several transcription factors are important in regulating plant responses to environmental stress (Chen et al., 2002; Rubio et al., 2017). In the present study, four genes encoding transcription factors, two ethylene response factors (ERF), elongated hypocotyl 5 (HY5)-like and nucleus accumbens associated 1 (NAC1), showed higher expression levels in roots of the condition T1N0 than in T0N0 roots. *ERF* genes play a role in the ethylene (ET)-dependent defense pathway, which is activated upon infection with different types of pathogens, including bacteria, fungi and oomycetes (Gimenez-Ibanez and Solano, 2013). ET is also an important phytohormone for plant growth, development, senescence, and abiotic stress tolerance. In addition, it is described that ERFs are not only involved in response to ET

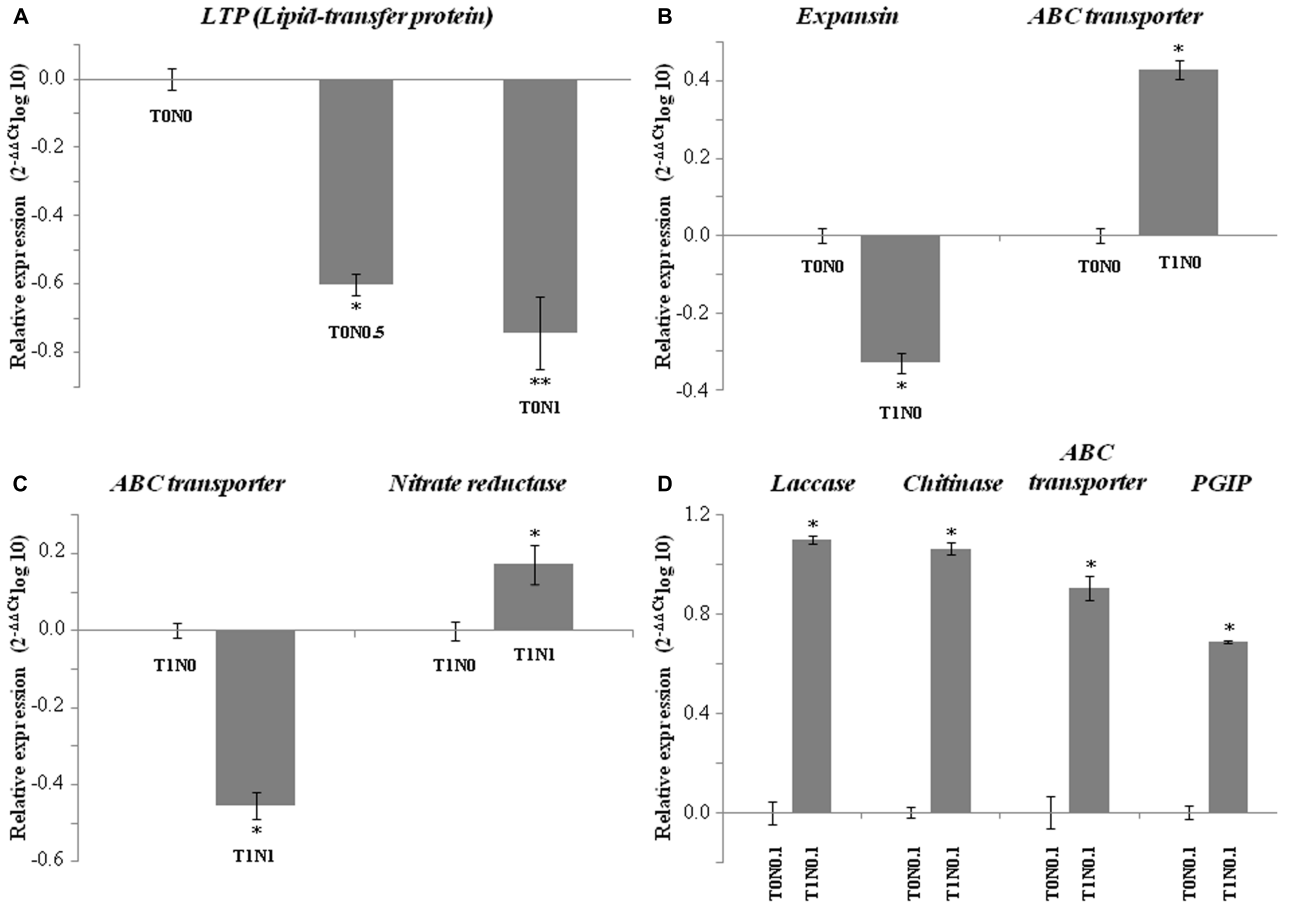

FIGURE 2 | qPCR expression analysis of seven International Wheat Genome Sequencing Consortium (IWGSC, v0.4)-referred genes of a set of 226 genes differently expressed in wheat seedling roots resulting from the GeneChip Wheat Genome Array analysis under eight different growth conditions with (T1) or without (T0) *Trichoderma harzianum* T34 and 0 (N0), 0.1 (N0.1), 0.5 (N0.5) or 1 (N1) mM calcium nitrate. Analyzed gene code for: **(A)** Lipid-transfer protein (LTP, ID TraesCS1A01G175200.1) (T0N0.5 and T0N1 compared to T0N0 conditions), **(B)** expansin (ID TraesCS4A01G034300.1) and ABC transporter (ID TraesCS5A01G016200.1) (T1N0 compared to T0N0), **(C)** ABC transporter and nitrate reductase (ID TraesCS6B01G024900.1) (T1N1 compared to T1N0), and **(D)** laccase (ID TraesCS3B01G489800.1), chitinase (ID TraesCS7A01G371600.1), ABC transporter, and polygalacturonase inhibitor (PGIP, ID TraesCS7B01G103900.1) (T1N0.1 compared to T0N0.1). Data are the mean of three technical replicates from two biological replicates and are displayed as the log10 of the relative quantity (RQ, 2^{-DDCt}) of target genes compared with the quantity of actin gene used as a reference. For each biological replicate, roots from ten plants were pooled.

signal transduction, but can also regulate ET biosynthesis in plant tissues (Hoang et al., 2017). HY5 is a master regulator of seedling development which modulates the expression of one third of the genes in *Arabidopsis* (Gangappa and Botto, 2016), being ERFs among them. HY5-ERF regulon restrains overproduction of ET, which is important for plant growth. According to this, it could be expected that T1N0 plants had a larger size than T0N0. In our study, length and fresh and dry weight values obtained from aerial wheat seedling parts, after 48 h growing in the presence of *T. harzianum* T34, were lower than those in absence of the fungus. This phetotype was reproducible in several independent experiments (**Figure 3**). An explanation might be the involvement of HY5 in the modulation of abscisic acid (ABA) and auxin pathways (Liu et al., 2018), and in the repression of cell elongation-responsive genes (Gangappa and Botto, 2016). In this sense, down-regulation of a gene coding an expansin 2 protein was detected in the condition T1N0 when compared to T0N0 (**Figure 2**). In wheat plants, expansins are involved in growth and developmental processes, as well as in tolerance to stress conditions, and their expression in other plants confers tolerance to salt, drought, cadmium and oxidative stresses (Zhang J.F. et al., 2018). In addition, down-regulation of a gene encoding a multicopper oxidase-like protein was also detected in the condition T1N0. It has been suggested that an homolog gene takes part in growth processes, possibly by participating in cell wall expansion in *Arabidopsis* (Sedbrook et al., 2002). In the same way, a reduced expression of *AKT1* potassium channel gene was detected. Potassium is a macronutrient for plants that is required for numerous physiological processes, such as membrane potential maintenance and turgor pressure, enzyme activation, osmotic pressure regulation, stomatal movement and tropism phenomena (Golldack et al., 2003). The induction

TABLE 1 | Short list of annotated hits for wheat genes that alter their expression in response to *Trichoderma* and/or calcium nitrate selected due to their putative role in plant defense or development.

	T0N0.5	T0N1	T1N0	T1N0.1	T1N0.5	T1N1
Up-regulated						
12-oxo-phyto dienoic acid reductase				■		
Acylglycerol-3-phosphate-*O*-acyltransferase						
Arginine decarboxylase			■			
Beta-1,6-*N*-acetylglucosaminyltransferase						
Chitinase				■	■	
Cysteine-rich receptor-like kinase						
Cytochrome P450			■			
Drug transmembrane transporter						
Endo-beta-1,3 glucanase (PR-2)				■		
Ethylene Response Factor (ERF)			■			
Expansin-B7-like protein				■		
Flavonoid 7-*O*-methyltransferase						
GTP-binding protein SAR1A			■			
Laccase				■		
NADPH-dependent 6′-deoxy chalcone synthase						
Non-annotated glycosyl hydrolase (GH)			■			
Omega-3 fatty acid desaturase				■		
Pectin-esterase					■	
Pleiotropic drug resistance (PDR)-type ABC transporter			■			
Polygalacturonase				■		
PR-1						
Protein LNK1-like						
Protein LNK4-like						
S-adenosylmethionine (SAM) decarboxylase			■			
Salutaridine reductase				■		
Somatic embryogenesis receptor kinase						
Stress-induced transcription factor NAC1			■			
Subtilisin-chymotrypsin inhibitors				■		
Thaumatine (PR-5)						
Thioredoxin						■
Transcriptional activator (gluthatione S-transferase)				■		
Transcription factor HY5-like			■			
Trehalose-6-phophate phosphatase				■		
UDP-glycosyltransferases			■			
Wall-associated receptor kinase					■	
Xylanase inhibitor			■			
Xyloglucan endotransglucosylase						■
Down-regulated						
24-methylene sterol C-methyl transferase 2					■	
AKT1 potassium channel gene			■			
Cysteine peptidase	■	■				
Expansin protein						
F-box protein		■				
Gliadin/LMW glutenin proteins						
Multicopper oxidase-like protein						
Non-specific lipid transfer protein	■	■				
Nitrate reductase					■	■
Pleiotropic drug resistance-type ABC transporter						
Phosphatidylinositide phosphatase SAC1				■		
Potassium channel AKT1			■			

(Continued)

TABLE 1 | Continued

	T0N0.5	T0N1	T1N0	T1N0.1	T1N0.5	T1N1
Polygalacturonase				■	■	
Putative ripening-related protein	■	■	■			
Repressor (MYB transcription factor)				■		
Transcriptor factor ILI6					■	
UDP-glycosyltransferase						■

Different growth conditions, including Trichoderma harzianum T34 (T1) or not (T0) and 0 (N0), 0.1 (N0.1), 0.5 (N0.5), or 1 (N1) mM calcium nitrate, were used for comparison.

of potassium channel genes by phytohormones like auxins gives them a central role in seedling growth and embryonic development. It has been shown that the potassium transporter AKT1 is required for the plant response to changes in external potassium, and subsequent regulation of potassium-dependent root growth and auxin redistribution in the root (Li J. et al., 2017).

In another way, the transcription factor family NAC has been reported to have pivotal functions in mediating plant responses against various abiotic stresses due to their ability to specifically bind to the sequence of ABA-responsive elements (Hoang et al., 2017). Although more than 100 NAC members are present in the bread wheat genome, NAC1 is a novel member of this family, which has dual roles in response to pathogens, since it may modulate plant jasmonic acid (JA)- and salicylic acid (SA)-signaling defense cascades (Wang et al., 2015). The up-regulation of *NAC1* gene in wheat seedling roots from the condition, T1N0, is indicative of defense response activation mediated by T34 strain, at the same time compromising the plant growth. It can be thought that ABA-dependent defenses are triggered by T34 strain. In this sense, four genes encoding cytochrome P450 monooxygenase were up-regulated in the condition, T1N0. Proteins of this class have been involved in ABA biosynthesis (Narusaka et al., 2004). Also, a gene coding for a pleiotropic drug resistance (PDR)-type ABC transporter was up-regulated, which seems to play a role in ABA transport (Kang et al., 2011; Curci et al., 2017). Several ABC transporters were also up-regulated in durum wheat roots stressed by N starvation when analyzed through an RNA-sequencing approach (Curci et al., 2017). These changes detected at a transcriptomic level are in a good agreement with the phenotypic differences observed between wheat seedlings of the T1N0 and T0N0 conditions (**Figure 3**), because elements like HY5, cytochrome P450 monooxygenase and ABC transporter would be able to trigger NAC1-dependent defense pathways by means of ABA (**Figure 4**).

Three genes encoding decarboxylases, enzymes involved in N and amino acid metabolism, were up-regulated in wheat seedlings in response to T34. Two of them encoded arginine decarboxylases and the third one coded for a *S*-adenosylmethionine (SAM) decarboxylase. Both enzymes participate in polyamine biosynthesis, being the arginine decarboxylase involved in the formation of putrescine from arginine, and the SAM decarboxylase in the spermidine and spermine biosynthesis process from putrescine. The activation of polyamine metabolism correlates with the smaller growth of the T1N0 seedlings since spermine and spermidine induce concentration-dependent oxidative damage, resulting in decreased wheat biomass (Szalai et al., 2017). Recently, an up-regulation of tomato genes included in categories such as "spermine and spermidine biosynthetic process" and "arginine catabolic process" has been associated with *T. atroviride* P1-tomato interactions (Coppola et al., 2019). Accumulation of polyamines, as well as the up-regulation of genes coding for SAM decarboxylase in wheat plants, under environmental stress conditions have been previously described (Li and Chen, 2000), highlighting the role of polyamines in plant resistance to adverse circumstances. Polyamine profiles analyzed in *Trichoderma-Arabidopsis* interactions have been related to the *Trichoderma* species used, the timing of the interaction and whether it occurred with physical contact or not, which may confer upon these compounds a role reprogramming the changes undergone by plants to fine tune their defense and growth responses (Salazar-Badillo et al., 2015). The relationship between polyamines and phytohormones has been also established since ET induces SAM descarboxylase in plants (Van de Poel et al., 2013) and endogenous SA and polyamine content have been linked in wheat plants (Szalai et al., 2017).

Different defense mechanisms could be activated by strain T34 in the wheat seedling roots. Supporting this, an up-regulation of three genes encoding glycosyl hydrolase (GH) proteins involved in "carbohydrate metabolism" (an non-annotated GH, an endo-β-1,3 glucanase and a 1,6-*N*-acetylglucosaminyl transferase) was observed in the condition T1N0. GHs catalyze the hydrolysis of glycosidic bonds and have been described to participate in plant defense and development processes. Within GHs, β-1,3 glucanases belong to the GH family 17 and are considered to be pathogenesis-related (PR) proteins, since they are coordinately expressed in response to various biotic and abiotic stress stimuli (Thomas et al., 2000). The up-regulation of a gene encoding a xylanase inhibitor was also observed. This enzyme inhibits microbial endoxylanases belonging to the GH family 11 (Raedschelders et al., 2004), and it has a role in the protection of wheat plants against biotic or abiotic stresses (Pollet et al., 2009). The up-regulation of a gene coding for a calcium binding protein can be related to plant defense because its involvement in wheat defense response to pathogens and abiotic stresses has been described (Feng et al., 2011). Since an up-regulation of two genes encoding UDP-glycosyltransferases was observed in the condition T1N0, it can be assumed that T34 strain is triggering the anthocyanin biosynthesis pathway in wheat seedlings. Anthocyanins, a main class of flavonoids, play multiple

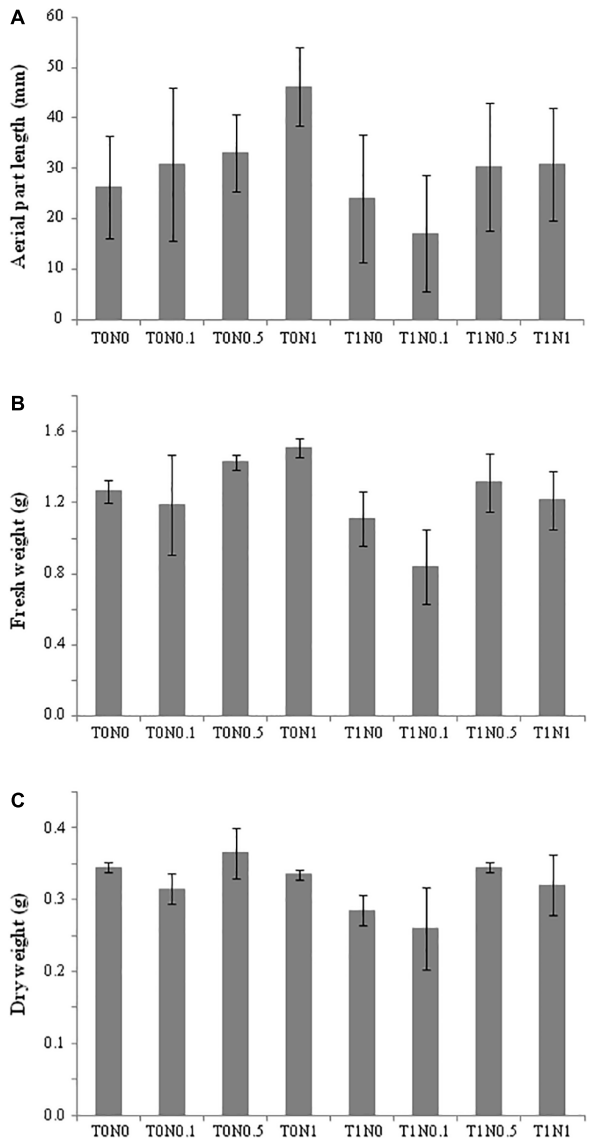

FIGURE 3 | Measurements of wheat seedlings after being growth for 48 h under eight different conditions: with (T0) or without (T1) *Trichoderma harzianum* T34 and 0 (N0), 0.1 (N0.1), 0.5 (N0.5) or 1 (N1) mM calcium nitrate as nitrogen source. **(A)** Aerial part length, **(B)** fresh weight, and **(C)** dry weight. For each measurement, mean values of 20 plants from two independent experiments are shown.

roles in higher plants since they provide colors, absorb UV and high light irradiation, act as insect and animal attractants and are also antioxidants. Apart from that, they are effective agents against pathogens in plants (Li D. et al., 2017).

Wheat gluten comprises glutenin and gliadin proteins that account for up to 80% of the total protein content in the mature grain and determine viscoelastic properties of wheat flour dough, which govern the behavior of dough processing and baking quality (Wan et al., 2013). Genes encoding glutenin and gliadin proteins are regulated by N supply in developing wheat grain (Wan et al., 2013). Currently, wheat crop yield and quality rely on chemical nitrogenous fertilizers application (Zörb et al., 2018). The present microarray analysis showed no differential expression in such kinds of genes after comparing data from T0N0 and T0N0.1, T0N0.5 or T0N1 conditions (**Supplementary Table S3**). However, a down-regulation of two genes encoding gliadin/Low Molecular Weight (LMW) glutenin proteins was detected in the condition T1N0 when compared with T0N0. Since we are analyzing changes in a root transcriptome, it is not possible to forecast that T34 strain will cause a decrease in gluten protein content of wheat grain. Recently, proteins with a gliadin domain have been identified as being involved in wheat plant immunity against *F. graminearum* (Zhang Y. et al., 2018). The observed down-regulation of glutenin genes in response to T34 may indicate that this strain of *T. harzianum* would not be triggering this novel plant defense mechanism.

The observed transcriptomic changes, together with the T1N0 seedling phenotype (**Figure 3**) would seem contradictory to some attributes associated with the beneficial effects of *Trichoderma*. Although, we ought not forget that the transcriptome had been analyzed when the *Trichoderma* colonization was still active. It would be reasonable to speculate that wheat seedlings, at least locally, and in response to T34 strain, increase defense to limit the fungal penetration to the outer layers of root cortical cells, being compromised the plant growth in return. Moreover, the up-regulation of *ERF*, *NAC1* and *HY5* genes in plants inoculated with *Trichoderma* indicates that, at least through these regulation hubs, the fungus adjusted the phytohormone networking leading to activate defenses, which in party explains the reduced size of the wheat seedlings treated with T34.

Wheat Genes Differentially Expressed in Response to $Ca(NO_3)_2$ and *Trichoderma* Combinations

The root transcriptional response of wheat seedlings to the combined application of *T. harzianum* T34 and different concentrations of N source (T1N0.1, T1N0.5 or T1N1 conditions) was analyzed, either taking as reference T1N0 (**Supplementary Table S5**) or T0N0.1, T0N0.5 and T0N1 conditions (**Supplementary Table S6**). The huge difference in the number of the differentially expressed genes between both comparatives, seven and 157, respectively, would be a good indicator of the important role that *Trichoderma* plays in the transcriptomic changes detected in wheat roots.

N Source Effect When Applied in Combination With *T. harzianum* T34

Only seven genes showed differential expression after comparing T1N0.1, T1N0.5 or T1N1 conditions with the condition T1N0. No differences in gene expression were detected when the conditions, T1N0 and T1N0.1, were compared. There were two and five genes that differed significantly in expression by at least twofold in wheat seedling roots between T1N0 and T1N0.5 or T1N1, respectively (**Supplementary Table S5**). One of the up-regulated genes (ID TraesCS6B01G024900.1), which was shared by both conditions (T1N0.5 and T1N1), codes for nitrate reductase. This enzyme catalyzes the reduction of nitrate

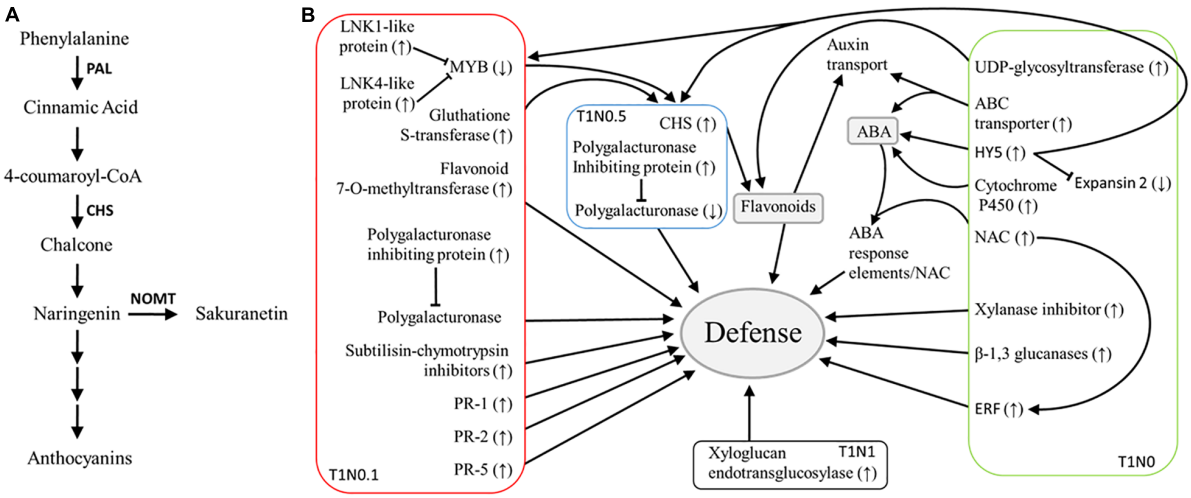

FIGURE 4 | Schematic representation of defense activation by *Trichoderma harzianum* T34 in wheat seedlings. **(A)** Scheme of the major branch pathway of flavonoid biosynthesis, seven genes differently expressed in wheat seedling roots resulting from the GeneChip Wheat Genome Array analysis under different growth conditions with *Trichoderma harzianum* T34 and 0 (T1N0, green), 0.1 (T1N0.1, red), 0.5 (T1N0.5, blue) or 1 (T1N1, black) mM calcium nitrate belong to this pathway. Enzyme names are abbreviated as follows: Chalcone synthase (CHS), Naringenin 7-*O*-methyltransferase (NOMT) and Phenylalanine ammonia-lyase (PAL). **(B)** Signaling networks involving major genes related to plant-*Trichoderma* interaction that show upregulation (↑) or downregulation (↓) in the current study.

to nitrite, which is highly toxic to plant cells and is reduced to ammonium by the enzyme nitrite reductase and finally, this ammonium can be used by the plant to produce amino acids and proteins (Krapp, 2015). Surprisingly, genes coding for N metabolism enzymes were not detected in response to an increase of the N source, that is when comparing T0N0.1, T0N0.5 or T0N1 conditions with the condition T0N0. However, this scenario changes when T34 strain is present, thus indicating that the fungus is able to modulate the plant N metabolism, at least at the two highest N concentrations tested. In order to confirm these microarray data, nitrate reductase activity was measured in the same root material employed for microarray analysis, as well as in the aerial part of wheat seedlings (**Table 2**). The highest nitrate reductase values were obtained in roots from T1N0.5 condition, likewise the aerial part of seedlings from T1N0.5 condition also gave the highest levels of this activity. Similar results were obtained in independent experiments. It has already been shown that changes in N concentration govern plant N metabolism, allowing them to mitigate the acclimatory effect to adverse environments (Vicente et al., 2016). Another up-regulated gene in the condition T1N1, with respect to T1N0, codes for a thioredoxin. Wheat thioredoxins have been involved in germination and seedling development by promoting mobilization of primary storage proteins, inactivation of small amylolytic enzyme inhibitors, and activation of calcium-dependent substrate-specific proteases (Pilcher et al., 2017). Previous studies have reported the induction of genes coding for thioredoxins by the herbicide metribuzin in wheat (Pilcher et al., 2017).

Three more genes, encoding an UDP-glycosyltransferase and two PDR-type ABC transporters, were down-regulated in seedling roots from T1N1 condition in comparison with T1N0 condition, one out of two transporter genes being up-regulated in roots of the condition T1N0 compared with T0N0 condition. These data were confirmed by qPCR analysis (**Figure 2**). The differences detected for this ABC transporter, for some of the assayed conditions, suggest that the scenario can be drastically changed when different N source concentrations and *Trichoderma* are applied in combination. Thus, great care must be taken for selecting the right combination to obtain the desired outcome.

TABLE 2 | Specific nitrate reductase activity, expressed as $\mu mol \cdot min^{-1}$ per mg protein, measured in either aerial part or root from wheat seedlings after growing for 48 h under eight different conditions: with or without *Trichoderma harzianum* T34 and 0, 0.1, 0.5, or 1 mM calcium nitrate as nitrogen source.

Conditions	Aerial part	Root
T0N0	13.43 ± 1.54^{a}	11.78 ± 1.06^{ab}
T0N0.1	12.10 ± 1.35^{ab}	11.18 ± 1.12^{ab}
T0N0.5	13.51 ± 1.06^{a}	10.58 ± 0.61^{ab}
T0N1	14.02 ± 0.99^{a}	10.43 ± 0.87^{ab}
T1N0	9.40 ± 2.47^{b}	9.50 ± 1.01^{b}
T1N0.1	11.83 ± 1.78^{ab}	10.01 ± 1.39^{ab}
T1N0.5	12.27 ± 0.71^{a}	12.20 ± 2.19^{a}
T1N1	12.88 ± 1.05^{a}	9.88 ± 1.03^{b}

Values are means of three technical replicates from two biological replicates with the corresponding standard deviation. For each biological replicate, roots or aerial part from ten plants were pooled. Values in the same column with different letters are significantly different according to Tukey's test ($P < 0.05$).

T. harzianum T34 Effect When Applied in Combination With Different N Inputs

The larger number of transcriptomic changes observed among all different conditions tested for wheat seedling roots was in the presence of T34 strain combined with the lowest N supply.

Almost 80% of differently expressed genes were up-regulated. Just in the presence of T34 strain without N source (T1N0), 67 genes were differentially expressed, but when N was included this number was higher, reaching 73 genes in the comparison between T1N0.1 and T0N0.1 conditions (**Supplementary Table S6**). Although less numerous, a great variety of changes, 61 and 23 genes, were detected when comparing T1N0.5 and T0N0.5 or T1N1 and T0N1 conditions, respectively. More than the half of the genes (56%) that differentially varied in their expression when T34 strain was applied in combination with different N supplies corresponded to hypothetical proteins with unknown function or had no matches in databases. The largest number of genes with putative function were associated with physiological processes included within the "metabolism" category (20.4%), being mainly affected the carbohydrate metabolism but also differential expression changes were detected for several genes related to lipid and fatty acid metabolism. The second largest set of genes was located within the "cellular processes and signaling" category (15.3%). In addition to the expected genes from subcategories, such as "transport" or "response to stimulus," it is noteworthy to mention that six genes from the "signaling" subcategory were up-regulated. Most of these last six genes code for kinase receptor proteins (**Supplementary Table S6**). On the basis of these results, we can conclude that the *Trichoderma* effect is more striking when low concentrations of $Ca(NO_3)_2$ are supplied, existing a correlation between an increase of N source applied in combination with T34 strain and a reduction in the number of transcriptomic changes in root of wheat seedlings, at least after 48 h of growing.

Overall, many of the genes differentially expressed in wheat seedling roots, due to a combined application of T34 and $Ca(NO_3)_2$ as an N source, have already been described as components of plant defense responses against pathogens. In wheat, PR-protein activation has been described in a resistant genotype as a defense response to infection by *F. graminearum,* in comparison with susceptible lines to this pathogen (Golkari et al., 2009). An up-regulation of endo-β-1,3 glucanase (PR-2) and chitinase genes was detected in wheat seedlings from T1N0.1 and T1N0.5 conditions. In addition, genes encoding proteins, such as PR-1, thaumatine (PR-5), and polygalacturonase and subtilisin-chymotrypsin inhibitors, which have been previously described and are involved in wheat defense against pests and pathogens (Caruso et al., 1999; Golkari et al., 2009), were differentially up-regulated in the T1N0.1 condition. In parallel to wheat defense activation, detected in response to the application of strain T34 combined with the lowest N concentration, the up-regulation of genes related to plant development was also detected. This is the case for the gene encoding trehalose-6-phophate phosphatase, an enzyme involved in trehalose production, which was up-regulated in T1N0.1 condition. It is well known that trehalose has a protector role in plant against abiotic stresses by preventing the denaturation of cellular proteins (Fernandez et al., 2010). However, trehalose-6-phosphate has emerged as an important signaling metabolite, regulating carbon assimilation and the sugar status in plants, thus having an essential role in development (Ponnu et al., 2011). Several genes that are also involved in cell wall structure modulation (Zhang J.F. et al., 2018) were up-regulated when T34 was applied along with different N concentrations. This is the case for genes coding for pectin-esterase (ID TraesCS3B01G258100.1) (T1N0.5), expansin-B7-like protein (ID TraesCS4B01G375600.1) (T1N0.1), laccase (ID TraesCS3B01G489800.1) (T1N0.1), and xyloglucan endotransglucosylase (ID TraesCS2A01G433500.1) (T1N1). On the other hand, some genes coding for proteins like polygalacturonase (ID TraesCS3B01G020300.1) (T1N0.1 and T1N0.5), 24-methylene sterol C-methyl transferase 2 (ID TraesCS1A01G204700.1) (T1N0.5), phosphatidylinositol phosphatase SAC1 (ID TraesCS1A01G020700.1) (T1N0.1), and the transcription factor ILI6 (ID TraesCS4A01G016300.1) (T1N0.5), which are involved in plant growth and development (Yang et al., 2018), were down-regulated. Transcriptomic analysis shows that the *Trichoderma* effect is more evident when it is applied in combination with low N supply. In this sense, the lowest number of differentially expressed genes was detected in the condition, T1N1, in comparison with those detected in T1N0.1 or T1N0.5. The hability of T34 strain to modulate plant defense and growth responses is remarkable.

It is noteworthy to mention that, in the condition T1N0.5, an important number of up-regulated genes were associated with the major physiological processes "signaling" or "response to stimulus stress" (**Table 1** and **Supplementary Table S6**), being annotated as receptor kinase or ABA-responsive protein, respectively. Such up-regulation observed in wheat roots is in good agreement with a previous study, in which up-regulation of ABA-related genes was described in *Arabidopsis* after 24 h of incubation in the presence of *T. harzianum* T34 (Morán-Diez et al., 2012). It is known that ABA plays a key role in the activation of plant cellular adaptation to abiotic stresses, and that, under adverse environmental conditions, this phytohormone functions as a growth inhibitor. Moreover, it is accepted that mitogen-activated protein kinase (MAPKs) mediates signal transduction cascades, they being central integrators of plant abiotic stress signaling since they link to cellular signaling, and metabolic and stress adaptative processes in the plant (Golldack et al., 2014). In view that an evident up-regulation of ABA-responsive element and receptor kinase genes was detected in the T1N0.5 condition, together with the above described up-regulation of ABA-related genes in T1N0, it could be thought that MAPKs and ABA also have a central role in plant defense responses to *Trichoderma* (**Figure 4**), linking primary metabolism and developmental processes. According to this scenario, it has recently been suggested that future plant holistic studies must consider biotic stress, abiotic stress and development processes (Bigeard and Hirt, 2018).

In a previous study, down-regulation of induced systemic resistance-linked genes was observed in *Arabidopsis* roots colonized by the endopolygalacturonase *Thpg1*-silenced transformant of *T. harzianum* T34 (Morán-Diez et al., 2009). Chalcone synthase (CHS) and xyloglucan endotransglucosylase genes were among the 10 *Arabidopsis* genes that were significantly affected by the silencing of *Thpg1* in T34, and in the present work, these two genes (**Table 1**) were up-regulated in wheat seedling roots from the conditions, T1N0.5 and T1N1, respectively. CHS is a member of the plant polyketide synthase superfamily, and it is

the key enzyme of the flavonoid biosynthesis pathway, providing the starting materials for the synthesis of these compounds (Dao et al., 2011) (**Figure 4**). An up-regulation of the CHS gene, accompanied by a down-regulation of a polygalacturonase gene, was observed in wheat seedling roots from the treatment T1N0.5. Moreover, genes involved in the flavonoid biosynthesis, such as flavonoid 7-*O*-methyltransferase gene, were differentially expressed in T1N0.1 condition (**Table 1**). In this regard, the up-regulation of genes encoding transcriptional activators (i.e., glutathione S-transferase) and coactivators (i.e., LNK1- and LNK4-like proteins) was observed, as well as the down-regulation of repressor genes (i.e., MYB transcription factor), indicative of an increased resistance in wheat seedling roots. In addition to the accumulation of flavonoids in plants, which have an important role in auxin regulation by inhibiting its polar transport, CHS is involved in the SA defense pathway. It is known that plants activate SA biosynthesis in response to *Trichoderma* root colonization to prevent the fungus from entering the vascular system (Alonso-Ramírez et al., 2014). Regarding flavonoids, it is worth highlighting that several genes involved in their biosynthesis were differentially expressed under T1N0, T1N0.1, and T1N0.5 conditions, thus reinforcing the relevance of such pathway during plant–*Trichoderma* interaction.

CONCLUSION

The early root transcriptomic changes observed in wheat seedling roots colonized by the *T. harzianum* T34 under different N supplies show that *Trichoderma* contributes to a larger extent than the N source to such changes. When the fungus is applied in combination with low N concentrations, the plant transcriptional changes are led to balance growth with the need for defense. Based on the fact that many changes observed affect the flavonoid biosynthesis pathway, we assume that *Trichoderma* induces plant defenses through such mechanism.

DATA AVAILABILITY STATEMENT

The microarray data are available at the GEO database with accession number GSE134903.

AUTHOR CONTRIBUTIONS

RH and EM conceived the research. MR, CN, and RH performed the experiments. MR and RH analyzed the data. EM and RH contributed reagents, materials, and analysis tools. MR, AM, and RH wrote the manuscript with the contributions from all other authors on the discussion of the data.

FUNDING

Research project funding was from the Spanish Government (Projects AGL2015-70671-C2 and RTI2018-099986-B-I00) and the Regional Government of Castile and Leon (Project SA270P18). AM was granted with a postdoctoral contract of the Regional Government of Castile and Leon (Project SA270P18).

SUPPLEMENTARY MATERIAL

The Supplementary Material for this article can be found online at: https://www.frontiersin.org/articles/10.3389/fmicb.2019.02444/full#supplementary-material

FIGURE S1 | Calcium nitrate [$Ca(NO_3)_2$] effect on the size of 72-h-old wheat seedlings after 48 h growing in a Phytatray box system. Aboveground plant length was measured for each $Ca(NO_3)_2$ concentration tested (0, 0.1, 0.5, 1, 2, 5, 7, and 10 mM), and as a result, three groups were set up: larger or equal than 13 cm, from 10 to 13 cm, and shorter or equal than 10 cm. Plant height percentages for each growth condition within either of the three groups are depicted by bars. The number of plants used to calculate these percentages is indicated above each bar. **(A)** $Ca(NO_3)_2$: 0, 2, 5, 7 and 10 mM, $n = 30$, and **(B)** $Ca(NO_3)_2$: 0, 0.1, 0.5, 1 and 2 mM, $n = 20$.

TABLE S1 | Primers used for quantitative real-time PCR (qPCR) analysis.

TABLE S2 | List of genes that showed at least a twofold significant change in expression using a P-value < 0.015 in at least one of the eight assayed conditions (as described in Materials and Methods).

TABLE S3 | Physiological processes differentially affected in wheat seedling roots in response to the nitrogen concentration in the plant growth media, 0.5 or 1 mM calcium nitrate [$Ca(NO_3)_2$] compared to nitrogen source absence.

TABLE S4 | Physiological processes differentially affected in wheat seedling roots in response to *Trichoderma harzianum* T34 in the absence of nitrogen source.

TABLE S5 | Physiological processes differentially affected in wheat seedling roots in response to the combined application of *Trichoderma harzianum* T34 and 0.5 or 1 mM calcium nitrate [$Ca(NO_3)_2$] in the plant growth medium compared to nitrogen source absence.

TABLE S6 | Physiological processes differentially affected in wheat seedling roots in response to the combined application of *Trichoderma harzianum* T34 and 0.1, 0.5, or 1 mM calcium nitrate [$Ca(NO_3)_2$] in the plant growth medium compared to T34 strain absence.

REFERENCES

Abenavoli, M. R., Longo, C., Lupini, A., Miller, A. J., Araniti, F., Mercati, F., et al. (2016). Phenotyping two tomato genotypes with different nitrogen use efficiency. *Plant Physiol. Biochem.* 107, 21–32. doi: 10.1016/j.plaphy.2016.04.021

Alonso-Ramírez, A., Poveda, J., Martín, I., Hermosa, R., Monte, E., and Nicolás, C. (2014). Salicylic acid prevents *Trichoderma harzianum* from entering the vascular system of roots. *Mol. Plant Pathol.* 15, 823–831. doi: 10.1111/mpp.12141

Altomare, C., Norvell, W. A., Bjorkman, T., and Harman, G. E. (1999). Solubilization of phosphate and micronutrients by the plant-growth-promoting and biocontrol fungus *Trichoderma harzianum* Rifai 1295-22. *Appl. Environ. Microbiol.* 65, 2926–2933.

Ashburner, M., Ball, C. A., Blake, J. A., Botstein, D., Butler, H., Cherry, J. M., et al. (2000). Gene ontology: tool for the unification of biology. *Nat. Genet.* 25, 25–29. doi: 10.1038/75556

Bigeard, J., and Hirt, H. (2018). Nuclear signaling of plant MAPKs. *Front. Plant Sci.* 9:469. doi: 10.3389/fpls.2018.00469

Botha, A. M., Kunert, K. J., and Cullis, C. A. (2017). Cysteine proteases and wheat (*Triticum aestivum* L) under drought: a still greatly unexplored association. *Plant Cell Environ.* 40, 1679–1690. doi: 10.1111/pce.12998

Boutrot, F., Guirao, A., Alary, R., Joudrier, P., and Gautier, A. F. (2005). Wheat non-specific lipid transfer protein genes display a complex pattern of expression in developing seeds. *Biochim. Biophys. Acta* 1730, 114–125. doi: 10.1016/j.bbaexp.2005.06.010

Brenchley, R., Spannagl, M., Pfeifer, M., Barker, G. L. A., D'Amore, R., Allen, A. M., et al. (2012). Analysis of the bread wheat genome using whole-genome shotgum sequencing. *Nature* 491, 705–710. doi: 10.1038/nature11650

Caruso, C., Chilosi, G., Caporale, C., Leonardi, L., Bertini, L., Magro, P., et al. (1999). Induction of pathogenesis-related proteins in germinating wheat seeds infected with *Fusarium culmorum*. *Plant Sci.* 140, 87–97. doi: 10.1016/S0168-9452(98)00199-X

Chang, Y. C., Chang, Y. C., Baker, R., Kleifeld, O., and Chet, I. (1986). Increased growth of plants in the presence of the biological control agent *Trichoderma harzianum*. *Plant Dis.* 70, 145–148. doi: 10.1094/PD-70-145

Chen, W., Provart, N. J., Glazebrook, J., Katagiri, F., Chang, H. S., Eulgem, T., et al. (2002). Expression profile matrix of *Arabidopsis* transcription factor genes suggest their putative functions in response to environmental stresses. *Plant Cell* 14, 559–574. doi: 10.1105/tpc.010410

Coppola, M., Diretto, G., Digilio, M. C., Woo, S. L., Giuliano, G., Molisso, D., et al. (2019). Transcriptome and metabolome reprogramming in tomato plants by *Trichoderma harzianum* strain T22 primes and enhances defense responses against aphids. *Front. Physiol.* 10:745. doi: 10.3389/fphys.2019.00745

Curci, P. L., Aiese-Cigliano, R., Zuluaga, D. L., Janni, M., Sanseverino, W., and Sonnante, G. (2017). Transcriptomic response of durum wheat to nitrogen starvation. *Sci. Rep.* 7:1176. doi: 10.1038/s41598-017-01377-0

Dao, T. T. H., Linthorst, H. J. M., and Verpoorte, R. (2011). Chalcone synthase and its functions in plant resistance. *Phytochem. Rev.* 10, 397. doi: 10.1007/s11101-011-9211-7

Fan, H., Ding, L., Xu, Y., and Du, C. (2017). Seed germination, seedling growth and antioxidant system responses in cucumber exposed to $Ca(NO_3)_2$. *Hortic. Environ. Biotechnol.* 58, 548–559. doi: 10.1007/s13580-017-0025-4

FAOSTAT (2018). *Food and Agriculture Data*. Available at: www.fao.org/faostat/en (January 18, 2019).

Feng, H., Wang, X., Sun, Y., Wang, X., Chen, X., and Guo, J. (2011). Cloning and characterization of calcium binding EF-hand protein gene *TaCab1* from wheat and its expression in response to *Puccinia striiformis* f. sp. *tritici* and abiotic stresses. *Mol. Biol. Rep.* 38, 3857–3866. doi: 10.1007/s11033-010-0501-8

Fernandez, O., Béthencourt, L., Quero, A., Sangwan, R. S., and Clément, C. (2010). Trehalose and plant stress responses: friend or foe? *Trends Plant Sci.* 15, 409–417. doi: 10.1016/j.tplants.2010.04.004

Gangappa, S. N., and Botto, J. F. (2016). The multifaceted roles of HY5 in plant growth and development. *Mol. Plant* 9, 1353–1365. doi: 10.1016/j.molp.2016.07.002

Gimenez-Ibanez, S., and Solano, R. (2013). Nuclear jasmonate and salicylate signaling and crosstalk in defense against pathogens. *Front. Plant Sci.* 4:72. doi: 10.3389/fpls.2013.00072

Golkari, S., Gilbert, J., Ban, T., and Procunier, J. D. (2009). QTL-specific microarray gene expression analysis of wheat resistance to Fusarium head blight in Sumai-3 and two susceptible NILs. *Genome* 52, 409–418. doi: 10.1139/g09-018

Golkari, S., Gilbert, J., Prashar, S., and Procunier, J. D. (2007). Microarray analysis of *Fusarium graminearum*-induced wheat genes: identification of organ-specific and differentially expressed genes. *Plant Biotechnol J.* 5, 38–49. doi: 10.1111/j.1467-7652.2006.00213.x

Golldack, D., Li, C., Mohan, H., and Probst, N. (2014). Tolerance to drought and salt stress in plants: unraveling the signaling networks. *Front. Plant Sci.* 5:151. doi: 10.3389/fpls.2014.00151

Golldack, D., Quigley, F., Michalowski, C. B., Kamasani, U. R., and Bohnert, H. J. (2003). Salinity stress-tolerant and -sensitive rice (*Oryza sativa* L.) regulate AKT1-type potassium channel transcripts differently. *Plant Mol. Biol.* 51, 71–81.

Harman, G. E. (2006). Overview of mechanisms and uses of *Trichoderma* spp. *Phytopathology* 96, 190–194. doi: 10.1094/PHYTO-96-0190

Hermosa, R., Viterbo, A., Chet, I., and Monte, E. (2012). Plant-beneficial effects of *Trichoderma* and of its genes. *Microbiology SGM* 158, 17–25. doi: 10.1099/mic.0.052274-0

Hoang, X. L. T., Nhi, D. N. H., Thu, N. B. A., Thao, N. P., and Tran, L. S. P. (2017). Transcription factors and their roles in signal transduction in plants under abiotic stresses. *Curr. Genom.* 18, 483–497. doi: 10.2174/1389202918666170227150057

International Wheat Genome Sequencing Consortium [IWGSC] (2018). Shifting the limits in wheat research and breeding using a fully annotated reference genome. *Science* 361:eaar7191. doi: 10.1126/science.aar7191

Kang, J., Park, J., Choi, H., Burla, B., Kretzschmar, T., Lee, Y., et al. (2011). Plant ABC transporters. *Arabidopsis Book* 9:e0153. doi: 10.1199/tab.0153

Krapp, A. (2015). Plant nitrogen assimilation and its regulation: a complex puzzle with missing pieces. *Curr. Opin. Plant Biol.* 25, 115–122. doi: 10.1016/j.pbi.2015.05.010

Laudencia-Chingcuanco, D., Ganeshan, S., You, F., Fowler, B., Chibbar, R., and Anderson, O. (2011). Genome-wide gene expression analysis supports a developmental model of low temperature tolerance gene regulation in wheat (*Triticum aestivum* S.). *BMC Genom.* 12:299. doi: 10.1186/1471-2164-12-299

Li, C., and Wong, W. H. (2001). Model-based analysis of oligonucleotide arrays: model validation, design issues and standard error application. *Genom. Biol.* 2:research0032. doi: 10.1186/gb-2001-2-8-research0032

Li, D., Wang, P., Luo, Y., Zhao, M., and Chen, F. (2017). Health benefits of anthocyanins and molecular mechanisms: update from recent decade. *Crit. Rev. Food Sci. Nutr.* 57, 1729–1741. doi: 10.1080/10408398.2015.1030064

Li, J., Wu, W.-H., and Wang, Y. (2017). Potassium channel AKT1 is involved in the auxin-mediated root growth inhibition in *Arabidopsis* response to low K^+ stress. *J. Integr. Plant Biol.* 59, 895–909. doi: 10.1111/jipb.12575

Li, Q., Wang, W., Wang, W., Zhang, G., Liu, Y., Wang, Y., et al. (2018). Wheat F-box protein gene *FaFBA1* is involved in plant tolerance to heat stress. *Front. Plant Sci.* 9:521. doi: 10.3389/fpls.2018.00521

Li, R. X., Cai, F., Pang, G., Shen, Q. R., Li, R., and Chen, W. (2015). Solubilization of phosphate and micronutrients by *Trichoderma harzianum* and its relationship with the promotion of tomato plant growth. *PLoS One* 10:e0130081. doi: 10.1371/journal.pone.0130081

Li, Z. Y., and Chen, S. Y. (2000). Isolation and characterization of a salt- and drought-inducible gene for S-adenosylmethionine decarboxylase from wheat (*Triticum aesticum* L.). *J. Plant Physiol.* 156, 386–393. doi: 10.1016/S0176-1617(00)80078-4

Liu, M., Chen, Y., Chen, Y., Shin, J.-H., Mila, I., Audran, C., et al. (2018). The tomato Ethylene Response Factor SI-ERF.B3 integrates ethylene and auxin signaling via direct regulation of *SI-Aux/IAA27*. *New Phytol.* 219, 631–640. doi: 10.1111/nph.15165

Livak, K. J., and Schmittgen, T. D. (2001). Analysis of relative gene expression data using real-time quantitative PCR and the 2(-delta delta CT) method. *Methods* 25, 402–408. doi: 10.1006/meth.2001.1262

Lullien, V., Barker, D. G., de Lajudie, P., and Huguet, T. (1987). Plant gene expression in effective and ineffective root nodules of alfalfa (*Medicago sativa*). *Plant Mol. Biol.* 9, 469–478. doi: 10.1007/BF00015878

Morán-Diez, E., Rubio, B., Domínguez, S., Hermosa, R., Monte, E., and Nicolás, C. (2012). Transcriptomic response of *Arabidopsis thaliana* after 24 h incubation with the biocontrol fungus *Trichoderma harzianum*. *J. Plant Physiol.* 169, 614–620. doi: 10.1016/j.jplph.2011.12.016

Morán-Diez, M. E., Hermosa, R., Ambrosino, P., Cardoza, R. E., Gutiérrez, S., Lorito, M., et al. (2009). The ThPG1 endopolygalacturonase is required for the *Trichoderma harzianum*-plant beneficial interaction. *Mol. Plant Microbe Int.* 22, 1021–1031. doi: 10.1094/MPMI-22-8-1021

Narusaka, Y., Narusaka, M., Seki, M., Umezawa, T., Ishida, J., Nakajima, M., et al. (2004). Crosstalk in the responses to abiotic and biotic stresses in *Arabidopsis*: analysis of gene expression in *cytochrome P450* gene superfamily by cDNA microarray. *Plant Mol. Biol.* 55, 327–342. doi: 10.1007/s11103-004-0685-1

Pilcher, W., Zandkamiri, H., Arceneaux, K., Harrison, S., and Baisakh, N. (2017). Genome-wide microarray analysis leads to identification of genes in response to herbicide, metribuzin in wheat leaves. *PLoS One* 12:e0189639. doi: 10.1371/journal.pone.0189639

Pitzschke, A., Datta, S., and Persak, H. (2014). Salt stress in *Arabidopsis*: lipid transfer protein AZI1 and its control by mitogen-activated protein kinase MPK3. *Mol. Plant* 7, 722–738. doi: 10.1093/mp/sst157

Pollet, A., Sansen, S., Raedschelders, G., Gebruers, K., Rabijns, A., Delcour, J. A., et al. (2009). Identification of structural determinants for inhibition strength

and specificity of wheat xylanase inhibitors TAXI-IA and TAXI-IIA. *FEBS J.* 276, 3916–3927. doi: 10.1111/j.1742-4658.2009.07105.x

Ponnu, J., Wahl, V., and Schmid, M. (2011). Trehalose-6-phosphate: connecting plant metabolism and development. *Front. Plant Sci.* 2:70. doi: 10.3389/fpls.2011.00070

Raedschelders, G., Debefve, C., Goesaert, H., Delcour, J. A., Volckaert, G., and Van Campenhout, S. (2004). Molecular identification and chromosomal localization of genes encoding *Triticum aestivum* xylanase inhibitor I-like protein in cereals. *Ther. Appl. Genet.* 109, 112–121. doi: 10.1007/s00122-004-1601-4

Rockström, J., Steffen, W., Noone, K., Persson, A., Stuart-Chapin, F., Lambin, E. F., et al. (2009). A safe operating space for humanity. *Nature* 461, 472–475. doi: 10.1038/climate.2009.92

Rubio, M. B., Hermosa, R., Vicente, R., Gómez-Acosta, F. A., Morcuende, R., Monte, E., et al. (2017). The combination of *Trichoderma harzianum* and chemical fertilization leads to the deregulation of phytohormone networking, preventing the adaptive responses of tomato plants to salt stress. *Front. Plant Sci.* 8:294. doi: 10.3389/fpls.2017.00294

Rubio, M. B., Quijada, N. M., Pérez, E., Domínguez, S., Monte, E., and Hermosa, R. (2014). Identifying beneficial qualities of *Trichoderma parareesei* for plants. *Appl. Environ. Microbiol.* 80, 1864–1873. doi: 10.1128/AEM.03375-13

Salazar-Badillo, F. B., Sanchez-Rangel, D., Becerra-Flora, A., Lopez-Gomez, M., Nieto-Jacobo, F., Mendoza-Mendoza, A., et al. (2015). *Arabidopsis thaliana* polyamine content is modified by the interaction with different *Trichoderma* species. *Plant Physiol. Biochem.* 95, 49–56. doi: 10.1016/j.plaphy.2015.07.003

Sedbrook, J. C., Carroll, K. L., Hung, K. F., Masson, P. H., and Somerville, C. R. (2002). The *Arabidopsis SKU5* gene encodes an extracellular glycosyl phosphatidylinositol-anchored glycoprotein involved in directional root growth. *Plant Cell* 14, 1634–1648. doi: 10.1105/tpc.002360

Shoresh, M., Harman, G. E., and Mastouri, F. (2010). Induced systemic resistance and plant responses to fungal biocontrol agents. *Annu. Rev. Phytopathol.* 48, 21–43. doi: 10.1146/annurev-phyto-073009-114450

Singh, A., Mantri, S., Sharma, M., Chaudhury, A., Tuli, R., and Roy, J. (2014). Genome-wide transcriptome study in wheat identified candidate genes related to processing quality, majority of them showing interaction (quality x development) and having temporal and spatial distributions. *BMC Genom.* 15:29. doi: 10.1186/1471-2164-15-29

Szalai, G., Janda, K., Darkó, E., Janda, T., Peeva, V., and Pál, M. (2017). Comparative analysis of polyamine metabolism in wheat and maize plants. *Plant Physiol. Biochem.* 112, 239–250. doi: 10.1016/j.plaphy.2017.01.012

Thomas, B. R., Romero, G. O., Nevins, D. J., and Rodriguez, R. E. (2000). New perspectives on the endo-beta-glucanases of glycosyl hydrolase Family 17. *Int. J. Biol. Macromol.* 27, 139–144. doi: 10.1016/S0141-8130(00)00109-4

Van de Poel, B., Bulens, I., Oppermann, Y., Hertog, M. L., Nicolai, B. M., Sauter, M., et al. (2013). S-adenosyl-L-methionine usage during climacteric ripening of tomato in relation to ethylene and polyamine biosynthesis and transmethylation capacity. *Physiol. Plant* 148, 176–188. doi: 10.1111/j.1399-3054.2012.01703.x

Vicente, R., Pérez, P., Martínez-Carrasco, R., Feil, R., Lunn, J. E., Watanabe, M., et al. (2016). Metabolic and transcriptional analysis of durum wheat responses to elevated CO_2 at low and high nitrate supply. *Plant Cell Physiol.* 57, 2133–2146. doi: 10.1093/pcp/pcw131

Vita, F., Giuntoli, B., Arena, S., Quaranta, F., Bertolini, E., Lucarotti, V., et al. (2018). Effects of different nitrogen fertilizers on two wheat cultivars: an integrated approach. *Plant Direct* 2:e00089. doi: 10.1002/pld3.89

Viterbo, A., Landau, U., Kim, S., Chernin, L., and Chet, I. (2010). Characterization of ACC deaminase from the biocontrol and plant growth-promoting agent *Trichoderma asperellum* T203. *FEMS Microbiol. Lett.* 305, 42–48. doi: 10.1111/j.1574-6968.2010.01910.x

Wan, Y., Gritsch, F., Hawkesford, M., and Shewry, P. (2013). Effects of nitrogen nutrition on the synthesis and deposition of the ω-gliadins of wheat. *Ann. Bot.* 113, 607–615. doi: 10.1093/aob/mct291

Wang, F., Lin, R., Feng, J., Chen, W., Qiu, D., and Xu, S. (2015). TaNAC1 acts as a negative regulator of stripe rust resistance in wheat, enhances susceptibility to *Pseudomonas syringae*, and promotes lateral root development in transgenic *Arabidopsis thaliana*. *Front. Plant Sci.* 6:108. doi: 10.3389/fpls.2015.00108

Yang, Y., Yu, Y., Liang, Y., Anderson, C. T., and Cao, J. (2018). A profusion of molecular scissors for pectins: classification, expression, and functions of plant polygalacturonase. *Front. Plant Sci.* 9:1208. doi: 10.3389/fpls.2018.01208

Zhang, Y., Hu, X., Islam, S., She, M., Peng, Y., Yu, Z., et al. (2018). New insights into the evolution of wheat avenin-like proteins in wild emmer wheat (*Triticum dicoccoides*). *Proc. Natl. Acad. Sci. U.S.A.* 115, 13312–13317. doi: 10.1073/pnas.1812855115

Zhang, J. F., Xu, Y. Q., Dong, J. M., Peng, L. N., Feng, X., Wang, X., et al. (2018). Genome-wide identification of wheat (*Triticum aestivum*) expansins and expansin expression analysis in cold-tolerant and cold-sensitive wheat cultivars. *PLoS One* 13:e0195138. doi: 10.1371/journal.pone.0195138

Zhao, S., Fung-Leung, W. P., Bittner, A., Ngo, K., and Liu, X. (2014). Comparison of RNA-seq and microarray in transcriptome profiling of activated T cells. *PLoS One* 9:e78644. doi: 10.1371/journal.pone.0078644

Zörb, C., Ludewig, U., and Hawkesford, M. J. (2018). Perspective on wheat yield and quality with reduced nitrogen supply. *Trends Plant Sci.* 23, 1029–1037. doi: 10.1016/j.tplants.2018.08.012

Conflict of Interest: The authors declare that the research was conducted in the absence of any commercial or financial relationships that could be construed as a potential conflict of interest.

frontiers in Microbiology

ORIGINAL RESEARCH
published: 31 January 2020
doi: 10.3389/fmicb.2019.03042

Commercial Formulates of *Trichoderma* Induce Systemic Plant Resistance to *Meloidogyne incognita* in Tomato and the Effect Is Additive to That of the *Mi-1.2* Resistance Gene

*Miriam Pocurull[1], Aïda M. Fullana[1], Miquel Ferro[1], Pau Valero[1], Nuria Escudero[1], Ester Saus[2,3], Toni Gabaldón[2,3,4] and F. Javier Sorribas[1]**

[1] Department of Agri-Food Engineering and Biotechnology, Universitat Politècnica de Catalunya, Barcelona, Spain, [2] Bioinformatics and Genomics Program, Centre for Genomic Regulation, Barcelona Institute of Science and Technology, Barcelona, Spain, [3] Department of Experimental and Health Sciences, Universitat Pompeu Fabra, Barcelona, Spain, [4] Catalan Institute for Research and Advance Studies (ICREA), Barcelona, Spain

OPEN ACCESS

Edited by:
Santiago Gutierrez,
Universidad de León, Spain

Reviewed by:
Danny Coyne,
International Institute of Tropical Agriculture (IITA), Kenya
Lee Robertson,
Department of Plant Protection, National Institute of Agricultural and Food Research and Technology, Spain

***Correspondence:**
F. Javier Sorribas
francesc.xavier.sorribas@upc.edu

Specialty section:
This article was submitted to Plant Microbe Interactions, a section of the journal Frontiers in Microbiology

Received: 16 September 2019
Accepted: 17 December 2019
Published: 31 January 2020

Citation:
Pocurull M, Fullana AM, Ferro M, Valero P, Escudero N, Saus E, Gabaldón T and Sorribas FJ (2020) Commercial Formulates of Trichoderma Induce Systemic Plant Resistance to Meloidogyne incognita in Tomato and the Effect Is Additive to That of the Mi-1.2 Resistance Gene. Front. Microbiol. 10:3042. doi: 10.3389/fmicb.2019.03042

Meloidogyne is the most damaging plant parasitic nematode genus affecting vegetable crops worldwide. The induction of plant defense mechanisms against *Meloidogyne* in tomato by some *Trichoderma* spp. strains has been proven in pot experiments, but there is no information for tomato bearing the *Mi-1.2* resistance gene or for other important fruiting vegetable crops. Moreover, *Trichoderma* is mostly applied for managing fungal plant pathogens, but there is little information on its effect on nematode-antagonistic fungi naturally occurring in soils. Thus, several experiments were conducted to determine (i) the ability of two commercial formulates of *Trichoderma asperellum* (T34) and *Trichoderma harzianum* (T22) to induce systemic resistance in tomato and cucumber against an avirulent *Meloidogyne incognita* population in split-root experiments; (ii) the effect of combining T34 with tomato carrying the *Mi-1.2* resistance gene to an avirulent *M. incognita* population in sterilized soil; and (iii) the effect of combining T34 with tomato carrying the *Mi-1.2* resistance gene to a virulent *M. incognita* population in two suppressive soils in which *Pochonia chlamydosporia* is naturally present, and the effect of T34 on the level of *P. chlamydosporia* egg parasitism. Both *Trichoderma* formulates induced resistance to *M. incognita* in tomato but not in cucumber. In tomato, the number of egg masses and eggs per plant were reduced by 71 and 54% by T34, respectively. T22 reduced 48% of the number of eggs per plant but not the number of egg masses. T34 reduced the number of eggs per plant of the virulent *M. incognita* population in both resistant and susceptible tomato cultivars irrespective of the suppressive soil, and its effect was additive with the *Mi-1.2* resistance gene. The percentage of fungal egg parasitism by *P. chlamydosporia* was not affected by the isolate T34 of *T. asperellum*.

Keywords: *Cucumis sativus*, induced resistance, nematode virulence, *Pochonia chlamydosporia*, root-knot nematodes, *Solanum lycopersicum*

INTRODUCTION

The root-knot nematodes (RKN), *Meloidogyne* spp., are the most damaging obligate plant-endoparasitic nematode worldwide in a wide range of plant species (Jones et al., 2013). Among the more than 100 species included in this genus, the tropical RKN species, *Meloidogyne arenaria*, *Meloidogyne incognita*, and *Meloidogyne javanica*, cause the majority of vegetable yield losses (Hallman and Meressa, 2018). For instance, maximum yield losses reported for fruiting solanaceous and cucurbit crops, the most cultivated worldwide, range from 30 to 100% (Giné et al., 2014, 2017; López-Gómez et al., 2014; Seid et al., 2015; Giné and Sorribas, 2017; Hallman and Meressa, 2018). Despite that several methods for control are available (Nyczepir and Thomas, 2009), most producers rely on the use of chemical nematicides (Djian-Caporalino, 2012; Talavera et al., 2012). Nonetheless, due to the risks and impacts on human health and the environment, its use must be reduced in favor of alternative methods according to legislative regulations, such as the European Directive 2009/128/EC. Sustainable and safe alternatives are required, such as plant resistance and biological control (Hallmann et al., 2009; Williamson and Roberts, 2009).

Plant resistance is defined as the ability of a plant to suppress infection, development, and/or reproduction of plant parasitic nematodes (Roberts, 2002). Resistance can be conferred by one or a few specific genes or quantitative trait loci (Williamson and Roberts, 2009) or be induced by microorganisms (Hallmann et al., 2009; Schouten, 2016). Plant resistance conferred by resistance genes (*R*-genes) is an effective and economically profitable control method against the tropical RKN species (Sorribas et al., 2005). However, the availability of commercial fruiting vegetable-resistant cultivars and rootstocks is currently restricted to solanaceous crops such as tomato, pepper, and aubergine. Therefore, the continuous cultivation of plant germplasm carrying the same *R*-gene will lead to the selection of virulent nematode populations (Verdejo-Lucas et al., 2009; Thies, 2011; Ros-Ibáñez et al., 2014; Expósito et al., 2019). Some fungal and bacterial species are able to induce resistance against RKN in vegetable crops (Hallmann et al., 2009), including some strains of *Trichoderma* spp., i.e., *Trichoderma asperellum* strain 203, *Trichoderma atroviride* strain T11, and *Trichoderma harzianum* strain T-78 in tomato (Sharon et al., 2009; de Medeiros et al., 2017; Martínez-Medina et al., 2017). Several *Trichoderma* spp. strains are approved by the EU legislation for controlling plant diseases caused by fungi but none of them for those caused by plant-parasitic nematodes.

The possibility of using *Trichoderma* spp. to induce resistance to RKN has been studied in susceptible tomato cultivars (Sharon et al., 2009; de Medeiros et al., 2017; Martínez-Medina et al., 2017) but never on tomato carrying the *Mi-1.2* resistance gene. Induction of resistance in plants carrying *R*-genes could contribute to limit the selection of virulent nematode populations and thus enhancing the resistance durability. On the other hand, if resistance can be induced in plant species for which no commercial RKN-resistant cultivars or rootstocks are available, such as cucurbits, or against virulent nematode populations, primed plants could be included in rotation schemes to manage RKN and reduce crop yield losses.

Trichoderma is a cosmopolitan genus of filamentous fungi in the order Hypocreales, with a flexible lifestyle that includes endophytic, saprophytic, and facultative mycoparasitic capabilities. Thus, *Trichoderma* spp. might limit growth of other soil microorganisms by predation or resource competition, including nematode antagonistic fungi such as *Pochonia (Metacordyceps) chlamydosporia*. This fungal species is frequently isolated from RKN eggs produced in vegetable crop roots cultivated in northeastern Spain (Giné et al., 2012) and has been reported as the main biotic factor responsible for soil suppressiveness to RKN in this area (Giné et al., 2016). In addition, it has been reported that some *P. chlamydosporia* strains can induce systemic resistance in tomato plants (Ghahremani et al., 2019). Consequently, the proper use of *Trichoderma* must consider the possible side effect on fungal nematode antagonists present in soils. Previous studies have shown that the effects of *Trichoderma* to *P. chlamydosporia* can vary depending on the analyzed fungal strains. For example, some harmful effects such as a reduction in mycelial growth due to volatile compounds produced by a strain of *Trichoderma* spp. from Brazil (Ferreira et al., 2008) or mycelium lysis by a strain of *T. harzinaum* from the Netherlands (Kok et al., 2001) have been reported. On the other hand, non-observable effects on percentage of RKN-parasitized eggs by *P. chlamydosporia* due to a strain of *T. harzianum* from Cuba was noticed (Puertas et al., 2006). However, as far as we know, there is no information regarding the effect of commercial formulates of *Trichoderma* spp. on the level of fungal egg parasitism by natural occurring antagonists in soil to avoid side effects.

Thus, in this work, several experiments were conducted to determine (i) the ability of commercial formulates of strains T34 of *T. asperellum* [T34 Biocontrol (10^{12} cfu kg^{-1}); Biocontrol Technologies S.L.] and T22 of *T. harzianum* [Trianum P (10^{9} cfu g^{-1}); Koppert] to induce systemic resistance in tomato and cucumber against *M. incognita* in split-root experiments; (ii) the effect of combining T34 with tomato carrying the *Mi-1.2* resistance gene to an avirulent *M. incognita* population in sterilized soil; and (iii) the effect of combining T34 with tomato carrying the *Mi-1.2* resistance gene to a virulent *M. incognita* population in two suppressive soils where *P. chlamydosporia* is naturally present, as well as the effect of T34 on the level of *P. chlamydosporia* egg parasitism.

MATERIALS AND METHODS

Plants, Fungi, and Nematodes

Susceptible (*mi/mi*) tomato cv. Durinta, resistant (*Mi/mi*) tomato cv. Monika (Cortada et al., 2008), and cucumber cv. Dasher II were used for this study. For the split-root and the combination of plant resistance with T34 to an avirulent *M. incognita* population experiments, seeds were surface sterilized following the procedure described in Ghahremani et al. (2019).

The commercial formulates of *T. asperellum* T34 (T34 Biocontrol; Biocontrol Technologies S.L.) and of *T. harzianum* T22 (Trianum P; Koppert) were used. These *Trichoderma* strains were selected because, despite the *T. asperellum* strain T203 and the T-78 of *T. harzianum* have been demonstrated to induce resistance to RKN in susceptible tomato (Sharon et al., 2009; Martínez-Medina et al., 2017), they are not currently approved in Europe. The strains used in this study are approved in Europe for the management of some fungal plant pathogens, and there are commercial formulates based on these strains available for producers in Spain. The viability of the inoculum was assessed by serial dilution from the commercial formulate and plating onto PDA, and the number of colony forming units were counted after 24 h of incubation at 25°C in the dark.

Second stage juveniles (J2) of the avirulent *M. incognita* population Agròpolis and the virulent population Agrovir were used in this study. The Agrovir population was selected from the Agròpolis population after cultivation of tomato grafted onto the resistant tomato rootstock cv. Aligator (Expósito et al., 2019). J2 were obtained from eggs extracted from resistant (Agrovir population) or susceptible (Agròpolis population) tomato roots by blender maceration in a 5% commercial bleach solution (40 g l^{-1} NaOCl) for 10 min (Hussey and Barker's, 1973). The suspension was passed through a 74-μm aperture sieve, and the eggs were collected on a 25-μm sieve. Eggs were placed on Baermann trays (Whitehead and Hemming, 1965) and incubated at 25 ± 2°C. J2 were collected daily for 7 days using a 25-μm sieve and stored at 9°C unless used.

Induction of Systemic Plant Resistance to an Avirulent *M. incognita* Population by *T. asperellum* T34 and *T. harzianum* T22

Tomato and cucumber were grown in a split-root system, following the procedure described in Ghahremani et al. (2019), in which the plant root is divided into two halves transplanted in two adjacent pots: the inducer, inoculated with the antagonist, and the responder, inoculated with the nematode. The main root of 5-day-old seedlings was excised, and plantlets were individually transplanted into seedling trays containing sterile vermiculite and maintained in a growth chamber at 25 ± 2°C with a 16/8 h (light/dark) photoperiod for 2 weeks for cucumber and 3 weeks for tomato plants. Afterward, plantlets were transferred to the split-root system by splitting roots into two halves planted in two adjacent 200-cm^3 pots filled with sterilized sand. The inducer part of the root was inoculated with a suspension of 10^5 cfu of *T. harzianum* T22 (T22) or *T. asperellum* T34 (T34) just before transplanting. This fungal dosage was selected because it was the same at which *P. chlamydosporia* induced resistance in tomato (Ghahremani et al., 2019). One week later, the responder part of the root was inoculated with the avirulent *M. incognita* population Agròpolis at a rate of 1 J2 cm^{-3} of soil (RKN). Five treatments were assessed: (i) the inducer inoculated with T22 and the responder with the nematode (T22-RKN), (ii) the inducer inoculated with T34 and the responder with the nematode (T34-RKN), (iii) the inducer non-inoculated with any fungal strain (None) and the responder inoculated with the nematode (None-RKN), (iv) the inducer inoculated with T22 and the responder non-inoculated (T22-None), (v) the inducer inoculated with T34 and the responder non-inoculated (T34-None), and (vi) neither inducer nor responder inoculated (None–None). Treatments (i)–(iii) served to assess the capability of each *Trichoderma* strain to induce plant resistant against the nematode, and treatments (iv)–(vi) were included to assess the effect of each *Trichoderma* strain on plant development. The non-inoculated inducer or responder parts of the root received the same volume of water than those inoculated with the fungal strains or the nematode. Each treatment was replicated 10 times. The plants were maintained in a growth chamber at 25 ± 2°C and photoperiod of 16-/8-h light/dark in a completely randomized design for 40 days. The plants were irrigated as needed and fertilized with Hoagland solution twice per week. Soil temperatures were recorded daily at 30-min intervals with a PT100 probe (Campbell Scientific, Ltd.) placed in the pots at a depth of 4 cm. At the end of the experiments, the foliar surface area of each single plant was measured with a Li-3100 AREA ETER (LI-COR, Inc., Lincoln, NE, United States). Afterward, the aboveground part of each plant was oven dried at 70°C for 2 days, and the dry shoot weight was recorded. The fresh weight of the inducer and responder part of the root system was also recorded. The number of egg masses produced in the responder part of the roots inoculated with the nematode was counted after being stained with a 0.01% erioglaucine solution for 45 min (Omwega et al., 1988). After that, the nematode eggs were extracted from the responder part of the roots by blender maceration in a 10% commercial bleach solution (40 g l^{-1} NaOCl) for 10 min following the Hussey and Barker's (1973) procedure and counted.

Combined Effect of *T. asperellum* T34 and Tomato-Resistant Germplasm to an Avirulent *M. incognita* Population

Resistant tomato cv. Monika and susceptible cv. Durinta plants were germinated as previously stated and grown in a growth chamber at 25 ± 2°C and photoperiod of 16/8 h light/dark. Three leaves stage plants were transferred to 200-cm^3 pots filled with sterilized sand. The experiment was composed by the following treatments: (i) susceptible tomato plants inoculated with 1 J2 cm^{-3} of soil, (ii) susceptible tomato plants inoculated with T34 7 days before nematode inoculation, (iii) resistant tomato plants inoculated with 1 J2 cm^{-3} of soil, and (iv) resistant tomato plants inoculated with T34 7 days before nematode inoculation. The *T. asperellum* T34 was applied at the rate recommended by the manufacturer, 0.01 g l^{-1} of soil as liquid suspension (2×10^6 cfu per plant). Each treatment was replicated 15 times. Plants were maintained in a growth chamber at the same conditions for 40 days. At the end of the experiment, roots were processed as previously described before the number of egg masses and eggs were counted.

Combined Effect of *T. asperellum* T34 and Tomato-Resistant Germplasm to a Virulent *M. incognita* Population and Effect of T34 on Natural Nematode Antagonism by *P. chlamydosporia*

Plants of the resistant tomato cv. Monika and the susceptible cv. Durinta supplied by Hishtil Gelpi Spain were used for the experiment. The experiment was conducted with soil taken from two sites located at the Tarragona Province (northeastern Spain), M10.23 and M10.55, where vegetables are commercially produced under organic standards in plastic greenhouse. The site M10.23 was a loam soil (45% sand, 40% silt, and 15% clay), pH 8.3, 5.8% organic matter (*w*/*w*), and 276 μS cm^{-1} electric conductivity. The site M10.55 was a sandy clay loam soil (68% sand, 0% silt, and 32% clay), pH 8.1, 2.5 organic matter (*w*/*w*), and 1,069 μS cm^{-1} electric conductivity. Both soils were previously characterized as suppressive to *Meloidogyne*, with *P. chlamydosporia* as the only fungal species recovered from RKN-parasitized eggs (Giné et al., 2016). Each soil was mixed with steam-sterilized sand at a ratio of 1:1 (dry w/dry w), to avoid soil compaction and to improve plant growth, and served as substrate for cropping tomato plants in 3-l pots. The population density of *Meloidogyne* J2 in the soil mixture was determined by counting the nematodes extracted from three 500-cm^3 samples of each soil mixture by Baermann trays (Whitehead and Hemming, 1965) and incubated at 27 ± 2°C for 1 week. The experiment consisted of four treatments per soil: (i) susceptible tomato plants inoculated in the seedling tray with T34 7 days before transplanting and also just after transplanting and with J2 of the virulent *M. incognita* Agrovir population to achieve 1 J2 cm^{-3} of mixed soil per pot, (ii) susceptible tomato plants inoculated with the virulent nematode population, (iii) resistant tomato plants inoculated in the seedling tray with T34 7 days before transplanting and just after transplanting and with the virulent nematode population, and (iv) resistant tomato plants inoculated with the virulent nematode population. The *T. asperellum* T34 was applied at the dose recommended by the manufacturer as liquid suspension, 0.5 g of T34 m^{-2} of seedling tray before transplanting (1.9×10^6 cfu per plantlet) and 0.01 g l^{-1} of soil (3×10^7 cfu per plant) just after transplanting. Each treatment was replicated 15 times per each soil (M10.23 and M10.55). Plants were maintained in a greenhouse for 40 days. In addition, three plants of each tomato cultivar growing in sterilized sand and inoculated with T34 at the same dose and timing were included to compare the ability of *T. asperellum* to colonize roots in non-sterilized mixed soil versus sterilized sand. At the end of the experiment, three egg masses per plant were taken for quantification of fungal egg parasitism as described in Giné et al. (2016). Afterward, eggs were extracted from roots and counted following the procedure previously described.

The detection and quantification of *T. asperellum* in tomato roots and in M10.23 and M10.55 soils were estimated using the TaqMan-quantitative PCR (qPCR) protocol specifically designed for this fungus by Gerin et al. (2018). Root colonization of plants grown in the M10.23 and M10.55 soils was estimated from three biological replicates per treatment. Each biological replicate consisted of a pool of 3-g, 1-g root per each of three plants. For plants cultivated in sterilized sand, each plant was considered an independent biological replicate. For soil replicates, the pooled soil from three independent pots per treatment was used. DNA extraction from roots was carried out as in Lopez-Llorca et al. (2010), while DNA was extracted from soil samples using the DNeasy PowerLyzer PowerSoil Kit (Qiagen) following the manufacturer's instructions. All DNA samples were quantified using Qubit dsDNA BR assay kit (Thermo Fisher Scientific). qPCR reactions were performed using the Sso AdvancedTM Universal Probes Supermix (Bio-Rad Laboratories, Hercules, CA, United States) in a final volume of 20 μl containing 40 ng of total DNA, 250 nM of each primer (5′ to 3′ direction) Ta_rpb2_fw (GGAGGTCGTTGAGGAGTACGAA) and Ta_rpb2_rev_3 (TTGCAGATAGGATTTACGACGAGT) and 150 nM of Ta_rpb2_probe (FAM-CGCTGAGGTATCCCCATGCGACA-BHQ1) (Gerin et al., 2018). Negative controls containing sterile water instead of DNA were included. Reactions were performed in duplicate in a 7900HT Fast Real-Time PCR System thermocycler (Applied Biosystems) using the following thermal cycling conditions: initial denaturation step at 95°C for 2 min, then 40 cycles at 95°C for 5 s, and 64.5°C for 30 s. Genomic DNA dilutions of the *T. asperellum* T34 were used to define a calibration curve from 10 pg to 100 ng. The specificity of the PCR amplicons was verified by agarose gel electrophoresis. *T. asperellum* DNA biomass was referred to the total DNA biomass (40 ng).

Statistical Analysis

Statistical analyses were performed using the JMP software v8 (SAS Institute, Inc., Cary, NC, United States). Both data normality and homogeneity of variances were assessed. When confirmed, a paired comparison using the Student's *t*-test was done, or Dunnett's test for multiple comparisons with a control. Otherwise, paired comparison was done using the non-parametric Wilcoxon test or multiple comparison using the Kruskal–Wallis test and groups separated by Dunn's test ($P \leq 0.05$).

RESULTS

Induction of Systemic Plant Resistance to an Avirulent *M. incognita* Population by *T. asperellum* T34 and *T. harzianum* T22

The split-root system did not influence tomato or cucumber root development since root fresh weight did not differ between the two halves of the split-root system of the None–None treatment ($P < 0.05$) (data not shown). Both tomato shoot dry biomass and leaf surface area did not differ ($P < 0.05$) between treatments (data not shown). In cucumber, shoot dry biomass did not differ, but the leaf surface area of the None–None treatment was lower ($P < 0.05$) than the remaining ones (**Figure 1**).

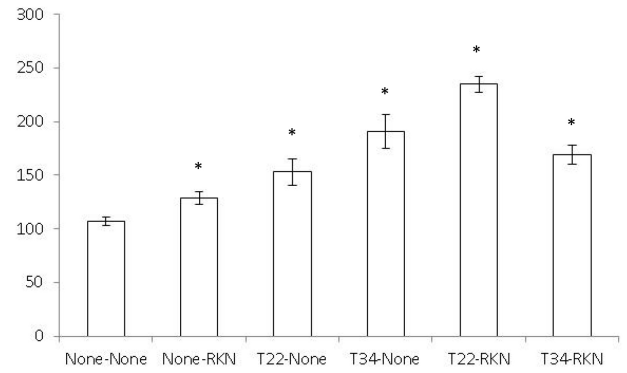

FIGURE 1 | Cucumber leaf area surface (cm^2) in a split-root system experiment conducted in two adjacent 200-ml pots (inducer–responder) in which the inducer part of the root was non-inoculated (None-) or inoculated with 10^5 cfu of *Trichoderma harzianum* T22 (T22-) or *T. asperellum* T34 (T34-) just before transplanting and the responder part of the root was non-inoculated (-None) or inoculated at a rate of 1 J2 cm^{-3} of soil of the avirulent *Meloidogyne incognita* population Agròpolis (-RKN) 1 week after fungal inoculation. Each value is mean (column) of 10 replications and the standard error (bar). Column with asterisk differ ($P < 0.05$) from the treatment None–None according to the Dunnett's test.

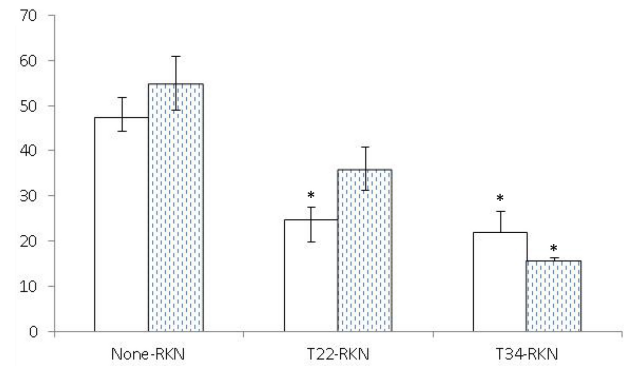

FIGURE 2 | Number of eggs ($\times 10^3$) (white column) and egg masses (spotted column) produced by the avirulent *M. incognita* population Agròpolis (-RKN) in the responder part of the root of the susceptible tomato cv. Durinta in a split-root system experiment conducted in two adjacent 200-ml pots (inducer–responder) in which the inducer part of the root was non-inoculated (None-) or inoculated with 10^5 cfu of *T. harzianum* T22 (T22-) or *T. asperellum* T34 (T34-) just before transplanting and the responder part of the root was non-inoculated (-None) or inoculated at a rate of 1 J2 cm^{-3} of soil of the avirulent *M. incognita* population Agròpolis 1 week after fungal inoculation. Each value is mean of 10 replications and the standard error (bar). Column for each variable with asterisk differ ($P < 0.05$) from the treatment None-RKN according to the Dunnett's test.

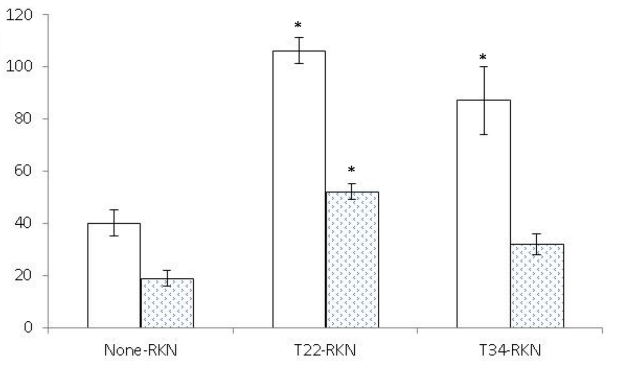

FIGURE 3 | Number of eggs ($\times 10^2$) (white column) and egg masses (spotted column) produced by the avirulent *M. incognita* population Agròpolis (-RKN) in the responder part of the root of the susceptible cucumber cv. Dasher II in a split-root system experiment conducted in two adjacent 200-ml pots (inducer–responder) in which the inducer part of the root was non-inoculated (None-) or inoculated with 10^5 cfu of *T. harzianum* T22 (T22-) or *T. asperellum* T34 (T34-) just before transplanting and the responder part of the root was non-inoculated (-None) or inoculated at a rate of 1 J2 cm^{-3} of soil of the avirulent *M. incognita* population Agròpolis 1 week after fungal inoculation. Each value is mean of 10 replications and the standard error (bar). Column for each variable with asterisk differ ($P < 0.05$) from the treatment None-RKN according to the Dunnett's test.

Both *Trichoderma* strains induced systemic resistance in tomato (**Figure 2**) but not in cucumber (**Figure 3**). *Trichoderma asperellum* T34 reduced both nematode infectivity and reproduction ($P < 0.05$) by 71 and 54%, respectively. Meanwhile, *T. harzianum* T22 suppressed nematode reproduction by 48%, but did not affect nematode infectivity ($P < 0.05$). For cucumber, the number of egg masses in the responder part of the root of the T22-RKN treatment was 2.7 times higher ($P < 0.05$) than in the None-RKN treatment, and the number of eggs in the responder part of the root of T22-RKN and T34-RKN treatments was 2.7 and 2.2 times higher ($P < 0.05$) than in the None-RKN treatment, respectively.

Combined Effect of *T. asperellum* T34 and Tomato-Resistant Germplasm to an Avirulent *M. incognita* Population

The infectivity and reproduction of the avirulent *M. incognita* population Agròpolis in the non-inoculated T34 resistant tomato were 97.7 and 97.2% lower ($P < 0.05$) than in the susceptible cultivar. For resistant tomato inoculated with T34, we observed a reduction of 98.2 and 98.7%, respectively, compared to the susceptible cultivar treated with T34 ($P < 0.05$).

The number of egg masses and eggs of *M. incognita* produced in the susceptible tomato plants inoculated with T34 were 20 and 30% lower ($P < 0.05$) than those observed in the non-inoculated susceptible plants. Regarding the resistant tomato, non-statistical differences ($P < 0.05$) were found between T34-inoculated and non-inoculated plants. Nonetheless, fewer egg masses and eggs per plant were recorded in the resistant tomato inoculated with T34 than in the non-inoculated (**Figure 4**).

Combined Effect of *T. asperellum* T34 and Resistant Tomato to a Virulent *M. incognita* Population and Effect of T34 on Natural Nematode Antagonism by *P. chlamydosporia*

In soil M10.23, resistant tomato plants presented a 46% reduction of eggs compared to susceptible tomato plants ($P < 0.05$)

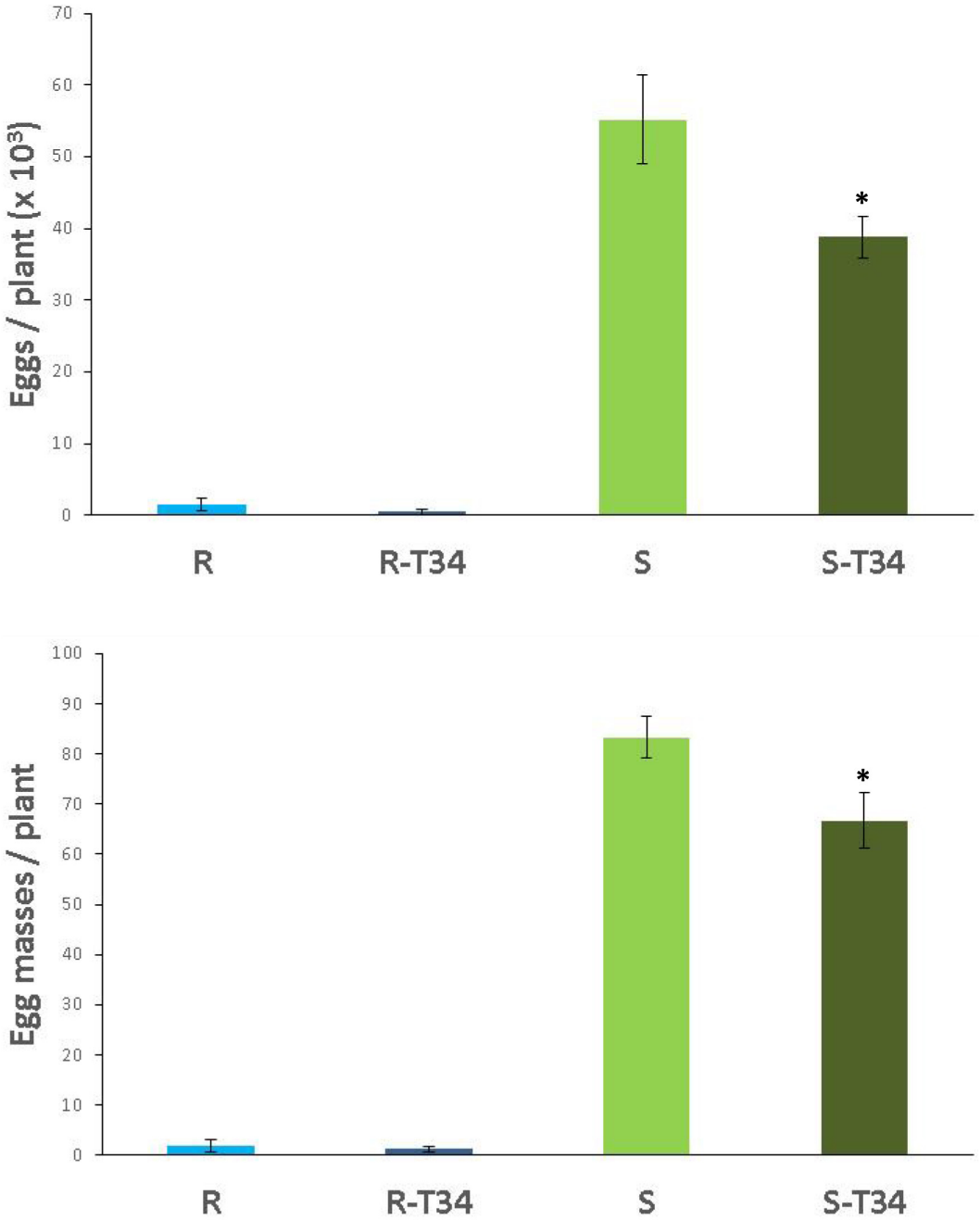

FIGURE 4 | Number of eggs ($\times 10^3$) and egg masses produced by the avirulent *M. incognita* population Agròpolis in the resistant tomato cv. Monika (R) and the susceptible cv. Durinta (S) cultivated in 200-ml pots inoculated with *Trichoderma asperellum* T34 (T34) at a rate of 0.01 g l^{-1} of soil (2×10^6 cfu per plant) just after transplanting and 7 days before inoculation with 1 J2 cm^{-3} of soil. Each value is mean (column) of 15 replications and the standard error (bar). Column with asterisk indicate differences ($P < 0.05$) between treatments within each tomato cultivar according to the Wilcoxon test.

independently of T34 treatment. In both tomato cultivars, the nematode produced 41% fewer eggs in T34-inoculated than in non-inoculated plants (**Figure 5A**). *P. chlamydosporia* was the only fungal species isolated from parasitized eggs. The percentage of parasitized eggs ranged from 21 to 28% and did not differ ($P < 0.05$) between tomato cultivars or between T34-inoculated and non-inoculated plants.

In soil M10.55, the nematode produced 77% fewer eggs ($P < 0.05$) in the resistant than in the susceptible tomato cultivar inoculated with T34, and 62% fewer eggs ($P < 0.05$) in the non-T34 inoculated resistant than susceptible tomato plants. The nematode produced 58% fewer ($P < 0.05$) eggs in T34-inoculated than in non-inoculated resistant tomato, and 31.6% fewer eggs in susceptible T34-inoculated tomato than

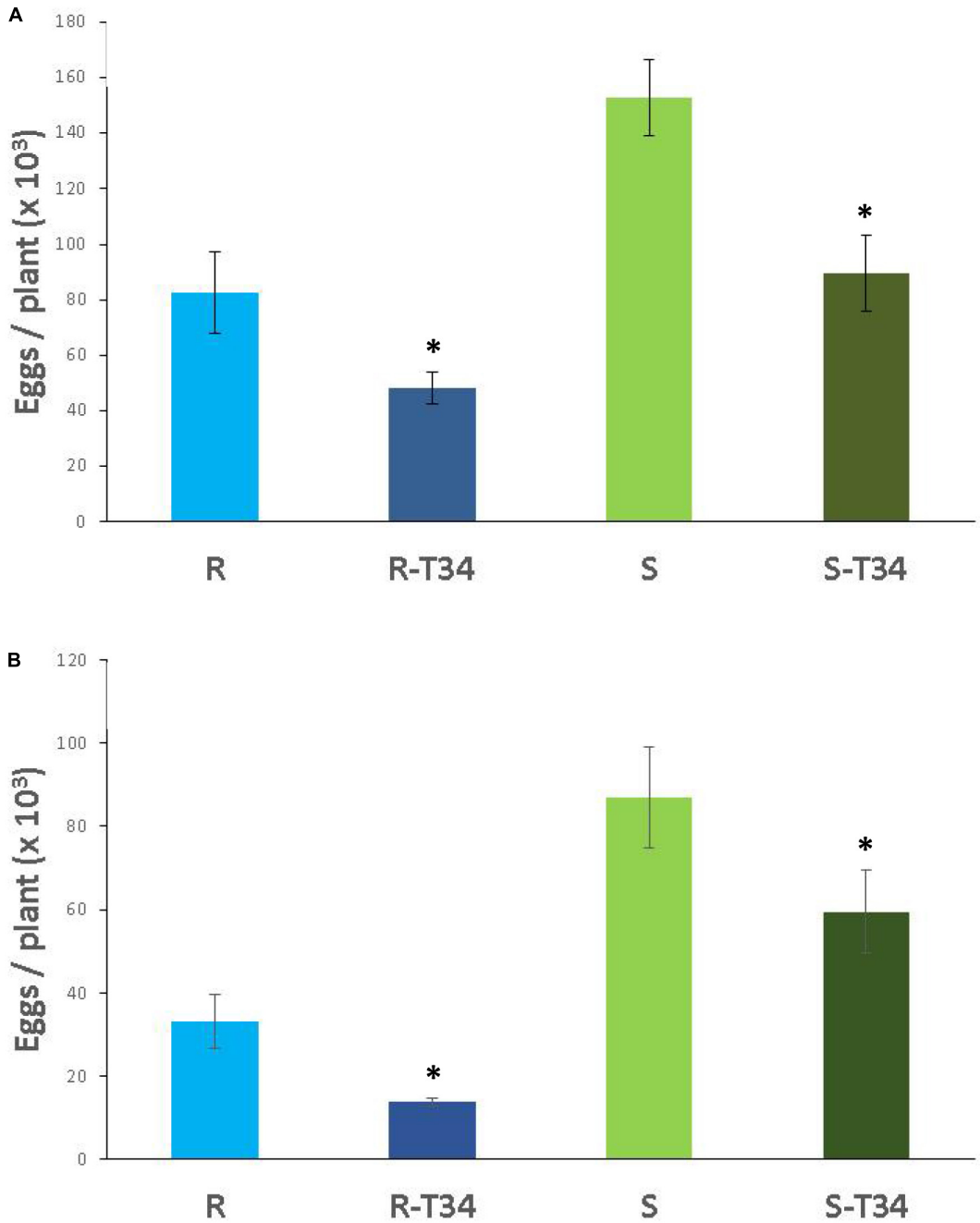

FIGURE 5 | Number of eggs ($\times 10^3$) produced by the virulent *M. incognita* population Agrovir in the resistant tomato cv. Monika (R) and the susceptible cv. Durinta (S) inoculated with *Trichoderma asperellum* T34 (T34) in the seedling trays at a rate of 0.5 g m^{-2} (1.9×10^6 cfu per plantlet) 7 days before transplanting, and at rate of 0.01 g l^{-1} of soil M10.23 **(A)** or M10.55 **(B)** at transplanting in 3-L pots (3×10^7 cfu per plant) and inoculated with J2 to achieve a rate of 1 J2 cm^{-3} of soil. Each value is mean (column) of 15 replications and the standard error (bar). Column with asterisk indicate differences ($P < 0.05$) between treatments within each tomato cultivar according to the Wilcoxon test.

in non-inoculated (**Figure 5B**). The percentage of parasitized eggs ranged from 25.4 to 28.9% and did not differ between tomato cultivars or T34-inoculated and non-inoculated plants. *P. chlamydosporia* was isolated from 90% of the total parasitized eggs, *T. asperellum* from 5%, and the remaining 5% were parasitized by an unidentified fungal species.

The standard curve for qPCR obtained by representing the cycle threshold (Ct) against log of 10-fold serial dilution of DNA from *T. asperellum* T34 was accurate and reproducible to estimate the DNA concentration of this fungal species ($y = -3.1479x + 24.79$; $R^2 = 0.9956$). The DNA concentration in the M10.23 and M10.55 soil samples was very low since

Ct values were higher than 35 cycles. Regarding the root samples, the DNA concentration was also very low except for two biological replicates of tomato cultivated in soil M10.55, one biological replicate of cv. Durinta inoculated with T34 and one of cv. Monika non-inoculated with T34 (**Supplementary Table S1**). Regarding the tomato plants cultivated in sterilized sand inoculated with T34, the majority of the Ct values was below 35 cycles, and the *T. asperellum* DNA concentration was estimated from those replicates. After analyzing 40 ng of DNA extracted from tomato roots, the estimated DNA content for *T. asperellum* did not differ ($P < 0.05$). It was 0.067 ± 0.018 ng in cv. Durinta and 0.087 ± 0.027 ng in cv. Monika.

DISCUSSION

This study provides evidence for the ability of two commercial *Trichoderma*-based formulates, T34 Biocontrol (*T. asperellum* strain T34) and Trianum P (*T. harzianum* strain T22), to induce systemic resistance in tomato against *M. incognita.* Systemic induction of plant defense mechanisms in tomato to RKN by different species and/or strains of *Trichoderma*, i.e., *T. asperellum* strain 203, *T. atroviride* strain T11, and *T. harzianum* strain T78, has been proven (Sharon et al., 2009; de Medeiros et al., 2017; Martínez-Medina et al., 2017). Martínez-Medina et al. (2017) studied the hormonal regulation pathways and proposed a three-phase model, that is, an early induction of the salicylic acid pathway suppressing RKN infection, a second phase mediated by jasmonic acid induction suppressing RKN reproduction and fecundity, and a final salicylic acid induction that affects root infection by the next J2 generation. Interestingly, the results of this study show that the resistance is also induced in tomato bearing the *Mi-1.2* resistance gene. The effect of combining *R*-genes with induced resistance by *Trichoderma* was more evident against the virulent nematode population than the avirulent one, which was highly suppressed by the *Mi-1.2* resistance gene although relatively less infection (34%) and reproduction (67%) was recorded in relation to the non-inoculated plants. Primed plants by *Trichoderma* can suppress the virulent nematode reproduction about 50%. Then, the resistance induced by *Trichoderma* is additive to that provided by the *Mi-1.2* gene. Thus, primed plants could be used as an additional sustainable tool to manage virulent nematode populations and also be useful for suppressing RKN species non-affected by the *M1.2* resistance gene such as *Meloidogyne hapla* (Liu and Williamson, 2006) and *Meloidogyne enterolobii* (Brito et al., 2007). Nonetheless, some -omic studies should be conducted to know the gene regulation and the physiological changes induced by the fungus in resistant tomato plants to foresee the possible medium to long-term consequences of using both types of resistance. If the additive effect is due to an overexpression of defense mechanisms usually expressed in *R*-gene-resistant plants, the probability for selecting virulent nematodes could be higher than if additional defense mechanisms are activated.

Interestingly, we found that the induction of resistance to *M. incognita* by both *Trichoderma* strains vary between plant species. Some reports have demonstrated the capability of *Trichoderma* strains to induce resistance in cucumber against several microbial plant pathogens (Khan et al., 2004; Shoresh et al., 2005; Segarra et al., 2007; Alizadeh et al., 2013; Sabbagh et al., 2017; Yuan et al., 2019). Segarra et al. (2007) found that *T. asperellum* T34 increased the concentration of salicylic acid and jasmonic acid in cotyledons of cucumber between 3 and 48 h suppressing *Pseudomonas syringae* pv. *lachrymans* inoculated 24 h after fungal inoculation. That experiment used a different inoculation regime, including a higher concentration of fungal spores, and thus, it is possible that the dosage used in the present work is sufficient to induce resistance in tomato but not in cucumber. *P. chlamydosporia* also induced systemic plant resistance against *M. incognita* in tomato but not in cucumber inoculated with 10^5 viable chlamydospores (Ghahremani et al., 2019). Increasing the inoculum density of *Trichoderma* per cucumber plant could modify this result and should be investigated. In addition to that, other causes could be responsible for the lack of induction of plant resistance to RKN. Recently, Chen et al. (2018) have reported that vanillic acid, a root exudate of cucumber, influences the fungal community in the rhizosphere and the abundance of *Trichoderma* and *Fusarium* species depending on the vanillic acid concentration. In our study, both *Trichoderma* strains increased the nematode reproduction in cucumber compared to the non-fungal-inoculated plants. As such, we cannot discard the possibility that *Trichoderma* might increase nematode susceptibility on cucumber plants. Further studies are needed to elucidate this.

T34 did not affect *P. chlamydosporia* egg parasitism that naturally occurred in soils M10.23 and M10.55. The ability of some *Trichoderma* spp. to parasitize nematode eggs and juveniles has been proven, and the mechanisms involved have been studied (summarized in Sharon et al., 2011; Szabó et al., 2012). The *T. asperellum* T34 used in this study can parasitize individual eggs in *in vitro* conditions (data not shown), but it was only isolated from 5% of the total *M. incognita* parasitized eggs produced in tomato cultivated in soil M10.55 inoculated with T34. This reduced ability of *Trichoderma* for parasitizing RKN eggs in comparison to other fungal egg parasites naturally occurring in soil can explain the lack of references regarding isolation of *Trichoderma* spp. from RKN eggs in vegetable growing areas from Spain (Olivares and López-Llorca, 2002; Verdejo-Lucas et al., 2002, 2013; Giné et al., 2012).

It is known that *Trichoderma* spp. strains can act as nematode antagonists affecting J2 motility, nematode development, egg hatching, nematode reproduction, and disease severity (summarized in Sharon et al., 2009; Wann et al., 2016), and also inducing resistance against RKN in susceptible tomato cultivars (Sharon et al., 2009; de Medeiros et al., 2017; Martínez-Medina et al., 2017). This study provides new evidence of the ability of some additional *Trichoderma* strains to induce resistance to RKN in susceptible tomato and demonstrate for the first time the ability to induce resistance in tomato carrying the *Mi-1.2* gene and that this resistance is additive to that provided by the *R*-gene against a virulent nematode population.

CONCLUSION

This study proves that the strains T34 of *T. asperellum* and T22 of *T. harzianum* induce resistance against *M. incognita* in tomato but not in cucumber, at least under our experimental conditions. Resistance conferred by the *Mi-1.2* resistance gene and that induced by T34 in tomato is additive. Finally, T34 does not affect the egg parasitism by the naturally occurring *P. chlamydosporia*. To foresee the potential selection for nematode virulence, future studies are needed to understand the genes related and the physiological changes involved in inducing resistance in tomato plants bearing the *Mi-1.2* gene. Moreover, the compatibility of commercial *Trichoderma* formulates with nematode antagonists that occurs naturally should be studied in deep to avoid potential detrimental effects.

DATA AVAILABILITY STATEMENT

All datasets generated for this study are included in the article/**Supplementary Material**.

AUTHOR CONTRIBUTIONS

FS and NE conceived, designed, and supervised the experiments, the data collection, and analyses. MP performed the split-root experiments and analyzed the data. AF, MF, and PV performed the experiments combining plant germplasm with T34 in different soils and analyzed the data. NE, ES, MF, and AF performed the molecular analysis. TG provided reagents, materials, and advice. NE, ES, TG, and FS wrote the manuscript.

FUNDING

Projects AGL2013-49040-C2-1-R and AGL2017-89785-R were financed by the Spanish Ministry of Economy and Competitiveness (MINECO) and the European Regional Development Fund (FEDER).

ACKNOWLEDGMENTS

Thanks are given to Ms. Sheila Alcala, Ms. Maria Julià, and Dr. Helio A. García-Mendívil for their technical support and to Dr. Miguel A. Naranjo-Ortíz for the critical revision of the manuscript.

SUPPLEMENTARY MATERIAL

The Supplementary Material for this article can be found online at: https://www.frontiersin.org/articles/10.3389/fmicb.2019.03042/full#supplementary-material

TABLE S1 | Threshold cycle (Ct) values, were obtained for quantifying *T. asperellum* using the primers and probe designed by Gerin et al. (2018) for every sample and technical replicates. The detection was carried out from roots of the susceptible tomato cv. Durinta, and the resistant cv. Monika non-inoculated or inoculated with *T. asperellum* T34 (T34) cultivated in two suppressive soils (M10.23 and M10.55) or in sterilized sand. The detection of the fungus was also assessed in soils M10.23 and M10.55. Root colonization of plants grown in the M10.23 and M10.55 soils was estimated from three biological replicates per treatment. Each biological replicate consisted of a pool of 3-g, 1-g root per each of three plants. For plants cultivated in sterilized sand, each plant was considered an independent biological replicate. For soil replicates, the pooled soil from three independent pots per treatment was used.

REFERENCES

Alizadeh, H., Behboudi, K., Ahmadzadeh, M., Javan-Nikkhah, M., Zamioudis, C., Pieterse, C. M. J., et al. (2013). Induced systemic resistance in cucumber and *Arabidopsis thaliana* by the combination of *Trichoderma harzianum* Tr6 and *Pseudomonas* sp. Ps14. *Biol. Control.* 65, 14–23. doi: 10.1016/j.biocontrol.2013.01.009

Brito, J. A., Stanley, J. D., Kaur, R., Cetintas, R., di Vito, M., Thies, J. A., et al. (2007). Effects of the Mi-1, N and *Tabasco* genes on infection and reproduction of *Meloidogyne mayaguensis* on tomato and pepper genotypes. *J. Nematol.* 39, 327–332.

Chen, S., Yu, H., Zhou, X., and Wu, F. (2018). Cucumber (*Cucumis sativus* L.) seedling *Rhizosphere trichoderma* and *Fusarium* spp. Communities altered by Vanillic acid. *Front. Microbiol.* 9:2195. doi: 10.3389/fmicb.2018.02195

Cortada, L., Sorribas, F. J., Ornat, C., Kaloshian, I., and Verdejo-Lucas, S. (2008). Variability in infection and reproduction of *Meloidogyne javanica* on tomato rootstocks with the Mi resistance gene. *Plant Pathol.* 57, 1125–1135. doi: 10.1111/j.1365-3059.2008.01906.x

de Medeiros, H. A., de Araújo Filho, J. V., de Freitas, L. G., Castillo, P., Rubio, M. B., Hermosa, R., et al. (2017). Tomato progeny inherit resistance to the nematode *Meloidogyne javanica* linked to plant growth induced by the biocontrol fungus *Trichoderma atroviride*. *Sci. Reps.* 7:40216. doi: 10.1038/srep40216

Djian-Caporalino, C. (2012). Root-knot nematode (*Meloidogyne* spp.), a growing problem in French vegetable crops. *EPPO Bull.* 42, 127–137. doi: 10.1111/j.1365-2338.2012.02530.x

Expósito, A., García, S., Giné, A., Escudero, N., and Sorribas, F. J. (2019). Cucumis metuliferus reduces *Meloidogyne incognita* virulence against the Mi1.2 resistance gene in a tomato–melon rotation sequence. *Pest Manag. Sci.* 77, 1902–1910. doi: 10.1002/ps.5297

Ferreira, P. A., Ferraz, S., Lopes, E. A., and de Freitas, L. G. (2008). Parasitismo de ovos de *Meloidogyne exigua* por fungos nematófagos e estudo da compatibilidade entre os isolados fúngicos. *Revista Trópica* 3, 15–21.

Gerin, D., Pollastro, S., Raguseo, C., De Miccolis Angelini, R. M., and Faretra, F. (2018). A ready-to-use single- and duplex-TaqMan-qPCR assay to detect and quantify the biocontrol Agents *Trichoderma asperellum* and *Trichoderma gamsii*. *Front. Microbiol.* 9:2073. doi: 10.3389/fmicb.2018.02073

Ghahremani, Z., Escudero, N., Saus, E., Gabaldón, T., and Sorribas, F. J. (2019). Pochonia chlamydosporia Induces plant-dependent systemic resistance to *Meloidogyne incognita*. *Front. Plant Sci.* 10:945. doi: 10.3389/fpls.2019.00945

Giné, A., Bonmatí, M., Sarro, A., Stchiegel, A., Valero, J., Ornat, C., et al. (2012). Natural occurrence of fungal egg parasites of root-knot nematodes, *Meloidogyne* spp. in organic and integrated vegetable production systems in Spain. *Biocontrol* 58, 407–416. doi: 10.1007/s10526-012-9495-6

Giné, A., Carrasquilla, M., Martínez-Alonso, M., Gaju, N., and Sorribas, F. J. (2016). Characterization of soil suppressiveness to root-knot nematodes in organic horticulture in plastic greenhouse. *Front. Plant Sci.* 7:164. doi: 10.3389/fpls.2016.00164

Giné, A., González, C., Serrano, L., and Sorribas, F. J. (2017). Population dynamics of *Meloidogyne incognita* on cucumber grafted onto the cucurbita hybrid RS841 or ungrafted and yield losses under protected cultivation. *Eur. J Plant. Pathol.* 148, 795–805. doi: 10.1007/s10658-016-1135-z

Giné, A., López-Gómez, M., Vela, M. D., Ornat, C., Talavera, M., Verdejo-Lucas, S., et al. (2014). Thermal requirements and population dynamics of root-knot nematodes on cucumber and yield losses under protected cultivation. *Plant Pathol.* 6, 1446–1453. doi: 10.1111/ppa.12217

Giné, A., and Sorribas, F. J. (2017). Quantitative approach for the early detection of selection for virulence of *Meloidogyne incognita* on resistant tomato in plastic greenhouses. *Plant Pathol.* 66, 1338–1344. doi: 10.1111/ppa.12679

Hallman, J., and Meressa, B. H. (2018). "Nematode parasites of vegetables," in *Plant Parasitic Nematodes in Subtropical and Tropical Agriculture*, eds R. A. Sikora, D. Coyne, J. Hallman, and P. Timper, (Wallingford: CABI International), 346–410. doi: 10.1079/9781786391247.0346

Hallmann, J., Davies, K. G., and Sikora, R. (2009). "Biological control using microbial pathogens, endophytes and antagonists," in *Root-knot Nematodes*, eds R. N. Perry, M. Moens, and J. L. Starr, (Wallingford: CABI international), 380–411. doi: 10.1079/9781845934927.0380

Hussey, R. S., and Barker, K. R. (1973). A comparison of methods of collecting inoculate of *Meloidogyne* spp. including a new technique. *Plant Dis. Rep.* 57, 1025–1028.

Jones, J. T., Haegeman, A., Danchin, E. G., Gaur, H. S., Helder, J., Jones, M. G., et al. (2013). Top 10 plant-parasitic nematodes in molecular plant pathology. *Mol. Plant Pathol.* 14, 946–961. doi: 10.1111/mpp.12057

Khan, J., Ooka, J. J., Miller, S. A., Madden, L. V., and Hoitink, H. A. J. (2004). Systemic resistance induced by *Trichoderma hamatum* 382 in cucumber against Phytophthora crown rot and leaf blight. *Plant Dis.* 88, 280–286. doi: 10.1094/PDIS.2004.88.3.280

Kok, C. J., Papert, A., and Hok-A-Hin, C. H. (2001). Microflora of *Meloidogyne* egg masses: species composition, population density and effect on the biocontrol agent *Verticillium chlamydosporium* (Goddard). *Nematology* 3, 729–734. doi: 10.1163/156854101753625236

Liu, Q. L., and Williamson, V. M. (2006). Host-specific pathogenicity and genome differences between inbred strains of *Meloidogyne hapla*. *J. Nematol.* 38, 158–164.

López-Gómez, M., Giné, A., Vela, M. D., Ornat, C., Sorribas, F. J., Talavera, M., et al. (2014). Damage function and thermal requirements of *Meloidogyne javanica* and *Meloidogyne incognita* on watermelon. *Ann. Appl. Biol.* 165, 466–473.

Lopez-Llorca, L. V., Gómez-Vidal, S., Monfort, E., Larriba, E., Casado-Vela, J., Elortza, F., et al. (2010). Expression of serine proteases in egg-parasitic nematophagous fungi during barley root colonization. *Fungal Genet. Biol.* 47, 342–351. doi: 10.1016/j.fgb.2010.01.004

Martínez-Medina, A., Fernandez, I., Lok, G. B., Pozo, M. J., Pieterse, C. M., and Van Wees, S. C. (2017). Shifting from priming of salicylic acid- to jasmonic acid-regulated defences by *Trichoderma* protects tomato against the root knot nematode *Meloidogyne incognita*. *New Phytol.* 213, 1363–1377. doi: 10.1111/nph.14251

Nyczepir, A. P., and Thomas, S. H. (2009). "Current and future management strategies in intensive crop production systems," in *Root-knot Nematodes*, eds R. N. Perry, M. Moens, and J. L. Starr, (Wallingford: CABI international), 412–443. doi: 10.1079/9781845934927.0412

Olivares, C. M., and López-Llorca, L. V. (2002). Fungal egg-parasites of plant-parasitic nematodes from Spanish soils. *Rev. Iberoam. Micol.* 19, 104–110.

Omwega, C., Thomason, I. J., and Roberts, P. A. (1988). A non-destructive technique for screening bean germ plasm for resistance to *Meloidogyne incognita*. *Plant Dis.* 72, 970–972.

Puertas, A. I., de la Noval, B. M., Martínez, B., Miranda, I., Fernández, F. E., and Hidalgo, L. (2006). Interacción de *Pochonia chlamydosporia* var. catenulata con *Rhizobium* sp., *Trichoderma harzianum* y Glomus clarum en el control de *Meloidogyne incognita*. *Revista de Protección Vegetal* 21, 80–89.

Roberts, P. A. (2002). "Concepts and consequences of resistance," in *Plant Resistance to Parasitic Nematodes*, eds J. L. Starr, R. Cook, and J. Bridge, (Wallingford: CABI International), 23–41. doi: 10.1079/9780851994666.0023

Ros-Ibáñez, C., Robertson, L., Martínez-Lluch, M., Cano-García, A., and Lacasa-Plasencia, A. (2014). Development of virulence to *Meloidogyne incognita* on resistant pepper rootstocks. *Span. J. Agric. Res.* 12, 225–232.

Sabbagh, S. K., Roudini, M., and Panjehkeh, N. (2017). Systemic resistance induced by *Trichoderma harzianum* and *Glomus mossea* on cucumber damping-off disease caused by *Phytophthora melonis*. *Arch. Phytopathol. Pfl* 50, 375–388. doi: 10.1080/03235408.2017.1317953

Schouten, A. (2016). Mechanisms involved in nematode control by endophytic fungi. *Annu. Rev. Phytopathol.* 54, 121–142. doi: 10.1146/annurev-phyto-080615-100114

Segarra, G., Casanova, E., Bellido, D., Odena, M. A., Oliveira, E., and Trillas, I. (2007). Proteome, salicylic acid, and jasmonic acid changes in cucumber plants inoculated with *Trichoderma asperellum* strain T34. *Proteomics* 7, 3943–3952. doi: 10.1002/pmic.200700173

Seid, A., Fininsa, C., Mekete, T., Decraemer, W., and Wesemael, W. M. L. (2015). Tomato (*Solanum lycopersicum*) and root-knot nematodes (*Meloidogyne* spp.) – a century-old battle. *Nematology* 17, 995–1009. doi: 10.1163/15685411-00002935

Sharon, E., Chet, I., Bar-Eyal, M., and Spiegel, Y. (2009). "Biocontrol of root-knot nematodes by *Trichoderma* – modes of action," in *Proceedings of IOBC Meeting on Multitrophic Interactions in Soil*, Vol. 42, (Dijon: IOBC/WPRS Bull), 159–163.

Sharon, E., Chet, I., and Spiegel, Y. (2011). "*Trichoderma* as a biological control agent," in *Biological Control of Plant-Parasitic Nematodes: Building Coherence Between Microbial Ecology and Molecular Mechanisms, Progress in Biological Control*, eds K. Davies, and Y. Spiegel, (Netherlands: Springer), 183–201. doi: 10.1007/978-1-4020-9648-8_8

Shoresh, M., Yedidia, I., and Chet, I. (2005). Involvement of jasmonic acid/ethylene signaling pathway in the systemic resistance induced in cucumber by *Trichoderma asperellum* T203. *Phytopathology* 95, 76–84. doi: 10.1094/PHYTO-95-0076

Sorribas, F. J., Ornat, C., Verdejo-Lucas, S., Galeano, M., and Valero, J. (2005). Effectiveness and profitability of the Mi-resistant tomatoes to control root-knot nematodes. *Eur. J. Plant. Pathol.* 111, 29–38. doi: 10.1007/s10658-004-1982-x

Szabó, M., Csepregi, K., Gálber, M., Virányi, F., and Fekete, C. (2012). Control plant-parasitic nematodes with *Trichoderma* species and nematode-trapping fungi: the role of chi18-5 and chi18-12 genes in nematode egg-parasitism. *Biol. Control* 63, 121–128. doi: 10.1016/j.biocontrol.2012.06.013

Talavera, M., Sayadi, S., Chirosa-Ríos, M., Salmerón, T., Flor-Peregrín, E., and Verdejo-Lucas, S. (2012). Perception of the impact of root-knot nematode-induced diseases in horticultural protected crops of south-eastern Spain. *Nematology* 14, 517–527. doi: 10.1163/156854112x635850

Thies, J. A. (2011). Virulence of *Meloidogyne incognita* to expression of N gene in pepper. *J. Nematol.* 43, 90–94.

Verdejo-Lucas, S., Blanco, M., Talavera, M., Stchigel, A. M., and Sorribas, F. J. (2013). Fungi recovered from root-knot nematodes infecting vegetables under protected cultivation. *Biocontrol Sci. Tech.* 23, 277–287. doi: 10.1080/09583157.2012.756459

Verdejo-Lucas, S., Cortada, L., Sorribas, F. J., and Ornat, C. (2009). Selection of virulent populations of *Meloidogyne javanica* by repeated cultivation of Mi-resistance gene tomato rootstocks under field conditions. *Plant Pathol.* 58, 990–998. doi: 10.1111/j.1365-3059.2009.02089.x

Verdejo-Lucas, S., Ornat, C., Sorribas, F. J., and Stchiegel, A. (2002). Species of root-knot nematodes and fungal egg parasites recovered from vegetables in Almería and Barcelona. *Spain. J. Nematol.* 34, 405–408.

Wann, S. B., Borah, B., Ahmed, R., Gogoi, B., Phukon, P., Baruah, J., et al. (2016). "Isolation, characterization of nematode-controlling bacteria and fungi from nature," in *Microbial Inoculants in Sustainable Agricultural Productivity, vol. 1: Research Perspectives*, eds D. P. Singh, H. B. Singh, and R. Prabha, (New Delhi: Springer India), 271–296.

Whitehead, A. G., and Hemming, J. R. (1965). A comparison of some quantitative methods of extracting small vermiform nematodes from soil. *Ann. Appl. Biol.* 55, 25–38. doi: 10.1111/j.1744-7348.1965.tb07864.x

Williamson, W. M., and Roberts, P. A. (2009). "Mechanisms and genetics of resistance," in *Root-knot Nematodes*, eds R. N. Perry, M. Moens, and J. L. Starr, (Wallingford: CABI international), 301–325.

Yuan, M., Huang, Y., Ge, W., Jia, Z., Song, S., Zhang, L., et al. (2019). Involvement of jasmonic acid, ethylene and salicylic acid signaling pathways behind the systemic resistance induced by *Trichoderma longibrachiatum* H9 in cucumber. *BMC Genom.* 20:144. doi: 10.1186/s12864-019-5513-8

Conflict of Interest: The authors declare that the research was conducted in the absence of any commercial or financial relationships that could be construed as a potential conflict of interest.

frontiers in Microbiology

REVIEW
published: 07 February 2020
doi: 10.3389/fmicb.2020.00041

Scent of a Killer: Microbial Volatilome and Its Role in the Biological Control of Plant Pathogens

*Bruno Tilocca[1,2], Aocheng Cao[3] and Quirico Migheli[2]**

[1]*Department of Health Sciences, University "Magna Græcia" of Catanzaro, Catanzaro, Italy,* [2]*Dipartimento di Agraria and NRD-Nucleo di Ricerca sulla Desertificazione, Università degli Studi di Sassari, Sassari, Italy,* [3]*Institute of Plant Protection, Chinese Academy of Agricultural Sciences, Beijing, China*

The use of synthetic fungicides represents the most common strategy to control plant pathogens. Excessive and/or long-term distribution of chemicals is responsible for increased levels of environmental pollution, as well as adverse health consequence to humans and animals. These issues are deeply influencing public perception, as reflected by the increasing demand for safer and eco-friendly agricultural commodities and their by-products. A steadily increasing number of research efforts is now devoted to explore the use of safer and innovative approaches to control plant pathogens. The use of microorganisms as biological control agents (BCAs) represents one of the most durable and promising strategies. Among the panoply of microbial mechanisms exerted by BCAs, the production of volatile organic compounds (VOCs) represents an intriguing issue, mostly exploitable in circumstances where a direct contact between the pathogen and its antagonist is not practicable. VOCs are potentially produced by all living microorganisms, and may be active in the biocontrol of phytopathogenic oomycetes, fungi, and bacteria by means of antimicrobial activity and/or other cross-talk interactions. Their biological effects, the reduced residuals in the environment and on agricultural commodities, and the ease of application in different agricultural systems make the use of VOCs a promising and sustainable approach to replace synthetic fungicides in the control of plant pathogens. In this review, we focus on VOCs produced by bacteria and fungi and on their role in the cross-talk existing between the plant pathogens and their host. Biologic systemic effect of the microbial volatile blends on both pathogen and host plant cells is also briefly reviewed.

Keywords: volatile organic metabolites, biocontrol, antagonist, yeast, eco-friendly agriculture

OPEN ACCESS

Edited by:
Francesco Vinale,
University of Naples Federico II, Italy

Reviewed by:
Tomislav Cernava,
Graz University of Technology, Austria
Raza Waseem,
Nanjing Agricultural University, China

****Correspondence:***
Quirico Migheli
qmigheli@uniss.it

Specialty section:
This article was submitted to Microbial Symbioses, a section of the journal Frontiers in Microbiology

Received: *01 November 2019*
Accepted: *09 January 2020*
Published: *07 February 2020*

Citation:
Tilocca B, Cao A and Migheli Q (2020) Scent of a Killer: Microbial Volatilome and Its Role in the Biological Control of Plant Pathogens. Front. Microbiol. 11:41. doi: 10.3389/fmicb.2020.00041

INTRODUCTION

Synthetic biocides are the major route to control plant pathogens (Irtwange, 2006). However, it has been widely demonstrated that prolonged usage of such agrochemicals is associated with unsustainable levels of environmental pollution, hence raising ecological concern. Long-term exposure to synthetic fungicides recorded a reduced treatment efficacy due to the development of resistance mechanisms by plant pathogens. This led farmers to increase chemical application, with a consequent accumulation of residues in the agricultural commodities and their by-products which, in turn, are responsible for harmful effects for both human and animal health (Pal and McSpadden Gardener, 2006). In addition, the appearance of

resistance mechanisms represents a clinical problem, and resistance to fungicides among human pathogenic fungi is being increasingly observed (Cowen et al., 2002; Mehta et al., 2018). A typical example is represented by the acquired resistance of *Aspergillus fumigatus* and other human pathogenic fungi to azoles (i.e., one of the major class of fungicides, widely used in both agricultural and clinical treatment) as reviewed by Deising et al. (2008).

These reasons have a strong influence on the public perception and market demand, posing the need to move toward the production of pesticide-free commodities, in a healthier and more ecologically friendly context. In this view, a promising pest management alternative is represented by the biological control approach, where the human intervention exploits the natural antagonistic effects of some agents (i.e., the biological control agents, or BCAs) to mitigate the detrimental effects of pathogenic (micro)organisms (Irtwange, 2006). Biological control mechanisms exerted by BCAs are diverse and depend on the specific peculiarities of both pathogen and the antagonist, as well as their density and the specificity of the interactions occurring among these species (Pal and McSpadden Gardener, 2006). A successful BCA is generally featured by the activation of a plurality of mechanisms and targets, synergistically aimed at controlling the pathogen and/or its detrimental effect (Droby et al., 2009). In addition, ideal BCAs do not produce toxic metabolites for both humans/animals and the environment (D'Alessandro et al., 2014; Velivelli et al., 2015). Direct antagonism (e.g., hyperparasitism and predation) occurs in the case of a very high affinity among the pathogen and its BCA (Wisniewski et al., 1991; Heydari and Pessarakli, 2010). Here, interacting species get directly in physical contact and the BCA exerts its suppressive effect without the need for any auxiliary activity from other microorganisms or the surrounding environment (Pal and McSpadden Gardener, 2006). Contrariwise, in the case of indirect antagonism (e.g., competition, or host resistance induction), no physical contact is required between the BCA and its target (Heydari and Pessarakli, 2010). Instead, the BCA acts as a "stimulus" to trigger the development of an unfavorable condition for the microbial growth, leading to a control of the pathogenic species (Pal and McSpadden Gardener, 2006).

Other pathogen suppression mechanisms include the production of volatiles, antibiotics, and other secondary metabolites of the microbial lifecycle. Volatile organic compounds (VOCs) production is gaining a constantly increasing interest by the scientific community, owing to the diverse advantages of their application. VOCs are a blend of volatile metabolites potentially produced by all living microorganisms and were observed to be active in the control of phytopathogenic oomycetes, fungi, and bacteria by means of antimicrobial activity and other cross-talk interactions. Their antimicrobial effects, along with the reduced hazard for both environment and human beings and their possible application without the need of a supplemental spray or drench, make the use of VOCs a promising and sustainable approach to replace fungicides of synthetic origin in the control of plant pathogens (Mercier and Jiménez, 2004; Fialho et al., 2010; Parafati et al., 2017).

In the current review, we focus our attention on the VOCs production by BCAs, intended as active effectors of the dynamic network of cross-relations existing among microbial entities and their host. Their potential exploitation as effective mechanisms to control the causal agents of diseases of economically relevant plants is discussed.

VOLATILE ORGANIC COMPOUNDS OF MICROBIAL ORIGIN

The volatile metabolites of both microbial and plant origin are gaining a steadily increasing interest, and the term "volatilome" has been relatively recently adopted to refer to this complex heterogeneous ensemble of metabolites (Maffei et al., 2011; Farbo et al., 2018).

Among the volatile metabolites produced by the microbial and/or plant metabolism, organic and inorganic molecules can be primarily differentiated. Inorganic volatile molecules such as CO, CO_2, H_2, N_2, O_2, NH_3, H_2S, NO_2^-, SO_2, SO_3, and HCN are the most relevant and are involved in a wide variety of biological functions ranging from electron acceptors/donor to acting as defense compound (Effmert et al., 2012). Moreover, a role in the interspecies communication (e.g., quorum sensing/quenching) and antibiotic resistance has been recently proved (Schmidt et al., 2015; Avalos et al., 2019). By acknowledging the important role of inorganic volatile metabolites under diverse biological and ecological aspects, the current review deals mainly with volatile organic compounds of microbial origin and their role in biological control of plant pathogens.

Volatile organic compounds are small (typically less than 300 Da), carbon-based molecules featured by a low water solubility and a high vapor pressure that makes them available in a gaseous status in the normal ambient conditions (i.e., 1 atm pressure and 25°C temperature) (Pagans et al., 2006; Vespermann et al., 2007; Morath et al., 2012). From a chemical point of view, VOCs are comprised of a heterogeneity of molecular classes, including hydrocarbons, alcohols, thioalcohols, aldehydes, ketones, thioesters, cyclohexanes, heterocyclic compounds, phenols, and benzene derivatives (Wheatley et al., 1997; Chiron and Micherlot, 2005; Morath et al., 2012). Examples of the most commonly investigated volatile molecules of bacterial and fungal origin are provided in **Figures 1A,B**, respectively.

In agriculture, the use of VOCs of microbial origin in the biocontrol of plant pathogens has received a reduced marginal in the past years; however, progresses recently made, along with the overall tendency of the scientific community toward the adoption of a holistic approach, highlighted the potential benefits of microbial VOCs in this field.

VOCs are generally effective already at a very low concentration (Mitchell et al., 2010; Raza et al., 2016). Being volatile, VOCs are capable of diffusing between the soil particles and spread in the atmosphere over large distances from their application point, where they can exert their inhibitory activity without requiring a direct or physical contact between the VOCs-producing microorganism and the target pathogen (Minerdi et al., 2009;

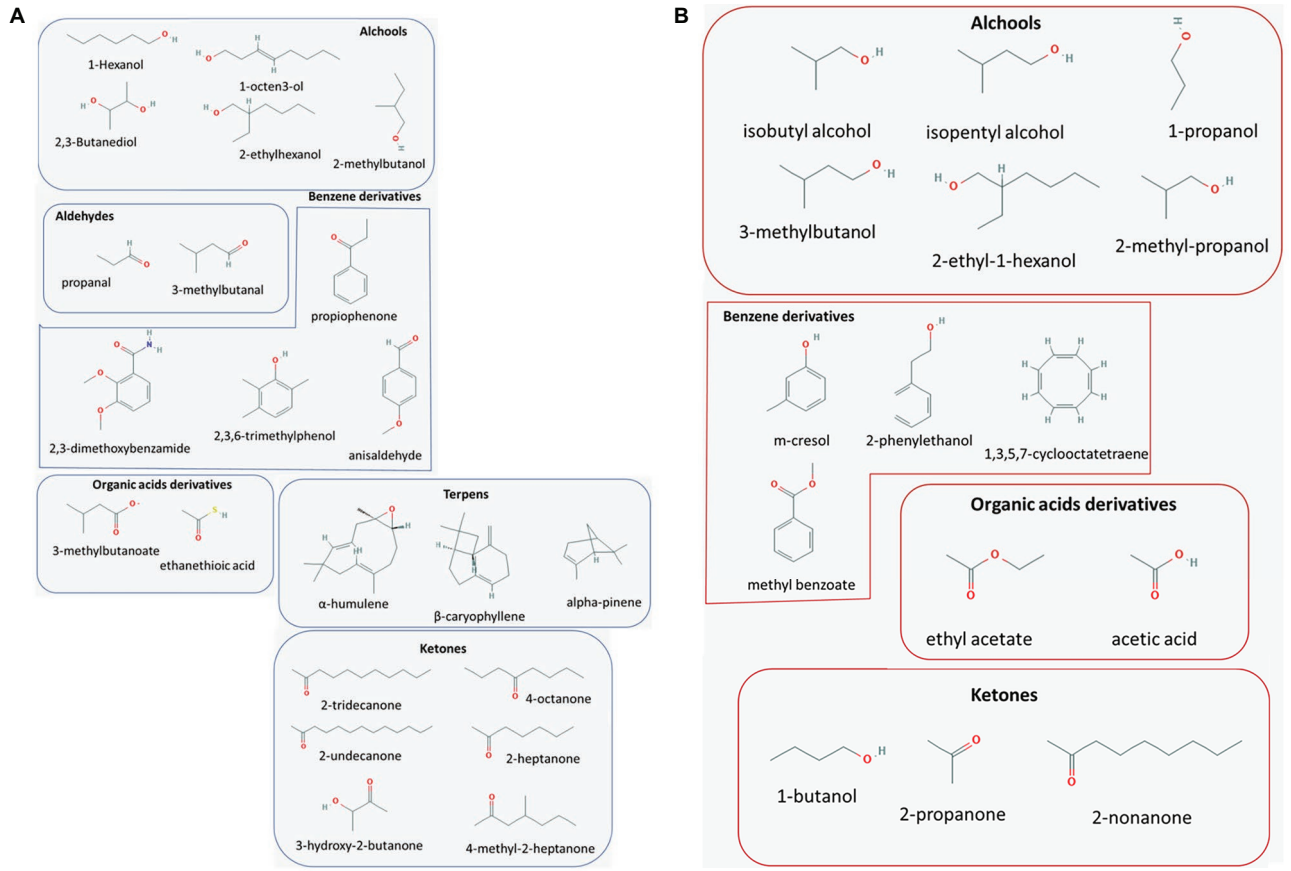

FIGURE 1 | Major volatile metabolites with antimicrobial properties. Molecular classes of bacterial (blue framed, panel **A**) and fungal (red framed, panel **B**) origin reported to exert promising antimicrobial activities, of actual or potential application in the biological control of plant pathogens.

Heydari and Pessarakli, 2010). Besides pathogen inhibition and the negative effects on fungal spore germination and the activity of morphogenesis enzymes (Fialho et al., 2011), microbial VOCs have also shown to be involved in a wide variety of processes (McKee and Robinson, 2009; Morath et al., 2012; Yuan et al., 2012). These include the capability of VOCs to kill plant-parasitic nematodes (Gu et al., 2007; Yang et al., 2012; Xu et al., 2015), the ability to promote plant growth (Ryu et al., 2003; Mercier and Manker, 2005; Minerdi et al., 2011), and the induction of resistance mechanisms in plants, preventing them from being colonized by pathogens (van Loon et al., 1998; Compant et al., 2005; Farag et al., 2006).

Biosynthetic pathways leading to the production of microbial VOCs are yet poorly understood; however, omics-based studies so far performed link the VOCs production to either metabolic transformation products of lipids, proteins, and other building blocks of living tissues, or as the result of degradation (i.e., end-products) of catabolic reactions (Serrano and Gallego, 2006; Tholl et al., 2006; van Dam and Poppy, 2008; Kännaste et al., 2014). On this basis, a dichotomic classification of VOCs as primary or secondary metabolites appears rather inappropriate; instead, VOCs are commonly classified on the basis of their molecular features, such as the number of carbon atoms, ring moieties, and substituent groups (Bennett et al., 2012).

The composition of microbial VOC blends depends on several factors. These include the microbial entities (e.g., bacteria, fungi) producing the VOCs, the substrate they are grown on, temperature, radiation, presence of other microorganisms, and the type of ecosystem (Pasanen et al., 1997; Nilsson et al., 2004; Fiedler et al., 2005). Also, VOCs composition of a given species is highly dynamic over time, resulting in a changing composition of the produced VOCs depending on the age of the VOCs-producing species (Wang et al., 2013).

Regardless of the emitting species and the specific VOCs blend composition, several studies are nowadays being performed with the aim to exploit the countless benefits of employing a natural antimicrobial mixture to prevent plant pathogens by replacing traditional chemical approaches. Unanimously, studies performed so far recommend VOCs application under air-tight environment, in order to rapidly saturate the atmosphere with the volatile antimicrobials. Particularly effective application of VOCs is reported in the control of storage pathogens on fresh fruit (e.g., citrus, peach, strawberry) but also other commodities such as nuts, grains, and seeds (**Table 1**; Strobel, 2006; Fialho et al., 2011; Wang et al., 2013; Chen et al., 2018; Gao et al., 2018).

TABLE 1 | Main biological control agents emitting volatile organic compounds, their target pathogen, framework application, and primary volatilome components.

Antagonist	Target	Application	Main VOCs	Reference
Aureobasidium pullulans	*Botrytis cinerea* *Colletotrichum acutatum* *Penicillium expansum* *Penicillium digitatum* *Penicillium italicum*	Post-harvest decay toxin contamination	2-Phenylethanol	Di Francesco et al. (2015)
Cyberlindnera jadinii *Lachancea thermotolerans* *Candida intermedia* *Candida friedrichii*	*Aspergillus carbonarius* *Aspergillus ochraceus*	Post-harvest decay toxin contamination	2-Phenylethanol	Farbo et al. (2018) Tilocca et al. (2019)
Saccharomyces cerevisiae	*Phyllosticta citricarpa*	Post-harvest decay	2-Phenylethanol	Fialho et al. (2010)
Wickerhamomyces anomalus	*Aspergillus flavus*	Toxin contamination	2-Phenylethanol	Hua et al. (2014)
Hanseniaspora uvarum *Pichia kluyveri* *Wickerhamomyces anomalus*	*Aspergillus ochraceus*	Toxin contamination	2-Phenylethyl acetate	Masoud et al. (2005)
Aureobasidium pullulans *Metschnikowia pulcherrima* *Saccharomyces cerevisiae* *Wickerhamomyces anomalus*	*Botrytis cinerea*	Pathogen prevention/inhibition	Whole volatilome	Parafati et al. (2015)
Candida sake	*Botrytis cinerea* *Penicillum expansum*	Post-harvest decay	Whole volatilome	Arrarte et al. (2017)
Bacillus amyloliquefaciens	*Fusarium oxysporum*	Pathogen prevention	2,3,6-Trimethyl-phenol Pentadecane Tetradecane	Yuan et al. (2012)
Bacillus atrophaeus	*Botrytis cinerea*	Pathogen prevention/inhibition	Hexadecane 2,3-Dimethoxybenzamide Oanisaldehyde	Zhang et al. (2013)
Burkholderia ambifaria	*Rhizoctonia solani* *Alternaria alternata*	Pathogen prevention/inhibition	Dimethyldisulfide 2-Undecanone dimethyltrisulfide 4-Octanone Methylmethanethiosulfonate Phenylpropanone	Groenhagen et al. (2013)
Burkholderia tropica	*Colletotrichum gloeosporioides* *Fusarium culmorum* *Fusarium oxysporum* *Athelia rolfsii*	Pathogen prevention/inhibition	Limonene Alpha-pinene Ocimene	Tenorio-Salgado et al. (2013)
Burkholderia gladioli	*Fusarium oxysporum* *Rhizoctonia solani*	Pathogen prevention/inhibition	Limonene	Elshafie et al. (2012)
Achromobacter sp. *Serratia* sp.	*Fusarium oxysporum*	Plant growth induction	Dimethyldisulfide Propanal 2-Ethyl-1-hexanol Dodecane Tridecane Tetradecane	Minerdi et al. (2009, 2011)
Bacillus spp.	Host	Resistance induction Plant growth induction	3-Hydroxy-2-butanone 2,3-Butanediol	Ryu et al. (2003) Rudrappa et al. (2010)
Enterobacter aerogenes	*Exserohilum turcicum*	Pathogen prevention/inhibition	2,3-Butanediol	D'Alessandro et al. (2014)
Phomopsis sp.	*Pythium* spp. *Phytophthora* spp. *Sclerotinia* spp. *Rhizoctonia* spp. *Fusarium* spp. *Botrytis* spp. *Verticillium* spp. *Colletotrichum* spp.	Pathogen prevention/inhibition	Sabinene 1-Butanol 3-Methylbenzeneethanol 1-Propanol 2-Methyl 2-Propanone	Zhou et al. (2014)
Phaeosphaeria nodorum	*Monilinia fructicola*	Pathogen prevention/inhibition	3-Methylbutanol Acetic acid 2-Propyl-1-ol Ethyl acetate	Naznin et al. (2012, 2014)
Wickerhamomyces anomalus	*Penicillium roqueforti*	Post-harvest decay	Ethyl acetate	Liu et al. (2014)

(Continued)

TABLE 1 | Continued

Antagonist	Target	Application	Main VOCs	Reference
Trichoderma viride	*Arabidopsis thaliana*	Plant growth induction	Isobutyl alcohol Isopentyl alcohol 3-Methylbutanal	Hung et al. (2013)
Talaromyces sp.	*Colletotrichum higginsianum*	Plant growth induction	β-Caryophyllene	Di Francesco et al. (2015)
Cladosporium sp.	*Pseudomonas syringae*	Resistance induction	m-Cresol	Di Francesco et al. (2015)
Ampelomyces sp.		pathogen Prevention/inhibition	Methylbenzoate	

Bacterial Volatilome as a Tool for the Biocontrol of Plant Pathogens

Bacteria produce volatile metabolites as part of their normal metabolism (**Figure 1A**). Bacterial VOCs are involved in the complex network of interconnections established among bacterial species, bacteria vs. other microorganisms, and bacteria vs. plants. Such interactions have a variable ecological role, ranging from beneficial cooperation (e.g., mutualism, symbiosis, host resistance induction) to antagonistic relationship occurring, for instance, in the case of microbicidal activity exerted by one of the interacting species (Maffei et al., 2011; Kanchiswamy et al., 2015). The recent awareness on the beneficial effects arising from bacteria-plant interaction opens new avenues in the use of bacterial volatilome to stimulate plant growth. Moreover, owing to the high versatility of bacteria-derived VOCs and their effectiveness in controlling other microorganisms, studies are focusing on exploiting the natural bacterial VOCs production as a strategy for the biocontrol of plant pathogens.

In this view, only a handful of studies have so far been performed to elucidate the metabolic effects of the bacterial volatilome on the target organism, while it is well known that bacteria-derived VOCs have a pivotal role in stimulating or repressing other bacterial species (Garbeva et al., 2014a; Kanchiswamy et al., 2015).

Bacillus amyloliquefaciens strain SQR-9 has been reported as effective against the tomato wilt pathogen *Ralstonia solanacearum* (Raza et al., 2016). A key role is played by the VOCs blend produced by the BCA, which provides effective inhibition of *R. solanacearum* in both synthetic media and in soil. Inhibitory effects of the bacterial VOCs have been confirmed by lack of inhibition observed in the case of treatment with a non-VOCs-producing bacterium as well as when *B. amyloliquefaciens* SQR-9 is applied in the presence of activated charcoal (i.e., a well-known gas adsorbent). Growth inhibition was dependent on the BCA load; however, the inhibitory effects produced by the bacterial VOCs were reversed by BCA removal, indicating a bacteriostatic effect of the *B. amyloliquefaciens*-derived VOCs on *R. solanacearum* (Raza et al., 2016). Bacteriostatic evidences were also observed in the volatilome of different strains of *Pseudomonas chlororaphis, Serratia plymuthica IC1270,* and *Serratia proteamaculans* 94, tested for their antagonistic potential against *Agrobacterium tumefaciens* C58 (Popova et al., 2014). In dual culture, all strains succeeded in total or partial inhibition of the phytopathogenic bacterium. An exception is represented by *S. proteamaculans* 94, resulting in a non-significant inhibition of the pathogen. Nevertheless, this strain scored a total inhibition of the cyanobacterium *Synechococcus* sp. PCC 7942 and other eukaryotic cells (Popova et al., 2014). This study confirms previous reports on the *in vitro* antagonistic potential of *S. plymuthica* IC1270, *P. fluorescens* Q8r1-96, and *P. fluorescens* B-4117 against phytopathogenic *A. tumefaciens* and *Agrobacterium vitis*. Here, authors indicated VOCs produced by the candidate BCAs as a valuable tool to prevent crown gall tumors on tomato plants (Dandurishvili et al., 2011).

Investigations on the composition and activity of the bacterial VOCs blend revealed a strain-specific VOCs mixture, with some molecular entities being exclusive to a given bacterial strain, whereas quantitative changes were observed among the other "commonly identified" volatile molecules. This might justify the diverse antagonistic features of candidate BCAs in regard to different pathogens (Dandurishvili et al., 2011; Popova et al., 2014; Garbeva et al., 2014b). Dimethyl disulfide (DMDS) was identified as the major volatile produced by *S. proteamaculans* 94 and other *Serratia* spp. (Dandurishvili et al., 2011; Popova et al., 2014); however, only traces of DMDS have been produced by *Pseudomonas* spp. strains, in favor of the production of ketones. Among these compounds, 2-nonanone, 2-heptanone, 2-undecanone, and 2-tridecanone are among the most represented bactericidal compounds as confirmed in subsequent VOCs experiments (Dandurishvili et al., 2011; Popova et al., 2014; Raza et al., 2016).

Bacteria-bacteria interaction does not necessarily result in the sole bactericidal (or bacteriostatic) effect; it may also imply a synergistic/cooperative activity among bacterial species. A recent investigation performed on soil bacteria showed that the volatilome of four genetically diverse isolates results in antithetical phenotypes of *P. fluorescens*. Here, VOCs released by *Collimonas pratensis* and *S. plymuthica* positively stimulated the growth of *P. fluorescens*, with *C. pratensis* volatiles even stimulating the production of antimicrobial compounds by *P. fluorescens*. On the other hand, *P. fluorescens* exposure to *Paenibacillus* and *Pedobacter* spp. did not stimulate the growth of *P. fluorescens*, but triggered a stress response mechanism in the bacterial model even though no significant inhibition was observed for any of the four different strains (Garbeva et al., 2014b).

Besides intra-kingdom interconnections, bacteria are also involved in sophisticated bi-directional cross-talks involving phylogenetically higher species such as fungi and plants: bacteria-fungi interactions are very dynamic, depending on the interacting species and are strongly exploited in the modern

agricultural practice to control important phytopathogenic taxa (Maffei et al., 2011).

Rhizobacteria such as *S. plymuthica*, *Serratia odorifera, Stenotrophomonas maltophilia*, *Stenotrophomonas rhizophila, P. fluorescens,* and *Pseudomonas trivialis* are known to produce VOCs mixtures with antifungal properties active against a wide array of both pathogenic and non-pathogenic fungi (Kai et al., 2010; Effmert et al., 2012; Kanchiswamy et al., 2015). Common volatile molecules known in the bacteria-fungi interaction are γ-patchoulene, 3-methylbutanal, 1-octen3-ol, 2-undecanone, 2-nonanone, 3-methylbutanoate, 2-methylbutan-1-ol, 4-methyl-2-heptanone, ethanethioic acid, and dimethyltrisulfide 2,3,6-trimethylphenol. Among these, several have already been tested for their antifungal activity.

A study on the antifungal activity of *B. amyloliquefaciens* NJN-6 volatilome demonstrated the ability of this bacterium to hinder growth and spore germination of the pathogenic *Fusarium oxysporum* f. sp. *cubense* causing fusarium wilt on banana. Analysis of its volatilome composition identified a total of 36 volatile molecules, including aromatic compounds, alkyls, ketones, alcohols, naphthyls, aldehydes, one ester and one ether compound. *In vitro* evaluation of the identified compounds suggested an important fungicidal activity of benzothiazoles phenol and 2,3,6-trimethylphenol. Other benzenic compounds, instead, were attributed to the "sole" inhibitory properties, owing to their inability to preclude the growth of the pathogenic fungus. The other identified compounds were able to inhibit almost completely *F. oxysporum* growth only when present in massive quantities, leading authors to exclude them as potential candidates to antagonize *F. oxysporum* growth (Yuan et al., 2012).

Volatiles released by *Streptomyces* spp. have also shown interesting antifungal properties, especially in the control of storage and mycotoxigenic fungi (Schöller et al., 2002; Li et al., 2010). A further study by Wang and colleagues confirmed the simultaneous antifungal activity of *Streptomyces alboflavus* TD-1 with regard to some of the most known mycotoxigenic fungi such as *F. moniliforme* (*syn. Fusarium fujikuroi*), *A. flavus, Aspergillus ochraceus, Aspergillus niger,* and *Penicillum citrinum* (Wang et al., 2013). Moreover, the investigation of its volatilome underlines a very complex and dynamic composition, with several molecules shared among taxonomically related species even though with high quantitative variability (Wilkins and Schöller, 2009; Li et al., 2010; Wang et al., 2013). In addition, some volatiles have been previously identified as components of essential oils of diverse plants with already supposed antifungal effects (Bajpai et al., 2008; Essien et al., 2011; Serrano et al., 2011; Shanthi et al., 2011; Wang et al., 2013; Gao et al., 2018). The mix of volatiles produced by *Bacillus atrophaeus* CAB-1 strains is mainly composed of hexadecane, 2,3-dimethoxybenzamide and oanisaldehyde. *In vitro* assay of the bacterial volatiles resulted in an effective inhibition of *Botrytis cinerea*, the causal agent of tomato gray mold (Zhang et al., 2013). In another study, DMDS, 2-undecanone, dimethyltrisulfide (DMTS), 4-octanone, S-methylmethanethiosulfonate, and 1-phenylpropan-1-one produced by *Burkholderia ambifaria* scored a significant inhibition of the growth of the pathogenic fungi *Rhizoctonia solani* and *Alternaria alternata* (Groenhagen et al., 2013). Similarly, the investigation of 15 strains of *Burkholderia tropica* resulted in a significant inhibition of the growth of four fungal pathogens, namely *Colletotrichum gloeosporioides, Fusarium culmorum, F. oxysporum*, and *Athelia rolfsii*, most likely due to their capability to produce VOCs, among which limonene, alpha-pinene, dimethyldisulfide (DMDS), and ocimene were considered as the most effective ones (Tenorio-Salgado et al., 2013). The antifungal activity of limonene was also confirmed in a further study, where the growth rate of *F. oxysporum* and *R. solani* has been hindered by the limonene emitted by *Bulkholderia gladioli* pv. *agaricola* (Elshafie et al., 2012).

Besides antagonism, VOCs from several bacterial species are also involved in ectosymbiotic relations occurring between bacteria and fungi. The bacterial volatiles of *Achromobacter* and *Serratia* spp. DMDS, propanal, 2-ethyl-1-hexanol, dodecane, tridecane, and tetradecane, are capable of stimulating *F. oxysporum* MSA35 to produce a higher amount of α-humulene and β-caryophyllene which, in turn, are known to favor lettuce growth (Minerdi et al., 2009, 2011).

Bacterial Volatilome Prevents Pathogen Infection by Conditioning Plant Physiology

Interactions occurring between plants and bacteria, by means of volatile emission, may have both beneficial and detrimental outcomes for the overall plant growth (Kai et al., 2009; Gutiérrez-Luna et al., 2010). Elucidating the complex cross-talk occurring between bacteria and their host allows a conscious human intervention that promotes plant growth by preventing plant colonization and/or by exploiting the direct beneficial effects that some bacteria exert on plants. Blom and co-workers screened over 40 bacterial species for their capability to stimulate plant growth. The study selected 36 bacterial volatiles and, of these, indole, 1-hexanol and pentadecene showed the most promising results in terms of plant growth stimulation (Blom et al., 2011). On the other hand, co-cultivation of *A. thaliana* in the presence of *Serratia odorifera* volatilome resulted in a severe inhibition of plant growth. Authors attributed the inhibitory effect to DMDS and ammonia volatiles (Vespermann et al., 2007; Kai et al., 2010). With regard to DMDS and its direct (i.e., plant growth stimulation) and indirect (e.g., disease prevention) effects on plants, controversial results are available in the literature. A study performed on *Nicotiana attenuata* reports DMDS as a volatile metabolite that directly alters plant metabolism, causing the downregulation of sulfur assimilation and methionine biosynthesis genes (Meldau et al., 2013). Contrariwise, a previous study linked the bacterial production of DMDS to a significantly increased growth of *A. thaliana* (Groenhagen et al., 2013). Accordingly, another study reported that DMDS produced by *Bacillus cereus* results in significant protection of tobacco and corn from the infection by *B. cinerea* and *Bipolaris maydis*, respectively (Huang et al., 2012a).

Other bacterial metabolites involved in bacteria-plant cross-talk include 3-hydroxy-2-butanone and 2,3-butanediol. These are produced by *Bacillus* spp. and are linked to a significantly enhanced total leaf surface area besides the induction of host systemic resistance (Ryu et al., 2003; Rudrappa et al., 2010).

This observation is also confirmed in another study highlighting 2,3-butanediol produced by *Enterobacter aerogenes* as involved in the induction of resistance against *Exserohilum turcicum* infection in corn plants (D'Alessandro et al., 2014).

Fungal Volatilome and Its Role in Biological Control

As for bacteria, several fungal species produce volatile metabolites (**Figure 1B**) taking part in diverse ecological relationships (Kanchiswamy et al., 2015), ranging from antagonism to symbiotic relations with other fungi (Schiestl et al., 2006), bacteria, and plants (Hung et al., 2013).

Among antagonistic fungi, *Muscodor albus*, an endophyte from *Cinnamomum zeylanicum* (cinnamon tree), represents the first commercially available BCA acting through its volatilome (Strobel et al., 2001; Strobel, 2006). This fungus produces a wide variety of volatiles comprising alcohol, acid, ester, and terpenoid derivatives, with antimicrobial properties against pathogens responsible of the post-harvest decay of fruits such as apple, peach, lemon, and grape. Moreover, it proved safe for humans and the environment, enabling its registration as a biopesticide at the US Environmental Protection Agency. The usage of bags containing a lyophilized culture of *M. albus* that is reactivated by hydration is advantageous for the biofumigation under air-tight environments, providing an effective prevention of fruit decay during storage and shipping (Strobel, 2006; Mercier et al., 2010). Moreover, due to its remarkable antagonistic activity, the use of *M. albus* was already proposed by Strobel and colleagues as a valuable alternative to replace methyl bromide fumigation, with comparable results (Strobel, 2006; Strobel et al., 2011). A risk assessment for the effects of VOCs on human health and the environment did not show important harmful potential since these compounds are produced in low amounts, do not contaminate treated food commodities, and dissipate rapidly in the atmosphere. Nevertheless, it has been recently demonstrated that a volatile molecule produced by *M. albus* raised human health issues, hence underlying the need to develop further studies/guidelines for a comprehensive assessment of the potential toxicity exerted by VOCs produced by BCAs (Braun et al., 2012; Jiménez et al., 2012; Romanazzi et al., 2012; Margolis, 2012, personal communication).

Other endophytic fungi have shown to promote plant growth through the release of volatile metabolites inhibiting the growth of plant pathogens. Investigations on endophytes from *Rosa x damascena* (Damask rose) yielded over 50 isolates, among which *A. niger* was found to produce high amounts of 2-phenylethanol (2-PE; Wani et al., 2010). In addition to the potential value in the cosmetic industry, this study is among the first ones linking the production of 2-PE with its potential application as fumigant, owing to its antimicrobial and antiseptic properties already exploited in pharmaceutics (Wani et al., 2010). Other studies indicated 2-PE as the major component of yeast volatile blends and described its role in limiting the growth of pathogenic *Aspergillus* spp. (Fialho et al., 2010; Hua et al., 2014; Liu et al., 2014; Chang et al., 2015; Farbo et al., 2018). *Phomopsis* spp. isolated by *Odontoglossum* sp. (*Orchidaceae*) emits a mixture of volatile metabolites including sabinene, 1-butanol, 3-methyl, benzene ethanol, 1-propanol, 2-methyl, and 2-propanone. An artificial mixture of such volatiles had remarkable antifungal properties against several oomycete and fungal pathogens, including *Pythium*, *Phytophthora*, *Sclerotinia*, *Rhizoctonia*, *Fusarium*, *Botrytis*, *Verticillium*, and *Colletotrichum* spp. In addition, the fungus was shown to tolerate and survive in the presence of the volatile metabolites produced by the antagonistic *M. albus* (Mercier and Jiménez, 2004; Singh et al., 2011). *Epichloe typhina* isolated from *Phleum pratense* emits sesquiterpene volatiles with antifungal activity against *Cladosporium phlei* (Kumar and Kaushik, 2012). *Phaeosphaeria nodorum*, a common endophyte of *Prunus domestica*, produces a blend of volatile metabolites comprising ethyl acetate, 3-methylbutan-1-ol, acetic acid, 2-propyl-1-ol, and 2-propenenitril. Altogether, these volatiles inhibit the pathogenic fungus *Monilinia fructicola*, by reducing its growth, hyphal width, and by provoking the disintegration of the hyphal content (Pimenta et al., 2012).

Yeast Volatilome and Its Effects Against Pathogenic and Mycotoxin-Producing Fungi

The application of yeasts as BCAs represents one of the most investigated alternatives to fungicides, due to the great ability of these microorganisms to grow and survive in heterogeneous ecological niches and under severe stress conditions (Muccilli and Restuccia, 2015). Moreover, the highly competitive activity of yeasts does not suffer the side effects (e.g., production of human allergenic compounds or toxic secondary metabolites) sometimes encountered with the application of other microbial species as BCAs, therefore extending their potential application to the eco-friendly safeguard of agricultural commodities and by-products (Droby et al., 2009; Janisiewicz et al., 2010; Liu et al., 2013; Muccilli and Restuccia, 2015). Early studies performed on *Wickerhamomyces anomalus* (syn. *Pichia anomala*) have shown that the antimicrobial effectiveness of yeast-derived volatilome is mainly attributed to ethyl acetate, enabling for a successful control of *Penicillium roqueforti* during air-tight storage of grain (Ädel Druvefors and Schnürer, 2005). Nevertheless, recent evidence confirmed the impossibility to determine a static inhibitory mechanism. As for bacteria, the yeast-pathogen interaction, as well as the chemical composition of the emitted blend of volatiles, is widely dynamic in relation to several factors such as the VOCs-producing yeast, the antagonized pathogen and the ecological niche where the cross-talking species are growing (Mari et al., 2012; Yuan et al., 2012; Parafati et al., 2017). Volatile metabolites produced by *Sporidiobolus pararoseus* effectively inhibited spore germination and mycelial growth of *B. cinerea*. Investigation of the volatile blend composition highlighted 2-ethyl-1-hexanol as the major compound (Huang et al., 2012b); whereas 1,3,5,7-cyclo octatetraene, 3-methyl-1-butanol, 2-nonanone, and phenylethyl alcohol are the major components of the VOCs produced by *Candida intermedia* antagonizing the same pathogen (*B. cinerea*) both *in vitro* and *in planta* (Huang et al., 2011).

Meyerozyma guilliermondii has shown antifungal activity against the rice blast pathogen *Pyricularia oryzae* by means of

VOCs production, with ethyl-acetate (Coda et al., 2013) and helvolic acid (Zhao et al., 2010) being the most effective molecules. More recent studies performed on *W. anomalus* identified 2-PE as the most effective compound in preventing spore germination, mycelial growth, and toxin production by *A. flavus* (Hua et al., 2014). Fiori et al. (2014) highlighted the effect of two non-fermenting (*Cyberlindnera jadinii* and *Candida friedrichii*) and of two low-fermenting (*C. intermedia* and *Lachancea thermotolerans*) yeast strains, resulting in the inhibition of both mycelial growth and toxigenic potential of the pathogen *Aspergillus carbonarius*. Subsequently, the chemical composition of the four yeast strains volatilome was characterized: although more than 20 different compounds were identified as components of the yeast-derived volatilome, 2-PE was found to be the most abundant one in all tested volatile blends (Farbo et al., 2018). A recent proteomic investigation aimed at assessing the role of *C. intermedia* volatilome in the inhibition of the ochratoxin A (OTA) producing fungus *A. carbonarius* revealed that yeast VOCs target a plurality of fungal metabolic routes, inducing a marked reduction of the protein biosynthetic activity, proliferative activity, energy metabolism, and inhibiting the fungal detoxification system. Nevertheless, exposure to the sole 2-PE (i.e., the major volatilome component) can only partially reproduce the metabolic alteration provoked by the whole yeast-derived volatilome, thereby suggesting that other minor and still unidentified yeast VOCs components are likely to involve a plurality of metabolic targets, resulting in a higher effectiveness of the treatment over the long-term period (Tilocca et al., 2019). In line with these observations, a very recent study reported the higher antagonistic efficiency of bacterial and fungal volatilome considered "as whole" when compared with the administration of the blend components in their pure form (Mülner et al., 2019).

Volatile organic compounds produced by *W. anomalus, Pichia kluyveri,* and *Hanseniaspora uvarum* inhibited the mycotoxigenic fungus *A. ochraceus* growth as well as OTA production during processing of coffee (Masoud et al., 2005; Masoud and Kaltoft, 2006).

Volatiles produced by *Aureobasidium pullulans* have been tested against *B. cinerea*, *Colletotrichum acutatum, P. expansum, P. digitatum*, and *P. italicum* resulting in an effective control of these post-harvest fruit pathogens growth both *in vitro* and *in planta* (Di Francesco et al., 2015). In a similar study, Parafati and colleagues attributed to VOCs produced by *W. anomalus*, *Metschnikowia pulcherrima*, *S. cerevisiae*, and *A. pullulans* a pivotal role in the biocontrol of *B. cinerea* vegetative growth and its infection rate on table grape berries (Parafati et al., 2015). Similarly, volatiles produced by *Candida sake* reduced the incidence of apple rot caused by the storage pathogens *P. expansum* and *B. cinerea* (Arrarte et al., 2017).

Exploiting Fungus-Plant Cross-Talk to Control Pathogens

Besides the pathogen-antagonist relationship, plant-fungi interactions are also widely exploited because of the beneficial effects exerted either directly or indirectly on the plant growth.

Direct effects of fungi on plant growth promotion are mainly investigated for endophytes, a group of plant-associated fungal symbionts emitting a wealth of volatile molecules with heterogenous physical, chemical, and biological properties (Khan et al., 2014; Waqas et al., 2014; Zhou et al., 2014; Kanchiswamy et al., 2015). Previous investigations showed that tobacco seedlings are improved by *Phoma* sp. GS8-3 volatiles, with a wide array of C4–C8 hydrocarbons being produced by this endophytic strain (Naznin et al., 2012). Although VOCs blend composition appeared highly dynamic over fungal growth, 2-methyl-propanol and 3-methyl-butanol were the most abundant compounds along the whole fungal cultivation period (Naznin et al., 2012). Volatile metabolites from endophytic fungi have demonstrated to induce plant growth when administered both as singular molecules and as a whole blend of compounds (Khan et al., 2014; Waqas et al., 2014; Zhou et al., 2014; Kanchiswamy et al., 2015). Quite remarkably, the application of low concentration of the volatiles blend has registered a better plant growth promotion than that observed upon exposure to higher concentrations (Naznin et al., 2012, 2014).

A total of 51 diverse volatiles have been identified from the fungal volatilome of *Trichoderma viride*, the most abundant of which included isobutyl alcohol, isopentyl alcohol, and 3-methylbutanal. Dual culture of *T. viride* with *A. thaliana* under air-tight condition revealed a significant plant growth promotion, stimulating bigger, taller, and earlier flowering plants (Hung et al., 2013).

Indirect effects of fungi on the plant growth concern primarily the induction of systemic resistance, providing the plants with the adequate resources to face infection by pathogenic species. The plant-growth promotion exerted by the fungi *Cladosporium* and *Ampelomyces* spp. can be partly attributed to their volatilome, with m-cresol and methyl benzoate, respectively, being the major players in eliciting host systemic resistance, hence resulting in a significantly decreased disease severity after experimental infection with *Pseudomonas syringae* pv. *tomato* DC3000 (Naznin et al., 2014). Another study, aiming at characterizing the volatilome of *Talaromyces* spp., identified several terpenoid-like molecules including β-caryophyllene. Subsequent investigation of the sole β-caryophyllene on *Brassica campestris* L. var. *perviridis* resulted in a significantly increased growth of seedlings and enhanced resistance against *Colletotrichum higginsianum* infection (Yamagiwa et al., 2011).

Volatile Organic Compounds Production by Mixed Microbial Consortia

It has been already proven that the heterogeneous ensemble of VOCs produced by a single organism may result in different biological outcomes (Tilocca et al., 2019). Analogously, multiple microbial specimens coexisting in the same ecological niche (e.g., the soil) might lead to differing biocontrol achievements compared to what observed and/or expected by the application of a single microbial entity. Many types of interaction can occur among microbial strains, genera, phyla, and even

kingdoms (Delory et al., 2016; Schulz-Bohm et al., 2017), leading to a diverse overall behavior of the microbiota, intended as a whole unique entity, whose biological and ecological role is the result of all interactions occurring among all microbiota members. It has been recently proved that interactions occurring among the microbiota members *Bacillus cereus Rs-MS53* and *Pseudomonas helmanticensis Sc-B94* result in enhanced effectiveness while controlling the pathogenic fungus *R. solani* (Mülner et al., 2019), supporting previous evidences of a strong strain compatibility and cooperative interaction (Lim et al., 1991; Dowling and O'Gara, 1994; Ait-Lahsen et al., 2001; Hong and Meng, 2003; Peighami-Ashnaei et al., 2009; Asari et al., 2016). Several strains of *Pseudomonas* and *Bacillus* spp. have shown to produce both volatile and nonvolatile antimicrobial compounds, resulting in either a direct inhibition of the pathogen or a conditioning of the whole microbial community that hampers pathogens growth and infection (Schulz-Bohm et al., 2017). Analogously, it has been reported that *Collimonas pratensis* and *Serratia plymuthica* inhibit the growth of pathogenic *Bacillus* sp. by means of an indirect stimulation of *Pseudomonas fluorescens* and its subsequent stimulation of antimicrobial compounds production (Garbeva et al., 2014b). Microbial cross-talk plays also a pivotal role in the microbial persistence, including antimicrobial resistance and optimal exploitation of scarce nutritional resources (Raza et al., 2016; Jones et al., 2017).

Microbiota investigation is still in its infancy under all applicative fields and further investigations are certainly needed. The soil-associated microbiota is rather complex, mostly because of the high biological diversity comprised in its architecture and the myriad of interfering molecules sampled along that hamper a fair and accurate analysis. Nevertheless, technical progress in the field of *meta-omics* sciences amended disciplines such as metagenomics, metatranscriptomics metaproteomics, and metabolomics, enabling a comprehensive investigation of the taxonomical composition, metabolic potential, and effective metabolic function of all microbial members. Such holistic approach would greatly benefit the comprehensive understanding of the whole microbial community and how it can be shaped by acting on key variables (e.g., physicochemical characteristics of the soil, inclusion of "probiotics"). Moreover, by analogy with animal-oriented research (Tröscher-Mußotter et al., 2019), investigating how the soil/plant microbiota interacts with its plant host, system biology would provide precious information to be exploited in diverse applicative field, including biological control.

PRACTICAL APPLICATION OF MICROBIAL VOLATILE ORGANIC COMPOUNDS

Volatile blends emitted by BCAs have resulted in a high effectiveness even at low concentrations. Moreover, the reduced release of residual and the negligible hazardous effects on both animals and the environment makes BCA volatilome an intriguing alternative to the use of synthetic pesticides and/or fertilizers. In addition, the high volatility of these molecules enables a wide and homogeneous diffusion both below- and above-ground level. On the other hand, volatility of these natural metabolites is also responsible for the major challenge to their massive application in open-field agricultural and horticultural practices. Drenching of 2,3-butanediol, 3-pentanol, and 2-butanone revealed reproducible outcomes (Cortes-Barco et al., 2010a,b). Moreover, open field application of the 3-pentanol and 2-butanone in a cucumber field has demonstrated a significant effectiveness against the bacterial angular leaf spot pathogen *Pseudomonas syringae* pv. *lachrymans* by inducing plant systemic acquired resistance mechanisms. In turn, the activation of the defense-related gene CsLOX stimulated the oxylipin pathway, which plays a role in recruiting *Coccinella septempunctata*, a natural enemy of the sucking insect aphid, *Myzus persicae* (Song and Ryu, 2013).

Similar observations were reported by a field study performed on red pepper (Choi et al., 2014). Treatment with *Bacillus amyloliquefaciens* strain IN937a on plant leaves resulted in an antagonistic effect against *Xanthomonas axonopodis* pv. *vesicatoria*. The 3-pentanol of bacterial origin has proved to be effective in the induction of plant resistance mechanism by priming salicylic acid, jasmonic acid, and ethylene defense signaling pathway. Another soundly piece of evidence supporting microbial VOCs in the open-field practices has been reported by D'Alessandro and colleagues, who demonstrated that field application on maize plants of acetoin and 2,3-butanediol produced by *Enterococcus aerogenes* triggers a higher resistance against the Northern corn leaf blight fungus *Setosphaeria turcica,* most likely by stimulating the plant defense system (D'Alessandro et al., 2014).

In a recent investigation performed on potato field, five bacterial strains, namely *Pseudomonas palleroniana* R43631, *Bacillus* sp. R47065, R47131, *Paenibacillus* sp. B3a R49541, and *Bacillus simplex* M3-4 R49538, were designed as suitable to improve potato yield by means of VOC production (Velivelli et al., 2015). Nevertheless, molecular details on how the single components of the volatilome exert their inhibitory activity are generally missing in field studies. On the other hand, studies carried out *in vitro* and/or greenhouse condition do generally succeed in the evaluation of the biological mechanisms triggered by the microbial VOCs, but lack to consider the practicability under open-field conditions. Undoubtedly, investigation of the microbial VOCs is still in its infancy and further complementary studies are needed to design appropriate methods for delivery and effective lasting of these innovative treatments (Velivelli et al., 2015; Chung et al., 2016; Schulz-Bohm et al., 2017).

To date, the most promising results were achieved by applying microbial VOCs for the control and prevention of storage pathogens. VOCs application under air-tight condition ensures a rapid saturation of the atmosphere and allows the maintaining of concentration levels of the microbial volatile blend above the minimal effective concentration required to succeed with

the pathogen control strategies. In this view, application of microbial VOCs in close environment condition may represent a valuable approach for investigating unique molecules and complex VOCs mixtures in relation to their potential biocontrol activity. Identification of bioactive molecules along with the dynamic cross-talk these compounds are involved in would greatly facilitate the development of suitable chemical forms (e.g., immobilized molecules, pro-bioactive compounds) that should allow better handling, storage, and safe deliver to open fields (Kanchiswamy et al., 2015).

CONCLUSION

Microbes produce a wide array of volatile metabolites linked to a complex network of interactions, involving intra- and inter-species relationship. Most of the studies so far performed have focused on the unidirectional effect of the microbial VOCs produced by a single microbial entity in regard to another microbial species or strain (Schulz-Bohm et al., 2015, 2017; Splivallo et al., 2015). Although of a great importance, this "foreshortening of the microbial reality" is rather simplistic and does not consider a wealth of biotic and abiotic factors that would facilitate a comprehensive understanding of the whole ecosystem the microbial species are coping with; thus, how modulating the ecosystem can shape the overall VOCs composition, in favor of a better control of the pathogen diffusion and plant growth stimulation.

Moreover, we are now suffering from a lack of knowledge related to VOCs emission by protists, archaea, or other rhizosphere organisms, such as nematodes or earthworms (Schulz-Bohm et al., 2017). These groups are currently understudied with respect to this aspect, yet their contribution to the overall VOCs composition and the inter-species cross-talk may be of crucial importance. In this view, we foresee that effort to validate this promising strategy will focus on expanding the knowledge on the microbial VOCs biodiversity along with the investigation of their effect on the living community through the adoption of holistic approaches such as -omics sciences and bioinformatics prediction tools.

AUTHOR CONTRIBUTIONS

All authors listed have made a substantial, direct and intellectual contribution to the work, and approved it for publication.

REFERENCES

Ädel Druvefors, U., and Schnürer, J. (2005). Mold-inhibitory activity of different yeast species during airtight storage of wheat grain. *FEMS Yeast Res.* 5, 373–378. doi: 10.1016/j.femsyr.2004.10.006

Ait-Lahsen, H., Soler, A. S., Rey, M., De, J. S., Cruz, L., Monte, E., et al. (2001). An antifungal exo-α-1,3-glucanase (AGN13.1) from the biocontrol fungus *Trichoderma harzianum*. *Appl. Environ. Microbiol.* 67, 5833–5839. doi: 10.1128/AEM.67.12.5833-5839.2001

Arrarte, E., Garmendia, G., Rossini, C., Wisniewski, M., and Vero, S. (2017). Volatile organic compounds produced by Antarctic strains of *Candida sake* play a role in the control of postharvest pathogens of apples. *Biol. Control* 109, 14–20. doi: 10.1016/j.biocontrol.2017.03.002

Asari, S., Matzén, S., Petersen, M. A., Bejai, S., and Meijer, J. (2016). Multiple effects of Bacillus amyloliquefaciens volatile compounds: plant growth promotion and growth inhibition of phytopathogens. *FEMS Microbiol. Ecol.* 92, 1–11. doi: 10.1093/femsec/fiw070

Avalos, M., Garbeva, P., Raaijmakers, J. M., and van Wezel, G. P. (2019). Production of ammonia as a low-cost and long-distance antibiotic strategy by *Streptomyces* species. *ISME J.* 2019, 1–15. doi: 10.1038/s41396-019-0537-2

Bajpai, V. K., Rahman, A., Dung, N. T., Huh, M. K., and Kang, S. C. (2008). *In vitro* inhibition of food spoilage and foodborne pathogenic bacteria by essential oil and leaf extracts of *Magnolia liliflora* Desr. *J. Food Sci.* 73, M314–M320. doi: 10.1111/j.1750-3841.2008.00841.x

Bennett, J. W., Hung, R., Lee, S., and Padhi, S. (2012). "Fungal and bacterial volatile organic compounds: an overview and their role as ecological signaling agents" in *The mycota (A Comprehensive Treatise on Fungi as Experimental Systems for Basic and Applied Research)*. ed. B. Hock (Berlin, Heidelberg: Springer), 373–393.

Blom, D., Fabbri, C., Connor, E. C., Schiestl, F. P., Klauser, D. R., Boller, T., et al. (2011). Production of plant growth modulating volatiles is widespread among rhizosphere bacteria and strongly depends on culture conditions. *Environ. Microbiol.* 13, 3047–3058. doi: 10.1111/j.1462-2920.2011.02582.x

Braun, G., Vailati, M., Prange, R., and Bevis, E. (2012). *Muscodor albus* volatiles control toxigenic fungi under controlled atmosphere (CA) storage conditions. *Int. J. Mol. Sci.* 13, 15848–15858. doi: 10.3390/ijms131215848

Chang, P. K., Hua, S. S. T., Sarreal, S. B. L., and Li, R. W. (2015). Suppression of aflatoxin biosynthesis in *Aspergillus flavus* by 2-phenylethanol is associated with stimulated growth and decreased degradation of branched-chain amino acids. *Toxins* 7, 3887–3902. doi: 10.3390/toxins7103887

Chen, P.-H., Chen, R.-Y., and Chou, J. Y. (2018). Screening and evaluation of yeast antagonists for biological control of *Botrytis cinerea* on strawberry fruits. *Mycobiology* 46, 33–46. doi: 10.1080/12298093.2018.1454013

Chiron, N., and Micherlot, D. (2005). Odeurs des champignons: chimie et rôle dans les interactions biotiques - une revue. *Cryptogam. Mycol.* 26, 299–364. https://hal.archives-ouvertes.fr/hal-00086256

Choi, H. K., Song, G. C., Yi, H., and Ryu, C. (2014). Field evaluation of the bacterial volatile derivative 3-pentanol in priming for induced resistance in pepper. *J. Chem. Ecol.* 40, 882–892. doi: 10.1007/s10886-014-0488-z

Chung, J. H., Song, G. C., and Ryu, C. M. (2016). Sweet scents from good bacteria: case studies on bacterial volatile compounds for plant growth and immunity. *Plant Mol. Biol.* 90, 677–687. doi: 10.1007/s11103-015-0344-8

Coda, R., Rizzello, C. G., Di Cagno, R., Trani, A., Cardinali, G., and Gobbetti, M. (2013). Antifungal activity of *Meyerozyma guilliermondii*: identification of active compounds synthesized during dough fermentation and their effect on long-term storage of wheat bread. *Food Microbiol.* 33, 243–251. doi: 10.1016/j.fm.2012.09.023

Compant, S., Duffy, B., Nowak, J., Clément, C., and Barka, E. A. (2005). Use of plant growth-promoting bacteria for biocontrol of plant diseases: principles, mechanisms of action, and future prospects. *Appl. Environ. Microbiol.* 71, 4951–4959. doi: 10.1128/AEM.71.9.4951-4959.2005

Cortes-Barco, A. M., Goodwin, P. H., and Hsiang, T. (2010a). Comparison of induced resistance activated by benzothiadiazole, (2R,3R)-butanediol and an isoparaffin mixture against anthracnose of *Nicotiana benthamiana*. *Plant Pathol.* 59, 643–653. doi: 10.1111/j.1365-3059.2010.02283.x

Cortes-Barco, A. M., Hsiang, T., and Goodwin, P. H. (2010b). Induced systemic resistance against three foliar diseases of *Agrostis stolonifera* by (2R,3R)-butanediol or an isoparaffin mixture. *Ann. Appl. Biol.* 157, 179–189. doi: 10.1111/j.1744-7348.2010.00417.x

Cowen, L. E., Anderson, J. B., and Kohn, L. M. (2002). Evolution of drug resistance in *Candida albicans*. *Annu. Rev. Microbiol.* 56, 139–165. doi: 10.1146/annurev.micro.56.012302.160907

D'Alessandro, M., Erb, M., Ton, J., Brandenburg, A., Karlen, D., Zopfi, J., et al. (2014). Volatiles produced by soil-borne endophytic bacteria increase plant pathogen resistance and affect tritrophic interactions. *Plant Cell Environ.* 37, 813–826. doi: 10.1111/pce.12220

Dandurishvili, N., Toklikishvili, N., Ovadis, M., Eliashvili, P., Giorgobiani, N., Keshelava, R., et al. (2011). Broad-range antagonistic rhizobacteria *Pseudomonas fluorescens* and *Serratia plymuthica* suppress *Agrobacterium* crown gall tumours on tomato plants. *J. Appl. Microbiol.* 110, 341–352. doi: 10.1111/j.1365-2672.2010.04891.x

Deising, H. B., Reimann, S., and Pascholati, S. F. (2008). Mechanisms and significance of fungicide resistance. *Braz. J. Microbiol.* 39, 286–295. doi: 10.1590/S1517-83822008000200017

Delory, B. M., Delaplace, P., Fauconnier, M., and du Jardin, P. (2016). Root-emitted volatile organic compounds: can they mediate belowground plant-plant interactions? *Plant Soil* 36, 361–368. doi: 10.1007/s11104-016-2823-3

Di Francesco, A., Ugolini, L., Lazzeri, L., and Mari, M. (2015). Production of volatile organic compounds by *Aureobasidium pullulans* as a potential mechanism of action against postharvest fruit pathogens. *Biol. Control* 81, 8–14. doi: 10.1016/j.biocontrol.2014.10.004

Dowling, D. N., and O'Gara, F. (1994). Metabolites of *Pseudomonas* involved in the biocontrol of plant disease. *Trends Biotechnol.* 12, 133–141.

Droby, S., Wisniewski, M., Macarisin, D., and Wilson, C. (2009). Twenty years of postharvest biocontrol research: is it time for a new paradigm? *Postharvest Biol. Technol.* 52, 137–145. doi: 10.1016/j.postharvbio.2008.11.009

Effmert, U., Kalderás, J., Warnke, R., and Piechulla, B. (2012). Volatile mediated interactions between bacteria and fungi in the soil. *J. Chem. Ecol.* 38, 665–703. doi: 10.1007/s10886-012-0135-5

Elshafie, H. S., Camele, I., Racioppi, R., Scrano, L., Iacobellis, N. S., and Bufo, S. A. (2012). *In vitro* antifungal activity of *Burkholderia gladioli* pv. *agaricicola* against some phytopathogenic fungi. *Int. J. Mol. Sci.* 13, 16291–16302. doi: 10.3390/ijms131216291

Essien, E., Aboaba, S. O., and Ogunwande, I. A. (2011). Constituents and antimicrobial properties of the leaf essential oil of *Gossypium barbadense* (Linn.). *J. Med.Plants Res.* 5, 702–705. doi: 10.5897/JMPR

Farag, M. A., Ryu, C. M., Sumner, L. W., and Paré, P. W. (2006). GC-MS SPME profiling of rhizobacterial volatiles reveals prospective inducers of growth promotion and induced systemic resistance in plants. *Phytochemistry* 67, 2262–2268. doi: 10.1016/j.phytochem.2006.07.021

Farbo, M. G., Urgeghe, P. P., Fiori, S., Marcello, A., Oggiano, S., Balmas, V., et al. (2018). Effect of yeast volatile organic compounds on ochratoxin A-producing *Aspergillus carbonarius* and *A. ochraceus*. *Int. J. Food Microbiol.* 284, 1–10. doi: 10.1016/j.ijfoodmicro.2018.06.023

Fialho, M. B., Ferreira, L. F. R., Monteiro, R. T. R., and Pascholati, S. F. (2011). Antimicrobial volatile organic compounds affect morphogenesis-related enzymes in *Guignardia citricarpa*, causal agent of citrus black spot. *Biocontrol Sci. Tech.* 21, 797–807. doi: 10.1080/09583157.2011.580837

Fialho, M. B., Toffano, L., Pedroso, M. P., Augusto, F., and Pascholati, S. F. (2010). Volatile organic compounds produced by *Saccharomyces cerevisiae* inhibit the *in vitro* development of *Guignardia citricarpa*, the causal agent of citrus black spot. *World J. Microbiol. Biotechnol.* 26, 925–932. doi: 10.1007/s11274-009-0255-4

Fiedler, N., Laumbach, R., Kelly-McNeil, K., Lioy, P., Fan, Z. H., Zhang, J., et al. (2005). Health effects of a mixture of indoor air volatile organics, their ozone oxidation products, and stress. *Environ. Health Perspect.* 113, 1542–1548. doi: 10.1289/ehp.8132

Fiori, S., Urgeghe, P. P., Hammami, W., Razzu, S., Jaoua, S., and Migheli, Q. (2014). Biocontrol activity of four non- and low-fermenting yeast strains against *Aspergillus carbonarius* and their ability to remove ochratoxin a from grape juice. *Int. J. Food Microbiol.* 189, 45–50. doi: 10.1016/j.ijfoodmicro.2014.07.020

Gao, H., Li, P., Xu, X., Zeng, Q., and Guan, W. (2018). Research on volatile organic compounds from *Bacillus subtilis* CF-3: biocontrol effects on fruit fungal pathogens and dynamic changes during fermentation. *Front. Microbiol.* 9:456. doi: 10.3389/fmicb.2018.00456

Garbeva, P., Hordijk, C., Gerards, S., and de Boer, W. (2014a). Volatiles produced by the mycophagous soil bacterium *Collimonas*. *FEMS Microbiol. Ecol.* 87, 639–649. doi: 10.1111/1574-6941.12252

Garbeva, P., Hordijk, C., Gerards, S., and de Boer, W. (2014b). Volatile-mediated interactions between phylogenetically different soil bacteria. *Front. Microbiol.* 5:289. doi: 10.3389/fmicb.2014.00289

Groenhagen, U., Baumgartner, R., Bailly, A., Gardiner, A., Eberl, L., Schulz, S., et al. (2013). Production of bioactive volatiles by different *Burkholderia ambifaria* strains. *J. Chem. Ecol.* 39, 892–906. doi: 10.1007/s10886-013-0315-y

Gu, Y. Q., Mo, M. H., Zhou, J. P., Zou, C. S., and Zhang, K. Q. (2007). Evaluation and identification of potential organic nematicidal volatiles from soil bacteria. *Soil Biol. Biochem.* 39, 2567–2575. doi: 10.1016/j.soilbio.2007.05.011

Gutiérrez-Luna, F. M., López-Bucio, J., Altamirano-Hernández, J., Valencia-Cantero, E., De La Cruz, H. R., and Macías-Rodríguez, L. (2010). Plant growth-promoting rhizobacteria modulate root-system architecture in *Arabidopsis thaliana* through volatile organic compound emission. *Symbiosis* 51, 75–83. doi: 10.1007/s13199-010-0066-2

Heydari, A., and Pessarakli, M. (2010). A review on biological control of fungal plant pathogens using microbial antagonists. *J. Biol. Sci.* 10, 273–290. doi: 10.3923/jbs.2010.273.290

Hong, T.-Y., and Meng, M. (2003). Biochemical characterization and antifungal activity of an endo-1,3-b-glucanase of *Paenibacillus* sp. isolated from garden soil. *Appl. Microbiol. Biotechnol.* 61, 472–478. doi: 10.1007/s00253-003-1249-z

Hua, S. S. T., Beck, J. J., Sarreal, S. B. L., and Gee, W. (2014). The major volatile compound 2-phenylethanol from the biocontrol yeast, *Pichia anomala*, inhibits growth and expression of aflatoxin biosynthetic genes of *Aspergillus flavus*. *Mycotoxin Res.* 30, 71–78. doi: 10.1007/s12550-014-0189-z

Huang, R., Che, H. J., Zhang, J., Yang, L., Jiang, D. H., and Li, G. Q. (2012b). Evaluation of *Sporidiobolus pararoseus* strain YCXT3 as biocontrol agent of *Botrytis cinerea* on post-harvest strawberry fruits. *Biol. Control* 62, 53–63. doi: 10.1016/j.biocontrol.2012.02.010

Huang, R., Li, G. Q., Zhang, J., Yang, L., Che, H. J., Jiang, D. H., et al. (2011). Control of postharvest Botrytis fruit rot of strawberry by volatile organic compounds of *Candida intermedia*. *Phytopathology* 101, 859–869. doi: 10.1094/phyto-09-10-0255

Huang, C. J., Tsay, J. F., Chang, S. Y., Yang, H. P., Wu, W. S., and Chen, C. Y. (2012a). Dimethyl disulfide is an induced systemic resistance elicitor produced by *Bacillus cereus* C1L. *Pest Manag. Sci.* 68, 1306–1310. doi: 10.1002/ps.3301

Hung, R., Lee, S., and Bennett, J. W. (2013). *Arabidopsis thaliana* as a model system for testing the effect of *Trichoderma* volatile organic compounds. *Fungal Ecol.* 6, 19–26. doi: 10.1016/j.funeco.2012.09.005

Irtwange, S. (2006). Application of biological control agents in pre-and postharvest operations. *Agric. Eng. Int. CIGR J.* 3, 3. Available at: http://cigrjournal.org/index.php/Ejounral/article/download/690/684; https://hdl.handle.net/1813/10564 (Accessed January 24, 2020).

Janisiewicz, W. J., Kurtzman, C. P., and Buyer, J. S. (2010). Yeasts associated with nectarines and their potential for biological control of brown rot. *Yeast* 27, 389–398. doi: 10.1002/yea.1763

Jiménez, J. I., Margolis, J. S., Baird, J. K., and Lego, S. F. (2012). Compounds derived from Muscodor fungi. US Patent 20120058058.

Jones, S. E., Ho, L., Rees, C. A., Hill, J. E., Nodwell, J. R., and Elliot, M. A. (2017). *Streptomyces* exploration is triggered by fungal interactions and volatile signals. *elife* 6:e21738. doi: 10.7554/eLife.21738

Kai, M., Crespo, E., Cristescu, S. M., Harren, F. J. M., Francke, W., and Piechulla, B. (2010). *Serratia odorifera*: analysis of volatile emission and biological impact of volatile compounds on *Arabidopsis thaliana*. *Appl. Microbiol. Biotechnol.* 88, 965–976. doi: 10.1007/s00253-010-2810-1

Kai, M., Haustein, M., Molina, F., Petri, A., Scholz, B., and Piechulla, B. (2009). Bacterial volatiles and their action potential. *Appl. Microbiol. Biotechnol.* 81, 1001–1012. doi: 10.1007/s00253-008-1760-3

Kanchiswamy, C. N., Malnoy, M., and Maffei, M. E. (2015). Chemical diversity of microbial volatiles and their potential for plant growth and productivity. *Front. Plant Sci.* 6:151. doi: 10.3389/fpls.2015.00151

Kännaste, A., Copolovici, L., and Niinemets, Ü. (2014). Gas chromatography-mass spectrometry method for determination of biogenic volatile organic compounds emitted by plants. *Methods Mol. Biol.* 1153, 161–169. doi: 10.1007/978-1-4939-0606-2_11

Khan, A. L., Waqas, M., Hussain, J., Al-Harrasi, A., Al-Rawahi, A., Al-Hosni, K., et al. (2014). Endophytes *Aspergillus caespitosus* LK12 and *Phoma* sp. LK13 of *Moringa peregrina* produce gibberellins and improve rice plant growth. *J. Plant Interact.* 9, 731–737. doi: 10.1080/17429145.2014.917384

Kumar, S., and Kaushik, N. (2012). Metabolites of endophytic fungi as novel source of biofungicide: a review. *Phytochem. Rev.* 11, 507–522. doi: 10.1007/s11101-013-9271-y

Li, Q., Ning, P., Zheng, L., Huang, J., Li, G., and Hsiang, T. (2010). Fumigant activity of volatiles of *Streptomyces globisporus* JK-1 against *Penicillium italicum* on *Citrus microcarpa*. *Postharvest Biol. Technol.* 58, 157–165. doi: 10.1016/j.postharvbio.2010.06.003

Lim, H.-S., Kim, Y.-S., and Kim, S.-D. (1991). *Pseudomonas stutzeri* YPL-1 genetic transformation and antifungal mechanism against *Fusarium solani*, an agent of plant root rot. *Appl. Environ. Microbiol.* 57, 510–516.

Liu, P., Cheng, Y., Yang, M., Liu, Y., Chen, K., Long, C. A., et al. (2014). Mechanisms of action for 2-phenylethanol isolated from *Kloeckera apiculata* in control of Penicillium molds of citrus fruits. *BMC Microbiol.* 14:242. doi: 10.1186/s12866-014-0242-2

Liu, J., Sui, Y., Wisniewski, M., Droby, S., and Liu, Y. (2013). Review: utilization of antagonistic yeasts to manage postharvest fungal diseases of fruit. *Int. J. Food Microbiol.* 167, 153–160. doi: 10.1016/j.ijfoodmicro.2013.09.004

Maffei, M. E., Gertsch, J., and Appendino, G. (2011). Plant volatiles: production, function and pharmacology. *Nat. Prod. Rep.* 28, 1359–1380. doi: 10.1039/c1np00021g

Mari, M., Martini, C., Guidarelli, M., and Neri, F. (2012). Postharvest biocontrol of *Monilinia laxa*, *Monilinia fructicola* and *Monilinia fructigena* on stone fruit by two *Aureobasidium pullulans* strains. *Biol. Control* 60, 132–140. doi: 10.1016/j.biocontrol.2011.10.013

Masoud, W., and Kaltoft, C. H. (2006). The effects of yeasts involved in the fermentation of *Coffea arabica* in East Africa on growth and ochratoxin a (OTA) production by *Aspergillus ochraceus*. *Int. J. Food Microbiol.* 106, 229–234. doi: 10.1016/j.ijfoodmicro.2005.06.015

Masoud, W., Poll, L., and Jakobsen, M. (2005). Influence of volatile compounds produced by yeasts predominant during processing of *Coffea arabica* in East Africa on growth and ochratoxin A (OTA) production by *Aspergillus ochraceus*. *Yeast* 22, 1133–1142. doi: 10.1002/yea.1304

McKee, N. D., and Robinson, P. M. (2009). Production of volatile inhibitors of germination and hyphal extension by *Geotrichum candidum*. *Trans. Br. Mycol. Soc.* 91, 157–160. doi: 10.1016/s0007-1536(88)80017-2

Mehta, H. H., Prater, A. G., and Shamoo, Y. (2018). Using experimental evolution to identify druggable targets that could inhibit the evolution of antimicrobial resistance. *J. Antibiot.* 71, 279–286. doi: 10.1038/ja.2017.108

Meldau, D. G., Meldau, S., Hoang, L. H., Underberg, S., Wunsche, H., and Baldwin, I. T. (2013). Dimethyl disulfide produced by the naturally associated bacterium *Bacillus* sp B55 promotes *Nicotiana attenuata* growth by enhancing sulfur nutrition. *Plant Cell* 25, 2731–2747. doi: 10.1105/tpc.113.114744

Mercier, J., and Jiménez, J. I. (2004). Control of fungal decay of apples and peaches by the biofumigant fungus *Muscodor albus*. *Postharvest Biol. Technol.* 31, 1–8. doi: 10.1016/j.postharvbio.2003.08.004

Mercier, J., Lego, S. F., and Smilanick, J. (2010). In-package use of *Muscodor albus* volatile-generating sachets and modified atmosphere liners for decay control in organic table grapes under commercial conditions. *Fruits* 65, 31–38. doi: 10.1051/fruits/2009039

Mercier, J., and Manker, D. C. (2005). Biocontrol of soil-borne diseases and plant growth enhancement in greenhouse soilless mix by the volatile-producing fungus *Muscodor albus*. *Crop Prot.* 24, 355–362. doi: 10.1016/j.cropro.2004.09.004

Minerdi, D., Bossi, S., Gullino, M. L., and Garibaldi, A. (2009). Volatile organic compounds: a potential direct long-distance mechanism for antagonistic action of *Fusarium oxysporum* strain MSA 35. *Environ. Microbiol.* 11, 844–854. doi: 10.1111/j.1462-2920.2008.01805.x

Minerdi, D., Bossi, S., Maffei, M. E., Gullino, M. L., and Garibaldi, A. (2011). *Fusarium oxysporum* and its bacterial consortium promote lettuce growth and expansin A5 gene expression through microbial volatile organic compound (MVOC) emission. *FEMS Microbiol. Ecol.* 76, 342–351. doi: 10.1111/j.1574-6941.2011.01051.x

Mitchell, A. M., Strobel, G. A., Moore, E., Robison, R., and Sears, J. (2010). Volatile antimicrobials from *Muscodor crispans*, a novel endophytic fungus. *Microbiology* 156, 270–277. doi: 10.1099/mic.0.032540-0

Morath, S. U., Hung, R., and Bennett, J. W. (2012). Fungal volatile organic compounds: a review with emphasis on their biotechnological potential. *Fungal Biol. Rev.* 26, 73–83. doi: 10.1016/j.fbr.2012.07.001

Muccilli, S., and Restuccia, C. (2015). Bioprotective role of yeasts. *Microorganisms* 3, 588–611. doi: 10.3390/microorganisms3040588

Mülner, P., Bergna, A., Wagner, P., Sarajlić, D., Gstöttenmayr, B., Dietel, K., et al. (2019). Microbiota associated with sclerotia of soilborne fungal pathogens – a novel source of biocontrol agents producing bioactive volatiles. *Phytobiomes Journal.* 3, 125–136. doi: 10.1094/PBIOMES-11-18-0051-R

Naznin, H. A., Kimura, M., Miyazawa, M., and Hyakumachi, M. (2012). Analysis of volatile organic compounds emitted by plant growth-promoting fungus *Phoma* sp. GS8-3 for growth promotion effects on tobacco. *Microbes Environ.* 28, 42–49. doi: 10.1264/jsme2.me12085

Naznin, H. A., Kiyohara, D., Kimura, M., Miyazawa, M., Shimizu, M., and Hyakumachi, M. (2014). Systemic resistance induced by volatile organic compounds emitted by plant growth-promoting fungi in *Arabidopsis thaliana*. *PLoS One* 9:e86882. doi: 10.1371/journal.pone.0086882

Nilsson, A., Kihlström, E., Lagesson, V., Wessén, B., Szponar, B., Larsson, L., et al. (2004). Microorganisms and volatile organic compounds in airborne dust from damp residences. *Indoor Air* 14, 74–82. doi: 10.1046/j.1600-0668.2003.00178.x

Pagans, E., Font, X., and Sánchez, A. (2006). Emission of volatile organic compounds from composting of different solid wastes: abatement by biofiltration. *J. Hazard. Mater.* 131, 179–186. doi: 10.1016/j.jhazmat.2005.09.017

Pal, K. K., and McSpadden Gardener, B. (2006). Biological control of plant pathogens. *Plant Health Instr.* 2, 1. doi: 10.1094/PHI-A-2006-1117-02

Parafati, L., Vitale, A., Restuccia, C., and Cirvilleri, G. (2015). Biocontrol ability and action mechanism of food-isolated yeast strains against *Botrytis cinerea* causing post-harvest bunch rot of table grape. *Food Microbiol.* 47, 85–92. doi: 10.1016/j.fm.2014.11.013

Parafati, L., Vitale, A., Restuccia, C., and Cirvilleri, G. (2017). Performance evaluation of volatile organic compounds by antagonistic yeasts immobilized on hydrogel spheres against gray, green and blue postharvest decays. *Food Microbiol.* 63, 191–198. doi: 10.1016/j.fm.2016.11.021

Pasanen, P., Korpi, A., Kalliokoski, P., and Pasanen, A. L. (1997). Growth and volatile metabolite production of *Aspergillus versicolor* in house dust. *Environ. Int.* 23, 425–432. doi: 10.1016/S0160-4120(97)00027-5

Peighami-Ashnaei, S., Sharifi-Tehrani, A., Ahmadzadeh, M., and Behboudi, K. (2009). Interaction of different media on production and biocontrol efficacy of *Pseudomonas fluorescens* P-35 and *Bacillus subtilis* B-3 against grey mould of apple. *J. Plant Pathol.* 91, 65–70. doi: 10.4454/jpp.v91i1.625

Pimenta, R. S., Moreira da Silva, J. F., Buyer, J. S., and Janisiewicz, W. J. (2012). Endophytic fungi from plums (*Prunus domestica*) and their antifungal activity against *Monilinia fructicola*. *J. Food Prot.* 75, 1883–1889. doi: 10.4315/0362-028X.JFP-12-156

Popova, A. A., Koksharova, O. A., Lipasova, V. A., Zaitseva, J. V., Katkova-Zhukotskaya, O. A., Eremina, S. I., et al. (2014). Inhibitory and toxic effects of volatiles emitted by strains of *Pseudomonas* and *Serratia* on growth and survival of selected microorganisms, *Caenorhabditis elegans*, and *Drosophila melanogaster*. *Biomed. Res. Int.* 2014:4. doi: 10.1155/2014/125704

Raza, W., Ling, N., Yang, L., Huang, Q., and Shen, Q. (2016). Response of tomato wilt pathogen *Ralstonia solanacearum* to the volatile organic compounds produced by a biocontrol strain *Bacillus amyloliquefaciens* SQR-9. *Sci. Rep.* 6:24856. doi: 10.1038/srep24856

Romanazzi, G., Lichter, A., Gabler, F. M., and Smilanick, J. L. (2012). Recent advances on the use of natural and safe alternatives to conventional methods to control postharvest gray mold of table grapes. *Postharvest Biol. Technol.* 63, 141–147. doi: 10.1016/j.postharvbio.2011.06.013

Rudrappa, T., Biedrzycki, M. L., Kunjeti, S. G., Donofrio, N. M., Czymmek, K. J., Paré, P. W., et al. (2010). The rhizobacterial elicitor acetoin induces systemic resistance in *Arabidopsis thaliana*. *Commun. Integr. Biol.* 3, 130–138. doi: 10.4161/cib.3.2.10584

Ryu, C.-M., Farag, M. A., Hu, C.-H., Reddy, M. S., Wei, H.-X., Pare, P. W., et al. (2003). Bacterial volatiles promote growth in Arabidopsis. *Proc. Natl. Acad. Sci. USA* 100, 4927–4932. doi: 10.1073/pnas.0730845100

Schiestl, F. P., Steinebrunner, F., Schulz, C., von Reuss, S., Francke, W., Weymuth, C., et al. (2006). Evolution of 'pollinator'-attracting signals in fungi. *Biol. Lett.* 2, 401–404. doi: 10.1098/rsbl.2006.0479

Schmidt, R., Cordovez, V., de Boer, W., Raaijmakers, J., and Garbeva, P. (2015). Volatile affairs in microbial interactions. *ISME J.* 9, 2329–2335. doi: 10.1038/ismej.2015.42

Schöller, C. E. G., Gürtler, H., Pedersen, R., Molin, S., and Wilkins, K. (2002). Volatile metabolites from actinomycetes. *J. Agric. Food Chem.* 5, 2615–2621. doi: 10.1021/jf0116754

Schulz-Bohm, K., Martín-Sánchez, L., and Garbeva, P. (2017). Microbial volatiles: small molecules with an important role in intra- and inter-kingdom interactions. *Front. Microbiol.* 8:2484. doi: 10.3389/fmicb.2017.02484

Schulz-Bohm, K., Zweers, H., de Boer, W., and Garbeva, P. (2015). A fragrant neighborhood: volatile mediated bacterial interactions in soil. *Front. Microbiol.* 6:1212. doi: 10.3389/fmicb.2015.01212

Serrano, A., and Gallego, M. (2006). Sorption study of 25 volatile organic compounds in several Mediterranean soils using headspace-gas chromatography-mass spectrometry. *J. Chromatogr.* 1118, 261–270. doi: 10.1016/j.chroma.2006.03.095

Serrano, C., Matos, O., Teixeira, B., Ramos, C., Neng, N., Nogueira, J., et al. (2011). Antioxidant and antimicrobial activity of *Satureja montana* L. extracts. *J. Sci. Food Agric.* 91, 1554–1560. doi: 10.1002/jsfa.4347

Shanthi, K., Gowri, P., and Gopu, M. (2011). Pharmacognosy, analysis of bioactive compounds form *Abutilon indicum* Linn. (Malvaceae) by using gas chromatography and mass spectrometry (GC-MS) in ethanol and hexane solvent. *J. Pharm. Res.* 4, 4795–4797.

Singh, S. K., Strobel, G. A., Knighton, B., Geary, B., Sears, J., and Ezra, D. (2011). An endophytic *Phomopsis* sp. possessing bioactivity and fuel potential with its volatile organic compounds. *Microb. Ecol.* 61, 729–739. doi: 10.1007/s00248-011-9818-7

Song, G. C., and Ryu, C. M. (2013). Two volatile organic compounds trigger plant self-defense against a bacterial pathogen and a sucking insect in cucumber under open field conditions. *Int. J. Mol. Sci.* 14, 9803–9819. doi: 10.3390/ijms14059803

Splivallo, R., Deveau, A., Valdez, N., Kirchhoff, N., Frey-Klett, P., and Karlovsky, P. (2015). Bacteria associated with truffle-fruiting bodies contribute to truffle aroma. *Environ. Microbiol.* 17, 2647–2660. doi: 10.1111/1462-2920.12521

Strobel, G. (2006). *Muscodor albus* and its biological promise. *J. Ind. Microbiol. Biotechnol.* 33, 514–522. doi: 10.1007/s10295-006-0090-7

Strobel, G. A., Dirkse, E., Sears, J., and Markworth, C. (2001). Volatile antimicrobials from *Muscodor albus*, a novel endophytic fungus. *Microbiology* 147, 2943–2950. doi: 10.1099/00221287-147-11-2943

Strobel, G., Singh, S. K., Riyaz-Ul-Hassan, S., Mitchell, A. M., Geary, B., and Sears, J. (2011). An endophytic/pathogenic *Phoma* sp. from creosote bush producing biologically active volatile compounds having fuel potential. *FEMS Microbiol. Lett.* 230, 87–94. doi: 10.1111/j.1574-6968.2011.02297.x

Tenorio-Salgado, S., Tinoco, R., Vazquez-Duhalt, R., Caballero-Mellado, J., and Perez-Rueda, E. (2013). Identification of volatile compounds produced by the bacterium *Burkholderia tropica* that inhibit the growth of fungal pathogens. *Bioengineered* 4, 236–243. doi: 10.4161/bioe.23808

Tholl, D., Boland, W., Hansel, A., Loreto, F., Röse, U. S., and Schnitzler, J. P. (2006). Practical approaches to plant volatile analysis. *Plant J.* 45, 540–560. doi: 10.1111/j.1365-313X.2005.02612.x

Tilocca, B., Balmas, V., Hassan, Z. U., Jaoua, S., and Migheli, Q. (2019). A proteomic investigation of *Aspergillus carbonarius* exposed to yeast volatilome or to its major component 2-phenylethanol reveals major shifts in fungal metabolism. *Int. J. Food Microbiol.* 306:108265. doi: 10.1016/j.ijfoodmicro.2019.108265

Tröscher-Mußotter, J., Tilocca, B., Stefanski, V., and Seifert, J. (2019). Analysis of the bacterial and host proteins along and across the porcine gastrointestinal tract. *Proteomes* 7:4. doi: 10.3390/proteomes7010004

van Dam, N. M., and Poppy, G. M. (2008). Why plant volatile analysis needs bioinformatics-detecting signal from noise in increasingly complex profiles. *Plant Biol.* 10, 29–37. doi: 10.1055/s-2007-964961

van Loon, L. C., Bakker, P. A. H. M., and Pieterse, C. M. J. (1998). Systemic resistance induced by rhizosphere bacteria. *Annu. Rev. Phytopathol.* 36, 453–483. doi: 10.1146/annurev.phyto.36.1.453

Velivelli, S. L. S., Kromann, P., Lojan, P., Rojas, M., Franco, J., Suarez, J. P., et al. (2015). Identification of mVOCs from andean rhizobacteria and field evaluation of bacterial and mycorrhizal inoculants on growth of potato in its center of origin. *Microb. Ecol.* 268, 285–292. doi: 10.1007/s00248-014-0514-2

Vespermann, A., Kai, M., and Piechulla, B. (2007). Rhizobacterial volatiles affect the growth of fungi and *Arabidopsis thaliana*. *Appl. Environ. Microbiol.* 73, 5639–5641. doi: 10.1128/AEM.01078-07

Wang, C., Wang, Z., Qiao, X., Li, Z., Li, F., Chen, M., et al. (2013). Antifungal activity of volatile organic compounds from *Streptomyces alboflavus* TD-1. *FEMS Microbiol. Lett.* 341, 45–51. doi: 10.1111/1574-6968.12088

Wani, M. A., Sanjana, K., Kumar, D. M., and Lal, D. K. (2010). GC-MS analysis reveals production of 2-phenylethanol from *Aspergillus niger* endophytic in rose. *J. Basic Microbiol.* 50, 110–114. doi: 10.1002/jobm.200900295

Waqas, M., Khan, A. L., and Lee, I. J. (2014). Bioactive chemical constituents produced by endophytes and effects on rice plant growth. *J. Plant Interact.* 9, 478–487. doi: 10.1080/17429145.2013.860562

Wheatley, R., Hackett, C., Bruce, A., and Kundzewicz, A. (1997). Effect of substrate composition on production of volatile organic compounds from *Trichoderma* spp. inhibitory to wood decay fungi. *Int. Biodeterior. Biodegrad.* 39, 199–205. doi: 10.1016/S0964-8305(97)00015-2

Wilkins, K., and Schöller, C. (2009). Volatile organic metabolites from selected *Streptomyces* strains. *Actinomycetologica* 23, 27–33. doi: 10.3209/saj.SAJ230202

Wisniewski, M., Biles, C., Droby, S., McLaughlin, R., Wilson, C., and Chalutz, E. (1991). Mode of action of the postharvest biocontrol yeast, *Pichia guilliermondii*. I. Characterization of attachment to *Botrytis cinerea*. *Physiol. Mol. Plant Pathol.* 39, 245–258. doi: 10.1016/0885-5765(91)90033-E

Xu, Y. Y., Lu, H., Wang, X., Zhang, K. Q., and Li, G. H. (2015). Effect of volatile organic compounds from bacteria on nematodes. *Chem. Biodivers.* 12, 1415–1421. doi: 10.1002/cbdv.201400342

Yamagiwa, Y., Inagaki, Y., Ichinose, Y., Toyoda, K., Hyakumachi, M., and Shiraishi, T. (2011). *Talaromyces wortmannii* FS2 emits β-caryphyllene, which promotes plant growth and induces resistance. *J. Gen. Plant Pathol.* 77, 336–341. doi: 10.1007/s10327-011-0340-z

Yang, Z., Yu, Z., Lei, L., Xia, Z., Shao, L., Zhang, K., et al. (2012). Nematicidal effect of volatiles produced by *Trichoderma* sp. *J. Asia Pac. Entomol.* 15, 647–650. doi: 10.1016/j.aspen.2012.08.002

Yuan, J., Raza, W., Shen, Q., and Huang, Q. (2012). Antifungal activity of *Bacillus amyloliquefaciens* NJN-6 volatile compounds against *Fusarium oxysporum* f. sp. *cubense*. *Appl. Environ. Microbiol.* 78, 5942–5944. doi: 10.1128/AEM.01357-12

Zhang, X., Li, B., Wang, Y., Guo, Q., Lu, X., Li, S., et al. (2013). Lipopeptides, a novel protein, and volatile compounds contribute to the antifungal activity of the biocontrol agent *Bacillus atrophaeus* CAB-1. *Appl. Microbiol. Biotechnol.* 97, 9525–9534. doi: 10.1007/s00253-013-5198-x

Zhao, J., Mou, Y., Shan, T., Li, Y., Zhou, L., Wang, M., et al. (2010). Antimicrobial metabolites from the endophytic fungus *Pichia guilliermondii* isolated from *Paris polyphylla* var. *yunnanensis*. *Molecules* 15, 7961–7970. doi: 10.3390/molecules15117961

Zhou, Z., Zhang, C., Zhou, W., Li, W., Chu, L., Yan, J., et al. (2014). Diversity and plant growth-promoting ability of endophytic fungi from the five flower plant species collected from Yunnan, Southwest China. *J. Plant Interact.* 9, 585–591. doi: 10.1080/17429145.2013.873959

Conflict of Interest: The authors declare that the research was conducted in the absence of any commercial or financial relationships that could be construed as a potential conflict of interest.

frontiers in Microbiology

ORIGINAL RESEARCH
published: 13 March 2020
doi: 10.3389/fmicb.2020.00300

Diversity, Bacterial Symbionts, and Antimicrobial Potential of Termite-Associated Fungi

Xiao Xu[1,2†], Mingwei Shao[1,2†], Caiping Yin[1], Zhenchuan Mao[3], Jingjing Shi[2], Xinyuan Yu[2], Ying Wang[2], Feifei Sun[2] and Yinglao Zhang[1,2]**

[1] School of Life Sciences, Anhui Agricultural University, Hefei, China, [2] College of Chemistry and Life Science, Zhejiang Normal University, Jinhua, China, [3] Institute of Vegetables and Flowers, Chinese Academy of Agricultural Sciences, Beijing, China

The phylogenetic diversity of fungi isolated from the *Odontotermes formosanus* was investigated by dilution-plate method, combined with morphological characteristics and 5.8S rDNA sequencing. Thirty-nine fungi were isolated and purified from *O. formosanus*, which were belonging to two phyla and four classes (Sordariomycetes, Dothideomycetes, Eurotiomycetes, Agaricomycetes). Furthermore, nine bacterial 16S rRNA sequences were obtained from total fungal genomic DNA. All bacterial symbionts were segmented into four genera: *Bacillus*, *Methylobacterium*, *Paenibacillus*, and *Trabulsiella.* The antimicrobial activities of all endophytic fungi extracts were tested by using the filter paper method against *Escherichia coli* (ATCC 8739), *Bacillus subtilis* (ATCC 6633), *Staphylococcus aureus* (ATCC 6538), and *Canidia albicans* (ATCC 10231). The results exhibited that 25 extracts (64%) exhibited antibacterial activity against at least one of the tested bacterial strains. Furthermore, the secondary metabolites **1** [5-hydroxyramulosin **(1a)**:biatriosporin M **(1b)** = 2:1] from the *Pleosporales* sp. BYCDW4 exhibited potent antimicrobial activities against *E. coli*, *C. albicans*, *B. subtilis*, and *S. aureus* with the inhibition zone diameter (IZD) of 13.67, 14.33, 12.17, and 11.33 mm, respectively, which were comparable with those of the positive control. 1-(2,5-Dihydroxyphenyl)-3-hydroxybutan-1-one (**2**) from the *Microdiplodia* sp. BYCDW8 showed medium inhibitory activities against *B. subtilis* and *S. aureus*, with the IZD range of 8.32–9.13 mm. In conclusion, the study showed the diversity of insect symbionts could be expected to develop the resource of new species and antibiotics.

Keywords: *Odontotermes formosanus*, fungal diversity, bacterial symbionts, antimicrobial activities, secondary metabolites

OPEN ACCESS

Edited by:
Santiago Gutierrez, Universidad de León, Spain

Reviewed by:
M. Oves, King Abdulaziz University, Saudi Arabia
Yeshi Yin, Hunan University of Science and Engineering, China

****Correspondence:***
Zhenchuan Mao
maozhenchuan@caas.cn
Yinglao Zhang
zhangyl@ahau.edu.cn

† These authors have contributed equally to this work

Specialty section:
This article was submitted to Microbial Symbioses, a section of the journal Frontiers in Microbiology

Received: *29 October 2019*
Accepted: *10 February 2020*
Published: *13 March 2020*

Citation:
Xu X, Shao M, Yin C, Mao Z, Shi J, Yu X, Wang Y, Sun F and Zhang Y (2020) Diversity, Bacterial Symbionts, and Antimicrobial Potential of Termite-Associated Fungi. Front. Microbiol. 11:300. doi: 10.3389/fmicb.2020.00300

INTRODUCTION

The symbiotic relationships, kinds of organisms including microorganisms, animals, and plants can be seen everywhere in the world (Blackwell and Vega, 2018; Grigorescu et al., 2018). For example, the first direct visual evidence of a not-yet-cultured CFB bacterium is detected in a mycorrhizal fungus (Barbieri et al., 2000). Many others with well-studied examples including the sponge and symbiotic strains, nitrogen-fixing bacteria, and legumes live in symbiotic association

(Trainer and Charles, 2006; Webster et al., 2008). Compared with other interactions, the insect symbiont interactions still represent a largely unknown field (Park et al., 2018).

There are few researches reported that symbioses of insects are an important unexploited microbial resource for human beings. For example, insect gut microbes, especially fungi in suppression of unwanted microorganisms (parasites, microorganic pathogens, etc.), protecting the hosts and maintaining the ordinary growth and behavior, are of interest to insects (Lu et al., 2016; Beemelmanns et al., 2017; Van Arnam et al., 2017). Based on this symbiosis, several new immunosuppressive polyketides were obtained from a fungus attached to mantis, *Daldinia eschscholzii* IFB-TL01 (Zhang et al., 2008, 2011). In addition, insect symbiosis is also an important source of new microorganisms. For instance, 57 entomopathogenic fungi were analyzed, including one species which was firstly reported (Nishi and Sato, 2017). Many new species were also isolated from aquatic insects, among which new genera were found (White and Lichtwardt, 2004; White et al., 2018). Nonetheless, extensive, methodical, and biologically correlative researches about the insect microorganisms were restricted, especially when the complexity of insect symbiotic system was taken into consideration.

Termites, belonging to the class Insecta and the order Isoptera in the phylum Arthropoda, are a kind of eusocial and hemimetabolous insects (Mathew et al., 2012). Multitudinous and particular microbial floras reside in the termites, most of which can help the host to digest and utilize their food (Zhu et al., 2012; Li et al., 2017). *Odontotermes formosanus* as a termite species is mainly distributed in south areas of the line between Yellow River and Yangtze River in China. As far as we know, research concentrated on *O. formosanus* fungi derived from China have been rather rare (Chou et al., 2007; Shinzato et al., 2007). Underexploited *O. formosanus* symbionts can offer a pathway to finding unreported biological resources, which will solve the dilemma that needs to be dealt with regarding new drugs, especially antibiotics, which we are in sore need of due to increasing bacterial resistance to existing antibiotics (Procópio et al., 2012; Bi et al., 2013; Elahwany et al., 2013). Herein, the study was intended to explore the phylogenetic diversity, bacterial symbionts, antimicrobial potency, and compounds of the fungi associated with *O. formosanus*.

MATERIALS AND METHODS

Sample Collection and Microbial Isolations

A total of 50 termite samples were collected from the rotten wood in a grove in Zhejiang Normal University (29°00′17.37″N, 119°29′54.84″E, Jinhua city, China) during early spring in March 2016. The 50 collected samples were starved for 12 h and surface-sterilized in 75% ethanol for 2 min, followed by rinsing in sterilized water three times (30 s each). Sterile forceps were used to dissect samples to get the guts. The guts and degutted bodies of termites were fully homogenized separately in 0.5 ml sterile water. Then, the homogenates were diluted in a 10-fold series (i.e., 10^{-1}, 10^{-2}, 10^{-3}), and aliquots of 200 μl from each dilution were spread onto 10 isolation media (**Supplementary Table S1**). Pure colonies of fungi from the appropriate dilution were transferred into new MEA medium. Isolated strains were preserved on MEA slants at 4°C until use. Fungal species were grouped via molecular sequence data. The fungi were stored at our institute.

DNA Sequencing

DNA sequencing was performed according to the methods detailed previously (Hoffman and Arnold, 2010; Shao et al., 2015). Symbiotic fungi were transferred into ME medium (20 g malt extract, 20 g sucrose, 1 g peptone in 1 L of distilled H_2O) and cultured at 28 ± 0.5°C on rotary shakers for 5–6 days. The growing fungal mycelia were used to afford samples for genomic DNA extraction. Fungal total DNA was amplified using the Fast DNA Extraction Kit (BioTeke, Beijing, China) as claimed by the manufacturer's specification. The genomic DNA was stored at 4°C until use. The primers ITS1/ITS4 and 27F/1492R were used to amplify 5.8S rDNA and 16S rRNA based on the fungal genomic DNA. Qualified PCR samples were used for sequencing (Sangon Biotech Co., Ltd., Shanghai, China).

Fungi's Identification and Phylogenetic Analyses

As described previously (Shao et al., 2015), all resulting sequences' affiliation which were returned from Sangon Biotech Company were recognized by the available data in BLAST from the National Center for Biotechnology Information (NCBI) database. Sequence alignment and neighbor-joining phylogenetic analysis were carried out using MEGA software version 5.1. Bootstrap analysis of tree construction on the strength of the sequences was accustomed to estimate the neighbor-joining information based on 1,000 replicates (Felsenstein, 1985). The 5.8S rDNA sequences that had been obtained were placed in NCBI with the accession numbers MG820065–MG820103. Besides, endosymbiotic bacterial 16S rRNA sequences were deposited in NCBI with the accession numbers MG825089–MG825096.

Fermentation

Every fungus was grown on MEA medium at 28 ± 0.5°C for 3–4 days. Then, pieces of fresh mycelium were inoculated into 1-L Erlenmeyer flasks each containing 150 ml of ME liquid medium, after 2–3 days of incubation at 28 ± 0.5°C in a shaker rotating at 180 rpm. A 20-ml suspension of the fungus was transferred as seed into 1-L Erlenmeyer flasks each containing 400 ml of ME liquid medium. The flask cultures were incubated at 28 ± 0.5°C for 1 week.

Isolation of Compounds From BYCDW4 and BYCDW8

A total of 26 L of fermentation broth of BYCDW4 was filtered and extracted with EtOAc (3 × 26 L) at room temperature. The solvent was then evaporated *in vacuo* to give a black-brown crude extract (13.5 g). The obtained extract was separated by column chromatography (CC) using silica gel (SiO_2: 200–300 mesh, 15 g) and eluting with a stepwise gradient of CH_2Cl_2/MeOH (100:0–100:16, *v*/*v*) to afford six primary fractions (A to F). Then the

white needle crystal (compound **1**, 5.84 g) were recrystallized by CH_2Cl_2/MeOH continuously up to no impurity.

The dark-yellow mixture of BYCDW8 (1.5 g) was obtained with the method as above. Compound **2** (14.5 mg) was isolated and purified from subfraction B-2, which was given from further chromatography over silica gel in fraction B (0.4 g, CH_2Cl_2/MeOH, 100:1).

Structural Elucidation of Metabolites

The structures of compounds **1** and **2** were primarily analyzed by mass and $^1H/^{13}C$-nuclear magnetic resonance (NMR) spectroscopies. The electrospray ionization mass spectrometry of the purified metabolites was recorded on a TripeTOF 4600 instrument (Bruker, Billerica, MA, United States). $^1H/^{13}C$ NMR spectra were measured with a Bruker AVANCE-600 (Bruker, Switzerland) spectrometer, and chemical shifts were reported as parts per million (δ) by referring to tetramethylsilane as internal standards. The structure of compound **1a** was further determined by single crystal X-ray.

Antimicrobial Activities

The antimicrobial activities of all the 39 fungal crude extracts and the secondary metabolites were evaluated using filter-paper method as described previously (Li et al., 2014). Three tested pathogens (*Escherichia* coli ATCC 8739, *Bacillus subtilis* ATCC 6633, *Staphylococcus aureus* ATCC 6538) were cultivated on NA medium (NaCl 3 g, peptone 10 g, beef extract 3 g, agar 18–20 g, distilled H_2O 1,000 ml) in 37℃, whereas the pathogenic *Candida albicans* (ATCC 10231) was inoculated on PDA medium in 28℃. Then 200 μl of the overnight fermentation broth of the pathogens was inoculated on the corresponding plate. Next, 5 μl of the tested objects including crude extracts, metabolites, and positive control drugs which were dissolved completely by acetone with the concentration of 6 mg/ml was pipetted onto a sterile filter disk with a diameter of 5 mm. Gentamicin sulfate and amphotericin B were used as the positive control of pathogenic bacteria and yeast, respectively. Then, all the processed filter papers were placed on the above pre-prepared medium. Each test was set up three repeats. Plates were cultivated at constant temperature incubator and the inhibition zone was measured at 24–36 h.

RESULTS

Phylogenetic Diversity of Cultivable Fungi From *O. formosanus*

In this study, a total of 39 symbiotic fungi were isolated from *O. formosanus* (**Table 1** and **Figure 1**). The ITS1-5.8S-ITS2 region of all strains were sequenced and compared with available GenBank reference sequences. Sequences analysis showed that all fungi were attached to the phyla Ascomycota and Basidiomycota, 35 strains of which were grouped into three classes [Sordariomycetes (23.1%), Dothideomycetes (53.8%), and Eurotiomycetes (15.4%)] within Ascomycota. The other three strains (8%) were distributed in the Agaricomycetes within the phylum Basidiomycota (**Figure 1**).

The fungi of Dothideomycetes were dominant species in phylogenetic diversity of cultivable fungi from *O. formosanus*. The largest number (21) of isolates was distributed in three orders, including the Capnodiales, Venturiales, and Pleosporales. Among of them, two strains belonging to Capnodiales showed highly similar to *Cladosporium cladosporioides* with identity of 99%. The strain BYCDW30 showed only 92% similarity to *O. constricta*, which indicated a potential new species. The most frequent order identified was the Pleosporales, which included six genera based on phylogenetic tree analysis (**Figure 1**).

The strains of Sordariomycetes (9) were mainly included in the three classes (Xylariales, Pleurotheciales, and Hypocreales). Four of them were grouped into the family Hyporcreaceae and were identified as *Fusarium verticillioides*, *Metacordyceps chlamydosporia*, *Nectria diminuta*, and *Trichoderma viride*, respectively (**Figure 1**). Two strains showed similar to *Phaeoisaria loranthacearum* with a low identity of 96%. Two other strains belonging to Xylariales were identified as *Pestalotiopsis hainanensis* and *P. microspora*, respectively.

Six isolates of the class Eurotiomycetes were mainly concentrated in the genus *Exophiala* grouped into the order Chaetothyriales. Four strains showed highly similar to *Exophiala jeanselmei* with an identity of more than 99%. Another two strains were similar to *E. bergeri* with sequence match of 94% and 99%, respectively. What was worth mentioning was that the BYCDW17 showed a sequence match of 94% with *E. bergeri*, which indicated that it might not have been deposited in the GenBank database or represent a potential new species (Landeweert et al., 2003).

The fungi of class Agaricomycetes belonging to the phylum Basidiomycota were mainly distributed in the orders Agaricales and Polyporales. The strain BYCDW26 of Agaricales was a *Termitomyces* fungus, which had the low similar sequence with an identity of 88.10%. Another two strains belonging to Polyporales were identified as *Irpex lacteus* and *Phellinus igniarius*, respectively.

Diversity of Bacterial Symbionts

A total of nine bacterial symbionts 16S rRNA was obtained from the fungi associated with *O. formosanus* in this study (**Supplementary Table S2**). These bacterial symbionts mainly pertained to the class Dothideomycetes and identified as Bacillales (*Bacillus*, *Paenibacillus*), Rhizobiales (*Methylobacterium*), and Enterobacterium (*Trabulsiella*). Furthermore, six bacteria were putatively divided into genus *Bacillus*.

Antimicrobial Activities of the Crude Extracts of Fungi

The antimicrobial results are shown in **Table 2**. Of the all isolates, 25 extracts (64%) exhibited antibacterial activity against at least one of the tested bacterial strains. Especially, BYCDW8, BYCDW4 (**Supplementary Figure S1**), BYCDW13, and BYCDW19 exhibited remarkable inhibitory activities against *S. aureus* (ATCC 6538) with the inhibition zone diameter (IZD) of more than 20 mm. These four fungi were all attached to

TABLE 1 | Phylogenetic analysis of cultivable fungi associated with *O. formosanus*.

Isolate code	Closest match	Accession no.	Proposed identity	Coverage/max ident	GenBank no.
BYCDW15	*Ascomycota* sp.	HQ607923	*Ascomycota* sp.	97/99	MG820065
BYCDW19	*Ascomycota* sp.	HQ607923	*Ascomycota* sp.	99/99	MG820066
*BYCDW1	*Ascomycota* sp.	HQ607923	*Ascomycota* sp.	99/97	MG820067
BYSTW10	*Ascomycota* sp.	KU535795	*Ascomycota* sp.	97/98	MG820068
BYCDW7	*Cladosporium cladosporioides*	KX258800	*Cladosporium cladosporioides*	100/99	MG820069
BYSTW6	*Cladosporium cladosporioides*	MF319902	*Cladosporium cladosporioides*	99/99	MG820070
BYCDW12	*Dothideomycetes* sp.	KM519287	*Dothideomycetes* sp.	98/99	MG820073
BYCDW3	*Exophiala bergeri*	JX473281	*Exophiala bergeri*	94/99	MG820091
*BYCDW17	*Exophiala bergeri*	JX473281	*Exophiala bergeri*	95/94	MG820075
BYSTW2	*Exophiala jeanselmei*	KY292527	*Exophiala jeanselmei*	98/99	MG820076
BYCDW10	*Exophiala jeanselmei*	KY292527	*Exophiala jeanselmei*	98/99	MG820077
BYSTW7	*Exophiala jeanselmei*	KY292527	*Exophiala jeanselmei*	98/99	MG820078
BYCDW6	*Exophiala jeanselmei*	KY292527	*Exophiala jeanselmei*	96/99	MG820079
BYCDW13	*Paraconiothyrium brasiliense*	FJ378076	*Paraconiothyrium brasiliense*	97/99	MG820080
BYCDW29	*Paraconiothyrium brasiliense*	FJ378076	*Paraconiothyrium brasiliense*	98/99	MG820081
BYSTW11	*Fusarium verticillioides*	KT587649	*Fusarium verticillioides*	99/99	MG820082
BYSTW1	*Irpex lacteus*	KC414252	*Irpex lacteus*	98/99	MG820083
*BYSTW9	*Leptosphaeria* sp.	KP747704	*Leptosphaeria* sp.	99/96	MG820084
*BYCDW9	*Leptosphaeria* sp.	KP747704	*Leptosphaeria* sp.	98/96	MG820085
BYCDW28	*Metacordyceps chlamydosporia*	KP216980	*Metacordyceps chlamydosporia*	96/99	MG820086
BYCDW5	*Microdiplodia* sp.	EU273518	*Microdiplodia* sp.	98/99	MG820071
BYCDW8	*Microdiplodia* sp.	EU273518	*Microdiplodia* sp.	98/99	MG820072
BYCDW27	*Nectria diminuta*	JX076962	*Nectria diminuta*	88/99	MG820087
*BYCDW30	*Ochroconis constricta*	KM056323	*Ochroconis constricta*	97/92	MG820088
*BYSTW5	*Pleosporales* sp.	HQ914849	*Pleosporales* sp.	97/99	MG820089
*BYCDW4	*Pleosporales* sp.	KP269012	*Pleosporales* sp.	99/99	MG820092
*BYSTW3	*Pleosporales* sp.	HQ914849	*Pleosporales* sp.	98/93	MG820090
*BYCDW20	*Pyrenochaeta* sp.	KJ207418	*Pyrenochaeta* sp.	97/99	MG820093
BYSTW8	*Pyrenochaeta* sp.	EU750693	*Pyrenochaeta* sp.	97/99	MG820094
BYCDW16	*Pleosporales* sp.	KY910236	*Pleosporales* sp.	97/100	MG820095
*BYCDW23	*Pleosporales* sp.	HQ914849	*Pleosporales* sp.	80/94	MG820091
BYCDW18	*Pestalotiopsis hainanensis*	GQ869902	*Pestalotiopsis hainanensis*	99/99	MG820096
*BYCDW24	*Phaeoisaria loranthacearum*	KR611888	*Phaeoisaria loranthacearum*	99/96	MG820097
*BYCDW25	*Phaeoisaria loranthacearum*	KR611888	*Phaeoisaria loranthacearum*	97/97	MG820098
BYCDW11	*Pestalotiopsis microspora*	KX755256	*Pestalotiopsis microspora*	97/97	MG820099
BYCDW22	*Phellinus igniarius*	KY703431	*Phellinus igniarius*	98/99	MG820100
BYCDW21	*Trichoderma viride*	KP689168	*Trichoderma viride*	98/100	MG820102
*BYCDW26	*Termitomyces* sp.	AB968241	*Termitomyces* sp.	98/95	MG820101
*BYCDW14	Uncultured fungus	FN397433	*Ascomycota* sp.	98/98	MG820103

**Potential new strain.*

Pleosporales in the class Dothideomycetes. Furthermore, the strain BYCDW4 possessed notable inhibitory effect against *E. coli* (ATCC 8739) with the IZD of 21.07 mm, which was stronger than the positive gentamicin sulfate with the IZD of 17.67 mm. However, other strains did not express remarkable activity against *E. coli*. The crude extracts of BYCDW3, BYCDW4, and BYCDW25 exhibited great inhibition effect on *C. albicans* (ATCC 10231), which were equivalent to that of amphotericin with the IZD of 19.17 mm. And among them, the crude extract of BYCDW25 was the most prominent. Further analysis showed that the inhibition activities of the fungal extracts against gram-positive bacteria was much better than the gram-negative bacteria. In addition, the potential new isolates BYCDW24 and BYCDW25 (in the order Pleurotheciales) presented moderate antimicrobial activities against several pathogens.

Identification of the Secondary Metabolites Isolated From BYCDW4 and BYCDW8

Secondary metabolites were identified by spectroscopic analyses, including HR–ESI-MS, NMR, and comparisons with the data described in the previous literatures. The constituents were identified as compound **1** [5-hydroxyramulosin **(1a)**:

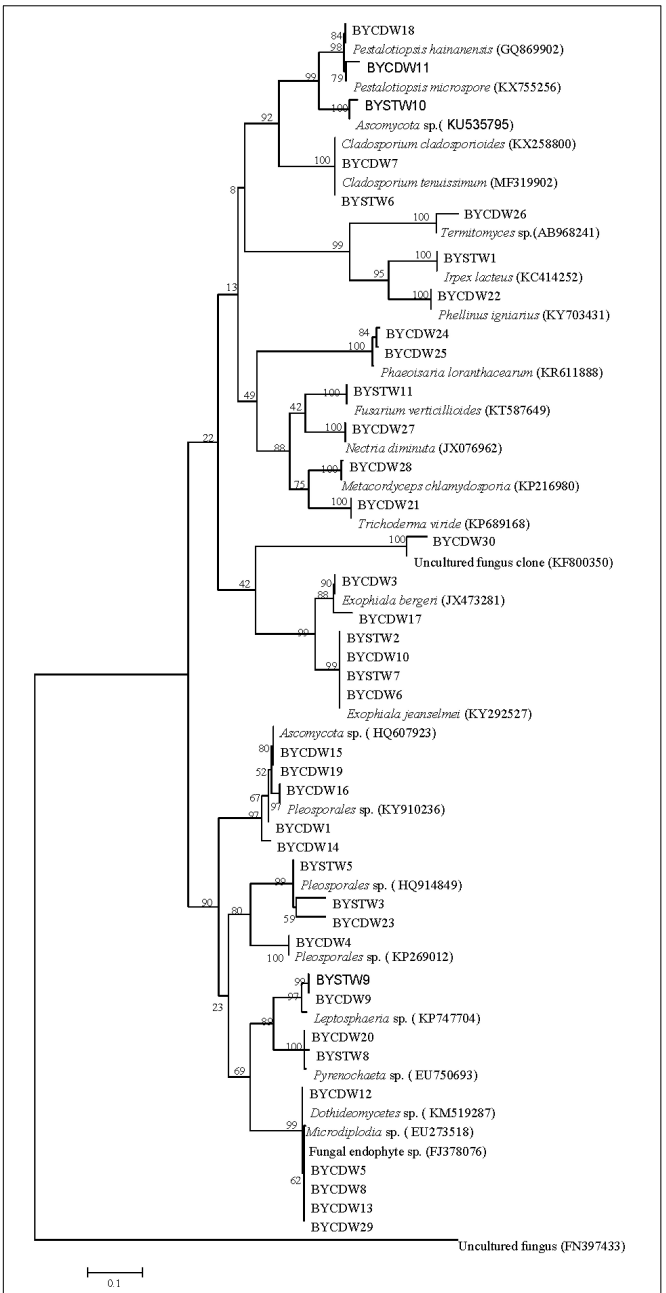

FIGURE 1 | Neighbor-joining phylogenetic tree of ITS rDNA sequences of *O. formosanus* fungal isolates. Bootstrap values were calculated using 1,000 replications.

TABLE 2 | Antimicrobial activities of 39 fungal crude extracts against pathogenic bacteria and yeast (mm).

Strains	*E. coli*	*C. albicans*	*B. subtilis*	*S. aureus*
BYCDW11	NI	NI	NI	7.83 ± 0.29
BYCDW3	8.17 ± 1.53	15.83 ± 1.15	11.50 ± 1.00	14.33 ± 2.57
BYCDW6	NI	NI	12.47 ± 0.38	14.90 ± 0.26
BYCDW23	14.00 ± 1.50	12.30 ± 2.25	12.13 ± 1.18	13.20 ± 1.25
BYCDW24	12.83 ± 1.26	NI	15.28 ± 6.26	NI
BYCDW5	11.67 ± 0.58	NI	14.75 ± 0.37	11.33 ± 1.53
BYCDW8	6.53 ± 0.25	NI	14.00 ± 1.80	22.33 ± 3.21
BYCDW4	21.07 ± 0.26	14.80 ± 0.84	18.45 ± 1.04	21.38 ± 0.12
BYCDW1	NI	NI	NI	8.03 ± 0.40
BYCDW29	11.23 ± 1.25	NI	NI	7.33 ± 0.21
BYCDW13	NI	NI	17.30 ± 0.83	20.4 ± 0.61
BYCDW25	NI	17.58 ± 0.60	11.55 ± 0.05	14.85 ± 0.26
BYCDW14	NI	NI	NI	NI
BYCDW20	NI	NI	NI	NI
BYCDW18	NI	NI	NI	NI
BYCDW19	NI	NI	NI	20.27 ± 0.64
BYCDW10	10.97 ± 0.15	NI	10.87 ± 0.15	NI
BYCDW26	NI	NI	NI	NI
BYCDW16	NI	NI	NI	NI
BYCDW30	NI	NI	NI	7.03 ± 0.12
BYCDW21	NI	NI	NI	6.97 ± 0.06
BYCDW28	NI	NI	NI	NI
BYCDW7	NI	NI	NI	NI
BYCDW9	NI	NI	NI	7.73 ± 0.25
BYCDW22	7.73 ± 0.06	NI	NI	NI
BYCDW15	NI	NI	NI	NI
BYCDW17	NI	NI	NI	NI
BYCDW12	NI	NI	NI	7.47 ± 0.46
BYCDW27	NI	10.02 ± 0.14	7.11 ± 0.14	12.42 ± 0.50
BYSTW11	12.67 ± 1.76	12.33 ± 0.76	12.33 ± 0.76	12.83 ± 0.76
BYSTW6	7.13 ± 0.85	NI	NI	6.40 ± 0.26
BYSTW1	NI	NI	10.68 ± 0.51	14.12 ± 0.83
BYSTW9	NI	NI	6.95 ± 0.10	7.06 ± 0.10
BYSTW7	NI	NI	6.67 ± 0.19	6.65 ± 0.10
BYSTW8	NI	NI	NI	NI
BYSTW2	NI	NI	NI	NI
BYSTW10	NI	NI	NI	NI
BYSTW3	8.40 ± 1.70	NI	NI	9.20 ± 1.84
BYSTW5	NI	NI	NI	10.53 ± 0.80
PC[a]	17.67 ± 0.29	19.17 ± 0.76	19.17 ± 0.29	21.33 ± 0.58

[a]*PC as the positive control, gentamicin sulfate and amphotericin as the positive control of pathogenic bacteria and yeast, respectively; results are presented as the mean ± standard; "NI" means not inhibited; the concentration for the test is 30 μg/filter paper.*

biatriosporin M **(1b)** = 2:1] from BYCDW4 and 1-(2,5-dihydroxyphenyl)-3-hydroxybutan-1-one (**2**) (**Figure 2**) from BYCDW8 based on the following data.

Compound **1** was obtained as a white needle crystal, which is a mixture (5-hydroxyramulosin (Osterhage et al., 2002) and biatriosporin M (Zhou et al., 2016)) with the proportion of 2:1 from the data of ^{1}H NMR. 5-Hydroxyramulosin (**1a**): HR–ESI-MS: $[M + H]^+$ *m/z* 199.0964 (calcd for 199.0970), $[M + Na]^+$ *m/z* 221.0785 (calcd for 221.0790); ^{1}H NMR ($CDCl_3$) δ: 13.30 (s, 1H), 4.48 (m, 1H), 4.05 (m, 1H), 2.68 (m, 1H), 2.59 (m, 1H), 2.38 (m, 1H), 2.05 (m, 1H), 1.72 (m, 1H), 1.96 (m, 1H), 1.84 (m, 1H), 1.42 (d, 6.3, 3H); ^{13}C NMR ($CDCl_3$) δ: 174.3, 172.4, 92.2, 76.2, 66.0, 37.4, 32.7, 27.9, 24.3, 21.8. Biatriosporin M (**1b**): HR–ESI-MS: $[M + H]^+$ *m/z* 197.0807 (calcd for 197.0814), $[M + Na]^+$ *m/z* 219.0625 (calcd for 219.0633); ^{1}H NMR ($CDCl_3$) δ: 12.70 (s, 1H), 6.66 (dd, 9.9, 5.4, 1H), 6.25 (d, 9.9, 1H), 4.50 (m, 1H), 3.99 (m, 1H), 2.81 (m, 1H), 1.88 (m, 1H), 1.80 (m, 1H), 1.47 (d,

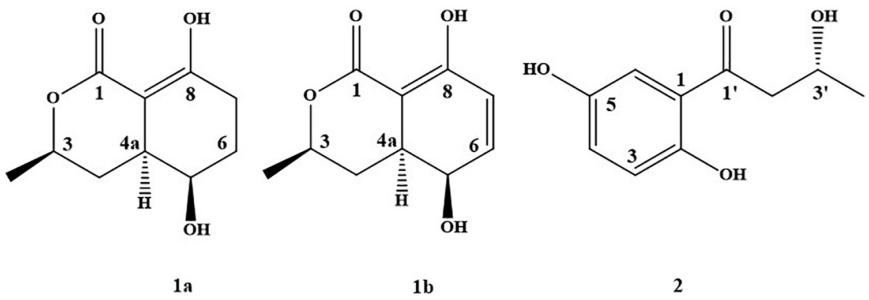

FIGURE 2 | The structure of compounds **1** and **2**.

6.3, 3H); ^{13}C NMR ($CDCl_3$) δ: 172.5, 166.0, 138.7, 125.8, 90.9, 75.9, 63.2, 36.0, 30.3, 21.6. Compound **1a** was further identified based on single-crystal X-ray diffraction data (**Supplementary Table S3** and **Supplementary Figure S2**). Compound **1b** was a dehydrogenated derivative of **1a**. Owing to their similar polarity, we were not able to isolate them by conventional separation methods. To the best of our knowledge, this was the first report that compound **1** was isolated from the fungus with high yield of 43.3% (compound/crude extract = 5.84 g:13.50 g). Worth mentioning was that compound **1a** (5-hydroxyramulosin) was reported with good antifungal activity against the fungal pathogen *Aspergillus niger* (IC_{50} = 2.10 μg/ml) and remarkable cytotoxicity to murine leukemia cells (IC_{50} = 2.10 μg/ml) (Santiago et al., 2012).

1-(2,5-Dihydroxyphenyl)-3-hydroxybutan-1-one (**2**) (Hong et al., 2018): light green-orange powder. HR-ESI-MS: $[M + H]^+$ *m/z* 197.0804 (calcd for 197.0814).^{1}H NMR (acetone-*d*6) δ: 11.77 (br s, 1H), 8.19 (br s, 1H), 7.34 (d, 2.94, 1H), 7.09 (dd, 2.94, 8.88, 1H), 6.80 (d, 8.88, 1H), 4.37 (m, 1H), 3.92 (br s, 1H), 3.19 (dd, 8.04, 17.52, 1H), 3.03 (dd, 4.62, 17.52, 1H), 1.26 (d, 6.20, 3H). ^{13}C NMR (acetone-*d*6) δ: 206.6, 156.6, 150.4, 125.6, 120.3, 119.3, 115.9, 64.8, 48.2, 23.7.

Antimicrobial Activities of Secondary Metabolites Isolated From BYCDW4 and BYCDW8

The antimicrobial activities of the compounds isolated from the strain BYCDW4 and BYCDW8 is shown in **Table 3**. Under the test concentration of 30 μg/filter paper, compound **1** [5-hydroxyramulosin **(1a)**:biatriosporin M **(1b)** = 2:1] exhibited some inhibitory activities against all the test pathogens. More specifically, the inhibitory effect on *E. coli* was the most significant with the IZD of 13.7 mm, which was slightly weaker than that of positive gentamicin sulfate with IZD of 17.7 mm. Compound **1** also showed good antimicrobial activities against *C. albicans*, *B. subtilis*, and *S. aureus* with the IZD of 14.33, 12.17, and 11.33 mm, respectively, which were comparable with those of the positive control. Compound **2** exhibited medium inhibitory activity against *B. subtilis* and *S. aureus*, with the IZD range of 8.32–9.13 mm, while it had no inhibition effect on *C. albicans*.

TABLE 3 | Antimicrobial activities of compounds isolated from BYCDW4 and BYCDW8 against the test pathogens (mm).

Compounds	*E. coli*	*C. albicans*	*B. subtilis*	*S. aureus*
1	13.67 ± 1.15	14.33 ± 2.57	12.17 ± 0.76	11.33 ± 0.58
2	6.53 ± 0.30	NI	8.32 ± 0. 07	9.13 ± 0.17
PC[a]	17.67 ± 0.29	19.17 ± 0.76	19.17 ± 0.29	21.33 ± 0.58

[a]*PC as the positive control, gentamicin sulfate and amphotericin as the positive control of pathogenic bacteria and yeast, respectively; results are presented as the mean ± standard; "NI" means not inhibited; the concentration for the test is 30 μg/filter paper.*

DISCUSSION

Microorganisms isolated from the bioprospecting underexploited environments with rich microbial biodiversity has been an important source of active natural products and new microorganism resources. A great variety of cultivable microbial flora was reported to exist in insects (Douglas, 2015; Shao et al., 2017; Blackwell and Vega, 2018). These important microbial resources were increasingly reported to be important sources of new natural products (Carr et al., 2012; Adnani et al., 2017; Xiao et al., 2017). In this study, the diversity of symbiotic fungi associated with *O. formosanus* and endophytic bacteria were studied. Thirty-nine fungi, including some potential new species, were isolated by culture-dependent method and molecular biological identification. To our knowledge, this is the first time that the phylogenetic diversity of cultivable and biological activity screening of secondary metabolites of fungi isolated from *O. formosanus* was studied, which will provide an important microbial resource for the discovery of new species and natural products.

Today, multidrug resistance of pathogens represents one of the major challenges to treat infectious diseases in community- and hospital-acquired infection diseases. There is also an urgent need for new antibiotics against gram-negative bacteria which have already been resistant to existing carbapenems and third-generation cephalosporins (Luther et al., 2019). In our study, the crude extract of potential new fungus BYCDW4 showed especially notable inhibitory effect against gram-negative *E. coli* (ATCC 8739) with the IZD of 21.07 mm, which was stronger than

that of the positive gentamicin sulfate. The inhibition effect of crude extract against *E. coli* was better than purified compound **1** with the IZD of 13.6 mm. This might be the result of the synergistic action of multiple compounds, or the more active compounds have not been separated from the crude extract. Further research on other metabolites of BYCDW4 will be expected to develop new antibiotics for the treatment of gram-negative bacteria.

The potential new isolates BYCDW24 and BYCDW25 (in the order Pleurotheciales) presented selectively antimicrobial activities against the pathogens. BYCDW25 had good inhibitory activity against *C. albicans* and nearly no inhibition to *E. coli*, while BYCDW24 showed certain inhibitory effect on *E. coli* but no effect on *C. albicans*. As we reported, the BYCDW24 and BYCDW25 shared the same evolutionary relationship except the BYCDW25 harboring one endophytic bacterium. Similar to endobacteria of insects, the endobacteria of fungi showed a range of behaviors from mutualism to antagonism (Bonfante and Desiro, 2017). It has been reported that endobacterium affects the activity of host fungus (Partida-Martinez and Hertweck, 2005; Lackner and Hertweck, 2011). Whether the endobacterium from BYCDW25 played an important role in the biological activity should be further explored.

It is reported that the majority of symbiotic bacteria was identified as *Bacillus* from the fungus-growing termite (Mathew et al., 2012; Zhu et al., 2012). In our experiments, 66.7% (6/9) symbiotic bacteria from the cultivable fungi were identified as *Bacillus*, which proved that these dominant bacterial symbionts can also inhabit fungi isolated from the gut of *O. formosanus*.

CONCLUSION

In this study, 39 fungi were isolated and identified from *O. formosanus*, which were belonging to two phyla and four classes. Furthermore, nine bacterial 16S rRNA sequences were obtained from total fungal genomic DNA. All bacterial symbionts belonged to four genera: *Bacillus*, *Methylobacterium*, *Paenibacillus*, and *Trabulsiella*. The antimicrobial bioassay showed that 25 fungal extracts (64%) exhibited antibacterial activities against at least one of the tested bacterial strains. Furthermore, the secondary metabolites **1** [5-hydroxyramulosin **(1a)**:biatriosporin M **(1b)** = 2:1] from the *Pleosporales* sp. BYCDW4 exhibited potent antimicrobial activities against all tested pathogens with the IZD of more than 11.3 mm, which were comparable with those of the positive control. 1-(2,5-Dihydroxyphenyl)-3-hydroxybutan-1-one (**2**) from the *Microdiplodia* sp. BYCDW8 showed medium antibacterial activities against *B. subtilis* and *S. aureus*. In conclusion, the report showed the diversity of insect symbionts had a potential to develop the resource of new species and antibiotics.

DATA AVAILABILITY STATEMENT

The raw data supporting the conclusions of this article will be made available by the authors, without undue reservation, to any qualified researcher.

AUTHOR CONTRIBUTIONS

YZ designed the research and supervised the study. XX, MS, CY, XY, FS, and ZM performed the experiments and analyzed the data. XX and MS wrote the manuscript. All authors revised the manuscript and approved the final version for submission.

FUNDING

This work was supported by the National Natural Science Foundation of China (NSFC) (31770007) and National Key R&D Program (2017YFD0200600).

SUPPLEMENTARY MATERIAL

The Supplementary Material for this article can be found online at: https://www.frontiersin.org/articles/10.3389/fmicb.2020.00300/full#supplementary-material

REFERENCES

Adnani, N., Rajski, S. R., and Bugni, T. S. (2017). Symbiosis-inspired approaches to antibiotic discovery. *Nat. Prod. Rep.* 34, 784–814. doi: 10.1039/c7np00009j

Barbieri, E., Potenza, L., Rossi, I., Sisti, D., Giomaro, G., Rossetti, S., et al. (2000). Phylogenetic characterization and in situ detection of a *Cytophaga–Flexibacter–Bacteroides* phylogroup bacterium in *Tuber borchii* Vittad, *Ectomycorrhizal mycelium*. *Appl. Environ. Microbiol.* 66, 5035–5042. doi: 10.1128/AEM.66.11.5035-5042.2000

Beemelmanns, C., Ramadhar, T. R., Kim, K. H., Klassen, J. L., Cao, S., Wyche, T. P., et al. (2017). Macrotermycins A-D, glycosylated macrolactams from a termite-associated *Amycolatopsis* sp. M39. *Org. Lett.* 19, 1000–1003. doi: 10.1021/acs.orglett.6b03831

Bi, S. F., Guo, Z. K., Jiang, N., Jiao, R. H., Ge, H. M., and Tan, R. X. (2013). New alkaloid from *Streptomyces koyangensis* residing in *Odontotermes formosanus*. *J. Asian Nat. Prod. Res.* 15, 422–425. doi: 10.1080/10286020.2013.76724

Blackwell, M., and Vega, F. E. (2018). Lives within lives: hidden fungal biodiversity and the importance of conservation. *Fungal Ecol.* 35, 127–134. doi: 10.1016/j.funeco.2018.05.011

Bonfante, P., and Desiro, A. (2017). Who lives in a fungus? The diversity, origins and functions of fungal endobacteria living in mucoromycota. *ISME J.* 11, 1727–1735. doi: 10.1038/ismej.2017.21

Carr, G., Poulsen, M., Klassen, J. L., Hou, Y., Wyche, T. P., Bugni, T. S., et al. (2012). Microtermolides A and B from termite-associated *Streptomyces* sp. and structural revision of vinylamycin. *Org. Lett.* 14, 2822–2825. doi: 10.1021/ol301043p

Chou, J. H., Sheu, S. Y., Lin, K. Y., Chen, W. M., Arun, A. B., and Young, C. C. (2007). *Comamonas odontotermitis* sp. nov., isolated from the gut of the termite *Odontotermes formosanus*. *Int. J. Syst. Evol. Microbiol.* 57, 887–891. doi: 10.1099/ijs.0.64632-0

Douglas, A. E. (2015). Multiorganismal insects: diversity and function of resident microorganisms. *Annu. Rev. Entomol.* 60, 17–34. doi: 10.1146/annurev-ento-010814-020822

Elahwany, A. M., Ghozlan, H. A., Elsharif, H. A., and Sabry, S. A. (2013). Phylogenetic diversity and antimicrobial activity of marine bacteria associated with the soft coral *Sarcophyton glaucum*. *J. Basic Microb.* 55, 2–10. doi: 10.1002/jobm.201300195

Felsenstein, J. (1985). Confidence limits on phylogenies: an approach using the bootstrap. *Evolution* 39, 783–791. doi: 10.1111/j.1558-5646.1985.tb00420.x

Lackner, G., and Hertweck, C. (2011). Impact of endofungal bacteria on infection biology, food safety, and drug development. *PLoS Pathog.* 7:e1002096. doi: 10.1371/journal.ppat.1002096

Grigorescu, A. S., Renoz, R., Sabri, A., Foray, V., Hance, T., and Thonart, P. (2018). Accessing the hidden microbial diversity of aphids: an illustration of how culture-dependent methods can be used to decipher the insect microbiota. *Microb. Ecol.* 75, 1035–1048. doi: 10.1007/s00248-017-1092-x

Hoffman, M. T., and Arnold, A. E. (2010). Diverse bacteria inhabit living hyphae of phylogenetically diverse fungal endophytes. *Appl. Environ. Microbiol.* 76:4063. doi: 10.1128/AEM.02928-09

Hong, Q. T., Cheol, K. D., Phan, V. K., Chau, V. M., Nguyen, X. N., Bui, H. T., et al. (2018). Macrolide and phenolic metabolites from the marine-derived fungus *Paraconiothyrium* sp. VK-13 with anti-inflammatory activity. *J. Antibiot.* 71, 826–830. doi: 10.1038/s41429-018-0073-8

Landeweert, R., Leeflang, P., Kuyper, T. W., Hoffland, E., Rosling, A., Wernars, K., et al. (2003). Molecular identification of ectomycorrhizal mycelium in soil horizons. *Appl. Environ. Microbiol.* 69, 327–333. doi: 10.1128/AEM.69.1.327-333.2003

Li, H., Yelle, D. J., Li, C., Yang, M., Ke, J., Zhang, R., et al. (2017). Lignocellulose pretreatment in a fungus-cultivating termite. *Proc. Natl. Acad. Sci. U.S.A.* 114, 4709–4714. doi: 10.1073/pnas.1618360114

Li, S., Shao, M. W., Lu, Y. H., Kong, L. C., Jiang, D. H., and Zhang, Y. L. (2014). Phytotoxic and antibacterial metabolites from *Fusarium proliferatum* ZS07 Isolated from the gut of long-horned grasshoppers. *J. Agric. Food Chem.* 62, 8997–9001. doi: 10.1021/jf502484n

Lu, Y. H., Jin, L. P., Kong, L. C., and Zhang, Y. L. (2016). Phytotoxic, antifungal and immunosuppressive metabolites from *Aspergillus terreus* QT122 isolated from the gut of dragonfly. *Curr. Microbiol.* 74, 1–6. doi: 10.1007/s00284-016-1157-y

Luther, A., Urfer, M., Zahn, M., Mueller, M., Wang, S. Y., Mondal, M., et al. (2019). Chimeric peptidomimetic antibiotics against Gram-negative bacteria. *Nature* 576, 452–458. doi: 10.1038/s41586-019-1665-6

Mathew, G. M., Ju, Y. M., Lai, C. Y., Mathew, D. C., and Huang, C. C. (2012). Microbial community analysis in the termite gut and fungus comb of *Odontotermes formosanus*: the implication of *Bacillus* as mutualists. *FEMS Microbiol. Ecol.* 79, 504–517. doi: 10.1111/j.1574-6941.2011.01232.x

Nishi, O., and Sato, H. (2017). Species diversity of the entomopathogenic fungi *Metarhizium anisopliae* and *M. flavoviride* species complexes isolated from insects in Japan. *Mycoscience* 58, 472–479. doi: 10.1016/j.myc.2017.06.008

Osterhage, C., König, G. M., Jones, P. G., and Wright, A. D. (2002). 5-Hydroxyramulosin, a new natural product produced by *Phoma tropica*, a marine-derived fungus isolated from the alga *Fucus spiralis*. *Planta Med.* 68, 1052–1054. doi: 10.1055/s-2002-35670

Park, J. M., You, Y. H., Back, C. G., Kim, H. H., Ghim, S. Y., and Park, J. H. (2018). Fungal load in *Bradysia agrestis*, a phytopathogen-transmitting insect vector. *Symbiosis* 74, 145–158. doi: 10.1007/s13199-017-0494-3

Partida-Martinez, L. P., and Hertweck, C. (2005). Pathogenic fungus harbours endosymbiotic bacteria for toxin production. *Nature* 437, 884–888. doi: 10.1038/nature03997

Procópio, R. E. D. L., Silva, I. R. D., Martins, M. K., Azevedo, J. L. D., and Araújo, J. M. D. (2012). Antibiotics produced by *Streptomyces*. *Braz. J. Infect. Dis.* 16, 466–471. doi: 10.1016/j.bjid.2012.08.014

Santiago, C., Fitchett, C., Munro, M. H., Jalil, J., and Santhanam, J. (2012). Cytotoxic and antifungal activities of 5-hydroxyramulosin, a compound produced by an endophytic fungus isolated from *Cinnamomum mollisimum*. *Evid Based Compl. Alt.* 2012:689310. doi: 10.1155/2012/689310

Shao, M. W., Lu, Y. H., Miao, S., Zhang, Y., Chen, T. T., and Zhang, Y. L. (2015). Diversity, bacterial symbionts and antibacterial potential of gut-associated fungi isolated from the *Pantala flavescens* Larvae in China. *PLoS One* 10:e0134542. doi: 10.1371/journal.pone.0134542

Shao, Y., Chen, B., Sun, C., Ishida, K., Hertweck, C., and Boland, W. (2017). Symbiont-derived antimicrobials contribute to the control of the *Lepidopteran* gut microbiota. *Cell Chem. Biol.* 24, 66–75. doi: 10.1016/j.chembiol.2016.11.015

Shinzato, N., Muramatsu, M., Matsui, T., and Watanabe, Y. (2007). Phylogenetic analysis of the gut bacterial microflora of the fungus-growing termite *Odontotermes formosanus*. *Biosci. Biotechnol. Biochem.* 71, 906–915. doi: 10.1271/bbb.60540

Trainer, M. A., and Charles, T. C. (2006). The role of PHB metabolism in the symbiosis of rhizobia with legumes. *Appl. Microbiol. Biotechol.* 71, 377–386. doi: 10.1007/s00253-006-0354-1

Van Arnam, E. B., Currie, C. R., and Clardy, J. (2017). Defense contracts: molecular protection in insect–microbe symbioses. *Chem. Soc. Rev.* 47, 1638–1651. doi: 10.1039/C7CS00340D

Webster, N. S., Cobb, R. E., and Negri, A. P. (2008). Temperature thresholds for bacterial symbiosis with a sponge. *ISME J.* 2, 830–842. doi: 10.1038/ismej.2008.42

White, M. M., and Lichtwardt, R. W. (2004). Fungal symbionts (*Harpellales*) in Norwegian aquatic insect larvae. *Mycologia* 96, 891–910. doi: 10.2307/3762122

White, M. M., Valle, L. G., Lichtwardt, R. W., Siri, A., Strongman, D. B., William, R. T., et al. (2018). New species and emendations of Orphella: taxonomic and phylogenetic reassessment of the genus to establish the orphellales, for stonefly gut fungi with a twist. *Mycologia* 110, 147–178. doi: 10.1080/00275514.2018.1448198

Xiao, Y. S., Zhang, B., Zhang, M., Guo, Z. K., Deng, X. Z., Shi, J., et al. (2017). Rifamorpholines A–E, potential antibiotics from locust-associated actinobacteria *Amycolatopsis* sp. Hca4. *Org. Biom. Chem.* 15, 3909–3916. doi: 10.1039/C7OB00614D

Zhang, Y. L., Ge, H. M., Zhao, W., Dong, H., Xu, Q., Li, S. H., et al. (2008). Unprecedented immunosuppressive polyketides from *Daldinia eschscholzii*, a mantis-associated fungus. *Angew Chem. Int. Ed.* 120, 5823–5826. doi: 10.1002/ange.200801284

Zhang, Y. L., Zhang, J., Jiang, N., Lu, Y. H., Wang, L., Xu, S. H., et al. (2011). Immunosuppressive polyketides from mantis-associated *Daldinia eschscholzii*. *J. Am. Chem. Soc.* 133, 5931–5940. doi: 10.1021/ja110932p

Zhou, Y. H., Zhang, M., Zhu, R. X., Zhang, J. Z., Xie, F., Li, X. B., et al. (2016). Heptaketides from an endolichenic fungus *Biatriospora* sp. and their antifungal activity. *J. Nat. Prod.* 79, 2149–2158. doi: 10.1021/acs.jnatprod.5b00998

Zhu, Y. H., Li, J., Liu, H. H., Yang, H., Xin, S., Zhao, F., et al. (2012). Phylogenetic analysis of the gut bacterial microflora of the fungus-growing termite *Macrotermes barneyi*. *Afr. J. Microbiol. Res.* 6, 2071–2078. doi: 10.5897/ajmr11.1345

Conflict of Interest: The authors declare that the research was conducted in the absence of any commercial or financial relationships that could be construed as a potential conflict of interest.

frontiers in Microbiology

ORIGINAL RESEARCH
published: 06 May 2020
doi: 10.3389/fmicb.2020.00664

Metabolomic Responses of Maize Shoots and Roots Elicited by Combinatorial Seed Treatments With Microbial and Non-microbial Biostimulants

Youssef Rouphael[1], Luigi Lucini[2], Begoña Miras-Moreno[3], Giuseppe Colla[4]*, Paolo Bonini[5] and Mariateresa Cardarelli[6]*

[1] Department of Agricultural Sciences, University of Naples Federico II, Portici, Italy, [2] Department for Sustainable Food Process, Research Centre for Nutrigenomics and Proteomics, Università Cattolica del Sacro Cuore, Piacenza, Italy, [3] Council for Agricultural Research and Economics-Research Centre for Genomics and Bioinformatics, Fiorenzuola d'Arda, Italy, [4] Department of Agriculture and Forest Sciences, University of Tuscia, Viterbo, Italy, [5] NGA Laboratory, Tarragona, Spain, [6] Consiglio per la Ricerca in Agricoltura el' Analisi dell'Economia Agraria, Centro di Ricerca Orticoltura e Florovivaismo, Pontecagnano Faiano, Italy

OPEN ACCESS

Edited by:
Santiago Gutierrez, Universidad de León, Spain

Reviewed by:
Katarzyna Turnau, Jagiellonian University, Poland
Michela Schiavon, University of Padova, Italy

***Correspondence:**
Luigi Lucini
luigi.lucini@unicatt.it
Giuseppe Colla
giucolla@unitus.it

Specialty section:
This article was submitted to Plant Microbe Interactions, a section of the journal Frontiers in Microbiology

Received: *03 February 2020*
Accepted: *23 March 2020*
Published: *06 May 2020*

Citation:
Rouphael Y, Lucini L, Miras-Moreno B, Colla G, Bonini P and Cardarelli M (2020) Metabolomic Responses of Maize Shoots and Roots Elicited by Combinatorial Seed Treatments With Microbial and Non-microbial Biostimulants. Front. Microbiol. 11:664. doi: 10.3389/fmicb.2020.00664

Microbial and non-microbial plant biostimulants have been successfully used to improve agriculture productivity in a more sustainable manner. Since the mode of action of biostimulants is still largely unknown, the present work aimed at elucidating the morpho-physiological and metabolomic changes occurring in maize (*Zea mays* L.) leaves and roots following seed treatment with (i) a consortium of two beneficial fungi [arbuscular mycorrhizal fungi (AMF) and *Trichoderma koningii* TK7] and rhizobacteria, (ii) a protein hydrolyzate-based biostimulant (PH) alone, or (iii) in combination with a consortium of *T. koningii* TK7 and rhizobacteria. The application of PH alone or in combination with *Trichoderma* elicited significant increases (+16.6%) in the shoot biomass compared to untreated maize plants, whereas inoculation with AMF + *Trichoderma* elicited significant increases in root dry biomass (+48.0%) compared to untreated plants. Distinctive metabolomic signatures were achieved from the different treatments, hence suggesting that different molecular processes were involved in the plants response to the biostimulants. The metabolic reprogramming triggered by the treatments including the protein hydrolyzate was hierarchically more pronounced than the application of microorganisms alone. Most of the differential metabolites could be ascribed to the secondary metabolism, with phenylpropanoids and terpenes being the most represented compounds. The application of PH triggered an accumulation of secondary metabolites, whereas the opposite trend of accumulation was seen in the case of microorganisms alone. The increase in biomass could be related to two processes, namely the modulation of the multilayer phytohormone interaction network and a possible increase in nitrogen use efficiency via the GS-GOGAT system.

Keywords: protein hydrolyzate, mycorrhiza, phytohormones, plant metabolomics, *Trichoderma*, *Zea mays* L.

INTRODUCTION

Nowadays, agriculture is facing new and concurrent challenges such as boosting crop productivity and coping with food insecurity. Considering that the global population will reach 10 billion by 2055 the environmental impact of agriculture has to be minimized and natural resources (i.e., soil quality and water) have to be preserved for future generations, both sustainability and low production costs are required to remain competitive in a globalized economy (FAO, 2009). Maize (*Zea mays* L.) has gained economic significance at a global level, contributing about 12.4% of the world's food demand (38% of cereals) and ranking first in production volume worldwide (1,135 million tons) (FAO, 2017). Enhancing resource use efficiency (e.g., water and nutrients) through novel, sustainable and eco-friendly strategies, is an urgent need to secure yield stability and food security while preserving soil quality and providing new business opportunities for farmers (Searchinger et al., 2018).

An eco-friendly, sustainable and innovative method that is able to tackle the upcoming challenges is the incorporation of biostimulant technology in the cropping system, especially biostimulants of plant origin (Chiaiese et al., 2018; Rouphael et al., 2018c). In a recent EU Regulation, "plant biostimulant" has been defined as an EU fertilizing product which is applied to crop plants or rhizospheres with the aim of modulating plant physiological functions and of improving crop productivity, efficiency of nutrient use, quality of crop products and abiotic stresses tolerance (EU, 2019). Plant biostimulants by this definition include several substances with bioactive properties: humic and fulvic acids, protein hydrolyzates, seaweed extracts, plant extracts and silicon, as well as plant growth promoting microorganisms: arbuscular mycorrhizal fungi (AMF), *Trichoderma*, and plant growth promoting rhizobacteria (PGPR) (Calvo et al., 2014; Battacharyya et al., 2015; Canellas et al., 2015; Colla and Rouphael, 2015; Colla et al., 2015a, 2017b; du Jardin, 2015; Rouphael and Colla, 2018, 2020).

Arbuscular mycorrhizal fungi and *Trichoderma* represent two major classes of beneficial microbes (López-Bucio et al., 2015; Rouphael et al., 2015). The biostimulant action of these endophytic fungi under both favorable and stressful soil or environmental conditions has been associated with several putative mechanisms including: (i) the production of key enzymes such as phosphatases and/or release of small peptides, volatiles, and active metabolites that have hormone-like activity, (ii) enhancing photosynthetic efficiency and water relations, (iii) the promotion of nitrate, phosphate and ammonia transporters, (iv) the accumulation of osmoprotectants and antioxidants, and (v) the modulation of plant root architecture through the increase of root length, density and branching, resulting in enhanced nutrient uptake (P, Fe, Mn, and Zn) (Contreras-Cornejo et al., 2009; Woo et al., 2014; López-Bucio et al., 2015; Rouphael et al., 2015; Fiorentino et al., 2018; Lucini et al., 2019; Saia et al., 2019, 2020).

Another prominent category of non-microbial plant biostimulants that has demonstrated beneficial effects on shoot and root stimulation, similar to those exerted by microbial-based biostimulants, is represented by protein hydrolyzates. In particular they contain a mixture of free amino acids and peptides obtained via the chemical or enzymatic partial hydrolysis of protein sources from either animal or vegetal origin (Calvo et al., 2014; Haplern et al., 2015). Direct and indirect modes of action underlying the biostimulant activity of plant- or animal-based protein hydrolyzates include: (i) the stimulation of C and N metabolism by triggering key enzymes, (ii) the induction of hormone-like activities, in particular those of auxins and gibberellins, (iii) the stimulation of secondary metabolism by increasing antioxidant capacity, (iv) the modulation of root growth which can consequently result in a '*nutrient acquisition response*' improving resource use efficiency (Schiavon et al., 2008; Ertani et al., 2009, 2013, 2017; Colla et al., 2015a,b, 2017a,b; Rouphael et al., 2017, 2018b; Sestili et al., 2018).

For field crop species such as maize, biostimulants (and in particular the microbial ones) are applied as a seed treatment or directly onto plant and soil. However, seed treatment has been proven to be an economical and efficient tool to introduce non-microbial and microbial biostimulants in the soil rhizosphere, compared to foliar spray or substrate/soil drench where a high quantity of the product is required (Tavares et al., 2013; Colla et al., 2015b).

Despite the significant advancements made in the last decade in terms of studying the effects of plant biostimulants on a broad spectrum of field and horticultural crops, there are two main bottlenecks that hamper scientists, private industries and farmers from extensively implementing plant biostimulants into agronomic practices. Firstly, an increase in knowledge about the molecular and physiological mechanisms underlying biostimulant action could substantially support and facilitate the diffusion of these products in the agricultural sector. Second, an increased awareness and knowledge about the combined application of microbial and/or non-microbial plant biostimulants may represent a valuable solution to render agriculture more resilient and sustainable.

From this perspective, the omics sciences, and in particular untargeted metabolomics, are considered to be a powerful tool to reveal the effects of biotic and abiotic factors on plant physiology (Tenenboim and Brotman, 2016). Metabolomics can help to shed light onto the biochemical processes involved in plant response to biostimulants (Bernardo et al., 2019; Wu et al., 2019). Therefore, the current research aims to overcome the above-reported bottlenecks by investigating the changes in shoot and root biomass and partitioning together with the metabolic reprogramming elicited on maize by either endophytic fungi (*Trichoderma koningii* TK7 and mycorrhiza: *Rhizoglomus irregulare* BEG72 and *Funneliformis mosseae* BEG 234), a legume-derived protein hydrolyzate, alone or as a combination of the both legume-derived protein hydrolyzate with *T. koningii* TK7. Finally, the insights from this work can improve the poor knowledge of the mode(s) of action and can address the development and optimization of plant biostimulants.

MATERIALS AND METHODS

Tested Crop, Greenhouse Growth Conditions, and Experimental Setup

The trial was conducted in the 2016 growing season in a polyethylene greenhouse located at the Experimental Farm 'Nello Lupori' of Tuscia University, central Italy (latitude 42°25′ N, longitude 12°08′ E, altitude 310 m). Inside the polyethylene greenhouse, ventilation was provided automatically when the air temperature exceeded 26°C, and light was provided only by natural solar radiation. During the experiment, daily mean values of solar radiation at crop level ranged from 16.1 to 22.3 MJ m^{-2}. The mean air temperature and relative humidity inside the greenhouse were 20°C and 60%, respectively. The trial was performed on maize (*Zea mays* L.) cultivar 'PR36B08' (Pioner, Gadesco-Pieve Delmona, Italy) belonging to FAO class 300.

Seeds of maize were surface sterilized with a solution containing 80% of ethanol. After sterilization (10 min), the seeds were washed two times with sterile distilled water. On May 4, maize seeds were sown in plastic pots (diameter of 18 cm) filled with 4.0 L of fluvial sand at a rate of five seeds per pot. Fluvial sand was previously washed with distilled water using 5 L of water for each liter of sand, and then sterilized in an autoclave twice to kill spores of bacteria and fungi. The experiment included the following four treatments:

(1) seed treatment with 3 g of a consortium of arbuscular mycorrhizal fungi (AMF), *T. koningii* TK7 and rhizosphere bacteria ('Covenant,' produced by Atens, Agrotecnologías Naturales, S. L., Tarragona, Spain, containing 230 spores g^{-1} of *Rhizoglomus irregulare* BEG72, 230 spores g^{-1} of *Funneliformis mosseae* BEG 234, 3×10^8 Colony-forming unit [CFU] g^{-1} of *T. koningii* TK7, 4×10^7 CFU g^{-1} of rhizosphere bacteria such as *Bacillus megaterium* MHBM77) per 1 kg of seed;
(2) seed treatment with a solution containing 0.3 g of a consortium of *T. koningii* TK7 and rhizosphere bacteria such as *Bacillus megaterium* MHBM77 ('Covenant Trichoderma,' produced by Atens, Agrotecnologías Naturales, S. L., Tarragona, Spain, containing 2×10^9 CFU g^{-1} of *T. koningii* TK7, 1×10^7 CFU g^{-1} of rhizosphere bacteria such as *Bacillus megaterium* MHBM77) plus 0.45 ml of a protein hydrolyzate-based biostimulant (PH) ('Coveron Stim' produced by Italpollina s.p.a, Rivoli Veronese, Italy, containing 70 g kg^{-1} of organic N) per 1 kg of seed;
(3) seed treatment with 0.45 ml of a protein hydrolyzate-based biostimulant ('Coveron Stim') per 1 kg of seed;
(4) untreated control.

The protein hydrolyzate included in the 'Covenant' and 'Coveron Stim' products was a legume-derived protein hydrolyzate obtained through enzymatic hydrolysis of proteins derived from legume seeds. It contains 50 g kg^{-1} of N as free amino acids, and soluble peptides. The aminogram of the product in g kg^{-1} was: Ala (12), Arg (18), Asp (34), Cys (3), Glu (54), Gly (12), His (8), Ile (13), Leu (22), Lys (18), Met (4), Phe (15), Pro (15), Thr (11), Trp (3), Tyr (11), Val (14). All three products contain a green natural colorant for verifying the uniformity of product distribution on seed surface.

Seed treatments were performed with a seed-treatment machine able to automatically spray the seed surface with a water suspension/solution containing the products at a rate of 10 ml per kg of seed. Treatments were arranged in a randomized block design with three replicates. Each experimental unit consisted of six pots. Besides the required pots (18 pots per treatment), 10 extra pots per treatment were also prepared. One week after the initial emergence of seedlings, pots having less than four plants were discarded.

Plants were fertirrigated starting 1 week after sowing. The basic nutrient solution used was a modified Hoagland and Arnon formulation having the following macro and micro mineral composition: 7.0 mM N–NO_3^-, 1.5 mM S, 0.2 mM P, 2.7 mM K, 5.5 mM Ca, 1.5 mM Mg, 20.0 μM Fe, 9.0 μM Mn, 0.3 μM Cu, 1.6 μM Zn, 20.0 μM B, and 0.3 μM Mo. The nutrient solution was prepared using de-mineralized water. The electrical conductivity and pH of the nutrient solution were 1.8 dS m^{-1} and 6.0, respectively.

Biomass Determination, Partitioning, and SPAD Index Measurement

At 16 days after sowing (May 19), all maize plants per experimental plot (i.e., the replicates) were harvested and the shoots (sum of leaves and stems) were separated from the roots. Shoots and roots were dried in a forced-air oven at 70°C for 72 h until constant weight, then the shoots and roots dry matter content were recorded. The root-to-shoot ratio was also calculated.

Plant Analysis Development (SPAD) index (i.e., a non-destructive measurement of chlorophyll content) was measured on undamaged maize leaves by means of a portable SPAD-502 chlorophyll meter (Konica-Minolta, Tokyo, Japan). Ten measurements were conducted on randomly picked maize leaves per experimental plot, then averaged to a single SPAD value for each replicate as described by Kumar et al. (2015).

Sampling and Untargeted Metabolomic Analysis

The first expanded maize leaf and terminal roots samples were collected from two plants per experimental plot (i.e., replicate) from each of the four tested treatments. Samples of maize leaf and roots (six samples of leaves and sx samples of roots per each treatment) were ground with liquid nitrogen using pestle and mortar, and then extracted as previously reported (Rouphael et al., 2018b). Briefly, an aliquot (1.0 g) was extracted in 10 mL of 0.1% HCOOH in 80% aqueous methanol using an Ultra-Turrax (Ika T-25, Staufen, Germany). The extracts were centrifuged (12000 × *g*) and the untargeted metabolomic screening was carried out using an UHPLC liquid chromatography system and a quadrupole-time-of-flight mass spectrometer equipped with an electrospray ionization source (UHPLC/Q-TOF), according to a previously reported set up

(Pretali et al., 2016). In more detail, a 1290 LC system was coupled to a G6550 quadrupole-time-of-flight mass spectrometer (Agilent Technologies Santa Clara, CA, United States). Chromatographic separation was achieved in reverse phase mode, using a C18 column (100 mm × 2.1 mm, 1.8 μm) and a binary gradient consisting of water and methanol (from 5 to 90% organic in 34 min) with a flow rate of 200 μL min^{-1}. The mass spectrometer operated in the positive polarity and in SCAN mode (range of 100–1200 m/z in extended dynamic range settings).

Compound annotation was achieved by combining both the monoisotopic accurate mass and isotopic pattern (i.e., isotope spacing and ratio), adopting a mass accuracy tolerance of <5 ppm and using the software Profinder B.07 (Agilent technologies) and a database exported from PlantCyc 9.6 (Plant Metabolic Network[1]). The annotation strategy corresponded to Level 2 (putatively annotated compounds) of COSMOS Metabolomics Standards Initiative[2]. A filter-by-frequency algorithm was then applied, retaining only those compounds present in 75% of replicates within at least one treatment.

Statistics and Chemometrics

The statistical analysis was carried out using IBM SPSS Statistics 20 (Chicago, IL, United States). The plant biomass and partitioning, as well as SPAD index, were subjected to one-way analysis of variance (ANOVA). Mean values were separated according to a Duncan test with $P = 0.05$.

Interpretation of the metabolomic analysis was initially carried out using Mass Profiler Professional 12.6 (Agilent Technologies) for log2 transformation of compound abundance, normalization at the 75th percentile, and baselining against the median of each compound in the dataset. Thereafter, hierarchical cluster analysis (Euclidean distance, Ward's linkage) was performed to investigate in an unsupervised manner the relatedness across treatments. The dataset was then imported into SIMCA 13 software (Umetrics, Malmö Municipality, Sweden) and elaborated through supervised orthogonal projection to latent structures discriminant analysis (OPLS-DA). The OPLS-DA model was cross validated (CV-ANOVA), inspected for outliers (Hotelling's T2), and thereafter model parameters (degree of correlation and prediction ability, R2Y and Q2Y respectively) were recorded. Overfitting was excluded through a permutation test (n = 100) and discriminant compounds selected by variables importance in projection (VIP) in the OPLS predictive model. The VIP score was calculated as a weighted sum of the squared correlations between the OPLS-DA components and the original variables. Compounds possessing a score > 1.32 were selected as discriminants. To gain a more in-depth knowledge about the individual effect of each biostimulant on the plant physiology Volcano analysis was also performed ($P < 0.01$, Bonferroni multiple testing correction; fold-change FC ≥ 2) and the differential compounds were exported to the PlantCyc pathway Tools software (Karp et al., 2010) to highlight the metabolic pathways and processes involved in plant response to treatments.

[1]http://www.plantcyc.org

[2]http://cosmos-fp7.eu/msi.html

RESULTS

Biostimulant Action of Microbial and Non-microbial Biostimulants on Growth Responses and SPAD Index

The results concerning plant biomass and partitioning as well as SPAD index in relation to microbial (AMF + *Trichoderma*) and non-microbial [protein hydrolyzate (PH) biostimulants alone or in combination with *Trichoderma* are presented in **Table 1**. Concerning the effects of biostimulant application on growth responses, our findings showed that the application of PH alone or in combination with *Trichoderma* elicited significant increases (+16.6%) in the shoots compared to untreated maize plants, whereas inoculation with AMF + *Trichoderma*, exhibited intermediate values. Regarding the root dry biomass, the inoculation with AMF + *Trichoderma* elicited significant increases (+48.0%) compared to untreated plants, whereas both PH and PH + *Trichoderma* combinations exhibited intermediate values (average +25% compared to the control treatment) (**Table 1**). The co-inoculation of maize plants with AMF and *T. koningii* TK7 enhanced the root-to-shoot ratio and SPAD index compared to the other three treatments (i.e., untreated or treated with PH and PH + *Trichoderma*; **Table 1**). Finally, the highest values of shoot and root dry matter content were recorded in PH and in both PH or PH + *Trichoderma* treatments, respectively (**Table 1**).

Implications of Microbial and Non-microbial Seed Tanning on the Metabolomic Profiling of Maize Leaves and Roots

In order to understand the effect of the different microbial and non-microbial biostimulants on maize at a molecular level, an untargeted metabolomic approach based on UHPLC-QTOF mass spectrometry was carried out. Overall, the metabolomic analysis lead us to putatively annotate more than 3,600 compounds in leaves and/or roots (**Supplementary Table 1**) that allowed us to discriminate the four treatments based on their metabolomic signatures.

In particular, an unsupervised hierarchical cluster analysis was first performed to identify similarities/dissimilarities among the treatments based on their metabolic profiles. The fold-change based heat map grouped the treatments in two main clusters (**Figure 1**). The combined treatment with microorganisms showed a less pronounced effect on both roots and leaves, as compared to the PH application, and considering that the AMF + *Trichoderma* treatment clustered together with the untreated control. However, a second well-separated cluster including the PH treatment and the combined PH + *Trichoderma* treatment was observed (**Figure 1**).

After the unsupervised analysis, a supervised multivariate analysis of the metabolomics-based data was produced to

TABLE 1 | Effect of seed treatments with a consortium of arbuscular mycorrhizal fungi (AMF), *Trichoderma koningii* TK7, and rhizosphere bacteria or with a consortium of *Trichoderma koningii* TK7 and rhizosphere bacteria (Tricho) plus a protein hydrolyzate-based biostimulant (PH), or with a protein hydrolyzate-based biostimulant (PH), on dry weight and dry matter of shoots and roots, root-to-shoot ratio and SPAD index in maize plants.

Treatment	Shoot		Roots		Root to shoot	SPAD index
	Dry weight (g plant^{-1})	Dry matter (%)	Dry weight (g plant^{-1})	Dry matter (%)		
Control	131.5b	10.9ab	29.8c	7.7b	0.21b	27.7b
AMF + Tricho	141.0ab	9.7b	44.1a	8.4ab	0.33a	30.8a
PH	155.0a	11.7a	36.6b	8.9a	0.24b	28.0b
PH + Tricho	151.8a	10.9ab	37.9b	8.8a	0.25b	28.6ab
Significance	*	*	***	*	**	*

, **, *, significant at P ≤ 0.05, 0.01, and 0.001, respectively. Different letters within each column indicate significant differences according to DuncanŠs multiple-range test (P = 0.05).*

better highlight the differences between treatments and identify discriminant compounds. Indeed, OPLS discriminant analysis was more effective in separating all the biostimulant-treated maize plants from the untreated control (**Figure 2**). The OPLS model indicators emphasized the predictivity of the model with R2Y (the goodness-of-fit) = 0.98 and 0.99 and Q2Y (goodness-of-prediction) = 0.52 and 0.64 for leaves and roots, respectively. The first latent vector could discriminate between the PH-containing treatment and the other groups, while the second vector accounted for the differences between the combined treatment with microbial biostimulants (AMF + *Trichoderma*) and the control treatment. Although the application of microorganisms induced a distinctive metabolic reprogramming, the PH-containing treatment showed the highest effect since the replicates were found to be completely separated from the other treatments in both leaves and roots. However, no separation was achieved between the PH treatment alone and the combined PH + *Trichoderma* treatment, thus strengthening the hypothesis of a hierarchically more pronounced effect of the PH-based products.

Overall, 216 compounds were recorded as discriminant in leaves by VIP analysis (**Supplementary Table 2**). Isoprenoids and phenylpropanoids were the most represented class of metabolites. Among isoprenoids, our results highlighted diterpenoids related to hormones biosynthetic such as kauralexin andent-kaurenal, as well as gibberellins, sesquiterpenes, and carotenoids. However, 133 compounds were pointed out as markers by VIP analysis in roots (**Supplementary Table 3**). Among these compounds, we underlined the presence of hormones including gibberellins, brassinosteroids and abscisic acid, together with jasmonate-related compounds.

The complete list of significant metabolites derived from Volcano analysis was consistent with the outcome of VIP analysis and is provided as **supplementary material** (**Supplementary Tables 4**, **5**). Interestingly, secondary metabolism was affected by all treatments in both leaves (**Figure 3**) and roots (**Figure 4**). Irrespective from the plant organ considered, the treatment with microorganisms in combination (AMF + *Trichoderma*) showed an effect on secondary metabolism with a general down-regulation, while PH alone or in combination with *Trichoderma* showed an up-regulation of secondary metabolism in leaves (**Figure 3**). It can be seen that secondary metabolism related compounds were the most involved, since over 150 compounds in leaves were affected by the treatments (**Table 2**). This PH-mediated response was characterized by the marked increase of phenylpropanoids (up-accumulated following PH application), at the expense of other phytoalexins, in contrast to the microorganism-treated plants. In fact L-phenylalanine, the upstream key compound in the phenylpropanoid biosynthetic pathway, as well as other amino acids and intermediate compounds, were up-regulated in leaves in the presence of PH. The omics viewer built-into PlantCyc allowed the visualization of some other groups of small molecules altered by the treatments including cofactors and prosthetic groups (tetrapyrroles and porphyrins), electron carriers (quinols and quinones), and vitamins. Similar metabolic trends could be observed in both the PH and PH + *Trichoderma* treatments. Although apparently displaying a similar response, the AMF + *Trichoderma* treatment showed a general down-accumulation of secondary metabolism, with several compounds (not affected by PH) being strongly decreased. In addition, the profile of phytohormones was also altered by the treatments. Gibberellin-related compounds were more abundant in the presence of PH alone or in combination with *Trichoderma*, whereas an opposite trend could be observed for abscisic acid. Although less evident, an accumulation of both brassinosteroids and cytokinins could be observed following PH application.

On the other hand, the treatments seemed to have a more pronounced effect on roots, since more than 500 compounds were found as discriminants by the Volcano analysis (as compared to about 330 compounds significantly affected in leaves) (**Supplementary Tables 4**, **5**). The effect of PH and PH + *Trichoderma* on the root metabolome was very similar (**Figure 4**) even though plants treated with AMF + *Trichoderma* showed a distinct signature. Consistently with leaves, the biosynthesis plot of PlantCyc showed that secondary metabolism was the most affected by the treatments. Indeed, over 200 metabolites involved in secondary pathways were identified overall (**Table 3**). The AMF + *Trichoderma* combined treatment caused a general decrease in secondary metabolites while the roots in the presence of PH, alone or in combination, showed an increase in this class of metabolites. Phenylpropanoids, N-containing compounds and terpenoids were the most down-regulated groups in the AMF + *Trichoderma* treatment. In

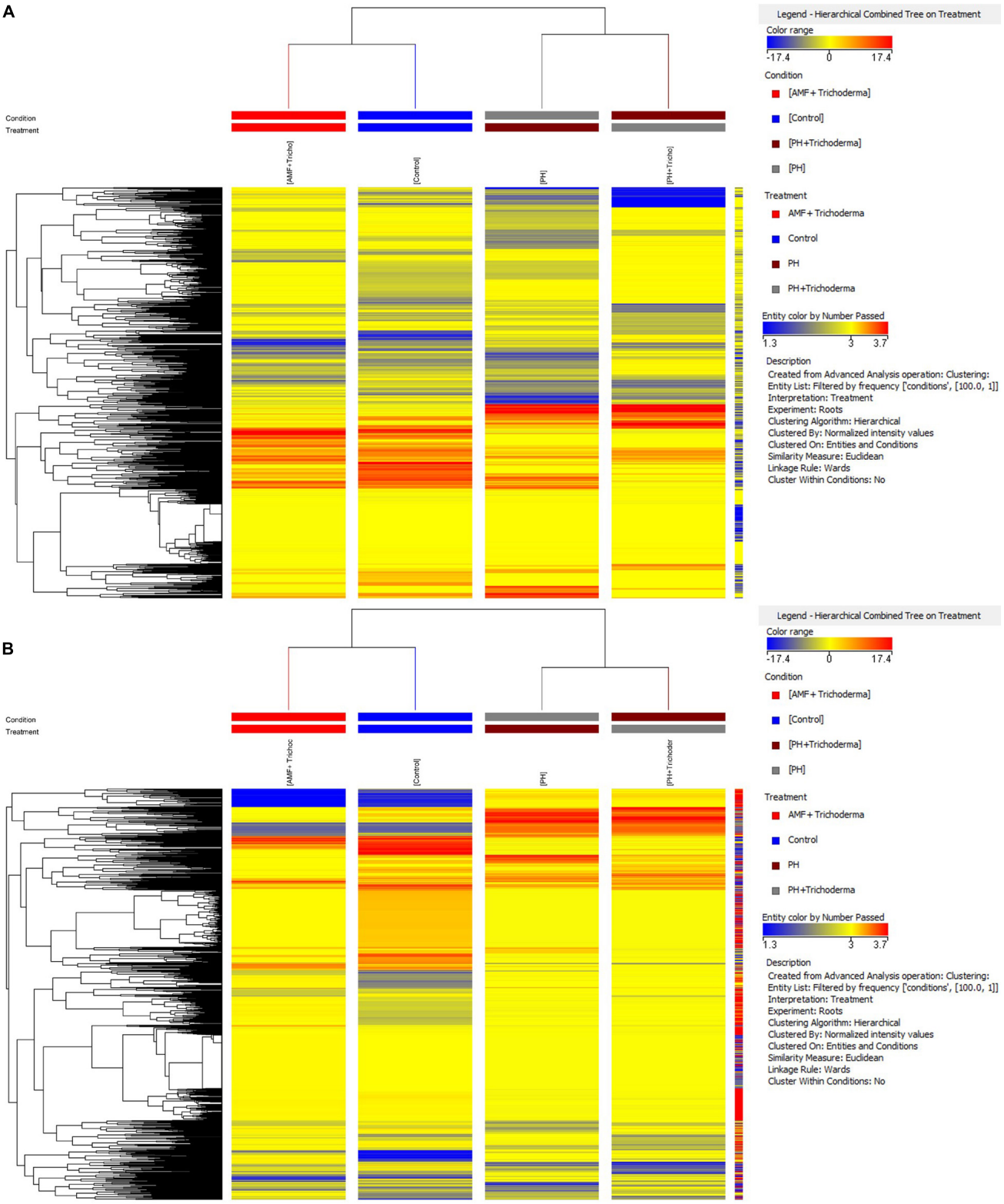

FIGURE 1 | Unsupervised hierarchical cluster analysis carried out from UHPLC-ESI/QTOF-MS metabolomic analysis of leaves **(A)** and roots **(B)** of maize plants treated with a consortium of arbuscular mycorrhizal fungi (AMF), *Trichoderma koningii* TK7, and rhizosphere bacteria or with a consortium of *Trichoderma koningii* TK7 and rhizosphere bacteria (Tricho) plus a protein hydrolyzate-based biostimulant (PH), or with a protein hydrolyzate-based biostimulant (PH). The fold-change based heat map was used to build hierarchical clusters (linkage rule: Ward; distance: Euclidean).

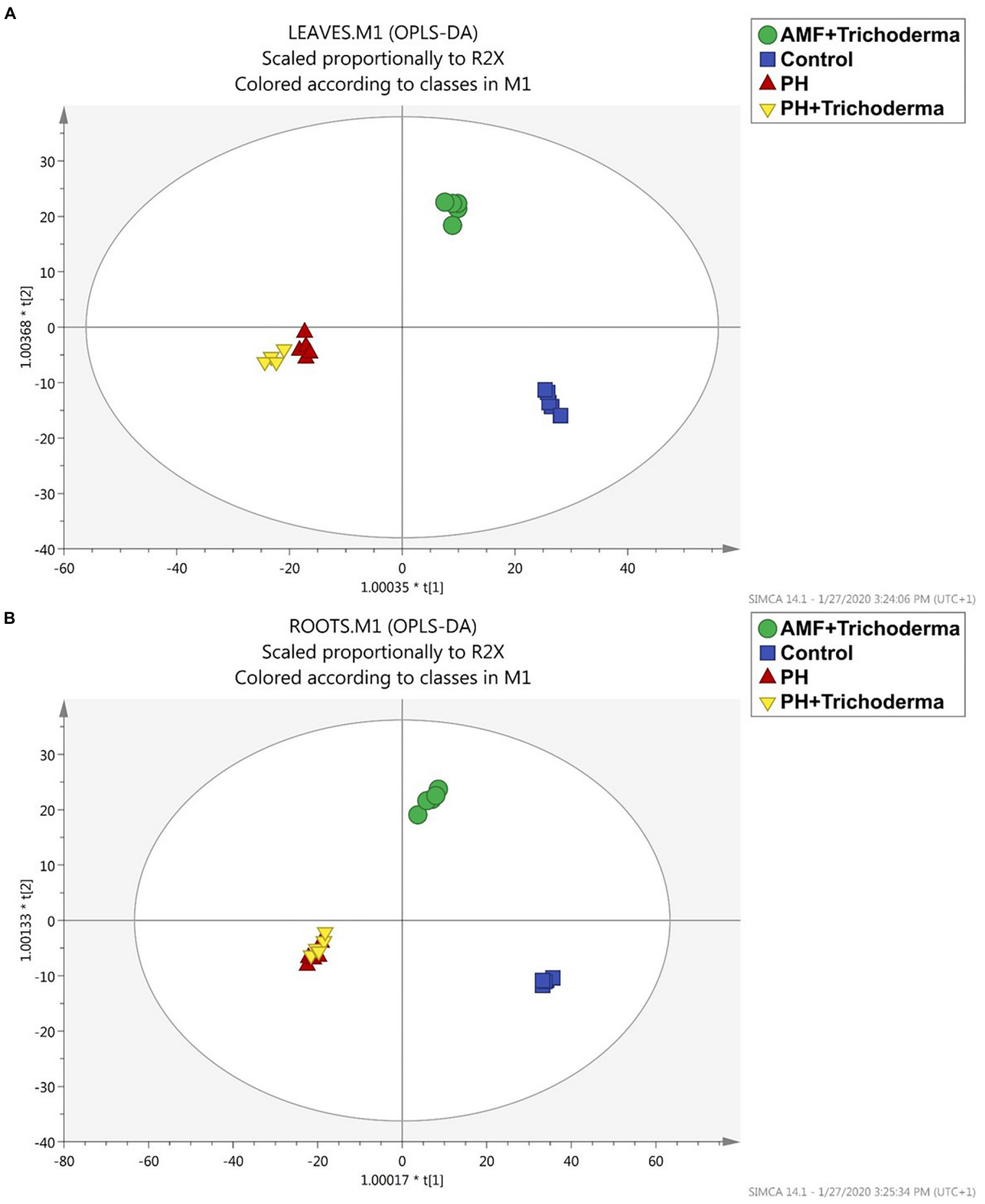

FIGURE 2 | Orthogonal projection to latent structures discriminant analysis (OPLS-DA) supervised modeling of leaves **(A)** and roots **(B)** of maize plants treated with a consortium of arbuscular mycorrhizal fungi (AMF), *Trichoderma koningii* TK7, and rhizosphere bacteria or with a consortium of *Trichoderma koningii* TK7 and rhizosphere bacteria (Tricho) plus a protein hydrolyzate-based biostimulant (PH), or with a protein hydrolyzate-based biostimulant (PH). The metabolomic dataset produced through UHPLC-ESI/QTOF-MS was Pareto scaled and then used for the multivariate OPLS-DA modeling.

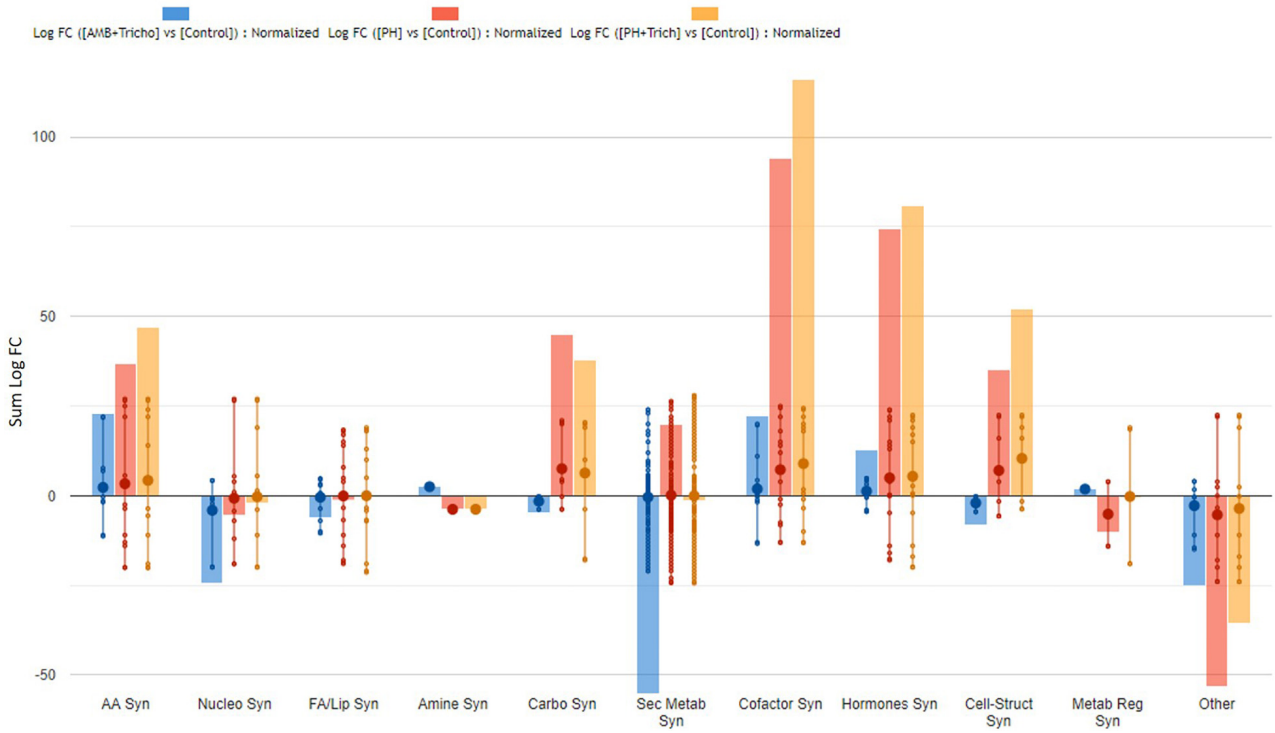

FIGURE 3 | Biosynthesis processes which take place in leaves of maize plants treated with a consortium of arbuscular mycorrhizal fungi (AMF), *Trichoderma koningii* TK7, and rhizosphere bacteria or with a consortium of *Trichoderma koningii* TK7 and rhizosphere bacteria (Tricho) plus a protein hydrolyzate-based biostimulant (PH), or with a protein hydrolyzate-based biostimulant (PH). The metabolomic dataset produced through UHPLC-ESI/QTOF-MS was subjected to a Volcano Plot analysis ($P < 0.01$, fold-change > 1.2) and differential metabolites were loaded into PlantCyc Pathway Tool (https://www.plantcyc.org/). The x-axis represents each set of subcategories while the y-axis corresponds to the cumulative fold-change.

contrast, these compounds together with other phytoalexins and polyketides, were the most up-regulated secondary compounds in the presence of PHs. As noted for leaves, the quinol and quinones pathway was significantly up-regulated in the presence of PH. The metabolic reprogramming induced by the treatments on phytohormones was also more pronounced in roots than leaves. A generalized increase of auxins and a decrease in jasmonates could be observed in all treatments, whereas the opposite trends could be observed when microorganisms were applied alone, compared to the treatments including PH. Gibberellin- and cytokinin-related compounds were more abundant following PH application and less abundant in presence of the microorganisms (AMF + *Trichoderma*), compared to the control. The same trend could be observed for brassinosteroids.

Finally, fatty acids, amino acids and their intermediate compounds showed an up-accumulation in the presence of PH or PH + *Trichoderma*. Interestingly, glutamate, glutamine and asparagine were accumulated in roots, whereas only asparagine accumulated in leaves following PH application. This may indicate that glutamine synthetase – glutamine oxoglutarate aminotransferase (GS-GOGAT) was involved in the maize response to the treatments including PH, thus suggesting the involvement of nitrogen assimilation and the subsequent export to shoots.

DISCUSSION

Biostimulants are EU fertilizing products having a beneficial effect on plants in low quantities because they are able to improve one or more of the following characteristics: (i) tolerance to abiotic stress, (ii) nutrient use efficiency, and (iii) quality traits (EU, 2019). These products include both substances and beneficial microorganisms (du Jardin, 2015). Since the mode of action of biostimulants is still largely unknown, the effect of microorganisms (in particular AMF and *T. koningii* TK7) in combination with PHs was investigated in order to shed light onto the molecular and biochemical processes following their application to plants. Diverse responses were found in plants treated with microorganisms alone rather than with PHs, differing by the specific pathways elicited in treated plants. Our results underline the nature of biostimulants as modulators of specific plant responses, since such responses were not generalized but rather depended on the treatment considered. From a phenotypic point of view, the application of PH alone or in combination with *Trichoderma* had the most positive effect on shoot biomass, followed by the co-inoculation with AMF and *Trichoderma*. The presumed mechanisms behind the desired effects on crop traits by PH or PH + *Trichoderma* could be related (i) to the release of signaling molecules with auxin and ethylene-like activity, in particular bioactive volatile compounds

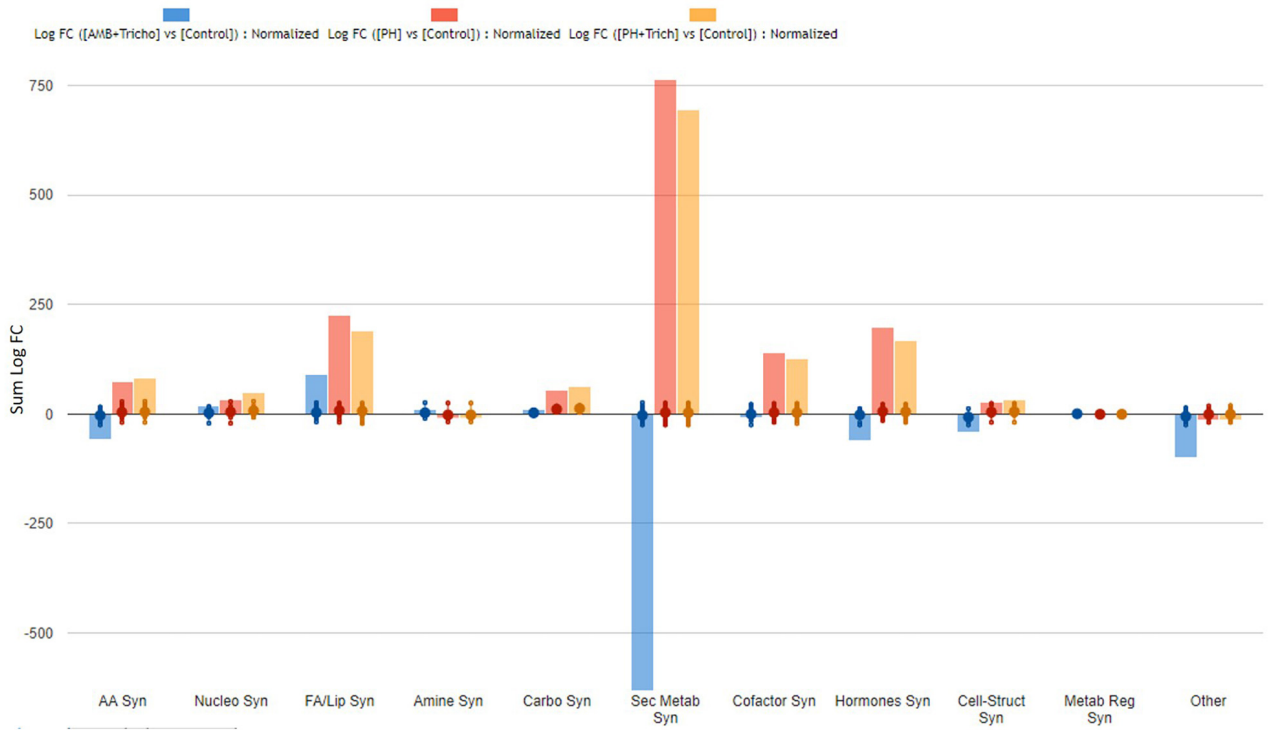

FIGURE 4 | Biosynthesis processes which take place in roots of maize plants treated with a consortium of arbuscular mycorrhizal fungi (AMF), *Trichoderma koningii* TK7, and rhizosphere bacteria or with a consortium of *Trichoderma koningii* TK7 and rhizosphere bacteria (Tricho) plus a protein hydrolyzate-based biostimulant (PH), or with a protein hydrolyzate-based biostimulant (PH). The metabolomic dataset produced through UHPLC-ESI/QTOF-MS was subjected to a Volcano Plot analysis ($P < 0.01$, fold-change > 1.2) and differential metabolites were loaded into PlantCyc Pathway Tool (https://www.plantcyc.org/). The x-axis represents each set of subcategories while the y-axis corresponds to the cumulative fold-change.

by *Trichoderma* and (ii) to the hormone-like activity (i.e., auxin and gibberellin-like activities) as well as the increase in the activity of key enzymes like glutamine synthetase and nitrate reductase by PH (Schiavon et al., 2008; Vinale et al., 2008; Matsumiya and Kubo, 2011; Colla et al., 2014; Sestili et al., 2018). The former biostimulant activity of PH alone or in combination with *Trichoderma* may have increased nutrient bioavailability to the plants, thus boosting biomass production. On the other hand, the co-inoculation with endophytic fungi stimulated the below ground root growth (higher root biomass) compared to PH, PH + *Trichoderma* and especially to the untreated control. A stimulation/modulation of root auxin production after the inoculation with AMF strains (*Rhizoglomus irregulare* BEG72 and *Funneliformis mosseae* BEG 234) may explain the increase of root biomass in mycorrhized plants, as reported previously in maize, tomato, pepper, lettuce, zucchini, and wheat (Colla et al., 2015a,b; Lucini et al., 2018; Saia et al., 2019, 2020).

The metabolomic profile of both maize leaves and roots were clearly affected by microbial and non-microbial biostimulants, as highlighted by unsupervised and supervised multivariate statistics. As expected, secondary metabolism in both leaves and roots was markedly modulated by the treatments. In general, microorganisms induced a down-regulation of phenylpropanoid, terpenoids, and N-containing secondary metabolites biosynthesis. These findings are supported by the fact that phenylalanine and tryptophan biosynthesis were decreased, although it has been reported that phenylalanine derivates play an important role in plant responses to AMF (Basu et al., 2018). However, in the presence of mycorrhizal fungi, glycolipids and phospholipids, as well as the biosynthetic intermediates of sterols, were up accumulated, mainly in roots. In this sense, several studies suggest that HMG-CoA reductase, a key enzyme of sterol biosynthesis, is involved in plant responses to AMF (MacLean et al., 2017). It is also known that lipids in membranes play an important role in microbial infection and some genes related to lipid metabolism are upregulated in plants following microbial attack. Lipidic metabolites could be involved as signal molecules or by modifying the lipid bilayers. Specifically, lipidic metabolites, such as choline, are involved in the metabolism of phosphatidic acid which is an important secondary messenger. Glycolipids and galactolipids in particular have a relevant function in plant–pathogen interactions and signal transduction (Siebers et al., 2016). The accumulation of these membrane lipids in our plants (mainly in the roots) after the application of microorganisms suggests the involvement of these metabolites in the plants response to microbial biostimulants.

On the other hand, plants treated with PH-containing biostimulants showed a higher number of metabolites involved in the response, as compared to microorganisms alone. Nonetheless, the response of PH and PH + *Trichoderma* were comparable.

TABLE 2 | Summarized biosynthesis processes highlighted in leaves of maize plants treated with a consortium of arbuscular mycorrhizal fungi (AMF), *Trichoderma koningii* TK7, and rhizosphere bacteria or with a consortium of *Trichoderma koningii* TK7 and rhizosphere bacteria (Tricho) plus a protein hydrolyzate-based biostimulant (PH), or with a protein hydrolyzate-based biostimulant (PH).

	AMF + *Trichoderma*			**PH**			**PH + *Trichoderma***		
	Number of compounds	**Average FC**	**Sum FC**	**Number of compounds**	**Average FC**	**Sum FC**	**Number of compounds**	**Average FC**	**Sum FC**
Amino acid	10	2.3	23.0	11	3.3	36.8	11	4.3	47.0
Nucleosides and Nucleotides	6	−4.1	−24.4	8	−0.7	−5.6	8	−0.3	−2.2
Fatty acid and Lipid	14	−0.4	−6.1	15	−0.1	−1.1	15	0.0	−0.1
Amines and Polyamines	1	2.5	2.5	1	−3.8	−3.8	1	−3.8	−3.8
Carbohydrates 3	−1.6	−4.7	6	7.5	45.1	6	6.3	37.9	
Secondary Metabolites	144	−0.4	−55.5	167	0.3	44.3	167	0.1	23.1
Cofactors, Prosthetic Groups, Electron Carriers	12	1.9	22.4	13	7.2	94.2	13	8.9	116.2
Hormones	10	1.3	12.7	15	5.0	74.4	15	5.4	81.0
Cell structures	4	−2.0	−8.1	5	4.0	35.2	5	10.4	52.0
Metabolic Regulators	1	1.8	1.8	2	−5.1	−10.3	2	−0.2	−0.5
Other biosynthesis	9	−2.8	−25.0	0	−5.3	−53.3	10	−3.5	−35.7

The metabolomic dataset produced through UHPLC-ESI/QTOF-MS was subjected to a Volcano Plot analysis (P < 0.01, fold-change > 1.2) and differential metabolites were loaded into PlantCyc Pathway Tool (https://www.plantcyc.org/). The average and summed Log fold-changes (Log FC) values, together with the number of compounds involved, is provided for each biosynthetic pathway and for each treatment.

TABLE 3 | Summarized biosynthesis processes highlighted in roots of maize plants treated with a consortium of arbuscular mycorrhizal fungi (AMF), *Trichoderma koningii* TK7, and rhizosphere bacteria or with a consortium of *Trichoderma koningii* TK7 and rhizosphere bacteria (Tricho) plus a protein hydrolyzate-based biostimulant (PH), or with a protein hydrolyzate-based biostimulant (PH).

	AMF + *Trichoderma*			**PH**			**PH + *Trichoderma***		
	Number of compounds	**Average FC**	**Sum FC**	**Number of compounds**	**Average FC**	**Sum FC**	**Number of compounds**	**Average FC**	**Sum FC**
Amino acid	18	−3.2	−58.5	19	4.0	75.3	19	4.4	82.7
Nucleosides and Nucleotides	7	2.5	17.8	7	4.5	31.6	7	7.2	50.6
Fatty acid and Lipid	29	3.1	90.0	29	7.8	225.6	29	6.5	189.5
Amines and Polyamines	4	2.7	10.8	4	−2.2	−8.7	4	−2.2	−8.7
Carbohydrates	4	2.6	10.4	5	10.8	54.0	5	12.4	61.9
Secondary Metabolites	224	−2.8	−621.6	242	3.3	809.2	244	3.0	741.1
Cofactors, Prosthetic Groups, Electron Carriers	43	−0.2	−7.4	44	3.2	141.1	44	2.9	126.5
Hormones	31	−2.0	−62.4	35	5.7	197.9	35	4.8	166.7
Cell structures	6	−7.2	−43.1	6	4.3	26.1	6	5.2	31.3
Metabolic Regulators	3	0.5	1.5	3	−0.7	−2.1	3	−0.7	−2.1
Other biosynthesis	19	−5.3	−100.7	20	−0.7	−13.1	20	−0.7	−14.9

The metabolomic dataset produced through UHPLC-ESI/QTOF-MS was subjected to a Volcano Plot analysis (P < 0.01, fold-change > 1.2) and differential metabolites were loaded into PlantCyc Pathway Tool (https://www.plantcyc.org/). The average and summed Log fold-changes (Log FC) values, together with the number of compounds involved, is provided for each biosynthetic pathway and for each treatment.

Despite a direct effect of PH on *Trichoderma* that cannot be excluded *a priori*, our findings suggest a hierarchically stronger effect of PH on plant physiology compared to microorganisms. Considering the pathways affected by PH application, this biostimulant could have a stronger metabolic reprogramming effect by modifying the essential metabolism of N and C. In this sense, it has been reported that PH acts by increasing, either directly or indirectly, the plant growth and crop yield by enhancing nutrient uptake and nutrient use efficiency in plants (Paul et al., 2019a,b). Several studies reveal that PHs stimulated some enzymes involved in N assimilation and C metabolism (Ertani et al., 2009; Colla et al., 2015a,b, 2017b). In our study, PH imposed a marked remodulation of the metabolic pathways of amino acids. Particularly interesting was the upregulation of the

phenylalanine biosynthetic pathway after PH application. This aromatic amino acid, biosynthesized *via* shikimate, is a precursor of phenylpropanoids which are linked to plant stress responses (Böttger et al., 2018). Consistently, other metabolites derived from shikimic acid such as chorismate were increased in the presence of PH, in agreement with the concurrent stimulation of the pathway of phenylpropanoid secondary metabolites.

Previous studies support the fact that the phenylpropanoid pathway is part of the reaction of plants to PHs (Lucini et al., 2015, 2018; Carillo et al., 2019). Some biostimulants are postulated to enhance the activity of PAL, a key enzyme in this pathway; Ertani et al. (2017) showed an increase in total phenolic compounds and an increase in the expression of PAL in tomato plants treated with an alfalfa-based PH. Other authors found an increase of PAL (ZmPAL1) gene expression and PAL activity in maize treated with 1 mg C/l of humic substances (Schiavon et al., 2010). These findings corroborate our results, suggesting a crucial role of phenylpropanoids in the response to PH biostimulants.

Hormones were also affected by PH, with a more evident modulation in the roots. The treatments induced reprogramming of the whole phytohormone profile. It is noteworthy that plant growth is known to be regulated by a complex and partially understood interaction network of hormones like auxins, cytokinins, and gibberellins (Liu et al., 2017). In fact, a regulation of all these hormones was triggered in maize roots by the treatments applied in this study, together with the modulation of brassinosteroids and jasmonates. Gibberellins, the most up accumulated phytohormones, play a crucial role in plant development comprising of shoot and root growth, leaf morphogenesis, germination dormancy, seed production, and flowering (Marzec, 2017). DELLA proteins have been related to the interaction between gibberellins and other hormones such as brassinosteroids, jasmonate, and ethylene (Liu et al., 2017). The concurrent increase in abscisic acid following PH treatment is also worth considering, since this hormone coordinates auxins to determine elongation, lateral root formation and architecture in general (Harris, 2015). In relation to hormones, it has been reported that PHs could affect the phytohormonal balance and elicit auxin- and gibberellin-like activities. Moreover, plant bioactive peptides has been noted to have hormone-like activities (Colla et al., 2015a,b, 2017b). In particular, Ertani et al. (2009) and Colla et al. (2014) reported that PHs could have auxin-like and gibberellin-like activity. Although the depiction of this hormonal coordinated network is complicated, we can postulate that the hormonal signatures induced by the treatments are involved in the improved plant growth we observed. The more distinctive phytohormone profile gained in plants treated with the microorganisms alone can also explain the differences in root growth and root-to-shoot ratio we observed from this treatment.

Another factor pertaining to the increased biomass we observed following the biostimulant treatments is the potential involvement of the GS-GOGAT nitrogen assimilation system. Indeed, this system represents the first step of incorporating both ammonium and nitrate into organic compounds. Glutamate and glutamine are the first results of this process, while asparagine is one of the most common ways to export nitrogen to shoots. Consistently, the former accumulated in roots whereas the latter accumulated in shoots. This opens the possibility that the treatments increased nitrogen use efficiency, although specific studies are advisable with this aim. Nonetheless, preliminary evidence that protein hydrolyzates can promote nitrogen use efficiency is present in prior literature (Colla et al., 2017a).

CONCLUSION

Over the past decade, the application of microbial and non-microbial biostimulants in intensive and extensive cropping systems has been on the rise, compelled by the increasing interest of growers, scientists, and private sectors. In fact, the agriculture industry has been requested to boost crop productivity in a sustainable manner, even for extensive crops such as maize. A biostimulant activity was observed in the current study in maize, demonstrating that the application of PH alone or in combination with *Trichoderma* as well as the co-inoculation with endophytic fungi (AMF + *Trichoderma*) can generate beneficial effects in terms of plant growth promotion. Co-inoculation with endophytic fungi or the application of PH alone or in combination distinctively modulated the metabolite profile of both maize leaves and roots. Untargeted metabolomics followed by multivariate statistics allowed us to shed light onto the biochemical processes elicited by the treatments. The specific metabolomic signatures achieved from the different treatments indicate that different molecular processes are involved in plant responses to biostimulants, thereby not excluding their combined use in order to provide complementary benefits. Nonetheless, PH induced a hierarchically more pronounced metabolomic response. In general, secondary metabolism (including phenylpropanoids and terpenes) was extensively affected by the different biostimulants, although the direction of regulation was different when only microorganisms (without PH) were used. The multilayer interaction network of phytohormones was also modulated by the treatments, thus supporting the hypothesis of a hormone-like activity ascribed to several biostimulants. For the first time, the treatments considered suggested that nitrogen use efficiency might be involved in the mechanism of the increased plant growth observed. This point is of particular interest and deserves future studies based on more targeted approaches.

DATA AVAILABILITY STATEMENT

All datasets generated for this study are included in the article/**Supplementary Material**.

AUTHOR CONTRIBUTIONS

YR wrote the first draft of the manuscript, followed the agronomic trial, and contributed to data analysis and interpretation. LL, BM-M, and PB performed the metabolomics analysis, data interpretation, and wrote the metabolomic part.

MC and GC were involved in agronomic trial, data analysis, data interpretation, and writing the manuscript. GC and LL coordinated the whole project, provided the intellectual input, set up the experiment, and corrected the manuscript.

SUPPLEMENTARY MATERIAL

The Supplementary Material for this article can be found online at: https://www.frontiersin.org/articles/10.3389/fmicb.2020.00664/full#supplementary-material

TABLE S1 | Whole dataset produced from untargeted metabolomic analysis carried out in leaves and roots of maize treated with biostimulants.

TABLE S2 | VIP discriminant compounds identified as discriminant from OPLS-DA in leaves following biostimulant application.

TABLE S3 | VIP discriminant compounds identified as discriminant from OPLS-DA in roots following biostimulant application.

TABLE S4 | Differential metabolites as derived from Volcano analysis (P-value < 0.01; FC > 1.2) of leaves following biostimulant application.

TABLE S5 | Differential metabolites as derived from Volcano analysis (P-value < 0.01; FC > 1.2) of roots following biostimulant application.

REFERENCES

Basu, S., Rabara, R. C., and Negi, S. (2018). AMF: the future prospect for sustainable agriculture. *Physiol. Mol. Plant Pathol.* 102, 36–45. doi: 10.1016/j.pmpp.2017.11.007

Battacharyya, D., Babgohari, M. Z., Rathor, P., and Prithiviraj, B. (2015). Seaweed extracts as biostimulants in horticulture. *Sci. Hortic.* 196, 39–48. doi: 10.1016/j.scienta.2015.09.012

Bernardo, L., Carletti, P., Badeck, F. W., Rizza, F., Morcia, C., Ghizzoni, R., et al. (2019). Metabolomic responses triggered by arbuscular mycorrhiza enhance tolerance to water stress in wheat cultivars. *Plant Physiol. Biochem.* 137, 203–212. doi: 10.1016/j.plaphy.2019.02.007

Böttger, A., Vothknecht, U., Bolle, C., and Wolf, A. (2018). *Lessons on Caffeine, Cannabis & Co*. Cham: Springer, 171–178.

Calvo, P., Nelson, L., and Kloepper, J. W. (2014). Agricultural uses of plant biostimulants. *Plant Soil* 383, 3–41. doi: 10.1007/s11104-014-2131-8

Canellas, L. P., Olivares, F. L., Aguiar, N. O., Jones, D. L., Nebbioso, A., Mazzei, P., et al. (2015). Humic and fulvic acids as biostimulants in horticulture. *Sci. Hortic.* 196, 15–27. doi: 10.1016/j.scienta.2015.09.013

Carillo, P., Colla, G., Fusco, G. M., Dell'Aversana, E., El-Nakhel, C., Giordano, M., et al. (2019). Morphological and physiological responses induced by protein hydrolysate-based biostimulant and nitrogen rates in greenhouse spinach. *Agronomy* 9:450. doi: 10.3390/agronomy9080450

Chiaiese, P., Corrado, G., Colla, G., Kyriacou, M. C., and Rouphael, Y. (2018). Renewable sources of plant biostimulation: microalgae as a sustainable means to improve crop performance. *Front. Plant Sci.* 9:1782. doi: 10.3389/fpls.2018.01782

Colla, G., Cardarelli, M., Bonini, P., and Rouphael, Y. (2017a). Foliar applications of protein hydrolysate, plant and seaweed extracts increase yield but differentially modulate fruit quality of greenhouse tomato. *HortScience* 52, 1214–1220. doi: 10.21273/hortsci12200-17

Colla, G., Hoagland, L., Ruzzi, M., Cardarelli, M., Bonini, P., Canaguier, R., et al. (2017b). Biostimulant action of protein hydrolysates: unraveling their effects on plant physiology and microbiome. *Front. Plant Sci.* 8:2202. doi: 10.3389/fpls.2017.02202

Colla, G., Nardi, S., Cardarelli, M., Ertani, A., Lucini, L., Canaguier, R., et al. (2015a). Protein hydrolysates as biostimulants in horticulture. *Sci. Hortic.* 196, 28–38. doi: 10.1016/j.scienta.2015.08.037

Colla, G., and Rouphael, Y. (2015). Biostimulants in horticulture. *Sci. Hortic.* 196, 1–2. doi: 10.1016/j.scienta.2015.10.044

Colla, G., Rouphael, Y., Canaguier, R., Svecova, E., and Cardarelli, M. (2014). Biostimulant action of a plant-derived protein hydrolysate produced through enzymatic hydrolysis. *Front. Plant Sci.* 5:448. doi: 10.3389/fpls.2014.00448

Colla, G., Rouphael, Y., Di Mattia, E., El-Nakhel, C., and Cardarelli, M. (2015b). Co-inoculation of *Glomus intraradices* and *Trichoderma atroviride* acts as a biostimulant to promote growth, yield and nutrient uptake of vegetable crops. *J. Sci. Food Agric.* 95, 1706–1715. doi: 10.1002/jsfa.6875

Contreras-Cornejo, H. A., Macias-Rodriguez, L., Cortes-Penagos, C., and López-Bucio, J. (2009). Trichoderma virens, a plant beneficial fungus, enhances biomass production and promotes lateral root growth through an auxin-pependent mechanism in *Arabidopsis*. *Plant Physiol.* 149, 1579–1592. doi: 10.1104/pp.108.130369

du Jardin, P. (2015). Plant biostimulants: definition, concept, main categories and regulation. *Sci. Hortic.* 196, 3–14. doi: 10.1016/j.scienta.2015.09.021

Ertani, A., Cavani, L., Pizzeghello, D., Brandellero, E., Altissimo, A., Ciavatta, C., et al. (2009). Biostimulant activities of two protein hydrolysates on the growth and nitrogen metabolism in maize seedlings. *J. Plant. Nutr. Soil. Sci.* 172, 237–244. doi: 10.1002/jpln.200800174

Ertani, A., Schiavon, M., Muscolo, A., and Nardi, S. (2013). Alfalfa plant-derived biostimulant stimulate short-term growth of salt stressed *Zea mays* L. plants. *Plant Soil* 364, 145–158. doi: 10.1007/s11104-012-1335-z

Ertani, A., Schiavon, M., and Nardi, S. (2017). Transcriptome-wide identification of differentially expressed genes in *Solanum lycopersicon* L. in response to an alfalfa-protein hydrolysate using microarrays. *Front. Plant Sci.* 8:1159. doi: 10.3389/fpls.2017.01159

EU (2019). *Regulation of the European Parliament and of the Council Laying Down Rules on the Making Available on the Market of EU Fertilising Products and Amending Regulations*. Italy: EU.

FAO (2009). *Global Agriculture Towards 2050, High-Level Expert Forum, How to Feed the World 2050*. Rome: Food and Agriculture Organization of the United Nations.

FAO (2017). *Food Balances (Old Methodology and Population)*. Rome: Food and Agriculture Organization of the United Nations.

Fiorentino, N., Ventorino, V., Woo, S. L., Pepe, O., De Rosa, A., Gioia, L., et al. (2018). *Trichoderma*-based biostimulants modulate rhizosphere microbial populations and improve N uptake efficiency, yield and nutritional quality of leafy vegetables. *Front. Plant Sci.* 9:743. doi: 10.3389/fpls.2018.00743

Haplern, M., Bar-Tal, A., Ofek, M., Minz, D., Muller, T., and Yermiyahu, U. (2015). The use of biostimulants for enhancing nutrient uptake. *Adv. Agron.* 130, 141–174. doi: 10.1016/bs.agron.2014.10.001

Harris, J. M. (2015). Abscisic acid: hidden architect of root system structure. *Plants* 4, 548–572. doi: 10.3390/plants4030548

Karp, P. D., Paley, S. M., Krummenacker, M., Latendresse, M., Dale, J. M., Lee, T. J., et al. (2010). Pathway tools version 13.0: integrated software for pathway/genome informatics and systems biology. *Brief. Bioinformatics* 11, 40–79. doi: 10.1093/bib/bbp043

Kumar, P., Lucini, L., Rouphael, Y., Cardarelli, C., Kalunke, R. M., and Colla, G. (2015). Insight into the role of grafting and arbuscular mycorrhiza on cadmium stress tolerance in tomato. *Front. Plant Sci.* 6:477. doi: 10.3389/fpls.2015.00477

Liu, J., Moore, S., Chen, C., and Lindsey, K. (2017). Crosstalk complexities between auxin, cytokinin, and ethylene in *Arabidopsis* root development: from experiments to systems modeling, and back again. *Mol. Plant* 10, 1480–1496. doi: 10.1016/j.molp.2017.11.002

López-Bucio, J., Pelagio-Flores, R., and Herrera-Estrella, A. (2015). *Trichoderma* as biostimulant: exploiting the multi level properties of a plant beneficial fungus. *Sci. Hortic.* 196, 109–123. doi: 10.1016/j.scienta.2015.08.043

Lucini, L., Colla, G., Miras Moreno, M. B., Bernardo, L., Cardarelli, M., Terzi, V., et al. (2019). Inoculation of *Rhizoglomus irregulare* or *Trichoderma atroviride* differentially modulates metabolite profiling of wheat root exudates. *Phytochemistry* 157, 158–167. doi: 10.1016/j.phytochem.2018.10.033

Lucini, L., Rouphael, Y., Cardarelli, M., Bonini, P., Baffi, C., and Colla, G. (2018). A vegetal biopolymer-based biostimulant promoted root growth in melon while triggering brassinosteroids and stress-related compounds. *Front. Plant Sci.* 9:472. doi: 10.3389/fpls.2018.00472

Lucini, L., Rouphael, Y., Cardarelli, M., Canaguier, R., and Kumar, P. G. (2015). The effect of a plant-derived biostimulant on metabolic profiling and crop performance of lettuce grown under saline conditions. *Sci. Hortic.* 182, 124–133. doi: 10.1016/j.scienta.2014.11.022

MacLean, A. M., Bravo, A., and Harrison, M. J. (2017). Plant signaling and metabolic pathways enabling arbuscular mycorrhizal symbiosis. *Plant Cell* 29, 2319–2335. doi: 10.1105/tpc.17.00555

Marzec, M. (2017). Strigolactones and gibberellins: a new couple in the phytohormone world? *Trends Plant Sci.* 22, 813–815. doi: 10.1016/j.tplants.2017.08.001

Matsumiya, Y., and Kubo, M. (2011). "Soybean peptide: novel plant growth promoting peptide from soybean," in *Soybean and Nutrition*, ed. H. El-Shemy (Rijeka: In Tech Europe Publisher), 215–230.

Paul, K., Sorrentino, M., Lucini, L., Rouphael, Y., Cardarelli, M., Bonini, P., et al. (2019a). A combined phenotypic and metabolomic approach for elucidating the biostimulant action of a plant-derived protein hydrolysate on tomato grown under limited water availability. *Front. Plant Sci.* 10:493. doi: 10.3389/fpls.2019.00493

Paul, K., Sorrentino, M., Lucini, L., Rouphael, Y., Cardarelli, M., Bonini, P., et al. (2019b). Understanding the biostimulant action of vegetal-derived protein hydrolysates by high-throughput plant phenotyping and metabolomics: a case study on tomato. *Front. Plant Sci.* 10:47. doi: 10.3389/fpls.2019.00047

Pretali, L., Bernardo, L., Butterfield, T. S., Trevisan, M., and Lucini, L. (2016). Botanical and biological pesticides elicit a similar induced systemic response in tomato (*Solanum lycopersicum*) secondary metabolism. *Phytochemistry* 130, 56–63. doi: 10.1016/j.phytochem.2016.04.002

Rouphael, Y., Cardarelli, M., Bonini, P., and Colla, G. (2017). Synergistic action of a microbial-based biostimulant and a plant derived-protein hydrolysate enhances lettuce tolerance to alkalinity and salinity. *Front. Plant Sci.* 8:131. doi: 10.3389/fpls.2017.00131

Rouphael, Y., and Colla, G. (2018). Synergistic biostimulatory action: designing the next generation of plant biostimulants for sustainable agriculture. *Front. Plant Sci.* 9:1655. doi: 10.3389/fpls.2018.01655

Rouphael, Y., and Colla, G. (2020). Editorial: biostimulants in agriculture. *Front. Plant Sci.* 11:40. doi: 10.3389/fpls.2020.00040

Rouphael, Y., Franken, P., Schneider, C., Schwarz, D., Giovannetti, M., Agnolucci, M., et al. (2015). Arbuscular mycorrhizal fungi act as biostimulants in horticultural crops. *Sci. Hortic.* 196, 91–108. doi: 10.1016/j.scienta.2015.09.002

Rouphael, Y., Kyriacou, M. C., Petropoulos, S. A., De Pascale, S., and Colla, G. (2018a). Improving vegetable quality in controlled environments. *Sci. Hort.* 234, 275–289. doi: 10.1016/j.scienta.2018.02.033

Rouphael, Y., Raimondi, G., Lucini, L., Carillo, P., Kyriacou, M. C., Colla, G., et al. (2018b). Physiological and metabolic responses triggered by omeprazole improve tomato plant tolerance to NaCl stress. *Front. Plant Sci.* 9:249. doi: 10.3389/fpls.2018.00249

Rouphael, Y., Spíchal, L., Panzarová, K., Casa, R., and Colla, G. (2018c). High-throughput plant phenotyping for developing novel biostimulants: from lab to field or from field to lab? *Front. Plant Sci.* 9:1197. doi: 10.3389/fpls.2018.01197

Saia, S., Aissa, E., Luziatelli, F., Ruzzi, M., Colla, G., Fica, A. G., et al. (2020). Growth-promoting bacteria and arbuscular mycorrhizal fungi differentially benefit tomato and corn depending upon the supplied form of phosphorus. *Mycorrhiza* 30, 133–147. doi: 10.1007/s00572-019-00927-w

Saia, S., Colla, G., Raimondi, G., Di Stasio, E., Cardarelli, M., Bonini, P., et al. (2019). An endophytic fungi-based biostimulant modulated lettuce yield, physiological and functional quality responses to both moderate and severe water limitation. *Sci. Hortic.* 256:108595. doi: 10.1016/j.scienta.2019.108595

Schiavon, M., Ertani, A., and Nardi, S. (2008). Effects of an alfaalfa protein hydrolysate on the gene expression and activity of enzymes of TCA cycle and N metabolism in *Zea mays* L. *J. Agric. Food Chem.* 56, 11800–11808. doi: 10.1021/jf802362g

Schiavon, M., Pizzeghello, D., Muscolo, A., Vaccaro, S., Francioso, O., and Nardi, S. (2010). High molecular size humic substances enhance phenylpropanoid metabolism in maize (*Zea mays* L.). *J. Chem. Ecol.* 36, 662–669. doi: 10.1007/s10886-010-9790-6

Searchinger, T., Waite, R., Hanson, C., Ranganathan, J., and Dumas, P. (2018). *World Resources Report: Creating a Sustainable Food Future*. Nairobi: UNEP, 1–97.

Sestili, F., Rouphael, Y., Cardarelli, M., Pucci, A., Bonini, P., Canaguier, R., et al. (2018). Protein hydrolysate stimulates growth in tomato coupled with N-dependent gene expression involved in N assimilation. *Front. Plant Sci.* 9:1233. doi: 10.3389/fpls.2018.01233

Siebers, M., Brands, M., Wewer, V., Duan, Y., Hölzl, G., and Dörmann, P. (2016). Lipids in plant–microbe interactions. *Biochim. Biophys. Acta Mol. Cell Biol. Lipids* 1861, 1379–1395.

Tavares, L. C., Rufino, C. A., Brunes, A. P., Friedrich, F. F., Barros, A. C. S. A., and Villela, F. A. (2013). Physiological performance of wheat seeds coated with micronutrients. *J. Seed Sci.* 35, 28–345. doi: 10.1590/s2317-15372013000100004

Tenenboim, H., and Brotman, Y. (2016). Omic relief for the biotically stressed: metabolomics of plant biotic interactions. *Trends Plant Sci.* 21, 781–791. doi: 10.1016/j.tplants.2016.04.009

Vinale, F., Sivasithamparam, K., Ghisalberti, E. L., Marra, R., Barbetti, M. J., Li, H., et al. (2008). A novel role for *Trichoderma* secondary metabolites in the interactions with plants. *Physiol. Mol. Plant Pathol.* 72, 80–86. doi: 10.1016/j.pmpp.2008.05.005

Woo, S. L., Ruocco, M., Vinale, F., Nigro, M., Marra, R., Lombardi, N., et al. (2014). *Trichoderma*-based products and their widespread use in agriculture. *Open Mycol. J.* 8, 71–126. doi: 10.2174/1874437001408010071

Wu, L., Gao, X., Xia, F., Joshi, J., Borza, T., and Wang-Pruski, G. (2019). Biostimulant and fungicidal effects of phosphite assessed by GC-TOF-MS analysis of potato leaf metabolome. *Physiol. Mol. Plant Pathol.* 106, 49–56. doi: 10.1016/j.pmpp.2018.12.001

Conflict of Interest: The authors declare that the research was conducted in the absence of any commercial or financial relationships that could be construed as a potential conflict of interest.

frontiers in Microbiology

REVIEW
published: 25 May 2020
doi: 10.3389/fmicb.2020.00992

Biological Control of Plant-Parasitic Nematodes by Filamentous Fungi Inducers of Resistance: *Trichoderma*, Mycorrhizal and Endophytic Fungi

Jorge Poveda[1,2†], *Patricia Abril-Urias*[1,3†] *and Carolina Escobar*[3,4*]

[1] Spanish-Portuguese Institute for Agricultural Research (CIALE), University of Salamanca, Salamanca, Spain, [2] Biological Mission of Galicia (MBG-CSIC), Pontevedra, Spain, [3] Facultad de Ciencias Ambientales y Bioquímica, Área de Fisiología Vegetal, Universidad de Castilla-La Mancha, Toledo, Spain, [4] International Research Organization for Advanced Science and Technology, Kumamoto University, Kumamoto, Japan

Plant-parasitic-nematodes represent a major threat to the agricultural production of different crops worldwide. Due to the high toxicity of chemical nematicides, it is necessary to develop new control strategies against nematodes. In this respect, filamentous fungi can be an interesting biocontrol alternative. The genus *Trichoderma*, mycorrhizal and endophytic fungi are the main groups of filamentous fungi studied and used as biological control agents (BCAs) against nematodes as resistance inducers. They are able to reduce the damage caused by plant-parasitic nematodes directly by parasitism, antibiosis, paralysis and by the production of lytic enzymes. But they also minimize harm by space and resource-competition, by providing higher nutrient and water uptake to the plant, or by modifying the root morphology, and/or rhizosphere interactions, that constitutes an advantage for the plant-growth. Besides, filamentous fungi are able to induce resistance against nematodes by activating hormone-mediated (salicylic and jasmonic acid, strigolactones among others) plant-defense mechanisms. Additionally, the alteration of the transport of chemical defense components through the plant or the synthesis of plant secondary metabolites and different enzymes can also contribute to enhancing plant defenses. Therefore, the use of filamentous fungi of the mentioned groups as BCAs is a promising durable biocontrol strategy in agriculture against plant-parasitic nematodes.

Keywords: plant-parasitic-nematodes, *Trichoderma*, mycorrhizal fungi, endophytic fungi, biocontrol, plant systemic resistance

OPEN ACCESS

Edited by:
Santiago Gutierrez, Universidad de León, Spain

Reviewed by:
Holger Heuer, Julius Kühn-Institut, Germany
Sofia R. Costa, University of Minho, Portugal

***Correspondence:**
Carolina Escobar
carolina.escobar@uclm.es

† These authors have contributed equally to this work

Specialty section:
This article was submitted to Plant Microbe Interactions, a section of the journal Frontiers in Microbiology

Received: *28 January 2020*
Accepted: *23 April 2020*
Published: *25 May 2020*

Citation:
Poveda J, Abril-Urias P and Escobar C (2020) Biological Control of Plant-Parasitic Nematodes by Filamentous Fungi Inducers of Resistance: Trichoderma, Mycorrhizal and Endophytic Fungi. Front. Microbiol. 11:992. doi: 10.3389/fmicb.2020.00992

INTRODUCTION

Over 4100 species of plant-parasitic nematodes were described to date, among which, a restricted group of genera is considered as major plant-pathogens, whereas others are specific to a more limited range of crops, both causing a high impact to economically important crops. Damage caused by plant nematodes has been estimated as a projected yield loss of 12.3% ($157 billion) worldwide (Singh et al., 2015), more significant damage comparing to invasive insects (around US$70 billion; Bradshaw et al., 2016). The full extent of worldwide nematode damage is likely to be

underestimated, since growers are often unaware of their presence because the symptoms caused in the plant are often non-specific, making difficult to attribute crop losses to nematode damage (Jones et al., 2013; Siddique and Grundler, 2018). Additional losses could be related to food quality and visual imperfections associated with infection symptoms (Palomares-Rius et al., 2017).

These nematodes are usually small soil-borne pathogens that can feed on all plant parts (including roots, stems, leaves, flowers and seeds), although most species feed on roots. They need a protrusible stylet for feeding that they use to penetrate the plant cells. The stylet is connected to three to five pharyngeal glands that produce effector molecules, which are often secreted, facilitating penetration, internal migration, and parasitism (Jones et al., 2013; Mejias et al., 2019). Based on their feeding habitats, plant-parasitic nematodes can be broadly categorized as either ectoparasitic or endoparasitic. However, the most important nematodes in terms of crop losses are sedentary endoparasites, the root-knot (*Meloidogyne* spp.) and cyst nematodes (*Heterodera* and *Globodera* spp.; Jones et al., 2013). Nowadays, there is an increasing need to supply more food to the growing population (FAO, 2017); therefore, the control of plant-parasitic nematodes is also a growing global demand.

Given the high economic impact caused by parasitic nematodes, a large number of strategies have been developed for nematode-control in agriculture, including the use of chemical nematicides. However, the need to deploy effective nematode resistance is intensified with the loss of pesticides due to EU regulations (EC No1107/2009) as they are harmful to human health and contaminant for the environment (Zhang et al., 2014, 2017). Strategies associated with biocontrol are proposed as a much safer alternative and highly practicable for plant-parasitic nematodes management. The term biological control (or biocontrol) applies to the use of living organisms to suppress the population density or impact to a specific pest organism, making it less abundant or less damaging than it would otherwise be. Specifically, biological control of nematodes is defined as the regulation of nematode populations and/or a reduction in nematode damage through the action of organisms antagonistic to them, which occur naturally or through the manipulation of the environment or the introduction of antagonists. The organism that suppresses the pathogen is referred to as the biological control agent (BCA) that can interact directly with the pathogen where we include antagonism (antibiosis and competition for nutrients or space among others) or interact indirectly with the pathogen through the host-plant as for example inducing plant-resistance (systemic acquired resistance or SAR and induced systemic resistance or ISR; Pal and Gardener, 2006; Stirling, 2018; Xiang et al., 2018). Nowadays, a wide variety of organisms are known to act as BCAs against plant-parasitic nematodes such as fungi, bacteria, viruses, protists, nematode antagonists and other invertebrates. BCAs, physical methods such as solarization and fallowing or cultural practices as crop rotation were proved in most cases viable applied in combination and/or with reduced doses of chemicals in a scenario of integrated pest management (Khan and Kim, 2007; D'Addabbo et al., 2019). Biocontrol of plant-parasitic nematodes using predatory nematodes dates back to the early 20th century; nevertheless, their potential has only begun to be studied in recent years. Apart from acting as BCAs against plant-parasitic nematodes, these nematodes play a main role in stimulating cycling of plant nutrients, which allow plants to defend themselves more effectively against the attack of pathogens. There are many examples described in the literature, among which we find for example *Odontopharynx longicaudata,* effective against *M. incognita* and *M. javanica* (among others) and *M. gaugleri*, effective against *Heterodera oryzae* and *M. incognita* (among others; Khan and Kim, 2007).

Interestingly, plant growth-promoting rhizobacterias (PGPRs) enhance plant growth by colonizing the plant root system, but some PGPR showed also nematicidal activity against plant-parasitic nematodes. One clear example is the secondary metabolites produced by *Pseudomonas fluorescens* CHA0 that induce mortality of nematode eggs and second-stage infective juveniles (J2s; Siddiqui and Shaukat, 2003). In a study conducted by Zhao et al. (2018), from 860 strains of bacteria collected from the rhizosphere, 5 showed high efficacy as BCAs against *Meloidogyne javanica*, i.e., *Bacillus cereus, B. subtilis, Pseudomonas putida, P. fluorescens,* and *Serratia proteamaculans.* Hence, PGPRs, in addition to benefit plants growth, have great potential through direct interaction against pathogens such as nematodes.

Plants also have a series of innate defensive strategies to defend themselves from the attack of pests and pathogens in a targeted manner. Once the attack occurred, the plants recognize non-specific molecules of the cell wall of the microorganisms [pathogen- and/or Microbial-Associated Molecular Patterns (PAMPs/MAMPs)], the oral secretions of the herbivores [herbivore-associated molecular patterns (HAMPs)] or signs of cell-plant damage [Damage-Associated Molecular Patterns (DAMPs)], by cell surface pattern recognition receptors (PRRs) (Mithöfer and Boland, 2008; Ramírez-Prado et al., 2018; Hou et al., 2019). Nematode-Associated Molecular Patterns (NAMPs) and its associated receptors have been scarcely described (reviewed in Ali et al., 2018). However, it is generally accepted that during the plant-pathogen interactions, the detection of PAMPs and DAMPs by PRRs triggers a complex network of intracellular signaling cascades leading to defense responses known as PAMP-triggered immunity (PTI). It involves the induction of plant responses coordinated by stress-hormones such as salicylic acid (SA), mostly associated to biotrophic pathogens, and jasmonic acid (JA), and ethylene (ET) against necrotrophic pathogens and herbivores. Additionally, the pathogens generate a diverse repertoire of effector proteins that avoid PTI, a phenomenon known as effector-triggered susceptibility (ETS), against which plants produce specific effector receptors that activate a specific effector-triggered immunity (ETI) (Shigenaga et al., 2017; Ramírez-Prado et al., 2018).

The plant innate immune system comprises local and systemic defense responses. After the attack of a biotroph pathogen and the occurrence of a programmed cell death response in plants, called hypersensitive response (HR), a broad-spectrum immunity to reinfection through the whole plant body, called systemic

acquired resistance (SAR) is activated in the plant. SAR signaling is mainly mediated by SA derived compounds, such as methyl-SA (MeSA). Similarly, numerous beneficial microorganisms are capable of inducing in the plant what is known as induced systemic resistance (ISR) against necrotrophic pathogens and herbivores. ISR is regulated mainly by JA/ethylene (ET) signaling, but dependence on SA signaling has also been reported (Van Wees et al., 2008; Martinez-Medina et al., 2016). Systemic resistance mediated by JA is also induced by wounding and is referred to as wound-induced resistance. This type of systemic resistance against the recognition of molecular patterns promotes an improved state of defenses in the plant, which causes the plant to respond much more quickly and effectively against a biotic attack. This process is known as defense priming, sensitization or trained immunity (Reimer-Michalski and Conrath, 2016; Mauch-Mani et al., 2017; Bürger and Chory, 2019).

While fungal pathogens have detrimental effects on plant physiology, mutualistic fungi augment host defense responses to pathogens and herbivores. Fungal partners secrete bioactive molecules such as small peptide effectors, enzymes and secondary metabolites that facilitate colonization and contribute to both symbiotic and defense against pathogenic relationships (Zeilinger et al., 2015). *Trichoderma* species, arbuscular mycorrhizas, ectomycorrhizas, endophytes, yeasts, and avirulent/hypovirulent strains of certain pathogens are among the main beneficial fungi with biocontrol capacity, also by induction of ISR (Martínez-Medina et al., 2013; Ghorbanpour et al., 2018). In this context, we will focus this review in those studies of the genus *Trichoderma*, mycorrhizal and endophytic fungi as BCAs for nematode control.

General Characteristics of Filamentous Fungi From the Genus *Trichoderma*, Mycorrhizal and Endophytic Fungi as BCAs

Genus *Trichoderma*

The *Trichoderma* genus includes a group of anamorphic filamentous fungi whose teleomorphic status has been described in several species, within the *Hypocrea* genus (Martínez et al., 2015). *Trichoderma* includes fungi characterized by rapid growth that produce large amounts of conidia whose pigmentation can vary from dark to light green. They grow naturally in different habitats in a wide range of climatic zones from polar to equatorial latitudes; hence, they are the most isolated fungi from the soil (Vinale et al., 2008; Martínez et al., 2015). The species of the genus *Trichoderma* are ubiquitous colonizers of cellulosic materials and, therefore, can be found wherever there is decaying plant material available, as well as in the plant rhizosphere. However, there are also species specifically limited to some geographic areas (López-Bucio et al., 2015).

A comparative analysis of the genomes of three species of the genus *Trichoderma*, *T. reesei*, *T. atroviride,* and *T. virens*, has determined that mycoparasitism is the ancestral way of life of this genus and that, subsequently, the rhizosphere colonization evolved. In this respect, the presence of pathogens in the soil and the exudates from the plant-roots favored a shift toward a more generalist way of life (Kubicek et al., 2011, 2019). The comparative genomics of these three specific species suggests that the saprotrophic species *T. reesei* has a smaller set of genes related to mycoparasitism, thus these genes should have subsequently been lost in *T. reesei* and other species (Kubicek et al., 2011).

Trichoderma acts as a symbiont capable of colonizing the roots (without reaching the vascular bundle, limited only to the outermost layers) establishing a complex molecular dialogue with the plant-host. This relationship, together with its easy adaptation to various climatic and edaphic conditions, and its growth speed, give this genus an advantage over many other filamentous fungi and make them excellent candidates as BCAs. Currently, several mechanisms of action of *Trichoderma* are recognized as BCA: mycoparasitism, antibiosis, competition with the pathogen, promotion of plant growth, enhanced plant-tolerance against abiotic stresses and stimulation of its defenses against pathogens (Hermosa et al., 2012; Poveda, 2020).

Mycorrhizal Fungi

Mainly used as biofertilizers, mycorrhizal fungi are obligate symbionts of the roots of 97% of the vascular plants. Ectomycorrhizal fungi (ECMF) and arbuscular mycorrhizal fungi (AMF) are the main groups and of great interest in forestry and agronomy, since the AMF are capable of forming symbiotic interactions with 80% of the plant species (Berruti et al., 2016; Ferlian et al., 2018). ECMF mainly include the filum Basidiomycota, some Ascomycota, and very few Zygomycota, capable of colonizing the intercellular space of roots from forest species and forming the so-called Hartig network (Domínguez-Núñez and Albanesi, 2019). Whereas, the AMF, belong to Glomeromycota and establish a root symbiosis intracellularly where they develop specialized structures called arbuscules in intimate contact with the plant cells cytosol (Berruti et al., 2016).

At present, molecular and paleo-biological studies have shown how the origin of AMF and of terrestrial plants occurred simultaneously over time (about 470 million years ago) from epiphytic fungi that grew on the surface of the first vascular plants. They were also necessary for the success of plant terrestrial colonization (Feijen et al., 2018; Rimington et al., 2018; Strullu-Derrien et al., 2018). Thus, ECMF emerged evolutionarily after AMF, once the plants had already colonized the earth (Hoeksema et al., 2018).

Development of a mycorrhizal symbiosis requires continuous signals exchange between the two symbionts, which triggers coordinated differentiation of both partners. Moreover, the intimate interaction of the arbuscules within the root cells requires also a partial suppression of plant defense responses (Liao et al., 2018). Mycorrhizal hyphae are able to colonize places in the soil where plant roots could never reach; besides, hyphae have the ability to absorb nutrients due to active transporters. The fungus can contribute mostly to the supply of phosphorus to the plant, but also other nutrients with low mobility, such as ammonium, potassium, copper, iron, sulfur, molybdenum or zinc. In response, the plant must provide carbohydrates to the fungus, which meet their needs, although it does not have a negative impact on the plant, due to photosynthetic compensation with the fungal supply of nutrients and reduced root development (Berruti et al., 2016; Chen et al., 2018).

Moreover, it is widely believed that the inoculation of mycorrhizal fungi provides tolerance to host plants against various stresses like heat, salinity, drought, metals and extremes of temperature (Begum et al., 2019).

The similarities between the fungi structural organs used for nutrient uptake between the biotrophic phytopathogenic fungi (haustoria form) and the AMF (arbuscules form), together with the establishment of a long-term relationship with their host, lead to an incorrect response by the plant. First, the plant recognizes PAMPs/MAMPs type molecular patterns (e.g., chitin), which triggers a generalist defensive response of the PTI or MAMP-triggered immunity type. Subsequently, the recognition of effectors released by the fungus in response to plant defenses activates a more specific defensive response (ETI). This part of the plant responses establishes the main difference between the pathogenic fungus and the symbiont fungi (Jacott et al., 2017). The continuous recognition of the AMF within the colonized cells causes the activation of a JA-mediated SAR through the plant termed as mycorrhizal induced resistance (MIR; Pozo and Azcón-Aguilar, 2007). Due to this mechanism, an increase in the systemic accumulation of different defense compounds, such as phytoalexins, suberin, callose, lignin, ROS, phenolic compounds, terpenoids, PR proteins and sulfur amino acids, was observed in mycorrhizal plants. Accordingly, enhanced enzymatic activity of chitinases, glucanases, proteases, ribonucleases, PALs, chalcone synthases and peroxidases was also detected (Hohmann and Messmer, 2017; Jacott et al., 2017; Hill et al., 2018).

Endophytic Fungi

The classic definition of plant endophytes refers to those microorganisms that can be isolated from plant tissues once they have been superficially disinfected. They also do not cause visible damage to plants. This group of microorganisms includes bacterial, archaeal, fungal and protist taxa. Among them, the fungal group play an important role in ecosystems, protecting plants against biotic and abiotic stresses (Lugtenberg et al., 2016; Yan et al., 2019). Numerous studies have indicated that these fungi have a wide biotechnological potential because they biosynthesize molecules, such as enzymes, that can be used as biocontrol and plant-growth-promoting agents as well as in bioremediation, biodegradation or biotransformation (Zheng et al., 2016). In turn, endophytic fungi also have a crucial role in nutrients cycling because, once the plant dies, they behave like saprophytes living from plant tissues (Saikkonen et al., 2015).

Although, endophytic fungi are found in a great variety of plants and ecosystems, there is a strong influence of the local environment in determining endophytic communities; hence, individual endophytes show a different niche occupancy (Glynou et al., 2016), accordingly, they are likely to be affected by future climate change (Giauque and Hawkes, 2016). Despite this geographical distribution, the systemic colonization of plant tissues by endophytic fungi is widely regulated by strong antagonism between the different species (which may run into hundreds), confirming that the systemic effects observed in plants by endophytic fungi are mostly due to chemical movement (Yan et al., 2015).

As mentioned before, endophytic fungi are capable of producing plant-associated metabolites and their analogs, bioactive compounds with diverse biotechnological applications, which have been extensively reviewed by numerous authors (Ludwig-Müller, 2015; Nisa et al., 2015; Saikkonen et al., 2016; Vasundhara et al., 2016; Yan et al., 2018). Among them, compounds with cytotoxic capacity against cancer cells and other diseases, such as taxol, podophyllotoxin, camptothecin, and vinca alkaloids have also been found (Gouda et al., 2016; Uzma et al., 2018). But, they are also capable of producing various mixtures of carbon-based compounds, which are known as volatile organic compounds (VOCs) with a direct application as pesticides (Kaddes et al., 2019).

The use of BCAs from endophytic fungi is a growing area of research as shown from numerous reviews on this topic (Chadha et al., 2015; Card et al., 2016; De Silva et al., 2019; Rabiey et al., 2019). The main mechanisms of direct interaction described include the production of lytic enzymes and/or secondary metabolites (antibiosis) and competition.

Endophytic fungi are also able to induce in plants SAR and ISR against the attack of pests and/or pathogens, but they also need to suppress, at least partially, the defenses of the plants to be able to colonize their tissues (Busby et al., 2016). *Epichloë* genus includes important endophytic fungi of grasses widely studied for their ability to protect the plants due to the synthesis of different alkaloids. Besides, these fungi enhance plant immunity against chewing insects by promoting endogenous defense responses mediated by the JA pathway (Bastias et al., 2017) and against leaf-fungi as *Bipolaris sorokiniana* in perennial ryegrass (*Lolium perenne*) by *Epichloë festucae* var. *lolii* (Li et al., 2018). JA-mediated defenses were also observed after the application of the endophytic fungus *Chaetomium cochlioides* on leaves of *Cirsium arvense* (Hartley et al., 2015). Furthermore, the application of *Penicillium citrinum* and *Aspergillus terreus* in sunflower against the stem rot caused by the fungus *Sclerotium rolfsii* increased the levels of SA and JA in the plant (Waqas et al., 2015).

Direct Interactions of Filamentous Fungi From the Genus *Trichoderma*, Mycorrhizal and Endophytic Fungi for Nematode Control

Genus *Trichoderma*

Sahebani and Hadavi (2008) reported that under greenhouse conditions, the inoculation of tomato seeds with *T. harzianum* significantly reduced the level of disease caused by the nematode *Meloidogyne javanica*; affecting their establishment, development and reproduction (i.e., parameters as the number of galls per plant, the number of egg masses per plant, as well as the number of eggs in each mass). Additionally, they observed a significant reduction in egg hatching, thus demonstrating that this species of the genus *Trichoderma* has significant potential as BCA against this plant parasite. Similarly, root colonization by *T. harzianum* impeded nematode performance locally at multiple stages of the parasitism: invasion, galling and reproduction in tomato (Martínez-Medina et al., 2017b).

Moreover, the effect of both the suspension culture and the exudates produced by different species of *Trichoderma*, in the control of *M. incognita* on tomato plants has been evaluated. The metabolites produced by the fungus, when growing in liquid culture, have a direct and very effective effect on *M. incognita*, since it significantly decreased eggs hatching and increased the mortality of the J2. Soil application of culture suspension (containing the fungus spores) affected more negatively to the population of J2s, in addition to increasing plant growth more effectively than fungus exudates (Khan et al., 2018). In both cases, the species with the best results in nematode control was *T. harzianum*. This study confirms the potential as BCAs against this nematode described previously by Sahebani and Hadavi (2008), but also the potential of other species of this genus as *T. viride*.

Furthermore, approximately 1 month after the penetration of the J2 from the root-knot nematodes (*Meloidogyne* spp.), the eggs are laid surrounded by a gelatinous matrix that constitutes an egg-mass secreted by the female, which is considered as a defensive envelope that protects the eggs against microorganisms allowing eggs survival on the soil. According to Sharon et al. (2007), the gelatinous matrix plays a key role in the process of *Trichoderma* conidial union to the nematode *M. javanica*, thus explaining the parasitism resulting from some species of this genus of fungi. However, it cannot be generalized for all species since, e.g., the growth of *T. harzianum* used in this study was inhibited by this matrix, thus not being effective in biocontrol against *M. javanica*.

The genus *Trichoderma* has an important potential as BCA, not only against root-knot nematodes but also against cyst-forming nematodes by direct parasitism of both eggs and larvae. It increase the level of extracellular enzymes like chitinase and protease, which allow the penetration of the fungus into the eggs by directly affecting very abundant structural components of the eggshell, thus reducing the number of eggs capable of hatching and therefore, the number of infective J2. Specifically, *T. longibrachiatum* has a strong inhibitory effect on the hatching of cysts produced by *Heterodera avenae*, since the spores completely cover the surface of these structures, causing their destruction, which is probably due to the production of enzymes (e.g., chitinases) that caused physiological alterations to the cysts (Zhang et al., 2014). *T. longibrachiatum* also showed an effect on females and on the development of both eggs and J2s of *H. avenae* (Zhang et al., 2017), hence *T. longibrachiatum* can be used as a BCA for the management of *H. avenae* in selected crop species. Within the cyst-forming nematodes, the specie *Globodera pallida* has also a high agronomic impact. Contina et al. (2017) used a strain of *T. harzianum* labeled with GFP as a biomarker to study the fungus-nematode interaction, confirming the reduced infection and reproduction of the nematode. The fungus was capable of negatively affecting both cysts and J2s of *G. pallida*, however, no effect was observed on the eggs. Besides, *T. harzianum* established hyphal colonization in the rhizoplane and the rhizosphere of the potato, possibly providing long-term protection to the infection. Therefore, to date, there are numerous studies that demonstrate the ability of the genus *Trichoderma* to effectively control plant-parasitic nematodes through direct interaction.

Mycorrhizal Fungi

Strictly direct mechanisms of mycorrhizal fungi against nematodes are not yet described as they normally act through the plant host, either providing the plant with higher nutrient and water uptake, altering root morphology by increasing root growth and branching, or making the plants more competitive for nutrients and space with other plants, or altered rhizosphere interactions (Schouteden et al., 2015; Wani et al., 2017). Recent studies have confirmed these mechanisms, for example, mycorrhizas (*Rhizophagus intraradices* and *Funneliformis mosseae*) reduce tomato root penetration by false root-knot nematode *Nacobbus aberrans* (Marro et al., 2018), in the same way as the application of *Glomus intraradices*, *G. mosseae,* and *G. etunicatum* against *M. javanica* in peach trees (Calvet et al., 2001). In contrast, the increment in root colonization by mycorrhizae (*Rhizophagus clarus, Claroideoglomus etunicatum, Gigaspora rosea, G. margarita, Scutellospora calospora,* and *S. heterogama*) caused an increase in the population of nematodes *Pratylenchus brachyurus* in maize crop (Brito et al., 2018) which is opposite to the effect in cotton (Ferreira et al., 2018). All these mechanisms and their effectiveness on the populations and the capacity of infection of the phytoparasitic nematodes will depend closely on the local environmental conditions. In this respect, alterations of potassium, phosphorus and moisture are the main factors negatively involved in the beneficial effect caused by mycorrhizal fungal (Ferreira et al., 2018). Despite some contradictory reports, the use of mycorrhizal fungi for the biological control of plant-parasitic nematodes has been widely studied in numerous crops, as maize (Alvarado-Herrejón et al., 2019), and even in energy crops such as switchgrass (*Panicum virgatum*) and miscanthus (Miscanthus × giganteus; Emery et al., 2017).

Endophytic Fungi

Regarding the nematode-control by endophytic fungi, there is still much speculation on the specific mechanisms by which these fungi antagonize nematodes in most cases, but they are likely quite diverse. Endophytic fungi can directly attack, kill, immobilize, or repel nematodes, confuse them when finding their host, interfere with nurse cell development, compete for resources, or employ a combination of those options (Schouten, 2016). For example, it has been observed how *Acremonium implicatum* can colonize the xylem of tomato roots and, in the soil, parasitize and destroy the eggs of *M. incognita* (Yao et al., 2015). Another example is *F. oxysporum* isolated from banana (*Musa* spp.) that paralyzes and kills the root-lesion nematode (*Pratylenchus goodeyi*; Mwaura et al., 2010). They can also produce nematicidal secondary metabolites, as e.g., chaetoglobosin A, chaetoglobosin B, flavipin, 3-methoxyepicoccone and 4,5,6-trihydroxy-7-methylphthalide produced by *Chaetomium globosum* against *M. incognita* (Khan et al., 2019), VOCs against *M. javanica* produced by *Daldinia cf. concentrica* (Liarzi et al., 2016), or the production of alternariol 9-methyl ether by *Alternaria* sp. against the pinewood nematode

or pine wilt nematode *Bursaphelenchus xylophilus* (Lou et al., 2016). Only a few reports show opposite results, such as the application of entomopathogenic fungus, e.g., *B. bassiana* that increased potato nematodes reproduction and potato tubers damage caused by *Ditylenchus destructor* and *D. dipsaci* (Mwaura et al., 2017).

Filamentous Fungi From the Genus *Trichoderma*, Mycorrhizal and Endophytic Fungi as Systemic Resistance Inducers for Nematode Control

Genus *Trichoderma*

Within their capacities as BCAs, it is worth highlighting the ability of filamentous fungi to stimulate plant defenses against pathogens. Calderón et al. (1993) showed for the first time, the induction of ISR mediated by *Trichoderma* in the grapevine, and one of the first clear demonstrations of induced resistance by *Trichoderma* showed that the treatment of soil with *T. harzianum* improved the resistance of bean plants to diseases caused by fungal pathogens *Botrytis cinerea* and *Colletotrichum lindemuthianu* (Bigirimana et al., 1997). Subsequently, numerous studies have shown that, by colonizing the plant roots, *Trichoderma* stimulates their defense mechanisms against numerous phytopathogenic microorganisms, including nematodes (Hermosa et al., 2012). Numerous attempts have been made to control plant-parasitic nematodes with this genus. *Trichoderma* is capable of inducing resistance in a wide variety of plant species, which leads to transcriptomic, proteomic and metabolomic modifications in the plant (Mukherjee et al., 2012). This systemic defense stimulation prepares the immune response of the plant, allowing a faster response after the priming against the subsequent attack of any kind of pathogen and thus reducing the possibility of disease spread (Hermosa et al., 2012; Bisen et al., 2016; Mendoza-Mendoza et al., 2018). In most cases, this ISR is regulated by a JA/ET signaling, as described by Leonetti et al. (2014). They observed that SA signaling is down-regulated in the early stages of *M. javanica* infection in tomato roots while, the response mediated by JA/ET is induced in tomato roots treated with the fungus, which indicates that the presence of *Trichoderma* activates the ISR within the plant. However, it has recently been described that the SA pathway also participates actively in this regulation (Martínez-Medina et al., 2017a,b). Similarly, the induction of defenses in tomato against *F. oxysporum* f. sp. *lycopersici* by *T. virens* is also, mediated through both JA and SA (Jogaiah et al., 2018). Numerous studies have shown how both hormones coordinate the resistance and susceptibility of plants to nematodes (Martínez-Medina et al., 2017a,b). In this respect, the root-knot nematode-plant interaction is highly dynamic, as plant responses differ significantly between the initial stages and the latest infection stages. Yet, the induction of defenses by *Trichoderma* is a plastic phenomenon. In the first phase, the presence of *T. harzianum* stimulates faster SA-mediated defense responses, to protect the roots against nematode invasion. In the second phase, when *M. incognita* suppresses JA-related defenses in the roots, *Trichoderma* stimulates the expression of JA-dependent defenses, thus antagonizing the suppression of defenses mediated by *M. incognita*, which leads to a reduction in development and reproduction of the nematodes. Once parasitism is established, the fungus increases the activation of SA-dependent defenses probably through the recognition of eggs, which can contribute to improving defenses against the invasion of new juveniles (Martínez-Medina et al., 2017b). Recently, it was proved not only the ability of *T. atroviride* to induce systemic resistance in tomato plants against the nematode *M. javanica*, but its heritability, as the offspring of those plants inoculated with *Trichoderma*, inherited the resistance against *M. javanica* (de Medeiros et al., 2017). This heritability extends to the growth promotion induced by this fungus during its interaction with the plant that is accompanied by a significant reduction in the defenses dependent on the SA and JA pathways. In this respect, it is very interesting to highlight how fungal symbiosis and nematode infection induce epigenetic changes in the plants probably guided by small RNAs (Cabrera et al., 2016; de Medeiros et al., 2017; Medina et al., 2017; Ruiz-Ferrer et al., 2018), that includes changes in plants methylomes (Hewezi et al., 2018). It has been recently demonstrated how epigenetic and post-transcriptional modifications control the interactions between the plants and their surrounding microorganisms, that is, these regulatory mechanisms play a key role in promoting plant resistance to pathogens facilitating the establishment of symbiotic relationships. Therefore, it is important to consider the role of these modifications in the adaptation of the plant to environmental stress, including the resistance of the plant to the pathogens and the formation of symbiotic relationships, as well as in the study of the interaction between plant-pathogen-beneficial microorganism, especially because symbiosis and pathogenesis share similar signaling mechanisms (Zogli and Libault, 2017; De Palma et al., 2019). Furthermore, it has been recently described that commercial formulates of some *Trichoderma* spp. strains induced resistance to *M. incognita* in tomato in split-root system experiments and additionally, an additive effect to that of the tomato *Mi 1.2* resistance gene was also observed (Pocurull et al., 2020). It opens possibilities for integrated pest management of root-knot nematodes with BCAs and other combined control methods.

The high-inoculum dose of *Trichoderma* can also trigger a SA-mediated SAR response similar to that caused by necrotrophic pathogens (Mukherjee et al., 2012; Bisen et al., 2016); hence, the defense induced by this genus can be mediated by ISR or SAR pathways and also by a complex signaling network that connects the SAR and ISR (Mendoza-Mendoza et al., 2018). Therefore, the induction of the SA, ET and JA pathways in the same plant when colonized by *Trichoderma* suggest the presence of alternative ISR pathways and a complex signaling network that connects the SAR and ISR defense response pathways. This varies upon the plant species, the *Trichoderma* strain and the pathogen against which the defense response is directed (Brotman et al., 2012; Nawrocka and Małolepsza, 2013).

Mycorrhizal Fungi

The control of mycorrhyzal symbiosis is a finely tuned process that involves multiple regulatory components functioning at

different levels. Research over the past few years revealed the critical roles of defense phytohormones in modulating mycorrhizal interactions, from early recognition/colonization events up to the final arbuscular formation and degradation (Liao et al., 2018). The ability of mycorrhizal fungi to activate ISR in the plant against the possible attack of pathogens and/or pests has been reviewed by numerous authors, highlighting Pozo and Azcón-Aguilar (2007), Hohmann and Messmer (2017), and Jacott et al. (2017). Mycorrhizal fungi initially trigger plant defense mechanisms similar to a biotrophic pathogen, but then modulate plant responses for successful colonization. In this sense, SA is known to activate responses against biotrophic pathogens, and it is enhanced by mycorrhizal fungi, although, it is subsequently downregulated, which finally allows the symbiotic interaction. Once the symbiosis is established, the microbe-induced resistance and priming regulated by JA is activated, similarly to the responses controlled by JA and ET pathways against necrotrophic pathogens (Hohmann and Messmer, 2017).

Plant resistance by mycorrhizal fungi against phytopathogenic nematodes have been described, however, in conventional pathogenic-assays, it is difficult to distinguish to what extent the decrease in infection is due solely to systemic resistance or to a direct effect. To try to determine the ability of mycorrhiza induced resistance against nematodes a good strategy is the use of split-root methodology. In this respect, Vos et al. (2012a) showed how the inoculation of tomato roots with *F. mosseae* in one of the compartments reduced the infection rates of *M. incognita* and *Pratylenchus penetrans* in the compartment without fungus, through altered root exudation. The mechanisms through which this increase in the systemic defensive capacity of the roots occurs are related to the activation of genes that encode chitinases, PR proteins, enzymes involved in the detoxification of ROS (whose accumulation occurs during hypertrophy and death cell caused by nematodes) such as glutathione S-transferase or the superoxide dismutase (SOD), enzymes involved in the lignin biosynthesis, and in the shikimate pathway which in turn, produces precursors of various aromatic secondary metabolites against nematodes (Schouteden et al., 2015; Sharma and Sharma, 2017b; Balestrini et al., 2019).

Concerning hormones not directly related to plant defensive responses, it is known that strigolactones, after being exuded from the root, activate hyphal branching and enhanced growth and energy metabolism of symbiotic AMF, and once the symbiosis is established, its production by the plant roots fades (Rochange et al., 2019). Regarding the nematodes, it has been proven that the strigolactones do not contribute to cyst nematode (*Heterodera schachtii*) hatching but they do play a role in host attraction and subsequent invasion (Martinez et al., 2019). In rice, signaling mediated by strigolactones suppresses jasmonate accumulation and promotes RKN infection (Lahari et al., 2019). In contrast, strigolactones play a positive role in nematode defense in tomato (Xu et al., 2018). Although, further research needs to be undertaken, another way to modulate plant responses by mycorrhization could be altering strigolactones -plants production, which might influence plant-nematode interaction.

Regarding the ECMF, colonization of pines (*Pinus thunbergii*) promoted a lasting SAR against the pine wilt nematode *Bursaphelenchus xylophilus*, which is transmitted by beetles of the genus *Monochamus* and feeds by colonizing the vascular bundles (Nakashima et al., 2016). Interestingly, those fungi do not only act systemically controlling nematodes-infection but enhance plant defenses against pathogens transmitted by the nematodes, as it is the case with the Grapevine Fanleaf Virus (GFLV) transmitted by the nematode vector *Xiphinema index*, against which AMF *R. intraradices* induces systemic protection (Hao et al., 2018).

Other examples of systemic resistance produced by AMF are a reduced nematode infection, due to the activity of phenolics and defensive plant enzymes, i.e., peroxidase (PO), polyphenol oxidase (PPO), and SOD, together with a significant reduction of malondialdehyde (MDA) and hydrogen peroxide (H_2O_2) content in tomato roots inoculated with *R. irregularis*, that also enhanced plant growth (Sharma and Sharma, 2017a). Similarly, the application of *G. mosseae* using a split-root system against the sedentary nematode *M. incognita* and the migratory nematode *P. penetrans*, in tomato indicated that the infection by both different types of nematodes can be controlled by AMF, but only systemically (Vos et al., 2012b). Similar results were observed in banana (*Musa* spp.) with split-roots using AMF *Glomus intraradices* against the migratory nematodes *Radopholus similis* and *Pratylenchus coffeae* (Elsen et al., 2008). In other cases, it is not clear whether ISR or a direct mechanism are acting against nematodes or even both mechanisms simultaneously. One example is the reduction of *P. penetrans* infestation in apple seedlings by AMF (Ceustermans et al., 2018), and of *Meloidogyne arenaria* in red ginger (*Alpinia purpurata*) by *Gigaspora albida*, *Claroideoglomus etunicatum,* and *Acaulospora longula* (Da Silva-Campos et al., 2017), or the control of the migratory endoparasitic nematode *Scutellonema bradys* in yam (*Dioscorea* spp.) by *F. mosseae* and *Glomus dussii* (Tchabi et al., 2016). In contrast, Frew et al. (2018) described that the root application of *Claroideoglomus entunicatum*, *Funneliformis coronatum*, *R. irregularis,* and *F. mosseae* in wheat produced an increase of the plant-parasitic nematode *Pratylenchus neglectus* populations. This fact is due to a decrease of root benzoxazinoid glucoside accumulation, an important defense metabolite against the nematode, probably necessary for the root colonization of the fungus itself.

Endophytic Fungi

The split root system methodology was also used to study systemic resistance induced by endophytic fungi, as *F. oxysporum* against the root-knot nematode *M. incognita* in *A. thaliana* (Martinuz et al., 2015), in tomato (Dababat and Sikora, 2007), and in banana against the burrowing nematode *Radopholus simili* (Vu et al., 2006). Another endophytic fungi, *Fusarium moniliforme* also ISR toward *Meloidogyne graminicola* in rice (Le et al., 2016). *Fusarium* spp. achieve this systemic induction due to the synthesis and release of chemical compounds such as 4-hydroxybenzoicacid, indole-3-acetic acid (IAA) and gibepyrone D, which, in addition to being toxic directly to the nematodes, induce defense mechanisms against nematodes in plants (Bogner et al., 2017). But endophytic fungi act also systemically causing the synthesis and transport of chemical defense components in the plant. This is the case of the secondary metabolite forskolin

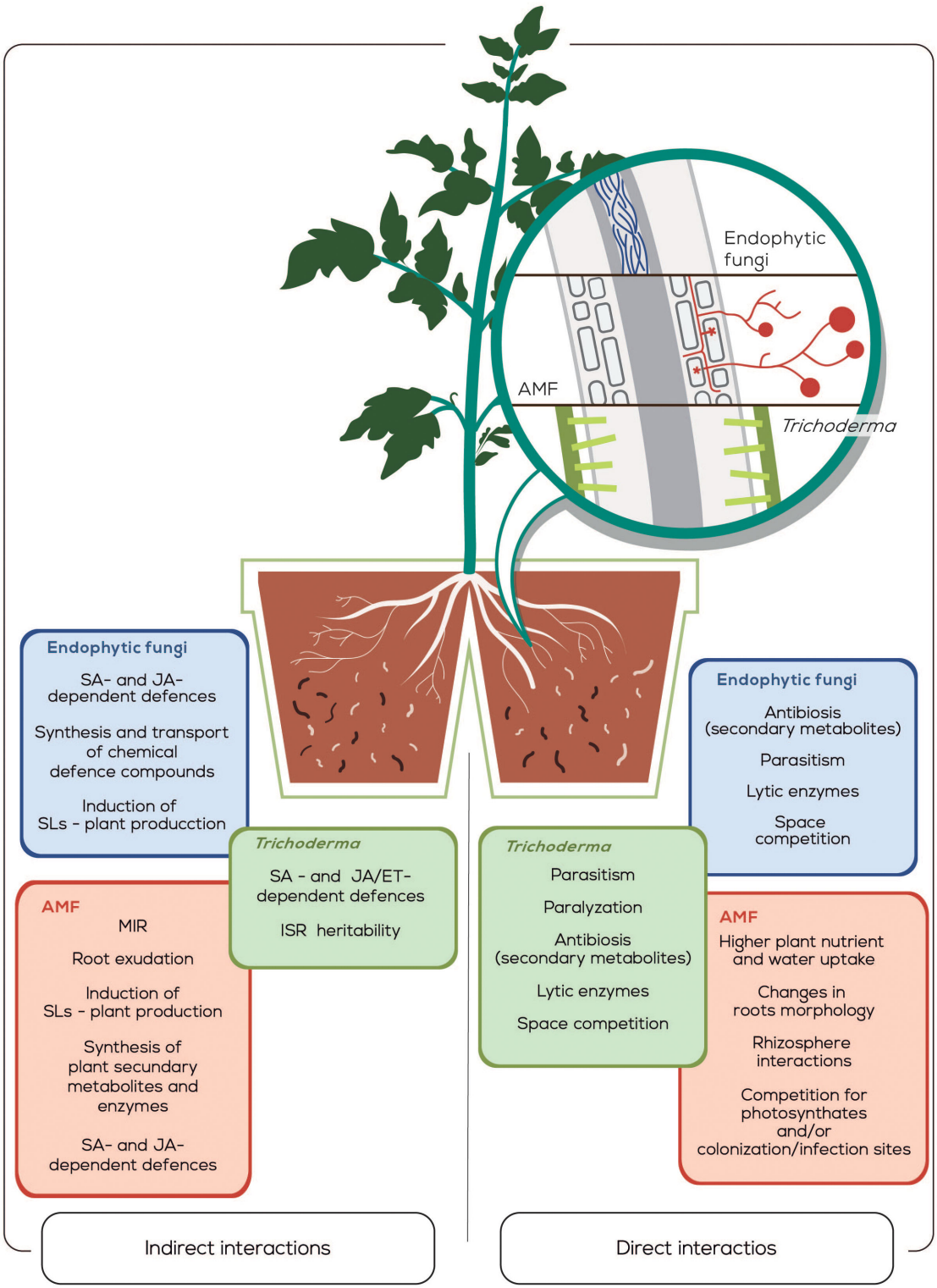

FIGURE 1 | Graphical representation of direct and induced resistance against plant-parasitic nematodes by filamentous fungi in a split-root system. The different tissue colonization strategies used by the three fungal groups are schematically represented in the microscopic enlargement of the roots. The mechanisms of fungus to induce resistance in plants either by direct or indirect interaction strategies against nematodes are indicated in colored boxes. The effects of the filamentous fungi on nematodes basically are: To increase J2 mortality, to decrease the hatching and/or nematodes infection rate, as well as to alter nematodes development inside the plant and/or their reproduction. Abbreviations correspond to arbuscular mycorrhizal fungi (AMF), salicylic acid (SA), jasmonic acid (JA), systemic acquired resistance (SAR), induced systemic resistance (ISR), strigolactones (SLs), and mycorrhizal induced resistance (MIR).

synthesized in the medicinal plant *Coleus forskohlii* after being inoculated with the endophytic fungi of the stem *Phialemoniopsis cornearis* and *Macrophomina pseudophaseolina* and radicular *Fusarium redolens*, as they enhance the expression of diterpene synthases, that enhances tolerance to *M. incognita* (Mastan et al., 2019). The ability of *P. indica* to modify plant stress-hormones has been extensively studied (Le-Xu et al., 2018). Although, several studies show that the application of this fungus against *M. incognita* (Varkey et al., 2018) and *Heterodera glycines* (Bajaj et al., 2015) reduces the incidence of the disease and improves plant growth, the exact role of systemic resistance is still unsolved. Similarly, *Phialemonium inflatum* in cotton against *M. incognita* (Zhou et al., 2018), *Nigrospora* sp. in sengon plant (*Paraserianthes falcataria*) against *Meloidogyne* spp. (Amin, 2015), *Penicillium brefeldianum* in melon against *M. incognita* (Miao et al., 2019) or *Fusarium solani* and *F. oxysporum* in tomato against *M. incognita* (Bogner et al., 2016) were described.

Pochonia chlamydosporia is a nematophagous fungus, but it is also a root endophyte that can colonize the roots of higher plants due to a partial suppression of defensive responses mediated by JA. They also reduce the flowering time, stimulate plant growth and increase seed production in *A. thaliana* (Zavala-González et al., 2017) and a greater root colonization was directly related to a lower incidence of *M. javanica* in tomato roots (Escudero et al., 2017). *P. chlamydosporia* induces systemic resistance against *M. javanica* in tomato (but not in cucumber) by activating a defensive response mediated by SA (Ghahremani et al., 2019). Interestingly, in the absence of nematodes, it is observed how it promotes systemic resistance mediated by JA in barley (Larriba et al., 2015). Another example in forest plant-species is that the presence of the endophytic fungi *Gaeumannomyces cylindrosporus*, *Paraphoma chrysanthemicola*, *Phialophora mustea*, *Exophiala salmonis* and *Cladosporium cladosporioides* modifies the systemic defensive responses reducing the incidence of the nematode *Bursaphelenchus xylophilus* in pine (Chu et al., 2019). On the other side, the attack of the nematodes can systematically alter the defenses of the plant and prevent its colonization by endophytic fungi. This has been observed in *Pinus tabulaeformis* after the infection of the pinewood nematode (*Bursaphelenchus xylophilus*) where the diversity of endophytic fungi in the roots was reduced to about 80% (Chu et al., 2018).

In the same way as for mycorrhizal fungi, strigolactones were necessary for the establishment of the beneficial interaction, at least in the case of the endophytic fungus *Mucor* sp. on *A. thaliana* roots. Once the symbiosis is established, the fungi decompose strigolactones *in planta* and downregulate the expression of strigolactones biosynthesis genes (Rozpądek et al., 2018), preventing, therefore, root invasion by nematodes (Martinez et al., 2019).

CONCLUSION

Biocontrol strategies for plant-parasitic-nematodes constitute a valid alternative to toxic chemical nematicides. Thereby, a wide diversity of effective strategies based on the use of filamentous fungi used as BCAs are described. They work through two main kinds of mechanisms of action, i.e., those that include the production of secondary metabolites (antibiosis), lytic enzymes, and space competition by *Trichoderma*. AMF directly acts providing higher nutrient and water uptake to the plant, modifying root morphology and altering the rhizosphere interactions, or competing for photosynthates or colonization/infection sites. Endophytic fungi reduce the attack of the plant-parasitic nematodes by parasitism, by paralyzing the nematodes, through antibiosis, by lytic enzymes production and also by space competition. The second group of action mechanisms are the induction of plant defenses, such as the activation of SAR and ISR by *Trichoderma*, which seems also heritable. As well as, the modification of roots exudates, strigolactones production, plant secondary metabolites and enzymes production by AMF. Finally, the induction of SAR and ISR, the transport of chemical defense components through the plant and the strigolactones production by endophytic fungi (**Figure 1**).

The scenario in agricultural systems is very complex as different microorganisms of the rhizosphere and plant-species are present; thus they may respond differently to BCAs. The integration of all microorganisms and plant-responses will determine the final output after the BCA treatment as it is a multifactorial response. Additionally, the strong influence of the local environment that for example, highly determine endophytic communities, is another complexity level to include in the agricultural systems. Therefore, BCAs can have variable control ability when established in different soils, and their success can be difficult to predict. However, there are commercial formulates with some of those filamentous fungi mentioned, effective for nematodes control in experimental conditions for particular crops, but scarce scientific information is still available of experiments on the field. The integration of empirical data knowledge in the field after the treatment with a particular fungi strain or formulate, together with detailed analysis of the plant responses at the molecular level in a particular crop could help to a deep understanding of those complex interactions. Yet, holistic approaches for soil-rhizosphere microbiota detection and characterization of specific plant responses could assist in identifying and predicting major problems as the presence of BCA antagonist in the soil or changes in the rhizosphere biota that may influence the final output. This would allow better practices for an effective nematode-control on a particular crop. Moreover, an in-depth knowledge on the molecular mechanisms of induced resistance by BCAs could allow perhaps to manipulate the plants directly, however, synergic effects derived for example of secondary metabolites induced also by some BCAs should also be integrated. Another question is that usually, BCAs based control methods are slow to implement as they may need time to increase their population up to the level required to be effective for PPN control. Yet, the growers need alternative control methods during this period. The durability of those BCA-based techniques is also a

great interrogate because of the mentioned complexity of the agricultural systems.

Perhaps, a feasible scenario would be to design integrated pest management based first on a well stablished method on a ground base, such as those chemically based, and slowly to introduce BCAs together with a detailed monitoring plan with the intention to gradually decrease the dependence on chemical control. We should not also discard the possible implementation of other complementary alternative control methods, including those based on host plant genotypes that may have an enhanced response in combination with BCAs.

In summary, the use of filamentous fungi of the genus *Trichoderma*, mycorrhizal and endophytic fungi as BCAs is a promising durable biocontrol strategy in agriculture against plant-parasitic nematodes (**Figure 1**) due mainly to the wide diversity of mechanisms of action described above, that in most of the cases act also in combination. However, there are still major question to address with further research. Moreover, recent reports point to a heritable biocontrol after BCAs infection possibly driven by still not well-known epigenetic mechanisms, opening a new field of research with special applied interest.

AUTHOR CONTRIBUTIONS

JP and PA-U contributed to the search for information and references in different databases, they gathered most of the peer-reviewed manuscript used on this topic, and highly contributed to the manuscript writing. CE contributed to the manuscript writing and the correction and critical reading, as well as to the knowledge on the nematode field.

FUNDING

This work was supported by the Spanish Government (AGL2016-75287-R to CE), by the Castilla–La Mancha Government (SBPLY/17/180501/000287 to CE) and by The Ministry of Science, Innovation and Universities (RED2018-102407-T to CE).

ACKNOWLEDGMENTS

Thanks to Darío Rodríguez-Prieto for preparing the infographic-summary of the entire manuscript.

REFERENCES

Ali, M. A., Anjam, M. S., Nawaz, M. A., Lam, H.-M., and Chung, G. (2018). Signal Transduction in Plant–Nematode Interactions. *Int. J. Mol. Sci.* 19:1648. doi: 10.3390/ijms19061648

Alvarado-Herrejón, M., Larsen, J., Gavito, M. E., Jaramillo-López, P. F., Vestberg, M., Martínez-Trujillo, M., et al. (2019). Relation between arbuscular mycorrhizal fungi, root-lesion nematodes and soil characteristics in maize agroecosystems. *Appl. Soil Ecol.* 135, 1–8. doi: 10.1016/j.apsoil.2018.10.019

Amin, N. (2015). Nematicidal activity of root exudates of sengon plant inoculated with endophytic fungi *Nigrospora* sp. to control of root-knot nematode *Meloidogyne* spp. *J. Chem. Pharm Res.* 7, 307–310.

Bajaj, R., Hu, W., Huang, Y., Chen, S., Prasad, R., Varma, A., et al. (2015). The beneficial root endophyte *Piriformospora indica* reduces egg density of the soybean cyst nematode. *Biol. Control* 90, 193–199. doi: 10.1016/j.biocontrol.2015.05.021

Balestrini, R., Rosso, L. C., Veronico, P., Melillo, M. T., De Luca, F., Fanelli, E., et al. (2019). Transcriptomic responses to water deficit and nematode infection in mycorrhizal tomato roots. *Front. Microbiol.* 10:1807. doi: 10.3389/fmicb.2019.01807

Bastias, D. A., Martínez-Ghersa, M. A., Ballaré, C. L., and Gundel, P. E. (2017). *Epichloë* fungal endophytes and plant defenses: not just alkaloids. *Trends Plant Sci.* 22, 939–948. doi: 10.1016/j.tplants.2017.08.005

Begum, N., Qin, C., Ahanger, M. A., Raza, S., Khan, M. I., Ahmed, N., et al. (2019). Role of arbuscular mycorrhizal fungi in plant growth regulation: implications in abiotic stress tolerance. *Front. Plant Sci.* 10:1068. doi: 10.3389/fpls.2019.01068

Berruti, A., Lumini, E., Balestrini, R., and Bianciotto, V. (2016). Arbuscular mycorrhizal fungi as natural biofertilizers: let's benefit from past successes. *Front. Microbiol.* 6:1559. doi: 10.3389/fmicb.2015.01559

Bigirimana, J., De Meyer, G., Poppe, J., Elad, Y., and Höfte, M. (1997). Induction of systemic resistance on bean (*Phaseolus vulgaris*) by *Trichoderma harziamum*. *Univ. Gent Fac. Landbouwwet. Meded.* 62, 1001–1007.

Bisen, K., Keswani, C., Patel, J. S., Sarma, B. K., and Singh, H. B. (2016). "*Trichoderma* spp.: efficient inducers of systemic resistance in plants," in *Microbial-Mediated Induced Systemic Resistance in Plants*, eds D. K. Choudhary, and A. Varma (Singapore: Springer), 185–195. doi: 10.1007/978-981-10-0388-2_12

Bogner, C. W., Kamdem, R. S., Sichtermann, G., Matthäus, C., Hölscher, D., Popp, J., et al. (2017). Bioactive secondary metabolites with multiple activities from a fungal endophyte. *Microb. Biotechnol.* 10, 175–188. doi: 10.1111/1751-7915.12467

Bogner, C. W., Kariuki, G. M., Elashry, A., Sichtermann, G., Buch, A. K., Mishra, B., et al. (2016). Fungal root endophytes of tomato from Kenya and their nematode biocontrol potential. *Mycol. Prog.* 15:30. doi: 10.1007/s11557-016-1169-9

Bradshaw, C. J., Leroy, B., Bellard, C., Roiz, D., Albert, C., Fournier, A., et al. (2016). Massive yet grossly underestimated global costs of invasive insects. *Nat. Commun.* 7, 1–8. doi: 10.1038/ncomms12986

Brito, O. D. C., Hernandes, I., Ferreira, J. C. A., Cardoso, M. R., Alberton, O., and Dias-Arieira, C. R. (2018). Association between arbuscular mycorrhizal fungi and *Pratylenchus brachyurus* in maize crop. *Chil. J. Agric. Res.* 78, 521–527. doi: 10.4067/S0718-58392018000400521

Brotman, Y., Lisec, J., Méret, M., Chet, I., Willmitzer, L., and Viterbo, A. (2012). Transcript and metabolite analysis of the *Trichoderma*-induced systemic resistance response to *Pseudomonas syringae* in *Arabidopsis thaliana*. *Microbiology* 158, 139–146. doi: 10.1099/mic.0.052621-0

Bürger, M., and Chory, J. (2019). Stressed out about hormones: how plants orchestrate immunity. *Cell Host Microbe* 26, 163–172. doi: 10.1016/j.chom.2019.07.006

Busby, P. E., Ridout, M., and Newcombe, G. (2016). Fungal endophytes: modifiers of plant disease. *Plant Mol. Biol.* 90, 645–655. doi: 10.1007/s11103-015-0412-0

Cabrera, J., Barcala, M., García, A., Rio-Machín, A., Medina, C., Jaubert-Possamai, S., et al. (2016). Differentially expressed small RNAs in *Arabidopsis galls* formed by *Meloidogyne javanica*: a functional role for miR390 and its TAS 3-derived tasi RNAs. *New Phytol.* 209, 1625–1640. doi: 10.1111/nph.13735

Calderón, A. A., Zapata, J. M., Muñoz, R., Pedreño, M. A., and Barceló, A. R. (1993). Resveratrol production as a part of the hypersensitive-like response of grapevine cells to an elicitor from *Trichoderma viride*. *New Phytol.* 124, 455–463. doi: 10.1111/j.1469-8137.1993.tb03836.x

Calvet, C., Pinochet, J., Hernández-Dorrego, A., Estaún, V., and Camprubí, A. (2001). Field microplot performance of the peach-almond hybrid GF-677 after inoculation with arbuscular mycorrhizal fungi in a replant soil infested with root-knot nematodes. *Mycorrhiza* 10, 295–300. doi: 10.1007/PL00009998

Card, S., Johnson, L., Teasdale, S., and Caradus, J. (2016). Deciphering endophyte behaviour: the link between endophyte biology and efficacious biological control agents. *FEMS Microbiol. Ecol.* 92:fiw114. doi: 10.1093/femsec/fiw114

Ceustermans, A., Van Hemelrijck, W., Van Campenhout, J., and Bylemans, D. (2018). Effect of arbuscular mycorrhizal fungi on *Pratylenchus penetrans* infestation in apple seedlings under greenhouse conditions. *Pathogens* 7:76. doi: 10.3390/pathogens7040076

Chadha, N., Mishra, M., Rajpal, K., Bajaj, R., Choudhary, D. K., and Varma, A. (2015). An ecological role of fungal endophytes to ameliorate plants under biotic stress. *Arch. Microbiol.* 197, 869–881. doi: 10.1007/s00203-015-1130-3

Chen, M., Arato, M., Borghi, L., Nouri, E., and Reinhardt, D. (2018). Beneficial services of arbuscular mycorrhizal fungi - from ecology to application. *Front. Plant Sci.* 9:1270. doi: 10.3389/fpls.2018.01270

Chu, H., Tang, M., Wang, H., and Wang, C. (2018). Pinewood nematode infection alters root mycoflora of *Pinus tabulaeformis* Carr. *J. Appl. Microbiol.* 125, 554–563. doi: 10.1111/jam.13883

Chu, H., Wang, C., Li, Z., Wang, H., Xiao, Y., Chen, J., et al. (2019). The dark septate endophytes and ectomycorrhizal fungi effect on *Pinus tabulaeformis* Carr. seedling growth and their potential effects to pine wilt disease resistance. *Forests* 10:140. doi: 10.3390/f10020140

Contina, J. B., Dandurand, L. M., and Knudsen, G. R. (2017). Use of GFP-tagged *Trichoderma harzianum* as a tool to study the biological control of the potato cyst nematode *Globodera pallida*. *Appl. Soil Ecol.* 115, 31–37. doi: 10.1016/j.apsoil.2017.03.010

Da Silva-Campos, M. A., Da Silva, F. S. B., Yano-Melo, A. M., De Melo, N. F., and Maia, L. C. (2017). Application of arbuscular mycorrhizal fungi during the acclimatization of *Alpinia purpurata* to induce tolerance to *Meloidogyne arenaria*. *Plant Pathol. J.* 33, 329–336. doi: 10.5423/PPJ.OA.04.2016.0094

Dababat, A. A., and Sikora, R. A. (2007). Induced resistance by the mutualistic endophyte, *Fusarium oxysporum* strain 162, toward *Meloidogyne incognita* on tomato. *Biocontrol Sci. Technol.* 17, 969–975. doi: 10.1080/09583150701582057

D'Addabbo, T., Laquale, S., Perniola, M., and Candido, V. (2019). Biostimulants for plant growth promotion and sustainable management of phytoparasitic nematodes in vegetable crops. *Agronomy* 9:616. doi: 10.3390/agronomy9100616

de Medeiros, H. A., de Araújo Filho, J. V., De Freitas, L. G., Castillo, P., Rubio, M. B., Hermosa, R., et al. (2017). Tomato progeny inherit resistance to the nematode *Meloidogyne javanica* linked to plant growth induced by the biocontrol fungus *Trichoderma atroviride*. *Sci. Rep.* 7:40216. doi: 10.1038/srep40216

De Palma, M., Salzano, M., Villano, C., Aversano, R., Lorito, M., Ruocco, M., et al. (2019). Transcriptome reprogramming, epigenetic modifications and alternative splicing orchestrate the tomato root response to the beneficial fungus *Trichoderma harzianum*. *Hortic. Res.* 6:5. doi: 10.1038/s41438-018-0079-1

De Silva, N. I., Brooks, S., Lumyong, S., and Hyde, K. D. (2019). Use of endophytes as biocontrol agents. *Fungal Biol. Rev.* 33, 133–148. doi: 10.1016/j.fbr.2018.10.001

Domínguez-Núñez, J. A., and Albanesi, A. S. (2019). "Ectomycorrhizal fungi as biofertilizers in forestry," in *Biostimulants in Plant Science*, eds A. Beck, S. Uhac, and A. A. De Marco (Rijeka: IntechOpen). doi: 10.5772/intechopen.88585

Elsen, A., Gervacio, D., Swennen, R., and De Waele, D. (2008). AMF-induced biocontrol against plant parasitic nematodes in *Musa* sp.: a systemic effect. *Mycorrhiza* 18, 251–256. doi: 10.1007/s00572-008-0173-6

Emery, S. M., Reid, M. L., Bell-Dereske, L., and Gross, K. L. (2017). Soil mycorrhizal and nematode diversity vary in response to bioenergy crop identity and fertilization. *GCB Bioenergy* 9, 1644–1656. doi: 10.1111/gcbb.12460

Escudero, N., Lopez-Moya, F., Ghahremani, Z., Zavala-Gonzalez, E. A., Alaguero-Cordovilla, A., Ros-Ibañez, C., et al. (2017). Chitosan increases tomato root colonization by *Pochonia chlamydosporia* and their combination reduces root-knot nematode damage. *Front. Plant Sci.* 8:1415. doi: 10.3389/fpls.2017.01415

FAO (2017). *The Future of Food and Agriculture*. Rome: Trends and challenges.

Feijen, F. A., Vos, R. A., Nuytinck, J., and Merckx, V. S. (2018). Evolutionary dynamics of mycorrhizal symbiosis in land plant diversification. *Sci. Rep.* 8:10698. doi: 10.1038/s41598-018-28920-x

Ferlian, O., Biere, A., Bonfante, P., Buscot, F., Eisenhauer, N., Fernandez, I., et al. (2018). Growing research networks on mycorrhizae for mutual benefits. *Trends Plant Sci.* 23, 975–984. doi: 10.1016/j.tplants.2018.08.008

Ferreira, B. S., Santana, M. V., Macedo, R. S., Silva, J. O., Carneiro, M. A., and Rocha, M. R. (2018). Co-occurrence patterns between plant-parasitic nematodes and arbuscular mycorrhizal fungi are driven by environmental factors. *Agric. Ecosyst. Environ.* 265, 54–61. doi: 10.1016/j.agee.2018.05.020

Frew, A., Powell, J. R., Glauser, G., Bennett, A. E., and Johnson, S. N. (2018). Mycorrhizal fungi enhance nutrient uptake but disarm defences in plant roots, promoting plant-parasitic nematode populations. *Soil Biol. Biochem.* 126, 123–132. doi: 10.1016/j.soilbio.2018.08.019

Ghahremani, Z., Escudero, N., Saus, E., Gabaldón, T., and Sorribas, F. J. (2019). *Pochonia chlamydosporia* induces plant-dependent systemic resistance to *Meloidogyne incognita*. *Front. Plant Sci.* 10:945. doi: 10.3389/fpls.2019.00945

Ghorbanpour, M., Omidvari, M., Abbaszadeh-Dahaji, P., Omidvar, R., and Kariman, K. (2018). Mechanisms underlying the protective effects of beneficial fungi against plant diseases. *Biol. Control* 117, 147–157. doi: 10.1016/j.biocontrol.2017.11.006

Giauque, H., and Hawkes, C. V. (2016). Historical and current climate drive spatial and temporal patterns in fungal endophyte diversity. *Fungal Ecol.* 20, 108–114. doi: 10.1016/j.funeco.2015.12.005

Glynou, K., Ali, T., Buch, A. K., Haghi Kia, S., Ploch, S., Xia, X., et al. (2016). The local environment determines the assembly of root endophytic fungi at a continental scale. *Environ. Microbiol.* 18, 2418–2434. doi: 10.1111/1462-2920.13112

Gouda, S., Das, G., Sen, S. K., Shin, H. S., and Patra, J. K. (2016). Endophytes: a treasure house of bioactive compounds of medicinal importance. *Front. Microbiol.* 7:1538. doi: 10.3389/fmicb.2016.01538

Hao, Z., van Tuinen, D., Fayolle, L., Chatagnier, O., Li, X., Chen, B., et al. (2018). Arbuscular mycorrhiza affects grapevine fanleaf virus transmission by the nematode vector *Xiphinema index*. *App. Soil Ecol.* 129, 107–111. doi: 10.1016/j.apsoil.2018.05.007

Hartley, S. E., Eschen, R., Horwood, J. M., Gange, A. C., and Hill, E. M. (2015). Infection by a foliar endophyte elicits novel arabidopside-based plant defence reactions in its host, *Cirsium arvense*. *New Phytol.* 205, 816–827. doi: 10.1111/nph.13067

Hermosa, R., Viterbo, A., Chet, I., and Monte, E. (2012). Plant-beneficial effects of *Trichoderma* and of its genes. *Microbiology* 158, 17–25. doi: 10.1099/mic.0.052274-0

Hewezi, T., Pantalone, V., Bennett, M., Stewart, C. N., and Burch-Smith, T. M. (2018). Phytopathogen-induced changes to plant methylomes. *Plant Cell Rep.* 37, 17–23. doi: 10.1007/s00299-017-2188-y

Hill, E. M., Robinson, L. A., Abdul-Sada, A., Vanbergen, A. J., Hodge, A., and Hartley, S. E. (2018). Arbuscular mycorrhizal fungi and plant chemical defence: effects of colonisation on aboveground and belowground metabolomes. *J. Chem. Ecol.* 44, 198–208. doi: 10.1007/s10886-017-0921-1

Hoeksema, J. D., Bever, J. D., Chakraborty, S., Chaudhary, V. B., Gardes, M., Gehring, C. A., et al. (2018). Evolutionary history of plant hosts and fungal symbionts predicts the strength of mycorrhizal mutualism. *Commun. Biol.* 1:116. doi: 10.1038/s42003-018-0120-9

Hohmann, P., and Messmer, M. M. (2017). Breeding for mycorrhizal symbiosis: focus on disease resistance. *Euphytica* 213:113. doi: 10.1007/s10681-017-1900-x

Hou, S., Liu, Z., and Wu, D. (2019). Damage-associated molecular pattern-triggered immunity in plants. *Front. Plant Sci.* 10:646. doi: 10.3389/fpls.2019.00646

Jacott, C., Murray, J., and Ridout, C. (2017). Trade-offs in arbuscular mycorrhizal symbiosis: disease resistance, growth responses and perspectives for crop breeding. *Agronomy* 7:75. doi: 10.3390/agronomy7040075

Jogaiah, S., Abdelrahman, M., Tran, L. S. P., and Ito, S. I. (2018). Different mechanisms of *Trichoderma virens*-mediated resistance in tomato against Fusarium wilt involve the jasmonic and salicylic acid pathways. *Mol. Plant Pathol.* 19, 870–882. doi: 10.1111/mpp.12571

Jones, J. T., Haegeman, A., Danchin, E. G., Gaur, H. S., Helder, J., Jones, M. G., et al. (2013). Top 10 plant-parasitic nematodes in molecular plant pathology. *Mol. Plant Pathol.* 14, 946–961. doi: 10.1111/mpp.12057

Kaddes, A., Fauconnier, M. L., Sassi, K., Nasraoui, B., and Jijakli, M. H. (2019). Endophytic fungal volatile compounds as solution for sustainable agriculture. *Molecules* 24:1065. doi: 10.3390/molecules24061065

Khan, B., Yan, W., Wei, S., Wang, Z., Zhao, S., Cao, L., et al. (2019). Nematicidal metabolites from endophytic fungus *Chaetomium globosum* YSC5. *FEMS Microbiol. Lett.* 366:fnz169. doi: 10.1093/femsle/fnz169

Khan, M. R., Ahmad, I., and Ahamad, F. (2018). Effect of pure culture and culture filtrates of *Trichoderma* species on root-knot nematode, *Meloidogyne incognita* infesting tomato. *Indian Phytopathol.* 71, 265–274. doi: 10.1007/s42360-018-0031-1

Khan, Z., and Kim, Y. H. (2007). A review on the role of predatory soil nematodes in the biological control of plant parasitic nematodes. *Appl. Soil Ecol.* 35, 370–379. doi: 10.1016/j.apsoil.2006.07.007

Kubicek, C. P., Herrera-Estrella, A., Seidl-Seiboth, V., Martinez, D. A., Druzhinina, I. S., Thon, M., et al. (2011). Comparative genome sequence analysis underscores mycoparasitism as the ancestral life style of *Trichoderma*. *Genome Biol.* 12:R40. doi: 10.1186/gb-2011-12-4-r40

Kubicek, C. P., Steindorff, A. S., Chenthamara, K., Manganiello, G., Henrissat, B., Zhang, J., et al. (2019). Evolution and comparative genomics of the most common *Trichoderma* species. *BMC Genomics* 20:485. doi: 10.1186/s12864-019-5680-7

Lahari, Z., Ullah, C., Kyndt, T., Gershenzon, J., and Gheysen, G. (2019). Strigolactones enhance root-knot nematode (*Meloidogyne graminicola*) infection in rice by antagonizing the jasmonate pathway. *New Phytol.* 224, 454–465. doi: 10.1111/nph.15953

Larriba, E., Jaime, M. D., Nislow, C., Martín-Nieto, J., and Lopez-Llorca, L. V. (2015). Endophytic colonization of barley (*Hordeum vulgare*) roots by the nematophagous fungus *Pochonia chlamydosporia* reveals plant growth promotion and a general defense and stress transcriptomic response. *J. Plant Res.* 128, 665–678. doi: 10.1007/s10265-015-0731-x

Le, H. T. T., Padgham, J. L., Hagemann, M. H., Sikora, R. A., and Schouten, A. (2016). Developmental and behavioural effects of the endophytic *Fusarium moniliforme* Fe14 towards *Meloidogyne graminicola* in rice. *Ann. Appl. Biol.* 169, 134–143.

Leonetti, P., Costanza, A., Zonno, M., Molinari, S., and Altomare, C. (2014). How fungi interact with nematode to activate the plant defence response to tomato plants. *Commun. Agric. Appl. Biol. Sci.* 79, 357–362.

Le-Xu, C. W., Oelmüller, R., and Zhang, W. (2018). Role of phytohormones in *Piriformospora indica*-induced growth promotion and stress tolerance in plants: more questions than answers. *Front. Microbiol.* 9:1646. doi: 10.3389/fmicb.2018.01646

Li, F., Christensen, M. J., Gao, P., Li, Y., and Duan, T. (2018). An arbuscular mycorrhizal fungus and *Epichloë festucae* var. lolii reduce *Bipolaris sorokiniana* disease incidence and improve perennial ryegrass growth. *Mycorrhiza* 28, 159–169. doi: 10.1007/s00572-017-0813-9

Liao, D., Wang, S., Cui, M., Liu, J., Chen, A., and Xu, G. (2018). Phytohormones regulate the development of arbuscular mycorrhizal symbiosis. *Int. J. Mol. Sci.* 19:3146. doi: 10.3390/ijms19103146

Liarzi, O., Bucki, P., Miyara, S. B., and Ezra, D. (2016). Bioactive volatiles from an endophytic *Daldinia* cf. concentrica isolate affect the viability of the plant parasitic nematode *Meloidogyne javanica*. *PLoS One* 11:e0168437. doi: 10.1371/journal.pone.0168437

López-Bucio, J., Pelagio-Flores, R., and Herrera-Estrella, A. (2015). *Trichoderma* as biostimulant: exploiting the multilevel properties of a plant beneficial fungus. *Sci. Hortic.* 196, 109–123. doi: 10.1016/j.scienta.2015.08.043

Lou, J., Yu, R., Wang, X., Mao, Z., Fu, L., Liu, Y., et al. (2016). Alternariol 9-methyl ether from the endophytic fungus *Alternaria* sp. *Samif*01 and its bioactivities. *Braz. J. Microbiol.* 47, 96–101. doi: 10.1016/j.bjm.2015.11.004

Ludwig-Müller, J. (2015). Plants and endophytes: equal partners in secondary metabolite production? *Biotechnol. Lett.* 37, 1325–1334. doi: 10.1007/s10529-015-1814-4

Lugtenberg, B. J., Caradus, J. R., and Johnson, L. J. (2016). Fungal endophytes for sustainable crop production. *FEMS Microbiol. Ecol.* 92:fiw194. doi: 10.1093/femsec/fiw194

Marro, N., Caccia, M., Doucet, M. E., Cabello, M., Becerra, A., and Lax, P. (2018). Mycorrhizas reduce tomato root penetration by false root-knot nematode *Nacobbus aberrans*. *Appl. Soil Ecol.* 124, 262–265. doi: 10.1016/j.apsoil.2017.11.011

Martínez, B., Infante, D., and Peteira, B. (2015). Taxonomía polifásica y variabilidad en el género *Trichoderma*. *Rev. Prot. Veg.* 30, 11–22.

Martinez, C. M. E., Guarneri, N., Overmars, H., van Schaik, C., Bouwmeester, H., Ruyter-Spira, C., et al. (2019). Distinct roles for strigolactones in cyst nematode parasitism of *Arabidopsis* roots. *Eur. J. Plant Pathol.* 154, 129–140. doi: 10.1007/s10658-019-01691-5

Martínez-Medina, A., Appels, F. V., and van Wees, S. C. (2017a). Impact of salicylic acid-and jasmonic acid-regulated defences on root colonization by *Trichoderma harzianum* T-78. *Plant Signal. Behav.* 12:e1345404. doi: 10.1080/15592324.2017.1345404

Martínez-Medina, A., Fernandez, I., Lok, G. B., Pozo, M. J., Pieterse, C. M., and Van Wees, S. C. (2017b). Shifting from priming of salicylic acid-to jasmonic acid-regulated defences by *Trichoderma* protects tomato against the root knot nematode *Meloidogyne incognita*. *New Phytol.* 213, 1363–1377. doi: 10.1111/nph.14251

Martínez-Medina, A., Fernández, I., Sánchez-Guzmán, M. J., Jung, S. C., Pascual, J. A., and Pozo, M. J. (2013). Deciphering the hormonal signalling network behind the systemic resistance induced by *Trichoderma harzianum* in tomato. *Front. Plant Sci.* 4:206. doi: 10.3389/fpls.2013.00206

Martinez-Medina, A., Flors, V., Heil, M., Mauch-Mani, B., Pieterse, C. M., Pozo, M. J., et al. (2016). Recognizing plant defense priming. *Trends Plant Sci.* 21, 818–822. doi: 10.1016/j.tplants.2016.07.009

Martinuz, A., Zewdu, G., Ludwig, N., Grundler, F., Sikora, R. A., and Schouten, A. (2015). The application of *Arabidopsis thaliana* in studying tripartite interactions among plants, beneficial fungal endophytes and biotrophic plant-parasitic nematodes. *Planta* 241, 1015–1025. doi: 10.1007/s00425-014-2237-5

Mastan, A., Bharadwaj, R. K. B., Kushwaha, R. K., and Babu, C. S. V. (2019). Functional fungal endophytes in Coleus forskohlii regulate labdane diterpene biosynthesis for elevated forskolin accumulation in roots. *Microb. Ecol.* 78, 914–926. doi: 10.1007/s00248-019-01376-w

Medina, C., da Rocha, M., Magliano, M., Ratpopoulo, A., Revel, B., Marteu, N., et al. (2017). Characterization of microRNAs from Arabidopsis galls highlights a role for miR159 in the plant response to the root-knot nematode *Meloidogyne incognita*. *New Phytol.* 216, 882–896. doi: 10.1111/nph.14717

Mejias, J., Truong, N. M., Abad, P., Favery, B., and Quentin, M. (2019). Plant proteins and processes targeted by parasitic nematode effectors. *Front. Plant Sci.* 10:970. doi: 10.3389/fpls.2019.00970

Mauch-Mani, B., Baccelli, I., Luna, E., and Flors, V. (2017). Defense priming: an adaptive part of induced resistance. *Annu. Rev. Plant Biol.* 68, 485–512. doi: 10.1146/annurev-arplant-042916-041132

Mendoza-Mendoza, A., Zaid, R., Lawry, R., Hermosa, R., Monte, E., Horwitz, B. A., et al. (2018). Molecular dialogues between *Trichoderma* and roots: role of the fungal secretome. *Fungal Biol. Rev.* 32, 62–85. doi: 10.1016/j.fbr.2017.12.001

Miao, G. P., Han, J., Zhang, K. G., Wang, S. C., and Wang, C. R. (2019). Protection of melon against *Fusarium* wilt-root knot nematode complex by endophytic fungi *Penicillium brefeldianum* HS-1. *Symbiosis* 77, 83–89. doi: 10.1007/s13199-018-0565-0

Mithöfer, A., and Boland, W. (2008). Recognition of herbivory-associated molecular patterns. *Plant Physiol.* 146, 825–831. doi: 10.1104/pp.107.113118

Mukherjee, M., Mukherjee, P. K., Horwitz, B. A., Zachow, C., Berg, G., and Zeilinger, S. (2012). *Trichoderma*–plant–pathogen interactions: advances in genetics of biological control. *Indian J. Microbiol.* 52, 522–529. doi: 10.1007/s12088-012-0308-5

Mwaura, P., Dubois, T., Losenge, T., Coyne, D., and Kahangi, E. (2010). Effect of endophytic *Fusarium oxysporum* on paralysis and mortality of *Pratylenchus goodeyi*. *Afr. J. Biotechnol.* 9, 1130–1134. doi: 10.5897/AJB09.964

Mwaura, P., Niere, B., and Vidal, S. (2017). Application of an entomopathogenic fungus (*Beauveria bassiana*) increases potato nematodes reproduction and potato tubers damage caused by *Ditylenchus destructor* and *D. dipsaci*. *Biol. Control* 115, 23–29. doi: 10.1016/j.biocontrol.2017.08.012

Nakashima, H., Eguchi, N., Uesugi, T., Yamashita, N., and Matsuda, Y. (2016). Effect of ectomycorrhizal composition on survival and growth of *Pinus thunbergii* seedlings varying in resistance to the pine wilt nematode. *Trees* 30, 475–481. doi: 10.1007/s00468-015-1217-0

Nawrocka, J., and Małolepsza, U. (2013). Diversity in plant systemic resistance induced by *Trichoderma*. *Biol. Control* 67, 149–156. doi: 10.1016/j.biocontrol.2013.07.005

Nisa, H., Kamili, A. N., Nawchoo, I. A., Shafi, S., Shameem, N., and Bandh, S. A. (2015). Fungal endophytes as prolific source of phytochemicals and other bioactive natural products: a review. *Microb. Pathog.* 82, 50–59. doi: 10.1016/j.micpath.2015.04.001

Pal, K. K., and Gardener, B. M. S. (2006). Biological control of plant pathogens. *Plant Health Instr.* 2, 1–25. doi: 10.1094/PHI-A-2006-1117-02

Palomares-Rius, J. E., Escobar, C., Cabrera, J., Vovlas, A., and Castillo, P. (2017). Anatomical alterations in plant tissues induced by plant-parasitic nematodes. *Front. Plant Sci.* 8:1987. doi: 10.3389/fpls.2017.01987

Pocurull, M., Fullana-Pons, A. M., Ferro, M., Valero, P., Escudero, N., Saus, E., et al. (2020). Commercial formulates of *Trichoderma* induce systemic plant resistance to Meloidogyne incognita in tomato and the effect is additive to that of the Mi-1.2 resistance gene. *Front. Plant Sci*. 1:1. doi: 10.3389/fmicb.2019.03042

Poveda, J. (2020). Trichoderma parareesei favors the tolerance of rapeseed (*Brassica napus* L.) to salinity and drought due to a chorismate mutase. *Agronomy* 10:118. doi: 10.3390/agronomy10010118

Pozo, M. J., and Azcón-Aguilar, C. (2007). Unraveling mycorrhiza-induced resistance. *Curr. Opin. Plant Biol.* 10, 393–398. doi: 10.1016/j.pbi.2007.05.004

Rabiey, M., Hailey, L. E., Roy, S. R., Grenz, K., Al-Zadjali, M. A., Barrett, G. A., et al. (2019). Endophytes vs tree pathogens and pests: can they be used as biological control agents to improve tree health? *Eur. J. Plant Pathol.* 155, 711–729. doi: 10.1007/s10658-019-01814-y

Ramírez-Prado, J. S., Abulfaraj, A. A., Rayapuram, N., Benhamed, M., and Hirt, H. (2018). Plant immunity: from signaling to epigenetic control of defense. *Trends Plant Sci.* 23, 833–844. doi: 10.1016/j.tplants.2018.06.004

Reimer-Michalski, E. M., and Conrath, U. (2016). Innate immune memory in plants. *Semin. Immunol.* 28, 319–327. doi: 10.1016/j.smim.2016.05.006

Rimington, W. R., Pressel, S., Duckett, J. G., Field, K. J., Read, D. J., and Bidartondo, M. I. (2018). Ancient plants with ancient fungi: liverworts associate with early-diverging arbuscular mycorrhizal fungi. *Proc. R. Soc. B* 285:20181600. doi: 10.1098/rspb.2018.1600

Rochange, S., Goormachtig, S., Lopez-Raez, J. A., and Gutjahr, C. (2019). "The role of strigolactones in plant–microbe interactions," in *Strigolactones-Biology and Applications*, eds H. Koltai, and C. Prandi (Cham: Springer), 121–142. doi: 10.1007/978-3-030-12153-2_4

Rozpądek, P., Domka, A. M., Nosek, M., Ważny, R., Jędrzejczyk, R. J., Wiciarz, M., et al. (2018). The role of strigolactone in the cross-talk between *Arabidopsis thaliana* and the endophytic fungus *Mucor* sp. *Front. Microbiol.* 9:441. doi: 10.3389/fmicb.2018.00441

Ruiz-Ferrer, V., Cabrera, J., Martinez-Argudo, I., Artaza, H., Fenoll, C., and Escobar, C. (2018). Silenced retrotransposons are major rasiRNAs targets in *Arabidopsis galls* induced by *Meloidogyne javanica*. *Mol. Plant Pathol.*ă19, 2431–2445. doi: 10.1111/mpp.12720

Sahebani, N., and Hadavi, N. (2008). Biological control of the root-knot nematode *Meloidogyne javanica* by *Trichoderma harzianum*. *Soil Biol Biochem.* 40, 2016–2020. doi: 10.1016/j.soilbio.2008.03.011

Saikkonen, K., Mikola, J., and Helander, M. (2015). Endophytic phyllosphere fungi and nutrient cycling in terrestrial ecosystems. *Curr. Sci.* 109, 121–126. doi: 10.1093/femsec/fiv095

Saikkonen, K., Young, C. A., Helander, M., and Schardl, C. L. (2016). Endophytic *Epichloë* species and their grass hosts: from evolution to applications. *Plant Mol. Biol.* 90, 665–675. doi: 10.1007/s11103-015-0399-6

Schouteden, N., De Waele, D., Panis, B., and Vos, C. M. (2015). Arbuscular mycorrhizal fungi for the biocontrol of plant-parasitic nematodes: a review of the mechanisms involved. *Front. Microbiol*. 6:1280. doi: 10.3389/fmicb.2015.01280

Schouten, A. (2016). Mechanisms involved in nematode control by endophytic fungi. *Annu. Rev. Phytopathol.* 54, 121–142. doi: 10.1146/annurev-phyto-080615-100114

Sharma, I. P., and Sharma, A. K. (2017a). Co-inoculation of tomato with an arbuscular mycorrhizal fungus improves plant immunity and reduces root-knot nematode infection. *Rhizosphere* 4, 25–28. doi: 10.1016/j.rhisph.2017.05.008

Sharma, I. P., and Sharma, A. K. (2017b). Physiological and biochemical changes in tomato cultivar PT-3 with dual inoculation of mycorrhiza and PGPR against root-knot nematode. *Symbiosis* 71, 175–183. doi: 10.1007/s13199-016-0423-x

Sharon, E., Chet, I., Viterbo, A., Bar-Eyal, M., Nagan, H., Samuels, G. J., et al. (2007). Parasitism of *Trichoderma* on *Meloidogyne javanica* and role of the gelatinous matrix. *Eur. J. Plant Pathol.* 118, 247–258. doi: 10.1007/s10658-007-9140-x

Shigenaga, A. M., Berens, M. L., Tsuda, K., and Argueso, C. T. (2017). Towards engineering of hormonal crosstalk in plant immunity. *Curr. Opin. Plant Biol.* 38, 164–172. doi: 10.1016/j.pbi.2017.04.021

Siddique, S., and Grundler, F. M. (2018). Parasitic nematodes manipulate plant development to establish feeding sites. *Curr. Opin. Microbiol.* 46, 102–108. doi: 10.1016/j.mib.2018.09.004

Siddiqui, I. A., and Shaukat, S. S. (2003). Suppression of root-knot disease by *Pseudomonas fluorescens* CHA0 in tomato: importance of bacterial secondary metabolite, 2, 4-diacetylpholoroglucinol. *Soil Biol. Biochem.* 35, 1615–1623. doi: 10.1016/j.soilbio.2003.08.006

Singh, S., Singh, B., and Singh, A. P. (2015). Nematodes: a threat to sustainability of agriculture. *Procedia Environ. Sci.* 29, 215–216. doi: 10.1016/j.proenv.2015.07.270

Stirling, G. R. (2018). "Biological control of plant-parasitic nematodes," in *Diseases of Nematodes*, eds G. O. Poinar and H. -B. Jansson (Boca Raton, FL: CRC Press), 103–150. doi: 10.1201/9781351071468

Strullu-Derrien, C., Selosse, M. A., Kenrick, P., and Martin, F. M. (2018). The origin and evolution of mycorrhizal symbioses: from palaeomycology to phylogenomics. *New Phytol.* 220, 1012–1030. doi: 10.1111/nph.15076

Tchabi, A., Hountondji, C. C., Ogunsola, B., Lawouin, L., Coyne, D. L., Wiemken, A., et al. (2016). Effect of two species of arbuscular mycorrhizal fungi inoculation on development of micro-propagated yam plantlets and suppression of *Scutellonema bradys* (Tylenchideae). *J. Entomol. Nematol.* 8, 1–10. doi: 10.5897/JEN2015.0149

Uzma, F., Mohan, C. D., Hashem, A., Konappa, N. M., Rangappa, S., Kamath, P. V., et al. (2018). Endophytic fungi-alternative sources of cytotoxic compounds: a review. *Front. Pharmacol.* 9:309. doi: 10.3389/fphar.2018.00309

Van Wees, S. C., Van der Ent, S., and Pieterse, C. M. (2008). Plant immune responses triggered by beneficial microbes. *Curr. Opin. Plant Biol.* 11, 443–448. doi: 10.1016/j.pbi.2008.05.005

Varkey, S., Anith, K. N., Narayana, R., and Aswini, S. (2018). A consortium of rhizobacteria and fungal endophyte suppress the root-knot nematode parasite in tomato. *Rhizosphere* 5, 38–42. doi: 10.1016/j.rhisph.2017.11.005

Vasundhara, M., Kumar, A., and Reddy, M. S. (2016). Molecular approaches to screen bioactive compounds from endophytic fungi. *Front. Microbiol.* 7:1774. doi: 10.3389/fmicb.2016.01774

Vinale, F., Sivasithamparam, K., Ghisalberti, E. L., Marra, R., Woo, S. L., and Lorito, M. (2008). *Trichoderma*–plant–pathogen interactions. *Soil Biol. Biochem.* 40, 1–10. doi: 10.1016/j.soilbio.2007.07.002

Vos, C., Claerhout, S., Mkandawire, R., Panis, B., De Waele, D., and Elsen, A. (2012a). Arbuscular mycorrhizal fungi reduce root-knot nematode penetration through altered root exudation of their host. *Plant Soil* 354, 335–345. doi: 10.1007/s11104-011-1070-x

Vos, C., Tesfahun, A. N., Panis, B., De Waele, D., and Elsen, A. (2012b). Arbuscular mycorrhizal fungi induce systemic resistance in tomato against the sedentary nematode *Meloidogyne incognita* and the migratory nematode *Pratylenchus penetrans*. *Appl. Soil Ecol.* 61, 1–6. doi: 10.1016/j.apsoil.2012.04.007

Vu, T., Sikora, R., and Hauschild, R. (2006). *Fusarium oxysporum* endophytes induced systemic resistance against *Radopholus similis* on banana. *Nematology* 8, 847–852. doi: 10.1163/156854106779799259

Wani, K. A., Manzoor, J., Shuab, R., and Lone, R. (2017). "Arbuscular mycorrhizal fungi as biocontrol agents for parasitic nematodes in plants," in *Mycorrhiza-Nutrient Uptake, Biocontrol, Ecorestoration*, eds A. Varma, R. Prasad, and N. Tuteja (Cham: Springer), 195–210. doi: 10.1007/978-3-319-68867-1_10

Waqas, M., Khan, A. L., Hamayun, M., Shahzad, R., Kang, S. M., Kim, J. G., et al. (2015). Endophytic fungi promote plant growth and mitigate the adverse effects of stem rot: an example of *Penicillium citrinum* and *Aspergillus terreus*. *J. Plant Interact.* 10, 280–287. doi: 10.1080/17429145.2015.1079743

Xiang, N., Lawrence, K. S., and Donald, P. A. (2018). Biological control potential of plant growth-promoting rhizobacteria suppression of *Meloidogyne incognita* on cotton and *Heterodera glycines* on soybean: a review. *J. Phytopathol.* 166, 449–458. doi: 10.1111/jph.12712

Xu, X., Fang, P., Zhang, H., Chi, C., Song, L., Xia, X., et al. (2018). Strigolactones positively regulate defense against root-knot nematodes in tomato. *J. Exp. Bot.* 70, 1325–1337. doi: 10.1093/jxb/ery439

Yan, J. F., Broughton, S. J., Yang, S. L., and Gange, A. C. (2015). Do endophytic fungi grow through their hosts systemically? *Fungal Ecol.* 13, 53–59. doi: 10.1016/j.funeco.2014.07.005

Yan, L., Zhao, H., Zhao, X., Xu, X., Di, Y., Jiang, C., et al. (2018). Production of bioproducts by endophytic fungi: chemical ecology, biotechnological

applications, bottlenecks, and solutions. *Appl. Microbiol. Biotechnol.* 102, 6279–6298. doi: 10.1007/s00253-018-9101-7

Yan, L., Zhu, J., Zhao, X., Shi, J., Jiang, C., and Shao, D. (2019). Beneficial effects of endophytic fungi colonization on plants. *Appl. Microbiol. Biotechnol.* 103, 3327–3340. doi: 10.1007/s0025

Yao, Y. R., Tian, X. L., Shen, B. M., Mao, Z. C., Chen, G. H., and Xie, B. Y. (2015). Transformation of the endophytic fungus *Acremonium implicatum* with GFP and evaluation of its biocontrol effect against *Meloidogyne incognita*. *World J. Microbiol. Biotechnol.* 31, 549–556. doi: 10.1007/s11274-014-1781-2

Zavala-González, E. A., Rodríguez-Cazorla, E., Escudero, N., Aranda-Martinez, A., Martínez-Laborda, A., Ramírez-Lepe, M., et al. (2017). *Arabidopsis thaliana* root colonization by the nematophagous fungus *Pochonia chlamydosporia* is modulated by jasmonate signaling and leads to accelerated flowering and improved yield. *New Phytol.* 213, 351–364. doi: 10.1111/nph.14106

Zeilinger, S., Gupta, V. K., Dahms, T. E., Silva, R. N., Singh, H. B., Upadhyay, R. S., et al. (2015). Friends or foes? Emerging insights from fungal interactions with plants. *FEMS Microbiol. Rev.* 40, 182–207. doi: 10.1093/femsre/fuv045

Zhang, S., Gan, Y., Ji, W., Xu, B., Hou, B., and Liu, J. (2017). Mechanisms and characterization of *Trichoderma longibrachiatum* T6 in suppressing nematodes (*Heterodera avenae*) in wheat. *Front. Plant Sci.* 8:1491. doi: 10.3389/fpls.2017.01491

Zhang, S., Gan, Y., Xu, B., and Xue, Y. (2014). The parasitic and lethal effects of *Trichoderma longibrachiatum* against *Heterodera avenae*. *Biol. Control* 72, 1–8. doi: 10.1016/j.biocontrol.2014.01.009

Zhao, D., Zhao, H., Zhao, D., Zhu, X., Wang, Y., Duan, Y., et al. (2018). Isolation and identification of bacteria from rhizosphere soil and their effect on plant growth promotion and root-knot nematode disease. *Biol. Control* 119, 12–19. doi: 10.1016/j.biocontrol.2018.01.004

Zheng, Y. K., Qiao, X. G., Miao, C. P., Liu, K., Chen, Y. W., Xu, L. H., et al. (2016). Diversity, distribution and biotechnological potential of endophytic fungi. *Ann. Microbiol.* 66, 529–542. doi: 10.1007/s1321

Zhou, W., Wheeler, T. A., Starr, J. L., Valencia, C. U., and Sword, G. A. (2018). A fungal endophyte defensive symbiosis affects plant-nematode interactions in cotton. *Plant Soil* 422, 251–266. doi: 10.1007/s11104-016-3147-z

Zogli, P., and Libault, M. (2017). Plant response to biotic stress: Is there a common epigenetic response during plant-pathogenic and symbiotic interactions? *Plant Sci.* 263, 89–93. doi: 10.1016/j.plantsci.2017.07.008

Conflict of Interest: The authors declare that the research was conducted in the absence of any commercial or financial relationships that could be construed as a potential conflict of interest.

frontiers in Microbiology

ORIGINAL RESEARCH
published: 12 June 2020
doi: 10.3389/fmicb.2020.01030

Whole Genome Sequencing Reveals Major Deletions in the Genome of M7, a Gamma Ray-Induced Mutant of *Trichoderma virens* That Is Repressed in Conidiation, Secondary Metabolism, and Mycoparasitism

*Shikha Pachauri[1,2], Pramod D. Sherkhane[1], Vinay Kumar[2,3] and Prasun K. Mukherjee[1,2]**

[1] Nuclear Agriculture and Biotechnology Division, Bhabha Atomic Research Centre, Mumbai, India, [2] Homi Bhabha National Institute, Mumbai, India, [3] Radiation Biology & Health Sciences Division, Bhabha Atomic Research Centre, Mumbai, India

OPEN ACCESS

Edited by:
Francesco Vinale,
University of Naples Federico II, Italy

Reviewed by:
Birinchi Kumar Sarma,
Banaras Hindu University, India
Eliane Ferreira Noronha,
University of Brasilia, Brazil
Vishukumar Aimanianda,
Institut Pasteur, France

***Correspondence:**
Prasun K. Mukherjee
prasunm@barc.gov.in;
prasunmukherjee1@gmail.com

Specialty section:
This article was submitted to Microbial Symbioses, a section of the journal Frontiers in Microbiology

Received: 03 February 2020
Accepted: 27 April 2020
Published: 12 June 2020

Citation:
Pachauri S, Sherkhane PD, Kumar V and Mukherjee PK (2020) Whole Genome Sequencing Reveals Major Deletions in the Genome of M7, a Gamma Ray-Induced Mutant of Trichoderma virens That Is Repressed in Conidiation, Secondary Metabolism, and Mycoparasitism. Front. Microbiol. 11:1030. doi: 10.3389/fmicb.2020.01030

Trichoderma virens is a commercial biofungicide used in agriculture. We have earlier isolated a mutant of *T. virens* using gamma ray-induced mutagenesis. This mutant, designated as M7, is defective in morphogenesis, secondary metabolism, and mycoparasitism. The mutant does not produce conidia, and the colony is hydrophilic. M7 cannot utilize cellulose and chitin as a sole carbon source and is unable to parasitize the plant pathogens *Rhizoctonia solani* and *Pythium aphanidermatum* in confrontation assay. Several volatile (germacrenes, beta-caryophyllene, alloaromadendrene, gamma-muurolene) and non-volatile (viridin, viridiol, gliovirin, heptelidic acid) metabolites are not detected in M7. In transcriptome analysis, many genes related to secondary metabolism, carbohydrate metabolism, hydrophobicity, and transportation, among others, were found to be downregulated in the mutant. Using whole genome sequencing, we identified five deletions in the mutant genome, totaling about 250 kb (encompassing 71 predicted ORFs), which was confirmed by PCR. This study provides novel insight into genetics of morphogenesis, secondary metabolism, and mycoparasitism and eventually could lead to the identification of novel regulators of beneficial traits in plant beneficial fungi *Trichoderma* spp. We also suggest that this mutant can be developed as a microbial cell factory for the production of secondary metabolites and proteins.

Keywords: *Trichoderma virens*, mutant, transcriptome, NGS, secondary metabolism

INTRODUCTION

Trichoderma virens is an agriculturally important fungus used for plant growth promotion and biocontrol of pathogens in commercial settings (Mukherjee et al., 2013b)[1,2]. Two strains of this fungus exist in nature: the "P" strains and the "Q" strains (Howell et al., 1993). Two isolates of *T. virens* have been widely used for genetic and biocontrol studies: Gv29-8, a "Q" strain,

[1] https://www.certisusa.com/pest_management_products/biofungicides/soilgard_12g_microbial_fungicide

[2] http://www.acceleronsas.com/products/Pages/QuickRoots-Corn.aspx

and IMI304061, a "P" strain (Mukhopadhyay et al., 1992; Djonović et al., 2006a,b, 2007a,b; Mukherjee et al., 2006, 2007; Bansal et al., 2018). *T. virens* is a mycoparasite on many plant pathogenic fungi and also produces several secondary metabolites, both volatile and non-volatile. Among these are gliotoxin (produced by "Q" strains), gliovirin (produced by "P" strains), viridin, viridiol, and heptelidic (koningic) acid, and several volatile sesquiterpenes, including beta-caryophyllene and germacrenes (Mukherjee et al., 2006; Crutcher et al., 2013; Zeilinger et al., 2016; Pachauri et al., 2019b). *T. virens* is also reported to induce systemic defense responses in plants (Djonović et al., 2007a; Gaderer et al., 2015; Mukherjee et al., 2018).

Whole genome of Gv29-8 and IMI304061 have been sequenced and analyzed, resulting in the identification of biosynthesis gene clusters for many unknown metabolites as well as for gliotoxin, gliovirin, viridin/viridiol, siderophores, and volatile sesquiterpenes (Kubicek et al., 2011; Crutcher et al., 2013; Sherkhane et al., 2017; Bansal et al., 2018; Mukherjee et al., 2018). Many hydrolytic enzymes and signal transduction proteins have been implicated to be involved in mycoparasitism of *Trichoderma* spp. on plant pathogenic fungi (Haran et al., 1996; Carsolio et al., 1999; Mendoza-Mendoza et al., 2003; Mukherjee et al., 2003; Druzhinina et al., 2011). A few elicitor proteins/peptides have been identified to be involved in triggering of plant defense (Djonović et al., 2006a; Viterbo et al., 2007; Mendoza-Mendoza et al., 2018). *T. virens* has also been studied for genomic presence and biological role of hydrophobins (Przylucka et al., 2006, 2017; Kubicek et al., 2008; Guzmán-Guzmán et al., 2017; Mendoza-Mendoza et al., 2018). Most of these studies involved bioinformatically identifying candidate genes, obtaining knockout mutants, and comparative phenotyping. Classical mutagenesis followed by complementation had earlier led to the discovery of several novel genes in many fungi (Mattern et al., 1992; Casselton and Zolan, 2002). In recent years, the advancements in whole genome sequencing tools have allowed for identification of mutations in classically induced mutants of fungi (McCluskey et al., 2011). The *Trichoderma reesei* strain RutC30 that is the major source of industrial cellulases was originally obtained by repeated chemical and physical mutagenesis of the wild type *T. reesei* strain QM6a. Using whole genome sequence analysis, a large deletion of 100 kb, 15 small deletions or insertions, and 223 single nucleotide variants were identified in RutC30 (Le Crom et al., 2009). We earlier obtained a mutant of *T. virens*, induced by gamma ray that does not produce conidia or detectable amounts of non-volatile secondary metabolites but has normal vegetative growth and produces excess chlamydospores (Mukherjee et al., 2006). Using SSH and this mutant, we identified a few genes involved in secondary metabolism and conidiation (Mukherjee et al., 2006; Crutcher et al., 2013; Bansal et al., 2019). Here, we describe several novel phenotypes associated with *T. virens* mutant M7, expand the repertoire of genes that are downregulated in this mutant by RNAseq and, using whole genome sequencing, attempt to identify the alterations in the genome composition of the mutant.

MATERIALS AND METHODS

Fungal Strains and Growth Conditions

Trichoderma virens (IMI 304061), *Pythium aphanidermatum*, and *Rhizactonia solani* (ITCC 4110) were used from our previous studies (Mukherjee et al., 2007). The non-conidiating mutant M7 of *T. virens* was obtained from our previous study (Mukherjee et al., 2006). The fungal cultures were grown in potato dextrose medium at 28°C and maintained at −80°C for long-term storage.

Test of Hydrophobicity

Wild-type *T. virens* and M7 mutant were grown for 5 days on PDA at 28°C, and hydrophobicity was tested by adding 0.5% aqueous aniline blue dye or water and recording the disappearance of the drop after 1 h.

Assays for Mycoparasitism

The mycoparasitic ability of wild-type and mutant M7 was determined using confrontation assay by pairing the *Trichoderma* and the test pathogens simultaneously on the same plate, placed opposite each other. Because *T. virens* wild-type takes 4–5 days to completely overgrow these test pathogens (Mukherjee et al., 2007), ability of wild-type or mutant to overgrow and lyse the mycelia of *P. aphanidermatum* and *R. solani* was recorded after 5 days of co-inoculation. *P. aphanidermatum* and *R. solani* cell walls are primarily composed of cellulose and chitin, respectively, and hence, we assessed the ability of wild-type and M7 to utilize chitin and cellulose as a carbon source by growing them in Vogel's minimal medium containing chitin or cellulose as the sole carbon source in liquid shake culture at 28°C and 150 rpm. For initiation of growth, 0.1% sucrose was added to the medium. All the experiments were conducted in four replicates.

Identification of Secondary Metabolites Produced by Wild-Type and M7

The non-volatile compounds were detected in wild-type *T. virens* and M7 using thin layer chromatography as described earlier (Mukherjee and Kenerley, 2010). WT and M7 cultures were grown for 3 days in potato dextrose broth and extracted with equal volumes of ethyl acetate. The extract was dried and reconstituted in 0.1 volume methanol, and 100 μl was spotted on precoated TLC plate. TLC plate was developed in acetone:chloroform:formic acid (28:70:2) and visualized under short-wavelength UV (254 nm). The spots were eluted with 100% methanol and subjected to LC-MS/MS analysis as described earlier (Bansal et al., 2018). For confirmation, LC-MS/MS analysis of standard viridin and viridiol (a kind gift from the late Dr. C. R. Howell) and heptelidic acid (Cayman Chemical Company, United States) were also analyzed and matched with the sample.

The head space solid-phase microextraction (HS-SPME) and gas chromatography–mass spectrometry (GC–MS) technique was used for volatile compound detection in wild-type *T. virens* and M7. The instrument used for analysis was GC–MS 2010 Plus (Shimadzu, Kyoto, Japan). The GC–MS instrument was equipped with an injection port having SPME glass liner (Supelco) and RTX-5 column (5% diphenyl dimethyl polysiloxane, 10

m × 0.1 mm I.D.; Restek Corporation, Bellefonte, PA, United States). The injection port was maintained at 270°C with no solvent cut. Helium was used as a carrier gas. GC column temperature was programmed as follows: 40°C for 5 min and then increased to 200°C at 4°C min^{-1}, held for 5 min and then increased to 280°C at 10°C min^{-1} with a final hold of 10 min. MS parameters were ionization voltage 70 eV, electron multiplier voltage 1 kV, and scan mode from m/z 35 to 350. Identification of the peaks was done by comparing their mass fragmentation pattern, Kovats retention indices and from the data available in the spectral (Wiley/NIST) libraries of the instrument. The experiments were conducted in three replicates and repeated once.

Transcriptome Analysis

Wild-type and M7 were grown on PDA plates overlaid with dialysis membrane (MWCO 12 kDa) opposite of *R. solani* for 2 days. For control, wild-type *T. virens* and M7 were confronted with self. Mycelial mat from the zone of contact was harvested with a sterile spatula and frozen in liquid nitrogen and stored at −80°C until further use. Cultures were grown in four replicates, and samples were pooled before RNA extraction. RNA was extracted with TriReagent, and transcriptome sequencing was performed on Illumina HiSeq 2500 platform at M/S Scigenom, Cochin, Kerala, India, as discussed earlier (Mukherjee et al., 2019). A paired-end library was prepared and sequenced, and Trinity software was used for assembly of the cleaned reads produced by standard data preprocessing methods, including adaptor trimming, quality filtering, and end trimming. Gene expression estimation was performed by aligning the trimmed reads to the assembled transcriptome using Bowtie2 program. DESeq program was employed for differential gene expression analysis, and an in-house pipeline CANoPI (Contig Annotator Pipeline) was used for transcriptome annotation. FPKM values were considered for fold-change calculation, and log2 fold change ≥ 2 was considered for comparison of gene expression.

Whole Genome Sequencing and Analysis

Total genomic DNA was extracted, and whole genome sequencing of the M7 mutant was performed using Illumina platform at M/S Xcelris Genomics, Ahmedabad, India. Illumina TruSeq Nano DNA HT Library Preparation Kit was used for paired end sequencing library preparation. The generated libraries were sequenced on Illumina Nextseq 500 using 2 × 150 bp chemistry. *T. virens* wild-type sequence (LQCH00000000) was used as a reference genome for M7 genome mapping using a Burrows-Wheeler Aligner (BWA) (v. 0.7.5a) program with optimized mapping parameters. The genome coverage, gene prediction, and total number of single nucleotide polymorphisms (SNPs) and insertion/deletion polymorphisms (INDELs) were analyzed and compared with the reference genome. Absence of the genes in the deleted regions was further confirmed by PCR amplification using gene specific primers (**Supplementary Table S1**) of representative genes using the following conditions: denaturation at 95°C for 5 min, annealing at 57°C for 45 s, extension at 72°C for 1 min, and 30 cycles.

RESULTS

M7 Mutant Is Deficient in Hydrophobicity in Addition to Conidiation

As reported earlier (Mukherjee et al., 2006), the M7 mutant does not conidiate while wild-type *T. virens* produces green pigmented conidia (**Supplementary Figure S1**). The deficiency in conidiation is associated with loss of hydrophobicity. Aqueous aniline blue dye or water drops stay on the wild-type colony for several hours but diffuse through M7 colony immediately after application (**Figure 1**).

M7 Is Defective in Mycoparasitism

A confrontation assay demonstrated that M7 is not able to overgrow the plant pathogens *R. solani* and *P. aphanidermatum* while wild-type *T. virens* completely overgrew the colonies in 5 days (**Figure 2**). Although wild-type showed mycoparasitic coiling on *R. solani* and *P. aphanidermatum*, M7 failed to do so (**Supplementary Figure S2**). Moreover, M7 could not utilize chitin and cellulose as a carbon source even when the medium was supplemented with 0.01% sucrose (**Supplementary Figure S3**).

M7 Is Downregulated in the Biosynthesis of Secondary Metabolites

The TLC profile of wild-type and M7 culture filtrate shows that none of the non-volatile metabolites, including viridin, viridiol, and heptelidic acid, are detected in M7 (**Figure 3A**). Similarly, GC–MS analysis of head-space gas shows that M7 is downregulated in biosynthesis of volatile metabolites that are present in wild-type *T. virens*; only 13 of 73 metabolites being detected in M7 mutant (**Figure 3B** and **Supplementary Table S2**).

Several Genes for Secondary Metabolism, Hydrolytic Enzymes, and Hydrophobicity Are Downregulated in M7

De novo transcriptome analysis of wild-type and M7, while interacting with self or *R. solani* (**Supplementary Figure S4**), indicated that as many as 463 genes are downregulated in M7 (**Supplementary Tables S3, S4**, **Supplementary Figures S5, S6**, and **Figures 4**, **5**). In self-confrontation, 294 genes were downregulated in M7 compared to wild-type (**Supplementary Table S3**). Among these are genes for secondary metabolism (including genes coding for NRPSs, PKSs, and terpene cyclases, modifying enzymes, transporters, and transcription factors), other cytochrome P450s (not associated with secondary metabolism gene clusters), carbohydrate-active enzymes (CAZymes), peptidases, and hydrophobins (**Figure 4**). In confrontation with the plant pathogen *R. solani*, a larger set of genes (375) were downregulated in M7, 206 genes being common under both the conditions (**Supplementary Table S4** and **Supplementary Figure S7**). A large number of genes involved in secondary metabolism (69), carbohydrate

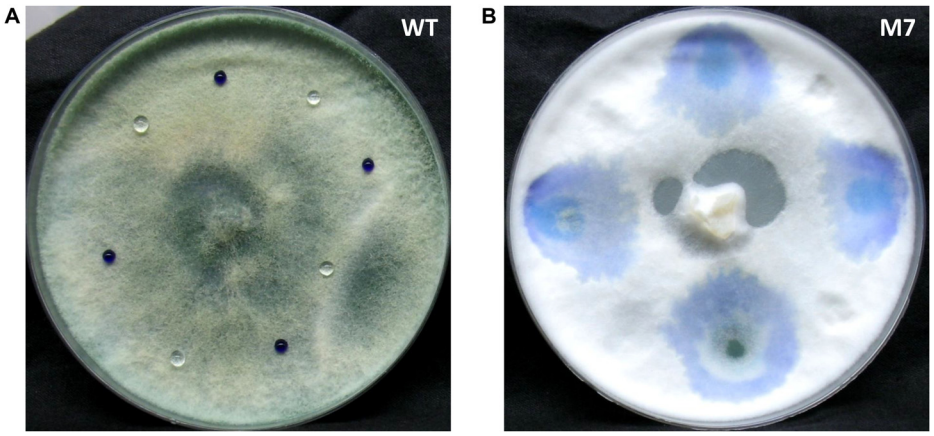

FIGURE 1 | Culture of *Trichoderma virens* wild-type and M7 with aniline blue dye and water placed on it. **(A)** Wild-type. **(B)** M7.

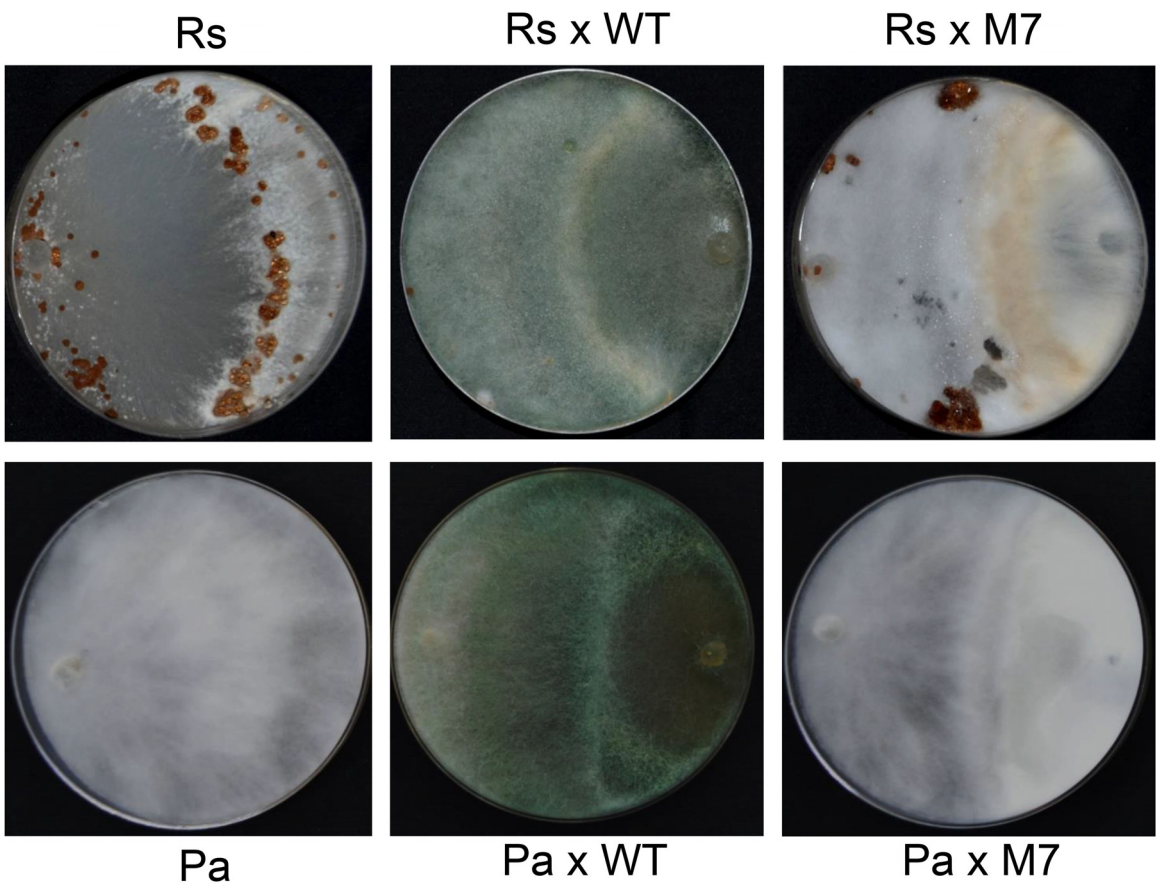

FIGURE 2 | Confrontation assay demonstrating that M7 is non-mycoparasitic in nature as it cannot overgrow and lyse *Rhizoctonia solani* (Rs) and *Pythium aphanidermatum* (Pa) after 5 days of co-inoculation, and wild-type (WT) *T. virens* is able to overgrow the test pathogens.

utilization (31), and transporters (30) are downregulated in M7 in confrontation with *R. solani* (**Figure 5**). This is in agreement with the fact that M7 does not produce detectable amount of secondary metabolites and also does not parasitize the plant pathogens *P. aphanidermatum* and *R. solani*. Six of the genes (protein IDs. TRIVIDRAFT_49849, TRIVIDRAFT_74289, TRIVIDRAFT_74291, TRIVIDRAFT_56195, TRIVIDRAFT_230740, TRIVIDRAFT_53375) that are downregulated in M7 were identified in our earlier study as under-expressed in M7 in RT-PCR analysis (Mukherjee et al., 2006).

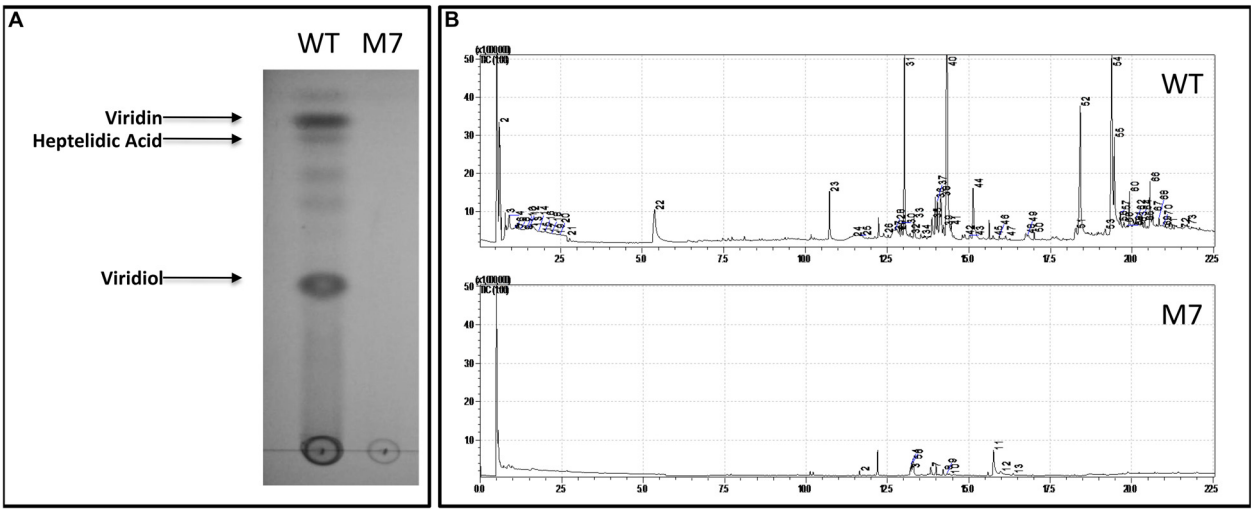

FIGURE 3 | Secondary metabolite profile of *T. virens* wild-type (WT) and M7. **(A)** Thin layer chromatography analysis of WT and M7 filtrate. **(B)** GC–MS analysis of WT and M7 head-space gas. The peak numbers correspond to the volatile metabolites detected as described in **Supplementary Table S2**.

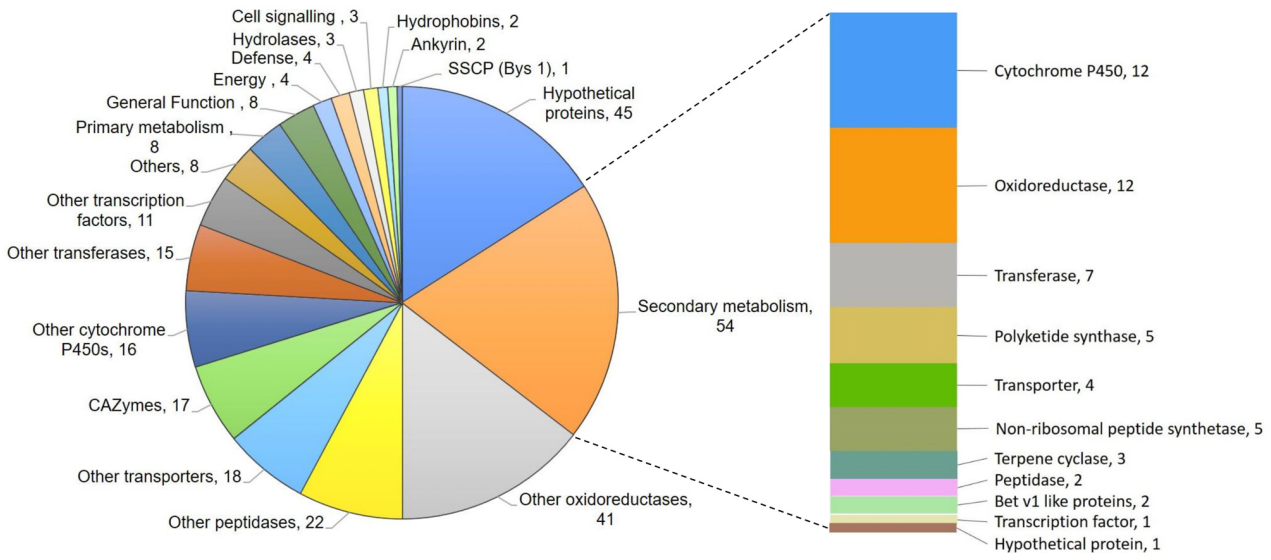

FIGURE 4 | Pie chart representing genes downregulated in M7 compared to the wild-type *T. virens*.

M7 Genome Has Large Deletions

Whole genome sequencing of the M7 mutant was performed using the Illumina platform to generate 2.1 GB data. The paired end sequencing library was of mean size 624 bp. The generated library was sequenced and mapped to *T. virens* wild-type assembly as a reference genome. A genome alignment revealed five deletions across three scaffolds (scaffold 1, 20, and 58) totaling about 250 Kb, comprising 71 genes (**Table 1**). Among the genes that are absent in the M7 genome are two large secondary metabolism gene clusters (PKS6 and Tex9 clusters), eight transcription factors (two associated with secondary metabolism gene clusters), five genes for carbohydrate metabolism, two genes related to cell signaling and as many as 11 oxidoreductases (**Table 1** and **Supplementary Figure S8**). To further confirm these deletions, PCR of representative genes was performed using wild-type and M7 genomic DNA as template. No amplification of these genes was obtained in M7, confirming the gene deletions (**Figure 6**). In addition, 118 SNPs and 57 small INDELs were also detected in M7 (**Supplementary Table S5**).

DISCUSSION

Trichoderma spp. are commercially important filamentous fungi and are used extensively in agriculture (Lorito et al., 2010;

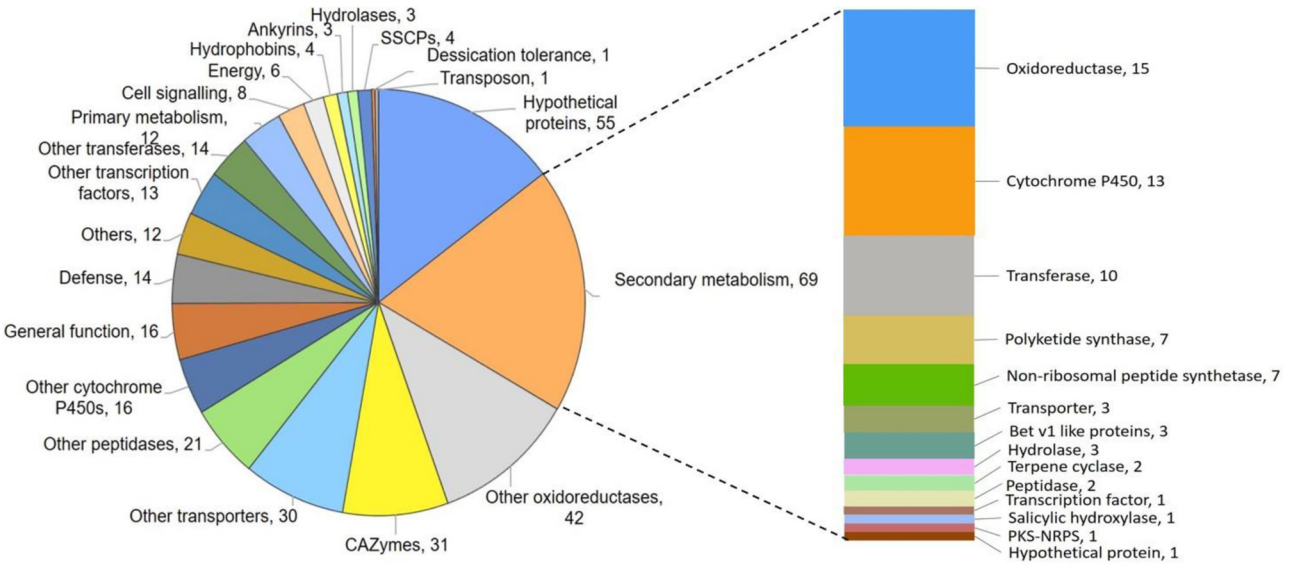

FIGURE 5 | Pie chart representing genes downregulated in M7 in confrontation with *Rhizoctonia solani*.

Mukherjee et al., 2013a). We had earlier isolated a non-conidiating mutant of the biocontrol agent *T. virens* that is also downregulated in secondary metabolite biosynthesis (Mukherjee et al., 2006). In the present study, we provide evidence that the mutant also lacks hydrophobicity. Hydrophobicity is imparted in fungi by small secreted cysteine-rich proteins known as hydrophobins. One hydrophobin (Trividraft_49849) was reported earlier to be downregulated in M7 (Mukherjee et al., 2006). In the transcriptome data, we noted one additional hydrophobin to be downregulated in the mutant. Hydrophobins are associated with conidiation (Wessels, 1996; Bayry et al., 2012) and loss of hydrophobicity in this non-conidiating mutant is not unexpected. *Trichoderma* hydrophobins also play important roles in attachment to root (Viterbo and Chet, 2006), elicitation of plant defense (Zhang et al., 2019), and tolerance to biotic and abiotic stresses (Przylucka et al., 2017). Hydrophobins are also involved in mycoparasitic interactions in *Trichoderma* (Guzmán-Guzmán et al., 2017). We have noticed two additional hydrophobins to be downregulated in the mutant in interaction with *R. solani* (**Supplementary Table S4**). These hydrophobins might, thus, be involved in mycoparasitism of *T. virens* on *R. solani*.

Trichoderma virens is an aggressive mycoparasite on many plant pathogenic fungi (Druzhinina et al., 2011). The mutant, however, has lost this property (**Figure 2** and **Supplementary Figure S2**), which can be explained by the lack of upregulation of a large number of CAZymes known to be involved in parasitism on other fungi (Haran et al., 1996; Carsolio et al., 1999; Djonović et al., 2006b, 2007b). CAZymes of glycoside hydrolase 2 (GH-2), GH-3, GH-18, GH-30, GH-47, GH-55, GH-75, and GH-92 families were downregulated in M7. Furthermore, the downregulation of CAZymes of GH-16, GH-20, GH-78, and GH-79 families only during confrontation with *R. solani* suggests the role of these CAZymes in mycoparasitism. Atanasova et al. (2013a) reported upregulation of many gene families, such as those involved in metabolism, transporters, signal transduction, transcriptional regulators, defense, etc., in *T. virens* during confrontation with *R. solani*. Similarly, in our study, we have detected downregulation of different groups of genes involved in secondary metabolism (69), genes for oxidoreductases (42), CAZymes (31), peptidases (21), transporters (30), transcription factors (13), transferases (14), and defense-related genes (14) in *T. virens* during confrontation with *R. solani*. Approximately twice the number of genes for transporters (30) and carbohydrate utilization groups (31) were downregulated in M7 during confrontation with *R. solani* as compared to confrontation with self, where only 18 genes for transporter and 17 for carbohydrate utilization were downregulated (**Figure 4**). These results indicate that the mutant, which cannot parasitize the host fungus *R. solani*, fails to respond to its presence. The role of most of these genes in mycoparasitism is not known, and further studies on the role of these genes could throw novel insights into the phenomenon of fungus–fungus interactions.

Trichoderma spp. produce a large number of useful secondary metabolites with diverse biological activities (Zeilinger et al., 2016; Pachauri et al., 2019b). A large number of genes for secondary metabolism (69) were downregulated in M7 during confrontation with *R. solani*. Viridin is one of the oldest known metabolites produced by *T. virens* possessing anti-cancer and anti-fungal activities, and viridiol is a phytotoxic agent produced by irreversible enzymatic conversion of viridin (Jones and Hancock, 1987; Howell et al., 1993). Gliovirin is a 'P' strain-specific non-ribosomal peptide with anti-oomycete activities (Howell and Stipanovic, 1983). Non-volatile compounds, such as viridin, viridiol, and heptelidic acid, were detected by TLC followed by LC-MS/MS analysis, and gliovirin was detected by LC-MS in *T. virens* wild-type (data not presented); the mutant does not produce these metabolites.

TABLE 1 | Genes deleted in *Trichoderma virens* mutant (M7) genome.

Gene ID (IMI 304061)	Size (aa)	Protein ID (*T. virens* Gv 29-8/ortholog)	Domains (NCBI CDD search)	Remarks/putative function
Deletion 1, Scaffold 1 (167 Kb)				
CDS375	421	33554 (Tv)	Glycoside hydrolase family 28 protein	CAZyme
CDS376	558	55166 (Tv)	Aryl sulfatase	Hydrolase
CDS377	223	34822 (Tv)	Glutathione *S*-transferase family (GST)	Transferase
CDS378	430	34910 (Tv)	Transcription factor, GAL4-like Zn(II)2Cys6 (or C6 zinc) binuclear cluster DNA-binding domain	Transcription factor
CDS379	157	XP_024770685 (Th)	Transcription factor bZIP	Transcription factor
CDS380	314	34863 (Tv)	Cysteine synthase family protein	Primary metabolism
CDS381	276	137438 (Tv)	Aromatic alcohol reductase	Secondary metabolism(PKS 6 cluster)
CDS382	447	34387 (Tv)	Acyl-CoA dehydrogenase	Secondary metabolism(PKS 6 cluster)
CDS383	612	140693 (Tv)	Abhydrolase 1 (esterase/lipase)	Secondary metabolism(PKS 6 cluster)
CDS384	1241	187765 (Tv)	Multi drug resistance-associated protein (MRP), ABC transporter	Secondary metabolism(PKS 6 cluster)
CDS385	1266	34120 (Tv)	ABC transporter	Secondary metabolism(PKS 6 cluster)
CDS386	201	XP_024768020 (Th)	Adenylate forming domain, Class I superfamily and peptide synthase	Secondary metabolism (NRPS like enzyme)
CDS387	153	62551 (Tv)	No hit	Secondary metabolism(PKS 6 cluster)
CDS388	296	140688 (Tv)	Domain of unknown function (DUF3328)	Secondary metabolism(PKS 6 cluster)
CDS389	2475	62549 (Tv)	Putative polyketide synthase (PKS6)	Secondary metabolism (PKS 6 cluster)
CDS390	329	62548 (Tv)	Transcription factor, GAL4 and AflR domain-containing protein	Secondary metabolism (PKS 6 cluster)
CDS391/392	3374	70819 (Tv)	Non-ribosomal peptide synthetase (NRPS), Tex9	Secondary metabolism (Tex 9 cluster)
CDS393	378	53253 (Tv)	No hit	Secondary metabolism (Tex 9 cluster)
CDS394	590	191897 (Tv)	Multicopper oxidase with three cupredoxin domains	Secondary metabolism (Tex 9 cluster)
CDS395	505	2412 (Tv)	Transcription factor, GAL4-like Zn(II)2Cys6 (or C6 zinc) binuclear cluster DNA-binding domain and middle homology region family	Secondary metabolism (Tex 9 cluster)
CDS396	318	131309 (Tv)	Domain of unknown function (DUF3328)	Hypothetical Protein
CDS397	98	222704 (Tv)	No hit	Hypothetical Protein
CDS398	382	222705 (Tv)	Class B metal beta-lactamase	Defense
CDS399	386	OPB40689 (Tg)	No hit	Hypothetical protein
CDS400	347	53264 (Tv)	Glycoside hydrolase family 10 protein	CAZyme
CDS401	534	127080 (Tv)	Transcription factor, GAL4-like Zn(II)2Cys6 (or C6 zinc) binuclear cluster DNA-binding domain and middle homology region family	Transcription factor
CDS402	506	151748 (Tv)	Amino acid permease (GABA permease)	Transporter
CDS403	390	151736 (Tv)	Agmatinase, arginase-like and histone-like hydrolases	Primary metabolism
CDS404	394	151735 (Tv)	Glycosyltransferase family A	CAZyme
CDS405	291	191903 (Tv)	Short-chain dehydrogenases/reductases (SDR)	Oxidoreductase
CDS406	606	191904 (Tv)	Acetyltransferase (GNAT) family	Transferase
CDS407	345	191905 (Tv)	Prostaglandin dehydrogenases	Oxidoreductase
CDS408	293	216175 (Tv)	Type 1 glutamine amidotransferase (GATase1)-like domain	Transferase
CDS409	680	191907 (Tv)	Transcription factor, GAL4-like Zn(II)2Cys6 (or C6 zinc) binuclear cluster DNA-binding domain and middle homology region family	Transcription factor
CDS410	635	230771 (Tv)	Ferric reductase and NADPH oxidase (NOX) like domain-containing protein	Oxidoreductase
CDS411	78	—NA—	No hit	Hypothetical protein
CDS412	179	53545 (Tv)	Copper transporter family protein	Transporter
CDS413	431	151414 (Tv)	Transferase family	Transferase
CDS414	361	53537 (Tv)	NAD/NADP octopine/nopaline dehydrogenase and Glycerol-3-phosphate dehydrogenase like domain-containing protein	Oxidoreductase

(Continued)

TABLE 1 | Continued

Gene ID (IMI 304061)	Size (aa)	Protein ID (*T. virens* Gv 29-8/ortholog)	Domains (NCBI CDD search)	Remarks/putativefunction
CDS416	513	59982 (Tv)	Cytochrome P450	P450
CDS417	217	53542 (Tv)	Lipid A phosphoethanol aminetransferase	Transferase
CDS418	534	191806 (Tv)	Major facilitator superfamily	Transporter
CDS419	672	XP_013944953 (Ta)	Transcription factor middle homology region (MHR)	Transcription factor
Deletion 2, Scaffold 1 (35 kb)				
CDS1017	349	222457 (Tv)	Short-chain dehydrogenases/reductases (SDR)	Oxidoreductase
CDS1018	469	222632 (Tv)	Transcription factor middle homology region (MHR)	Transcription factor
CDS1019	622	53406 (Tv)	Alpha/beta hydrolases (abhydrolase)	Hydrolase
CDS1020	455	53401 (Tv)	2-Polyprenyl-6-methoxyphenol hydroxylase and related FAD-dependent oxidoreductases	Oxidoreductase
CDS1021	136	222635 (Tv)	No hit	Hypothetical protein
CDS1022	163	XP_023915254 (Qs)	Major facilitator superfamily	Transporter
CDS1023	622	201619 (Tv)	Alpha/beta hydrolases (abhydrolase)	Hydrolase
CDS1024	368	213077 (Tv)	No hit	Hypothetical protein
CDS1025	223	191847 (Tv)	Soluble inorganic pyrophosphatase	Primary metabolism
CDS1026	307	XP_024754708 (Tas)	Camphor resistance (CrcB) family protein	Defense
CDS1027	433	53420 (Tv)	Enolase superfamily	Primary metabolism
CDS1028	242	70901 (Tv)	Alginate lyase (polysaccharide lyase family 7 protein)	CAZyme
CDS1029	177	191851 (Tv)	Short-chain dehydrogenases/reductases (SDR)	Oxidoreductase
Deletion 3, Scaffold 1 (0.3 kb)				
CDS2538	81	65480 (Tv)	Protein tyrosine phosphatase-like protein	Post-translational modifications, signaling
Deletion 4, Scaffold 20 (8.5 kb)				
CDS6746	809	90966 (Tv)	Cytochrome P450 (No methyl transferase)	P450
CDS6747	667	202324 (Tv)	No hit	Hypothetical protein
CDS6748	318	51663 (Tv)	Alpha/beta hydrolase family (abhydrolase 6)	Hydrolase
Deletion 5, Scaffold 58 (40 kb)				
CDS11382	217	66994 (Tv)	No hit	Hypothetical protein
CDS11383	410	128312 (Tv)	Lactonase	Defense
CDS11384	261	EMR68722 (Ul)	No hit	Hypothetical protein
CDS11385	410	70730 (Tv)	No hit	Hypothetical protein
CDS11386	1167	201824 (Tv)	Catalytic domain of phospholipase D superfamily proteins	Cell signaling
CDS11387	378	152027 (Tv)	Glycosyl hydrolase families: GH43, GH62, GH32, GH68, GH117, CH130 and fungal-type cellulose-binding like domain-containing protein	CAZyme
CDS11388	390	52963 (Tv)	No hit	Hypothetical protein
CDS11389	735	KID82061 (Mg)	hAT family C-terminal dimerization region	Transposase
CDS11390	312	60120 (Tv)	S1/P1 nucleases	Primary metabolism
CDS11391	608	KAE8412673 (Ap)	Tetratricopeptide repeat	Involved in cell division
CDS11392	553	193258 (Tv)	Berberine and berberine and FAD binding like domain-containing protein	Oxidoreductase

Tv: Trichoderma virens, Mg: Metarhizium guizhouense, Ap: Aspergillus pseudocaelatus, Tas: Trichoderma asperellum, Qs: Quercus suber, Ta: Trichoderma atroviride, Tg: Trichoderma guizhouense, Th: Trichoderma harzianum, Ul: Eutypa lata.

In addition, M7 is downregulated in biosynthesis of volatile organic compounds, including volatile sesquiterpenes, such as germacrenes, caryphyllene, alloaromadendrene, and gamma-muurolene, all having important biological activities (**Figure 3** and **Supplementary Table S2**). Volatile compounds produced by *Trichoderma* spp. promote plant growth and have antimicrobial effects against plant pathogens (Vinale et al., 2008; Hung et al., 2013). In transcriptome analysis, many secondary metabolism-related genes and gene clusters were downregulated in M7 (**Supplementary Tables S3, S4**). The viridin biosynthesis gene cluster comprises of 21 genes (Bansal et al., 2018), out of which, 16 genes were detected to be downregulated in M7. Similarly, the gliovirin biosynthetic gene cluster has 22 genes (Sherkhane et al., 2017), of which 16 genes were detected to be downregulated in M7. All the eight genes from the "*vir*" cluster, which are associated with volatile sesquiterpene compound production (Crutcher et al., 2013; Pachauri et al., 2019a), were downregulated in M7. In addition, eight NRPSs, one NRPS/PKS,

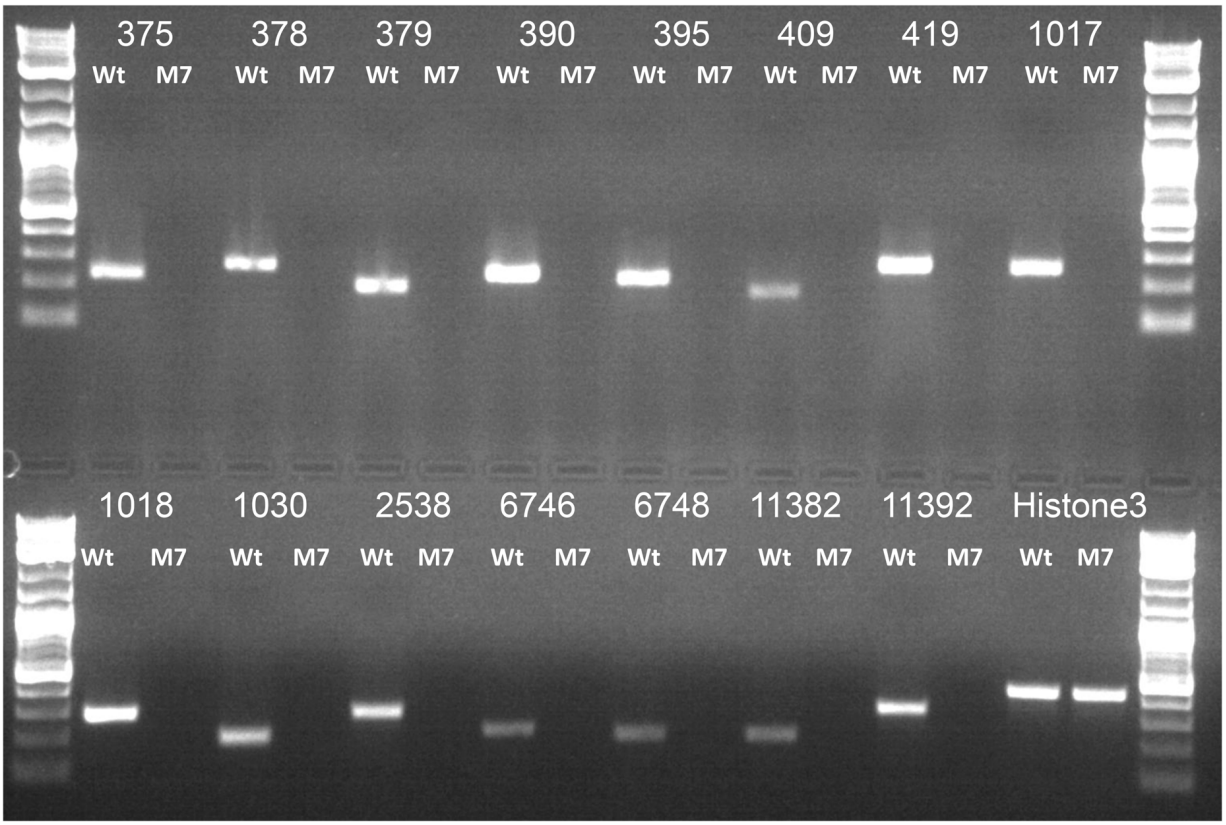

FIGURE 6 | PCR analysis of representative genes that are deleted in M7, using genomic DNA as template. Histone 3 was used as a positive control. The number corresponds to gene IDs as per **Table 1**. Ladder: Quick-Load Purple 1 kb Plus DNA Ladder (NEB).

seven PKSs, and three terpene cyclase genes were downregulated in M7. The NRPS genes that are downregulated in transcriptome analysis of M7 are Tex1, Tex2, Tex5, Tex7, Tex21, Glv21, NRPS (Trividraft 50383), NRPS-like (Trividraft_222800) (NRPSs), and Tex14 (NRPS/PKS). In addition, certain genes belonging to the Tex6, Tex8, Tex10 (NRPSs), and Tex12 (NRPS/PKS) clusters were also downregulated in M7. Tex1 and Tex2 code for peptaibol synthetase (Wiest et al., 2002; Mukherjee et al., 2011). Tex10 is involved in the biosynthesis of intracellular siderophore ferricrocin while Tex21 is responsible for the biosynthesis of extracellular siderophores (Mukherjee et al., 2018). The metabolites produced by Tex5 and Tex7-NRPS genes and Tex12 and Tex14-NRPS/PKS hybrid genes are not known. Of these NRPS genes, Tex5, Tex14, and Tex21 are downregulated in M7 during confrontation with *R. solani* (**Supplementary Table S4**). Seven PKS genes, namely PKS4, PKS8, PKS14, and PKS17, one un-annotated PKS (Trividraft_53518), and two orthologs of *Arthroderma benhamiae* (Acc. Nos. DAA76265 and EGE05473) PKSs were downregulated in M7 during confrontation with *R. solani*. The biosynthetic products of none of these PKS genes are known. In addition, some members of PKS3 and PKS6 gene clusters were also found to be downregulated in M7. PKS4 is an ortholog of pigment-forming PKS from *T. reesei* responsible for green conidial pigment biosynthesis and is involved in mechanical stability and stress tolerance (Atanasova et al., 2013a). Because M7 does not produce conidia, it is not surprising that the pigment PKS4 gene is downregulated in M7. In addition to PKS4, another gene (*con6*) that is associated with conidiation in *Neurospora crassa* (White and Yanofsky, 1993) was also downregulated in M7.

Having noted that the mutant M7 has a deficiency in conidiation, hydrophobicity, secondary metabolism, and mycoparasitism (all traits that dictate the success of *Trichoderma* spp. as plant beneficial fungi), which was apparent from the phenotyping and transcriptome data analysis, we did a whole genome sequence analysis of the mutant vis-à-vis the wild-type strain. It was interesting to note that the M7 genome has five deletions comprising as many as 71 genes. Because the mutant was generated using gamma ray-induced mutagenesis, deletions may be expected. Two large secondary metabolism-related gene clusters (PKS6 and Tex9) are deleted in the mutant. Four genes for glycoside hydrolase (GH) are also deleted, and so are several oxidoreductases. Because the data set of genes that are under-expressed in M7 is much larger that the number of genes that are deleted in the genome, it is likely that one or a few of these genes that are deleted or affected due to other mutations (**Table 1** and **Supplementary Table S5**) could have a pleiotropic phenotype regulating a big set of genes.

Our findings identify possible candidates for future research leading to identification of master regulator gene(s) in *Trichoderma*, a biotechnologically important fungal genus. Also, because the mutant is under-regulated in secondary metabolism and a large number of carbohydrate active enzymes, it could be possible to develop this mutant as a microbial cell factory for production of secondary metabolites and proteins.

We have recently reported the isolation and characterization of a mutant (G2) of *T. virens* that is upregulated in secondary metabolite biosynthesis (Mukherjee et al., 2019). A total of 140 genes were found to be upregulated in G2 over wild-type when grown on PDA medium. Of these, as many as 45 genes are downregulated in M7, including genes for CAZymes (13), secondary metabolism (5), Cytochrome P450 (3), SSCPs (2), oxidoreductase (3), peptidases (3), metabolism (5), hydrophobins (3), hypothetical proteins (5), transporter (1), and others (2). G2 and M7, thus, seem to be two contrasting "gene-regulation" mutants of *T. virens*. Although G2 has been developed as an improved biocontrol formulation (Mukherjee et al., 2019), M7 can serve as an excellent genetic tool for understanding *Trichoderma* biology.

CONCLUSION

We have identified a mutant of the plant beneficial fungus *T. virens* that is downregulated in conidiation, hydrophobicity, secondary metabolism, carbohydrate metabolism, and mycoparasitism. These traits are important for development of formulations, enzyme production, plant interactions, and biocontrol applications. By transcriptome analysis, we have also identified novel candidate genes for future research. We have also been able to identify 71 ORFs that are deleted in the mutant, which could be further studied for a role as novel regulator(s) of morphogenesis, secondary metabolism, and biocontrol properties in these plant beneficial fungal bioagents.

DATA AVAILABILITY STATEMENT

The datasets generated for this study can be found in the attached **Supplementary Material**. This Whole Genome Shotgun project has been deposited at DDBJ/ENA/GenBank under the accession JABENJ000000000. The version described in this manuscript is version JABENJ010000000.

AUTHOR CONTRIBUTIONS

SP and PS performed the laboratory experiments. PM and VK conceptualized, designed, and coordinated the studies. SP and PM analyzed the data. SP, PM, and VK wrote the manuscript.

FUNDING

SP was supported by a fellowship from the Department of Atomic Energy, Government of India.

ACKNOWLEDGMENTS

PM thanks Dr. P. Suprasanna, Head, NA&BT Division and Dr. V. P. Venugopalan, Associate Director, Bioscience Group, BARC, for encouragement and support. We would like to acknowledge Dr. Sumit Gupta, Food Technology Division, BARC for helping us in GC–MS analysis and Dr. Kaushik Banerjee, NRC-Grapes, Pune, for LC-MS/MS analysis of the metabolites.

SUPPLEMENTARY MATERIAL

The Supplementary Material for this article can be found online at: https://www.frontiersin.org/articles/10.3389/fmicb.2020.01030/full#supplementary-material

REFERENCES

Atanasova, L., Crom, S. L., Gruber, S., Coulpier, F., Seidl-Seiboth, V., Kubicek, C. P., et al. (2013a). Comparative transcriptomics reveals different strategies of *Trichoderma* mycoparasitism. *BMC Genomics* 14:121. doi: 10.1186/1471-2164-14-121

Atanasova, L., Knox, B. P., Kubicek, C. P., Druzhinina, I. S., and Baker, S. E. (2013b). The polyketide synthase gene pks4 of *Trichoderma reesei* provides pigmentation and stress resistance. *Eukaryot. Cell* 12, 1499–1508. doi: 10.1128/EC.00103-13

Bansal, R., Mukherjee, M., Horwitz, B. A., and Mukherjee, P. K. (2019). Regulation of conidiation and antagonistic properties of the soil-borne plant beneficial fungus *Trichoderma virens* by a novel proline-, glycine-, tyrosine-rich protein and a GPI-anchored cell wall protein. *Curr. Genet.* 65, 953–964. doi: 10.1007/s00294-019-00948-0

Bansal, R., Sherkhane, P. D., Oulkar, D., Khan, Z., Banerjee, K., and Mukherjee, P. K. (2018). The viridin biosynthesis gene cluster of *Trichoderma virens* and its conservancy in the bat white-nose fungus *Pseudogymnoascus destructans*. *Chem. Select.* 3, 1289–1293. doi: 10.1002/slct.201703035

Bayry, J., Aimanianda, V., Guijarro, J. I., Sunde, M., and Latgé, J. P. (2012). Hydrophobins-unique fungal proteins. *PLoS Pathog.* 8:e1002700. doi: 10.1371/journal.ppat.1002700

Carsolio, C., Benhamou, N., Haran, S., Cortés, C., Gutierrez, A., Chet, I., et al. (1999). Role of the *Trichoderma harzianum* endochitinase gene, ech42, in mycoparasitism. *Appl. Environ. Microbiol.* 65, 929–935. doi: 10.1128/aem.65.3.929-935.1999

Casselton, L., and Zolan, M. (2002). The art and design of genetic screens: Filamentous fungi. *Nat. Rev. Genet.* 3, 683–697. doi: 10.1038/nrg889

Crutcher, F. K., Parich, A., Schuhmacher, R., Mukherjee, P. K., Zeilinger, S., and Kenerley, C. M. (2013). A putative terpene cyclase, vir4, is responsible for the biosynthesis of volatile terpene compounds in the biocontrol fungus *Trichoderma virens*. *Fungal Genet. Biol.* 56, 67–77. doi: 10.1016/j.fgb.2013.05.003

Djonović, S., Pozo, M. J., Dangott, L. J., Howell, C. R., and Kenerley, C. M. (2006a). Sm1, a proteinaceous elicitor secreted by the biocontrol fungus *Trichoderma virens* induces plant defense responses and systemic resistance. *Mol. Plant Microbe Interact.* 19, 838–853. doi: 10.1094/mpmi-19-0838

Djonović, S., Pozo, M. J., and Kenerley, C. M. (2006b). Tvbgn3, a β-1,6-glucanase from the biocontrol fungus *Trichoderma virens*, is involved in mycoparasitism and control of *Pythium ultimum*. *Appl. Environ. Microbiol.* 72, 7661–7670. doi: 10.1128/aem.01607-06

Djonović, S., Vargas, W., Kolomiets, M., Horndeski, M., Wiest, A., and Kenerley, C. (2007a). A Proteinaceous Elicitor Sm1 from the beneficial fungus *Trichoderma*

virens is required for induced systemic resistance in Maize. *Plant Physiol.* 145, 875–889. doi: 10.1104/pp.107.103689

Djonović, S., Vittone, G., Mendoza-Herrera, A., and Kenerley, C. M. (2007b). Enhanced biocontrol activity of *Trichoderma virens* transformants constitutively coexpressing β-1,3- and β-1,6-glucanase genes. *Mol. Plant Pathol.* 8, 469–480. doi: 10.1111/j.1364-3703.2007.00407.x

Druzhinina, I. S., Seidl-Seiboth, V., Herrera-Estrella, A., Horwitz, B. A., Kenerley, C. M., Monte, E., et al. (2011). *Trichoderma*: the genomics of opportunistic success. *Nat. Rev. Microbiol.* 9, 749–759. doi: 10.1038/nrmicro2637

Gaderer, R., Lamdan, N. L., Frischmann, A., Sulyok, M., Krska, R., Horwitz, B. A., et al. (2015). Sm2, a paralog of the *Trichoderma* cerato-platanin elicitor Sm1, is also highly important for plant protection conferred by the fungal-root interaction of *Trichoderma* with maize. *BMC Microbiol.* 15:2. doi: 10.1186/s12866-014-0333-0

Guzmán-Guzmán, P., Alemán-Duarte, M. I., Delaye, L., Herrera-Estrella, A., and Olmedo-Monfil, V. (2017). Identification of effector-like proteins in *Trichoderma* spp. and role of a hydrophobin in the plant-fungus interaction and mycoparasitism. *BMC Genet.* 18:16. doi: 10.1186/s12863-017-0481-y

Haran, S., Schickler, H., and Chet, I. (1996). Molecular mechanisms of lytic enzymes involved in the biocontrol activity of *Trichoderma harzianum*. *Microbiology* 142, 2321–2331. doi: 10.1099/00221287-142-9-2321

Howell, C. R., and Stipanovic, R. D. (1983). Gliovirin, a new antibiotic from Gliocladium virens, and its role in the biological control of Pythium ultimum. *Can. J. Microbiol.* 29, 321–324. doi: 10.1139/m83-053

Howell, C. R., Stipanovic, R. D., and Lumsden, R. D. (1993). Antibiotic production by strains of *Gliocladium virens* and its relation to the biocontrol of cotton seedling diseases. *Biocontrol Sci. Techn.* 3, 435–441. doi: 10.1080/09583159309355298

Hung, R., Lee, S., and Bennett, J. W. (2013). Arabidopsis thaliana as a model system for testing the effect of *Trichoderma* volatile organic compounds. *Fungal Ecol.* 6, 19–26. doi: 10.1016/j.funeco.2012.09.005

Jones, R. W., and Hancock, J. G. (1987). Conversion of viridin to viridiol by viridin-producing fungi. *Can. J. Microbiol.* 33, 963–966. doi: 10.1139/m87-169

Kubicek, C. P., Baker, S., Gamauf, C., Kenerley, C. M., and Druzhinina, I. S. (2008). Purifying selection and birth-and-death evolution in the class II hydrophobin gene families of the ascomycete *Trichoderma/Hypocrea*. *BMC Evol. Biol.* 8:4. doi: 10.1186/1471-2148-8-4

Kubicek, C. P., Herrera-Estrella, A., Seidl-Seiboth, V., Martinez, D. A., Druzhinina, I. S., Thon, M., et al. (2011). Comparative genome sequence analysis underscores mycoparasitism as the ancestral life style of *Trichoderma*. *Genome Biol.* 12:R40. doi: 10.1186/gb-2011-12-4-r40

Le Crom, S., Schackwitz, W., Pennacchio, L., Magnuson, J. K., Culley, D. E., Collett, J. R., et al. (2009). Tracking the roots of cellulase hyperproduction by the fungus *Trichoderma reesei* using massively parallel DNA sequencing. *PNAS* 106, 16151–16156. doi: 10.1073/pnas.0905848106

Lorito, M., Woo, S. L., Harman, G. E., and Monte, E. (2010). Translational research on *Trichoderma*: from 'Omics to the Field. *Annu. Rev. Phytopathol.* 48, 395–417. doi: 10.1146/annurev-phyto-073009-114314

Mattern, I. E., van Noort, J. M., van den Berg, P., Archer, D. B., Roberts, I. N., and van den Hondel, C. A. M. J. J. (1992). Isolation and characterization of mutants of *Aspergillus niger* deficient in extracellular proteases. *Mol. Gen. Genet.* 234, 332–336. doi: 10.1007/bf00283855

McCluskey, K., Wiest, A. E., Grigoriev, I. V., Lipzen, A., Martin, J., Schackwitz, W., et al. (2011). Rediscovery by whole genome sequencing: classical mutations and genome polymorphisms in *Neurospora crassa*. *G3* 1, 303–316. doi: 10.1534/g3.111.000307

Mendoza-Mendoza, A., Pozo, M. J., Grzegorski, D., Martínez, P., García, J. M., Olmedo-Monfil, V., et al. (2003). Enhanced biocontrol activity of *Trichoderma* through inactivation of a mitogen-activated protein kinase. *PNAS* 100, 15965–15970. doi: 10.1073/pnas.2136716100

Mendoza-Mendoza, A., Zaid, R., Lawry, R., Hermosa, R., Monte, E., Horwitz, B. A., et al. (2018). Molecular dialogues between *Trichoderma* and roots: role of the fungal secretome. *Fungal Biol. Rev.* 32, 62–85. doi: 10.1016/j.fbr.2017.12.001

Mukherjee, M., Horwitz, B. A., Sherkhane, P. D., Hadar, R., and Mukherjee, P. K. (2006). A secondary metabolite biosynthesis cluster in *Trichoderma virens*: evidence from analysis of genes underexpressed in a mutant defective in morphogenesis and antibiotic production. *Curr. Genet.* 50, 193–202. doi: 10.1007/s00294-006-0075-0

Mukherjee, P. K., and Kenerley, C. M. (2010). Regulation of morphogenesis and biocontrol properties in *Trichoderma virens* by a VELVET protein, Vel1. *Appl. Environ. Microbiol.* 76, 2345–2352. doi: 10.1128/AEM.02391-09

Mukherjee, M., Mukherjee, P. K., and Kale, S. P. (2007). cAMP signalling is involved in growth, germination, mycoparasitism and secondary metabolism in *Trichoderma virens*. *Microbiology* 153, 1734–1742. doi: 10.1099/mic.0.2007/005702-0

Mukherjee, P. K., Horwitz, B. A., Herrera-Estrella, A., Schmoll, M., and Kenerley, C. M. (2013a). *Trichoderma* research in the genome era. *Annu. Rev. Phytopathol.* 51, 105–129.

Mukherjee, P. K., Horwitz, B. A., Singh, U. S., Mukherjee, M., and Schmoll, M. (eds) (2013b). *Trichoderma Biology and Applications*. Wallingford: CABI.

Mukherjee, P. K., Hurley, J. F., Taylor, J. T., Puckhaber, L., Lehner, S., Druzhinina, I., et al. (2018). Ferricrocin, the intracellular siderophore of *Trichoderma virens*, is involved in growth, conidiation, gliotoxin biosynthesis and induction of systemic resistance in maize. *Biochem. Biophys. Res. Commun.* 505, 606–611. doi: 10.1016/j.bbrc.2018.09.170

Mukherjee, P. K., Latha, J., Hadar, R., and Horwitz, B. A. (2003). TmkA, a mitogen-activated protein kinase of *Trichoderma virens*, is involved in biocontrol properties and repression of conidiation in the dark. *Eukaryot. Cell.* 2, 446–455. doi: 10.1128/ec.2.3.446-455.2003

Mukherjee, P. K., Mehetre, S. T., Sherkhane, P. D., Muthukathan, G., Ghosh, A., Kotasthane, A. S., et al. (2019). A novel seed-dressing formulation based on an improved mutant strain of *Trichoderma virens*, and its field evaluation. *Front. Microbiol.* 10:1910. doi: 10.3389/fmicb.2019.01910

Mukherjee, P. K., Wiest, A., Ruiz, N., Keightley, A., Moran-Diez, M. E., McCluskey, K., et al. (2011). Two classes of new peptaibols are synthesized by a single non-ribosomal peptide synthetase of *Trichoderma virens*. *J. Biol. Chem.* 286, 4544–4554. doi: 10.1074/jbc.M110.159723

Mukhopadhyay, A. N., Shrestha, S. M., and Mukherjee, P. K. (1992). Biological seed treatment for control of soil-borne plant pathogens. *FAO Plant Prot. Bull.* 40, 21–30.

Pachauri, S., Chatterjee, S., Kumar, V., and Mukherjee, P. K. (2019a). A dedicated glyceraldehyde-3-phosphate dehydrogenase is involved in the biosynthesis of volatile sesquiterpenes in *Trichoderma virens*—evidence for the role of a fungal GAPDH in secondary metabolism. *Curr Genet.* 65, 243–252. doi: 10.1007/s00294-018-0868-y

Pachauri, S., Sherkhane, P., and Mukherjee, P. K. (2019b). "Secondary metabolism in trichoderma: chemo- and geno-diversity" in *Microbial Diversity in Ecosystem Sustainability and Biotechnological Applications*, eds T. Satyanarayana, S. K. Das, and B. N. Johri (Berlin: Springer Nature)

Przylucka, A., Akcapinar, G. B., Chenthamara, K., Cai, F., Grujic, M., Karpenko, J., et al. (2006). Multiple roles and effects of a novel Trichoderma hydrophobin. *Mol. Plant Pathol.* 7, 249–258. doi: 10.1094/MPMI-07-14-0194-R

Przylucka, A., Akcapinar, G. B., Chenthamara, K., Cai, F., Grujic, M., Karpenko, J., et al. (2017). HFB7 – A novel orphan hydrophobin of the *Harzianum* and *Virens* clades of *Trichoderma*, is involved in response to biotic and abiotic stresses. *Fungal Genet. Biol.* 102, 63–76. doi: 10.1016/j.fgb.2017.01.002

Sherkhane, P. D., Bansal, R., Banerjee, K., Chatterjee, S., Oulkar, D., Jain, P., et al. (2017). Genomics-driven discovery of the gliovirin biosynthesis gene cluster in the plant beneficial fungus *Trichoderma virens*. *ChemistrySelect* 2, 3347–3352. doi: 10.1002/slct.201700262

Vinale, F., Sivasithamparam, K., Ghisalberti, E. L., Marra, R., Woo, S. L., and Lorito, M. (2008). *Trichoderma*–plant–pathogen interactions. *Soil Biol. Biochem.* 40, 1–10.

Viterbo, A., and Chet, I. (2006). TasHyd1, a new hydrophobin gene from the biocontrol agent *Trichoderma asperellum*, is involved in plant root colonization. *Mol. Plant Pathol.* 7, 249–258. doi: 10.1111/j.1364-3703.2006.00335.x

Viterbo, A., Wiest, A., Brotman, Y., Chet, I., and Kenerley, C. (2007). The 18mer peptaibols from *Trichoderma virens* elicit plant defence responses. *Mol Plant Pathol.* 8, 737–746. doi: 10.1111/j.1364-3703.2007.00430.x

Wessels, J. G. H. (1996). Fungal hydrophobins: proteins that function at an interface. *Trends Plant Sci.* 1, 9–15. doi: 10.1016/s1360-1385(96)80017-3

White, B. T., and Yanofsky, C. (1993). Structural characterization and expression analysis of the *Neurospora* conidiation gene con-6. *Dev. Biol.* 160, 254–264. doi: 10.1006/dbio.1993.1303

Wiest, A., Grzegorski, D., Xu, B. W., Goulard, C., Rebuffat, S., Ebbole, D. J., et al. (2002). Identification of peptaibols from *Trichoderma virens* and cloning of a peptaibol synthetase. *J. Biol. Chem.* 277, 20862–20868. doi: 10.1074/jbc.m201654200

Zeilinger, S., Gruber, S., Bansal, R., and Mukherjee, P. K. (2016). Secondary metabolism in *Trichoderma* - Chemistry meets genomics. *Fungal Biol. Rev.* 30, 74–90. doi: 10.1016/j.fbr.2016.05.001

Zhang, H., Ji, S., Guo, R., Zhou, C., Wang, Y., Fan, H., et al. (2019). Hydrophobin HFBII-4 from *Trichoderma asperellum* induces antifungal resistance in poplar. *Braz. J. Microbiol.* 50, 603–612. doi: 10.1007/s42770-019-00083-5

Conflict of Interest: The authors declare that the research was conducted in the absence of any commercial or financial relationships that could be construed as a potential conflict of interest.

frontiers in Microbiology

ORIGINAL RESEARCH
published: 17 June 2020
doi: 10.3389/fmicb.2020.01196

Antifungal Effects of Volatiles Produced by *Bacillus subtilis* Against *Alternaria solani* in Potato

Dai Zhang[1], Shuiqing Yu[1], Yiqing Yang[1], Jinglin Zhang[2], Dongmei Zhao[1], Yang Pan[1], Shasha Fan[1], Zhihui Yang[1] and Jiehua Zhu[1]**

[1] College of Plant Protection, Hebei Agricultural University, Baoding, China, [2] Beijing Laboratory for Food Quality and Safety, Beijing Technology and Business University, Beijing, China

OPEN ACCESS

Edited by:
Francesco Vinale,
University of Naples Federico II, Italy

Reviewed by:
Frédérique Reverchon,
Instituto de Ecología (INECOL), Mexico
Hafiz Abdul Samad Tahir,
Ministry of National Food Security and Research, Pakistan

***Correspondence:**
Zhihui Yang
bdyzh@hebau.edu.cn
Jiehua Zhu
zhujiehua356@126.com

Specialty section:
This article was submitted to Microbial Symbioses, a section of the journal Frontiers in Microbiology

Received: 24 March 2020
Accepted: 12 May 2020
Published: 17 June 2020

Citation:
Zhang D, Yu S, Yang Y, Zhang J, Zhao D, Pan Y, Fan S, Yang Z and Zhu J (2020) Antifungal Effects of Volatiles Produced by Bacillus subtilis Against Alternaria solani in Potato. Front. Microbiol. 11:1196. doi: 10.3389/fmicb.2020.01196

Antifungal activities of plant-beneficial *Bacillus* have been widely studied in recent years. Numerous studies have studied the antifungal mechanisms of soluble non-volatile bioactive compounds such as lipopeptides and proteins produced by *Bacillus* against soil-borne diseases. However, the antagonistic mechanisms of volatile organic compounds (VOCs) from *Bacillus* against airborne phytopathogens are still largely unknown, and the function of *Alternaria solani* pathogenic genes has not been well identified. Here, we first isolated a *Bacillus* strain with strong antifungal activity and finally identified it as *B. subtilis* ZD01. Then, the antagonistic mechanisms of VOCs produced by strain ZD01, against *A. solani*, an airborne fungal pathogen that can cause early blight diseases of potato, were studied. We showed that VOCs produced by strain ZD01 can reduce the colony size and mycelial penetration and can cause serious morphological changes of *A. solani*. Scanning electron microscope (SEM) observation showed that VOCs released by ZD01 could cause more flaccid and gapped hyphae of *A. solani*. Also, we found that VOCs produced by ZD01 can inhibit the conidia germination and reduce the lesion areas and number of *A. solani in vivo* significantly. Meanwhile, based on gas chromatography/mass spectrometry (GC/MS) analysis, 29 volatile compounds produced by strain ZD01 were identified. Out of 29 identified VOCs, 9 VOCs showed complete growth inhibition activities against *A. solani*. Moreover, we identified two virulence-associated genes (*slt2* and *sod*) in *A. solani*. *slt2* is a key gene that regulates the mycelial growth, penetration, sporulation, and virulence *in vivo* in *A. solani*. In addition, *sod* plays a significant role in the SOD synthetic pathway in *A. solani*. Results from qRT-PCR showed that the transcriptional expression of these two genes was down-regulated after being treated by VOCs produced by ZD01. These results are useful for a better understanding of the biocontrol mechanism of *Bacillus* and offer a potential method for potato early blight disease control.

Keywords: antifungal activity, *Bacillus subtilis*, volatile organic compounds, airborne phytopathogens, *Alternaria solani*

INTRODUCTION

Alternaria solani is a kind of fungal pathogen that can cause early blight disease of tomato, potato, tobacco, and many other vegetables and crops, and lead to huge losses in agricultural production. Potato is one of the most important crops in the world. Early blight disease on potato can cause up to 80% of annual yield losses in some regions of the world (Morgan et al., 2002; Pasche et al., 2004; Peters et al., 2008). Nowadays, chemical fungicides are the most effective agents to control early blight. However, the indiscriminate using and even abuse of chemical fungicides have already caused the appearance of resistant pathogens, which will further threaten the food safety and human health. Due to this, there is a rising interest to seek for alternative antifungal agents for plant disease control.

Bacillus species are known for their capacity to produce a great variety of antifungal compounds to suppress or kill fungal pathogens (Chaurasia et al., 2005). Among them, non-ribosomal cyclic lipopeptides (Nakano et al., 1988; Munimbazi and Bullerman, 1998; Kim et al., 2004; Timmusk et al., 2005) are the most well-studied ones. However, these non-volatile antibiotics cannot spread over long distances. In recent years, volatile organic compounds (VOCs) produced by *Bacillus* have been evaluated as a new approach for plant fungal disease control. Due to their capability of diffusing between the soil particles and spreading into the atmosphere over very large distances from their original application point, VOCs can exert their inhibitory activity without direct or physical contact between the VOC-producing microorganisms and the target pathogens (Minerdi et al., 2009; Heydari and Pessarakli, 2010). Their strong antifungal activities, along with the characteristic of harmless to both environment and human beings, make VOCs a promising and sustainable agent to replace fungicides for plant pathogen control in the future (Fialho et al., 2010; Parafati et al., 2017; Tilocca et al., 2020).

In many previous studies, VOCs emitted by *Bacillus* species were shown to be potential antifungal agent against many soil-borne pathogens. For instance, VOCs produced by *B. amyloliquefaciens* NJN-6 could hinder growth and spore germination of the pathogenic *Fusarium oxysporum* f. sp. *cubense* causing fusarium wilt on banana (Yuan et al., 2012). Moreover, numerous identified volatiles released by *Bacillus* have demonstrated to inhibit fungal growth, including dimethyl disulfide, 1-undecene, benzaldehyde, benzothiazole, dimethyl trisulfide, cyclohexanol, decanal, 2-ethyl-1-hexanol (Kai et al., 2009). For instance, co-cultured with 2-nonone and 2-heptanone released by *B. amyloliquefaciens*, the mycelia of *F. oxysporum* f. sp. *niveum* stopped growth completely (Wu et al., 2019).

However, limited knowledge is known about bacterial VOCs controlling airborne plant fungal pathogens, especially *A. solani*. In several recent studies, VOCs produced by *Bacillus* species have been identified to inhibit the airborne pathogens, mainly as *Botrytis cinerea*, the causal agent of tomato gray mold. Two *Bacillus velezensis* strains 5YN8 and DSN012 could suppress the growth and spore formation of *B. cinerea* by releasing numbers of VOCs (Jiang et al., 2018). The VOCs of *B. velezensis* ZSY-1 strain exhibit significant antifungal activity against *B. cinerea* (Gao et al., 2017). The mixed volatiles produced by *B. atrophaeus* CAB-1 strains, mainly composed of hexadecane, 2,3-dimethoxybenzamide, and oanisaldehyde, resulted in an effective inhibition of *B. cinerea* (Zhang et al., 2013).

In this study, *B. subtilis* ZD01, an effective antifungal strain, was isolated and identified from potato rhizosphere, and the antifungal effects of VOCs produced by it on *A. solani* were investigated by both *in vivo* and *in vitro* experiments. We demonstrated that VOCs of *B. subtilis* have great potential to be used as a biologically synthesized fungicide in the agricultural field.

RESULTS

B. subtilis ZD01 Showed Strong Inhibitory Activity Against *A. solani*

A total of 103 isolated *Bacillus* strains were obtained from rhizosphere of potato in Shandong and Hebei Province in China. Among them, 34 isolates showed a certain inhibition effect on *A. solani* (**Supplementary Table S1**). Notably, strain ZD01 showed the strongest antagonistic activity against *A. solani* (**Supplementary Table S1**). Then, ZD01 were tested for inhibitory activity mediated by volatile against *A. solani* using face-to-face Petri dish method (Gao et al., 2017). The result showed that the growth rates of *A. solani* mycelia were reduced by 50.1 ± 2.1% in the presence of volatiles released by ZD01 (**Figure 1A**). **Figures 1C,D** showed that a broad range of pathogens were also inhibited by the volatiles released from strain ZD01.

Strain ZD01 was then identified by 16s rRNA and complete genome sequencing. We performed BLAST search using the DNA sequence of the16S rRNA gene of ZD01 as a query against the NCBI GenBank database. Furthermore, we sequenced the complete genome of ZD01 by Pacbio RSII. After that, a single circularized chromosome of 4,015,360 bp in length with a GC content of 43.71% from ZD01 was obtained (**Figure 1B**, CP046448). According to the BLAST and complete genome sequencing results, we found that strain ZD01 showed extremely high similarity (identity 99%, *E*-value = 0) to *B. subtilis*. We finally classified the strain ZD01 as *B. subtilis*.

VOCs Produced by ZD01 Changed the Mycelia Morphology and Inhibited the Conidia Germination of *A. solani*

Inhibition of fungal mycelia growth and spore germination is conventional mechanism of biocontrol agents for disease controlling. So, the suppression of VOCs produced by ZD01 on mycelia growth and conidia germination were evaluated. The result showed that the inhibition rate of *A. solani* growth by VOCs was 50.1 ± 2.1% compared with the control after 6 days, suggesting that the VOCs from ZD01 showed a strong inhibitory activity on fungal mycelia growth. Moreover, with the treatment of VOCs produced by *B. subtilis* ZD01, the mycelia of *A. solani* became denser and thicker, and the color of the colony turned into white (**Figure 1A**). In addition, strong decrease in

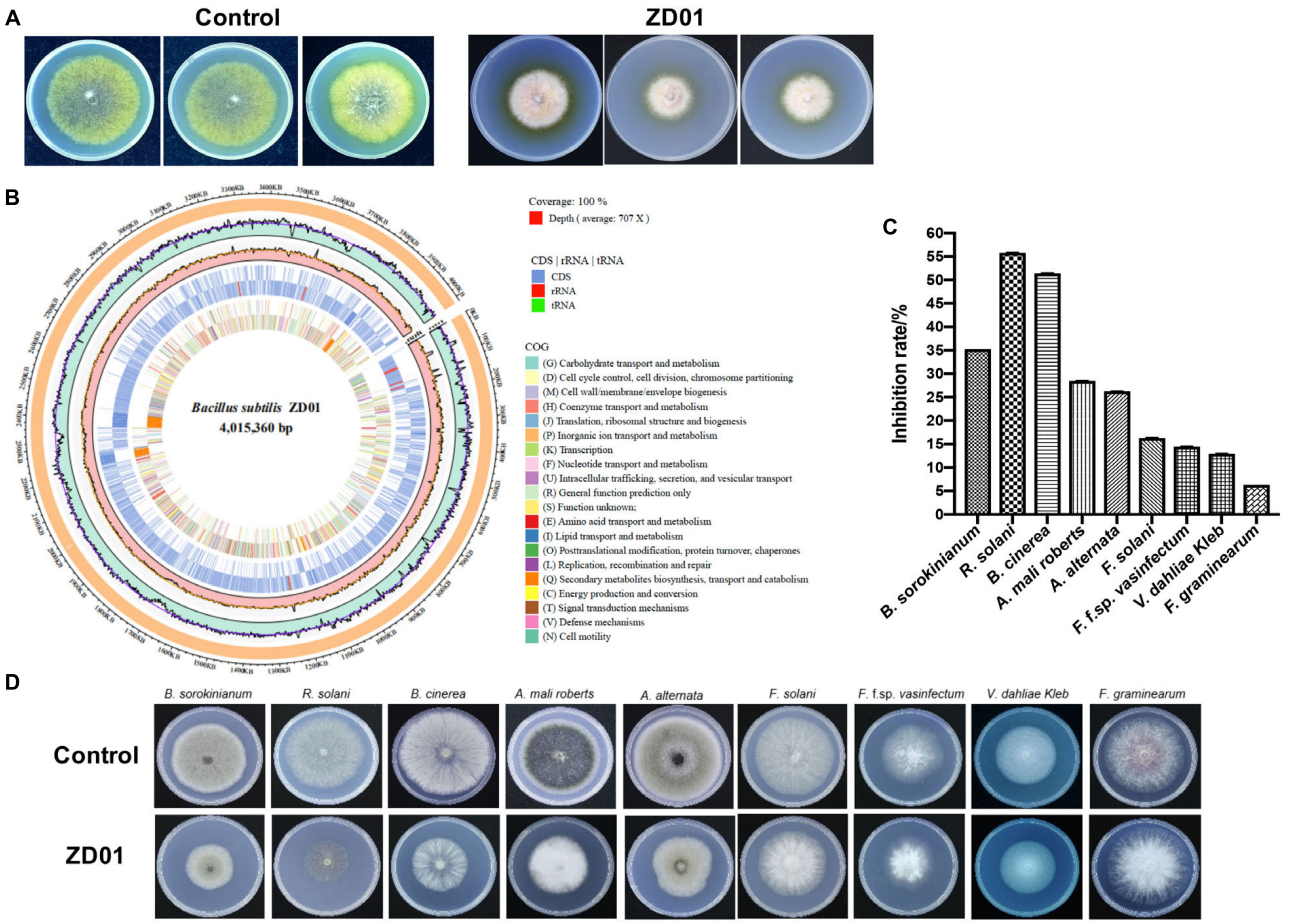

FIGURE 1 | Isolation and identification of ZD01 volatiles for *A. solani* control. **(A)** Antagonistic activity of ZD01 volatiles against *A. solani*. **(B)** The circularized genome map of *Bacillus subtilis* ZD01. **(C,D)** Antagonistic activity of VOCs produced by ZD01 against nine plant pathogens, including *Bipolaris sorokinianum*, *Rhizoctonia solani*, *Botrytis cinerea*, *Alternaria mali roberts*, *Alternaria alternata*, *Fusarium solani*, *Fusarium oxysporum* f. sp. *vasinfectum*, *Verticillium dahliae Kleb*, and *Fusarium graminearum*. Control represents *A. solani* without treatment of ZD01 VOCs; ZD01 represents *A. solani* with treatment of ZD01 VOCs.

mycelial penetration was observed after treatment. Mycelia in control groups were able to penetrate cellophane sheets during the cellophane penetration assay with the colony diameter of 5.5 ± 1.6 cm. However, the *A. solani* colony co-cultured with VOCs produced by ZD01 did not grow after the cellophane was removed, which indicated that the penetration ability of mycelia lost completely (**Figure 2A**).

A scanning electron microscope (SEM) was used to investigate detailed morphological changes of *A. solani* hyphae caused by VOCs. Morphological changes in *A. solani* cells are shown in **Figure 2B**. Regular length and intact cell walls with uniform composition and structure were present in the hyphae of *A. solani* in the control group (**Figure 2B**). However, hyphae treated with VOCs from ZD01 exhibited substantial structural destruction (**Figure 2B**). In detail, some of the hyphae became expanded, and the formation of empty segments was presented (red arrows, **Figure 2B**). Treated mycelium appeared with a more flaccid hyphae, and the surface of the cell walls became uneven (yellow arrows, **Figure 2B**). Also, thin or gapped structures presenting a retracted protoplasm were seen in **Figure 2B** (green arrows). The broken structures might lead to the leakage of cytoplasmic components. Thus, volatiles produced by ZD01 could change the morphology of *A. solani* seriously, and decompose the cell walls and membrane.

Spore germination plays a crucial role during the infection of fungal pathogens, so the conidia germination suppression capacity of VOCs produced by *B. subtilis* ZD01 was evaluated. As shown in **Figures 2C,D**, the *B. subtilis* ZD01 could inhibit the germination of *A. solani* conidia significantly ($P < 0.05$) by releasing some VOCs compared with the control group. In the control group, conidia began to germinate and germ tube formed. Then, the germ tubes formed regular hyphae (black arrow, **Figure 2C**), which can directly penetrate the host epidermal cell junctions and formed infection hyphae on leaf. However, some conidia treated with VOCs from ZD01 could not germinate completely (blue arrow, **Figure 2C**), and some conidia formed irregular germ tubes, which were much shorter than those in the control group (red arrows, **Figure 2C**). The inhibition rate of VOCs from ZD01 on conidia germination was 19.2 ± 2.1% (**Figure 2D**).

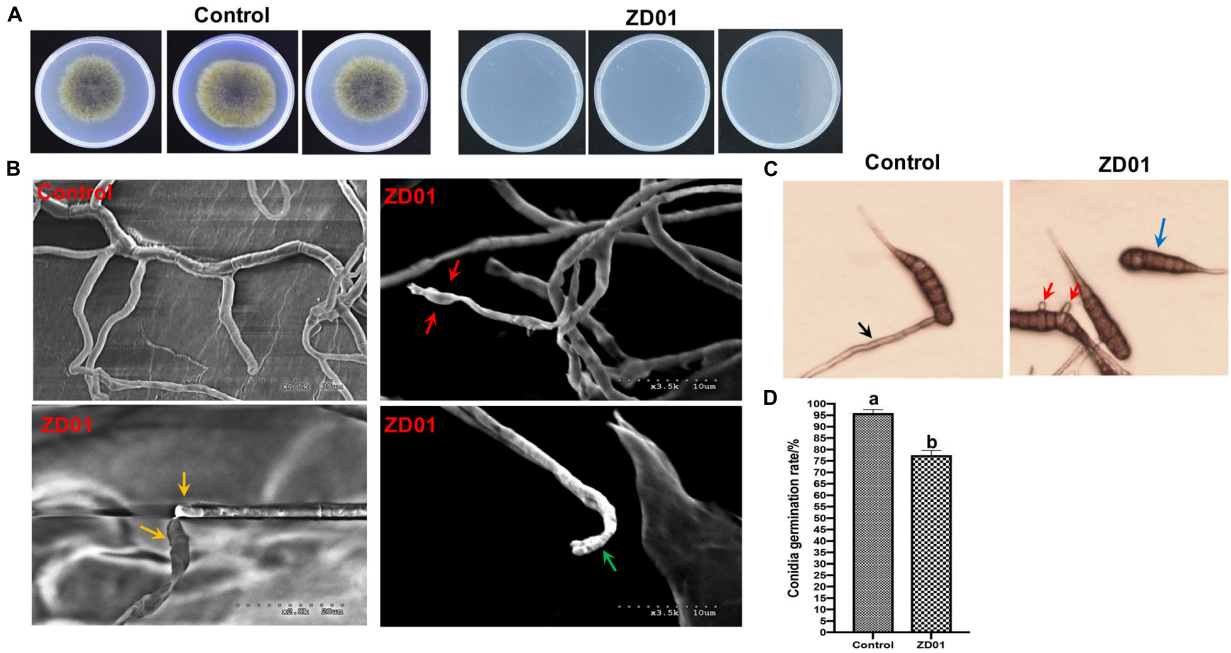

FIGURE 2 | Effects of strain ZD01 volatiles on mycelia penetration and morphology as well as conidia germination of *A. solani*. **(A)** Mycelia penetration inhibition by ZD01 volatiles. **(B)** Scanning electron micrographs of *A. solani* co-cultured with ZD01 volatiles. **(C,D)** Reduction of conidia germination of *A. solani* with the treatment of ZD01 volatiles. Control represents *A. solani* without treatment of ZD01 VOCs; ZD01 represents *A. solani* with treatment of ZD01 VOCs. Data presented are the mean ± s.d. (n = 3). The same letter on the bars for each column indicates no significant difference according to a LSD test at P = 0.05.

VOCs Produced by *B. subtilis* ZD01 Reduced the Symptoms of Early Blight Disease on Potato Leaf

The development and expansion of disease symptom induced by *A. solani* was inhibited effectively by VOCs produced by strain ZD01 in *in vivo* leaf test. As shown in **Figure 3A**, the lesion areas on potato leaves (cultivar Helan 15) inoculated by *A. solani* were significantly reduced ($P < 0.05$) after co-cultivation with ZD01 volatiles by divided plate method. For leaves in the control group with no treatment of ZD01 volatiles, the lesion areas extended to 5.2 ± 1.7 cm^2 after 5–7 days incubation at 25°C, whereas for the leaves exposed to volatiles from ZD01, the lesion areas were limited to 0.8 ± 0.3 cm^2 (**Figure 3B**). These results corresponded to relative pathogen copy numbers per milligram leaf of 3.98 ± 0.67 × 10^8 and 1.08 ± 0.22 × 10^8 for control and treatment, respectively (**Figure 3C**).

Identification and Antifungal Activity of VOCs Produced by *B. subtilis* ZD01

The VOCs produced by strain ZD01 were analyzed by solid-phase microextraction–gas chromatography/mass spectrometry (SPME-GC/MS). In total, 29 VOCs were identified from ZD01, including 6 ketones, 17 aromatic compounds, 1 furan, 1 pyrazine, 3 alcohols, and 1 ester (**Figures 4A,B** and **Table 1**).

To determine the antagonistic effect of VOCs produced by ZD01, 25 of the identified VOCs were tested using face-to-face plate method (Gong et al., 2015). Among the 25 volatile chemicals, nine chemicals including acetophenone, 2-nonanone, m-tolunitrile, 2-ethylhexanol, 2-heptanone, benzylacetone, 6-methyl-2-heptanone, benzothiazole, and 5-methyl-2-hexanone completely inhibited the growth of *A. solani*. Aniline, 4-methylanisole, benzoxazole, valerophenone, and 2,5-dimethylpyrazine showed strong antagonistic effect, and their inhibition rates against *A. solani* were 93.6 ± 0.3, 91.7 ± 1.6, 88.5 ± 4.6, 88.8 ± 0.5, and 77.7 ± 6.0%, respectively. The remaining compounds showed weak or no inhibitory activity (**Figures 4C,D**). Among these active VOCs, acetophenone, 6-methyl-2-heptanone, and aniline have larger peak areas than others, with 18.5, 8.9, and 31.4%, respectively (**Table 1**), which indicated that these compounds are potential agents for controlling potato early blight.

slt2 and *sod* Are Virulence-Associated Genes in *A. solani*

Identification of virulence-associated genes is important to reveal the pathogenic mechanisms and biological control approaches of fungal pathogens. The complete genome sequence of *A. solani* HWC-168 has been sequenced and analyzed in our previous study (Zhang et al., 2018). We compared the whole genome sequence of HWC-168 with its well-studied *Saccharomyces cerevisiae* (EF058927.1) and close relative *A. alternate* (GQ414510.1). After that, two typical pathogenic genes (*slt2* and *sod*) were found in the genome of HWC-168. Then, the functions of these two genes were determined through gene knockout and phenotype verification.

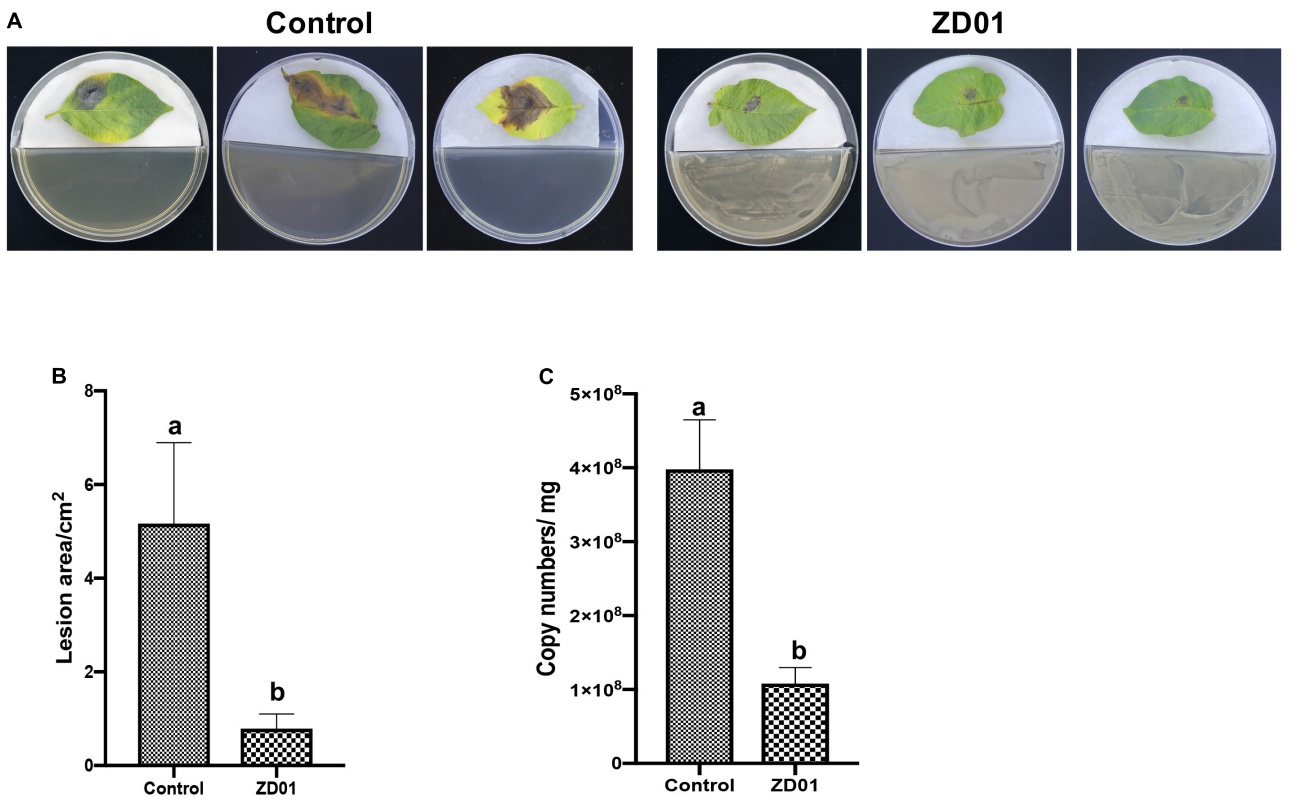

FIGURE 3 | Antagonistic effects of VOCs produced by strain ZD01 against *A. solani* on potato leaf. **(A)** Effect of VOCs produced by ZD01 on development of early blight symptoms on Potato leaf. **(B)** Lesion areas of potato leaf with or without the treatment by ZD01 volatiles. **(C)** *A. solani* copy numbers per leaf were detected in potato leaf. Control represents *A. solani* without treatment of ZD01 VOCs; ZD01 represents *A. solani* with treatment of ZD01 VOCs. Data presented are the mean ± s.d. (n = 3). The same letter on the bars for each column indicates no significant difference according to a LSD test at P = 0.05.

To determine whether *slt2* and *sod* affects the pathogenicity of *A. solani*, we compared the deletion mutants with the wild-type strain and complementation strains in mycelia growth, sporulation, and virulence by *in vivo* potato leaf tests. Compared with the wild-type strain and complementation strains, the mycelium of *slt2* mutant was significantly denser, and the color of colony was gray-white without pigments (**Figure 5A**). The colony diameter of *slt2* deletion mutants was 2.79 ± 0.52 cm, while that of wild-type strain and complementation strains were 6.18 ± 0.14 and 6.18 ± 0.08 cm, respectively (**Figure 5E**). No obvious changes of the colony morphology and diameter of *sod* deletion mutant were observed (**Figures 5A,E**), while the colony diameter of Δ*sod* and its complementation strain (Δ*sod*-C) were 6.04 ± 0.14 and 6.11 ± 0.27 cm, respectively. These results suggested that *slt2* is the key gene involved in the regulation of mycelium growth and development. Also, we found that the *slt2* gene was critical for the penetration ability of *A. solani*. As shown in **Figure 5B**, the wild-type and complemented strains of *slt2* but not the mutants were able to penetrate cellophane sheets in the cellophane penetration assay.

We next tested whether the *slt2* and *sod* genes are also responsible for the sporulation of *A. solani*. The results showed that *slt2* mutant lost the capacity of conidia production and the yield of conidia of *sod* deletion mutant per area was 514 ± 149/cm^2, while the wild-type strain was 2131 ± 301/cm^2 (**Figure 5D**). Compared with the wild-type strain, the sporulation yield of *slt2* and *sod* deletion mutants per area decreased significantly (P < 0.05). Through the complementation strain, the yield of sporulation increased to 2073 ± 415/cm^2 and 1709 ± 171/cm^2, respectively. The sporulation ability of the *slt2* deletion mutant was completely lost, and the sporulation ability of the *sod* deletion mutants was weakened compared to that of the wild-type strain, suggesting that *slt2* is a key gene regulating the sporulation in *A. solani*. Meanwhile, a reduction of Δ*sod* mutant in superoxide dismutase (SOD) content was detected. The content of SOD in mutant was 86.8 ± 1.4 and 89.6 ± 3.2 ng/L, respectively, after 1 and 2 days incubation as compared to the wild-type HWC-168, which was 127.7 ± 9.2 and 134.2 ± 12.0 ng/L, respectively (**Figure 5G**). In addition, SOD contents in complementation strains were similar to those of the wild type (124.0 ± 3.2 ng/L, 133.5 ± 3.9 ng/L). These results suggested that *sod* has a significant role in the SOD synthetic pathway in *A. solani*.

In *in vivo* tests, potato leaves inoculated with wild-type HWC-168, and complementation strains of Δ*slt2-C* and Δ*sod-C* showed obvious lesions and yellow halos (**Figure 5C**). The lesion diameter extended to 0.99 ± 0.16, 1.01 ± 0.02, and 1.03 ± 0.09 cm after 7 days incubation at 25°C, whereas for

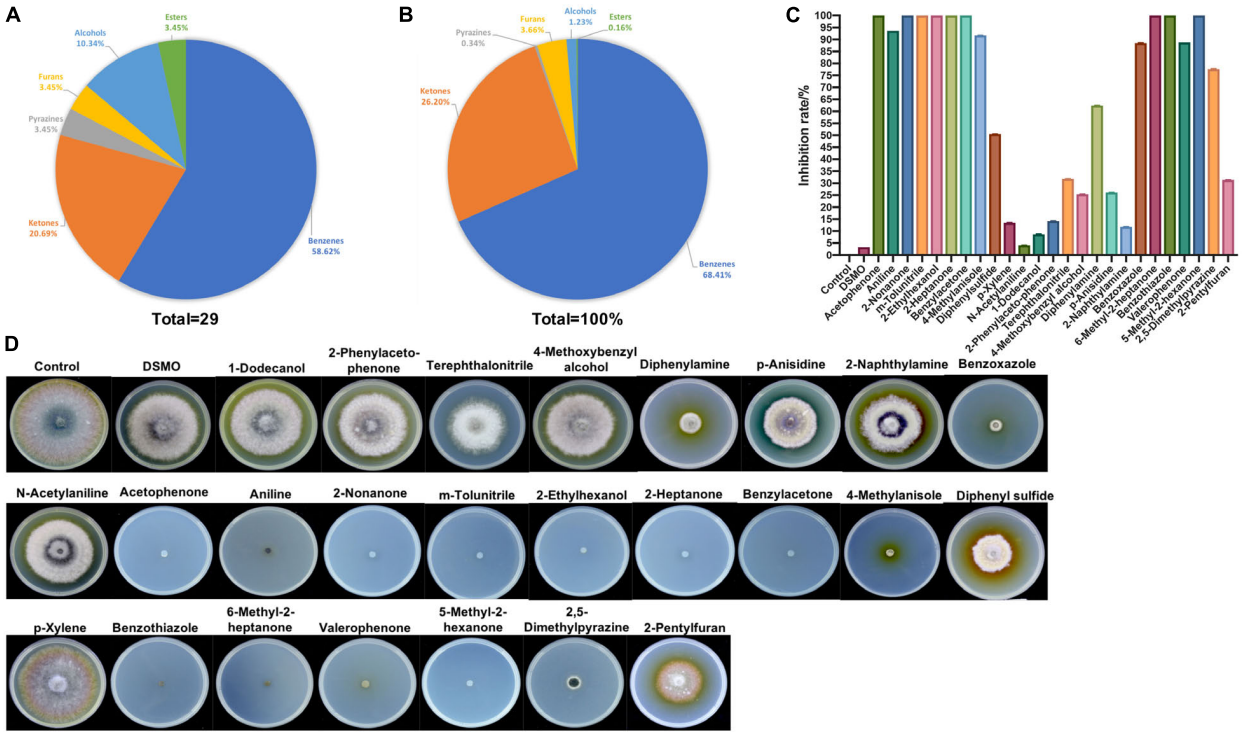

FIGURE 4 | Identification of ZD01 volatiles and inhibition effects of selected VOCs on *A. solani*. **(A)** Classification of VOCs produced by ZD01. **(B)** Peak area of six identified classes of VOCs from ZD01. **(C)** Inhibition rate of 25 identified VOCs against *A. solani*. **(D)** Colony diameter of *A. solani* co-cultured with 25 identified VOCs. Control represents *A. solani* without treatment of pure identified VOCs.

the leaves inoculated with Δ*slt2* and Δ*sod* mutants, the lesion diameters were limited to 0.00 ± 0.00 cm and 0.73 ± 0.07 cm, respectively (**Figure 5F**). The result showed that the deletion of *slt2* and *sod* can significantly reduce the pathogenicity of *A. solani* ($P < 0.05$).

B. subtilis ZD01 Volatiles Down-Regulated the Expression of Virulence-Associated Genes in *A. solani*

The transcriptional expression profiles of *slt2* and *sod* under condition of co-culture with ZD01 volatiles were investigated by real-time RT-PCR. The results showed that after *A. solani* strain HWC-168 was exposed to volatiles emitted by ZD01 for 3 days, the transcriptional expression of *sod* was strongly induced (∼2.45-fold) compared with the control group and then repressed (∼0.61-fold) after 4 days (**Figure 5H**). The expression of *slt2* was strongly repressed (∼0.83- and 0.40-fold) in the presence of VOCs after 3- and 4-day co-culture (**Figure 5H**). The down-regulated expression of *slt2* was consistent with the virulence reduction in *A. solani*.

DISCUSSION

Many plant-beneficial *Bacillus* species exhibit their biocontrol capacity to plant pathogens through non-volatile antibiotic production, nutrients, and niche competitions, as well as induction of plant systemic resistance (Pliego et al., 2008; Lemfack et al., 2014; Farag et al., 2017; Xie et al., 2018). However, limited knowledge is known about the antifungal mechanisms of volatiles produced by *Bacillus* strains. Most studies just focus on mycelia morphology and penetration and spore germination at a cellular level. However, the molecular mechanisms of antifungal activity have not been revealed. For example, transmission electron microscopy observation of fumigated and untreated *B. cinerea* showed excessive vesication or thickened cell walls in exposed conidia and increased strong retraction of plasma membrane in exposed hyphae (Li et al., 2012). The VOCs of *B. velezensis* 5YN8 can suppress the mycelium growth and conidia formation of *B. cinerea* BC1301 (Jiang et al., 2018). In this study, the insights into the mechanisms of *B. subtilis* ZD01 volatiles against *A. solani* showed similar biocontrol strategies. The hyphae penetration, conidia germination, and virulence of *A. solani* were significantly reduced when treated with VOCs produced by ZD01 ($P < 0.05$). Scanning electron microscopy showed thin, inward or gapped structures and altered surface morphology in the majority of *A. solani* cells after co-culture with strain ZD01 volatiles. Meanwhile, *A. solani* cells exposed to VOCs produced by strain ZD01 formed swollen part of hyphae with defective ability, leading to aborted invasion to the plant barrier. These results were consistent with the reduced pathogenicity *in vivo*. All of these findings indicated that the mode of action of volatiles can be explained, at least in part, by their activities that lead to the functional degradation through the damage

TABLE 1 | Volatile compounds produced by *B. subtilis* ZD01.

Chemicals	CAS	Retaining time (min)	Similarity degree	Retention index	Peak area ratio (%)
5-methyl-2-hexanone	110-12-3	7.57	94	853	1.99
p-xylene	106-42-3	7.88	90	863	0.78
2-heptanone	110-43-0	8.68	90	888	1.05
2,5-dimethylpyrazine	123-32-0	9.34	94	908	0.34
6-methyl-2-heptanone	928-68-7	10.91	97	954	8.88
5-methyl-2-heptanone	18217-12-4	11.2	90	962	12.81
Aniline	62-53-3	11.55	97	973	31.39
2-pentylfuran	3777-69-3	12.12	86	990	3.66
Benzoxazole	273-53-0	12.88	85	1013	0.08
4-methylanisole Anisole	104-93-8	12.98	80	1016	0.17
2-ethylhexanol	104-76-7	13.38	90	1028	0.42
2-Nonanone	821-55-6	14.2	90	1054	1.30
Acetophenone	98-86-2	14.47	98	1062	18.54
Allypropyl ether	1471-03-0	15.37	90	1090	0.16
m-tolunitrile	620-22-4	15.65	92	1098	0.56
Acrylophee	768-03-6	17.26	91	1151	2.18
Propiophenone	93-55-0	17.57	92	1161	1.63
p-anisidine	104-94-9	19.16	91	1215	0.55
Benzothiazole	95-16-9	19.31	98	1220	3.01
Benzylacetone	2550-26-7	19.89	92	1240	0.17
Terephthalonitrile	623-26-7	20.42	86	1259	0.11
4-methoxybenzyl alcohol	105-13-5	20.99	86	1279	0.62
Valerophenone	1009-14-9	23.03	92	1354	2.21
N-acetylaniline	103-84-4	23.57	94	1374	0.28
2-naphthylamine	91-59-8	25.79	91	1459	3.53
1-dodecanol	112-53-8	26	94	1467	0.19
Diphenyl sulfide	139-66-2	28.83	92	1587	0.43
Diphenylamine	122-39-4	29.49	90	1620	0.69
2-Phenylacetophenone	451-40-1	31.34	94	1731	2.28

of mycelium structure, killing *A. solani* cells partially, and the reduction of spore germination (**Figure 6**).

All of the active volatiles produced by bacteria so far can be grouped into alcohols, ketones, aldehydes, alkenes, alkynes, benzenes, esters, terpenoids, heterocycles, and sulfur-containing compounds (Fernando et al., 2005; Corcuff et al., 2011; Lemfack et al., 2014). Among nine identified chemicals with strong antifungal effects, the antifungal effects of 6-methyl-2-heptanone, acetophenone, 2-pentylfuran, 2,5-dimethyl pyrazine, and benzothiazole have also been analyzed. 6-Methyl-2-heptanone produced by *B. subtilis* completely inhibited mycelial growth of *F. oxysporum* f. sp. *lactucae* (Liu et al., 2018). Acetophenone released by *Streptomyces globisporus* and *Paenibacillus polymyxa* can inhibit *Penicillium italicum* and *F. oxysporum* growth, respectively (Li et al., 2010; Raza et al., 2015). The multiple functions of 2-pentylfuran have also been identified. 2-Pentylfuran isolated from the volatile products of bacterial strains presented strong inhibition on both mycelial growth and conidia germination of *F. oxysporum* (Wu et al., 2015; Liu et al., 2018). 2-Pentylfuran fumigated from *Bacillus megaterium* strain XTBG34 could significantly promote plant growth of *Arabidopsis thaliana* (Zou et al., 2010). Moreover, 2,5-dimethylpyrazine can significantly inhibit growth of several plant pathogens such as *Magnaporthe oryzae*, *Phytophthora capsici*, and *A. solani* (Munjal et al., 2016; Gao et al., 2017), and it can also be used as a food additive at low concentration (Müller and Rappert, 2010). Benzothiazole produced by *Bacillus* species can inhibit growth of *F. oxysporum* (Raza et al., 2015), and it can also be used to produce riluzole and pramipexole (Powell, 2015; Faridbod et al., 2016).

In this study, benzenes and ketones are the most abundant volatiles produced by strain ZD01. The aniline and acetophenone, which belonged to benzene compounds, could completely inhibit the growth of *A. solani* at certain concentrations and also exhibited high yield, as indicated by the peak areas of the GCs, so it was likely that they are main VOCs that play key roles during the antifungal process. For the VOCs that belong to ketones, 2-nonanone, 5-methyl-2-hexone, and 2-heptanone exhibited 100% inhibition of *A. solani* under certain concentrations when we did *in vitro* inhibition test, but their yields were relatively low among VOCs produced by ZD01, as indicated by GC-MS. However, 6-methyl-2-heptanone exhibited large peak areas on the GCs, and it did show strong antifungal effects against *A. solani* with 100% inhibition. Considering both contents and antifungal effects, aniline, acetophenone, and 6-methyl-2-heptanone might be considered active antifungal compounds.

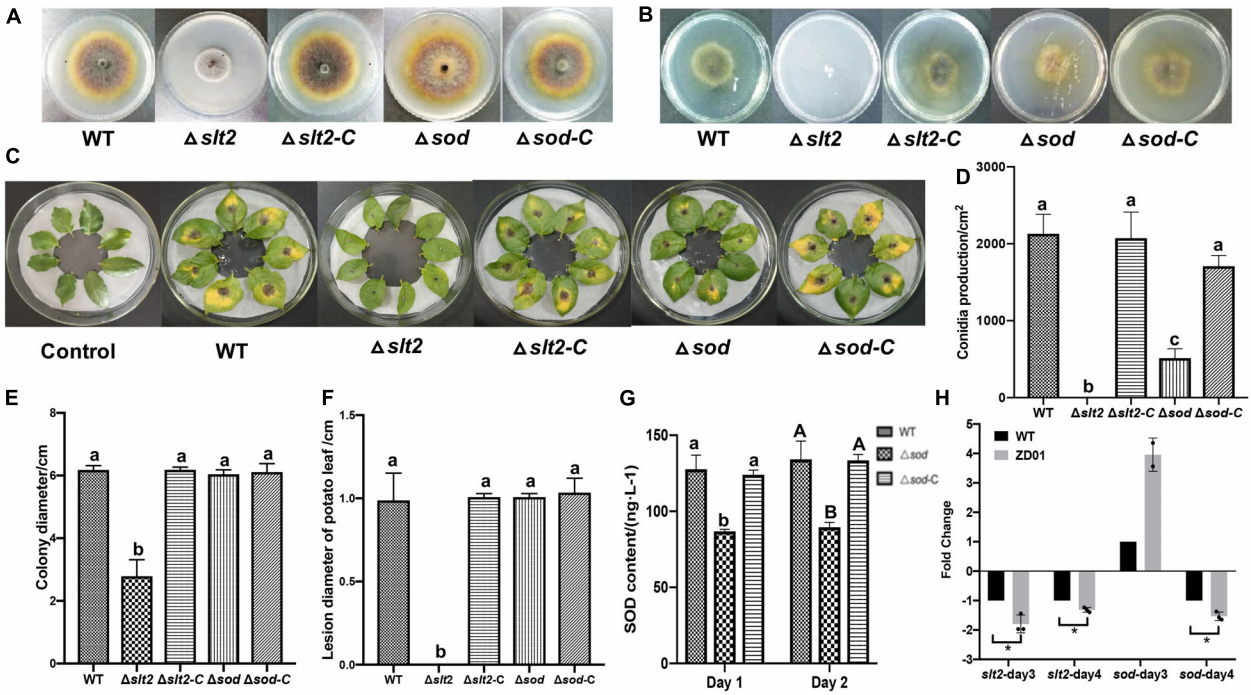

FIGURE 5 | *slt2* and *sod* are key virulence related genes in *A. solani*. **(A)** Colony morphology of wild-type *A. solani* (WT), mutants (Δ*slt2* and Δ*sod*) and complementation strains (Δ*slt2*-C and Δ*sod*-C). **(B)** Mycelia penetration ability of wild-type *A. solani* (WT), mutants (Δ*slt2* and Δ*sod*), and complementation strains (Δ*slt2*-C and Δ*sod*-C). **(C)** Symptoms of early blight disease on potato leaf caused by sterile water (Control), wild-type *A. solani* (WT), mutants (Δ*slt2* and Δ*sod*), and complementation strains (Δ*slt2*-C and Δ*sod*-C). **(D,E)** Conidia production and colony diameter of wild-type *A. solani* (WT), mutants (Δ*slt2* and Δ*sod*), and complementation strains (Δ*slt2*-C and Δ*sod*-C). **(F)** Lesion diameter early blight disease on potato leaf caused by wild-type *A. solani* (WT), mutants (Δ*slt2* and Δ*sod*), and complementation strains (Δ*slt2*-C and Δ*sod*-C). **(G)** SOD contents in wild-type *A. solani* (WT), mutants (Δ*slt2* and Δ*sod*), and complementation strains (Δ*slt2*-C and Δ*sod*-C). **(H)** Transcriptional expression profiles of *slt2* and *sod* after co-culture with ZD01 VOCs for 3 and 4 days. WT represents *A. solani* without treatment of ZD01 VOCs; ZD01 represents *A. solani* with treatment of ZD01 VOCs. Data presented are the mean ± s.d. (n = 3). The same letter on the bars for each column indicates no significant difference according to a LSD test at P = 0.05.

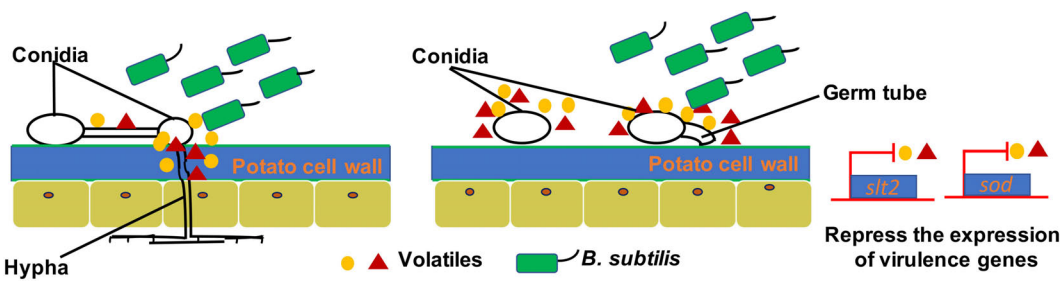

FIGURE 6 | A model for the mode of action of VOCs produced by ZD01 against *A. solani*. Volatiles produced by ZD01 mediate the conidia germination and mycelium penetration of *A. solani*. Acetophenone, 6-methyl-2-heptanone, and aniline biosynthesized by ZD01 is the major antifungal compounds against *A. solani*. These volatiles produced by ZD01 target the conidia and mycelium, which subsequently leads to suppression of fungal growth, mycelium penetration, conidia germination, and pathogenicity of *A. solani* as well as virulence gene expression.

Based on whole genome sequences and annotation of *A. solani* strain HWC-168 (Zhang et al., 2018), two virulence-related genes *slt2* and *sod* were predicted. In some fungal pathogens, like *Colletotrichum lagenarium*, *B. cinerea*, and *Mycosphaerella graminicola*, the role of virulence-related gene *slt2* has also been well studied, involved in the maintenance of cell-wall integrity and various aspects of saprotrophic and pathogenic growth (Kojima et al., 2002; Mehrabi et al., 2006; Rui and Hahn, 2007). In *B. cinerea*, a mutant defective in the *slt2* homolog *mp3* was defective in penetration and non-pathogenic infection (Rui and Hahn, 2007). Meanwhile, the biological role of *sod* gene has been extensively investigated in the model organism *S. cerevisiae*. However, the roles of these two genes in *A. solani* are still unclear. Here, we present the functions of *slt2* and *sod* in *A. solani* identified by knock-out mutant construction and phenotypical characterization. We

found that *slt2* is a key gene involved in mycelial growth, hyphae penetration, and sporulation of *A. solani*, which could further affect its pathogenicity. Meanwhile, we also found that *sod* is responsible for the synthesis of SOD in *A. solani* and its deletion mutant can reduce virulence of *A. solani* to some extent. Furthermore, we found that VOCs produced by *B. subtilis* ZD01 can decrease the transcriptional expression of these two genes. The down-regulated expression of *slt2* was consistent with the reduced virulence in *A. solani*. However, the expression of *sod* was induced co-cultured with VOCs produced by strain ZD01 after 3 days. *A. solani* responds to and resists the biocontrol agent, *B. subtilis* VOCs, resulting to produce the high level of reactive oxygen species (ROS). SOD, encoded by *sod*, is involved in scavenging the high level of ROS into molecular oxygen and hydrogen peroxide. Then, with the accumulation of VOCs emitted by strain ZD01, the pathogenicity of *sod* decreased along with the increasing VOCs. In addition, VOC composition of a given species is highly dynamic over time, resulting in a changing composition of the produced VOCs depending on the age of the VOC-producing species (Wang et al., 2013). That would be the reason for the induced *sod* response after 3 days and repression after 4 days. These results reveal the molecular mechanism by which VOCs antagonize *A. solani*.

This study shed light on the interaction mechanisms between *A. solani* and VOCs produced by *B. subtilis*, and a potential biocontrol method for potato early blight disease caused by *A. solani*.

EXPERIMENTAL PROCEDURES

Strains and Culture Conditions

Soil samples were collected from four different fields (Chengde, Hebei; Zhang Jiakou, Hebei; Qinhuangdao, Hebei; Tengzhou, Shandong) which had serious potato early blight disease by a five-spot sampling method (Chen et al., 2018) in China. Briefly, five soil samples that were 0–20 cm away from infected potato plants (Helan 15) were collected and then pooled as one sample. After that, the dilution plating method with miner modification was used for spore-forming bacteria isolation (López-Berges et al., 2010). In brief, soil sample was homogenized and placed in a sterilized beaker. Macerated samples were heated in a water bath for 15 min at 80°C to kill non-spore-forming bacteria and vegetative cells of spore-forming bacteria. The resulting supernatants were serially diluted in sterile 0.85% NaCl solution and plated onto LB agar plates. Plates were incubated at 37°C for 1 day.

Collected strains were tested for antagonistic activity. Briefly, bacterial antagonistic activities toward *A. solani* were tested by dual-culture assay on PDA (Hu et al., 2014), which support the vegetative growth of either bacteria or fungi. The bacterial strains (5 μl, 1×10^8 CFU/ml) were inoculated 2 cm away from *A. solani*. Four strains were spotted in each dish, and the blank control without bacterial strains was set. All isolates were tested in triplicate, and their inhibition zones were measured after 7 days of dual culture at 25°C.

Isolated bacterial strains were cultured in LB medium at 37°C. Strain ZD01 was then identified by 16S rRNA gene analysis and whole genome sequencing (CP046448). The genome of ZD01 was sequenced using the PacBio RSII sequencing platform (Pacific Biomarkers, CA, United States). All the strains used in this study are listed in **Supplementary Table S2**.

Antagonistic Assay of VOCs Against Fungal Pathogens

By following the methods of Gong et al. (2015), two Petri dishes were placed face to face. The bottom Petri dish contained LB agar (1.5%, wt/vol), which was inoculated with ZD01 (200 μl, 1×10^8 CFU/ml), or pure identified VOCs (100 μl; 1 g/ml) were added. All the commercial solid VOCs were dissolved in dimethyl sulfoxide (DMSO). Purchase information of all the used reagents is listed in **Supplementary Table S3**. The top Petri dish contained 1.5% of potato dextrose agar (PDA). For the growth inhibition test, plugs (5 mm in diameter) of plant pathogenic fungi were placed onto the center of PDA plates. All the used fungal pathogens are listed in **Supplementary Table S2**. For the conidia germination inhibition test, 100 μl of conidia solution (10^5 CFU/ml) was added. The top and bottom Petri dishes were sealed together with parafilm and incubated at 25°C. After 4–7 days, the diameters of the fungal colonies were measured. Inhibition of *A. solani* conidia germination by VOCs was determined after 8 h of incubation. LB plates without bacterial inoculum were used as control. Inhibition rate of mycelium growth and conidia germination was calculated by the following formulas:

$$\begin{aligned}&\text{Inhibition rate of mycelium growth}(\%)\\&= (\text{the diameter of control} - \text{the diameter of treatment group})/\\&\quad \text{the diameter of control} \times 100\%\end{aligned}$$

$$\begin{aligned}&\text{Inhibition rate of conidia germination}(\%)\\&= (\text{the conidia germination of control} - \text{the conidia germination}\\&\quad \text{of treatment group})/\text{the conidia germination of control} \times 100\%\end{aligned}$$

Penetrability Assays

The penetration ability of each *A. solani* strain was examined on grown PDA plates covered with cellophane membranes, as described previously (López-Berges et al., 2010). Briefly, each strain was grown on PDA plates covered with a cellophane membrane. For the VOC treatment groups, plugs (5 mm in diameter) of wild-type *A. solani* were spotted onto the center of PDA plate with a cellophane. Then, the wild-type strains were co-cultured with VOCs produced by strain ZD01 in LB plate (200 μl, 10^8 CFU/ml) for 3 days at 25°C using the face-to-face Petri dishes. For another 3 days, the wild-type strain was grown without VOC treatment and the cellophane membrane on the PDA plate was removed. Then, the penetrability halo was examined. LB plates without bacterial inoculum were used as control. For mutants and complementation strains, plugs (5 mm in diameter) of wild type, mutants of Δ*slt2* and Δ*sod*, and complementation strains of *A. solani* were spotted onto the center

of the PDA plate covered with the cellophane, respectively. After 3 days of incubation at 25°C, the cellophane membrane with the colony was removed from each plate. Each strain was grown for another 3 days at 25°C. Then, penetrated mycelial growth on each plate was examined after incubation. The experiment was repeated three times.

Scanning Electron Microscopy

The mycelia morphologies of *A. solani* in control groups or those treated with VOCs released by ZD01 were visualized by SEM. To observe structural changes on *A. solani*, the wild-type strains were co-cultured with VOCs produced by strain ZD01 for 6 days at 25°C using the face-to-face Petri dishes. Mycelia of each group were harvested and fixed in 2% glutaraldehyde at 4°C and then dehydrated with gradient ethanol solutions (30, 50, 80, 90, and 100%). After that, ethanol was replaced by 100% tertiary butyl ethanol. Cells were then freeze-dried, coated with gold, and imaged using a Hitachi S-3500N field emission SEM (Hitachi, Tokyo, Japan). The experiment was repeated three times.

In vivo Antagonistic Activity of VOCs Produced by ZD01

Strain ZD01 was inoculated in 2 ml of LB broth and grown overnight. 1% of overnight culture was re-inoculated into 50 ml of fresh LB broth and incubated at 37°C under the shaking condition of 200 rpm for 12 h. Subsequently, 200 μl of cell-free supernatant was transferred into one compartment of the divided Petri dish with 1.5% of LB agar and spread out. One piece of fresh potato leaf (Helan 15) was placed onto the other compartment with 0.5% water agar containing 10 μg/ml tetracycline hydrochloride and 20 μl of *A. solani* conidia suspension (10^5 CFU/ml) was inoculated onto the center of the leaf. LB plates without ZD01 were used as control. For the pathogenicity of different *A. solani* strains, 5-mm plugs of the wild type, Δ*slt2* and Δ*sod* mutants, and complementation strains were inoculated onto the center of one piece of fresh potato leaf. After 5 days of growth with 12 h of light and 12 h of darkness alternately at 25°C, the lesion areas were measured.

SOD Concentration Measurement of *A. solani*

The concentrations of SOD in wild-type, Δ*sod* mutant, and complementation strains of *A. solani* were determined by double antibody sandwich method using a commercial kit. One gram of ground mycelium was resuspended in 9 ml of PBS buffer (pH 7.2–7.4) and then centrifuged at 3,000 rpm for 20 min. The supernatant was then collected for SOD concentration measurement using the Enzyme Immunoassay Kit for Superoxide Dismutase (Omega Bio-Tek, Norcross, GA, United States) according to the manufacturer's instructions.

Collection of VOCs With SPME and Analysis by GC-MS

For VOC extraction, the *Bacillus* strain was inoculated into 6 ml of LB medium in a 20-ml vial. After incubation at 37°C for 4 days, samples were used for analysis. To provide a repeatability of the experiment, four samples were prepared and the LB medium without the antagonistic bacteria was set up as a control.

Volatile organic compounds were analyzed using solid phase microextraction (SPME) coupled with gas-chromatography tandem mass spectrometry (GC-MS) analysis. The SPME fiber (2 cm, 50/30 μm divinylbenzene/carboxen/polydimethylsiloxane fiber, DVB/CAR/PDMS) was inserted into the headspace of the vial and then placed at 50°C for 40 min. Compounds were then desorbed for 10 min in the injection port of the gas chromatograph at 220°C with the purge valve off (split-less mode).

An HP-5 capillary column (30.0 m × 0.25 mm × 0.25 μm, Thermo) and helium as the carrier gas were used for GC-MS. A Thermo Trace 1300-ISQ MS was used for peak separation and detection. Each run was performed for 45 min. The initial oven temperature of 40°C was held for 4 min, ramped up at a rate of 5°C/min to 150°C holding for 1 min, further ramped up at a rate of 10°C/min to 280°C, and held for 5 min. The mass spectrometer was operated in the electron ionization mode at 70 eV with a source temperature of 280°C, and a continuous scan from 35 to 400 m/z was used. The analysis was performed in full-scan mode. Mass spectral data of the volatile compounds were compared with data in the National Institute of Standards and Technology (NIST) Mass Spectrum Library.

Construction of Fungal Deletion and Complementation Strains

Gene deletion vector construction and transformation of *A. solani* were generated by the double-joint PCR method with minor modification (Yu et al., 2004). The primers used for flanking sequences amplification for each gene are listed in **Supplementary Table S4**. Open reading frames (ORFs) of *slt*2 and *sod* were replaced with a hygromycin resistance cassette (hyg) and the constructed fragment was inserted into the pEASY-T1 cloning vector (**Supplementary Table S2**). After transforming the constructed plasmid into HWC-168, the subsequent deletion mutants were verified by PCR with slt2-F/R and sod-F/R (**Supplementary Table S4**). For complementation, the respective ORFs were fused to a neomycin selection marker (neo) and introduced into the corresponding deletion mutants. Specific primers slt2-F/R and sod-F/R and marker gene primers neo-F/R (**Supplementary Table S4**) were used for verification.

Quantitative Real-Time PCR

Total RNAs of *A. solani* cells co-cultured with volatiles produced by ZD01 after 3 and 4 days were extracted by using the Bacterial RNA Kit (Omega Bio-Tek, Norcross, GA, United States) according to the manufacturer's instructions. First-strand cDNA was obtained using reverse transcriptase (TransGen Biotech, Beijing, China) with random hexamer primers. Real-time PCR was performed with SYBR Premix Ex Taq^{TM} (TransGen Biotech, Beijing, China). ITS gene was used as an internal reference gene. The specific primers used are listed in **Supplementary Table S4**. The relative expression of specific genes was calculated by using the $2^{-\Delta\Delta CT}$ method (Livak and Schmittgen, 2001).

Statistical Analysis

Three independent experiments were performed for each assay. Data were analyzed by SPSS20.0 Windows Software (SPSS Inc., Chicago, IL, United States). Least significant differences (LSD) were calculated to compare the results at the 0.05 level.

DATA AVAILABILITY STATEMENT

The datasets generated for this study can be found in the online repositories. The names of the repository/repositories and accession number(s) can be found: https://www.ncbi.nlm.nih.gov/genbank/, CP046448.

AUTHOR CONTRIBUTIONS

DaZ, SY, YY, JinZ, and SF performed the experiments. DoZ and YP provided technical assistance. DaZ, ZY, and JieZ designed the experiments. DaZ, ZY, and JieZ wrote the manuscript. All authors contributed to the manuscript and approved the submitted version.

FUNDING

This work was supported by the National Key Research and Development Program of China (2018YFD0200806), the Earmarked Fund for Modern Agro-industry Technology Research System (CARS-09-P18), and the Earmarked Fund for Modern Agro-industry Technology Research System in Hebei Province, China (HBCT2018080205).

SUPPLEMENTARY MATERIAL

The Supplementary Material for this article can be found online at: https://www.frontiersin.org/articles/10.3389/fmicb.2020.01196/full#supplementary-material

REFERENCES

Chaurasia, B., Pandey, A., Palni, L. M. S., Trivedi, P., Kumar, B., and Colvin, N. (2005). Diffusible and volatile compounds produced by an antagonistic *Bacillus subtilis* strain cause structural deformations in pathogenic fungi in vitro. *Microbiol. Res.* 160, 75–81. doi: 10.1016/j.micres.2004.09.013

Chen, Y., Wang, J., Yang, N., Wen, Z., Sun, X., Chai, Y., et al. (2018). Wheat microbiome bacteria can reduce virulence of a plant pathogenic fungus by altering histone acetylation. *Nat. Communi.* 9, 1–14.

Corcuff, R., Mercier, J., Tweddell, R., and Arul, J. (2011). Effect of water activity on the production of volatile organic compounds by Muscodor albus and their effect on three pathogens in stored potato. *Fungal Biol.* 115, 220–227. doi: 10.1016/j.funbio.2010.12.005

Farag, M. A., Song, G. C., Park, Y.-S., Audrain, B., Lee, S., Ghigo, J.-M., et al. (2017). Biological and chemical strategies for exploring inter-and intra-kingdom communication mediated via bacterial volatile signals. *Nat. Protoc.* 12, 1359–1377. doi: 10.1038/nprot.2017.023

Faridbod, F., Jamshidpour, T., and Ganjali, M. R. (2016). Pramipexole symmetric and asymmetric potentiometric PVC membrane sensors. *Int. J. Electrochem. Sci.* 11, 7990–8001. doi: 10.20964/2016.09.64

Fernando, W. D., Ramarathnam, R., Krishnamoorthy, A. S., and Savchuk, S. C. (2005). Identification and use of potential bacterial organic antifungal volatiles in biocontrol. *Soil Biol. Biochem.* 37, 955–964. doi: 10.1016/j.soilbio.2004.10.021

Fialho, M. B., Toffano, L., Pedroso, M. P., Augusto, F., and Pascholati, S. F. (2010). Volatile organic compounds produced by *Saccharomyces cerevisiae* inhibit the in vitro development of *Guignardia citricarpa*, the causal agent of citrus black spot. *World J. Microbiol. Biotechnol.* 26, 925–932. doi: 10.1007/s11274-009-0255-4

Gao, Z., Zhang, B., Liu, H., Han, J., and Zhang, Y. (2017). Identification of endophytic *Bacillus velezensis* ZSY-1 strain and antifungal activity of its volatile compounds against *Alternaria solani* and *Botrytis cinerea*. *Biol. Control* 105, 27–39. doi: 10.1016/j.biocontrol.2016.11.007

Gong, A.-D., Li, H.-P., Yuan, Q.-S., Song, X.-S., Yao, W., He, W.-J., et al. (2015). Antagonistic mechanism of iturin A and plipastatin A from *Bacillus* amyloliquefaciens S76-3 from wheat spikes against *Fusarium graminearum*. *PLoS One* 10:e0116871. doi: 10.1371/journal.pone.0116871

Heydari, A., and Pessarakli, M. (2010). A review on biological control of fungal plant pathogens using microbial antagonists. *J. Biol. Sci.* 10, 273–290. doi: 10.3923/jbs.2010.273.290

Hu, W., Gao, Q., Hamada, M. S., Dawood, D. H., Zheng, J., Chen, Y., et al. (2014). Potential of *Pseudomonas* chlororaphis subsp. aurantiaca strain Pcho10 as a biocontrol agent against *Fusarium graminearum*. *Phytopathology* 104, 1289–1297. doi: 10.1094/phyto-02-14-0049-r

Jiang, C.-H., Liao, M.-J., Wang, H.-K., Zheng, M.-Z., Xu, J.-J., and Guo, J.-H. (2018). *Bacillus velezensis*, a potential and efficient biocontrol agent in control of pepper gray mold caused by *Botrytis cinerea*. *Biol. Control* 126, 147–157. doi: 10.1016/j.biocontrol.2018.07.017

Kai, M., Haustein, M., Molina, F., Petri, A., Scholz, B., and Piechulla, B. (2009). Bacterial volatiles and their action potential. *Appl. Microbiol. Biotechnol.* 81, 1001–1012. doi: 10.1007/s00253-008-1760-3

Kim, P., Bai, H., Bai, D., Chae, H., Chung, S., Kim, Y., et al. (2004). Purification and characterization of a lipopeptide produced by *Bacillus thuringiensis* CMB26. *J. Appl. Microbiol.* 97, 942–949. doi: 10.1111/j.1365-2672.2004.02356.x

Kojima, K., Kikuchi, T., Takano, Y., Oshiro, E., and Okuno, T. (2002). The mitogen-activated protein kinase gene MAF1 is essential for the early differentiation phase of appressorium formation in *Colletotrichum lagenarium*. *Mol. PlantMicrobe Interact.* 15, 1268–1276. doi: 10.1094/mpmi.2002.15.12.1268

Lemfack, M. C., Nickel, J., Dunkel, M., Preissner, R., and Piechulla, B. (2014). mVOC: a database of microbial volatiles. *Nucleic Acids Res.* 42, D744–D748.

Li, Q., Ning, P., Zheng, L., Huang, J., Li, G., and Hsiang, T. (2010). Fumigant activity of volatiles of *Streptomyces globisporus* JK-1 against *Penicillium italicum* on *Citrus microcarpa*. *Postharvest Biol. Technol.* 58, 157–165. doi: 10.1016/j.postharvbio.2010.06.003

Li, Q., Ning, P., Zheng, L., Huang, J., Li, G., and Hsiang, T. (2012). Effects of volatile substances of *Streptomyces globisporus* JK-1 on control of *Botrytis cinerea* on tomato fruit. *Biol. Control* 61, 113–120. doi: 10.1016/j.biocontrol.2011.10.014

Liu, C., Yin, X., Wang, Q., Peng, Y., Ma, Y., Liu, P., et al. (2018). Antagonistic activities of volatiles produced by two Bacillus strains against *Monilinia fructicola* in peach fruit. *J. Sci. Food Agric.* 98, 5756–5763. doi: 10.1002/jsfa.9125

Livak, K. J., and Schmittgen, T. D. (2001). Analysis of relative gene expression data using real-time quantitative PCR and the 2- ΔΔCT method. *Methods* 25, 402–408. doi: 10.1006/meth.2001.1262

López-Berges, M. S., Rispail, N., Prados-Rosales, R. C., and Di Pietro, A. (2010). A nitrogen response pathway regulates virulence functions in *Fusarium oxysporum* via the protein kinase TOR and the bZIP protein MeaB. *Plant Cell* 22, 2459–2475. doi: 10.1105/tpc.110.075937

Mehrabi, R., van der Lee, T., Waalwijk, C., and Kema, G. H. (2006). MgSlt2, a cellular integrity MAP kinase gene of the fungal wheat pathogen *Mycosphaerella graminicola*, is dispensable for penetration but essential for invasive growth. *Mol. Plant Microbe Interact.* 19, 389–398. doi: 10.1094/mpmi-19-0389

Minerdi, D., Bossi, S., Gullino, M. L., and Garibaldi, A. (2009). Volatile organic compounds: a potential direct long-distance mechanism for antagonistic action of *Fusarium oxysporum* strain MSA 35. *Environ. Microbiol.* 11, 844–854. doi: 10.1111/j.1462-2920.2008.01805.x

Morgan, G., Stevenson, W., MacGuidwin, A., Kelling, K., Binning, L., and Zhu, J. (2002). Plant pathogen population dynamics in potato fields. *J. Nematol.* 34, 189–193.

Müller, R., and Rappert, S. (2010). Pyrazines: occurrence, formation and biodegradation. *Appl. Microbiol. Biotechnol.* 85, 1315–1320. doi: 10.1007/s00253-009-2362-4

Munimbazi, C., and Bullerman, L. (1998). Isolation and partial characterization of antifungal metabolites of *Bacillus pumilus*. *J. Appl. Microbiol.* 84, 959–968. doi: 10.1046/j.1365-2672.1998.00431.x

Munjal, V., Nadakkakath, A. V., Sheoran, N., Kundu, A., Venugopal, V., Subaharan, K., et al. (2016). Genotyping and identification of broad spectrum antimicrobial volatiles in black pepper root endophytic biocontrol agent. *Bacillus megaterium* BP17. *Biol/ Control* 92, 66–76. doi: 10.1016/j.biocontrol.2015.09.005

Nakano, M. M., Marahiel, M., and Zuber, P. (1988). Identification of a genetic locus required for biosynthesis of the lipopeptide antibiotic surfactin in *Bacillus subtilis*. *J. Bacteriol.* 170, 5662–5668. doi: 10.1128/jb.170.12.5662-5668.1988

Parafati, L., Vitale, A., Restuccia, C., and Cirvilleri, G. (2017). Performance evaluation of volatile organic compounds by antagonistic yeasts immobilized on hydrogel spheres against gray, green and blue postharvest decays. *Food Microbiol.* 63, 191–198. doi: 10.1016/j.fm.2016.11.021

Pasche, J., Wharam, C., and Gudmestad, N. (2004). Shift in sensitivity of *Alternaria solani* in response to QoI fungicides. *Plant Dis.* 88, 181–187. doi: 10.1094/pdis.2004.88.2.181

Peters, R., Drake, K., Gudmestad, N., Pasche, J., and Shinners-Carnelley, T. (2008). First report of reduced sensitivity to a QoI fungicide in isolates of *Alternaria solani* causing early blight of potato in Canada. *Plant Dis.* 92, 1707–1707. doi: 10.1094/pdis-92-12-1707b

Pliego, C., De Weert, S., Lamers, G., De Vicente, A., Bloemberg, G., Cazorla, F. M., et al. (2008). Two similar enhanced root-colonizing *Pseudomonas* strains differ largely in their colonization strategies of avocado roots and *Rosellinia necatrix* hyphae. *Environ. Microbiol.* 10, 3295–3304. doi: 10.1111/j.1462-2920.2008.01721.x

Powell, L. A. (2015). *). Synthesis of Novel Riluzole Analogues*. Huddersfield: University of Huddersfield.

Raza, W., Yuan, J., Ling, N., Huang, Q., and Shen, Q. (2015). Production of volatile organic compounds by an antagonistic strain *Paenibacillus polymyxa* WR-2 in the presence of root exudates and organic fertilizer and their antifungal activity against *Fusarium oxysporum* f. sp. niveum. *Biol. Control* 80, 89–95. doi: 10.1016/j.biocontrol.2014.09.004

Rui, O., and Hahn, M. (2007). The Slt2-type MAP kinase Bmp3 of *Botrytis cinerea* is required for normal saprotrophic growth, conidiation, plant surface sensing and host tissue colonization. *Mol. Plant Pathol.* 8, 173–184. doi: 10.1111/j.1364-3703.2007.00383.x

Tilocca, B., Cao, A., and Migheli, Q. (2020). Scent of a Killer: microbial volatilome and its role in the biological control of plant pathogens. *Front. Microbiol.* 11:41. doi: 10.3389/fmicb.2020.00041

Timmusk, S., Grantcharova, N., and Wagner, E. G. H. (2005). *Paenibacillus polymyxa* invades plant roots and forms biofilms. *Appl. Environ. Microbiol.* 71, 7292–7300. doi: 10.1128/aem.71.11.7292-7300.2005

Wang, C., Wang, Z., Qiao, X., Li, Z., Li, F., Chen, M., et al. (2013). Antifungal activity of volatile organic compounds from *Streptomyces alboflavus* TD-1. *FEMS Microbiol. Lett.* 341, 45–51.

Wu, Y., Yuan, J. E. Y., Raza, W., Shen, Q., and Huang, Q. (2015). Effects of volatile organic compounds from *Streptomyces albulus* NJZJSA2 on growth of two fungal pathogens. *J. Basic Microbiol.* 55, 1104–1117. doi: 10.1002/jobm.201400906

Wu, Y., Zhou, J., Li, C., and Ma, Y. (2019). Antifungal and plant growth promotion activity of volatile organic compounds produced by *Bacillus amyloliquefaciens*. *Microbiol. Open* 8:e00813.

Xie, S., Zang, H., Wu, H., Uddin Rajer, F., and Gao, X. (2018). Antibacterial effects of volatiles produced by *Bacillus* strain D13 against *Xanthomonas oryzae* pv. oryzae. *Mol. Plant Pathol.* 19, 49–58. doi: 10.1111/mpp.12494

Yu, J.-H., Hamari, Z., Han, K.-H., Seo, J.-A., Reyes-Domínguez, Y., and Scazzocchio, C. (2004). Double-joint PCR: a PCR-based molecular tool for gene manipulations in filamentous fungi. *Fungal Genet. Biol.* 41, 973–981. doi: 10.1016/j.fgb.2004.08.001

Yuan, J., Raza, W., Shen, Q., and Huang, Q. (2012). Antifungal activity of *Bacillus amyloliquefaciens* NJN-6 volatile compounds against *Fusarium oxysporum* f. sp. cubense. *Appl. Environ. Microbiol.* 78, 5942–5944. doi: 10.1128/aem.01357-12

Zhang, D., He, J.-Y., Haddadi, P., Zhu, J.-H., Yang, Z.-H., and Ma, L. (2018). Genome sequence of the potato pathogenic fungus *Alternaria solani* HWC-168 reveals clues for its conidiation and virulence. *BMC Microbiol.* 18:176. doi: 10.1186/s12866-018-1324-3

Zhang, X., Li, B., Wang, Y., Guo, Q., Lu, X., Li, S., et al. (2013). Lipopeptides, a novel protein, and volatile compounds contribute to the antifungal activity of the biocontrol agent *Bacillus atrophaeus* CAB-1. *Appl. Microbiol. Biotechnol.* 97, 9525–9534. doi: 10.1007/s00253-013-5198-x

Zou, C., Li, Z., and Yu, D. (2010). *Bacillus megaterium* strain XTBG34 promotes plant growth by producing 2-pentylfuran. *J. Microbiol.* 48, 460–466. doi: 10.1007/s12275-010-0068-z

Conflict of Interest: The authors declare that the research was conducted in the absence of any commercial or financial relationships that could be construed as a potential conflict of interest.

frontiers in Microbiology

ORIGINAL RESEARCH
published: 03 July 2020
doi: 10.3389/fmicb.2020.01364

Trichoderma Applications on Strawberry Plants Modulate the Physiological Processes Positively Affecting Fruit Production and Quality

Nadia Lombardi[1†], Simonetta Caira[2†], Antonio Dario Troise[1,2], Andrea Scaloni[2], Paola Vitaglione[1], Francesco Vinale[3,4], Roberta Marra[1], Anna Maria Salzano[2], Matteo Lorito[1,4,5] and Sheridan Lois Woo[4,5,6*]*

[1] Department of Agricultural Sciences, University of Naples Federico II, Naples, Italy, [2] Proteomics and Mass Spectrometry Laboratory, ISPAAM, National Research Council, Naples, Italy, [3] Department of Veterinary Medicine and Animal Productions, University of Naples Federico II, Naples, Italy, [4] Institute for Sustainable Plant Protection, National Research Council, Portici, Italy, [5] Task Force on Microbiome Studies, University of Naples Federico II, Naples, Italy, [6] Department of Pharmacy, University of Naples Federico II, Naples, Italy

OPEN ACCESS

Edited by:
Vincenzo Lionetti,
Sapienza University of Rome, Italy

Reviewed by:
Juan Carlos Díaz Ricci,
Universidad Nacional de Tucumán, Argentina
Manuel Benedetti,
University of L'Aquila, Italy

***Correspondence:**
Anna Maria Salzano
annamaria.salzano@cnr.it
Sheridan Lois Woo
woo@unina.it

[†] These authors have contributed equally to this work

Specialty section:
This article was submitted to Plant Microbe Interactions, a section of the journal Frontiers in Microbiology

Received: 23 December 2019
Accepted: 27 May 2020
Published: 03 July 2020

Citation:
Lombardi N, Caira S, Troise AD, Scaloni A, Vitaglione P, Vinale F, Marra R, Salzano AM, Lorito M and Woo SL (2020) Trichoderma Applications on Strawberry Plants Modulate the Physiological Processes Positively Affecting Fruit Production and Quality. Front. Microbiol. 11:1364. doi: 10.3389/fmicb.2020.01364

Many *Trichoderma* spp. are successful plant beneficial microbial inoculants due to their ability to act as biocontrol agents with direct antagonistic activities to phytopathogens, and as biostimulants capable of promoting plant growth. This work investigated the effects of treatments with three selected *Trichoderma* strains (T22, TH1, and GV41) to strawberry plants on the productivity, metabolites and proteome of the formed fruits. *Trichoderma* applications stimulated plant growth, increased strawberry fruit yield, and favored selective accumulation of anthocyanins and other antioxidants in red ripened fruits. Proteomic analysis of fruits harvested from the plants previously treated with *Trichoderma* demonstrated that the microbial inoculants highly affected the representation of proteins associated with responses to stress/external stimuli, nutrient uptake, protein metabolism, carbon/energy metabolism and secondary metabolism, also providing a possible explanation to the presence of specific metabolites in fruits. Bioinformatic analysis of these differential proteins revealed a central network of interacting molecular species, providing a rationale to the concomitant modulation of different plant physiological processes following the microbial inoculation. These findings indicated that the application of *Trichoderma*-based products exerts a positive impact on strawberry, integrating well with previous observations on the molecular mechanisms activated in roots and leaves of other tested plant species, demonstrating that the efficacy of using a biological approach with beneficial microbes on the maturing plant is also able to transfer advantages to the developing fruits.

Keywords: ***Fragaria x ananassa*, *Trichoderma*, proteomics, antioxidant, phenolics, anthocyanins**

Abbreviations: ASA/DHA, ascorbic acid/dehydroascorbic acid ratio; BCAs, biological control agents; DRPs, differentially represented proteins; GSH/GSSG, reduced glutathione/oxidized glutathione ratio; MRM, multiple reaction monitoring; MS, mass spectrometry; MS/MS, tandem mass spectrometry; TMT, tandem mass tagging.

INTRODUCTION

For centuries, the fruits of strawberry (*Fragaria x ananassa* Duch.) have been consumed, appreciated for their taste and nutritional properties. Their cultivation has augmented in recent years, with productivity increasing to more than 9 million tons worldwide in 2017 (Food and Agriculture Organization of the United Nations, 2018)[1]. Human health benefits derived from eating strawberry fruits include heart protection, reduced blood pressure, as well as anticancer and anti-inflammatory activities (Liu et al., 2000; Joseph et al., 2014). These effects are related to the high content of phenolic compounds, vitamin C, anthocyanins, proanthocyanidins (cyanidin and pelargonidin derivatives) and other antioxidants, which contrast oxidative stress and retard cellular aging (Hanhineva et al., 2011; Giampieri et al., 2012; Joseph et al., 2014; Park et al., 2017). Anthocyanins represent the main flavonoid class in strawberry fruits that play an active role in the determination of the red pigmentation and in the evaluation of fruit ripeness (da Silva et al., 2007). Ripened strawberries contain high concentrations of pelargonidin glycosides, including pelargonidin 3-*O*-glucoside, pelargonidin 3-*O*-malonyl-glucoside, pelargonidin 3-*O*-rutinoside and cyanidin 3-*O*-glucoside, which may represent up to 95, 33, 7, and 6%, respectively, of the total anthocyanins (Aaby and Remberg, 2015). Previous studies reported that the biosynthesis of antioxidant metabolites (and the corresponding concentration in the fruit) is strongly influenced by the interaction of the plant genotype and cultivation practices, i.e., fertilization, with the growth environment (Anttonen et al., 2006; Buendia et al., 2010; Aaby et al., 2012). The metabolomic dynamics are also affected by the nutritional status of the plant, as noted with iron- and phosphorus- deficiencies in the rhizosphere, often compensated by the regulation of root exudates that influence nutrient bioavailability and uptake determining fruit quality (Valentinuzzi et al., 2015). Furthermore, metabolite composition of strawberry are also associated with the phenology of the plant, developmental stages of the fruit, vegetative structure and interactions with biotic and abiotic stress factors that correspond to plant responses to the pathogen/pest attack and to adverse factors in the environment (Hanhineva et al., 2011).

Recent findings reinforce the concept that some microbial biological control agents (BCAs) may have multiple beneficial effects on plants, that not only include disease control, but also the stimulation of plant growth, increased yield, enhanced bioavailability and uptake of nutrients, as well as improvement of crop quality (Pascale et al., 2017; Woo and Pepe, 2018; Marra et al., 2019). Numerous fungi belonging to the genus *Trichoderma* have been widely studied as BCAs for their antagonistic and plant biostimulant activities; they are present as active ingredients in more than 200 products marketed worldwide as biofungicides, biofertilizers, biostimulants, and soil probiotics for agriculture (Woo et al., 2014). Furthermore, many *Trichoderma* spp. applied as biofungicides and considered as alternatives to chemical phytosanitary products of synthesis, are proven efficient antagonists of many causal disease agents of strawberry such as *Botrytis* or *Colletotrichum* (Tronsmo and Dennis, 1977; Freeman et al., 2004; Porras et al., 2007).

Several *Trichoderma* strains are endophytes able to establish a complex molecular crosstalk network in interactions with other rhizosphere microorganisms and the plant, which improve plant feedback to different stresses, and the ability to improve crop development and productivity (Vinale et al., 2008; Hermosa et al., 2012; Lombardi et al., 2018).

Since the early observations of the plant growth promotion effects by *Trichoderma* treatments to the plant (Baker, 1988; Klefield and Chet, 1992; Ousley et al., 1994), investigations in this field of research have been steadily intensified in an attempt to understand the mechanisms involved. Root colonization by *Trichoderma* spp. was found to be associated with enhanced plant nutrient uptake as result of an improved efficient solubilization of macro- and micro-nutrients (Altomare et al., 1999; Yedidia et al., 2001; de Santiago et al., 2011) that modified the metabolism of several crops (Harman, 2004; Vinale et al., 2008, 2012; Hermosa et al., 2012). Modern technologies in the "omics" era permitted functional studies on the beneficial fungus (Lorito et al., 2010), the host plant (Harman et al., 2004a), as well as on the interactions between *Trichoderma*, plant and pathogens (Marra et al., 2006). Proteomic and transcriptomic approaches were used to characterize metabolic pathways and molecular processes underlying the plant response to treatments with *Trichoderma* preparations, specifically regarding the plant defense responses (Yedidia et al., 2000) and induced systemic resistance (Shoresh et al., 2010). The various studies that described the plant responses to these beneficial microbes were performed on root and leaf tissues obtained from diverse plant species, i.e., bean, maize, tomato, cucumber and grapevine. These plants were treated with *T. harzianum* or *T. virens* in order to evaluate the differential quantitative changes in proteins/genes related to specific signaling cascades and metabolic pathways involved in defense responses, redox stresses and carbon/energy metabolism (Marra et al., 2006; Segarra et al., 2007; Shoresh and Harman, 2008; Perazzolli et al., 2016; Manganiello et al., 2018; Nogueira-Lopez et al., 2018; De Palma et al., 2019). Although proteomics and metabolomics have found a large application in the characterization of the physiological changes occurring during development, ripening and post-harvest of diverse fruits (Guarino et al., 2007; D'Ambrosio et al., 2013; Molassiotis et al., 2013; Salzano et al., 2018, 2019), including strawberry (Bianco et al., 2009; Li et al., 2013, 2015), the objectives have been largely focused on the quality of the harvested products and the effects of conservation conditions.

The principle method to administer the biological products containing *Trichoderma* in agricultural production is by direct applications to the seed or the developing plant (Woo et al., 2014), and any positive changes noted by the treatments are observed on the growing plant (biomass) and the developing fruit, which are reflected in the biometric parameters important for evaluating yield quantity. However, only a very few reports have provided information on specific genes or enzymatic activities in the fruits, when the corresponding plants have been inoculated with *T. harzianum* preparations; the only case is for tomato (Chacón et al., 2007; Singh et al., 2018). No dedicated investigations have

[1] www.fao.org

been performed on fruits collected from plants treated with microbial BCAs in order to evaluate the metabolic pathways and molecular changes that can influence the quality and beneficial health characteristics in the harvested products.

To investigate the outcome of *Trichoderma* on strawberry, in particular on the fruit, this study was undertaken to determine the effects of treatments with different *Trichoderma* strains on the productivity of strawberry, on the plant growth promotion of above/below ground vegetative structures, and the reproductive structures determining fruit yield. Moreover, multiple approaches assayed the physiological characteristics of strawberry after the application of these beneficial fungi to the mother plant, which could have an effect on the corresponding formed fruits, anthocyanin and antioxidant compound content, and the representation of proteins associated with signaling, energetic and metabolic processes, as well as with plant response to biotic/abiotic stresses. This study provides evidences that *Trichoderma* can have positive effects on above-mentioned plant physiological parameters, as well as on beneficial compounds that highly influence food quality and consumer health.

MATERIALS AND METHODS

Fungal Strains

Trichoderma harzianum strains T22 and TH1, and *T. virens* strain GV41 were obtained from a microbial collection available at the Department of Agricultural Sciences of the University of Naples Federico II, Portici, Italy, and cultivated bimonthly on Potato Dextrose Agar (HI-MEDIA, Pvt. Ltd., Mumbai, India), at 25°C. *Trichoderma* propagules were produced by solid-state fermentation on sterile rice bran (500 g) inoculated with a spore suspension (1×10^6 spores/mL), and incubated at 25°C. After 7 days, the spores were collected washing the rice bran with sterile water. Spore suspensions were adjusted to the desired concentration by using a haemocytometer. *T. harzianum* strain T-22 and *T. virens* strain G-41 (GV41) are registered mBCA Plant Protection Products, components biofungicides on the agricultural market that meet safety criteria established by EPA and EU governing bodies. *T. harzianum* strain TH1 does not produce noted toxic compounds as determined by metabolomic analysis (Vinale and Woo, data not shown).

Plant Material, Treatments and Sampling

Experiments were carried out in the greenhouse at the Department of Agricultural Sciences of the University of Naples Federico II, Portici, Italy, under natural, seasonal environmental conditions. Fresh transplants of uniform size of *Fragaria x ananassa* cv. Sabrina were transplanted in October 2016 into 25 cm-diameter pots (one plant per pot) filled with sterile soil. The trial was arranged in a completely randomized block design with 2 biological replicates per treatment and 10 plants in each replicate. Fungal spore suspensions (T22, TH1, and GV41) were tested at 10^7 spores/mL in water. They were applied once by root dip (15 min) immediately prior to transplanting, and monthly by irrigation (25 mL) until 7 days before the first harvest. Controls consisted in water-treated plants (CTR). Throughout the duration of the field experiment, the disease incidence of the most common strawberry pathogens was monitored on plants and fruits.

Ripe fruits were harvested at the commercial stage from *Trichoderma*-treated and control plants once per week from April to June 2017 and individually counted and weighed. All strawberry plants were harvested at the end of June 2017, and thoroughly washed under running tap water to remove soil particles. Plants were dried in oven at 65°C for about 72 h, until achieving a constant weight. For each treatment, total yield (TY), number of fruits/plant (NF), root length (RL), root fresh weight (RFW), and root dry weight (RDW) were measured.

Preparation of Fruit Samples for Chemical and Proteomic Analyses

Red ripe fruits from *Trichoderma*-treated and control plants were immediately ground in liquid N_2 and stored at −80°C until their use. For chemical analyses, individual freeze-dried strawberries were stored in a desiccator, at room temperature, in the dark, and then pulverized by using a knife mill Grindomix GM 200 (Retsch, Haan, Germany). Powdered strawberry samples were pooled according to treatment and used for further chemical analyses.

For proteomic analysis, individual frozen strawberries were pooled according to treatment, grounded in a blender and finally grinded in a mortar, using copious liquid N_2 to avoid tissue defrosting. Samples were then lyophilized, and immediately processed for further proteomic analysis.

Determination of Total Antioxidant Capacity and Total Phenolic Content in Fruits

The 2,2-diphenyl-1-picrylhydrazyl (DPPH) free radical assay was used to measure total antioxidant capacity (TAC) of strawberry fruit hydroalcoholic extracts (Sharma and Bhat, 2009). Briefly, 1 mL of a solution 1% v/v formic acid in methanol:water (70:30 v/v) was added to 10 mg of each sample, which was then homogenized; the suspension was vortexed and then centrifuged (14800 rpm, 4°C, for 10 min). DPPH was dissolved in methanol (0.4 mg/mL) and the absorbance at a wavelength of 517 nm was adjusted to 0.9 ± 0.02 by using a T92+ UV double beam spectrophotometer (PG Instruments, Leicester, United Kingdom). Scavenging capacity was evaluated by dissolving 0.2 mL of each hydroalcoholic extract in 0.9 mL of DPPH solution; after incubation at 25°C, for 10 min, the absorbance was measured at 517 nm. Percentage of inhibition was calculated with respect to a solution of 1% v/v formic acid in methanol:water (70:30 v/v). A trolox calibration curve was built in the range 10-120 μM, and TAC was expressed as μmol of trolox equivalent per gram of dry matter. Each extraction was performed in duplicate for a whole of eight observations for each sample.

Total phenolic content (TPC) was measured through the colorimetric Folin-Ciocalteu method, following the procedure of Singleton et al. (1998). Gallic acid was used as a standard, and a series of calibration solutions was prepared in the concentration range 0.020–0.150 mg/mL. Sample hydroalcoholic suspensions

were prepared as described above. A 0.1 mL sample aliquot was mixed with 0.5 mL of distilled water and 125 μL of Folin-Ciocalteu solution. The mixture was vortexed (1000 rpm), left for 6 min at room temperature and added with 1.25 mL of 0.70 M sodium carbonate. The mixture was vigorously vortexed and incubated for 90 min, at room temperature. The absorbance of samples was measured at 760 nm.

Determination of Ascorbic Acid Content in Fruits

Strawberry samples (500 mg) were extracted with 5 mL of an aqueous solution containing 3% v/v metaphosphoric acid and 8% v/v acetic acid. Upon vortexing and centrifugation (4000 rpm, at 4°C, for 10 min), acid extracts were titrated using an indophenol solution (25% w/v 2,6-dichloroindophenol, 21% w/v $NaHCO_3$), until a light pink color appeared. Different concentrations of ascorbic acid were titrated with above-mentioned indophenol solution in order to build up a standard calibration curve (Ramirez et al., 1996).

Analysis of Anthocyanins in Fruits by LC–DAD–ESI-MS/MS

Samples were extracted according to Holzwarth et al. (2012), with minor modifications. Strawberry dried samples (50 mg) were suspended in 3 mL of 5% v/v formic acid in methanol, sonicated for 10 min, at 40°C, and finally placed in a water bath (40°C), under agitation. Samples were centrifuged (4000 rpm, at 4°C, for 10 min), and 1 mL of each supernatant was dried at 40°C in a Savant centrifugal evaporator (Thermo-Fisher, Bremen, Germany). Dried extracts were dissolved in 0.3 mL of 5% v/v formic acid, filtered with modified cellulose filters (0.22 μm, Phenomenex, Torrance, CA, United States), and 10 μL of each solution was injected into the LC system. Quantitative analysis of anthocyanins was performed by using a Shimadzu LC10AD binary system (Shimadzu, Kyoto, Japan) equipped with a SPD-M10A diode array detector (DAD, Shimadzu) and a Series 200 autosampler (Perkin Elmer, Billerica, MA, United States). Chromatographic separation was achieved through a Kinetex XB-C18 column (150 × 4.6 mm, 5 μm, 100 Å, Phenomenex) equipped with a C18 ODS guard column (4.0 × 3.0 mm), at 25°C, with a flow rate of 0.8 mL/min. Mobile phase A was 5% v/v formic acid and mobile phase B was 5% v/v formic acid in methanol. The following binary gradient (min/%B) was used: (0/20), (3/20), (15/55), (18/55), (22/90), (25/90). Typical benzopyrylium and flavylium ions of anthocyanins were monitored at 520 nm.

For peak assignment, samples were injected into an API2000 triple quadrupole tandem mass spectrometer (AB Sciex, Carlsbad, CA, United States) by using the same chromatographic conditions listed above. Positive electrospray ionization was used for the detection; source parameters were as follows: spray voltage 5.5 kV; capillary temperature 300°C, dwell time 100 ms. The chromatographic profile was recorded in multiple reaction monitoring mode (MRM). Tentative identification of individual anthocyanins was achieved according to Määttä-Riihinen et al. (2004) by using mass transitions given in parentheses: cyanidin 3-*O*-glucoside (*m/z* 449 → 287), pelargonidin 3-*O*-glucoside (*m/z* 433 → 271), pelargonidin 3-*O*-rutinoside (*m/z* 579 → 271), pelargonidin 3-*O*-malonyl-glucoside (*m/z* 519 → 271), pelargonidin 3-*O*-acetyl-glucoside (*m/z* 475 → 271) and cyanidin derivative (*m/z* 449 → 287). Individual anthocyanins were quantified using calibration curves of pelargonidin 3-*O*-glucoside, while cyanidin was used for the quantification of anthocyanidins (aglycone form). Three sets of calibration curves were built in the range 0.1–50 μg/mL according to the limit of detection and the limit of quantitation (Armbruster and Pry, 2008). Three replicates of the solutions 50 ng/mL were injected into the LC-DAD system to verify the lowest concentration for which the signal to noise ratio was higher than three. The r^2 value was calculated plotting the area counts against the injected concentrations. Each point of the calibration curves was injected three times in the same day (intraday assay for the repeatability) and three times in three different days (interday assay for the reproducibility); the accuracy was reported as the discrepancies between nine calibration curves performed intraday and interday. Slope among the calibration curves was calculated and compared to each point of each calibration curve. Results were expressed as relative standard deviation (%). Each sample was extracted and injected twice for a total of 4 observations; results were reported as μg/g of fruit sample. In case of lacking standards, the calibration of structurally related compounds was used and corrected by a molecular weight factor (Chandra et al., 2001).

Fruit Protein Extraction, Digestion and Peptide Fractionation

Lyophilized samples from pooled frozen fruits of *Trichoderma*-treated and control strawberry plants (9 fruits collected from 3 plants for each condition) were quickly extracted in parallel for proteins through a slightly modified phenol-extraction method followed by ammonium acetate–methanol precipitation (Li et al., 2015). Thus, 1 g of lyophilized powder of each sample was mixed in a mortar with 1% w/w polyvinylpyrrolidone, and resuspended in 10 mL of 0.7 M sucrose, 0.1 M KCl, 0.5 M Tris–HCl, 50 mM EDTA, 40 mM DTT, pH 8.5, containing a protease inhibitors cocktail for plant tissues (Sigma-Aldrich, United States). Homogenization was performed in an Ultra-Turrax tissue processor (IKA, Werke GmbH, Germany) for 1 min, at 6000 rpm. Tris-buffered phenol, pH 8.0 (Sigma-Aldrich) was added to the suspension (1:1, v/v) and the sample was mixed thoroughly and centrifuged at 10,000 × *g*, for 15 min, at 4°C. The extraction was repeated twice and phenol phases were collected and precipitated with 5 vol of cold 0.1 M ammonium acetate in methanol, at −20°C, overnight. Protein pellets were washed twice with ice-cold methanol and finally with cold acetone containing 20 mM DTT, and then air-dried. Protein pellets (5 mg) were solubilized in 250 μL of 7 M urea, 2 M thiourea, 50 mM triethylammonium bicarbonate (TEAB), 2% SDS, 10 mM DTT, pH 8.5, and added with plant specific protease inhibitors (Sigma-Aldrich). Samples were vortexed and incubated for 1 h, at 30°C, under shaking. Samples were

centrifuged at 12,000 × *g* for 5 min, at 5°C, and the taken of the supernatant containing the corresponding protein extract. Protein concentration was determined using the Bio-Rad Protein Assay (Bio-Rad, Hercules, CA, United States), according to manufacturer's instructions. Relative quantification of individual proteins was obtained by a tandem mass tagging (TMT)-labeling experiment using a TMT10plex Isobaric Label Reagent Kit (Thermo-Fisher Scientific, United States); protein samples were prepared according to manufacturer's instructions. Thus, an aliquot of each protein sample (100 μg) was adjusted to a 100 μL final volume with 100 mM TEAB, and then treated as reported in the manufacturer's instructions. Each sample was digested with freshly prepared trypsin (enzyme to protein ratio 1:50 w/w) in 100 mM TEAB, at 37°C, overnight. Resulting peptides from each protein sample were labeled with the TMT10plex Label Reagent Set (Thermo-Fisher Scientific), at 25°C, following manufacturer's instructions, according to the labeling scheme: Ctrl-TMT10-126, T22-2-TMT10-127N, TH1-TMT10-127C, and GV41-TMT10-128N. After 1 h of reaction, 8 μL of 5% w/v hydroxylamine was added in each tube and mixed for 15 min, in order to quench the derivatization reaction. For a set of comparative experiments, tagged peptide mixtures were mixed in equal-molar ratios (1:1:1:1) and vacuum-dried under rotation. Then, pooled TMT-labeled peptide mixtures were suspended in 0.1% v/v trifluoroacetic acid, and fractionated by using the Pierce High pH Reversed-Phase Peptide fractionation kit (Thermo-Fisher Scientific) according to manufacturer's instructions. After fractionation, eight fractions of TMT-labeled peptides were collected, vacuum-dried and finally reconstituted in 0.1% v/v formic acid for subsequent mass spectrometric analysis.

NanoLC-ESI-Q-Orbitrap MS/MS Analysis of Fruit Protein Digests

Tandem mass tagging-labeled peptide fractions were analyzed with a nanoLC-ESI-Q-Orbitrap-MS/MS platform consisting of an UltiMate 3000 HPLC RSLC nano system (Dionex, United States) coupled to a Q Exactive Plus mass spectrometer through a Nanoflex ion source (Thermo-Fisher Scientific). Peptides were loaded on an Acclaim PepMap RSLC C18 column (150 mm × 75 μm ID, 2 μm particles, 100 Å pore size, Thermo-Fisher Scientific), and eluted with a gradient of solvent B (19.92/80/0.08 v/v/v water/acetonitrile/formic acid) in solvent A (99.9/0.1 v/v water/formic acid), at a flow rate of 300 nL/min. The gradient of solvent B started at 5%, increased to 60% over 125 min, raised to 95% over 1 min, remained at 95% for 8 min. The mass spectrometer operated in data-dependent mode, using a full scan (*m/z* range 375–1500, nominal resolution of 70,000), followed by MS/MS scans of the 10 most abundant ions. MS/MS spectra were acquired in a scan *m/z* range 110–2000, using a normalized collision energy of 32%, an automatic gain control target of 100,000, a maximum ion target of 120 ms, and a resolution of 17,500. A dynamic exclusion value of 30 s was also used.

Bioinformatics for Protein Identification and Quantitation

Raw data files were analyzed for protein identification and relative protein quantification with Proteome Discoverer v. 2.1 software (Thermo Scientific), enabling the database search by Mascot algorithm v. 2.6 (Matrix Science, United Kingdom) using the following criteria: NCBI protein database (Viridiplantae, 6216064 protein sequences, 12/2018) including the most common protein contaminants; carbamidomethylation of Cys and TMT modification of lysine and peptide N-terminal as fixed modifications; oxidation of Met, deamidation of Asn and Gln, pyroglutamate formation of Gln as variable modifications. Peptide mass tolerance was set to ±10 ppm and fragment mass tolerance to ±0.02 Da. Proteolytic enzyme and maximum number of missed cleavages were set to trypsin and 2, respectively. Protein candidates assigned on the basis of at least 2 sequenced peptides and an individual Mascot Score ≥ 30 were considered as confidently identified. For quantification, ratios of TMT reporter ion intensities in the MS/MS spectra from raw datasets were used to calculate fold changes between samples. Results were filtered to 1% false discovery rate. Proteomic data have been deposited to the ProteomeXchange consortium (Vizcaíno et al., 2016) with the PRIDE partner repository with the dataset identifier PXD016951.

Bioinformatics for Protein Functional Analysis

Identified proteins were subjected to BLAST sequence homology search using command line NCBI applications against the *Arabidopsis thaliana* protein sequence database TAIR 10 from The Arabidopsis Information Resource repository[2]. Functional categorization of differentially represented proteins (DRPs) was obtained using Mercator pipeline[3] for automated sequence annotation. Final outputs were integrated with data from available literature. Hierarchical clustering analysis of $\log_2$ transformed abundance ratios of DRPs from *Trichoderma*-treated strawberry plants was performed using Genesis 1.8.1 platform (Sturn et al., 2002). Person's correlation as distance and average linkage clustering were chosen as parameters. Protein interaction networks were obtained with STRING v. 11[4] using the *A. thaliana* database. Venn diagrams were depicted using a web tool at http://bioinformatics.psb.ugent.be/webtools/Venn.

Statistical Analysis

Biometric data (TY, NF, RL, RFW, and RDW), and total antioxidant capacity, ascorbic acid, total phenolic compounds, total anthocyanins and single anthocyanin content of samples were examined by one-way ANOVA using SPSS software (v.15.0 IBM, Armonk, NY, United States). Significant differences among treatments were separated using SNK (Student–Newman–Keuls) and Fisher's Least Significant Difference (LSD) *post hoc* tests, at the 0.05 level of significance.

[2]www.arabidopsis.org

[3]http://mapman.gabipd.org/web/guest/app/mercator

[4]http://string-db.org

RESULTS

Strawberry Growth and Yield of Strawberry Plants

Treatments with *Trichoderma harzianum* strains T22 and TH1, and *T. virens* strain GV41 significantly enhanced total yield (TY) ($P < 0.05$) of strawberry plants, as compared to control (CTR) (**Table 1**). In particular, the strains T22, TH1, and GV41 increased TY by 35, 38, and 29%, respectively. Applications of *T. harzianum* strains T22 and TH1 were also found to significantly increase ($P < 0.05$) the number of fruits per plant (NF) by 17 and 39%, respectively, while a lower effect (6%) was observed in the case of *T. virens* strain GV41.

All *Trichoderma* treatments slightly enhanced root length (RL), root fresh weight (RFW) and root dry weight (RDW), and GV41 showed the highest increase of RL (11%), RFW (17%) and RDW (21%) compared to CTR, as outlined in **Table 1**.

In addition, no incidence of disease was observed on the plants or fruits subjected to the *Trichoderma* biological treatments monitored for the duration of the experiment (data not shown).

Antioxidant Properties of Strawberry Fruits

Treatments with *Trichoderma* strains variably affected the antioxidant capacity of fruits, as well as the corresponding total polyphenol, ascorbic acid and total anthocyanin content. In particular, application of the strain GV41 exhibited a slight increase (8%) of antioxidant activity in strawberry samples respect to CTR ($P < 0.05$), together with a significant accumulation of ascorbic acid (23%) and total anthocyanins (31%) ($P < 0.05$) (**Table 2**). Conversely, strain TH1 only promoted a significant increase (66%) of total anthocyanin levels ($P < 0.05$).

Quali-Quantitative Characterization of Individual Anthocyanins in Strawberry Fruits

To better evaluate anthocyanin content in strawberry fruits from *Trichoderma*-treated plants, a dedicated quali-quantitative characterization of individual compounds was undertaken. To this purpose, mass spectrometry (MS) transitions were tentatively identified and assigned according to previous studies (Chandra et al., 2001; Määttä-Riihinen et al., 2004; Holzwarth et al., 2012); the results are reported in **Supplementary Table S1**, while **Supplementary Figure S1** depicts a representative anthocyanin profile of a fruit sample recorded at 520 nm. Peaks 1 and 6 were assigned to cyanidin 3-*O*-glucoside (cya 3-*O*-glc) and cyanidin derivative (cya der), respectively; both compounds exhibited an $[M^+]$ signal at *m/z* 449, releasing cyanidin as fragment at *m/z* 287 in MS/MS experiments. As expected based on chromatographic gradient and cationic selectivity of the column, cya 3-*O*-glc eluted earlier than cya der. Peaks 2, 3, 4, and 5 were tentatively assigned to pelargonidin glycosides since each component showed the flavylium ion signal at *m/z* 271 (pelargonidin flavylium ion) in MS/MS experiments. In agreement with previous investigations (Holzwarth et al., 2012), the predominant

TABLE 1 | Effects of different *Trichoderma* strains (T22, TH1, and GV41) on the growth and productivity of strawberry plants under greenhouse conditions.

Treatment	Total Yield (TY) (g/plant)	Number of fruits/plant (NF)	Root length (RL) (cm/plant)	Root fresh weight (RFW) (g/plant)	Root dry weight (RDW) (g/plant)
	Mean ± SD (%)	Mean ± SD (%)	Mean ± SD (%)	Mean ± SD (%)	Mean ± SD (%)
CTR	125.4 ± 21.8 a	6.4 ± 1.2 ab	22.0 ± 1.9 a	62.9 ± 5.4 ab	13.5 ± 1.1 bc
T22	168.9 ± 25.2 b (35)	7.5 ± 1.2 c (17)	24.5 ± 2.2 b (11)	69.3 ± 7.8 bcd (10)	15.1 ± 1.3 cd (12)
TH1	173.1 ± 24.2 b (38)	8.9 ± 1.2 d (39)	24.0 ± 3.2 ab (9)	64.8 ± 7.7 abc (3)	15.1 ± 1.8 cd (12)
GV41	161.6 ± 24.1 b (29)	6.8 ± 1.2 bc (6)	24.5 ± 2.7 b (11)	73.7 ± 5.4 d (17)	16.4 ± 1.5 a (21)

Treatments were applied at the time of transplant (by root dip) and monthly by irrigation. Data represent the mean value of 10 biological replicates ± standard deviation (SD). Different letters in a single column indicate statistically significant differences for P < 0.05. Increments or decrements compared to control (CTR) are shown in percent (%) and are reported in parenthesis.

TABLE 2 | Effects of the application of different *Trichoderma* strains (T22, TH1, and GV41) on the antioxidant properties of strawberry fruits.

Treatment	Antioxidant capacity [μmol eq Trolox/g]	Total polyphenols [mg/g]	Ascorbic acid [mg/100g]	Total anthocyanins [μg/g]
	Mean ± SD (%)	Mean ± SD (%)	Mean ± SD (%)	Mean ± SD (%)
CTR	54.0 ± 10.7 bc	10.9 ± 0.1 a	116.8 ± 12.6 bc	809.0 ± 13.0 bc
T22	47.9 ± 0.9 abc (−11)	8.6 ± 2.9 a (−21)	107.0 ± 13.1 b (−8)	818.1 ± 23.5 bc (1)
TH1	42.8 ± 16.7 a (−21)	9.5 ± 8.4 a (−13)	102.8 ± 30.8 ab (−12)	1340.7 ± 15.6 a (66)
GV41	58.3 ± 0.3 c (8)	10.4 ± 2.5 a (−5)	144.2 ± 2.5 d (23)	1056.6 ± 1.9 b (31)

Treatments were applied at the transplant (root dip) and monthly by irrigation. Data represent the mean value of eight biological replicates ± standard deviation (SD). Different letters in a single column indicate statistically significant differences for P < 0.05. Increments or decrements compared to control (CTR) are reported as % values in parenthesis.

anthocyanin (peak 2) was pelargonidin 3-*O*-glucoside (pel 3-*O*-glc) with a $[M^+]$ signal at *m/z* 433. On the other hand, peak 3, 4 and 5 were assigned to pelargonidin 3-*O*-rutinoside (pel 3-*O*-rut), pelargonidin 3-*O*-malonyl-glucoside (pel 3-*O*-mal-glc) and pelargonidin 3-*O*-acetyl-glucoside (pel 3-*O*-ac-glc) based on corresponding $[M^+]$ signals at *m/z* 579, 519 and 475, respectively.

Based on above-mentioned results, LC–DAD-assisted quantitative measurements of individual anthocyanins in fruits from plants exposed to the *Trichoderma* spore suspensions (**Figure 1**) confirmed the increment of total compounds already detected by colorimetric test **(Table 2**). The highest increases were observed with the application of strain TH1, which promoted the accumulation of cya 3-*O*-glc (82%), pel 3-*O*-glc (70%), pel 3-*O*-rut (77%), pel 3-*O*-ac-glc (24%) and cya der (72%) ($P < 0.05$), compared to CTR; no significant differences were envisaged for pel 3-*O*-mal-glc. Similarly, the strain GV41 increased the accumulation of all the individual anthocyanins ($P < 0.05$), with the exception of cya der. Finally, the application of strain T22 only determined a 24% increase in pel 3-*O*-ac-glc content ($P < 0.05$).

Proteomic Analysis of Strawberry Fruits

With the aim of evaluating molecular effectors/metabolic pathways that underlie the above-mentioned effects of *Trichoderma* spp. on strawberry fruits, and obtaining original information on fruits from a plant treated with BCAs, protein extracts from berry samples of plants inoculated with *Trichoderma* strains T22, TH1, and GV41 were comparatively evaluated to the control by a TMT-based proteomic approach. This quantitative analysis allowed the identification of 3294 proteins and measuring the relative quantitative levels of 3014 plant proteins (data available in PRIDE repository with dataset identifier PXD016951) that found a counterpart in 3262 and 2982 redundant *Arabidopsis thaliana* entries in TAIR 10 database, respectively, plus additional 32 plant sequence entries not having a homolog in the same sequence data inventory. This proteomic analysis of the strawberry did not note the presence of *Trichoderma* proteins in the fruit extracts. Above-mentioned proteins were further filtered for abundance fold changes $\geq$1.50 or $\leq$0.66 (T22, TH1, and GV41 *vs.* CTR) ($P \leq 0.05$) and accession redundancy, thus ascertaining 333 differentially represented proteins (DRPs) associated with various *Trichoderma* treatments (**Supplementary Table S2**). The latter corresponded to 323 non-redundant *A. thaliana* sequence entries in TAIR 10 database plus additional 10 plant sequence entries not having an *A. thaliana* counterpart. In particular, 75, 45, and 253 DRPs were observed for *Trichoderma* strains T22, TH1, and GV41, respectively. A Venn diagram representation of these DRPs showed a number of unique and shared components between different *Trichoderma* treatments (**Figure 2**). Hierarchical clustering of abundance ratios and distribution of DRPs between different *Trichoderma* strains highlighted that most significant quantitative changes occurred after treatment with *T. virens* GV41, followed by that with *T. harzianum* T22 and TH1 (data not shown and **Figure 2**). Resultant DRPs were functionally indexed through an initial assignment obtained with Mercator software, followed by a functional group cataloguing including information from the Bevan classification (Bevan et al., 1998) and recent literature data (**Figure 3** and **Supplementary Table S3**). This analysis attributed a function to all proteins, except 23 molecular species that were not assigned to any known ontology or functional group. Thus, DRPs were mostly related to the functional category of protein metabolism (including components involved in protein biosynthesis, protein degradation and protein translocation) (20%), stress response (including components associated with redox homeostasis, external stimuli response and protein modification) (17%), carbon and energy metabolism (including enzymes related to carbohydrate metabolism, energy and photosynthesis) (14%), vesicle trafficking (9%), and secondary metabolism (including enzymes catalyzing biosynthesis/degradation of secondary metabolites and phytohormones) (7%), thus highlighting prominent molecular mechanisms and metabolic pathways modified following *Trichoderma* treatments. No major differences in the functional distribution were observed when DPRs from plants treated with strains T22, TH1, and GV41 were considered singularly (data not shown). Functional enrichments of above-mentioned proteins for biological processes, and molecular functions and KEGG pathways confirmed the involvement of most DRPs in the response to different chemical stimuli, in binding to ions/small molecules and catalytic activity, or in the biosynthesis of secondary metabolites, oxidative phosphorylation, and carbon and protein metabolism, respectively (**Supplementary Table S4**). Heat-map pictures originated from hierarchical clustering of quantity ratios of DRPs for each functional group were reported in **Figure 4** and **Supplementary Figures S2–S9**. These figures describe the relative quantitative representation profile of the different strawberry proteins as result of the different *Trichoderma* treatments, as related to CTR. A general coherent qualitative trend of DRPs between the various treatments with *Trichoderma* strains was observed, with a very limited number of exceptions. In the subsequent sections focused on the most represented protein functional groups, these heat-map pictures are discoursed together with corresponding DRPs and metabolic pathways/molecular processes.

Bioinformatic analysis of DRPs with STRING allowed predicting a strawberry functional protein association map based on *A. thaliana* homolog counterparts, which at high confidence (0.7) revealed a predominant highly ramified network linking together 182 components, plus twelve binary/ternary molecular complexes (**Figure 5** and **Supplementary Table S5**). The involvement of most DRPs (54.6% of total number) in this major network emphasized the occurrence of a functional assembly bridging different deregulated metabolic pathways and molecular processes, which underlies the physiological adaptation of strawberry fruits to the occurrence of *Trichoderma* strains in plant roots. As mentioned above, most of the knots present in this network were associated with DRPs from treatment with *T. virens* GV41. When a medium confidence (0.4) was used, a unique highly ramified network linking together 287 DRPs (86.2% of their total number) was observed (data not shown). Overall, above-mentioned proteomic results suggested that various

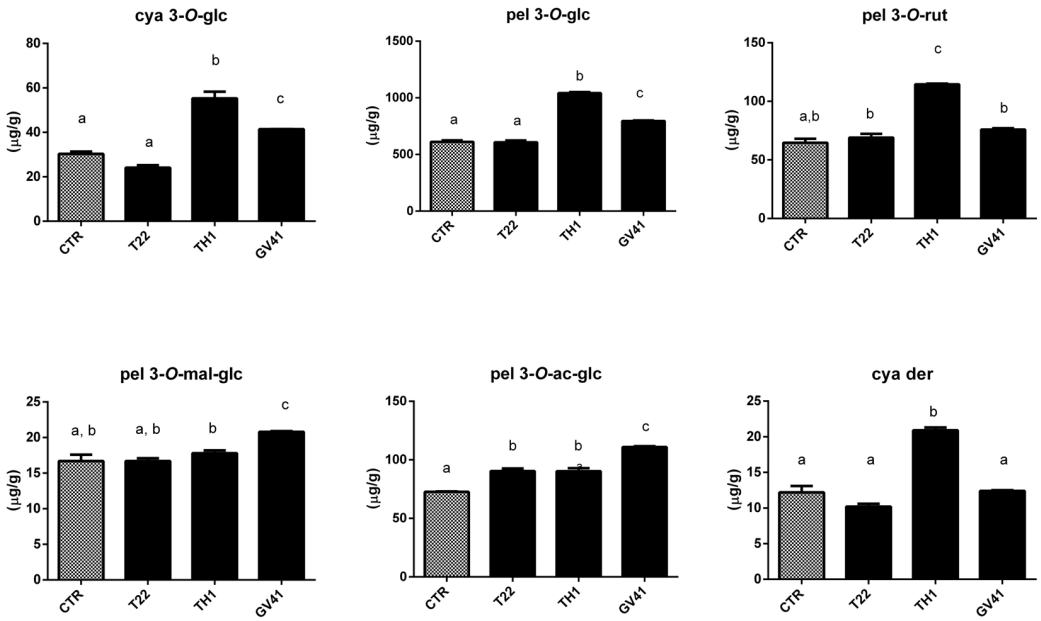

FIGURE 1 | Concentration of individual anthocyanins in strawberry fruits produced by plants subjected to the treatment with *Trichoderma* strains (T22, TH1, and GV41), as compared to control (CTR). Results on cyanidin 3-*O*-glucoside (cya 3-*O*-glc), pelargonidin 3-*O*-glucoside (pel 3-*O*-glc), pelargonidin 3-*O*-rutinoside (pel 3-*O*-rut), pelargonidin 3-*O*-malonyl-glucoside (pel 3-*O*-mal-glc), pelargonidin 3-*O*-acetyl-glucoside (pel 3-*O*-ac-glc) and cyanidin derivative (cya der) are shown. Data were reported as µg/g sample, and represent the mean value of 8 biological replicates ± standard deviation (SD). Different letters on the bars indicate statistically significant differences ($P < 0.05$).

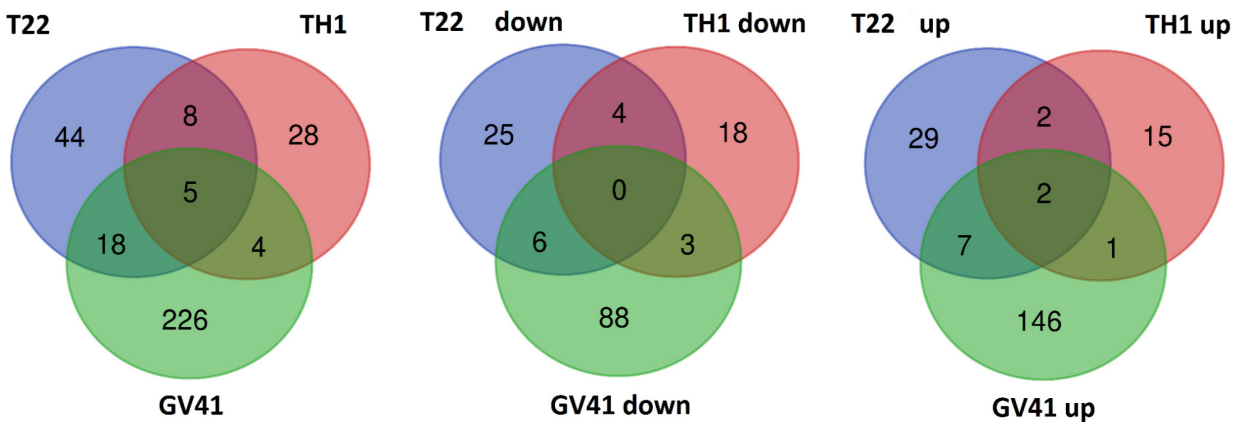

FIGURE 2 | Venn diagram showing differentially represented proteins present in strawberry fruits produced by plants subjected to the treatment with *Trichoderma* strains (T22, TH1, and GV41), as compared to control. Diagrams refer to all differentially represented proteins **(left)**, those down-represented **(middle)** and over-represented **(right)**, respectively.

metabolic, energetic and signaling processes, together with a number of plant external stimuli-/stress-responsive mechanisms, are simultaneously regulated in strawberry fruits as result of the plant treatment with different *Trichoderma* strains.

DISCUSSION

Fungi belonging to the genus *Trichoderma* are used as successful plant growth enhancers, biostimulants, biofertilizers, and as effective biocontrol agents against various pathogens (Woo et al., 2014; Lorito and Woo, 2015). Some of these positive effects have been related to the microbial release of bioactive metabolites and elicitor proteins in the plant rhizosphere (Harman et al., 2004a,b; Vinale et al., 2014). Proteomic and transcriptomic studies on plant root, leaf tissues, and seedlings suggested that this growth-promoting activity of *Trichoderma* spp. is associated with different molecular events in the host, such as: (i) an increased nutrient uptake (Altomare et al., 1999); (ii) variations in phytohormone levels and corresponding

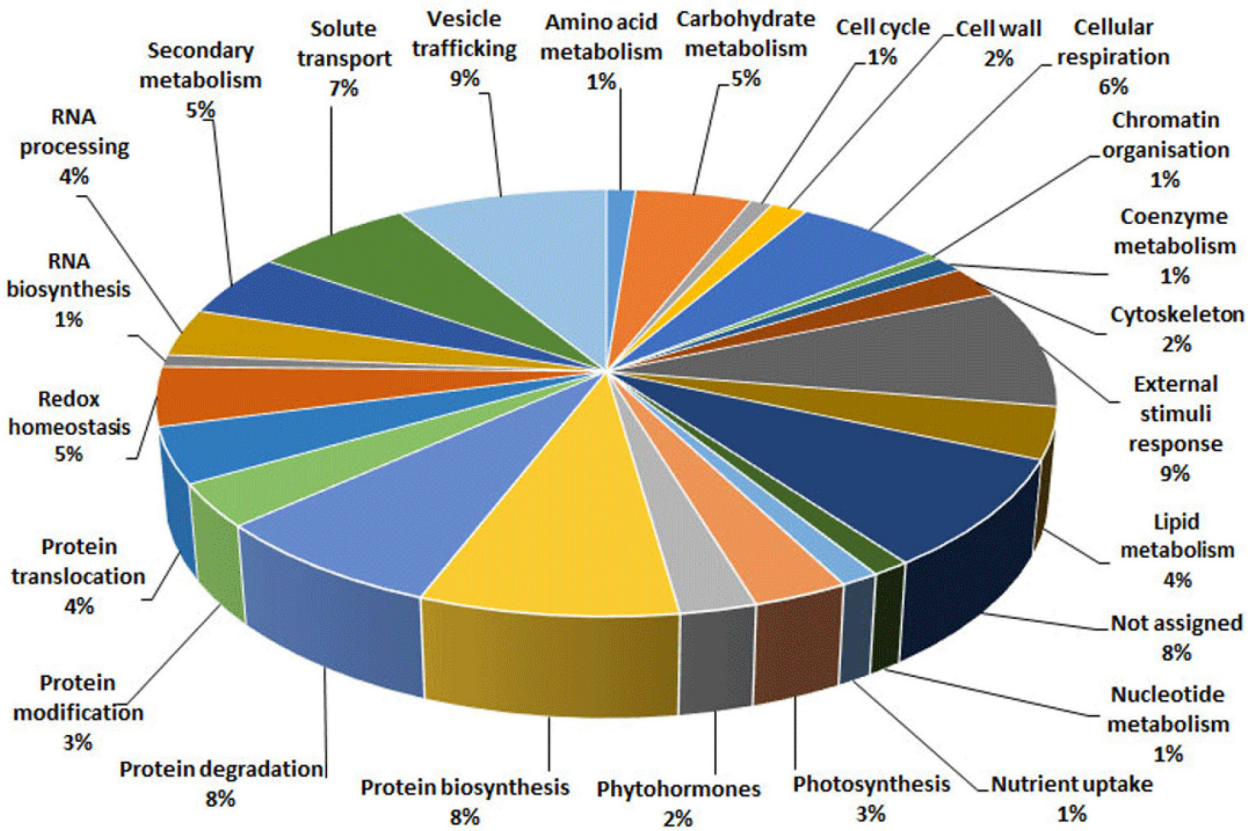

FIGURE 3 | Functional distribution of differentially represented proteins present in strawberry fruits produced by plants subjected to the treatment with *Trichoderma* strains (T22, TH1, and GV41), as compared to control (CTR). Identified protein species were initially assigned with Mercator software (**Supplementary Table S3**), followed by a functional group cataloguing including information from the Bevan classification (Bevan et al., 1998) and recent literature data.

induced metabolic processes (Harman et al., 2004a; Caporale et al., 2014); (iii) a general augmented carbon and energy metabolism (Shoresh et al., 2010); (iv) a higher photosynthetic efficiency (Shoresh et al., 2010). Molecular data on fruit tissues are scant in the literature and mainly limited to specific genes/proteins/metabolites (Singh et al., 2018).

Growth Promotion and Related Molecular Mechanisms

This study on strawberry plants and fruits confirmed the ability of the selected *T. harzianum* (T22 and TH1) and *T. virens* (GV41) strains to act as growth-promoting agents. In fact, these treatments increased significantly strawberry plant total yield (from a value of 29% for GV41 to 38% for TH1), augmented the number of corresponding fruits (from a value of 6% for GV41 to 39% for TH1) and promoted corresponding root growth (from a value of 12% for TH1 and T22 to 38% for GV41), when compared to control.

It has already been reported that the yield in strawberry plants is strongly dependent on micronutrient availability in the soil (Valentinuzzi et al., 2015). Our proteomic results on strawberry fruits confirmed the positive effect of *Trichoderma* strains in facilitating plant nutrient uptake, as demonstrated by the observed over-representation of membrane proteins devoted to (neutral and ionic) solute transport (**Supplementary Table S4**) and, in general, by the functional enrichment of biological processes related to the response to various chemicals (**Supplementary Table S4**). This phenomenon was more evident for GV41, but also detectable in T22 and TH1. Among the above-mentioned augmented proteins, worth mentioning are plasma membrane intrinsic proteins 1;4, 2, 2A and 2;5 allowing the cellular import of water and small neutral molecules (Wang et al., 2016), as well as membrane transporters for ATP/ADP, malate, nucleotide derivatives, and xanthine/uracil/ascorbate (**Supplementary Figure S2**). The selective over-representation of the latter protein in *Trichoderma* GV41-treated plants may be related to the augmented levels of ascorbic acid measured in the corresponding fruit (**Table 2**). In the above-mentioned context, it could also be considered the observed over-representation of five H^+-translocating and two Ca^{2+}-translocating ATPases, which couple the well-known ion fluxes associated with plant response to BCAs (Shoresh et al., 2010) to energy production (**Supplementary Figure S2**). Additional over-represented membrane components devoted to phytohormone, oxidant and proton translocation were ABCG transporters (3 pleiotropic drug resistance proteins) (see below) and two

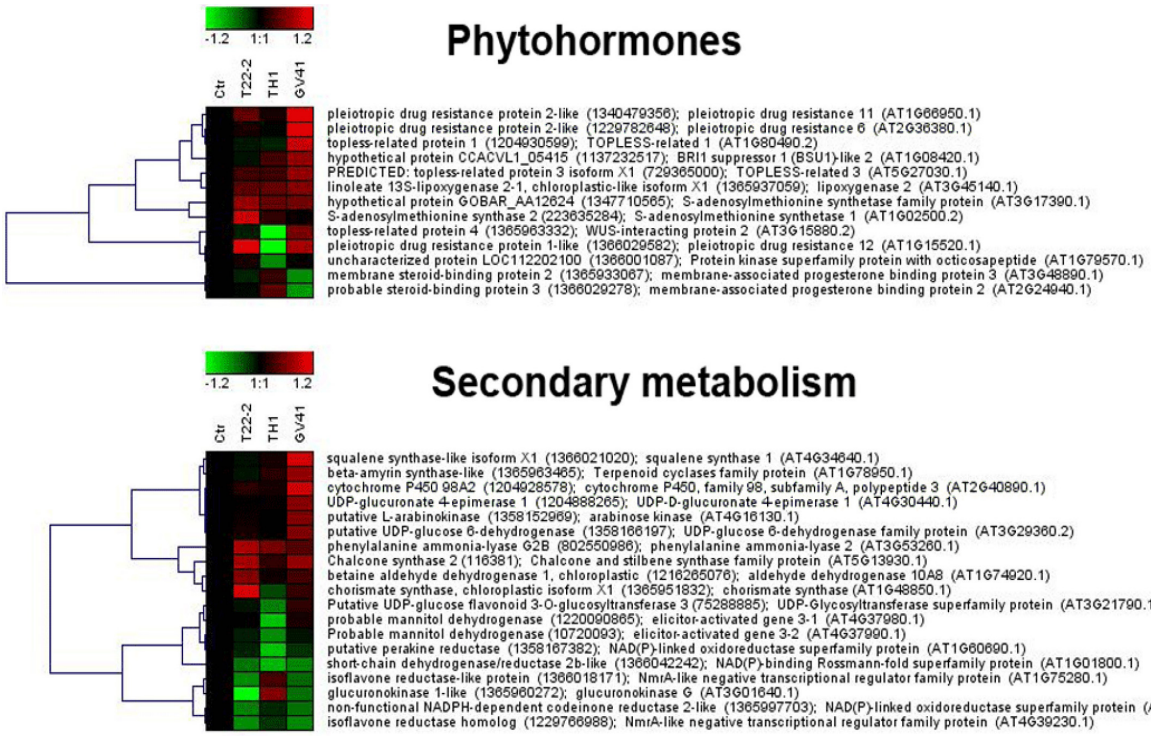

FIGURE 4 | Heat-map representation and hierarchical clustering analysis of proteins related to phytohormone metabolism **(upper panel)** and secondary metabolism **(lower panel)**, which were differentially represented in strawberry fruits produced by plants subjected to the treatments with *Trichoderma* strains (T22, TH1, and GV41), as compared to control (CTR). Proteins shown are those with abundance fold changes ≥1.50 or ≤0.66 compared to control ($P \leq 0.05$) (**Supplementary Table S3**). Data are reported as $\log_2$ transformed abundance ratio values. Hierarchical clustering analysis of DRPs was performed using Genesis 1.8.1 platform (Institute for Genomics and Bioinformatics, Graz University of Technology).

H^+-exporting pyrophosphatases. The latter proteins have been widely recognized to play an essential role in auxin-mediated leaf/fruit development, biomass accumulation and crop yield increase (Li et al., 2005; Schilling et al., 2014; Yang et al., 2014). On the other hand, the observed down-representation of the nutrient-related chloroplast nitrogen regulatory protein PII (GlnB) in fruits from treated plants was in line with previous observations on the reduced transcription of the corresponding gene in the presence of elevated levels of N-containing metabolites (Hsieh et al., 1998; **Supplementary Figure S2**). GlnB also played an essential role in regulating target proteins in response to cellular ADP/ATP levels and 2-oxoglutarate status, thereby coordinating the plant carbon/nitrogen balance and regulating specific metabolic pathways (Uhrig et al., 2009). In the whole, our gel-free proteomic approach revealed abundance changes of membrane nutrient transporter proteins already ascertained by transcriptomic studies (De Palma et al., 2016, 2019), but whose solubility hampered corresponding detection in previous gel-based methods.

In addition to above-mentioned H^+- and Ca^{2+}-translocating ATPase machineries, proteomic analysis of strawberry fruits also provided information on additional mechanisms ensuring the greater energy supply requested in *Trichoderma*-treated plants to sustain the observed plant growth and development. Thus, different proteins involved in carbohydrate (starch, sucrose and nucleotide-sugar) metabolism (β-galactosidase, β-fructofuranosidase, granule-bound starch synthase 1, sucrose synthase 1F, 4 and 6, xyloglucan 6-xylosyltransferase, UDP-glucuronate 4-epimerase 1, glucuronokinase 1, UDP-glucose 6-dehydrogenase, sorbitol dehydrogenase and arabinose kinase), glycolysis and tricarboxylic acid cycle (two phosphofructokinase isoforms, pyruvate kinase, isocitrate dehydrogenase, ATP lyase and 2-oxoglutarate dehydrogenase), and alcoholic fermentation (two pyruvate decarboxylase isoforms) showed augmented levels in fruit after *Trichoderma* treatments (**Supplementary Figure S3**). This effect was again more evident in *Trichoderma* GV41-treated plants, confirming the already-mentioned strain-dependent potential of BCAs (Tucci et al., 2011; Fiorentino et al., 2018; Marra et al., 2019). These results were in good agreement with previous proteomic observations on root and leaf tissues from maize, tomato, cucumber and grapevine plants (Segarra et al., 2007; Shoresh and Harman, 2008; Shoresh et al., 2010; Palmieri et al., 2012; Manganiello et al., 2018). Conversely, all mitochondrial components of the mitochondrial ATP synthase and cytochrome C reductase complexes showed reduced levels after microbial treatments (**Supplementary Figure S3**), while a mixed behavior was observed for proteins involved in photosynthesis. The first phenomenon may be related to a

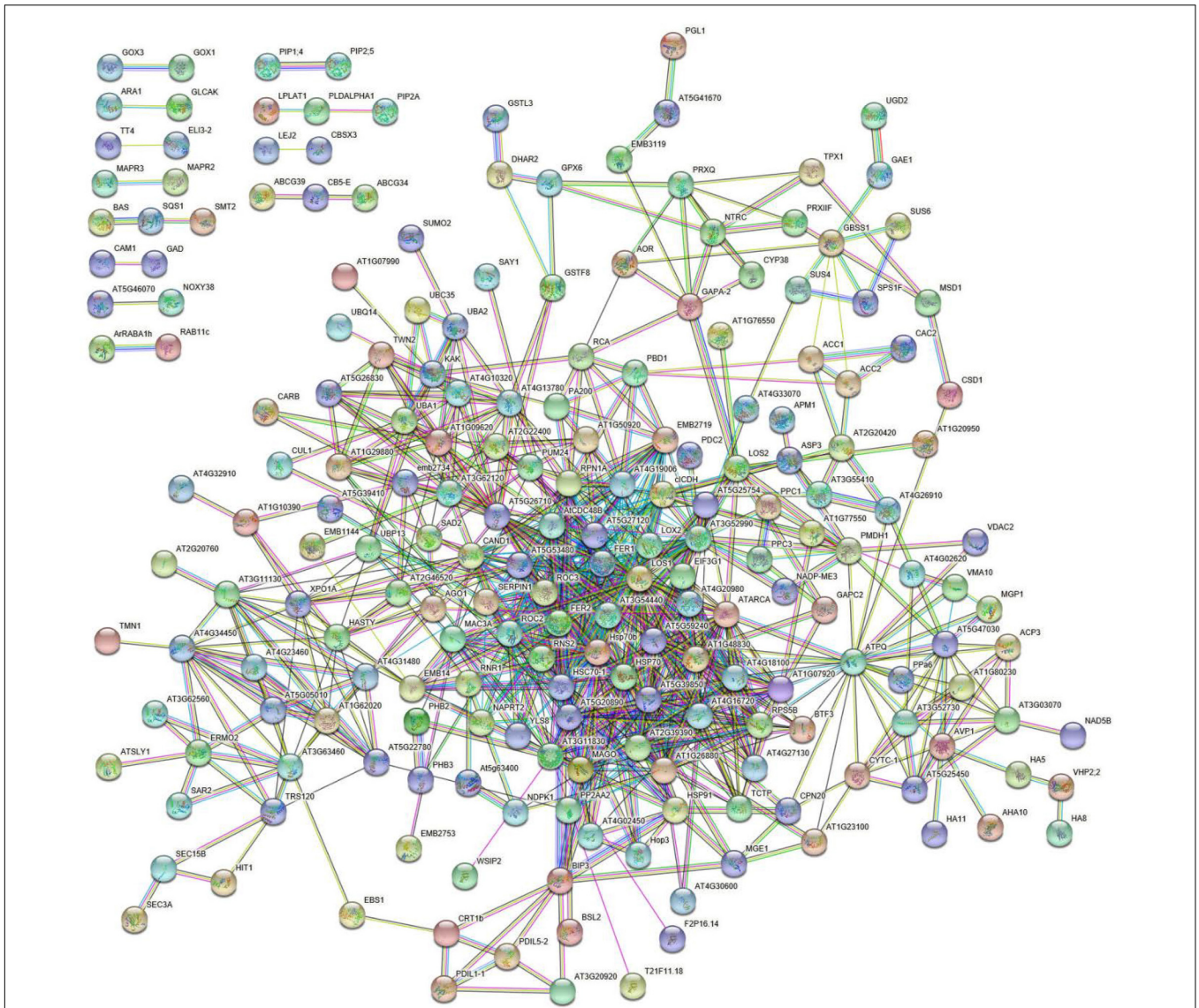

FIGURE 5 | STRING analysis of differentially represented proteins present in strawberry fruits produced by plants subjected to the treatments with *Trichoderma* strains (T22, TH1, and GV41), as compared to control (CTR). Functional protein associations were based on data recorded for *A. thaliana* protein homologs. Only high-confidence interactions (0.7) are shown. Protein codes are reported in **Supplementary Table S5**.

cell attempt to limit generation of reactive oxygen species (ROS) side products during oxidative phosphorylation, in a physiological plant condition where plant cells are already exposed to significant oxidant fluxes (see below) (Shoresh et al., 2010). On the other hand, components of the NADH dehydrogenase complex (complex I), which is believed to belong to the minimal assembly required for the transfer of electrons from NADH to the respiratory chain, showed augmented levels after *Trichoderma* treatments.

Observed plant growth and development in *Trichoderma*-treated plants also corresponded to increased fruit representation levels of a number of components present in protein biosynthetic machineries involved in: (i) RNA biosynthesis and processing (2 and 8 in number, respectively); (ii) production of amino acid-tRNAs (8 in number); (iii) assembling of large/small ribosomal subunits (8 in number); (iv) polypeptide chain translation initiation/elongation activities (translation initiation factor 3 subunits G and L, and elongation factor G); (v) protein translocation from cytoplasm to cell nucleus and endoplasmic reticulum (3 and 7 in number, respectively) (**Supplementary Figures S6, S7**). Sporadic proteins showing an opposite quantitative trend were also observed. Above-mentioned components seemed essential to fuel novel enzymes and structural proteins to developing fruit cells and growing tissues (Shoresh and Harman, 2008), as revealed by the number of over-represented species mentioned in the previous paragraphs and the augmented levels of constitutive elements present in evolving cell wall (5 in number) and cytoskeleton (5 in number)

compartments (**Supplementary Figure S8**). In the latter group can also be included the cell division protein FtsZ that, together with all other strawberry deregulated components present in the cell cycle catalog, also showed augmented levels after *Trichoderma* treatment. This protein is a structural homolog of tubulin and mediates ring formation at the chloroplast division site, and thus is essential for plant growth (Vitha et al., 2001). A request for augmented protein levels in treated plants has also to be considered in light of the need of additional defensive components (see below).

Secondary Metabolites and Related Biosynthetic Pathways

This study also showed that *Trichoderma* spp. treatment of plants favored accumulation of anthocyanins and other antioxidants in strawberry fruits, with a pattern that was strain-dependent. In particular, application of two microorganisms increased significantly total content of anthocyanins (31 and 66% for GV41 and TH1, respectively), ascorbic acid (23% for GV41) and corresponding antioxidant capacity (8% for GV41). Chromatographic measurements of individual anthocyanins confirmed the above-mentioned total increment, highlighting the accumulation of all measured compounds except pel 3-*O*-mal-glc and pel 3-*O*-ac-glc in TH1 and GV41, respectively. Induction of antioxidant metabolites in plant tissues of BCA-treated plants has already been reported; for example, *T. harzianum* inoculation was described to increase polyphenolic content and antioxidant activity in grape (Pascale et al., 2017), as well as GSH/GSSG and ASA/DHA ratios in tomato seedlings (Mastouri et al., 2012). Similarly, *T. asperellum* root colonization of cucumber plants augmented total antimicrobial polyphenols (Yedidia et al., 2003). Our proteomic measurement of enzymes involved in biosynthesis of secondary metabolites provided a rationale to the above-mentioned increase of anthocyanins in strawberry fruits. Indeed, it demonstrated augmented levels of phenylalanine-ammonia lyase (PAL) and chorismate synthase, which control the first reaction steps of the phenylpropanoid pathway yielding phenolic compounds (including anthocyanins), and other enzymes (chalcone and stilbene synthase, UDP-glucuronate 4-epimerase, glucokinase, UDP-glucose 6-dehydrogenase, arabinose kinase) assisting the conversion of corresponding intermediates into final compounds, or forming UDP-sugar moieties to be included into corresponding structures (**Figure 4**). To increase anabolic efficiency toward anthocyanin production, proteins (elicitor-activated gene 3-1 and 3-2, and two isoflavone reductases) catalyzing transformation of above-mentioned secondary metabolites into lignin derivatives were also down-represented. These results well resembled the augmented PAL levels already reported in roots and leaves of other *Trichoderma*-treated plants (Shoresh and Harman, 2008; Shoresh et al., 2010; De Palma et al., 2016).

Additional deregulated secondary metabolism enzymes showing augmented levels after *Trichoderma* application were squalene synthase and β-amyrin synthase, which are involved in the biosynthesis of sesquiterpenoids/triterpenoids (**Figure 4**). Terpenoids represent important constituents of herbivore-induced plant volatiles that deter herbivores and/or attract their predators (Sharma et al., 2017). They serve as airborne signals that can induce defense responses in systemic undamaged parts of the plant, and prime defense responses in neighboring plants. Our determinations were in good agreement with those on corresponding metabolic pathways and metabolites in tomato plants challenged with *T. harzianum* (Manganiello et al., 2018), confirming that fungal treatment can influence the plant defensive volatilome.

Antioxidant Enzymes and Related Molecular Processes

Augmented production of antioxidant metabolites in strawberry fruits may occur as consequence of the induction of different defense mechanisms (Contreras-Cornejo et al., 2011), which follow plant interactions with specific BCAs or pathogens. For example, expression of *Pal* genes is induced by jasmonic acid (JA)/ethylene (ET) signaling during plant defense response (Shoresh et al., 2010), and augmented levels of anthocyanins have already been reported to attenuate the effects of ROS produced to generate an hostile environment in plant tissues after microorganism challenge (Figueroa-Balderas et al., 2006; Senthil-Kumar and Mysore, 2010; Mathys et al., 2012). In particular, it has already been demonstrated that plant co-cultivation with *T. asperellum* increased anthocyanin production in *A. thaliana* leaves (Contreras-Cornejo et al., 2011). Our proteomic experiments showed that this augmented production of antioxidants in fruits from treated plants corresponded to a widespread down-representation of enzymes limiting the detrimental effects of ROS (15 in number and corresponding to different redox protective machineries) (**Supplementary Figure S4**). These findings apparently contrast with previous observations on root and leaf tissues of *Trichoderma*-challenged plants, which report an over-representation of antioxidant and toxicant-scavenging enzymes therein [Segarra et al., 2007; Shoresh and Harman, 2008; Shoresh et al., 2010; Mastouri et al., 2012; De Palma et al., 2016, 2019; Perazzolli et al., 2016; Zhang et al., 2017; Manganiello et al., 2018), although in some cases a coherent quantitative trend was also described (Vitti et al., 2015; Rubio et al., 2017). Thus, our results on this antioxidant metabolite-rich fruit suggested that either the increased concentration of these small protective compounds after fungal challenge was enough to remodulate ROS levels, without the need of augmented antioxidant protein machineries that are repressed to save plant energy, or the biosynthesis of the latter components was selectively down-regulated to allow high basal levels of detrimental oxidants to contrast bacterial challenge. Future investigations are required in this context.

Defense Processes and Related Molecular Mechanisms

Proteomic analysis of *Trichoderma*-treated plants also highlighted defensive signaling pathways and corresponding down-stream mechanisms modulated following fungus-plant interaction; a number of them have already been reported to prevent pathogen colonization (Shoresh et al., 2010;

Pérez and Goossens, 2013; Guerreiro et al., 2016; Yuan et al., 2017; Aldon et al., 2018; Yu et al., 2018). In particular, signaling pathways involving Ca^{2+}, JA, ET and brassinosteroid (BR) effectors appear to be modulated in strawberry fruits following the interaction with *Trichoderma*. This was suggested from the observed modified levels of: (i) a number of Ca^{2+}-binding sensors and a MAP3K (10 in number, all showing down-representation except coherent Ca^{2+}-translocating ATPase concentrations ensuring ion expulsion from the cell); (ii) lipoxygenase 2 involved in JA biosynthesis (showing over-representation); (iii) S-adenosylmethionine synthase 1 and 2 involved in ET biosynthesis (showing over-representation); (iv) BR-related membrane-associated progesterone-binding proteins 2 and 3, and BRI suppressor 1 and 2 (showing a mixed but coherent quantitative trend); and (v) topless-related protein 1, 2 and 3 (**Figure 4** and **Supplementary Figures S2, S7**). Some proteins mentioned above (especially those sensitive to Ca^{2+}) are involved in signal decoding and transduction mechanisms leading to a rapid down-stream activation of cellular ROS burst, protein phosphorylation and transcriptional reprogramming events, as well as to the biosynthesis of defense-related phytohormones JA, ET, and salicylic acid (SA). A number of these quantitative protein changes were in agreement with those already determined in other proteomic/transcriptomic studies on root/leaf tissues from *Trichoderma*-treated maize, tomato and cucumber plants (Segarra et al., 2007; Shoresh et al., 2010; Manganiello et al., 2018; Nogueira-Lopez et al., 2018; De Palma et al., 2019). Notwithstanding this investigation strongly suggested the activation of JA- and ET-mediated defense processes also in fruits from *Trichoderma*-treated strawberry plants, a real comprehension of those involving Ca^{2+} and BR action will deserve future dedicated studies (on other plant tissues and according to a time-basis). In fact, Ca^{2+}, BR, and ET concentration changes are also known to modulate plant growth and to proceed with different rates (Hepler, 2005; Yu et al., 2018), and variable levels of these molecules have been reported in other tissues after fungal challenge (Navazio et al., 2007).

This study also demonstrated a clear activation (23 over-represented proteins) of a number of protein machineries involved in cellular vesicle trafficking in fruits from treated plants (**Supplementary Figure S8**); these vesicles have been reported as essential structures to dump out high- and low-mass compounds involved in plant innate immunity. In fact, since antimicrobials are also toxic to plant cells themselves, they have to be safely delivered to target sites in a separate compartment (Yun and Kwon, 2017). Because immune responses generally require energy otherwise used for the other metabolic processes, it is also very important to properly control duration/strength of these secretory activities. This can be achieved by regulating the sensing of immune signals and the delivery/discharge of extracellular immune molecules, all of which are controlled by membrane trafficking in plant cells. Thus, components of the clathrin coated vesicle machinery, coat protein I and II coatomer machineries, or regulating membrane tethering and fusion were over-represented in fruits from *Trichoderma*-treated plants, suggesting also in this case the occurrence of this physiological phenomenon (**Supplementary Figure S8**). Among above-mentioned immunity-related components, worth mentioning are exocyst complexes that were already reported to transport anthocyanins between different plant cell subcellular compartments (Pecenková et al., 2017). Preliminary evidence of quantitative changes in few of the above-mentioned protein families were observed in leaves of grapevine plants challenged with *T. harzianum* T39 (Perazzolli et al., 2016).

Finally, a number of proteins (52 in number) known to elicit a protective action against biotic/abiotic stresses showed variable quantitative levels in fruits from fungal-treated plants, highlighting a significant remodeling of the corresponding defense effector molecular machineries (**Supplementary Figures S4, S7**). Significant differences were observed among either the effect of different *Trichoderma* strains (with most frequent changes in GV41) and components belonging to the same protein family. Regarding heat shock proteins (HSPs), chaperones and protein disulfide-isomerases (PDIs), *T. virens* GV41 was observed to increase the representation of different HSP70 isoforms, HSP91 and DNAJ protein, while it decreased the concentration of various chaperones and HSP20; depending on the isoform, PDIs showed variable levels (**Supplementary Figure S4**). No significant changes were observed in the case of *T. harzianum* T22 and TH1. On the other hand, a number of proteins involved in the plant response to abiotic stresses also showed quantitative variations. This is the case of some CBS domain-containing protein and late embryogenesis abundant protein isoforms, as well as temperature-induced lipocalin, stress-inducible protein, stress induced protein, universal stress protein A, stress response protein, mucin 22-like protein and metallothionein, which were generally down-represented in *T. virens* GV41 and over-represented in *T. harzianum* T22 (**Supplementary Figures S4, S7**). A similar quantitative trend was also observed for proteins involved in the plant response to biotic stresses, namely cysteine and serine protease inhibitors, thaumatin domain-containing protein, MLP-like protein 28, Bet v I type allergen, Fra a 1-E allergen chain A and Fra A3 allergen chain B, which generally showed reduced levels in *T. virens* GV41 and a higher representation in *T. harzianum* T22 and TH1. Data on antioxidant proteins have already been described in previous paragraphs. Various defense components reported above have already been demonstrated to show quantitative variations in root and leaf tissues of bean, maize, tomato, cucumber, and grapevine plants treated with *Trichoderma* strains (Marra et al., 2006; Segarra et al., 2007; Shoresh and Harman, 2008; Perazzolli et al., 2016; Manganiello et al., 2018; Nogueira-Lopez et al., 2018; De Palma et al., 2019). The distinct pattern of the allergens present in strawberry fruits depending on the *Trichoderma* spp. used for plant treatment prompts us to suggest the development of future investigations with the aim of evaluating novel food products with specific characteristics for human consumption.

CONCLUSION

This study demonstrated that the treatment of strawberry plants with different *Trichoderma* can either influence the relative

yield, growth and productivity, as well as the accumulation of anthocyanins and other antioxidants in the corresponding fruits. These findings indicated that the positive effects observed by the application of *Trichoderma*-based products to the developing plant are also transferred to fruits, thus modulating different physiological processes and describing the molecular mechanisms that positively influence food quality and consumer health.

In recent years, with the changing perception by governing bodies to implement precautionary measures that reduce the use of chemical phytosanitary products in agriculture, a great effort has been spent in the development of alternative methods for crop protection. In addition to the valuable influence that *Trichoderma* treatments have demonstrated on the plant, increased strawberry fruit production and enhanced nutritional properties, plus its known success as a biological control agent and its acceptance as a natural product for use in diverse crop production systems, confirms the important role that this beneficial microbe can play in sustainable agricultural while safeguarding the well-being of the consumer and the environment.

DATA AVAILABILITY STATEMENT

All datasets generated for this study are included in the article/**Supplementary Material**.

AUTHOR CONTRIBUTIONS

NL and SW planned and designed the experiments. NL performed the field research, sample collection, and biometric analysis. AMS, SC, and AS performed the proteomics analysis and interpretation of the data. SW, AS, NL, RM, and FV assisted in the interpretation of results and in the writing of the manuscript. AT and PV defined the experimental protocols for the antioxidant capacity, total phenolic, ascorbic acid, and anthocyanins content in fruits, and performed data elaboration and analyses. All authors contributed to the article and approved the submitted version.

FUNDING

This work was supported by the following projects: MIURPON (grant number Linfa 03PE_00026_1; grant number Marea 03PE_00106), POR FESR CAMPANIA 2014/2020- O.S. 1.1 (grant number Bioagro 559); MISE CRESO (grant number Protection n. F/050421/01-03/X32); PSR Veneto 16.1.1 (grant number Divine n. 3589659); European Union Horizon 2020 Research and Innovation Program, ECOSTACK (grant agreement no. 773554); ProBio IZSM (Portici), n. D01 6309, 14/12/2016; CNR project NUTR-AGE (FOE-2019, DSB.AD004.271).

ACKNOWLEDGMENTS

The authors thank Dr. Luigi De Vitto for providing the strawberry plants, and Koppert Biological Systems, Rotterdam, Netherlands for fungal inocula.

SUPPLEMENTARY MATERIAL

The Supplementary Material for this article can be found online at: https://www.frontiersin.org/articles/10.3389/fmicb.2020.01364/full#supplementary-material

REFERENCES

Aaby, K., Mazur, S., Nes, A., and Skrede, G. (2012). Phenolic compounds in strawberry (*Fragaria* x *ananassa* Duch.) fruits: composition in 27 cultivars and changes during ripening. *Food Chem.* 132, 86–97. doi: 10.1016/j.foodchem.2011.10.037

Aaby, K., and Remberg, S. F. (2015). "Strawberry phenolics and impact of ripening," in *Processing and Impact on Active Components in Food*, ed. V. R. Preedy (Cambridge, MA: Academic Press).

Aldon, D., Mbengue, M., Mazars, C., and Galaud, J. P. (2018). Calcium signalling in plant biotic interactions. *Int. J. Mol. Sci.* 19:665. doi: 10.3390/ijms19030665

Altomare, C., Norvell, W. A., Bjorkman, T., and Harman, G. E. (1999). Solubilization of phosphates and micronutrients by the plant-growth-promoting and biocontrol fungus *Trichoderma harzianum* Rifai 1295-22. *Appl. Environ. Microbiol.* 65, 2926–2933. doi: 10.1128/aem.65.7.2926-2933.1999

Anttonen, M. J., Hoppula, K. I., Nestby, R., Verheul, M. J., and Karjalainen, R. O. (2006). Influence of fertilization, mulch color, early forcing, fruit order, planting date, shading, growing environment, and genotype on the contents of selected phenolics in strawberry (*Fragaria* x *ananassa* Duch.) fruits. *J. Agric. Food Chem.* 54, 2614–2620. doi: 10.1021/acs.jafc.7b0381

Armbruster, D. A., and Pry, T. (2008). Limit of blank, limit of detection and limit of quantitation. *Clin. Biochem.* 29(Suppl 1), S49–S52.

Baker, R. (1988). *Trichoderma* spp. as plant-growth stimulants. *CRC Crit. Rev. Biotechnol.* 7, 97–106.

Bevan, M., Bancroft, I., Bent, E., Love, K., Goodman, H., Dean, C., et al. (1998). Analysis of 1.9 Mb of contiguous sequence from chromosome 4 of *Arabidopsis thaliana*. *Nature* 391, 485–488. doi: 10.1038/35140

Bianco, L., Lopez, L., Scalone, A. G., Di Carli, M., Desiderio, A., Benvenuto, E., et al. (2009). Strawberry proteome characterization and its regulation during fruit ripening and in different genotypes. *J. Proteomics* 72, 586–607. doi: 10.1016/j.jprot.2008.11.019

Buendia, B., Gil, M. I., Tudela, J. A., Gady, A. L., Medina, J. J., Soria, C., et al. (2010). HPLC-MS analysis of proanthocyanidin oligomers and other phenolics in 15 strawberry cultivars. *J. Agric. Food Chem.* 58, 3916–3926. doi: 10.1021/jf9030597

Caporale, A. G., Sommella, A., Lorito, M., Lombardi, N., Azam, S. M., Pigna, M., et al. (2014). *Trichoderma* spp. alleviate phytotoxicity in lettuce plants (*Lactuca sativa* L.) irrigated with arsenic-contaminated water. *J. Plant Physiol.* 171, 1378–1384. doi: 10.1016/j.jplph.2014.05.011

Carbone, F., Preuss, A., De Vos, R. C. H., D'Amico, E., Perrotta, G., Bovy, A. G., et al. (2009). Developmental, genetic and environmental factors affect the expression of flavonoid genes, enzymes and metabolites in strawberry fruits. *Plant Cell Environ.* 32, 1117–1131. doi: 10.1111/j.1365-3040.2009.01994

Chacón, M. R., Rodríguez Galán, O., Benítez Fernández, C. T., Sousa, S., Rey, M., Llobell González, A., et al. (2007). Microscopic and transcriptome analyses of early colonization of tomato roots by" *Trichoderma harzianum* ". *Int. Microbiol.* 10, 19–27. doi: 10.2436/20.1501.01.4

Chandra, A., Rana, J., and Li, Y. (2001). Separation, identification, quantification, and method validation of anthocyanins in botanical supplement raw materials by HPLC and HPLC - MS. *J. Agric. Food Chem.* 49, 3515–3521. doi: 10.1021/jf010389p

Contreras-Cornejo, H. A., Macías-Rodríguez, L., Beltrán-Peña, E., Herrera-Estrella, A., and López-Bucio, J. (2011). *Trichoderma*-induced plant immunity likely involves both hormonal-and camalexin-dependent mechanisms in *Arabidopsis thaliana* and confers resistance against necrotrophic fungi *Botrytis cinerea*. *Plant Signal. Behav.* 6, 1554–1563. doi: 10.4161/psb.6.10.17443

da Silva, F. L., Escribano-Bailón, M. T., Alonso, J. J. P., Rivas-Gonzalo, J. C., and Santos-Buelga, C. (2007). Anthocyanin pigments in strawberry. *LWT Food Sci. Technol.* 40, 374–382. doi: 10.1016/j.lwt.2005.09.018

D'Ambrosio, C., Arena, S., Rocco, M., Verrillo, F., Novi, G., Viscosi, V., et al. (2013). Proteomic analysis of apricot fruit during ripening. *J. Proteomics* 78, 39–57. doi: 10.1016/j.jprot.2012.11.008

De Palma, M., D'Agostino, N., Proietti, S., Bertini, L., Lorito, M., Ruocco, M., et al. (2016). Suppression subtractive hybridization analysis provides new insights into the tomato (*Solanum lycopersicum* L.) response to the plant probiotic microorganism *Trichoderma longibrachiatum* MK1. *J. Plant Physiol.* 190, 79–94. doi: 10.1016/j.jplph.2015.11.005

De Palma, M., Salzano, M., Villano, C., Aversano, R., Lorito, M., Ruocco, M., et al. (2019). Transcriptome reprogramming, epigenetic modifications and alternative splicing orchestrate the tomato root response to the beneficial fungus *Trichoderma harzianum*. *Hortic. Res.* 6:5. doi: 10.1038/s41438-018-0079-1

de Santiago, A., Quintero, J. M., Avilés, M., and Delgado, A. (2011). Effect of *Trichoderma asperellum* strain T34 on iron, copper, manganese, and zinc uptake by wheat grown on a calcareous medium. *Plant Soil* 342, 97–104. doi: 10.1007/s11104-010-0670-1

Figueroa-Balderas, R. E., García-Ponce, B., and Rocha-Sosa, M. (2006). Hormonal and stress induction of the gene encoding common bean acetyl- coenzyme A carboxylase. *Plant Physiol.* 142, 609–619. doi: 10.1104/pp.106.085597

Fiorentino, N., Ventorino, V., Woo, S. L., Pepe, O., De Rosa, A., Gioia, L., et al. (2018). *Trichoderma*-based biostimulants modulate rhizosphere microbial populations and improve N uptake efficiency, yield, and nutritional quality of leafy vegetables. *Front. Plant Sci.* 9:743. doi: 10.3389/fpls.2018.00743

Freeman, S., Minz, D., Kolesnik, I., Barbul, O., Zveibil, A., Maymon, M., et al. (2004). *Trichoderma* biocontrol of *Colletotrichum acutatum* and *Botrytis cinerea* and survival in strawberry. *Eur. J. Plant Pathol.* 110, 361–370. doi: 10.1023/b:ejpp.0000021057.93305.d9

Giampieri, F., Tulipani, S., Alvarez-Suarez, J. M., Quiles, J. L., Mezzetti, B., and Battino, M. (2012). The strawberry: composition, nutritional quality, and impact on human health. *Nutrition* 28, 9–19. doi: 10.1016/j.nut.2011.08.009

Guarino, C., Arena, S., De Simone, L., D'Ambrosio, C., Santoro, S., Rocco, M., et al. (2007). Proteomic analysis of the major soluble components in Annurca apple flesh. *Mol. Nutr. Food Res.* 51, 255–262. doi: 10.1002/mnfr.200600133

Guerreiro, A., Figueiredo, J., Sousa Silva, M., and Figueiredo, A. (2016). Linking jasmonic acid to grapevine resistance against the biotrophic oomycete *Plasmopara viticola*. *Front. Plant Sci.* 7:565. doi: 10.3389/fpls.2016.00565

Hanhineva, K., Kärenlampi, S., and Aharoni, A. (2011). Recent advances in strawberry metabolomics. Genomics, transgenics, molecular breeding and biotechnology of strawberry. *Genes Genomes Genomics* 5, 65–75.

Harman, G. E. (2004). Overview of new insights into mechanisms and uses of *Trichoderma* based products. *Phytopathology* 94:138.

Harman, G. E., Howell, C. R., Viterbo, A., Chet, I., and Lorito, M. (2004a). *Trichoderma* species – opportunistic, avirulent plant symbionts. *Nat. Rev. Microbiol.* 2, 43–56. doi: 10.1038/nrmicro797

Harman, G. E., Lorito, M., and Lynch, J. M. (2004b). Uses of *Trichoderma* spp. to alleviate or remediate soil and water pollution. *Adv. Appl. Microbiol.* 56, 313–330. doi: 10.1016/S0065-2164(04)56010-0

Hepler, P. K. (2005). Calcium: a central regulator of plant growth and development. *Plant Cell* 17, 2142–2155. doi: 10.1105/tpc.105.032508

Hermosa, R., Viterbo, A., Chet, I., and Monte, E. (2012). Plant-beneficial effects of *Trichoderma* and of its genes. *Microbiology* 158, 17–25. doi: 10.1099/mic.0.052274-0

Holzwarth, M., Korhummel, S., Carle, R., and Kammerer, D. R. (2012). Evaluation of the effects of different freezing and thawing methods on color, polyphenol and ascorbic acid retention in strawberries (*Fragaria* × *Ananassa* Duch.). *Food Res. Int.* 48, 241–248. doi: 10.1016/j.foodres.2012.04.004

Hsieh, M. H., Lam, H. M., van de Loo, F. J., and Coruzzi, G. A. (1998). PII-like protein in *Arabidopsis*: putative role in nitrogen sensing. *Proc. Natl. Acad. Sci. U.S.A.* 95, 13965–13970. doi: 10.1073/pnas.95.23.13965

Joseph, S. V., Edirisinghe, I., and Burton-Freeman, B. M. (2014). Berries: anti-inflammatory effects in humans. *J. Agric. Food Chem.* 62, 3886–3903. doi: 10.1021/jf4044056

Klefield, O., and Chet, I. (1992). *Trichoderma harzianum* - interaction with plants and effect on growth response. *Plant Soil* 144, 267–272. doi: 10.1007/bf00012884

Li, J., Yang, H., Peer, W. A., Richter, G., Blakeslee, J., Bandyopadhyay, A., et al. (2005). Arabidopsis H+-PPase AVP1 regulates auxin-mediated organ development. *Science* 310, 121–125. doi: 10.1126/science.1115711

Li, L., Luo, Z., Huang, X., Zhang, L., Zhao, P., Ma, H., et al. (2015). Label-free quantitative proteomics to investigate strawberry fruit proteome changes under controlled atmosphere and low temperature storage. *J. Proteomics* 120, 44–57. doi: 10.1016/j.jprot.2015.02.016

Li, L., Song, J., Kalt, W., Forney, C., Tsao, R., Pinto, D., et al. (2013). Quantitative proteomic investigation employing stable isotope labeling by peptide dimethylation on proteins of strawberry fruit at different ripening stages. *J. Proteomics* 94, 219–239. doi: 10.1016/j.jprot.2013.09.004

Liu, S., Manson, J. E., Lee, I. M., Cole, S. R., Hennekens, C. H., Willett, W. C., et al. (2000). Fruit and vegetable intake and risk of cardiovascular disease: the women's health study. *Am. J. Clin. Nutr.* 72, 922–928. doi: 10.1093/ajcn/72.4.922

Lombardi, N., Vitale, S., Turrà, D., Reverberi, M., Fanelli, C., Vinale, F., et al. (2018). Root exudates of stressed plants stimulate and attract *Trichoderma* soil fungi. *Mol. Plant Microbe Interact.* 31, 982–994. doi: 10.1094/MPMI-12-17-0310-R

Lorito, M., and Woo, S. L. (2015). "*Trichoderma*: a multi-purpose tool for integrated pest management," in *Principles of Plant-Microbe Interactions*, ed. B. Lugtenberg (Cham: Springer), 345–353. doi: 10.1007/978-3-319-08575-3_36

Lorito, M., Woo, S. L., Harman, G. E., and Monte, E. (2010). Translational research on *Trichoderma*: from 'omics to the field. *Annu. Rev. Phytopathol.* 48, 395–417. doi: 10.1146/annurev-phyto-073009-114314

Määttä-Riihinen, K. R., Kamal-Eldin, A., and Törrönen, A. R. (2004). Identification and quantification of phenolic compounds in berries of *Fragaria* and *Rubus* species (family *Rosaceae*). *J. Agric. Food Chem.* 52, 6178–6187. doi: 10.1021/jf049450r

Manganiello, G., Sacco, A., Ercolano, M. R., Vinale, F., Lanzuise, S., Pascale, A., et al. (2018). Modulation of tomato response to *Rhizoctonia solani* by *Trichoderma harzianum* and its secondary metabolite harzianic acid. *Front. Microbiol.* 9:1966. doi: 10.3389/fmicb.2018.01966

Marra, R., Ambrosino, P., Carbone, V., Vinale, F., Woo, S. L., Ruocco, M., et al. (2006). Study of the three-way interaction between *Trichoderma atroviride*, plant and fungal pathogens by using a proteomic approach. *Curr. Genet.* 50, 307–321. doi: 10.1007/s00294-006-0091-0

Marra, R., Lombardi, N., d'Errico, G., Troisi, J., Scala, G., Vinale, F., et al. (2019). Application of *Trichoderma* strains and metabolites enhances soybean productivity and nutrient content. *J. Agric. Food Chem.* 67, 1814–1822. doi: 10.1021/acs.jafc.8b06503

Mastouri, F., Björkman, T., and Harman, G. E. (2012). *Trichoderma harzianum* enhances antioxidant defense of tomato seedlings and resistance to water deficit. *Mol. Plant Microbe Interact.* 25, 1264–1271. doi: 10.1094/MPMI-09-11-0240

Mathys, J., De Cremer, K., Timmermans, P., Van Kerkhove, S., Lievens, B., Vanhaecke, M., et al. (2012). Genome-wide characterization of ISR induced in *Arabidopsis thaliana* by *Trichoderma hamatum* T382 against *Botrytis cinerea* infection. *Front. Plant Sci.* 3:108. doi: 10.3389/fpls.2012.00108

Molassiotis, A., Tanou, G., Filippou, P., and Fotopoulos, V. (2013). Proteomics in the fruit tree science arena: new insights into fruit defense, development, and ripening. *Proteomics* 13, 1871–1884. doi: 10.1002/pmic.201200428

Navazio, L., Moscatiello, R., Genre, A., Novero, M., Baldan, B., Bonfante, P., et al. (2007). A diffusible signal from arbuscular mycorrhizal fungi elicits a transient cytosolic calcium elevation in host plant cells. *Plant Physiol.* 144, 673–681. doi: 10.1104/pp.106.086959

Nogueira-Lopez, G., Greenwood, D. R., Middleditch, M., Winefield, C., Eaton, C., Steyaert, J. M., et al. (2018). The apoplastic secretome of *Trichoderma virens* during interaction with maize roots shows an inhibition of plant defence and scavenging oxidative stress secreted proteins. *Front. Plant. Sci.* 9:409. doi: 10.3389/fpls.2018.00409

Ousley, M. A., Lynch, J. M., and Whipps, J. M. (1994). Potential of *Trichoderma* spp. as consistent plant growth stimulators. *Biol. Fertil. Soils* 17, 85–90. doi: 10.1007/bf00337738

Palmieri, M. C., Perazzolli, M., Matafora, V., Moretto, M., Bachi, A., and Pertot, I. (2012). Proteomic analysis of grapevine resistance induced by *Trichoderma harzianum* T39 reveals specific defence pathways activated against downy mildew. *J. Exp. Bot.* 63, 6237–6251. doi: 10.1093/jxb/ers279

Park, D., Park, Y., Lee, Y. H., Choi, I. Y., Park, K. C., Park, S. U., et al. (2017). A comparative study of phenolic antioxidant activity and flavonoid biosynthesis related gene expression between summer and winter strawberry cultivars. *J. Food Sci.* 82, 341–349. doi: 10.1111/1750-3841.13600

Pascale, A., Vinale, F., Manganiello, G., Nigro, M., Lanzuise, S., Ruocco, M., et al. (2017). *Trichoderma* and its secondary metabolites improve yield and quality of grapes. *Crop Prot.* 92, 176–181. doi: 10.1016/j.cropro.2016.11.010

Pecenková, T., Markovic, V., Sabol, P., Kulich, I., and Žárskı, V. (2017). Exocyst and autophagy-related membrane trafficking in plants. *J. Exp. Bot.* 69, 47–57. doi: 10.1093/jxb/erx363

Perazzolli, M., Palmieri, M. C., Matafora, V., Bachi, A., and Pertot, I. (2016). Phosphoproteomic analysis of induced resistance reveals activation of signal transduction processes by beneficial and pathogenic interaction in grapevine. *J. Plant Physiol.* 195, 59–72. doi: 10.1016/j.jplph.2016.03.007

Pérez, A. C., and Goossens, A. (2013). Jasmonate signalling: A copycat of auxin signalling? *Plant Cell Environ.* 36, 2071–2084. doi: 10.1111/pce.12121

Porras, M., Barrau, C., Arroyo, F. T., Santos, B., Blanco, C., and Romero, F. (2007). Reduction of *Phytophthora cactorum* in strawberry fields by *Trichoderma* spp. and soil solarization. *Plant Dis.* 91, 142–146. doi: 10.1094/PDIS-91-2-0142

Ramirez, R. G., Haelein, T. A., Reyna, J., McDowell, L. R., Russel, L., Aganga, A. A., et al. (1996). Association of official analytical chemists. Official methods of analysis. *J. Biol. Sci.* 5, 7–16.

Rubio, M. B., Hermosa, R., Vicente, R., Gómez-Acosta, F. A., Morcuende, R., Monte, E., et al. (2017). The combination of *Trichoderma harzianum* and chemical fertilization leads to the deregulation of phytohormone networking, preventing the adaptive responses of tomato plants to salt stress. *Front. Plant Sci.* 8:294. doi: 10.3389/fpls.2017.00294

Salzano, A. M., Renzone, G., Sobolev, A. P., Carbone, V., Petriccione, M., Capitani, D., et al. (2019). Unveiling Kiwifruit metabolite and protein changes in the course of postharvest cold storage. *Front. Plant Sci.* 4:71. doi: 10.3389/fpls.2019.00071

Salzano, A. M., Sobolev, A., Carbone, V., Petriccione, M., Renzone, G., Capitani, D., et al. (2018). A proteometabolomic study of *Actinidia deliciosa* fruit development. *J. Proteomics* 172, 11–24. doi: 10.1016/j.jprot.2017.11.004

Schilling, R. K., Marschner, P., Shavrukov, Y., Berger, B., Tester, M., Roy, S. J., et al. (2014). Expression of the *Arabidopsis* vacuolar H^+-pyrophosphatase gene (AVP1) improves the shoot biomass of transgenic barley and increases grain yield in a saline field. *Plant Biotechnol. J.* 12, 378–386. doi: 10.1111/pbi.12145

Segarra, G., Casanova, E., Bellido, D., Odena, M. A., Oliveira, E., and Trillas, I. (2007). Proteome, salicylic acid, and jasmonic acid changes in cucumber plants inoculated with *Trichoderma asperellum* strain T34. *Proteomics* 7, 3943–3952. doi: 10.1002/pmic.200700173

Senthil-Kumar, M., and Mysore, K. S. (2010). Assessing functional role of three water deficit stress-induced genes in nonhost disease resistance using virus-induced gene silencing in *Nicotiana benthamiana*. *Plant Signal. Behav.* 5, 586–590. doi: 10.4161/psb.11497

Sharma, E., Anand, G., and Kapoor, R. (2017). Terpenoids in plant and arbuscular mycorrhiza-reinforced defence against herbivorous insects. *Ann. Bot.* 119, 791–801. doi: 10.1093/aob/mcw263

Sharma, O. P., and Bhat, T. K. (2009). DPPH antioxidant assay revisited. *Food Chem.* 113, 1202–1205. doi: 10.1016/j.foodchem.2008.08.008

Shoresh, M., and Harman, G. E. (2008). The molecular basis of shoot responses of maize seedlings to *Trichoderma harzianum* T22 inoculation of the root: a proteomic approach. *Plant Physiol.* 147, 2147–2163. doi: 10.1104/pp.108.123810

Shoresh, M., Harman, G. E., and Mastouri, F. (2010). Induced systemic resistance and plant responses to fungal biocontrol agents. *Annu. Rev. Phytopathol.* 48, 21–43. doi: 10.1146/annurev-phyto-073009-114450

Singh, U. B., Malviya, D., Khan, W., Singh, S., Karthikeyan, N., Imran, M., et al. (2018). Earthworm grazed-*Trichoderma harzianum* biofortified spent mushroom substrates modulate accumulation of natural antioxidants and biofortification of mineral nutrients in tomato. *Front. Plant Sci.* 9:1017. doi: 10.3389/fpls.2018.01017

Singleton, V. L., Orthofer, R., and Lamuela-Raventós, R. M. (1998). Analysis of total phenols and other oxidation substrates and antioxidants by means of folin-ciocalteu reagent. *Methods Enzymol.* 5, 759–766. doi: 10.1016/S0076-6879(99)99017-1

Sturn, A., Quackenbush, J., and Trajanoski, Z. (2002). Genesis: cluster analysis of microarray data. *Bioinformatics* 18, 207–208. doi: 10.1093/bioinformatics/18.1.207

Tronsmo, A., and Dennis, C. (1977). The use of *Trichoderma* species to control strawberry fruit rots. *Netherlands J. Plant Pathol.* 83:449. doi: 10.1007/bf03041462

Tucci, M., Ruocco, M., De Masi, L., De Palma, M., and Lorito, M. (2011). The beneficial effect of *Trichoderma* spp. on tomato is modulated by the plant genotype. *Mol. Plant Pathol.* 12, 341–354. doi: 10.1111/J.1364-3703.2010.00674.X

Uhrig, R. G., Ng, K. K., and Moorhead, G. B. (2009). PII in higher plants: a modern role for an ancient protein. *Trends Plant Sci.* 14, 505–511. doi: 10.1016/j.tplants.2009.07.003

Valentinuzzi, F., Pii, Y., Vigani, G., Lehmann, M., Cesco, S., and Mimmo, T. (2015). Phosphorus and iron deficiencies induce a metabolic reprogramming and affect the exudation traits of the woody plant *Fragaria* × *ananassa*. *J. Exp. Bot.* 66, 6483–6495. doi: 10.1093/jxb/erv364

Vinale, F., Sivasithamparam, K., Ghisalberti, E. L., Marra, R., Woo, S. L., and Lorito, M. (2008). *Trichoderma*–plant–pathogen interactions. *Soil Biol. Biochem.* 40, 1–10. doi: 10.1016/j.soilbio.2007.07.002

Vinale, F., Sivasithamparam, K., Ghisalberti, E. L., Ruocco, M., Woo, S., and Lorito, M. (2012). *Trichoderma* secondary metabolites that affect plant metabolism. *Nat. Prod. Commun.* 7, 1545–1550. doi: 10.1177/1934578X1200701133

Vinale, F., Sivasithamparam, K., Ghisalberti, E. L., Woo, S. L., Nigro, M., Marra, R., et al. (2014). *Trichoderma* secondary metabolites active on plants and fungal pathogens. *Open Mycol. J.* 8, 127–139. doi: 10.2174/1874437001408010127

Vitha, S., McAndrew, R. S., and Osteryoung, K. W. (2001). FtsZ ring formation at the chloroplast division site in plants. *J. Cell Biol.* 153, 111–120. doi: 10.1083/jcb.153.1.111

Vitti, A., La Monaca, E., Sofo, A., Scopa, A., Cuypers, A., and Nuzzaci, M. (2015). Beneficial effects of *Trichoderma harzianum* T-22 in tomato seedlings infected by Cucumber mosaic virus (CMV). *BioControl* 60, 135–147. doi: 10.1007/s10526-014-9626-3

Vizcaíno, J. A., Csordas, A., del-Toro, N., Dianes, J. A., Griss, J., Lavidas, I., et al. (2016). Update of the PRIDE database and its related tools. *Nucleic Acids Res.* 44, 447–456. doi: 10.1093/nar/gkw880

Wang, M., Ding, L., Gao, L., Li, Y., Shen, Q., and Guo, S. (2016). The interactions of aquaporins and mineral nutrients in higher plants. *Int. J. Mol. Sci.* 17:1229. doi: 10.3390/ijms17081229

Woo, S. L., and Pepe, O. (2018). Microbial consortia: promising probiotics as plant biostimulants for sustainable agriculture. *Front. Plant Sci.* 9:1801. doi: 10.3389/fpls.2018.01801

Woo, S. L., Ruocco, M., Vinale, F., Nigro, M., Marra, R., Lombardi, N., et al. (2014). *Trichoderma*-based products and their widespread use in agricolture. *Open Mycol. J.* 8, 71–126. doi: 10.3389/fpls.2018.01801

Yang, H., Zhang, X., Gaxiola, R. A., Xu, G., Peer, W. A., and Murphy, A. S. (2014). Over-expression of the *Arabidopsis* proton-pyrophosphatase AVP1 enhances transplant survival, root mass, and fruit development under limiting phosphorus conditions. *J. Exp. Bot.* 65, 3045–3053. doi: 10.1093/jxb/eru149

Yedidia, I., Benhamou, N., Kapulnik, Y., and Chet, I. (2000). Induction and accumulation of PR proteins activity during early stages of root colonization by the mycoparasite *Trichoderma harzianum* strain T-203. *Plant Physiol. Biochem.* 38, 863–873. doi: 10.1016/s0981-9428(00)01198-0

Yedidia, I., Shoresh, M., Kerem, Z., Benhamou, N., Kapulnik, Y., and Chet, I. (2003). Concomitant induction of systemic resistance to *Pseudomonas syringae* pv. *lachrymans* in cucumber by *Trichoderma asperellum* (T-203) and

accumulation of phytoalexins. *Appl. Environ. Microbiol.* 69, 7343–7353. doi: 10.1128/AEM.69.12.7343-7353.2003

Yedidia, I., Srivastva, A. K., Kapulnik, Y., and Chet, I. (2001). Effect of *Trichoderma harzianum* on microelement concentrations and increased growth of cucumber plants. *Plant Soil* 235, 235–242.

Yu, M. H., Zhao, Z. Z., and He, J. X. (2018). Brassinosteroid signaling in plant-microbe interactions. *Int. J. Mol. Sci.* 19:4091. doi: 10.3390/ijms19124091

Yuan, P., Jauregui, E., Du, L., Tanaka, K., and Poovaiah, B. W. (2017). Calcium signatures and signaling events orchestrate plant-microbe interactions. *Curr. Opin. Plant Biol.* 38, 173–183. doi: 10.1016/j.pbi.2017.06.003

Yun, H. S., and Kwon, C. (2017). Vesicle trafficking in plant immunity. *Curr. Opin. Plant Biol.* 40, 34–42. doi: 10.1016/j.pbi.2017.07.001

Zhang, F., Chen, C., Zhang, F., Gao, L., Liu, J., Chen, L., et al. (2017). *Trichoderma harzianum* containing 1-aminocyclopropane-1-carboxylate deaminase and chitinase improved growth and diminished adverse effect caused by *Fusarium oxysporum* in soybean. *J. Plant Physiol.* 210, 84–94. doi: 10.1016/j.jplph.2016.10.012

Conflict of Interest: The authors declare that the research was conducted in the absence of any commercial or financial relationships that could be construed as a potential conflict of interest.

frontiers in Microbiology

ORIGINAL RESEARCH
published: 14 July 2020
doi: 10.3389/fmicb.2020.01475

A Genetic and Metabolomic Perspective on the Production of Indole-3-Acetic Acid by *Pantoea agglomerans* and Use of Their Metabolites as Biostimulants in Plant Nurseries

*Francesca Luziatelli[1†], Anna Grazia Ficca[1†], Paolo Bonini[2], Rosario Muleo[3], Lorenzo Gatti[3], Massimiliano Meneghini[4], Michele Tronati[1], Francesca Melini[1,5] and Maurizio Ruzzi[1]**

[1] Department for Innovation in Biological, Agro-food and Forest systems (DIBAF), University of Tuscia, Viterbo, Italy, [2] Next-Generation Agronomics (NGA) Laboratory, Tarragona, Spain, [3] Department of Agricultural and Forestry Sciences (DAFNE), University of Tuscia, Viterbo, Italy, [4] Vivai Piante Battistini soc. agr. s.s., Cesena, Italy, [5] Council for Agricultural Research and Economics (CREA), Research Centre for Food and Nutrition, Rome, Italy

OPEN ACCESS

Edited by:
Francesco Vinale,
University of Naples Federico II, Italy

Reviewed by:
Sabrina Sarrocco,
University of Pisa, Italy
Eloisa Pajuelo,
Universidad de Sevilla, Spain
Hassan Etesami,
University of Tehran, Iran

***Correspondence:**
Maurizio Ruzzi
ruzzi@unitus.it

† These authors have contributed equally to this work

Specialty section:
This article was submitted to Plant Pathogen Interactions, a section of the journal Frontiers in Microbiology

Received: 31 March 2020
Accepted: 05 June 2020
Published: 14 July 2020

Citation:
Luziatelli F, Ficca AG, Bonini P, Muleo R, Gatti L, Meneghini M, Tronati M, Melini F and Ruzzi M (2020) A Genetic and Metabolomic Perspective on the Production of Indole-3-Acetic Acid by Pantoea agglomerans and Use of Their Metabolites as Biostimulants in Plant Nurseries. Front. Microbiol. 11:1475. doi: 10.3389/fmicb.2020.01475

The species *Pantoea agglomerans* includes strains that are agronomically relevant for their growth-promoting or biocontrol traits. Molecular analysis demonstrated that the IPDC pathway involved in the conversion of tryptophan (Trp) to indole-3-acetic acid (IAA) is highly conserved among *P. agglomerans* strains at both gene and protein levels. Results also indicated that the promoter region controlling the inducible expression of *ipdC* gene differs from the model system *Enterobacter cloacae*, which is in accordance with the observation that *P. agglomerans* accumulates higher levels of IAA when cells are collected in the exponential phase of growth. To assess the potential applications of these microorganisms for IAA production, *P. agglomerans* C1, an efficient auxin-producer strain, was cultivated in 5 L fermenter so as to evaluate the effect of the medium formulation, the physiological state of the cells, and the induction timing on the volumetric productivity. Results demonstrated that higher IAA levels were obtained by using a saline medium amended with yeast extract and saccharose and by providing Trp, which acts both as a precursor and an inducer, to a culture in the exponential phase of growth. Untargeted metabolomic analysis revealed a significant effect of the carbon source on the exometabolome profile relative to IAA-related compounds and other plant bioactive signaling molecules. The IAA-enriched metabolites secreted in the culture medium by *P. agglomerans* C1 were used as plant biostimulants to run a series of trials at a large-scale nursery farm. Tests were carried out with *in vitro* and *ex vitro* systems following the regular protocols used for large-scale plant tree agamic propagation. Results obtained with 4,540 microcuttings of *Prunus* rootstock GF/677

and 1,080 plantlets of *Corylus avellana* L. showed that metabolites from strain C1 improved percentage of rooted-explant, number of adventitious root formation, plant survival, and quality of plant as vigor, with an increase in the leaf area between 17.5 and 42.7% compared to IBA-K (indole-3-butyric acid potassium salt)–treated plants.

Keywords: plant growth promotion, auxin, *Pantoea*, indole-3-pyruvate decarboxylase (*ipdC*) gene, culture condition, Q-TOF LC/MS, *Prunus* rootstock, *Corylus avellana* L.

INTRODUCTION

Indole-3-acetic acid (IAA) is the most abundant member of the auxin family of phytohormones, and its biosynthesis in plants and bacteria proceeds through distinct biosynthetic routes: both tryptophan (Trp)–dependent and Trp-independent pathways have been described (Eckardt, 2001; Ljung et al., 2002). Based on the distinct intermediates involved in Trp-dependent IAA biosynthesis, five different pathways have been characterized in bacteria, namely, indole-3-acetamide (IAM), indole-3-pyruvic acid (IPyA), indole-3-acetonitrile (IAN), tryptamine (TAM), and Trp side-chain oxidase pathway (Patten et al., 2013; Doktycz, 2019). Although the Trp-independent pathway is thought to occur in bacteria as well (Prinsen et al., 1993), no specific enzymes in this pathway have been characterized.

The IPyA pathway is operational in plant-beneficial bacteria, such as *Azospirillum brasilense* and representative members of *Enterobacter cloacae* complex and is subjected to extremely tight regulation. In this pathway, there is transamination of Trp to IPyA, followed by decarboxylation to indole-3-acetaldehyde (IAAld) by the enzyme indole-3-pyruvate decarboxylase (IPDC; EC 4.1.1.74), and then oxidation of IAAld to IAA. The key enzyme in this pathway, IPDC, is encoded by *ipdC*, and deletion or functional inactivation of *ipdC* gene affects IAA biosynthesis in some strains, such as *Enterobacter ludwigii* (formerly, *E. cloacae*) UW5, *A. brasilense*, *Pantoea agglomerans* 299R, and *Pantoea* species YR343 (Koga et al., 1991; Brandl and Lindow, 1997; Malhotra and Srivastava, 2008; Garcia et al., 2019). The IPDC genes code for polypeptides of approximately 550 amino acids in length, corresponding to a molecular mass of 60 kDa per subunit. The homotetrameric IPDC from *E. ludwigii* UW5, characterized both at biochemical and structural levels, has a molecular mass of 240 kDa and binds four molecules of the cofactors thiamine diphosphate (ThDP) and Mg^{2+} (Schutz et al., 2003). The *ipdC* gene from *E. ludwigii* UW5 is activated by the transcription factor TyrR and increases in response to the aromatic amino acid Trp, tyrosine, and phenylalanine (Ryu and Patten, 2008; Coulson and Patten, 2015). However, regulation varies across bacterial species: constitutive in *Agrobacterium*; regulated by specific transcriptional factors, such as RpoS or RpoN, in some *Pseudomonas* and *Enterobacter* strains; regulated by the global signal transduction system GacS/GacA that controls secondary metabolism in several plant-associated gram-negative bacteria (Spaepen et al., 2007).

Indole-3-acetic acid plays an important role in the regulation of growth and development of vascular plants, including cell division, cell extension, and cell differentiation (Kasahara, 2016). It specifically plays a crucial role in root initiation, apical dominance, tropisms, and senescence (Zhao, 2010). In addition, IAA is produced by plants, as well as by some beneficial bacteria in the rhizosphere, where it acts as a signaling molecule with significant effects on the communication between plants and microorganisms, and on plant growth (Spaepen and Vanderleyden, 2011; Duca et al., 2014).

In recent years, several studies have reported alternative approaches to the application of phytohormones and plant growth regulators, such as the use of symbiotic organisms and/or natural biostimulants from microbial and non-microbial organisms in agriculture systems and in tissue cultures, which are also environment friendly, as for microbial biostimulants (Ruzzi and Aroca, 2015; Orlikowska et al., 2017; Rouphael and Colla, 2018). Within this framework, the species *P. agglomerans* has drawn attention for its plant growth–promoting activity.

Classification of *P. agglomerans* into the biosecurity group 2 and the fact that sometimes this species causes human infections particularly in immunocompromised people prevent its utilization as bioinoculant in Europe (Dutkiewicz et al., 2016a; Büyükcam et al., 2018). However, increasing evidence has shown that selected members of the *P. agglomerans* species can have a great potential as plant growth–promoting bacteria (Paredes-Páliz et al., 2016a,b, 2017) and comprise strains that are agronomically relevant for their growth-promoting or biocontrol traits and have been increasingly regarded as ideal candidates among plant growth–promoting rhizobacteria to be used as a biocontrol agent (Dutkiewicz et al., 2016b).

In details, *P. agglomerans* strain C1, isolated from the phyllosphere of lettuce plants (*Lactuca sativa* L.) treated with plant-derived protein hydrolysates (Luziatelli et al., 2016), has been studied for its potential as novel biostimulant in sustainable agriculture. It has been specifically characterized for its heavy metal resistance and metabolic capacities (Luziatelli et al., 2019b, 2020), as well as for its ability to solubilize phosphate, to inhibit plant pathogens, to produce IAA and siderophores, and to improve the use of rock phosphates and the growth of corn (*Zea mays* L.) and tomato (*Solanum lycopersicum* L.) in pot experiments (Luziatelli et al., 2019a, 2020; Saia et al., 2020). In particular, when *P. agglomerans* strain C1 is grown onto medium rich in Trp, large amounts of IAA are produced, which makes it a natural biostimulant suitable to be used in the rooting phase of micropropagation instead of the synthetic auxins (Luziatelli et al., 2020).

Micropropagation allows a rapid multiplication of several plant species in large-scale clonal plants and is becoming a widespread technique for rootstocks and crops species propagation (Loberant et al., 2010). On the nursery farming scale, micropropagation has a strong economic impact,

because in a relatively short time period, reduced space and growing controlled conditions are required independently of environmental conditions and season period (Akin-Idowu et al., 2009). Micropropagation starts, in fact, from a small part of selected elite plant and allows the production thousands of plants that can be produced in a continuous process (Pierik and Scholten, 1994). However, rhizogenesis and root growth are critical morphophysiological events for plant survival in *ex vitro* conditions and are achieved by auxin treatment of unrooted microshoots as the last phase of *in vitro* culture and/or the first phase of *in vivo* acclimatization phase.

In micropropagation of woody crops, it has been observed that, besides IAA, synthetic molecules with strong auxin activities can be used. Among them, indole-3-butyric acid (IBA) is the compound of choice, thanks to its higher stability in the culture medium (Nissen and Sutter, 1990; Bhatti and Jha, 2010). Moreover, it has been assumed that, among the metabolites making up the pool of excreted molecules (exometabolome), there are molecules that could have a synergistic activity with auxin and/or elicitor roles, acting on the regulation pathways of adventitious rooting events and quality of roots.

The study was designed to test the biostimulant properties of metabolites excreted by *P. agglomerans* strain C1 on root induction and plant development of some woody fruit crop species in large-scale nurseries, at the phase of *in vitro* and *ex vitro* rooting and acclimation.

MATERIALS AND METHODS

Strain and Media

Pantoea agglomerans C1 is an environmental strain isolated from the phyllosphere of lettuce (Luziatelli et al., 2016, 2019a). Strain C1 was maintained as LB Lennox (Lennox, 1955)–glycerol 20% (vol/vol) stocks at −80°C and revived on LB broth at 30°C under agitation [180 revolutions/min (rpm)]. For production of IAA, the strain can be cultivated on both saline and rich media supplemented with Trp (4 mM). A total of six media were used: LB broth Lennox (per liter, tryptone 10 g, yeast extract 5 g, NaCl 5 g); saline M9-glucose medium (Maniatis et al., 1982); yeast extract sucrose (YES) and yeast extract glucose (YEG) medium [1 × M9 saline solution, yeast extract 5 g L^{-1}, carbon source (sucrose or glucose), 5 g L^{-1}]; and reinforced YES/YEG medium (rYES and rYEG medium containing double the amount of yeast extract, 10 g L^{-1}).

Pathway and Gene Identification

As a preliminary step, a database of bacterial proteins that are associated to the five major IAA biosynthetic pathways was constructed following a comprehensive search of the literature. Then, the complete set of 4497 protein sequences encoded by *P. agglomerans* C1 (Luziatelli et al., 2020) was compared against this manually curated set of IAA biosynthetic genes using the Basic Local Alignment Search Tool (BLAST; Altschul et al., 1990). Multiple protein sequence alignments were generated using ClustalW algorithm (Thompson et al., 1994). Bacterial promoter prediction program, BPROM[1], was used to identify the position of the promoter, that is, -10 box and -35 box in the input sequence. The PATRIC BLASTN and BLASTP services were used to perform homology searches against *P. agglomerans* genomes available at PATRIC Website[2] using, as queries, nucleotide/protein sequences of strain C1 corresponding to (1) the 4 kb *ipdC*-containing region; (2) the 5′ upstream region of *ipdC* gene; (3) the genes encoding aminotransferase (peg.1678), IPDC (*ipdC*; peg.1955), and IAAld dehydrogenase (peg.576 and peg.879); (4) the deduced protein sequences of peg.1678, peg.1955, peg.576, and peg.879. The resulting hits were filtered at 100% query coverage and ≥ 80% of sequence identity.

Growth Conditions

Seed cultures, from a freeze glycerol stock of *P. agglomerans* strain C1, were inoculated into 500 Erlenmeyer flasks containing 50 mL of LB medium and incubated at 30°C with agitation (180 rpm).

Seed cultures in the late exponential phase of growth [optical density at 600 nm (OD_{600}) of 4.5–4.8] were used to inoculate, with an initial OD_{600} of 0.1, 25 mL of production medium amended with Trp (4 mM), and growth was monitored by measuring the wet weight of cells. In addition, LB + Trp (4 mM) was used as reference media for IAA biosynthesis.

After 24 h of growth at 30°C and 180 rpm, cells were removed by centrifugation (10 min at 8,000 g), and the supernatant was filter-sterilized through a 0.22 μm filter and stored at -20°C until use.

Fermentation and Optimization of the Induction Conditions

To evaluate the relationship between the physiological state of the cells and the IAA production level, *P. agglomerans* strain C1 was grown in a BioFlo 120 bench-top stirred tank reactor (Eppendorf S.r.l., Milan, Italy) equipped with a 7.5-L vessel, two Rushton impellers, digital ISM probes for dissolved oxygen (DO), and pH (Mettler-Toledo S.p.A., Milan, Italy) and a platinum RTD (Pt100) sensor for the temperature. The growth was carried out in YES medium (5 L) at 30°C under aerobic conditions. The oxygen concentration was maintained greater than 20% of saturation (oscillation between 25 and 40%), blowing sterile air at an aeration rate of 0.2–1.5 (vol/vol/m), and by regulating the impellers speed from 150 rpm (initial condition) to 525 rpm (end of the exponential phase of growth). The initial pH of the medium was adjusted to 6.6 by addition of 1 M HCl or 2 M of NaOH, and growth was carried out without pH control.

The reactor was inoculated at 5% (vol/vol) with an initial optical density (OD_{600}) of 0.4, using an LB culture grown at 180 rpm and 30°C up to the late exponential phase. After 3, 3.5, 4, 4.5, 5, and 6 h of growth, 100 mL aliquots were collected from the fermenter, and the cells recovered by centrifugation (8,000 rpm for 10 min) were resuspended in fresh YES medium to obtain a final OD_{600} of 10 and used to inoculate shaken flasks containing YES medium (25 mL) amended with Trp (4 mM). All cultures were inoculated at the same initial OD_{600} of 0.5 and incubated

[1]http://www.softberry.com/berry.phtml?topic=bprom&group=programs&subgroup=gfindb

[2]https://patricbrc.org/

at 180 rpm and 30°C for 18 h. For each time point, experiments were carried out in triplicate. To measure the accumulation of IAA in the culture medium, 1 mL samples were taken at intervals of 60 min for the first 2 h and at the end of the growth (18 h) and treated as reported before.

Spectrophotometric Determination of Indole Auxins

Auxin production was measured using Salkowski reagent as described previously (Luziatelli et al., 2020). In brief, 1 mL of filter-sterilized (0.22 μm) supernatant was added to 2 mL of Salkowski reagent (0.5 M $FeCl_3$, 35% vol/vol $HClO_4$), and the mixture was incubated at room temperature (in the dark) for 20 min. The presence of IAA and other indole auxins were detected measuring pink color development at 535 nm using a Cary 50 UV-Vis spectrophotometer (Agilent, Santa Clara, CA, United States). A series of IAA standard solutions of known concentrations were prepared to set up the calibration curve.

Metabolome Analysis by Quadrupole Time-of-Flight Liquid Chromatography–Mass Spectroscopy

For untargeted metabolomics, the sample (1 mL) was extracted in 5 mL of cold (−20°C) acidified (0.1% HCOOH) 80/20 methanol/water using an Ultra-Turrax Homogenizer (Ika T-25, Staufen, Germany), centrifuged at 1200 rpm and filtered through a 0.2 μm cellulose membrane. The analysis was carried out on an Agilent 6550 Q-TOF with ESI source, coupled with an Agilent 1290 UHPLC. A BEH C18 column from Waters (100 × 2.1 mm internal diameter, 1.7 μm) was used according to the procedure and gradient described in Tsugawa et al. (2019). Injection volume was 2 μL for all samples. A pooled quality control was obtained by mixing 10 μL of each sample and acquired in tandem mass spectroscopy mode using iterative function five consecutive times to increase the number of compounds with associate MS2 spectra. Blank filtering, alignment, and identification were accomplished using MS-DIAL (Tsugawa et al., 2015) and MS-FINDER (Tsugawa et al., 2016), with the procedure described by Blaženović et al. (2019).

The table with all compound peaks height was exported from MS-DIAL into MS-FLO (DeFelice et al., 2017) to reduce false positives and duplicates. Then, an internal developed workflow in R was employed for fold change and Benjamini-Hochberg corrected *p*-value, PLSDA analysis (Thévenot et al., 2015), and chemical enrichment analysis (Barupal et al., 2012).

Plant Inoculation

In vitro shoot tips of peach clonal rootstock "GF677" (*Prunus persica* × *Prunus amygdalus*) of 10 mm in length and *in vitro* shoot tips of hazelnut cv. "Fertile de Coutard" (*Corylus avellana* L.) of 15 mm in length were cultured on proliferation medium, containing a modified Quirin and Lepoivre (QL; Quoirin and Lepoivre, 1977) and Driver and Kuniyaki Walnut (DKW; Driver and Kuniyuki, 1984) basal salt solution, respectively, and enriched by 30 g L^{-1} sucrose and solidified by 6.8 g L^{-1} agar. The growth regulators added to the medium were as follows: 2.22 μM of 6-benzyladenine (BA), 0.05 μM of α-naphthalene acetic acid for the rootstock GF677; 10 μM of BA, 0.05 μM of IBA for the cv. Fertile de Coutard. The pH of the medium was adjusted to 6.3 ± 0.1 for the rootstock GF677, and 6.0 ± 0.1 for the cv. Fertile de Coutard, before addition of agar and sterilization at 120°C for 20 min. Shoots of rootstock GF677 were subcultured at a 4-week interval, while shoots of cv. Fertile de Coutard were subcultured at a 6-week interval, under 16 h light photoperiod, using white fluorescent lamps Philips TL-D 58/865-MASTER (Philips, Italia), at 40 μM m^{-2} s^{-1} photon flux at constant temperature of 23°C ± 1°C.

After the proliferation step, microcuttings were transferred for 15 days in Murashige and Skoog (MS) elongation medium (Murashige and Skoog, 1962), supplemented with 14 μM gibberellic acid (GA3) and 20 g L^{-1} sucrose. The medium was sterilized at 120°C (2 bars), for 20 min after addition of 6.8 g L^{-1} agar and pH titration to 6.5. Glass jars of 500 mL in volume, each containing 100 mL of culture medium, were used as culture vessels.

At the beginning of the acclimatization, before the transfer into the cell plug tray, plantlets were immersed for 10 s in an auxin solution containing either an appropriate dilution of IAA-enriched excretome from *P. agglomerans* strain C1 (indole auxins final concentration of 1 μM) or 10 μM IBA potassium salt (IBA-K). *Ex vitro* acclimatization started on April 2018 by transferring the treated plantlets into 360 cells plug tray (Jiffy, Netherlands), with a volume of each cell cavity of 7 cm^3.

Trays were placed under controlled misting of the greenhouse (temperature 28°C ± 4°C, RH 90%), at natural photoperiod and photosynthetic active radiation varying daily between 300 and 500 μM m^{-2} s^{-1}.

All on-farm trials, two with *Prunus* rootstock GF677 and one with hazelnut, were carried out in agreement with the company's production cycle. In the first trial with rootstock GF677, 720 plants (two trays of 360 cells) were treated by dipping with secreted metabolites from strain C1, and an equal number of plants were treated with IBA-K solution. In the second trial, 3,780 plants (10.5 trays of 360 cells) were treated with C1 metabolites, and 1,800 plants (five trays of 360 cells) with IBA-K. In both experiments, after 10 days from the dip treatment, plants were treated again by spraying fine drops of the same solution until the complete wetting of the leaves was achieved.

For hazelnut adventitious rooting induction experiments, 1,440 plantlets were treated by dipping with secreted metabolites from strain C1, and 1,080 plantlets were treated with IBA-K.

On the 20th day of the *ex vitro* acclimatization, the percentage of rooted plantlets, the number of roots per plantlet, the root length, and the elongation of plantlet stem were recorded.

After 1 month, all plantlets were transferred into 60 preloaded cells plug tray (Jiffy), each cell plug with a volume of 117 cm^3. Two weeks later, the survival ratio of plant was determined, and the total leaf area per plant was detected by Android "CANOPEO" application[3] on a total of 600 randomly chosen plants (300 for control and 300 *Pantoea*-treated).

[3]www.canopeoapp.com

Since the beginning of the transfer *in vivo*, every 20 days, plants were fertilized with NUTRIGREEN AD (GREEN HAS ITALIA S.p.A.), through the fertigation system at the amount of 2 mL L^{-1}.

Statistical Analysis

Statistically significant differences between the means were determined by the one-way analysis of variance using the SigmaStat 3.1 package (Systat Software Inc., San Jose, CA, United States).

RESULTS

Identification of the IAA-Biosynthetic Genes

Genes encoding enzymes involved in IAA synthesis were identified in *P. agglomerans* C1 genome by BLASTx analysis using the sequences of 11 different enzymes associated with alternative IAA pathways, as queries (**Table 1**). This analysis revealed the presence, in strain C1, of the whole set of genes of only one of the five IAA pathways occurring in bacteria and plants: the indole-3-pyruvic acid (IPyA) pathway (**Table 1** and **Figure 1**). Noteworthy, for each of the three enzymes involved in this pathway, the identity, at amino acid level, with sequences of other *Pantoea* strains was between 81 and 92% along the entire protein length (**Table 1**). For the same proteins, the identity between sequences from strain C1 and strains belonging to other genera, including *Azospirillum*, *Pseudomonas*, *Enterobacter*, *Azospirillum*, and *Arthrobacter*, varied between 25 and 56% (**Table 1**).

Proteins with weak similarity to (i) indole acetamide hydrolase (pathway IAM) and (ii) Trp decarboxylase and amine oxidase (pathway TAM) were also identified (**Table 1** and **Figure 1**). In contrast, no sequence related to Trp aminotransferase and YUCCA enzymes (pathway IPyA-YUCCA) or nitrilases (pathway IAN) was detected (**Table 1**).

Sequence Comparison of IPDC Proteins

BLAST analysis of the ThDP-binding indolepyruvate decarboxylase (IPDC EC 4.1.1.74) revealed (**Table 1**) that the deduced amino acid sequence encoded by C1_peg1955 from *P. agglomerans* C1 ($IPDC_{Pa\_C1}$) shares a 92% of identity with IPDC from *P. agglomerans* (formerly *Erwinia herbicola*) strain 299R ($IPDC_{Pa\_299R}$; Brandl and Lindow, 1996) and 73% of identity with IPDC1 from *Pantoea* species strain YR343 ($IPDC1_{Psp\_YR343}$; Garcia et al., 2019). To gain more information about $IPDC_{Pa\_C1}$, a comparative analysis was carried out between this protein and IPCD from *E. ludwigii* (previously misidentified as *Pseudomonas putida* and subsequently as *E. cloacae*) strain UW5 ($IPDC_{Ec\_UW5}$). The structural model of $IPDC_{Ec\_UW5}$ has been published almost 10 years ago by Schutz et al. (2003), and the authors demonstrated that $IPDC_{Ec\_UW5}$ is a homotetrameric enzyme in which each monomer has defined domains involved in the binding of both the substrate and the cofactors (Mg^{2+} and ThDP). Using the MULTALIN tool (Corpet, 1988), IPDC sequences from strain C1, *E. ludwigii* UW5 and other *Pantoea* strains were aligned as reported in **Table 1**. This analysis allowed demonstrating that several amino acids, which were found to be essential for the activity of $IPDC_{Ec\_UW5}$, were conserved or conservatively replaced in all *Pantoea* strains (**Figure 2**). In detail, 90% of the active site residues of $IPDC_{Ec\_UW5}$ are conserved in $IPDC_{Pa\_C1}$, suggesting that the two enzymes might have a similar catalytic mechanism.

Organization of the IPDC Coding Region

DNA sequence analysis of the genomic region surrounding the *ipd*C gene from *P. agglomerans* C1 revealed the presence of two ORFs encoding a 330-amino acid protein, annotated as L-glyceraldehyde 3-phosphate reductase (ORF1), and a 322-amino acid protein, with high homology to glucokinase, respectively (**Figure 3**). Interestingly, a similar genetic structure occurs in *E. ludwigii* UW5 (Coulson and Patten, 2015) and *Pantoea* species YR343 (Garcia et al., 2019; **Figure 3**), as well as in 45 of 50 *P. agglomerans* genomes sequenced so far. In the latter case, the identity over the entire 4 kb sequence of the ORF1-*ipdC*-ORF2 gene cluster was between 88 and 100%, with a mean value of 99% (**Figure 4**, lane A). Surprisingly, a high sequence identity (mean value = 98%) was also observed (**Figure 4**, lane C*g*-F*g*) comparing the DNA sequence of all *P. agglomerans* genes of the IPyA pathway, the genes encoding amino transferase, IPDC and IAAld decarboxylase (peg.1678, peg.1955, peg.576, and peg.879 in strain C1; **Figure 1**). The remarkable evolutionary conservation of the IPyA pathway among the members of the *P. agglomerans* species was also confirmed analyzing the variability at the level of protein sequence that varied between 1 and 2% and the kernel density plot (**Figure 4**, lane C*p*-F*p*). A similar observation was done analyzing the *ipdC* promoter region, which, as shown by the density of the data in the violin plot reported in **Figure 4** (lane B), is more conserved than the IPCD coding sequence.

Analysis of the *ipdC* Promoter

A search of functional motifs carried out with BPROM annotation package (Softberry Inc., Mount Kisco, NY, United States) revealed the presence, in the promoter region upstream of *P. agglomerans* C1 *ipd*C gene, of sequences that resemble to the *Escherichia coli* RpoD (s^{70}) -10 and -35 elements, matching the *E. coli* consensus sequences at four of six nucleotides (-10), and five of six nucleotides (-35), respectively. Interestingly, the *ipd*C putative regulatory sites of C1 showed significant similarity with those predicted in the *ipd*C promoter of other *Pantoea* strains (YR343 and 299R) and *E. ludwigii* UW5 (**Figure 5**).

Inspection of the 5′ untranslated region upstream from the C1_*ipd*C start codon showed no detectable *cis*-regulatory element such as the inverted repeats identified in the *ipd*C promoter of *A. brasilense* (Vande Broek et al., 2005) or the two 18-bp consensus sequences (weak and strong TyrR boxes) recognized by TyrR, which regulates the expression of the *ipd*C gene in *E. ludwigii* UW5 (Coulson and Patten, 2015). Sequences with weak similarity to the TyrR consensus motif (TGTAAA-N_6-TTTACA) were found in the *ipdC* promoter region from *Pantoea* strains, but they do not meet the minimum molecular

TABLE 1 | Identification of protein encoding genes (peg) and enzymes involved in IAA biosynthesis in *P. agglomerans* strain C1 based on a systematic computational approach.

Pathway	Enzymes	Query source	C1 representatives	Template sequence identity/coverage (%/%)
IPyA	Aminotransferase (EC 1.4.3.2) (EC 2.6.1.27) (EC 2.6.1.99)	> AEB97257.1 HisC1 [*Azospirillum brasilense* Sp7][§]	peg.1678	28/91
		>PMI_01811_Am_Trf1[*Pantoea* speciesYR343][§]		88/100
	Indole-3-pyruvate decarboxylase (EC 4.1.1.74)	> AAB06571 [*Pantoea agglomerans*_299R][§]	peg.1955	92/100
		>PMI_00059_IPDC1 [*Pantoea* speciesYR343][§]		73/100
		>AKM88529[*Enterobacter ludwigii* UW5, formely *E. cloacae* UW5][§]		56/99
		>AAG00523 [*Pseudomonas putida* GR12-2][§]		56/99
		>BAA14242 [*Enterobacter cloacae* FERM BP-1529][§]		56/94
		>AAC36886 [*A. brasilense* Sp245][§]		27/92
		>ABV24338[*Paenibacillus polymyxa* E681][§]		25/80
	Indole-3-acetaldehyde dehydrogenase (EC 1.2.1.3) (EC 1.2.3.7)	> WP_040136836.1 [*A. brasilense*][§]	peg.1406	42/96
		> AAC49575 [*Ustilago maydis*][§]	peg.766	42/94
		> NP_789951[*Pseudomonas syringae* DC3000][§]	peg.1613	41/95
		> NP_792480 [*P. syringae* DC3000][§]	peg.3848	40/96
		> WP_042703524.1[*Azospirillum* species B506]	peg.1614	39/94
		> ELT45240.1 [*Arthrobacter nitrophenolicus* SJCon]	peg.1183	36/96
		> PMI39_00794 IALDH7[*Pantoea* speciesYR343][§]	peg.879	81/100
		> PMI39_04236 IALDH16[*Pantoea* speciesYR343][§]	peg.576	87/100
IPyA-YUCCA	Indole-3-pyruvate monooxygenase	> Q9SZY8.1 YUCCA1 [*Arabidopsis thaliana*]	–	–
		>BAS07733.1 YUCCA3 [*Arthrobacter* species Hiyo4]		
IAM	Trp-monoxygenase	> AGL87350.1 IaaM [*Pseudomonas protegens* CHA0][§]	–	–
		>AAD30489.1 [*Agrobacterium fabrum* str. C58][§]		
	Indole acetamide hydrolase (EC 3.5.1.4)	> WP_087872787.1 [*Arthrobacter globiformis*]	peg.1593	34/97
		> P0A2 × 0 [*Agrobacterium tumefaciens* pTiA6 plasmid][§]	peg.13	27/97
		> AAA17679.1 [*P. syringae* Y30][§]	peg.3060	40/61
IAN	Oxidoreductase	> O81346.2 [*A. thaliana*]	–	–
		>Q501D8.1[*A. thaliana*]		
	Acetaldoxime dehydratase	> BAA90461.1 [*Bacillus* species OxB-1]	–	–
		>BAD17969.1 [*Rhodococcus erythropolis* N-771]		
	Nitrile hydratase	> AFY20546.1 [*Pseudomonas* species UW4]	–	–
		>AFY20547.1 [*Pseudomonas* species UW4]		
TAM	Trp decarboxylase (EC 4.1.1.28) (EC 4.1.1.105)	> 4OBV_A Chain A [*Ruminococcus gnavus* ATCC29149][§]	peg.2389	31/80
			peg.2288	30/80
	Amine oxidase (EC 1.4.3.22) (EC 1.4.3.4)	> EZQ09285 [*A. brasilense* Az39]	peg.2873	24/93

[§]*Proteins whose function is supported by biochemical evidences.*

requirements for TyrR-mediated regulation: the presence of a strong TyrR box or a weak box with an adjacent strong box; the presence in the TyrR box of the G-C residues, essential for TyrR binding, spaced 14 bp apart (**Figure 5**). These evidences strongly support the hypothesis that the transcription of the *ipdC* gene in *P. agglomerans* is not controlled by the TyrR regulatory system.

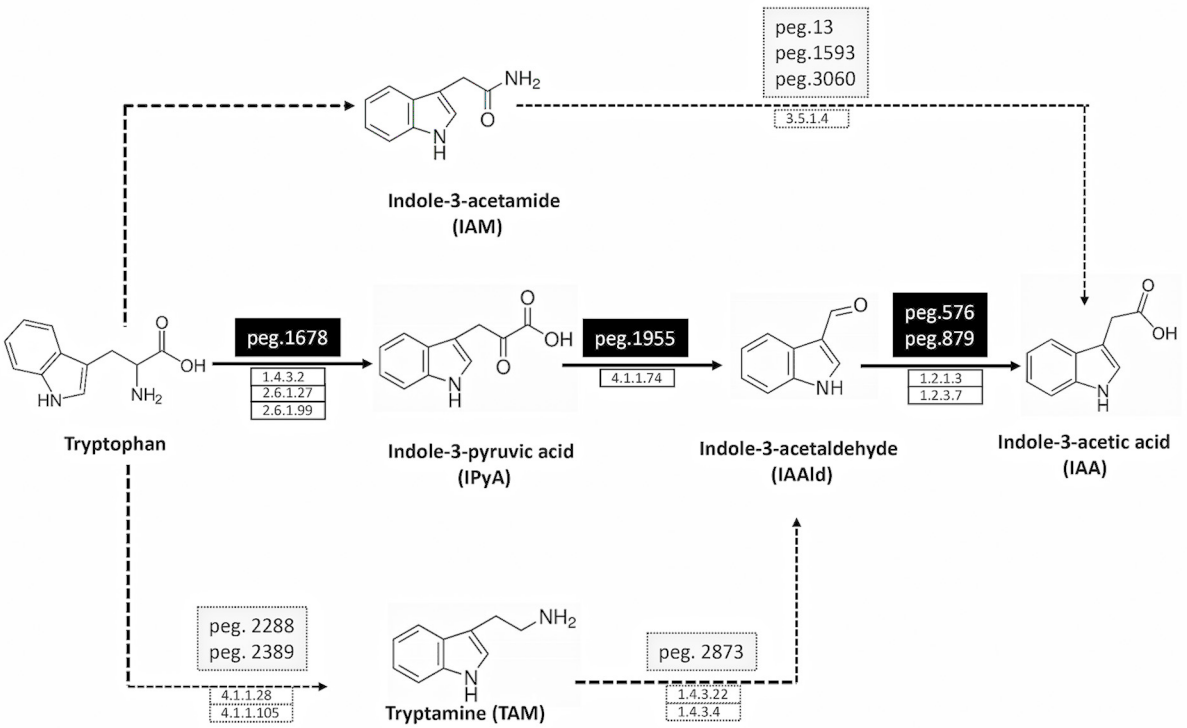

FIGURE 1 | Deduced pathways for IAA biosynthesis in *P. agglomerans* strain C1. The solid line indicates the principal pathway for IAA biosynthesis, and the dotted ones the pathways that are not fully supported by molecular evidences (low identity with known proteins; see **Table 1** for details). The names of the pathways indicate the name of their first products. The names of the protein encoding genes (peg) and the definition of the protein coding enzymes (EC number) are reported on the top and the bottom of the arrows, respectively.

Selection of the Growth Medium for IAA Production

In preliminary experiments, it was observed that, in contrast to LB, when *P. agglomerans* C1 cells were grown on saline M9-glucose medium without Trp, no basal level of IAA was produced. Providing Trp (as inducer and precursor) at 4 mM concentration, no significant difference was observed in the IAA final titer (54 ± 0.9 mg L^{-1}) shifting from LB to M9-glucose medium. To further investigate the possibility to use a medium that has equivalent performances of LB but is free of animal-derived ingredients, the ability of C1 cells to grow and produce IAA on a simplified culture medium containing a saline phosphate buffer (M9 saline solution), a sugar, as a carbon source, and yeast extract, as a source of organic nitrogen, vitamins, and other growth factors, was investigated. For this purpose, glucose or sucrose, as a carbon source, was used alternatively, in combination with two concentrations of yeast extract (5 or 10 g L^{-1}). All four media were amended with Trp (4 mM), and LB-Trp was used as a control.

Results reported in **Figure 6** indicate that IAA production occurred in all tested conditions and, independently from the carbon source and the amount of yeast extract that was used, was higher in saline medium compared to the control medium (LB-Trp). In particular, the higher level of biomass (64.1 ± 3.1 g [wet weight] L^{-1}) and IAA (120.5 ± 0.9 μg mL^{-1}) were obtained cultivating the microorganism in the presence of both sucrose and yeast extract at a final concentration of 0.5% (wt/vol) (SYE medium; **Figure 5**). Surprisingly, an increase in the organic nitrogen content, with double the amount of yeast extract [from 0.5 to 1% (wt/vol)], did not affect IAA production (80.13 ± 0.11 μg mL^{-1} in rGYE and 88.1 ± 0.44 μg mL^{-1} in rSYE) and biomass yield (47.1 ± 2.5 or 48.7 ± 2.2 g [wet weight] L^{-1}) (**Figure 6**).

Interestingly, there was no significant difference in the biomass yield when cells were grown on GYE or LB medium (40.8 ± 3.3 g [wet weight] L^{-1} and 40.3 ± 2.5 g [wet weight] L^{-1}), but the IAA-specific productivity shifting from LB to GYE had approximately 1.8-fold increase (**Figure 6**). These results suggested that LB was not an optimal medium for IAA production by *P. agglomerans* strain C1.

Overall Impact of the Carbon Source on the Metabolites Secreted by *P. agglomerans* C1

Results obtained in shake-flask experiments indicated that, in contrast to previous finding obtained with *P. agglomerans* 299R (Brandl and Lindow, 1997), the production of IAA from strain C1 was affected by the carbon source. For this reason, the

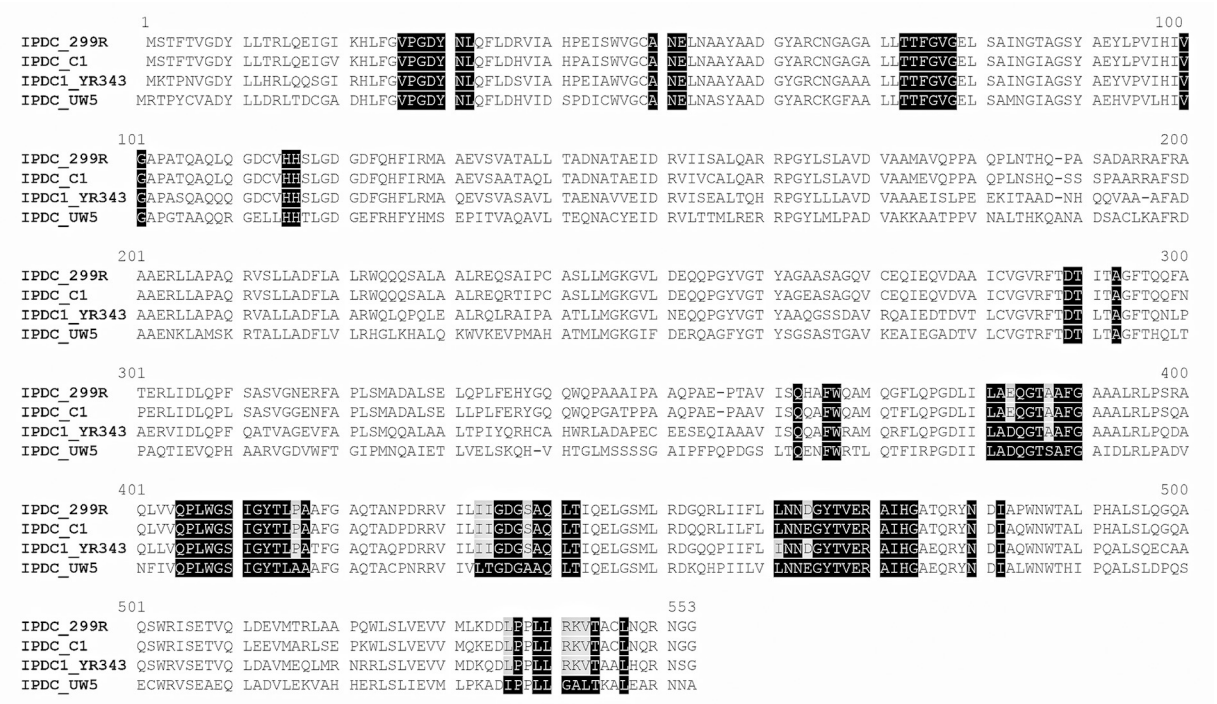

FIGURE 2 | Sequence alignment of peg.1955 encoded protein from *P. agglomerans* strain C1 and functionally characterized IPDC from *E. ludwigii* and other *Pantoea* strains. Residues in IPDC sequence from *E. ludwigii* UW5 that have been identified by crystal structure analysis as being at the active site or involved in either ThDP or substrate binding are highlighted in black. In the alignment, the amino acid residues of these regions that are conserved among all or almost all different sequences are highlighted in black or gray.

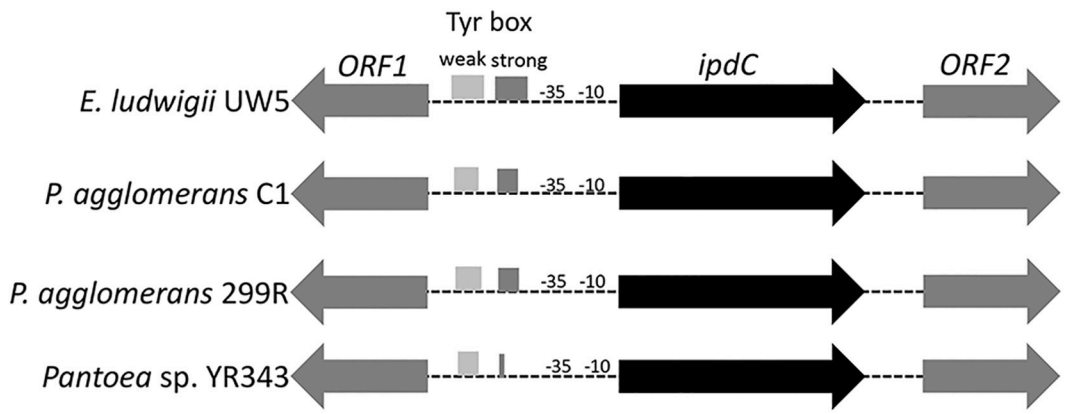

FIGURE 3 | Organization of the chromosome region surrounding *ipdC* across different species. The boxes in the *ipdC* promoter region indicate the location of the sequences with partial similarity to the two TyrR binding boxes occurring in *E. ludwigii* EW5. The predicted -10 and -35 elements for *ipdC* gene are also shown.

effect of the carbon source on the production of IAA and IAA-related compounds was studied in more detail by analyzing the exometabolome of *P. agglomerans* C1 using an untargeted metabolomics approach. Of the 528 features detected in the exhausted growth medium, when cells were cultured on YES or YEG amended with Trp, a total of 381 were more than twofold higher, and 94 were more than twofold lower when sucrose was used as a carbon source. ChemRICH analysis showed that a total of 58 metabolite clusters were significantly different ($P > 0.05$) between YES and YEG (**Figure 7** and **Supplementary Table S1**). For 27 of these clusters, the differences arise from an increased level in all the compounds of the cluster, and for other 10 clusters, the enriched molecules represented 75–95% of the total compounds of the cluster. As shown in **Figure 7**, in sucrose-grown cultures, the classes of metabolites with the highest elevated level were as follows: dipeptides and cyclic peptides; triterpenes; compounds belonging to new clusters 1, 21, and 49. Clustering analysis also revealed

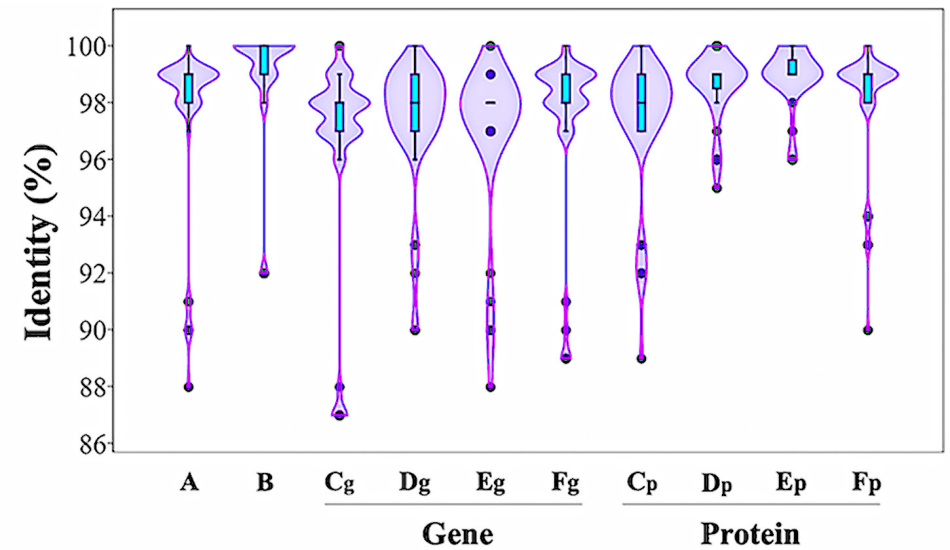

FIGURE 4 | Distribution of sequence identity matches of *P. agglomerans* strain C1 to other *P. agglomerans* DNA and protein sequences related to IPyA pathway. The violin plots show the distribution of sequence identities of the *ipdC* gene cluster (A), the *ipdC* promoter region (B), the IPDC gene (C_g) and protein (C_p), the amino transferase gene (D_g) and protein (D_p), and the two IAAld dehydrogenase genes (E_g and F_g) and proteins (E_p and E_p).

Sigma 70 DNA binding motif

Strain	-35 TTGACA	-10 TATAAT
P. agglomerans		
C1	CGCCTTTCCAGCCATTGCGGCT-------GGCTAAAATAG	
299R	CGTCTTGCCAGGCATTGCGGCT-------GGTTAAAATAGC	
***Pantoea* sp YR343**	TGC-TTGCCACAAATCAGCACCACACGATGGTGAATATCTC	
***E. ludwigii* UW5**	TTC-TGGACAGCCATCACGCTTCTTT------AATACTC--	

Consensus TyrR binding motif TGTAAA N6 TTTACA

Strain	weak Tyr box (24 bp)	strong TyrR box (22 bp)
E. ludwigii UW5	AGTGTATACGTTTACATTTACATG	TTTGTAAAGCATTCTTTCCATG
P. agglomerans C1	AGTGTATACGgTTACAcT-cagTG	TTTtTAcAGaAT--aTTCC--G
P. agglomerans 299R	AGTGTATACGgTTACAcTTA-gTG	TTTt-TAcAGaAT--aTTCC--G
Pantoea sp YR343	AGTGTATgCGTTTACAcT------	TTatctgtcgtcgtaacgaATG

FIGURE 5 | Alignment of relevant elements of the *ipdC* promoter sequence of *E. ludwigii* UW5, *P. agglomerans* C1, *P. agglomerans* 299R, and *Pantoea* species YR343. The conserved nucleotides in the -10 and -35 region (upper panel) and putative TyrR binding sites (lower panel) are highlighted in black.

significant differences in the concentration level of single metabolites belonging to the indole-oligopeptides clusters and to the flavonoids cluster. In the first two clusters, we observed an increase of some bisindole alkaloids, such as the guaiaflavine (140-fold); an increase of some monoindole alkaloids, such as the indole-3-carbinol (I3C; 4.3-fold) and the IAA (2.2-fold); an increase of some amide-linked-IAA-L-amino acid conjugates (IAA-aa), such as indole-3-acetyl-L-valine (39-fold) and indole-3-acetyl-L-leucine (2.4-fold); a threefold decrease of aldehyde derivatives, such as IAAld and ^{1}H-indole-3-carboxaldehyde (I3A) (**Supplementary Table S2**). In the flavonoids cluster, a significant increase in N-containing flavonoids, such as phyllospadine (54-fold increase), was observed. These results clearly indicate that in *P. agglomerans* C1 the levels of secreted metabolites were significantly affected by the medium carbon source.

Optimization of the Growth Conditions in Bench-Top Fermenter

In contrast with previous findings obtained with *Enterobacter* and *Agrobacterium*, in which the *ipdC* gene is under the

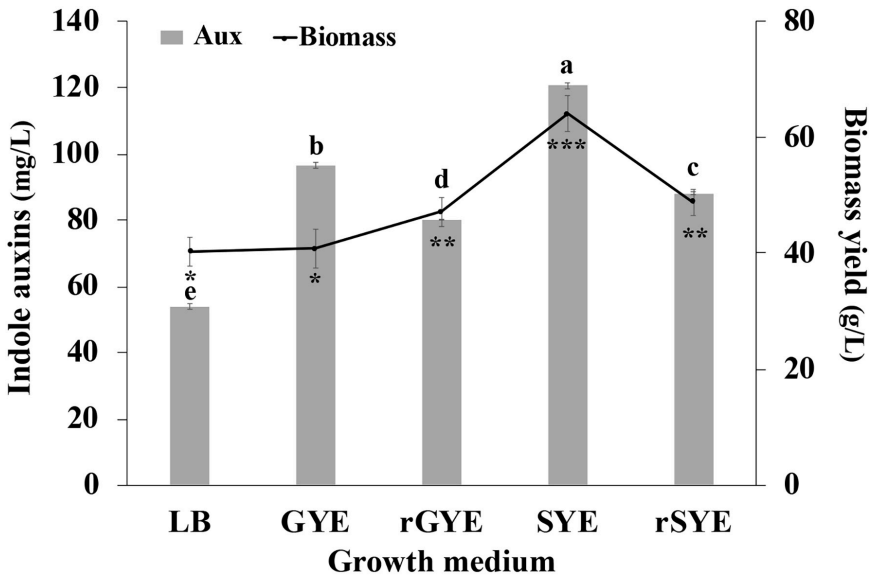

FIGURE 6 | Effect of culture medium on IAA production (mg L^{-1}) and biomass concentration (g [wet weight] L^{-1}). LB, YEG, and YES contained 5 g L^{-1} of yeast extract; in reinforced media (rYEG and rYES) the concentration of this ingredient is doubled (10 g L^{-1}). Differences in letters and symbols indicate that the values are significantly different ($P > 0.05$).

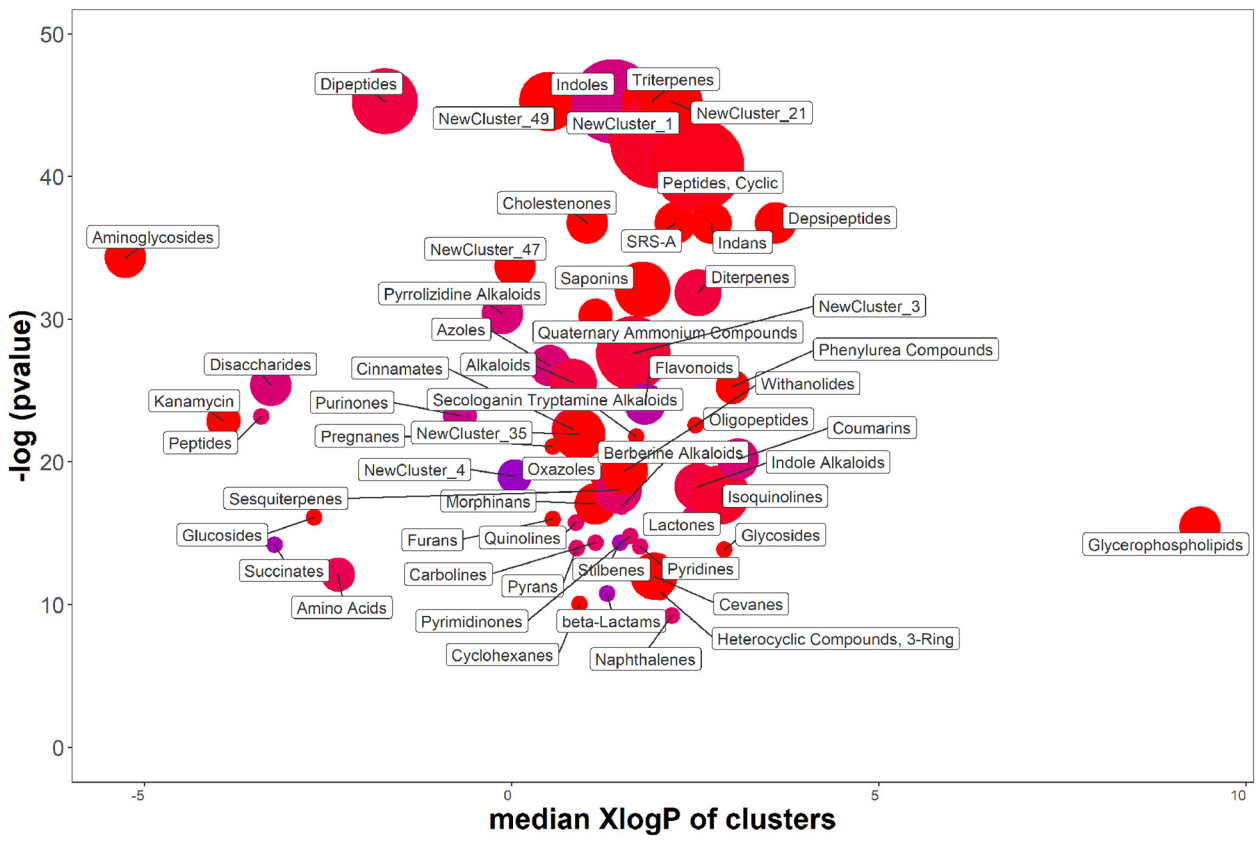

FIGURE 7 | ChemRich analysis of exometabolome of *P. agglomerans* C1 grown on YES vs. YEG medium. Red clusters associated with higher outcomes, and the blue ones associated with lower outcomes.

control of TyrR and the accumulation of IAA occurred only after entrance in the stationary phase (Ryu and Patten, 2008), when *P. agglomerans* strain C1 was grown on LB medium, as well as on M9 glucose, no significant production of IAA was detected when Trp was provided to resting cells or to stationary-phase cultures. To better understand the link between the cell physiological state and the biosynthesis of IAA in *P. agglomerans*, strain C1 was grown under controlled bioreactor conditions ensuring optimum oxygen uptake and temperature control and high growth rates.

Analyzing the growth profile of C1 cultures grown at 30°C on YES medium under aerobic conditions (DO level > 20% of saturation), a lag phase of 30 min was observed followed by an acceleration phase (up to 1.5 h) during which the growth rate gradually increased (**Figure 8**). In the exponential phase, which reached its maximum at approximately 4 h, the specific growth rate was 1.63 h^{-1}. Between the 4th and the 5.5th hour, the specific growth rate decreased to approximately 67% (from 1.63 to 0.53 h^{-1}) and at approximately 5.5 h the culture entered in the stationary phase (**Figure 8**). Interestingly, during the first 3.5 h of growth, medium pH decreased slowly from 6.6 to 6.5, at a rate of approximately 0.028 unit per hour (**Figure 8**). In YES medium, when the culture reached the end of the exponentially phase (4 h), the pH started to decrease rapidly (at a rate of 0.87 unit per hour) and reached a minimum value of 6.22 at 5 h. Later, at the beginning of the stationary phase, the medium pH increased from 6.22 up to 6.34 and remained constant up to the end of the fermentation (**Figure 8**). Variations in the medium pH between the 3.5th and the 5.5th hour occurred concurrently with changes in the oxygen consumption rate that were controlled by DO-dependent modifications of the agitation speed and the airflow using a closed-loop system. As shown in **Supplementary Figures S1B,C**, the oxygen demand suddenly increased between 4 and 4.5 h (agitation speed increased > 10% in 30 min, from 400 to 450 rpm) and then remained stable up the beginning of the stationary phase (5.5 h).

The growth of *P. agglomerans* strain C1 in bioreactor allowed increasing the biomass yield compared to shake-flask cultures of about sixfold, up to 292.5 ± 4.8 g [wet weight] L^{-1}.

Influence of the Physiological State of the Inoculum on IAA Production

Cells collected at different time points during the growth in bioreactor were transferred in medium containing Trp, so as to evaluate the effect of the physiological state of the cells used for inoculation on the IAA production. The growth was carried out in shake flasks at 30°C, and the IAA production was monitored during the first 2 h and at the end of the growth. In all tested conditions, no significant difference was observed in the initial rate of IAA production that was approximately 42 ± 2 g L^{-1} h^{-1}. Surprisingly, at the end of the growth, a significant influence of the inoculum was observed on the IAA titer that varied between 161.58 ± 4.91 (6 h old inoculum) and 263.33 ± 8.25 mg/L (4 h old inoculum; **Figure 9**).

Use of IAA-Enriched Excretome From *P. agglomerans* C1 in Plant Nursery

The efficacy of the exhausted culture medium, containing IAA and other secreted metabolites from *P. agglomerans* strain C1, named IAA-E_{C1} (for IAA-enriched Excretome from strain C1) was tested on a total of 4,540 plants of *Prunus* rootstock GF/677 and 1,080 plants of hazelnut cv. Fertile de Coutard. The experiments were carried out in a large-scale nursery farm (Vivai Piante Battistini, Cesena, Italy) according to the protocols used for large agamic propagation of fruit crop trees.

Plant Survival Experiments

The inductive activity of adventitious rooting of exometabolites from strain C1 was tested *in vitro* on two sets of 760 plantlets of rootstock GF677 treated with either a 3 μM IBA-K solution or an appropriate volume of IAA-E_{C1} to achieve a final concentration of auxins of 1 μM. After 10 days of rooting stage, when plantlets were transferred to 360-cell plug tray, the percentage of survival was 85% for IAA-E_{C1}–treated plants and 97% for IBA-treated plants; after 1 month of *ex vitro* acclimation, this value resulted 95% for IAA-E_{C1}–treated plants and only 80% for IBA-treated plants. Taken together, these values indicate an overall increase of about 3% in plant survival when bacterial metabolites were used in alternative to IBA-K.

Ex vitro Experiments

After 20 days of *ex vitro* acclimatization, regardless of the inductive treatments, the percentage of rooting was 100%. However, the number of roots per rooted explant was significantly higher for IAA-E_{C1}–treated plants (5.2 ± 0.5 roots per explant), compared to an average of 3.6 ± 0.5 of roots for IBA-K–treated plants. The quality of the roots also resulted improved after the treatment with IAA-EC (**Figure 10**). No significant difference was, instead, detected for the elongation of roots, which was approximately 14 mm for all plants, as well as for the plant survival percentage that, after 3 weeks from the beginning of the experiments, was 85% ± 1%. Finally, the average total leaf area per plant was higher in IAA-E_{C1}–treated (115 ± 2 mm^2) with respect to IBA-K–treated plants (102 ± 8 mm^2).

The inductive role of adventitious rooting by IAA-E_{C1} was also investigated on hazelnut microcuttings of cv. Fertile de Coutard using the same experimental protocol applied for *Prunus* rootstock. This experiment was carried out on two distinct pools of 1,080 and 1,440 binodal cuttings that were treated with IBA-K (3 μM solution) and IAA-E_{C1} (a 1:1000 diluted solution with an indole auxins final concentration of 1 μM), respectively. The percentage of rooted cuttings and number of roots per rooted explants resulted to be not significantly affected by the treatments, with the rooted ratio being between 64 and 75% and the value of root number being between 1.1 ± 0.1 and 1.3 ± 0.2 (**Table 2**). The root length was significantly affected by C1 metabolites and increased about 1.3-fold after treatment with IAA-E_{C1} compared to IBA-K (**Table 2**). A similar positive effect was also observed analyzing the stem elongation and the leaf area which both increase of about 1.4-fold in IAA-E_{C1}–treated plants (**Figure 11**). It is worth mentioning that the treatment with C1 metabolites

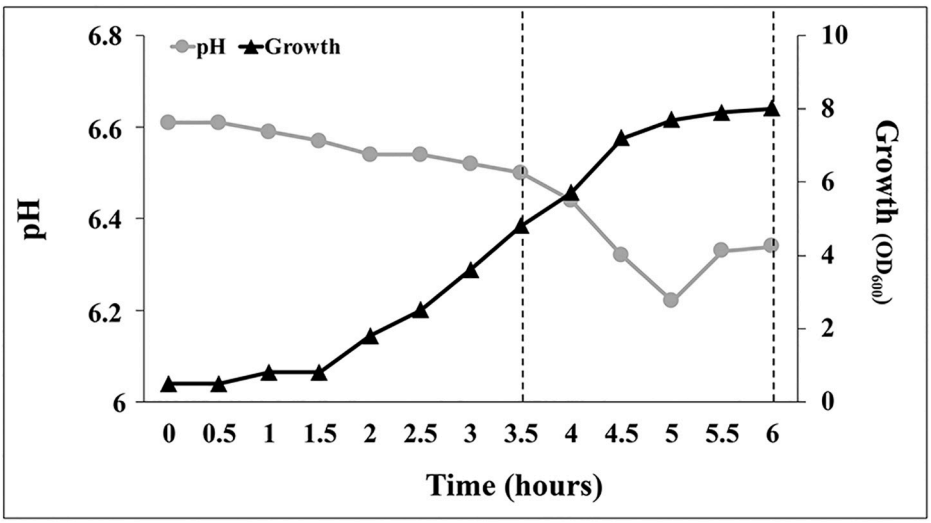

FIGURE 8 | Growth pattern and pH evolution during batch scale tests in YES medium under aerobic conditions at 30°C. Data points are mean values of duplicate fermentations.

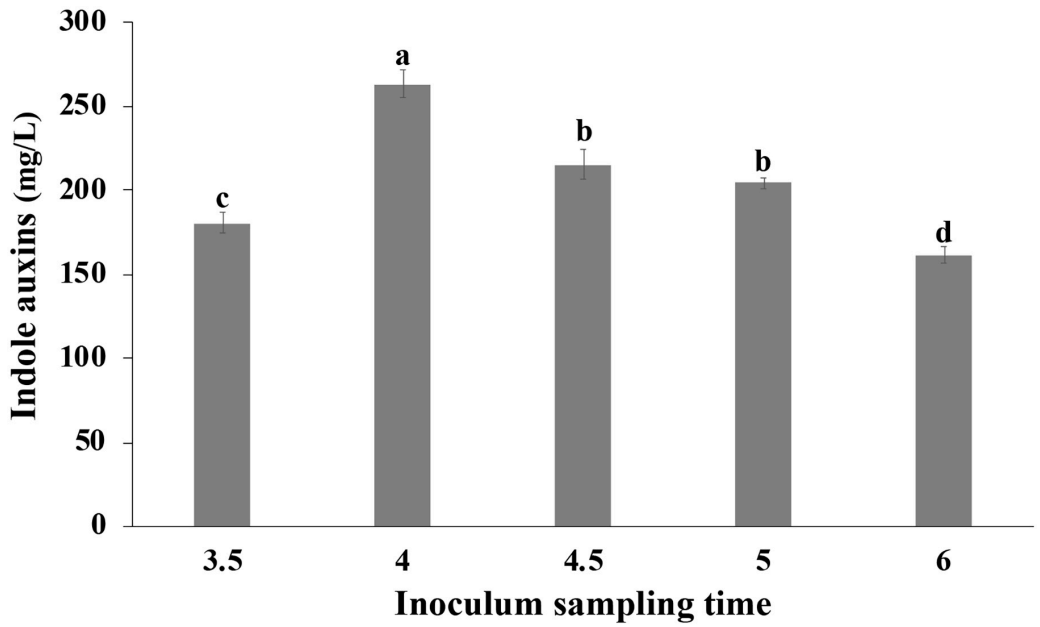

FIGURE 9 | Effect of the physiological state of the cells used for inoculation on IAA production. *Pantoea agglomerans* strain C1 was cultivated on YES-tryptophan medium for 18 h, and cells used for the inoculum (OD = 0.5) were collected by the fermenter at the time points indicated on the *x*-axis. Differences in letters indicate that the values are significantly different ($P > 0.05$).

determined a development of adventitious roots that are not present in IBA-K–treated plants (**Figure 12**).

DISCUSSION

Indole-3-acetic acid production is widespread among plant growth–promoting bacteria and varies from species to species and also among strains belonging to the same species (Spaepen and Vanderleyden, 2011; Duca et al., 2014). Auxins and other plant growth–promoting metabolites obtained from non-pathogenic *P. agglomerans* strains can be successfully applied in agriculture systems as plant biostimulants. It has been demonstrated that *P. agglomerans* strain C1 produces IAA and siderophores, and the metabolites secreted by this strain can be utilized as biostimulants to improve the root surface area in tomato cuttings (Luziatelli et al., 2020). This strain is also able to solubilize phosphates and can improve the use of rock

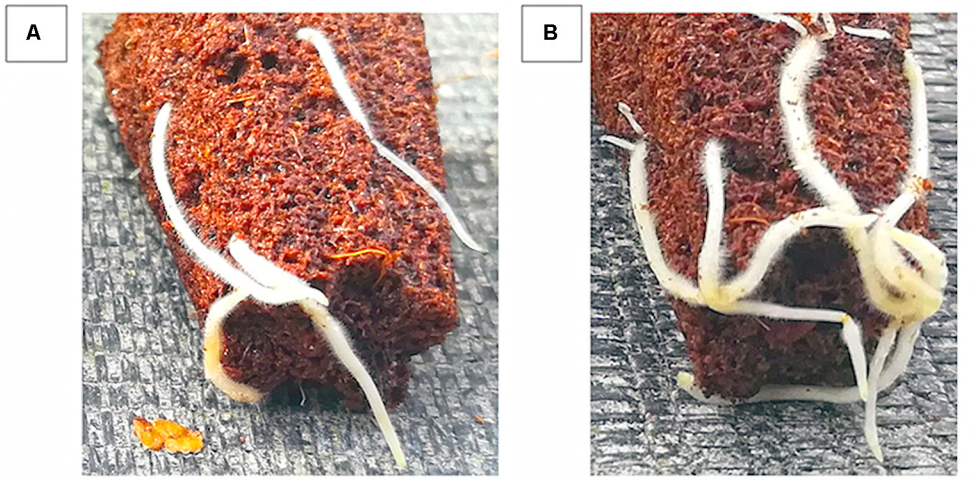

FIGURE 10 | Effect of different auxin treatments on morphology of rootstock GF677 roots. **(A)** IBA-K (3 μM); **(B)** diluted IAA-E_{C1} solution (IAA = 1 μM).

phosphates by corn (*Zea mays* L.) and tomato (*S. lycopersicum* L.) (Saia et al., 2020).

The application of comparative genetics, metabolomics, and fermentation technology in this study allowed analyzing in more detail the possibility of using this strain for production of a novel cell-free biostimulants. Whole-genome analysis demonstrated that *P. agglomerans* C1 has several genes connected with the production of IAA from Trp and all the genes of the IPyA pathway (**Table 1** and **Figure 1**). In GenBank, there are several sequences encoding indolepyruvate decarboxylase, the key enzyme of the IPyA pathway, and homologous enzymes, but only in few cases that the corresponding proteins have been isolated and characterized for their biochemical properties. The 1,653 bp peg1955 gene from *P. agglomerans* C1 encodes a 551-amino acid protein, which shares high identity with well-characterized IPDC from other *Pantoea* strains: 92% identity with the IPDC from *P. agglomerans* 299R (Brandl and Lindow, 1996) and 73% identity with IPDC1 from *Pantoea* species YR343 (Garcia et al., 2019; **Table 1** and **Figure 2**). Interestingly, the results obtained in this study demonstrated that, with few exceptions, in most of the sequenced genomes of isolates belonging to *P. agglomerans* species (45 of 50), the genes encoding enzymes of the IPyA pathway share an identity higher than 95% over the full-length of the sequence (**Figure 4**). This unusually high sequence conservation among bacteria occurring in diverse natural environments has never been reported before for IAA genes belonging to other species. This is a strong evidence of the evolutionary importance of this functional trait for the interaction between *P. agglomerans* and host plants.

Molecular data presented in this work also indicate that strain C1 produces IAA through the IPyA route, which is usually associated to beneficial bacteria, whereas the IAM pathway, linked to plant pathogens using auxin synthesis as a virulence factor (Patten et al., 2013), is not present. These observations encourage the exploitation of strain C1 and its metabolites as a plant growth promoter.

Interestingly, comparative genomics also allowed demonstrating that the non-coding region upstream of the *ipdC* gene is highly conserved among member of *P. agglomerans* species (**Figure 4**) and that this gene is not regulated by TyrR (**Figures 3**, **5**). TyrR is a transcriptional regulator that controls the expression of a number of genes involved in the biosynthesis, catabolism, and transport of aromatic amino acids in *E. coli* (Pittard et al., 2005) and regulates expression of *ipdC* gene in *E. ludwigii* UW5 (Coulson and Patten, 2015). The *ipdC* promoter from strain UW5 contains two TyrR binding motifs, a strong (highly conserved) and a weak Tyr-box, which are not present in *Pantoea* strains (**Figure 5**). This result agrees with the observation that in *P. agglomerans* C1 the IAA production occurs in exponential phase of growth and not in stationary phase as in species in which *ipdC* gene is under the control of TyrR. The regulatory mechanism that control expression of the genes involved in IPyA pathway in *P. agglomerans* has not been elucidated yet, although there is evidence that multiple regulatory mechanisms may exist. For example, Brandl and Lindow (1997) demonstrated that in *P. agglomerans* strain 299R *ipdC* gene was expressed at low levels when cells were cultured in *in vitro* liquid cultures (independently from the presence of Trp or the growth phase of the culture) and was fully induced only when cells were grown on plants under water stress. In contrast, IAA production in *P. agglomerans* C1 is Trp-dependent and is

TABLE 2 | Effect of different auxin treatments on plant length, leaf area, number of roots per cutting, and root length of hazelnut cv. "Fertile de Coutard."

Treatment	Plant length (cm)	Leaf area (cm^2)	No. roots per cutting	Root length (cm)
IBA-K (3 μM)	17.8 ± 1.5^b	164 ± 5^b	1.3 ± 0.2^a	9.4 ± 0.5^b
IAA-E_{C1} (1 μM*)	25.7 ± 1.7^a	234 ± 5^a	1.1 ± 0.1^a	12.2 ± 0.5^a

*Means followed by the same letter were not significantly different ($P < 0.05$). *IAA conc.*

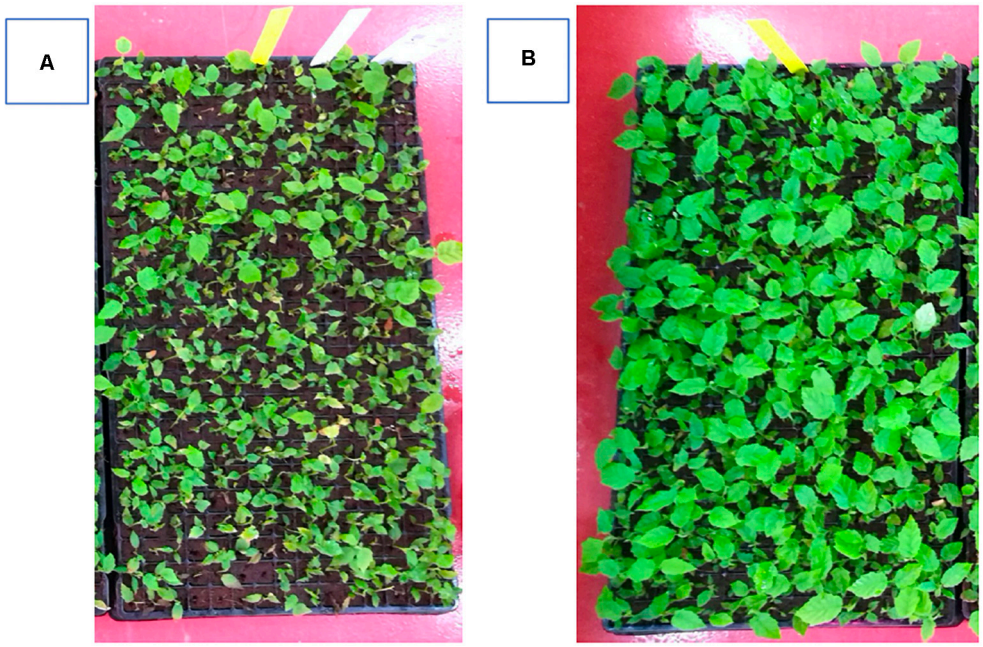

FIGURE 11 | Effect of different auxin treatments on plant growth of *Corylus avellana* L. cv. "Fertile de Coutard." **(A)** IBA-K (3 μM); **(B)** diluted IAA-E_{C1} solution (IAA = 1 μM).

FIGURE 12 | Effect of different auxin treatments on morphology of *Corylus avellana* L. cv. "Fertile de Coutard" roots. **(A)** IBA-K (3 μM); **(B)** diluted IAA-E_{C1} solution (IAA = 1 μM).

significantly affected from the carbon source (**Figure 6**) and the physiological state of the cells (**Figure 9**). Moreover, cultivation in bench-top fermenter indicated that with strain C1 there is a correlation between the amount of IAA produced after induction with Trp and the preparation of the inoculum (**Figure 9**). This observation agrees with the findings of a previous work with recombinant *E. coli* cells, where the production of aromatic compounds in enteric bacteria is enhanced with cells in exponential phase of growth in which the availability of ATP is higher (Luziatelli et al., 2019c).

Untargeted metabolomics allowed demonstrating that *P. agglomerans* C1, on medium containing sucrose as a carbon source, produces, together with IAA, other IAA-related compounds, such as I3C and IAA-leucine, which can either

modulate the effect of an excess of IAA (Katz et al., 2015) or increase the availability of this compound (Sanchez Carranza et al., 2016). In the exometabolome of *P. agglomerans* C1, other classes of compounds are also present, such as peptides and cyclopeptides that crosstalk with auxins or affect auxin transport or turnover.

Finally, the results obtained from studies run on a large scale on both one of the most diffuse *Prunus* rootstock and plant hazelnut confirmed that metabolites secreted by indole auxin–producing cells of *P. agglomerans* C1 have a high stimulating effect on adventitious rooting induction and adaption and plant growth *in vitro*. Interestingly, the excretome of strain C1 can also play relevant roles in root morphology (**Figures 10**, **12**) and plant growth (**Figure 11**) in *ex vitro* conditions. It is worth noting that these effects, as shown by the control experiments with IBA-K, are only in part dependent on auxins and with IAA-E_{C1} can be achieved at a molar concentration of IAA_{equ} threefold lower than the synthetic auxin (1 vs. 3 μM). Both *in vitro* and *extra vitro* procedures have shown that IAA-E_{C1} improved the performance and quality of micropropagated plant production. It should be emphasized that evaluation of the applicability of *Pantoea* metabolites in plant nursery industry was carried out following standard operation procedures used for large-scale production. Best practices for plant production rely on a careful control of microbial contamination of the production lines and equipment, the growing media, and the plant containers. In this specific context, the use of microbial inocula that can be beneficial for some plant cultures and not appropriate for others is always questionable and potentially dangerous. Under this respect, the use of liquid products, which are cell-free and contain only microbial metabolites, reduces contamination risks, is more compatible with the automation systems, and facilitates the adoption of this technology in plant nurseries.

CONCLUSION

In conclusion, the use of metabolites secreted by selected strains of *P. agglomerans* species can provide a valuable contribute for production of innovative biostimulants that can comply with current EU legislation. Further studies on gene expression will help to decipher the regulatory network that control IAA biosynthesis in *P. agglomerans* and provide more insight into the mechanisms by which *Pantoea* metabolites elicit plant growth promotion.

DATA AVAILABILITY STATEMENT

All datasets presented in this study are included in the article/**Supplementary Material**.

AUTHOR CONTRIBUTIONS

FL, AF, PB, RM, and MR contributed to the conception and design of the study and wrote the first draft of the manuscript. FL, AF, PB, LG, RM, MM, MT, and MR contributed to define the methodology. FL, AF, PB, and MR contributed to software analysis and data validation. FL, AF, PB, LG, RM, MM, MT, FM, and MR contributed to investigation. FL, AF, RM, FM, and MR wrote and edited the final version of the manuscript. All authors have read and agreed to the published version of the manuscript.

FUNDING

LG was supported by a Ph.D. grant of Minister for Education, University and Research (MIUR), Department of Excellence project SAFE-Med (Law 232/2016). The funder was not involved in the study design, collection, analysis, interpretation of data, the writing of this article or the decision to submit it for publication.

ACKNOWLEDGMENTS

We are grateful to the NGA Laboratory and Atens, Agrotecnologias Naturales S.L. (Spain) for helping us in the metabolomics analysis and metabolite annotation.

SUPPLEMENTARY MATERIAL

The Supplementary Material for this article can be found online at: https://www.frontiersin.org/articles/10.3389/fmicb.2020.01475/full#supplementary-material

REFERENCES

Akin-Idowu, P. E., Ibitoye, D. O., and Ademoyegun, O. T. (2009). Tissue culture as a plant production technique for horticultural crops. *African J. Biotechnol.* 8, 3782–3788. doi: 10.5897/AJB2009.000-9374

Altschul, S. F., Gish, W., Miller, W., Myers, E. W., and Lipman, D. J. (1990). Basic local alignment search tool. *J. Mol. Biol.* 215, 403–410. doi: 10.1016/S0022-2836(05)80360-2

Barupal, D. K., Haldiya, P. K., Wohlgemuth, G., Kind, T., Kothari, S. L., Pinkerton, K. E., et al. (2012). MetaMapp: mapping and visualizing metabolomic data by integrating information from biochemical pathways and chemical and mass spectral similarity. *BMC Bioinf.* 13:99. doi: 10.1186/1471-2105-13-99

Bhatti, S., and Jha, G. (2010). Current trends and future prospects of biotechnological interventions through tissue culture in apple. *Plant Cell. Rep.* 29, 1215–1225. doi: 10.1007/s00299-010-0907-8

Blaženović, I., Kind, T., Sa, M. R., Ji, J., Vaniya, A., Wancewicz, B., et al. (2019). Structure annotation of all mass spectra in untargeted metabolomics. *Anal. Chem.* 91, 2155–2162. doi: 10.1021/acs.analchem.8b04698

Brandl, M. T., and Lindow, S. E. (1996). Cloning and characterization of a locus encoding an indolepyruvate decarboxylase involved in indole-3-acetic acid synthesis in *Erwinia herbicola*. *Appl. Environ. Microbiol.* 62, 4121–4128.

Brandl, M. T., and Lindow, S. E. (1997). Environmental signals modulate the expression of an indole-3-acetic acid biosynthetic gene in *Erwinia herbicola*. *MPMI* 10, 499–505. doi: 10.1094/MPMI.1997.10.4.499

Büyükcam, A., Tuncer, Ö, Gür, D., Sancak, B., Ceyhan, M., Cengiz, A. B., et al. (2018). Clinical and microbiological characteristics of *Pantoea agglomerans* infection in children. *J. Infect. Public Health* 11, 304–309. doi: 10.1016/j.jiph.2017.07.020

Corpet, F. (1988). Multiple sequence alignment with hierarchical clustering. *Nucl. Acids Res.* 16, 10881–10890.

Coulson, T. J., and Patten, C. L. (2015). Complete genome sequence of *Enterobacter cloacae* UW5, a rhizobacterium capable of high levels of indole-3-acetic acid production. *Genome Announc.* 3:e00843-15. doi: 10.1128/genomeA.00843-15

DeFelice, B. C., Mehta, S. S., Samra, S., Čajka, T., Wancewicz, B., Fahrmann, J. F., et al. (2017). Mass spectral feature list optimizer (MS-FLO): a tool to minimize false positive peak reports in untargeted liquid chromatography–mass spectroscopy (LC-MS) data processing. *Anal. Chem.* 89, 3250–3255. doi: 10.1021/acs.analchem.6b04372

Doktycz, M. J. (2019). Computationally guided discovery and experimental validation of indole-3-acetic acid synthesis pathways. *ACS Chem. Biol.* 14, 2867–2875. doi: 10.1021/acschembio.9b00725

Driver, J. A., and Kuniyuki, A. H. (1984). In vitro propagation of *Paradox* walnut rootstock. *Hort. Sci.* 19, 507–509.

Duca, D., Lorv, J., Patten, C. L., Rose, D., and Glick, B. R. (2014). Indole-3-acetic acid in plant-microbe interactions. *Antonie Leeuwenhoek* 106, 85–125. doi: 10.1007/s10482-013-0095-y

Dutkiewicz, J., Mackiewicz, B., Lemieszek, M. K., Golec, M., and Milanowski, J. (2016a). *Pantoea agglomerans*: a mysterious bacterium of evil and good. Part III. Deleterious effects: infections of humans, animals and plants. *Ann. Agric. Environ. Med.* 23, 197–205. doi: 10.5604/12321966.1203878

Dutkiewicz, J., Mackiewicz, B., Lemieszek, M. K., Golec, M., and Milanowski, J. (2016b). *Pantoea agglomerans*: a mysterious bacterium of evil and good. Part IV. Beneficial effects. *Ann. Agric. Environ. Med.* 23, 206–222. doi: 10.5604/12321966.1203879

Eckardt, N. A. (2001). New insights into auxin biosynthesis. *Plant Cell* 13, 1–3. doi: 10.1105/tpc.13.1.1

Garcia, D. C., Cheng, X., Land, M. L., Standaert, R. F., Morrell-Falvey, J. L., Mitchel, J., et al. (2019). A cheminformatics approach to characterize metabolomes in stable-isotope-labeled organisms. *Nat. Methods* 16, 295–298. doi: 10.1038/s41592-019-0358-2

Kasahara, H. (2016). Current aspects of auxin biosynthesis in plants. *Biosci. Biotechnol. Biochem.* 80, 34–42. doi: 10.1080/09168451.2015.1086259

Katz, E., Nisani, S., Yadav, B. S., Woldemariam, M. G., Shai, B., Obolski, U., et al. (2015). The glucosinolate breakdown product indole-3-carbinol acts as an auxin antagonist in roots of *Arabidopsis thaliana*. *Plant J.* 82, 547–555. doi: 10.1111/tpj.12824

Koga, J., Adachi, T., and Hidaka, H. (1991). Molecular cloning of the gene for indolepyruvate decarboxylase from *Enterobacter cloacae*. *Mol. Gen. Genet.* 226, 10–16. doi: 10.1007/bf00273581

Lennox, S. (1955). Transduction of linked genetic characters of the host by bacteriophage P1. *Virology* 1, 190–206. doi: 10.1016/0042-6822(55)90016-7

Ljung, K., Hull, A. K., Kowalczyk, M., Marchant, A., Celenza, J., Cohen, J. D., et al. (2002). Biosynthesis, conjugation, catabolism and homeostasis of indole-3-acetic acid in *Arabidopsis thaliana*. *Plant Mol. Biol.* 50, 309–332. doi: 10.1023/A:1015298812300

Loberant, B., Altman, A., and Smith, R. H. (2010). "Micropropagation of plants," in *Encyclopedia of Industrial Biotechnology: Bioprocess, Bioseparation, and Cell Technology*, ed. M. C. Flickinger, (New York, NY: Wiley), 1–17.

Luziatelli, F., Brunetti, L., Ficca, A. G., and Ruzzi, M. (2019c). Maximizing the efficiency of vanillin production by biocatalyst enhancement and process optimization. *Front. Bioeng. Biotechnol.* 7:279. doi: 10.3389/fbioe.2019.00279

Luziatelli, F., Ficca, A. G., Cardarelli, M. T., Melini, F., Cavalieri, A., and Ruzzi, M. (2020). Genome sequencing of *Pantoea agglomerans* C1 provides insights into molecular and genetic mechanisms of plant growth-promotion and tolerance to heavy metals. *Microorganisms* 8:153. doi: 10.3390/microorganisms8020153

Luziatelli, F., Ficca, A. G., Colla, G., Baldassarre Švecová, E., and Ruzzi, M. (2019a). Foliar application of vegetal derived bioactive compounds stimulates the growth of beneficialbacteria and enhances microbiome biodiversity in lettuce. *Front. Plant Sci.* 10:60. doi: 10.3389/fpls.2019.00060

Luziatelli, F., Ficca, A. G., Melini, F., and Ruzzi, M. (2019b). Genome sequence of the plant growth-promoting rhizobacterium (PGPR) *Pantoea agglomerans* C1. *Microbiol. Resour. Announc.* 8:e00828-19. doi: 10.1128/mra.00828-19

Luziatelli, F., Ficca, A. G., Colla, G., Švecová, E., and Ruzzi, M. (2016). Effects of a protein hydrolysate-based biostimulant and two micronutrient based fertilizers on plant growth and epiphytic bacterial population of lettuce. *Acta Hortic.* 1148, 43–48. doi: 10.17660/ActaHortic.2016

Malhotra, M., and Srivastava, S. (2008). Organization of the *ipd*C region regulates IAA levels in different *Azospirillum brasilense* strains: molecular and functional analysis of *ipd*C in strain SM. *Environ Microbiol.* 10, 1365–1373. doi: 10.1111/j.1462-2920.2007.01529.x

Maniatis, T., Fritsch, E. F., and Sambrook, J. (1982). *Molecular Cloning: A Laboratory Manual*. Cold Spring Harbor, NY: Cold Spring Harbor.

Murashige, T., and Skoog, F. (1962). A revised medium for rapid growth and bioassays with tobacco tissue cultures. *Physiol. Plant.* 15, 473–497. doi: 10.1111/j.1399-3054.1962.tb08052.x

Nissen, S. J., and Sutter, E. G. (1990). Stability of IAA and IBA in nutrient medium to several tissue culture procedures. *Hort. Sci.* 25, 800–802. doi: 10.21273/HORTSCI.25.7.800

Orlikowska, T., Nowak, K., and Reed, B. (2017). Bacteria in the plant tissue culture environment. *Plant Cell Tiss. Organ. Cult.* 128, 487–508. doi: 10.1007/s11240-016-1144-9

Paredes-Páliz, K. I., Caviedes, M. A., Doukkali, B., Mateos-Naranjo, E., Rodríguez-Llorente, I. D., and Pajuelo, E. (2016a). Screening beneficial rhizobacteria from *Spartina maritima* for phytoremediation of metal polluted salt marshes: comparison of gram-positive and gram-negative strains. *Environ. Sci. Pollut. Res.* 23, 19825–19837. doi: 10.1007/s11356-016-7184-1

Paredes-Páliz, K. I., Pajuelo, E., Doukkali, B., Caviedes, M. Á, Rodríguez-Llorente, I. D., and Mateos-Naranjo, E. (2016b). Bacterial inoculants for enhanced seed germination of *Spartina densiflora*: implications for restoration of metal polluted areas. *Mar. Pollut. Bull.* 110, 396–400. doi: 10.1016/j.marpolbul.2016.06.036

Paredes-Páliz, K. I., Mateos-Naranjo, E., Doukkali, B., Caviedes, M. A., Redondo-Gómez, S., Rodríguez-Llorente, I. D., et al. (2017). Modulation of *Spartina densiflora* plant growth and metal accumulation upon selective inoculation treatments: a comparison of gram negative and gram positive rhizobacteria. *Mar. Pollut. Bull.* 125, 77–85. doi: 10.1016/j.marpolbul.2017.07.072

Patten, C. L., Blakney, A. J., and Coulson, T. J. (2013). Activity, distribution and function of indole-3-acetic acid biosynthetic pathways in bacteria. *Crit. Rev. Microbiol.* 39, 395–415. doi: 10.3109/1040841X.2012.716819

Pierik, R. L. M., and Scholten, H. J. (1994). "Micropropagation, an essential tool in modern agriculture, horticulture, forestry and plant breeding," in *Plant Production on the Threshold of a New Century*, Vol. 61, eds P. C. Struik, W. J. Vredenberg, J. A. Renkema, J. E. Parlevliet, and Develop Plant Soil Sci, (Dordrecht, DE: Springer).

Pittard, J., Camakaris, H., and Yang, J. (2005). The TyrR regulon. *Mol. Microbiol.* 55, 16–26. doi: 10.1111/j.1365-2958.2004.04385.x

Prinsen, E., Costacurta, A., Michiels, K., Vanderleyden, J., and Van Onckelen, H. (1993). *Azospirillum brasilense* indole-3-acetic acid biosynthesis: evidence for a non-tryptophan dependent pathway. *Mol. Plant Microbe Interact.* 6, 609–615. doi: 10.1046/j.1432-1327.1999.00033.x

Quoirin, M., and Lepoivre, P. (1977). Etudes de milieux adaptes aux cultures in vitro de Prunus. *Acta Hortic.* 78, 437–442.

Rouphael, Y., and Colla, G. (2018). Synergistic biostimulatory action: designing the next generation of plant biostimulants for sustainable agriculture. *Front. Plant Sci.* 9:1655. doi: 10.3389/fpls.2018.01655

Ruzzi, M., and Aroca, R. (2015). Plant growth-promoting rhizobacteria act as biostimulants in horticulture. *Sci. Hortic.* 196, 124–134. doi: 10.1016/j.scienta.2015.08.042

Ryu, R. J., and Patten, C. L. (2008). Aromatic amino acid-dependent expression of indole-3-pyruvate decarboxylase is regulated by TyrR in *Enterobacter cloacae* UW5. *J. Bacteriol.* 190, 7200–7208. doi: 10.1128/JB.00804-08

Saia, S., Aissa, E., Luziatelli, F., Ruzzi, M., Colla, G., Fiacca, A. G., et al. (2020). Growth-promoting bacteria and arbuscular mycorrhizal fungi differentially benefit tomato and corn depending upon the supplied form of phosphorus. *Mycorrhiza* 30, 133–147. doi: 10.1007/s00248-009-9531-y

Sanchez Carranza, A. P., Singh, A., Steinberger, K., Panigrahi, K., Palme, K., Dovzhenko, A., et al. (2016). Hydrolases of the ILR1-like family of *Arabidopsis*

thaliana modulate auxin response by regulating auxin homeostasis in the endoplasmic reticulum. *Sci. Rep.* 6:24212. doi: 10.1038/srep24212

Schutz, A., Golbik, R., Tittmann, K., Svergun, D. I, Koch, M. H., Hübner, G., et al. (2003). Studies on structure function relationships of indolepyruvate decarboxylase from *Enterobacter cloacae*, a key enzyme of the indole acetic acid pathway. *Eur. J. Biochem.* 270, 2322–2331. doi: 10.1046/j.1432-1033.2003.03602.x

Spaepen, S., and Vanderleyden, J. (2011). Auxin and plant-microbe interactions. *CSH Perspect. Biol.* 3:a001438. doi: 10.1101/cshperspect.a001438

Spaepen, S., Vanderleyden, J., and Remans, R. (2007). Indole-3-acetic acid in microbial and microorganism-plant signaling. *FEMS Microbiol. Rev.* 31, 425–448. doi: 10.1111/j.1574-6976.2007.00072.x

Thévenot, E. A., Roux, A., Xu, Y., Ezan, E., and Junot, C. (2015). Analysis of the human adult urinary metabolome variations with age, body mass index, and gender by implementing a comprehensive workflow for univariate and OPLS statistical analyses. *J. Proteome Res.* 14, 3322–3335. doi: 10.1021/acs.jproteome.5b00354

Thompson, J. D., Higgins, D. G., and Gibson, T. J. (1994). CLUSTAL W: improving the sensitivity of progressive multiple sequence alignment through sequence weighting, position-specific gap penalties and weight matrix choice. *Nucleic Acids Res.* 22, 4673–4680. doi: 10.1093/nar/22.22.4673

Tsugawa, H., Cajka, T., Kind, T., Ma, Y., Higgins, B., Ikeda, K., et al. (2015). MS-DIAL: data-independent MS/MS deconvolution for comprehensive metabolome analysis. *Nat. Methods* 12, 523–526. doi: 10.1038/nmeth.3393

Tsugawa, H., Kind, T., Nakabayashi, R., Yukihira, D., Tanaka, W., Cajka, T., et al. (2016). Hydrogen rearrangement rules: computational MS/MS Fragmentation and structure elucidation using MS-FINDER software. *Anal. Chem.* 88, 7946–7958. doi: 10.1021/acs.analchem.6b00770

Tsugawa, H., Nakabayashi, R., Mori, T., Yamada, Y., Takahashi, M., Rai, A., et al. (2019). A cheminformatics approach to characterize metabolomes in stable-isotope-labeled organisms. *Nat. Methods* 16, 295–298. doi: 10.1038/s41592-019-0358-2

Vande Broek, A., Gysegom, P., Ona, O., Hendrickx, N., Prinsen, E., Van Impe, J., et al. (2005). Transcriptional analysis of the *Azospirillum brasilense* indole-3-pyruvate decarboxylase gene and identification of a *cis*-acting sequence involved in auxin responsive expression. *Mol. Plant–Microb. Interact.* 18, 311–323. doi: 10.1094/MPMI-18-0311

Zhao, Y. (2010). Auxin biosynthesis and its role in plant development. *Annu. Rev. Plant Biol.* 61, 49–64. doi: 10.1146/annurev-arplant-042809-112308

Conflict of Interest: PB was employed by Next-Generation Agronomics Laboratory. MM was employed by the company Vivai Piante Battistini soc. agr. s.s.

The remaining authors declare that the research was conducted in the absence of any commercial or financial relationships that could be construed as a potential conflict of interest.

frontiers in Microbiology

ORIGINAL RESEARCH
published: 18 August 2020
doi: 10.3389/fmicb.2020.02044

Development and Application of Low-Cost and Eco-Sustainable Bio-Stimulant Containing a New Plant Growth-Promoting Strain *Kosakonia pseudosacchari* TL13

Ida Romano[1†], Valeria Ventorino[1†], Patrizia Ambrosino[2], Antonino Testa[1], Fatima Ezzahra Chouyia[1,3] and Olimpia Pepe[1]*

[1] Department of Agricultural Sciences, University of Naples Federico II, Naples, Italy, [2] Agriges S.r.l. – Nutrizione Speciale per L'Agricoltura Biologica e Integrata, San Salvatore Telesino, Italy, [3] Department of Biology, Faculty of Sciences and Techniques, Hassan II University of Casablanca, Casablanca, Morocco

OPEN ACCESS

Edited by:
Santiago Gutierrez, Universidad de León, Spain

Reviewed by:
Bruno Brito Lisboa, Secretaria Estadual da Agricultura, Pecuária e Irrigação, Brazil
Vasvi Chaudhry, Eberhard Karls University of Tübingen, Germany

***Correspondence:**
Olimpia Pepe
olipepe@unina.it

[†] These authors have contributed equally to this work and share first authorship

Specialty section:
This article was submitted to Microbial Symbioses, a section of the journal Frontiers in Microbiology

Received: 29 April 2020
Accepted: 03 August 2020
Published: 18 August 2020

Citation:
Romano I, Ventorino V, Ambrosino P, Testa A, Chouyia FE and Pepe O (2020) Development and Application of Low-Cost and Eco-Sustainable Bio-Stimulant Containing a New Plant Growth-Promoting Strain Kosakonia pseudosacchari TL13. Front. Microbiol. 11:2044. doi: 10.3389/fmicb.2020.02044

The use of beneficial microbes as inoculants able to improve fitness, growth and health of plants also in stress conditions is an attractive low-cost and eco-friendly alternative strategy to harmful chemical inputs. Thirteen potential plant growth-promoting bacteria were isolated from the rhizosphere of wheat plants cultivated under drought stress and nitrogen deficiency. Among these, the two isolates TL8 and TL13 showed multiple plant growth promotion activities as production of indole-3-acetic acid (IAA), siderophores, ammonia, and 1-aminocyclopropane-1-carboxylic acid (ACC) deaminase production, the ability to solubilize phosphate as well as exerted antimicrobial activity against plant pathogens as *Botrytis* spp. and *Phytophthora* spp. The two selected strains were identified as *Kosakonia pseudosacchari* by sequencing of 16S rRNA gene. They resulted also tolerant to abiotic stress and were able to efficiently colonize plant roots as observed *in vitro* assay under fluorescence microscope. Based on the best PGP properties, the strain *K. pseudosacchari* TL13 was selected to develop a new microbial based formulate. A sustainable and environmentally friendly process for inoculant production was developed using agro-industrial by-products for microbial growth. Moreover, the application of *K. pseudosacchari* TL13- based formulates in pot experiment improved growth performance of maize plants.

Keywords: inoculant, PGPR, rhizocompetence, bio-formulate, organic by-products

INTRODUCTION

According to the Food and Agriculture Organization (FAO), the estimated world population for 2025 will be nearly 8.5×10^9 inhabitants (Timmusk et al., 2017). Such an increase in agricultural production of 60% within the next years could be required to satisfy global food demand (Berger et al., 2018). Actually, in order to maintain a high quality of agricultural productions and eliminate or minimize yield loss, chemicals (fertilizers, pesticides, herbicides, etc.), hormones and antibiotics

are commonly used for crops. The use of agrochemicals at industrial level allows to produce a large number of agricultural products at low costs with high profits for farmers. However, serious concerns regarding human and environmental health resulting from chemical residues in soil, water and food as well as farm workers' exposure have posed great attention (Alori and Babalola, 2018). Indeed, in the last two decades, the demand for organically grown agricultural products increased as consequence to the request for healthy and safe products (Dorais and Alsanius, 2016). Therefore, new eco-compatible strategies to improve agricultural systems and crop production are needed. The use of plant beneficial microorganisms as inoculants offers an attractive eco-friendly alternative strategy to chemical inputs to ensure crop yield and nutritional quality (Fiorentino et al., 2018) acting as agricultural probiotics. Probiotics are live microorganisms that offer benefits to the host providing nutritional inputs and protecting it from pathogens (Hossain et al., 2017). Among the beneficial microbes employed in agriculture, plant growth-promoting rhizobacteria (PGPR) are the most commonly used. These microbes are able by a wide range of mechanisms to improve nutrient availability in soil, plant nutrient uptake and assimilation [i.e., nitrogen fixation, phosphate solubilization, siderophore, indole-3-acetic acid (IAA), and ammonia production] and/or providing protection against plant pathogens (Backer et al., 2018; Woo and Pepe, 2018). Indeed, these microbes could also act as bio-stimulants ameliorating plant growth and crop production in response to abiotic stress in hostile environments (Viscardi et al., 2016; Van Oosten et al., 2017).

Important examples of PGPR include *Pseudomonas*, *Bacillus*, *Azotobacter*, *Azospirillum*, *Burkholderia*, *Sphingomonas* (Sharma et al., 2011; Singh et al., 2013; Castanheira et al., 2017; Dal Cortivo et al., 2017; Kandel et al., 2017; Khalid et al., 2017). However, in the last few years, it is rising the interest around the genus *Kosakonia* for its potential PGP activities. Recently, several members of this genus have been recognized as endophyte of different agricultural plants and it was demonstrated their growth-promoting effects and crop yield improvement (Kämpfer et al., 2016; Berger et al., 2017). However, this genus being relatively young, it is poorly studied and many of its features remain still unexplored.

Actually, the establishment of a low-cost and eco-sustainable process, as well as an effective and stable formulation, are among the main biotechnological challenges for the development of microbial inoculants. The use of agro-industrial organic waste and by-products as carbon source for the growth and production of microbial biomass is an attractive strategy to reduce the production costs, to valorize organic waste and by-products and to develop a sustainable and environmentally friendly process for inoculant production at industrial level. Moreover, it is also very important the form (solid or liquid) of microbial inoculant as well as its shelf-life. In fact, the form of the inoculant could influence its cost production, affect its efficiency and determine the method of application in agriculture on large scale (Alori and Babalola, 2018). The inoculant must be easy to handle in the field but it should maintain its features during the process and an adequate viability and shelf-life since it is required that it should be stable for at least 6 months (Berger et al., 2018).

This work aimed to isolate, select and characterize rhizobacteria with multiple PGP properties and antimicrobial activity. The selected plant growth-promoting bacteria (PGPB) strains were also tested for their ability to tolerate abiotic stress and to be able to efficiently colonize plant roots in *in vitro* experiments. Additionally, the selected strain was used to develop a new inoculant using agro-industrial by-products as sole carbon source for microbial growth and the new low-cost and eco-sustainable bio-formulates were finally tested in two forms (solid or liquid) in pot experiment to improve growth performance of maize plant.

MATERIALS AND METHODS

Soil Sampling and Microbial Isolation

Rhizosphere samples were collected according to Romano et al. (2020) from wheat plants grown, under drought stress and nitrogen deficiency, in a greenhouse at the experimental station of the University of Naples Federico II (Bellizzi, Italy; 43°31′N, 14°58′E, 60 m a.s.l.). Ten grams of samples were shaken for 30 min in 90 mL of quarter strength Ringer's solution (Oxoid, Milan, Italy) containing tetrasodium pyrophosphate (16% w/v) as previously described (Ventorino et al., 2012a). After shaking, tenfold serial dilutions (1:10) were performed and used to inoculate liquid Augier medium (Pepe et al., 2013) for the detection of free-living (N_2)-fixing aerobic bacteria. After incubation for 14 days at 28°C, the brown rings formed by microorganisms grew in the liquid medium were used to inoculate LG agar medium (Aquilanti et al., 2004). The plates were incubated for 7 days at 28°C. Isolated colonies were picked from plates, purified by streaking on the same isolation medium, characterized by different morphologies examined by microscopy, gram staining and catalase reaction and stored at 4°C as slant cultures until their characterization.

Preliminary Screening for Plant Growth Promoting Traits

Thirteen bacterial isolates were screened on the basis of their potential plant growth promotion activities. Detection and quantification of IAA production was determined by the Salkowski colorimetric assay using Nutrient Broth (Oxoid) with and without l-tryptophan (2 mg L^{-1}; Sigma-Aldrich, Milan, Italy) as previously described (Ventorino et al., 2014).

Semi-quantitative agar spot method was used to determine the ability of bacterial isolates to produce siderophores by Chrome azurol S (CAS) assay as described by Silva-Stenico et al. (2005). After 14–21 days of incubation at 28°C, the formation of an orange or yellow halo around the colony indicated the production of siderophores by the microorganism.

Determination of 1-aminocyclopropane-1-carboxylic acid (ACC) deaminase activity of isolates was performed by assessing the growth on nitrogen-free minimal medium (MM) agar supplemented with 3 mM ACC (Sigma-Aldrich) after incubation at 28°C in the dark for 7 days as described by

Jaemsaeng et al. (2018). MM agar supplemented with 2 g L^{-1} $(NH_4)_2SO_4$ was used as control.

Identification of Selected Strains

The bacterial isolates showing the highest plant growth promoting activities were selected for further investigations and identified by the sequencing of the 16S rRNA gene. In detail, total genomic DNA of selected strains was extracted by boiling for 10 min and then used as template for the PCR assay. The PCR mixture was employed according to Alfonzo et al. (2012) using the primers fD1 (5′-AGAGTTTGATCCTGGCTCAG-3′) and rD1 (5′-AAGGAGGTGATCCAGCC-3′). The PCR conditions were as described by Ventorino et al. (2017). PCR products were purified using the QIAquick PCR Purification Kit (Quiagen, Milan, Italy) according to the supplier's recommendations and sequenced as previously reported (Ventorino et al., 2016). The DNA sequences were compared to the GenBank nucleotide data library using the BLAST software at the National Centre for Biotechnology Information website[1].

The nearly full-length 16S rRNA sequences of the selected bacterial strain and 31 type strains belonging to different genera related to *Kosakonia pseudosacchari* species as described by Kämpfer et al. (2016) and Wang et al. (2019) were used to perform multiple nucleotide alignments using the ClustalW program (Thompson et al., 1994) from MEGA version X (Kumar et al., 2018; Stecher et al., 2020). The nucleotide sequences of the type strains were retrieved from the Ribosomal Database Project (RDP)[2] and from the National Center for Biotechnology Information (NCBI)[3]. The phylogenetic tree was inferred using the Neighbor-Joining method with the Maximum Composite Likelihood model in the MEGAX program, with bootstrap values based on 1,000 replications.

The 16S rRNA gene sequences obtained from selected bacterial strains were deposited in the GenBank nucleotide database under accession numbers MN607213 and MN607214 (see footnote 3).

Characterization of Selected Strains for PGP Traits and Antimicrobial Activity

Phosphate solubilization ability was quantified by molybdenum blue quantitative assay in Pikovskaya's (PVK) liquid medium. Briefly, 10 mL of PVK medium was inoculated with 0.1 mL of bacterial cultures (approximately 1.5×10^8 CFU mL^{-1}) and incubated for 15 days at 30°C. After incubation, cultures were centrifuged (5 min at 18,620 × *g*) and supernatant was collected to estimate released soluble phosphorus (P) as described by Murphy and Riley (1962). The concentration of P solubilized was determined by spectroscopic absorbance measurements at 430 mμ according to the standard curve (Murphy and Riley, 1962).

Ammonia production of selected strains was estimated by inoculating the microorganisms in 5 mL of peptone water according to Cappuccino and Sherman (1987) and incubating under shaking (100 rpm) at 30°C for 7 days. The presence of ammonia was detected by the development of a brown to yellow color after adding 0.5 mL of Nessler's reagent (Sigma-Aldrich) to the culture and then quantified by spectroscopic absorbance measurements at 420 nm according to the standard curve (Passari et al., 2017).

The presence of the target gene *nif*H, encoding nitrogenase reductase enzyme, was assessed by PCR assay using the synthetic oligonucleotide primers *nif*H-F (5′-AAAGGYGGWAT CGGYAARTCCACCAC-3′; Rösch et al., 2002) and *nif*H-R, (5′-TTGTTSGCSGCRTACATSGCCATCAT-3′; Rösch et al., 2002) using conditions reported by Fiorentino et al. (2016). The presence of the target gene was assessed by visualization of a 475 bp band by agarose (1.5% w/v) gel electrophoresis (100 V for about 1 h).

A 1-aminocyclopropane-1-carboxylic acid deaminase activity was quantified according to Penrose and Glick (2003) by measuring the amount of α-ketobutyrate (Sigma-Aldrich) produced when the enzyme ACC deaminase cleaves ACC. In detail, bacterial strains were inoculated in 5 mL of Dworkin and Foster (DF) minimal salt medium containing $(NH_4)_2SO_4$ as sole nitrogen source (Penrose and Glick, 2003). After incubation at 30°C for 48 h, the cultures were used to inoculate 5 mL of DF salt medium containing 3 mM ACC (Oxoid) as nitrogen source. The amount of α-ketobutyrate (μmol) produced was estimated by measuring the absorbance at 540 nm according to the standard curve (α-ketobutyrate concentration ranged from 0.1 to 100 μmol).

Quantitative estimation of siderophores was performed according to Arora and Verma (2017) using CAS reagent and expresses as percent siderophore unit (psu) using the following formula (Payne, 1993):

$$psu = [(Ar - As)x100]/Ar$$

where Ar is the absorbance of reference (CAS solution and uninoculated medium), and As is the absorbance of sample (CAS solution and cell-free sample supernatant).

Antimicrobial antagonism was evaluated using the dual culture method described by Hammami et al. (2013) against eight pathogenic eukaryotic strains belonging to the microbial collection of Division of Biology and Protection of Agricultural and Forest Systems (Department of Agricultural Sciences, University of Naples Federico II): *Botrytis cinerea* B11, *B. cinerea* B12, *Fusarium oxysporum* F3, *F. oxysporum* F5, *Aspergillus niger* A31, *Phytophthora infestans* ph1, *Phytophthora cactorum* ph3, and *Phytophthora cryptogea* ph4. Fungi were grown on Potato Dextrose Agar (PDA, Oxoid) at 28°C for 7 days, while Oomycetes were grown on V8 agar (200 mL of V8 juice, 2.5 g $CaCO_3$, 800 mL of distilled water and 17 g of bacteriological agar) at 28°C for 21 days. Conidia were harvested from the surface of plates by flooding the cultures with 9 mL of sterilized distilled water and gently scraping with a sterilized glass rod. The conidial concentration was determined using the counting chamber Thoma (Hawksley, United Kingdom). An over-layer agar (agar 0.7%) containing a concentration of 10^5 conidia mL^{-1} of each plant pathogen was poured on Brain Heart Infusion (BHI)

[1]http://www.ncbi.nlm.nih.gov/Blast.cgi

[2]https://rdp.cme.msu.edu/

[3]https://www.ncbi.nlm.nih.gov

agar plates previously spotted with the bacterial strains. After incubation for 7 or 21 days at 28°C, the antimicrobial activity of the bacterial strains was highlighted by the presence of a halo around the colony without fungal growth.

Tolerance to Abiotic Stress

The two selected bacterial strains were tested for their salt tolerance in liquid medium as previously described Ventorino et al. (2012b). Briefly, 5 mL of BHI medium supplemented with NaCl up to 15% (w/v) was inoculated with each bacterial strain. The standard BHI medium with 0.5% (w/v) NaCl was used as control. Bacterial growth was determined by observing the development of turbidity of cultures at 24 and 48 h and comparing them with McFarland Turbidity Standard.

Similarly, temperature tolerance was investigated comparing bacterial growth in BHI liquid medium with McFarland Turbidity Standard after 24 and 48 h of incubation at 28, 30, 37, and 42°C.

Finally, pH tolerance was determined by evaluating the growth of bacterial strains in BHI liquid medium in which pH was adjusted at pH 5, 6, 7, and 8 by the addition of HCl or NaOH. After incubation, bacterial growth was estimated at 24 and 48 h comparing their turbidity to McFarland Turbidity Standard.

Rhizosphere Competence

Tomato seeds (*Solanum lycopersicum* var. *cerasiforme*) were carefully de-husked without damaging the embryo and surface sterilized as described by Banik et al. (2016). Briefly, seeds were treated with 2% sodium hypochlorite (5 min) followed by washing with sterile distilled water, then seeds were treated with 75% ethanol (5 min), washed again with sterile water and treated with 30% hydrogen peroxide (2 min) as suggested by Amarasinghe et al. (2018); finally, they were carefully rinsed ten times with sterile distilled water. Seeds sterility was checked by plating on Plate Count Agar (PCA; Oxoid). Seeds germination took place in darkness at 30 ± 2°C.

Microbial cells were grown in BHI medium (30 ± 2°C, 24 h). Cells were harvested by centrifugation (2000 × *g* for 5 min) at the end of their exponential phase of growth, washed twice in HEPES buffer (0.1 M) and then suspended in quarter strength Ringer's solution (Oxoid) until achieving microbial concentration of approximately 5×10^8 CFU mL^{-1} (counting chamber Thoma 0.02 depth, Hawksley United Kingdom). Finally, tomato seedlings were treated with bacterial suspension for 48 h at 30 ± 2°C and then rinsed five times with sterile HEPES buffer (0.1 M) to remove the loosely associated bacteria from the radicle surface. Tomato seedlings treated with sterile water were used as control. Bacteria-infected radicles and controls were treated with LIVE/DEAD® BacLight™ bacterial viability kit (Thermo Fisher Scientific) following the manufacturer's instructions. Treated radicles were observed by fluorescence microscope (Axiovert 200M, Zeiss, Göttingen, Germany) under UV light (50-W mercury lamp) and using a Green Fluorescent Protein Filter (38 HE-GFP; excitation wavelength of 450–490 nm) and Rhodamine Filter (Rh-20; excitation wavelength of 540–552 nm).

Production of a Low-Cost Bacterial Inoculants

Study of Bacterial Growth

The strain TL13 was inoculated in 200 μL of BHI using 96-well flat-bottom microplate in a Microplate Reader (BioTek Elx808) and incubated at 30°C for 24 h with moderate shaking every 30 min. $O.D_{600\,nm}$ measurements were performed every 30 min to define the growth curve.

Preliminary batch growth tests were performed to assess the best growth conditions for the strain TL13. In details, 500 mL flasks filled with BHI medium were inoculated with 2% bacterial cells suspension (8.45 ± 0.20 CFU mL^{-1}) and incubated at 30°C for 24 h using three different growth conditions: (1) Batch 1, shaking at 130 rpm (Grant-bio, Orbital Shaker-Incubator ES80); (2) Batch 2, shaking at 130 rpm and sterile air sparging at 0.5 vvm; control, no shaking and no air sparging. Samples were withdrawn every 2 h and cell growth was determined by viable counting on BHI medium.

A scale-up batch experiment was performed in a 14 L fermentor (New Brunswick BioFlo®/CelliGen® 115, Eppendorf) to evaluate the microbial growth using the best conditions assessed in the preliminary batch experiments. The experiment was performed in a working volume of 4 L of BHI medium inoculated with 2% bacterial cells suspension (8.67 ± 0.40 CFU mL^{-1}), using the following parameters: 30°C, pH 7.00, agitation of 130 rpm, air sparging at 0.5 vvm, 40 mL of a solution 3% of Antifoam 204 (Sigma-Aldrich) added at the beginning of the process. Samples were withdrawn every 2 h and cell growth was determined by viable counting on BHI medium. After 24 h, the culture was centrifuged (45 min at 3428 × *g*) and recovered cells were suspended in a 5% sucrose solution at the ratio 1:5 (w:v). The strain was freeze-dried, and cell viability was determined by counting on BHI medium immediately after freeze-drying and after 3 and 6 months of storage at room temperature.

Microbial Growth in Liquid Media Containing Food By-Products

The strain TL13 was inoculated in several liquid media containing agro-food industrial by-products to find a low-cost carbon source useful for its growth. To this end, the strain was inoculated into 10 mL of liquid substrates containing 1, 5 or 10% of whey, protein hydrolysate, exhausted yeasts, molasse or vinasse, kindly provided by Agriges S.r.l. (San Salvatore Telesino, Benevento, Italy). The strain TL13 grown in BHI was used as control. Samples were withdrawn after 48 h of incubation at 30°C, to determine bacterial growth.

Production of Bacterial Inoculants on Nutrient-Supplemented Vermiculite

Solid state fermentation (SSF) was performed in gas permeable polypropylene bags (SacO2, Belgium). Growth on inert support was carried out by adopting the procedures described by Graham-Weiss et al. (1987). Sterile vermiculite, moistened with BHI broth or with a solution of exhausted yeasts and vinasse, was inoculated with the selected strain TL13 (10^6 bacterial cells per g of vermiculite). After incubation (15 days at 30 ± 1°C),

an aliquot was used to develop liquid inoculants recovering the bacterial cells and added them in a raw castor oil/alginate based emulsion following the protocol described by Fravel et al. (1985) with some modifications. Another amount of inoculated vermiculite was dried for 15 days at 30 ± 2°C to achieve a microbial-based solid formulation. Samples were withdrawn immediately after incubation and after the development of formulations to determine bacterial growth by viable counting on BHI medium.

Pot Trials

The ability of the selected strain TL13 to promote plant growth was evaluated in growth chamber pot trials. The experimental set up was performed according to standard procedure (DM 27/01/2014, 2014) with some modifications. Maize (*Zea mays*, Class FAO 400/gg 120) seeds were surface sterilized by 5 min washing in NaClO 5% solution and germinated on damp tissue paper for 48 h. Seeds were planted in 10 cm Ø plastic pots filled with 0.5 kg of unsterilized soil (35% clay, 27% silt and 38% sand; pH-H_2O 7.7; electrical conductivity 0.6 dS m^{-1}; $CaCO_3$ 37 g kg^{-1}; organic matter 16.3 g kg^{-1}; organic carbon 9.5 g kg^{-1}; total nitrogen 1.2 g kg^{-1}; C/N ratio 7.9; phosphorus available 59 mg kg^{-1}; potassium exchangeable 296 mg kg^{-1}; calcium exchangeable 2089 mg kg^{-1}; magnesium exchangeable 111 mg kg^{-1}; sodium exchangeable 57 mg kg^{-1}; Cation Exchange Capacity 12.1 cmol(+) kg^{-1}). At planting, soil was inoculated with the strain TL13 at a concentration of approximately 1×10^6 cells g^{-1}.

The strain TL13 was inoculated in three different formulates: raw castor oil/alginate based emulsion (E-TL13), dried vermiculite (V-TL13) and recovered cells (R-TL13) diluted in sterile Ringer's solution (Oxoid). Un-inoculated soil (C) was used as control. All tests were performed in triplicate and three seeds were planted for each pot.

Plants were grown under controlled conditions with a constant temperature of 28 ± 0.5°C, a 16 h light/8 h dark photoperiod, relative moisture 70% and daily watered for 15 days.

After 15 days, the plants were sampled and were measured vegetative parameters as total plant length, root and shoot length, root and shoot fresh weight, root and shoot dry weight percentage.

Statistical Analyses

Data were analyzed by one-way ANOVA followed by Duncan's HSD *post hoc* for pairwise comparison of means (at $P < 0.05$) using SPSS 19.0 statistical software package (SPSS Inc., Cary, NC, United States).

RESULTS

Plant Growth Promoting Activities of Bacterial Isolates

A total of 13 bacterial isolates (from TL1 to TL13) were obtained from the rhizosphere of wheat plants using Augier liquid medium followed by streaking on LG agar medium. Isolates were preliminarily screened for their potential plant growth promoting activities, as IAA and siderophores production and ACC-deaminase activity (**Table 1**).

The results indicated that about 85% of isolates were able to synthetize IAA, although most of them at low amounts (ranging from 1.32 to 5.98 mg L^{-1}). The two isolates, TL8 and TL13, showed the highest IAA production up to 13.20 ± 1.80 or 22.16 ± 2.67 and 12.91 ± 0.64 or 33.26 ± 1.67 mg L^{-1}, respectively, in the absence and in the presence of L-tryptophan (**Table 1**).

Ten isolates produced siderophores showing orange haloes around the colony in CAS agar ranging from 10 to 35 mm (**Table 1**). Among these, the isolates TL3, TL4, and TL13 exhibited the highest siderophores production (halo dimension 30–33 mm); while, the isolates TL1, TL3, TL7, TL8, and TL12 produced haloes ranging approximately from 20 to 23 mm.

Moreover, seven isolates (TL1, TL2, TL4, TL6, TL7, TL8, and TL13), corresponding to about 54%, revealed ACC-deaminase activity because they were able to grow on MM medium supplemented with ACC (**Table 1**).

Identification and Phylogenetic Analysis of Selected Strains

The preliminary screening for the assessment of plant growth promotion activities allowed for the selection of the TL8 and TL13 isolates. The nearly full-length sequence of 16S rRNA gene (about 1,450 bp) of the strains TL8 and TL13 revealed an identity of 99% with *Kosakonia sacchari*, *K. pseudosacchari*, *Kosakonia oryzae*, and *Kosakonia radicincitans* species using Blast software. To establish the identification of the two selected strains, a phylogenetic tree generated from the distance data using the Neighbor-Joining method with the Maximum Composite

TABLE 1 | Preliminary screening for the assessing the plant growth-promoting activities of bacterial isolates obtained from wheat rhizosphere.

Isolate	IAA† in NB (mg L^{-1})	IAA§ in NB + TRP (mg L^{-1})	Siderophores# (mm)	ACC-deaminase activity*
TL1	$2.59 \pm 0.06^{g-m}$	0.00 ± 0.00^{n}	20.0 ± 0.00^{cd}	++
TL2	$3.16 \pm 0.50^{g-i}$	$1.82 \pm 0.31^{i-m}$	0.00 ± 0.00^{f}	+
TL3	$1.56 \pm 0.07^{l-n}$	1.32 ± 0.02^{mn}	30.0 ± 0.00^{ab}	–
TL4	$3.40 \pm 0.02^{f-h}$	4.90 ± 0.63^{de}	33.33 ± 5.77^{a}	+
TL5	$1.62 \pm 0.02^{l-m}$	1.42 ± 0.00^{mn}	23.33 ± 5.77^{bc}	–
TL6	5.98 ± 1.03^{d}	$3.95 \pm 0.33^{e-g}$	10.0 ± 0.00^{e}	++
TL7	5.89 ± 0.60^{d}	5.15 ± 0.51^{de}	23.33 ± 5.77^{bc}	++
TL8	13.20 ± 1.80^{c}	12.91 ± 0.64^{c}	23.33 ± 11.55^{bc}	++
TL9	0.00 ± 0.00^{n}	0.00 ± 0.00^{n}	0.00 ± 0.00^{f}	–
TL10	$1.68 \pm 0.67^{i-m}$	$4.69 \pm 1.32^{d-f}$	0.00 ± 0.00^{f}	–
TL11	$2.23 \pm 0.02^{h-m}$	0.00 ± 0.00^{n}	13.33 ± 5.77^{e}	–
TL12	1.43 ± 0.02^{mn}	$3.05 \pm 0.07^{g-l}$	20.0 ± 0.00^{cd}	–
TL13	22.16 ± 2.67^{b}	33.26 ± 1.67^{a}	30.0 ± 0.00^{ab}	++

†*IAA production in Nutrient Broth without L-tryptophan, values represent the means ± SD of three replicates.* §*IAA production in Nutrient Broth supplemented with L-tryptophan, values represent the means ± SD of three replicates.* #*Halo size (mm) = diameter of clearing or halo zone/colony diameter, values represent the means ± SD of three replicates. Different letters after values indicate significant differences ($P < 0.05$).* **– no growth; + middle growth; ++ high growth.*

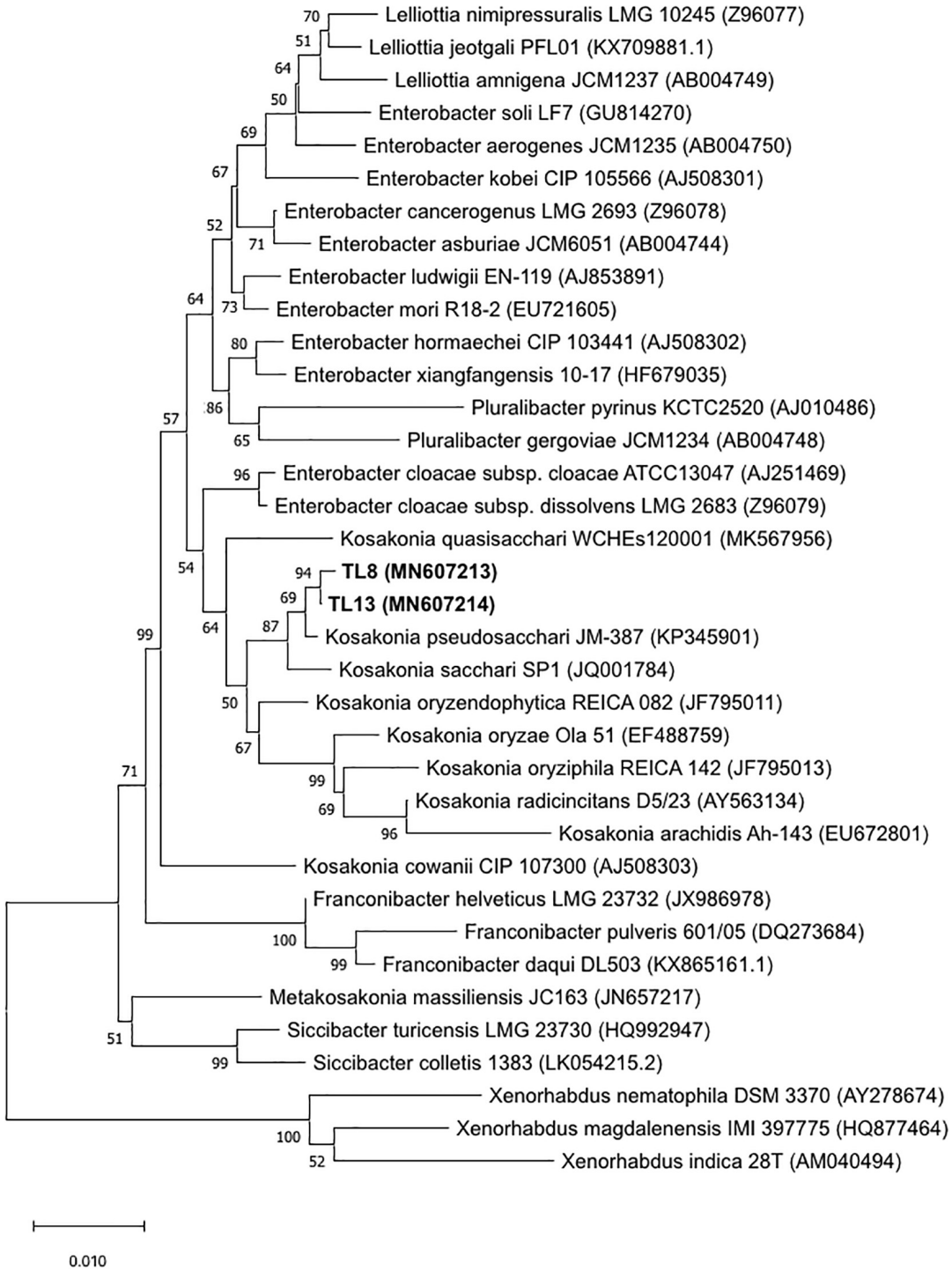

FIGURE 1 | Neighbor-Joining tree based on the comparison of 16S rRNA gene sequences of bacterial strains TL8 and TL13 and 31 type strains related to genus *Kosakonia* sequences from RDP and NCBI. Bootstrap values (expressed as percentages of 1,000 replications) are given at the nodes. The sequence accession numbers used for the phylogenetic analysis are shown in parentheses following the species name. *Xenorhabdus* type strain sequences were used as out group. The scale bar estimates the number of substitutions per site.

Likelihood model in the MEGAX Program was constructed including the 16S rRNA sequences of type strains related to *Kosakonia* genus (**Figure 1**). High bootstrap values, ranging from 50 to 100%, were observed and indicated significant branching points in the phylogenetic tree. The phylogenetic tree indicated that the closest relative species of the two selected strains

was *K. pseudosacchari* (cluster with bootstrap value of 69%), demonstrating that the strains TL8 and TL13 can be classified as belonging to this species (**Figure 1**).

PGP Traits, Phenotypic Characteristics and Rhizosphere Competence of *Kosakonia pseudosacchari* Strains

The selected strains *K. pseudosacchari* TL8 and TL13 were further characterized to evaluate other plant growth promotion activities as well as antagonistic behaviors. Quantitative estimation of phosphate solubilization by molybdenum blue assay in PKV liquid medium indicated that the strains TL8 and TL13 were able to solubilize up to 348.05 ± 12.77 and 346.05 ± 25.62 mg L^{-1} of phosphate starting from dicalcium phosphate (**Table 2**). Measurement of ammonia in peptone water liquid medium by quantitative Nessler's reagent test highlighted that both bacterial strains TL8 and TL13 were capable to produce ammonia (2.24 ± 0.03 and 2.37 ± 0.03 mg L^{-1}, respectively; **Table 2**) in medium without nitrogen source. Moreover, *K. pseudosacchari* TL8 and *K. pseudosacchari* TL13 were potentially able to fix atmospheric nitrogen (N_2) due to the presence of the *nif*H gene detected by specific PCR amplification as well as exhibited ACC deaminase activity producing up to 3.04 ± 0.10 and 3.31 ± 0.11 μM of α-ketobutyrate protein mg^{-1} in 30 min (**Table 2**). As reported in **Table 2**, quantitative assay showed a siderophore concentration produced by the strains *K. pseudosacchari* TL8 and TL13 equal to 32.00 ± 0.92 and 29.77 ± 1.8 psu, respectively. Indeed, both strains exerted antimicrobial activity against soil-borne plant pathogens (**Table 2**) revealed by a considerable reduction of mycelium growth of *B. cinerea* B12, *P. infestans* ph1, *P. cactorum* ph3, and *P. cryptogea* ph4, in respect to the control plates.

Kosakonia pseudosacchari TL8 and TL13 were found to be salt-tolerant because they were able to grow in the liquid culture medium containing up to 13% w/v of NaCl (**Table 2**). In detail, no differences were found in the bacterial growth up to 8.0% w/v of NaCl reaching a concentration of about 1×10^8 CFU mL^{-1} after 24 h of incubation (**Table 2**). At higher NaCl concentration (from 9.0 to 13% w/v) the two strains grew slowly reaching a bacterial growth of two orders of magnitude lower (about 1×10^6 CFU mL^{-1}) after 48 h of incubation (**Table 2**). The two strains *K. pseudosacchari* TL8 and TL13 grew also up to about 1×10^8 CFU mL^{-1} after 24 h of incubation at different temperatures (28, 30, 37, and 42°C). Finally, both strains tolerated a pH range between 4.0 and 8.0 reaching a final concentration of about 1×10^8 CFU mL^{-1} after 24 h (**Table 2**).

In order to test the ability of the two selected strains *K. pseudosacchari* strains TL8 and TL13 to colonize the root surface, sterile tomato radicles were inoculated and observed by fluorescence microscope after staining with the LIVE/DEAD® BacLight™ kit reagents. As shown in **Figure 2**, bacterial cells were clearly visualized on plant tissues highlighting that both *K. pseudosacchari* TL8 and *K. pseudosacchari* TL13 successfully colonized tomato's radicle. In particular, bacterial cells of the strains TL8 resulted congregated on root surfaces (**Figure 2a**); whereas, cells of the strain TL13 appeared scattered (**Figure 2b**).

Investigation and Optimization of Growth Conditions

On the basis of PGP traits, the strain *K. pseudosacchari* TL13 was selected for further investigations in order to produce an innovative bacterial inoculant.

The first step was to explore and define the best growth conditions of the strain *K. pseudosacchari* TL13. To this end, a kinetic growth curve of the strain TL13 was obtained by Microplate Reader test. This preliminary investigation showed that the exponential phase started after 4 h of incubation and continued until 10 h, when begun the stationary phases (data not shown).

Batch experiments were then performed to investigate the effect of agitation and air sparging on the bacterial growth. The highest bacterial concentration in the shorter time was recorded in the batch 2 reaching a value of 8.87 ± 0.02 log CFU mL^{-1} after 8 h of incubation (**Figure 3**), after that, a significant decrease in its concentration was observed. Similarly, in the batch 1 was detected an increase of three orders of magnitude at 10 and 12 h (8.88 ± 0.00 log CFU mL^{-1} and

TABLE 2 | Differential phenotypic characteristics and plant growth-promoting traits of bacterial strains *Kosakonia pseudosacchari* TL8 and TL13.

Characteristic/ Activity	*Kosakonia pseudosacchari* TL8	*Kosakonia pseudosacchari* TL13
IAA in NB† (mg L^{-1})	13.20 ± 1.80	22.16 ± 2.67
IAA in NB + T§ (mg L^{-1})	12.91 ± 0.64	33.26 ± 1.67
Siderophores production (psu)	32.00 ± 0.92	29.77 ± 1.8
ACC-deaminase activity (μM of α-ketobutyrate protein mg^{-1} in 30 min)	3.04 ± 0.10	3.31 ± 0.11
Ca_2HPO_4 solubilization (mg L^{-1})	348.05 ± 12.77	346.05 ± 25.62
*Nif*H gene	+	+
Ammonia accumulation (mg L^{-1})	2.24 ± 0.03	2.37 ± 0.03
NaCl tolerance range (w/v, 0.5–8%) 24 h	1×10^8 CFU mL^{-1}	1×10^8 CFU mL^{-1}
NaCl tolerance range (w/v, 9–13%) 48 h	1×10^6 CFU mL^{-1}	1×10^6 CFU mL^{-1}
pH range at 24 h	5–8	5–8
Temperature range (°C) at 24 h	28–42	28–42
Antagonistic activity	+ against *Botrytis cinerea* B12, *Phytophthora infestans* ph1, *Phytophthora cactorum* ph3, *Phytophthora cryptogea* ph4	+ against *Botrytis cinerea* B12, *Phytophthora infestans* ph1, *Phytophthora cactorum* ph3, *Phytophthora cryptogea* ph4

†*NB = Nutrient Broth.* §*NB + T = Nutrient Broth supplemented with L-tryptophan.*

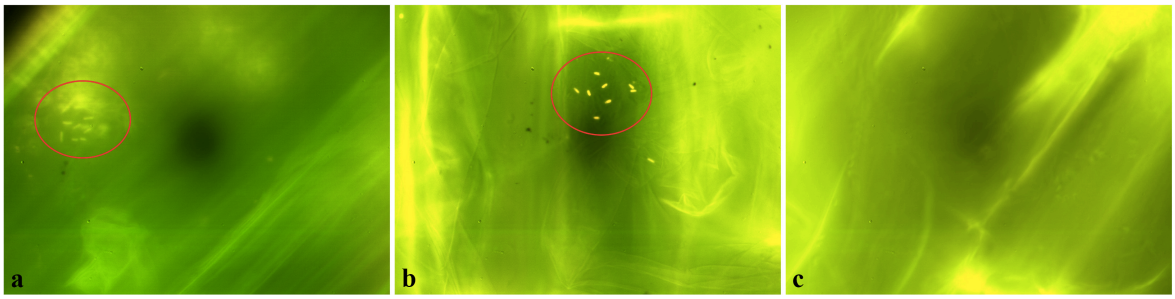

FIGURE 2 | Colonization of tomato's radicles by *Kosakonia pseudosacchari* TL8 **(a)**, *Kosakonia pseudosacchari* TL13 **(b)**, and uninoculated control **(c)** detected by LIVE/DEAD BacLigh bacterial viability kit and observed under fluorescence microscope.

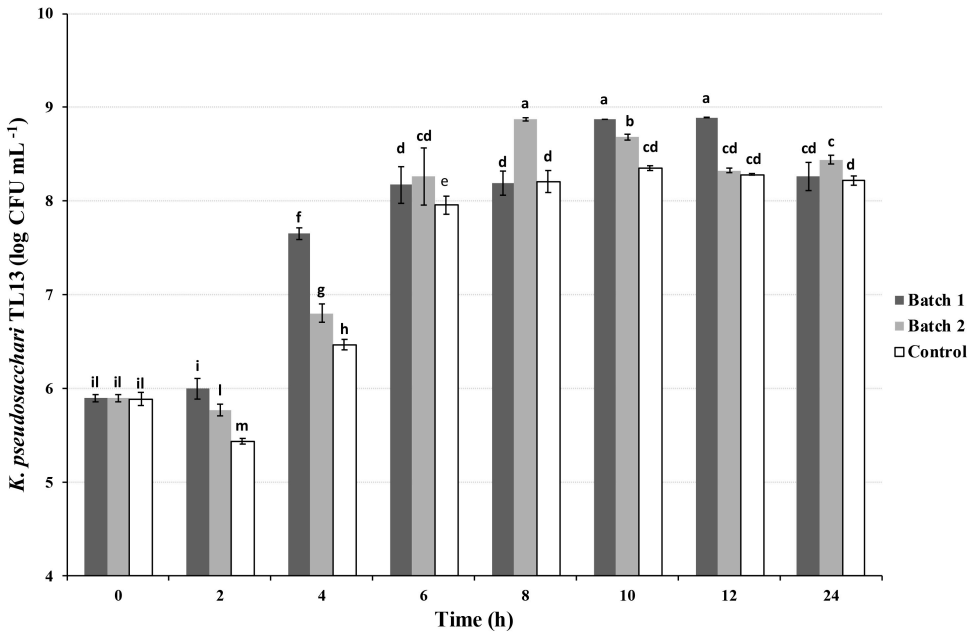

FIGURE 3 | Viable count of *Kosakonia pseudosacchari* TL13 during its growth in batch experiments using BHI medium (30°C and pH 7.00). Batch 1: shaking at 130 rpm; Batch 2: shaking at 130 rpm and air sparging at 0.5 vvm; Control: no shaking and no air sparging. The error bars represent the means ± SD of three replicates. Different letters indicate significant differences ($P < 0.05$).

8.89 ± 0.00 log CFU mL^{-1}) in respect to the beginning of the experiment (0 h; 5.90 ± 0.04 log CFU mL^{-1}), decreasing up to 8.26 ± 0.15 log CFU mL^{-1} at 24 h (**Figure 3**). However, in both conditions, the *K. pseudosacchari* TL13 load was approximately one order of magnitude greater than that recovered in the control at the same sampling time (ranging from 5.89 ± 0.07 to 8.35 ± 0.03 log CFU mL^{-1}; **Figure 3**).

On the basis of these results, growth conditions of batch 2 (shaking at 130 rpm and air sparging at 0.5 vvm) were chosen to perform the scale-up of the experiment in a 10 L fermentor. In this condition, although at 8 h was detected a bacterial concentration (8.66 ± 0.02 log CFU mL^{-1}) similar to that recorded in the previous batch experiment, the exponential phase persisted up to 24 h reaching a bacterial load of 9.33 ± 0.18 log CFU mL^{-1} (**Figure 4**). Moreover, to explore the tolerance of the strain *K. pseudosacchari* TL13 to desiccation and to test its shelf-life, the viability of freeze-dried bacterial cells obtained by fermentor experiment was estimated over time. Immediately after freeze-drying, a bacterial concentration of 10.43 ± 0.10 log CFU g^{-1} was determined. This value remained constant after 3 months of storage (10.40 ± 0.06 log CFU g^{-1}) and decrease of about 1 log after 6 months reaching a concentration of 9.57 ± 0.14 log CFU g^{-1}.

Production of Eco-Friendly and Low-Cost Bacterial Inoculants

Different agro-food industrial by-products were used to obtain an eco-sustainable and cheap carbon source for the growth at industrial level of *K. pseudosacchari* TL13 and its use as inoculant. The strain TL13 resulted able to grow in presence of several carbon sources (whey, protein hydrolysate, exhausted yeasts, or

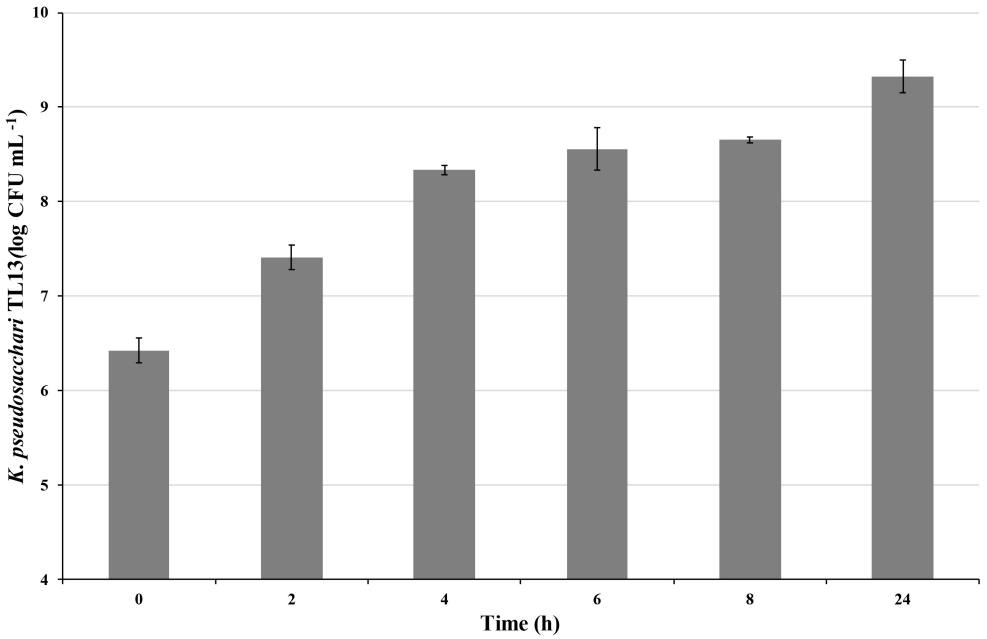

FIGURE 4 | Viable count of *Kosakonia pseudosacchari* TL13 during its growth in 10 L fermentor at 30°C, pH 7.00, shaking at 130 rpm and air sparging at 0.5 vvm. The error bars represent the means ± SD of two replicates.

vinasse) at different concentrations (1, 5 and 10%) reaching a bacterial load of about 8–9 log CFU mL^{-1} (**Table 3**). The only exception was the liquid medium containing molasse that determined the lowest bacterial growth at 5% (7.08 ± 0.18 log CFU mL^{-1}) and no growth at 1 and 10% (**Table 3**). The highest bacterial growth was detected in the medium containing 10% exhausted yeasts (8.86 ± 0.21 log CFU mL^{-1}), that was comparable to the optimal synthetic medium used as control (8.93 ± 0.01 log CFU mL^{-1}), followed by the liquid medium containing 5% vinasse (8.81 ± 0.07 log CFU mL^{-1}; **Table 3**). Therefore, SSF on nutrient-supplemented vermiculite of the strain *K. pseudosacchari* TL13 for the production of inoculant was performed using a solution of exhausted yeasts and vinasse. Microbial concentration increased after 15 days of incubation of about three orders of magnitude from 6.81 ± 0.05 to 9.34 ± 0.11 log CFU g^{-1}. No significant differences ($P > 0.05$) were detected between *K. pseudosacchari* TL13 grown on vermiculite moistened with exhausted yeasts and vinasse and the vermiculite moistened with BHI used as control (9.20 ± 0.65 log CFU g^{-1}).

Solid state fermentation products were used to develop solid and liquid inoculants containing a microbial load of about 6.7–6.9 log CFU g^{-1} or mL^{-1}, which remained constant up to 28 days.

IN VIVO POT EXPERIMENTS

Maize plants were positively affected by inoculation with the strain *K. pseudosacchari* TL13. Indeed, several plant growth parameters significantly increased in the soils treated with solid or liquid inoculants as shown in **Table 4**. In particular, E-TL13 treatment (raw castor oil/alginate based emulsion containing *K. pseudosacchari* TL13 cells) showed the best results, in which a significant increase ($P < 0.05$) of total plant length (63.83 ± 4.51 cm), root length (23.67 ± 2.57 cm), and root fresh weight (1.28 ± 0.11 g) was recorded in E-TL13 treated plants in respect to the un-inoculated control (49.17 ± 3.40 cm, 11.06 ± 0.90 cm, and 0.80 ± 0.13 g, respectively; **Table 4**). Similarly, a significant increase in the root length was also observed in the V-TL13 (dried vermiculite containing *K. pseudosacchari* TL13 cells) and R-TL13 (*K. pseudosacchari* TL13 cells diluted in sterile Ringer's solution) treatments reaching values of 18.50 ± 2.26 and 23.13 ± 1.99 cm, respectively (**Table 4**). Interestingly, V-TL13 treatment induced a significant increase

TABLE 3 | Viable counts of *Kosakonia pseudosacchari* TL13 (log CFU mL^{-1}) after 48 h of growth at 30°C in several liquid media containing different agro-industrial by-products as carbon source at three percentage (1, 5, and 10%).

Agro-industrial by-products	Percentage of by-products in the liquid medium		
	1%	5%	10%
Whey	8.18 ± 0.02^{e}	7.98 ± 0.07^{fg}	7.95 ± 0.03^{fg}
Protein hydrolysate	8.05 ± 0.01^{f}	8.30 ± 0.03^{d}	8.18 ± 0.07^{e}
Exhausted Yeast	8.30 ± 0.09^{d}	8.48 ± 0.08^{c}	8.86 ± 0.21^{ab}
Molasse	0.00 ± 0.00^{i}	7.08 ± 0.18^{h}	0.00 ± 0.00^{i}
Vinasse	7.94 ± 0.02^{g}	8.81 ± 0.07^{b}	7.98 ± 0.02^{fg}
BHI (control)	–	8.93 ± 0.01^{a}	–

Values represent the means ± SD of three replicates. Different letters indicate significant differences ($P < 0.05$).

TABLE 4 | Effect of different inoculant formulations on total plant length (cm), root length (cm), shoot length (cm), root fresh weight (g), shoot fresh weight (g), root dry weight (%), shoot dry weight (%) of maize plants.

	Soil treatment			
Plant parameters	**V-TL13**	**E-TL13**	**R-TL13**	**C**
Total plant length (cm)	51.50 ± 4.63^{ab}	63.83 ± 4.5^{a}	58.56 ± 4.78^{ab}	49.17 ± 3.40^{b}
Root length (cm)	18.50 ± 2.26^{ab}	23.67 ± 2.57^{a}	23.13 ± 1.99^{a}	11.06 ± 0.90^{b}
Shoot length (cm)	33.00 ± 2.87^{a}	40.17 ± 2.55^{a}	35.44 ± 3.68^{a}	38.11 ± 2.77^{a}
Root fresh weight (g)	1.01 ± 0.15^{ab}	1.28 ± 0.11^{a}	0.81 ± 0.15^{b}	0.80 ± 0.13^{b}
Shoot fresh weight (g)	1.19 ± 0.21^{a}	1.58 ± 0.14^{a}	1.54 ± 0.30^{a}	1.30 ± 0.27^{a}
Root dry weight (%)	15.30 ± 1.64^{a}	15.03 ± 1.52^{a}	19.73 ± 1.08^{a}	17.25 ± 2.42^{a}
Shoot dry weight (%)	9.62 ± 0.29^{a}	7.75 ± 0.64^{ab}	8.53 ± 0.83^{ab}	6.84 ± 0.40^{b}

V-TL13, soil inoculated with dried vermiculite containing K. pseudosacchari TL13; E-TL13, soil inoculated with raw castor oil/alginate based emulsion containing K. pseudosacchari TL13; R-TL13, soil inoculated with K. pseudosacchari TL13 cells diluted in sterile Ringer's solution; C, un-inoculated soil. Values represent the means ± SD of three replicates. Different letters indicate significant differences ($P < 0.05$).

of shoot dry weight percentage (9.62 ± 0.29%) compared to un-inoculated control (6.84 ± 0.40%; **Table 4**). However, also E-TL13 and R-TL13 treatments showed a similar trend of this plant parameter although no significant differences were detected ($P > 0.05$; **Table 4**).

DISCUSSION

PGP Traits, Phenotypic Characteristics and Rhizosphere Competence

In the last decades, the development and the use of microbial inoculants have elicited great interest as an ecofriendly alternative strategy to the application of synthetic fertilizers for plant growth promotion and pest management. This approach improves the sustainability of agricultural systems by reducing environmental and human health risks due to the application of chemical fertilizers and pesticides in crop production (Rahman et al., 2018). In this context, it is necessary to find new microorganisms that can exert multiple plant beneficial activities to develop a low-cost inoculant. The ecological approach developed in this study enabled the isolation of new plant growth-promoting strains *K. pseudosacchari* TL8 and *K. pseudosacchari* TL13. This species belongs to the phylum Proteobacteria, and in particular to the γ-proteobacteria class. This bacterial class, that commonly colonize the rhizosphere of crop plants (Sheridan et al., 2017) or is associated to plant biomass (Montella et al., 2017), is ubiquitous in the soil environment (Ventorino et al., 2019). Indeed, it includes different species that were known to synthesize substances which promote plant growth (i.e., hormones such as IAA, ethylene, and gibberellins), to increase nutrient availability (i.e., N, P, Fe) and their uptake in soil (Kim et al., 2011) and they act as plant disease-suppressive bacteria (Kobayashi et al., 2002; Haas and Défago, 2005). Therefore, the presence of these populations in the soil highlight its high biological fertility potential because they could improve the growth, fitness and health of agricultural plants playing an important role in the bionetwork function of soils (Ventorino et al., 2018). Although many members belonging to the genus *Kosakonia*, as *K. radicincitans*, are known to interact and exert beneficial effects on plant growth (Bergottini et al., 2015; Kämpfer et al., 2016; Berger et al., 2017; Brock et al., 2018), PGP properties in *K. pseudosacchari* species are poorly investigated. Indeed, it was recognized as a novel endophyte species only recently (Kämpfer et al., 2016) and siderophore production was the sole PGP activity previously documented (Arora and Verma, 2017). The main PGP activity by the new PGPR strain *K. pseudosacchari* TL13 was the production of IAA. About 80% of rhizospheric microorganisms are able to produce and release auxins as a secondary metabolite, among these IAA is the most common that can contribute to plant-microbe interaction (Olanrewaju et al., 2017). It is an important growth enhancer because it plays a central role in cell division, elongation, fruit development and senescence, and it has a significant effect on plant root system development (Duca et al., 2014). The concentration of IAA produced by the strain TL13 is similar or higher to that recovered in *K. radicincitans* YD4 strain (about 24 $\mu g\ mL^{-1}$) by Bergottini et al. (2015). Interestingly, an increase of 50% of this phytohormone synthesis was observed in the strain grown in the presence of L-tryptophan suggesting a tryptophan-dependent IAA biosynthesis pathway. The synthesis and secretion of IAA could also be linked to the synthesis of ACC synthase in the plant to catalyze the formation of ACC (Glick, 2014). Synthesis of ACC deaminase is also one of the crucial bacterial traits that can facilitate plant growth in the presence of several abiotic or biotic stress (Ali et al., 2014; Glick, 2014). Indeed, *K. pseudosacchari* strains isolated in this work were able to produce ACC deaminase. As for IAA, this is the first work reporting ACC deaminase activity in *K. pseudosacchari* species.

Another interesting PGP activity is the production of siderophores. These are iron-chelating agents with low molecular masses (200–2000 Da), which are produced by microorganisms especially when the bioavailability of Fe is low (Ahmed and Holmström, 2014). Siderophore producing bacteria can improve plant growth by reducing the Fe availability for the phytopathogens and increasing nutrient availability to the plant (Ahmed and Holmström, 2014). As expected, the two *K. pseudosacchari* strains TL8 and TL13 were able to produce iron chelating siderophores, a trait commonly present in *Kosakonia* genus as largely reported by the

literature (Arora and Verma, 2017; Chimwamurombe et al., 2016; Lambrese et al., 2018). Siderophore production could be involved also in disease suppression. Indeed, PGPR could act also as biocontrol agents against soil-borne plant pathogens by different ways like competing for nutrients or space, limiting available Fe supply through producing siderophores or by the production of lytic enzymes and antibiosis (Bhattacharyya and Jha, 2012). *K. pseudosacchari* TL8 and TL13 exerted antagonistic activity against *Botrytis* and *Phytophthora* species. To the best of our knowledge, this is the first work reporting suppressive effect against plant pathogens in *K. pseudosacchari* species highlighting that these strains could use also for pest control in agricultural plants.

In addition, *K. pseudosacchari* TL8 and TL13 were also able to solubilize phosphate. Phosphorus is one of the major growth-limiting nutrients required by plants due to its limited availability. There is a great interest in searching phosphate solubilizing bacteria that are able to increase phosphate content and bioavailability in the soil and therefore they are considered promising bio-fertilizers for agriculture enhancement (Kalayu, 2019). Within genus *Kosakonia* this ability was previously reported only in the strain *Kosakonia* sp. A37 (Chakdar et al., 2018).

It is known that some PGPB can fix atmospheric nitrogen into ammonium, and consequently increase the availability of this nutrient in the rhizosphere. The use of these microorganisms in agriculture could decrease the use of chemical N-based fertilizers and therefore their negative impact on the environment as soil quality depletion, pollution and human health (Noar and Bruno-Bárcena, 2018). According to previous works in which several *Kosakonia* species were described as N_2-fixing bacteria (Chen et al., 2014; Chin et al., 2017; Sun et al., 2018), the new strains *K. pseudosacchari* TL8 and TL13 were able to produce ammonia and potentially able to fix atmospheric nitrogen due to the presence of the *nif*H gene encoding nitrogenase reductase enzyme.

Kosakonia pseudosacchari TL8 and *K. pseudosacchari* TL13 showed also interesting abiotic stress tolerance because they were able to grow in a wide range of temperature, pH and salt. These phenotypic properties could help the tolerance of crops cultivated in stress conditions. In particular, salinity is one of the most common abiotic stress in modern agriculture because the irrigation of summer crops with saline water, especially in the coastal regions, lead to an increase of soil salinization in many areas of the world causing major problems for the productivity of agricultural crops and reducing the soil microbial activity (Kumar and Verma, 2018).

As observed *in vitro* assay under fluorescence microscope after treatment with BacLight bacterial viability kit, *K. pseudosacchari* TL8 and TL13 were able to colonize tomato radicles. This result was in according to Kämpfer et al. (2016) which describe *K. pseudosacchari* species as an endophyte of maize plants. Moreover, this ability was also described for other *Kosakonia* species as *K. radicincitans*, able to colonize the root surface of winter wheat (Witzel et al., 2017), or of cucumbers (Sun et al., 2018).

Production of a Low-Cost and Eco-Sustainable Bacterial Inoculants and Their Effectiveness in Inoculated Plants

Based on PGP traits, the strain *K. pseudosacchari* TL13 was selected for the production of a new low-cost and eco-sustainable bacterial inoculant. In order to develop new bacterial inoculants and to ensure the application of a suitable number of viable and active microbial cells, high biomass production, formulation and shelf life are crucial steps (Bashan et al., 2014). Preliminary investigations in synthetic medium allowed us to assess the growth curve and the best growth condition and parameters to increase bacterial biomass and to obtain a suitable microbial concentration of the strain *K. pseudosacchari* TL13. Besides, microbial cells of TL13 were also subjected to freeze-drying, a common method for preserving bacteria, in order to evaluate their shelf life over time. Although freeze-dried *K. pseudosacchari* TL13 remained viable up to 6 months, this approach could not be suitable at industrial level for its higher production costs than others as foam drying (Morgan et al., 2006). Indeed, production costs of a bio-formulate, which include raw material, equipment and staff, must be competitive in relation to that for the production of chemical fertilizers (Lobo et al., 2019). In general, the use of a low-cost culture medium for the growth and production of microbial biomass is an important issue (Liu et al., 2014; Xu et al., 2015). In this work, to reduce the costs and to develop an eco-sustainable inoculant, the use of several agro-industrial by-products as carbon source was evaluated for the production of *K. pseudosacchari* TL13 by SSF on vermiculite. Indeed, valorization of organic waste biomass and by-products derived from agriculture and food processing factories by a sustainable and harmless disposal have generated interest in microbial biotechnologies (Pagliano et al., 2019). This new approach to by-products management is eco-friendly, easy to be conducted and economically advantageous. Interestingly, *K. pseudosacchari* TL13 was able to use different organic by-products as carbon source although the highest bacterial growth was observed in liquid media containing exhausted yeasts or vinasse. This approach allowed to obtain a suitable bacterial concentration (10^6 CFU mL^{-1} or g^{-1}) in the two final, solid (vermiculite-based) or liquid (raw castor oil/alginate-based emulsion), bio-formulations. The development of two kinds of formulations was important to evaluate their different advantages. Indeed, liquid emulsion formulation allowed to protect the bio−inoculant from desiccation as well as from osmotic and oxidative stress (John et al., 2010); whereas, solid vermiculite-based inoculants were very stable, require no special storage and has good seed-sticking properties (Graham-Weiss et al., 1987). Although, both *K. pseudosacchari* TL13 formulations exerted positive effects on maize plants cultivated in unsterilized soil, the liquid raw castor oil/alginate-based emulsion showed the best results increasing several plant parameters. Liquid formulations are often preferred by users because the product is ready to use. However, the stable and low-cost solid vermiculite-based formulation could be used in agricultural crops for increasing dry matter. These results are in accord with previous

works in which inoculum of *Kosakonia* sp. strains were able to exert positive effects in various crops as radish (Berger et al., 2015), yerba mate (Bergottini et al., 2015), tomato (Berger et al., 2017), and maize (Berger et al., 2018).

CONCLUSION

The *K. pseudosacchari* strains isolated in this study showed multiple PGP traits as well as antimicrobial activity against several soilborne plant pathogens. In particular, the new selected strain *K. pseudosacchari* TL13 was able to colonize plant roots and improve plant growth. To our knowledge, this is the first work reporting effective multiple PGP abilities and antimicrobial activity in *K. pseudosacchari* species. Moreover, the ability of *K. pseudosacchari* TL13 to efficiently use agro-industrial organic by-products as carbon source for its metabolism makes this strain a promising candidate for the development of new biofertilizers for sustainable agriculture.

DATA AVAILABILITY STATEMENT

The datasets presented in this study can be found in online repositories. The names of the repository/repositories and accession number(s) can be found at: https://www.ncbi.nlm.nih.gov/genbank/, MN607213 and MN607214.

AUTHOR CONTRIBUTIONS

IR performed the experiments, analyzed the data, and drafted the manuscript. VV significantly contributed in results interpretation and drafted the manuscript. PA coordinated the development of bio-formulates and *in vivo* experiments. FC contributed to plant-growth promoting assays and evaluation of microbial growth in liquid media containing agro-industrial by-products. AT provided the soilborne plant pathogens. OP conceived the study and participated in its design and coordination. All authors approved and reviewed the manuscript.

FUNDING

This work was supported by FSE-FESR PON R&I 2014-2020, Ph.D. program on "Sustainable agricultural and forestry systems and food security" – XXXIII cycle and by Agriges S.r.l. within the research project "BENEVEGEFIT", MISE—Agrifood PON I&C 2014-2020.

ACKNOWLEDGMENTS

The authors thank Alessandro Robertiello for technical support in batch and fermentor experiments.

REFERENCES

Ahmed, E., and Holmström, S. J. M. (2014). Siderophores in environmental research: roles and applications. *Microb. Biotechnol.* 7, 196–208. doi: 10.1111/1751-7915.12117

Alfonzo, A., Lo Piccolo, S., Conigliaro, G., Ventorino, V., Burruano, S., and Moschetti, G. (2012). Antifungal peptides produced by *Bacillus amyloliquefaciens* AG1 active against grapevine fungal pathogens. *Ann. Microbiol.* 62, 1593–1599. doi: 10.1007/s13213-011-0415-2

Ali, S., Charles, T. C., and Glick, B. R. (2014). Amelioration of high salinity stress damage by plant growth-promoting bacterial endophytes that contain ACC deaminase. *Plant. Physiol. Bioch* 80, 160–167. doi: 10.1016/j.plaphy.2014.04.003

Alori, E. T., and Babalola, O. O. (2018). Microbial inoculants for improving crop quality and human health in Africa. *Front. Microbiol.* 9:2213. doi: 10.3389/fmicb.2018.02213

Amarasinghe, R. M. N. T., Wang, J.-H., Xie, W. X., Peng, L. C., Li, S.-F., and Li, H. (2018). Seed-sterilization of rhododendron wardii for micropropagation, Sri Lanka. *J. Food Agric.* 4, 9. doi: 10.4038/sljfa.v4i1.51

Aquilanti, L., Favilli, F., and Clementi, F. (2004). Comparison of different strategies for isolation and preliminary identification of azotobacter from soil samples. *Soil Biol. Biochem.* 36, 1475–1483. doi: 10.1016/j.soilbio.2004.04.024

Arora, N. K., and Verma, M. (2017). Modified microplate method for rapid and efficient estimation of siderophore produced by bacteria. *3 Biotech.* 7:381. doi: 10.1007/s13205-017-1008-y

Backer, R., Rokem, J. S., Ilangumaran, G., Lamont, J., Praslickova, D., Ricci, E., et al. (2018). Plant growth-promoting rhizobacteria: context, mechanisms of action, and roadmap to commercialization of biostimulants for sustainable agriculture. *Front. Plant Sci.* 9:1473. doi: 10.3389/fpls.2018.01473

Banik, A., Mukhopadhaya, S. K., Sahana, A., Das, D., and Dangar, T. K. (2016). Fluorescence resonance energy transfer (FRET)-based technique for tracking of endophytic bacteria in rice roots. *Biol. Fertil. Soils* 52, 277–282. doi: 10.1007/s00374-015-1064-6

Bashan, Y., de-Bashan, L. E., Prabhu, S. R., and Hernandez, J.-P. (2014). Advances in plant growth-promoting bacterial inoculant technology: formulations and practical perspectives (1998-2013). *Plant Soil* 378, 1–33. doi: 10.1007/s11104-013-1956-x

Berger, B., Baldermann, S., and Ruppel, S. (2017). The plant growth-promoting bacterium *Kosakonia radicincitans* improves fruit yield and quality of *Solanum lycopersicum*. *J. Sci. Food Agric.* 97, 4865–4871. doi: 10.1002/jsfa.8357

Berger, B., Patz, S., Ruppel, S., Dietel, K., Faetke, S., Junge, H., et al. (2018). Successful formulation and application of plant growth-promoting *Kosakonia radicincitans* in maize cultivation. *Biomed. Res. Int.* 2018, 1–8. doi: 10.1155/2018/6439481

Berger, B., Wiesner, M., Brock, A. K., Schreiner, M., and Ruppel, S. (2015). *K. radicincitans*, a beneficial bacteria that promotes radish growth under field conditions. *Agron. Sustain. Dev.* 35, 1521–1528. doi: 10.1007/s13593-015-0324-z

Bergottini, V. M., Otegui, M. B., Sosa, D. A., Zapata, P. D., Mulot, M., Rebord, M., et al. (2015). Bio-inoculation of yerba mate seedlings (Ilex paraguariensis St. Hill.) with native plant growth-promoting rhizobacteria: a sustainable alternative to improve crop yield. *Biol. Fertil. Soils* 51, 749–755. doi: 10.1007/s00374-015-1012-5

Bhattacharyya, P. N., and Jha, D. K. (2012). Plant growth-promoting rhizobacteria (PGPR): emergence in agriculture. *World J. Microbiol. Biotechnol.* 28, 1327–1350. doi: 10.1007/s11274-011-0979-9

Brock, A. K., Berger, B., Schreiner, M., Ruppel, S., and Mewis, I. (2018). Plant growth-promoting bacteria *Kosakonia radicincitans* mediate anti-herbivore defense in *Arabidopsis thaliana*. *Planta* 248, 1383–1392. doi: 10.1007/s00425-018-2964-0

Cappuccino, J. G., and Sherman, N. (1987). *Microbiology: A Laboratory Manual*, 3rd Edn, New York, NY: Benjamin-Cummings Publishing Company.

Castanheira, N. L., Dourado, A. C., Pais, I., Semedo, J., Scotti-Campos, P., Borges, N., et al. (2017). Colonization and beneficial effects on annual ryegrass by mixed inoculation with plant growth promoting bacteria. *Microbiol. Res.* 198, 47–55. doi: 10.1016/j.micres.2017.01.009

Chakdar, H., Dastager, S. G., Khire, J. M., Rane, D., and Dharne, M. S. (2018). Characterization of mineral phosphate solubilizing and plant growth promoting bacteria from termite soil of arid region. *3 Biotech.* 8:463. doi: 10.1007/s13205-018-1488-4

Chen, M., Zhu, B., Lin, L., Yang, L., Li, Y., and An, Q. (2014). Complete genome sequence of *Kosakonia sacchari* type strain SP1T. *Stand. Genomic Sci.* 9, 1311–1318. doi: 10.4056/sigs.5779977

Chimwamurombe, P. M., Grönemeyer, J. L., and Reinhold-Hurek, B. (2016). Isolation and characterization of culturable seed-associated bacterial endophytes from gnotobiotically grown Marama bean seedlings. *FEMS Microbiol. Ecol.* 92:fiw083. doi: 10.1093/femsec/fiw083

Chin, C. F. S., Furuya, Y., Zainudin, M. H. M., Ramli, N., Hassan, M. A., Tashiro, Y., et al. (2017). Novel multifunctional plant growth-promoting bacteria in co-compost of palm oil industry waste. *J. Biosci. Bioeng.* 124, 506–513. doi: 10.1016/j.jbiosc.2017.05.016

Dal Cortivo, C., Barion, G., Visioli, G., Mattarozzi, M., Mosca, G., and Vamerali, T. (2017). Increased root growth and nitrogen accumulation in common wheat following PGPR inoculation: assessment of plant-microbe interactions by ESEM. *Agric. Ecosyst. Environ.* 247, 396–408. doi: 10.1016/j.agee.2017.07.006

DM 27/01/2014 (2014). Metodi Di Analisi Per Il Controllo Ufficiale Dei Fertilizzanti. Supplemento n. 12. Gazzetta Ufficiale 42 Del 20/02/2014.

Dorais, M., and Alsanius, B. W. (2016). Recent advances in organic horticulture technology and management. *Sci. Hortic.* 208, 1–2. doi: 10.1016/j.scienta.2016.07.006

Duca, D., Lorv, J., Patten, C. L., Rose, D., and Glick, B. R. (2014). Indole-3-acetic acid in plant-microbe interactions. *Antonie Van Leeuwenhoek* 106, 85–125. doi: 10.1007/s10482-013-0095-y

Fiorentino, N., Ventorino, V., Bertora, C., Pepe, O., Giancarlo, M., Grignani, C., et al. (2016). Changes in soil mineral N content and abundances of bacterial communities involved in N reactions under laboratory conditions as predictors of soil N availability to maize under field conditions. *Biol. Fertil. Soils* 52, 523–537. doi: 10.1007/s00374-016-1095-7

Fiorentino, N., Ventorino, V., Woo, S. L., Pepe, O., De Rosa, A., Gioia, L., et al. (2018). Trichoderma-based biostimulants modulate rhizosphere microbial populations and improve N uptake efficiency, yield, and nutritional quality of leafy vegetables. *Front. Plant Sci.* 9:743. doi: 10.3389/fpls.2018.00743

Fravel, D. R., Marois, J. J., Lumsden, R. D., and Connick, W. J. Jr. (1985). Encapsulation of potential biocontrol agents in an alginate-clay matrix. *Phytopathology* 75, 774–777. doi: 10.1094/phyto-75-774

Glick, B. R. (2014). Bacteria with ACC deaminase can promote plant growth and help to feed the world. *Microbiol. Res.* 169, 30–39. doi: 10.1016/j.micres.2013.09.009

Graham-Weiss, L., Bennett, M. L., and Paau, A. S. (1987). Production of bacterial inoculants by direct fermentation on nutrient-supplemented vermiculite. *Appl. Environ. Microbiol.* 53, 2138–2141. doi: 10.1128/aem.53.9.2138-2141.1987

Haas, D., and Défago, G. (2005). Biological control of soil-borne pathogens by fluorescent pseudomonads. *Nat. Rev. Microbiol.* 3, 307–319. doi: 10.1038/nrmicro1129

Hammami, I., Hsouna, A. B., Hamdi, N., Gdoura, R., and Triki, M. A. (2013). Isolation and characterization of rhizosphere bacteria for the biocontrol of the damping-off disease of tomatoes in Tunisia. *C. R. Biol.* 336, 557–564. doi: 10.1016/j.crvi.2013.10.006

Hossain, M. I., Sadekuzzaman, M., and Ha, S. D. (2017). Probiotics as potential alternative biocontrol agents in the agriculture and food industries: a review. *Food Res. Int.* 100, 63–73. doi: 10.1016/j.foodres.2017.07.077

Jaemsaeng, R., Jantasuriyarat, C., and Thamchaipenet, A. (2018). Molecular interaction of 1-aminocyclopropane-1-carboxylate deaminase (ACCD)-producing endophytic *Streptomyces* sp. *GMKU* 336 towards salt-stress resistance of *Oryza sativa* L. cv. KDML105. *Sci. Rep.* 8:1950. doi: 10.1038/s41598-018-19799-9

John, R. P., Tyagi, R. D., Brar, S. K., and Prévost, D. (2010). Development of emulsion from rhizobial fermented starch industry wastewater for application as medicago sativa seed coat. *Eng. Life Sci.* 10, 248–256. doi: 10.1002/elsc.201000002

Kalayu, G. (2019). Phosphate solubilizing microorganisms: promising approach as biofertilizers. *Int. J. Agron.* 2019:4917256. doi: 10.1155/2019/4917256

Kämpfer, P., McInroy, J. A., Doijad, S., Chakraborty, T., and Glaeser, S. P. (2016). Kosakonia pseudosacchari sp. nov., an endophyte of *Zea mays*. *Syst. Appl. Microbiol.* 39, 1–7. doi: 10.1016/j.syapm.2015.09.004

Kandel, S. L., Joubert, P. M., and Doty, S. L. (2017). Bacterial endophyte colonization and distribution within plants. *Microorganisms* 5:E77. doi: 10.3390/microorganisms5040077

Khalid, M., Hassani, D., Bilal, M., Asad, F., and Huang, D. (2017). Influence of bio-fertilizer containing beneficial fungi and rhizospheric bacteria on health promoting compounds and antioxidant activity of *Spinacia oleracea* L. *Bot. Stud.* 58:35. doi: 10.1186/s40529-017-0189-3

Kim, W. I., Cho, W. K., Kim, S. N., Chu, H., Ryu, K. Y., Yun, J. C., et al. (2011). Genetic diversity of cultivable plant growth-promoting rhizobacteria in Korea. *J. Microbiol. Biotechnol.* 21, 777–790. doi: 10.4014/jmb.1101.01031

Kobayashi, D. Y., Reedy, R. M., Bick, J. A., and Oudemans, P. V. (2002). Characterization of a chitinase gene from *Stenotrophomonas* maltophilia strain 34S1 and its involvement in biological control. *Appl. Environ. Microbiol.* 68, 1047–1054. doi: 10.1128/aem.68.3.1047-1054.2002

Kumar, A., and Verma, J. P. (2018). Does plant—Microbe interaction confer stress tolerance in plants: a review? *Microbiol. Res.* 207, 41–52. doi: 10.1016/j.micres.2017.11.004

Kumar, S., Stecher, G., Li, M., Knyaz, C., and Tamura, K. (2018). MEGA X: molecular evolutionary genetics analysis across computing platforms. *Mol. Biol. Evol.* 35, 1547–1549. doi: 10.1093/molbev/msy096

Lambrese, Y., Guiñez, M., Calvente, V., Sansone, G., Cerutti, S., Raba, J., et al. (2018). Production of siderophores by the bacterium *Kosakonia radicincitans* and its application to control of phytopathogenic fungi. *Bioresour. Technol. Rep.* 3, 82–87. doi: 10.1016/j.biteb.2018.06.003

Liu, J., Yang, J., Liang, X., Zhao, Y., Cade-Menun, B. J., and Hu, Y. (2014). Molecular speciation of phosphorus present in readily dispersible colloids from agricultural soils. *Soil Sci. Soc. Am. J.* 78, 47–53. doi: 10.2136/sssaj2013.05.0159

Lobo, C. B., Juárez Tomás, M. S., Viruel, E., Ferrero, M. A., and Lucca, M. E. (2019). Development of low-cost formulations of plant growth-promoting bacteria to be used as inoculants in beneficial agricultural technologies. *Microbiol. Res.* 219, 12–25. doi: 10.1016/j.micres.2018.10.012

Montella, S., Ventorino, V., Lombard, V., Henrissat, B., Pepe, O., and Faraco, V. (2017). Discovery of genes coding for carbohydrate-active enzyme by metagenomic analysis of lignocellulosic biomasses. *Sci. Rep.* 7:42623. doi: 10.1038/srep42623

Morgan, C. A., Herman, N., White, P. A., and Vesey, G. (2006). Preservation of micro-organisms by drying. A review. *J. Microbiol. Methods* 66, 183–193. doi: 10.1016/j.mimet.2006.02.017

Murphy, J., and Riley, J. P. (1962). A modified single solution method for the determination of phosphate in natural waters. *Anal. Chim. Acta* 27, 31–36. doi: 10.1016/s0003-2670(00)88444-5

Noar, J. D., and Bruno-Bárcena, J. M. (2018). Azotobacter vinelandii: the source of 100 years of discoveries and many more to come. *Microbiology* 164, 421–436. doi: 10.1099/mic.0.000643

Olanrewaju, O. S., Glick, B. R., and Babalola, O. O. (2017). Mechanisms of action of plant growth promoting bacteria. *World J. Microbiol. Biotechnol.* 33:197. doi: 10.1007/s11274-017-2364-9

Pagliano, G., Ventorino, V., Panico, A., Romano, I., Pirozzi, F., and Pepe, O. (2019). Anaerobic process for bioenergy recovery from dairy waste: meta-analysis and enumeration of microbial community related to intermediates production. *Front. Microbiol.* 9:3229. doi: 10.3389/fmicb.2018.03229

Passari, A. K., Mishra, V. K., Singh, G., Singh, P., Kumar, B., Gupta, V. K., et al. (2017). Insights into the functionality of endophytic actinobacteria with a focus on their biosynthetic potential and secondary metabolites production. *Sci. Rep.* 7:11809. doi: 10.1038/s41598-017-12235-4

Payne, S. M. (1993). Iron acquisition in microbial pathogenesis. *Trends Microbiol.* 1, 66–69. doi: 10.1016/0966-842x(93)90036-q

Penrose, D. M., and Glick, B. R. (2003). Methods for isolating and characterizing ACC deaminase-containing plant growth-promoting rhizobacteria. *Physiol. Plant.* 118, 10–15. doi: 10.1034/j.1399-3054.2003.00086.x

Pepe, O., Ventorino, V., and Blaiotta, G. (2013). Dynamic of functional microbial groups during mesophilic composting of agro-industrial wastes and free-living (N2)-fixing bacteria application. *Waste Manag.* 33, 1616–1625. doi: 10.1016/j.wasman.2013.03.025

Rahman, M., Sabir, A. A., Mukta, J. A., Khan, M. M. A., Mohi-Ud-Din, M., Miah, M. G., et al. (2018). Plant probiotic bacteria *Bacillus* and paraburkholderia improve growth, yield and content of antioxidants in strawberry fruit. *Sci. Rep.* 8:2504. doi: 10.1038/s41598-018-20235-1

Romano, I., Ventorino, V., and Pepe, O. (2020). Effectiveness of plant beneficial microbes: overview of the methodological approaches for the assessment of root colonization and persistence. *Front. Plant Sci.* 11:6. doi: 10.3389/fpls.2020.00006

Rösch, C., Mergel, A., and Bothe, H. (2002). Biodiversity of denitrifying and dinitrogen-fixing bacteria in an acid forest soil. *Appl. Environ. Microbiol.* 68, 3818–3829. doi: 10.1128/aem.68.8.3818-3829.2002

Sharma, S. D., Kumar, P., Bhardwaj, S. K., and Yadav, S. K. (2011). Screening and selecting novel AM fungi and *Azotobacter* strain for inoculating apple under soilsolarization and chemical disinfestation with mulch practices for sustainable nursery management. *Sci. Hortic.* 130, 164–174. doi: 10.1016/j.scienta.2011.06.032

Sheridan, C., Depuydt, P., De Ro, M., Petit, C., Van Gysegem, E., Delaere, P., et al. (2017). Microbial community dynamics and response to plant growth-promoting microorganisms in the rhizosphere of four common food crops cultivated in hydroponics. *Microb. Ecol.* 73, 378–393. doi: 10.1007/s00248-016-0855-0

Silva-Stenico, M. E., Pacheco, F. T. H., Rodrigues, J. L. M., Carrilho, E., and Tsai, S. M. (2005). Growth and siderophore production of *Xylella fastidiosa* under iron-limited conditions. *Microbiol. Res.* 160, 429–436. doi: 10.1016/j.micres.2005.03.007

Singh, S. R., Zargar, M. Y., Najar, G. R., Peer, F. A., and Ishaq, M. (2013). Microbial dynamics, root colonization, and nutrient availability as influenced by inoculation of liquid bioinoculants in cultivars of apple seedlings. *Commun. Soil Sci. Plant Anal.* 44, 1511–1523. doi: 10.1080/00103624.2012.760571

Stecher, G., Tamura, K., and Kumar, S. (2020). Molecular evolutionary genetics analysis (MEGA) for macOS. *Mol. Biol. Evol.* 37, 1237–1239. doi: 10.1093/molbev/msz312

Sun, S., Chen, Y., Cheng, J., Li, Q., Zhang, Z., and Lan, Z. (2018). Isolation, characterization, genomic sequencing, and GFP-marked insertional mutagenesis of a high-performance nitrogen-fixing bacterium, *Kosakonia radicincitans* GXGL-4A and visualization of bacterial colonization on cucumber roots. *Folia Microbiol.* 63, 789–802. doi: 10.1007/s12223-018-0608-1

Thompson, J. D., Higgins, D. G., and Gibson, T. J. (1994). CLUSTAL W: improving the sensitivity of progressive multiple sequence alignment through sequence weighting, position-specific gap penalties and weight matrix choice. *Nucleic Acids Res.* 22, 4673–4680. doi: 10.1093/nar/22.22.4673

Timmusk, S., Behers, L., Muthoni, J., Muraya, A., and Aronsson, A. C. (2017). Perspectives and challenges of microbial application for crop improvement. *Front. Plant Sci.* 8:49. doi: 10.3389/fpls.2017.00049

Van Oosten, M. J., Pepe, O., De Pascale, S., Silletti, S., and Maggio, A. (2017). The role of biostimulants and bioeffectors as alleviators of abiotic stress in crop plants. *Chem. Biol. Technol. Agric.* 4:5. doi: 10.1186/s40538-017-0089-5

Ventorino, V., Caputo, R., De Pascale, S., Fagnano, M., Pepe, O., and Moschetti, G. (2012a). Response to salinity stress of *Rhizobium leguminosarum* bv. viciae strains in the presence of different legume host plants. *Ann. Microbiol.* 62, 811–823. doi: 10.1007/s13213-011-0322-6

Ventorino, V., De Marco, A., Pepe, O., De Santo, A. V., and Moschetti, G. (2012b). "Impact of innovative agricultural practices of carbon sequestration on soil microbial community," in *Carbon Sequestration in Agricultural Soils. A Ultidisciplinary Approach to Innovative Methods*, ed. A. Piccolo (Berlin: Springer), 145–177. doi: 10.1007/978-3-642-23385-2_6

Ventorino, V., Ionata, E., Birolo, L., Montella, S., Marcolongo, L., de Chiaro, A., et al. (2016). Lignocellulose-adapted endo-cellulase producing *Streptomyces* strains for bioconversion of cellulose-based materials. *Front. Microbiol.* 7:2061. doi: 10.3389/fmicb.2016.02061

Ventorino, V., Pascale, A., Adamo, P., Rocco, C., Fiorentino, N., Mori, M., et al. (2018). Comparative assessment of autochthonous bacterial and fungal communities and microbial biomarkers of polluted agricultural soils of the Terra dei Fuochi. *Sci. Rep.* 8:14281. doi: 10.1038/s41598-018-32688-5

Ventorino, V., Pascale, A., Fagnano, M., Adamo, P., Faraco, V., Rocco, C., et al. (2019). Soil tillage and compost amendment promote bioremediation and biofertility of polluted area. *J. Clean. Prod.* 239:118087. doi: 10.1016/j.jclepro.2019.118087

Ventorino, V., Robertiello, A., Cimini, D., Argenzio, O., Schiraldi, C., Montella, S., et al. (2017). Bio-based succinate production from *Arundo donax* hydrolysate with the new natural succinic acid-producing strain *Basfia succiniciproducens* BPP7. *Bioenergy Res.* 10, 488–498. doi: 10.1007/s12155-017-9814-y

Ventorino, V., Sannino, F., Piccolo, A., Cafaro, V., Carotenuto, R., and Pepe, O. (2014). *Methylobacterium populi* VP2: plant growth-promoting bacterium isolated from a highly polluted environment for polycyclic aromatic hydrocarbon (PAH) biodegradation. *Sci. World J.* 2014, 931793. doi: 10.1155/2014/931793

Viscardi, S., Ventorino, V., Duran, P., Maggio, A., De Pascale, S., Mora, M. L., et al. (2016). Assessment of plant growth promoting activities and abiotic stress tolerance of *Azotobacter chroococcum* strains for a potential use in sustainable agriculture. *J. Soil Sci. Plant Nutr.* 16, 848–863. doi: 10.4067/s0718-95162016005000060

Wang, C., Wu, W., Wei, L., Feng, L., Kang, M., Xie, Y., et al. (2019). *Kosakonia quasisacchari* sp. nov. recovered from human wound secretion in China. *Int. J. Syst. Evol. Microbiol.* 69, 3155–3160. doi: 10.1099/ijsem.0.003606

Witzel, K., Strehmel, N., Baldermann, S., Neugart, S., Becker, Y., Becker, M., et al. (2017). *Arabidopsis thaliana* root and root exudate metabolism is altered by the growth-promoting bacterium *Kosakonia radicincitans* DSM 16656T. *Plant Soil* 419, 557–573. doi: 10.1007/s11104-017-3371-1

Woo, S. L., and Pepe, O. (2018). Microbial consortia: promising probiotics as plant biostimulants for sustainable agriculture. *Front. Plant Sci.* 9:1801. doi: 10.3389/fpls.2018.01801

Xu, S., Bai, Z., Jin, B., Xiao, R., and Zhuang, G. (2015). Bioconversion of wastewater from sweet potato starch production to *Paenibacillus polymyxa* biofertilizer for tea plants. *Sci. Rep.* 4:4131. doi: 10.1038/srep04131

Conflict of Interest: PA was employed by Agriges S.r.l.

The authors declare that this study received funding from Agriges S.r.l. The funder had the following involvement in the study: coordination of the development of bio-formulates and *in vivo* experiments.

frontiers in Plant Science

ORIGINAL RESEARCH
published: 05 November 2020
doi: 10.3389/fpls.2020.567388

A Microbial-Based Biostimulant Enhances Sweet Pepper Performance by Metabolic Reprogramming of Phytohormone Profile and Secondary Metabolism

Paolo Bonini[1], Youssef Rouphael[2], Begoña Miras-Moreno[3], Byungha Lee[1], Mariateresa Cardarelli[4], Gorka Erice[5], Veronica Cirino[5], Luigi Lucini[3] and Giuseppe Colla[6]*

[1] Next Generation Agronomics Laboratory (NGAlab), La Riera de Gaia, Tarragona, Spain, [2] Department of Agricultural Sciences, University of Naples Federico II, Portici, Italy, [3] Department for Sustainable Food Process, Research Centre for Nutrigenomics and Proteomics, Università Cattolica del Sacro Cuore, Piacenza, Italy, [4] Consiglio per la ricerca in agricoltura e l'analisi dell'economia agraria, Centro di ricerca Orticoltura e Florovivaismo, Pontecagnano Faiano, Italy, [5] Atens, La Riera de Gaia, Tarragona, Spain, [6] Department of Agriculture and Forest Sciences, Università degli Studi della Tuscia, Viterbo, Italy

Microbial-based biostimulants can improve crop productivity by modulating cell metabolic pathways including hormonal balance. However, little is known about the microbial-mediated molecular changes causing yield increase. The present study elucidates the metabolomic modulation occurring in pepper (*Capsicum annuum* L.) leaves at the vegetative and reproductive phenological stages, in response to microbial-based biostimulants. The arbuscular mycorrhizal fungi *Rhizoglomus irregularis* and *Funneliformis mosseae*, as well as *Trichoderma koningii*, were used in this work. The application of endophytic fungi significantly increased total fruit yield by 23.7% compared to that of untreated plants. Multivariate statistics indicated that the biostimulant treatment substantially altered the shape of the metabolic profile of pepper. Compared to the untreated control, the plants treated with microbial biostimulants presented with modified gibberellin, auxin, and cytokinin patterns. The biostimulant treatment also induced secondary metabolism and caused carotenoids, saponins, and phenolic compounds to accumulate in the plants. Differential metabolomic signatures indicated diverse and concerted biochemical responses in the plants following the colonization of their roots by beneficial microorganisms. The above findings demonstrated a clear link between microbial-mediated yield increase and a strong up-regulation of hormonal and secondary metabolic pathways associated with growth stimulation and crop defense to environmental stresses.

Keywords: ***Funneliformis mosseae*, *Rhizoglomus irregularis*, *Trichoderma koningii*, *Capsicum annuum* L., plant metabolomics, metabolic reprogramming**

OPEN ACCESS

Edited by:
Santiago Gutierrez, Universidad De León, Spain

Reviewed by:
Francesca Mapelli, University of Milan, Italy
Mara Novero, University of Turin, Italy

****Correspondence:***
Paolo Bonini
pb@ngalab.com

Specialty section:
This article was submitted to Plant Pathogen Interactions, a section of the journal Frontiers in Plant Science

Received: *29 May 2020*
Accepted: *15 October 2020*
Published: *05 November 2020*

Citation:
Bonini P, Rouphael Y, Miras-Moreno B, Lee B, Cardarelli M, Erice G, Cirino V, Lucini L and Colla G (2020) A Microbial-Based Biostimulant Enhances Sweet Pepper Performance by Metabolic Reprogramming of Phytohormone Profile and Secondary Metabolism. Front. Plant Sci. 11:567388. doi: 10.3389/fpls.2020.567388

INTRODUCTION

Three major current global challenges are food security, environmental degradation, and climate change. The first may be augmented, and the latter two diminished by improving nutrient (nitrogen, phosphorus) use efficiency in agricultural crop production and stabilizing yield by practicing sustainable agriculture (Searchinger et al., 2018). The application of plant biostimulants

such as beneficial microbes [arbuscular mycorrhizal fungi (AMF), *Trichoderma* spp., plant growth-promoting rhizobacteria (PGPR)], and bioactive substances (humic and fulvic acids, macroalgae and microalgae, protein hydrolysates and silicon) used either separately or in combination may help crops contend with the challenges mentioned above (Rouphael and Colla, 2020).

Plant biostimulants were recently defined in the Regulations of the European Parliament and Council (Regulation EU 2019/1009) as "*. . .EU fertilising product(s) able to stimulate plant nutrition processes independently of the product's nutrient content with the sole aim of improving one or more of the following characteristics of the plant or the plant rhizosphere: (1) nutrient use efficiency, (2) tolerance to abiotic stress, (3) quality traits, or (4) availability of confined nutrients in the soil or rhizosphere*". AMF comprise a very important category of biostimulants (Rouphael et al., 2015; Bitterlich et al., 2018). They are members of the *Glomeromycotina* subphylum and establish mutualistic relationships with 74% of all terrestrial plant species (Spatafora et al., 2016). AMF boost productivity and enhance tolerance to abiotic stress (high temperature, drought, and salinity) in crops (Rouphael et al., 2015). These findings are due to the AMF-mediated enhancement of (1) growth and vigor of the root apparatus in terms of biomass, length, density, and branching; (2) macronutrient (N, P, and Fe) and micronutrient (Mn and Zn) uptake and assimilation; (3) water relations and photosynthetic activity; (4) secondary metabolism; (5) release of low- and high-molecular-weight organic compounds such as amino acids, phenolics, organic acids, and proteins into the rhizosphere; (6) phytohormone signaling (Rouphael et al., 2015, 2020b; Yakhin et al., 2017; Rouphael and Colla, 2018). The indirect and direct mechanisms of AMF influence shoot and root function and augment crop agronomic performance. Other plant beneficial endophytic fungi include *Trichoderma* spp. Several of them are registered as microbial biological control agents (López-Bucio et al., 2015; Rouphael et al., 2020a). However, several studies reported that certain *Trichoderma* spp. including *T. atroviride*, *T. koningii*, *T. harzianum,* and *T. virens* are other plant biostimulants that boost crop performance (Colla et al., 2015) and nutrient use efficiency and/or endue plants with abiotic stress tolerance (Saia et al., 2020). The direct and indirect mechanisms of the biostimulant action of *Trichoderma* strains include (i) improvement of lateral root development, (ii) induction of plant mitogen-activated protein 6, and (iii) production and rhizosphere excretion of auxins and secondary metabolites such as volatile and non-volatile substances that stimulate various plant responses and enhance crop nutrient uptake, resilience, and productivity (López-Bucio et al., 2015).

The beneficial effects of combinations of AMF and *Trichoderma* on vegetable crops were previously demonstrated under both optimal and suboptimal conditions (Colla et al., 2015; Saia et al., 2020). However, the physiological and molecular mechanisms underlining biostimulant action have not been fully elucidated. One strategy to clarify biostimulant efficacy is to analyze metabolic profiling. In turn, this process serves as a basis for subsequent transcriptomic analyses. The metabolomic phytochemical characterization could identify numerous physiological processes and metabolic pathways modulated by biostimulants (Yakhin et al., 2017). The above approach has been never used in an important vegetable crop such as pepper (*Capsicum* spp.) where biostimulant applications (e.g., vegetal-derived substances, arbuscular mycorrhizal fungi, plant growth-promoting microorganisms) have proven to be beneficial in ameliorating the growth, yield and nutritional value of fruits (Ertani et al., 2014; Pereira et al., 2016).

It has been hypothesized that AMF and *Trichoderma* can induce and enhance fruit yield by modulating the hormonal balance and secondary metabolic pathways.

In the present study, then, an untargeted metabolomics approach was conducted on greenhouse pepper. The objectives were to illuminate metabolomic reprogramming by microbial biostimulants in leaf tissue at the vegetative and reproductive phenological stages, elucidate biostimulant regulation of key phytohormones, and correlate these molecular-level biostimulant-promoted changes to observed fruit yield and quality variations.

MATERIALS AND METHODS

Growth Conditions, Plant Material, Crop Management, and Experimental Design

The trial was conducted in a greenhouse located at Paraje Águilas Bajas, Santa María del Águila, Almería, Spain (36°47′39″N 2°46′32″W). The greenhouse was composed of polycarbonate walls and a roof made of tri-laminated low-density polyethylene (LDPE) film (200 μm thickness) with ∼60% spectral transmittance in the photosynthetically active radiation (PAR) region. The greenhouse was unheated and passively ventilated with lateral side panels and flap roof windows. It had an east-west orientation and a north-south crop row alignment. The air temperature and relative humidity inside the greenhouse were in the ranges of 12–32 °C and 50–70%, respectively. Transplants of the sweet pepper (*Capsicum annuum* L.) hybrid 'SV1204PB' (Seminis, Montornés del Vallés, Barcelona, Spain) at the 4–5 true-leaf stage were planted in "Enarenado" sandy soil commonly used in greenhouse production in Almería. This soil is formed by placing a 20 cm layer of sandy loam soil, imported from a quarry, over the original stony, loam soil. A 10 cm layer of coarse river sand is placed over the imported sandy loam soil as a mulch (Thompson et al., 2007). The planting date was 19 July 2017, and the planting density was 2.0 m^{-2}. The soil composition was 13.5% (w/w) clay, 72.8% (w/w) sand, and 13.7% (w/w) silt. Soil pH was 7.52, with an organic matter content of 0.71%, and total nitrogen, available phosphorus, and exchangeable potassium of 690, 51.4, and 321 mg kg^{-1}, respectively. Aerial drip irrigation was used. The in-line emitters were positioned at 0.30 m intervals, and the emitter flow rate was 3.4 L h^{-1}. Preplant fertilizer was broadcast at 90 kg · ha^{-1} P, 120 kg · ha^{-1} K, and 15 kg · ha^{-1} Mg and incorporated into the soil. Additional fertilizer in the form of K_2SO_4 (80 kg · ha^{-1} K) was applied through the drip irrigation system. Nitrogen was applied via fertigation in the form of 27% NH_4NO_3 soluble fertilizer starting 10 days after transplanting until day 83. The

total N supply was split into 10 weekly dressings. Powdery mildew caused by *Leveillula taurica* was controlled by three foliar applications of penconazole (Topas 10EC; Syngenta, Madrid, Spain) at the label-recommended rate. Aphids and spider mites were controlled by one foliar application each of imidacloprid (Confidor 200 SL; Bayer Crop Science, Valencia, Spain) and fenpyroximate (Miro; Bayer Crop Science, Valencia, Spain), respectively. Weeds were controlled by hand hoeing. The control and microbial-based biostimulant treatments were compared in a randomized block design with four replicates for a total of eight experimental plots. Each experimental plot was 30 m^2 and contained 60 plants in four single rows. The microbial-based biostimulants were applied through a drip irrigation system. The first application was made at 15 days after transplanting (DAT) (3 August 2017) at the rates of 1×10^6 spores ha^{-1} *Rhizoglomus irregularis* BEG72 and 1×10^6 spores ha^{-1} *Funneliformis mosseae* BEG234 in the form of 2.0 kg ha^{-1} Team Horticola (Agrotecnologías Naturales, S.L., Tarragona, Spain) plus 1×10^{12} CFU ha^{-1} *Trichoderma koningii* TK7 in the form of 1.0 kg ha^{-1} Condor Shield (Agrotecnologías Naturales, S.L., Tarragona, Spain). The second treatment was applied 43 DAT (31 August 2017) at the rate of 5×10^{11} CFU ha^{-1} *Trichoderma koningii* TK7 as 0.5 kg Condor Shield (Agrotecnologías Naturales, S.L., Tarragona, Spain). Multiple applications of *Trichoderma* inoculum are recommended especially in long-term crops like greenhouse pepper under soils with low organic matter to raise the population of this saprophytic beneficial fungus in the soil rhizosphere. Because arbuscular mycorrhizal fungi such as *Rhizoglomus irregularis* and *Funneliformis mosseae* are symbiotic microorganisms, it is usually sufficient the application of mycorrhizal inoculum just once at the beginning of cropping cycle (Colla et al., 2008).

Yield Measurements and Arbuscular Mycorrhizal Fungi (AMF) Root Colonization

Fully mature pepper fruits were harvested from 139 DAT (5 December 2017) to 272 DAT (17 April 2018) on 26 plants per each plot. Mean fruit weight and number and marketable yield were determined for each experimental plot (replicate). Rotten fruit and those weighing < 100 g were considered unmarketable yield.

At the end of the trial, the roots of six pepper plants per experimental plot were rinsed, and subsamples were used to evaluate AMF root colonization. The root samples were cleared with 10% (w/v) KOH, stained with 0.05% (w/v) trypan blue in lactophenol, and microscopically (Stereo microscope Leica EZ4V, 32x—Leica Microsystems Srl, Buccinasco, Italy) examined for AMF colonization. The percentage of colonized root segments was determined by the grid line intersect method (Giovannetti and Mosse, 1980).

Quantitative Real-Time PCR (qPCR) for Determining Concentration of Strain TK7 in Soil

At the end of the trial, rhizosphere soil was collected by shaking the roots collected from 10 plants per plot. The concentration of *T. koningii* TK7 in the rhizosphere was determined using a qPCR approach with two strain-specific primers, named RM3 (GGAGGCTTGAATGGGA) and RM4 (CAAAACGCTGCTAAGG), targeting to a coding sequence annotated as hypothetical protein. The DNA template used in qPCR experiments was extracted from the soil samples with a DNeasy® Powersoil® kit (Cat. No. 12888-50; Qiagen, Hilden, Germany) according to Qiacube (Qiagen, Hilden, Germany) automation procedures. Amplification reactions were carried out in a 20 μL final volume on a Rotor-Gene Q apparatus (Qiagen, Hilden, Germany). Reactions contained: 4 μL of DNA sample;10 μL of QuaniNova™ SYBR® Green Supermix (2x); 0.14 μL of 25 μM primers; 4.72 10-μL of water. The qPCR cycling conditions were as follows: initial incubation at 95°C for 2 min, 45 cycles of 95°C for 5 s each, and 60°C for 12 s. Two technical replicates were performed per sample. After qPCR, the number of colony forming unit (CFU) equivalent per gram of soil was calculated by interpolation of calibration curves obtained using serial dilutions (1:1,000, 1:10,000, and 1:100,000) of a DNA preparation extracted from 10^9 CFU mL^{-1} culture aliquots of the target strain.

Sample Collection and Untargeted Metabolomics

Four leaves in the third position from the branch tip were harvested for untargeted metabolomics at 43 DAT (31 August 2017) and at 131 DAT (27 November 2017). The leaves were flash-frozen in liquid nitrogen and stored at −80 °C until subsequent metabolomic analysis.

The four leaves from each replicate were pooled and homogenized, then 1.0 g was extracted in 0.1% HCOOH in 80% methanol using an ultra-turrax, as previously described (Paul et al., 2019). An untargeted metabolomics approach was conducted in the UHPLC 1290 chromatographic system coupled to a hybrid quadrupole-time-of-flight (Q-TOF) G6550 mass spectrometer (UHPLC/Q-TOF) (Agilent Technologies, Santa Clara, CA, United States). A Waters Acquity UPLC® BEH C18 column (100 × 2.1 mm i.d., 1.7 μm) (Waters Corp., Milford, MA, United States) was used for reverse-phase chromatographic separation. The binary gradient consisted of water and acetonitrile and the Riken Plasma method was followed (Tsugawa et al., 2019). The injection volume was 2 μL and the mass spectrometer was run in positive polarity and SCAN mode (range: 100–1,700 m/z; extended dynamic range setting). Quality controls (QC) were prepared by pooling 10 μL samples. Five QCs were acquired in data-dependent mode (auto MS/MS) at 1 Hz, 10 precursors/cycle, collision energies of 10 V, 30 V, and 50 V), and in iterative mode with active exclusion to increase the number of compounds targeted for tandem MS fragmentation.

Alignment, blank filtration, and identification were performed in MSDIAL v. 4.0 (Riken, Tokyo, Japan) using the publicly available library MoNA (Mass Bank of North America) and an internal standard compound library as specified in the **Supplementary Table 1**. Compounds lacking experimental MS/MS spectra were annotated with MSFINDER (Riken, Tokyo, Japan) following the procedure described in Blaženović et al. (2019). The alternatives were filtered by retention time prediction (Bonini et al., 2020). MSI (metabolomics standards

initiative) levels for each identified compound are listed in **Supplementary Table 1**.

Statistics and Data Analysis

Data were statistically analyzed with SPSS v. 21 (IBM Corp., Armonk, NY, United States). The microbial-based biostimulant effects on mycorrhizal root colonization, *Trichoderma* population, fruit yield and yield components were analyzed by an unpaired Student's *t*-test. A *p*-value of less than or equal to 0.05 was considered to indicate significant difference. Values are presented as means plus/minus standard deviation.

Concerning metabolomics, the compound intensity table exported from MSDIAL v. 4.0 (Riken, Tokyo, Japan) (Tsugawa et al., 2015) was uploaded into MS-FLO (Riken, Tokyo, Japan) (De Felice et al., 2017) to reduce false positives and duplicates. The output was then imported into R v. 3.6.0 for centring (normalization against the median), scaling, PCA, and calculation of fold changes, ANOVA (Benjamini-Hochberg FDR multiple testing correction, $P < 0.05$). Venn diagrams were plotted to identify metabolites common to 43 and 131 DAT sampling points but not exclusive to a particular growth stage. Compounds with $P < 0.05$ were imported into ChemRICH (Barupal and Fiehn, 2017) for enrichment analysis based on their chemical similarity and MetaMapp (Barupal et al., 2012) for chemical network analysis. Cytoscape (Saito et al., 2012) displayed exported MetaMapp data and plotted the final images.

RESULTS

Soil Fungal Concentration and Crop Yield

By the end of the trial, the percentage of mycorrhizal root colonization was significantly ($P < 0.01$) higher under the microbial inoculation treatment (33.6 ± 11.7%) than it was under the uninoculated control treatment (8.0 ± 4.9%). The total number of *Trichoderma* colonies estimated by qPCR in the rhizosphere of inoculated pepper plants was significantly ($P < 0.01$) higher than that recorded for the untreated control ($2.2 \times 10^5 \pm 0.6 \times 10^5$ vs. $1.2 \times 10^3 \pm 0.4 \times 10^3$ CFU g^{-1}, respectively). It is worth mentioning that the weak PCR amplification signal observed in control experiments with metagenome from not inoculated soil did not interfere with the quantitative PCR analysis.

Relative to the uninoculated control, inoculation with AMF and *Trichoderma koningii* significantly increased fruit yield at single harvests (139, 174, 272 DAT) and as a total (**Table 1**); moreover, the biostimulant-mediated yield increase was more pronounced during the first part of the reproductive cycle, namely, early yield (139 and 174 DAT) (**Table 1**). The comparatively higher production rates measured at 139 DAT and 272 DAT for pepper plants inoculated with microbial-based biostimulant was due to an increase in mean fruit weight. In contrast, the relatively higher fruit yield determined for 174 DAT was attributed to increases in both fruit number per plant and mean fruit mass (**Tables 1–3**). The microbial-based biostimulant significantly improved cumulative fruit yield by an average of 23.7% relative to uninoculated pepper plants (**Table 1**).

Yields and Modulation of Metabolomic Profile

In the present study, we inoculated pepper plants with the AMF species *Rhizoglomus irregularis* and *Funneliformis mosseae* and *Trichoderma koningii*. Microbial treatments accelerated and increased total crop yield by 24%, relative to uninoculated plants (**Table 1**). Such increase in pepper yield was attributed to the gain in fruit weight and/or number. Ultra-high-performance liquid chromatography quadrupole-time-of-flight high-resolution mass spectrometry (UHPLC-QTOF) and annotation in publicly available databases and large metabolite groups were conducted

TABLE 1 | Effect of microbial-based biostimulant application on fruit yield of greenhouse-grown peppers at different days after transplanting (DAT).

Treatment	Fruit yield (kg plant^{-1})					
	139 DAT	**174 DAT**	**243 DAT**	**264 DAT**	**272 DAT**	**Total**
	139 DAT	**174 DAT**	**243 DAT**	**264 DAT**	**272 DAT**	**Total**
Control	0.57 ± 0.04	0.85 ± 0.07	0.59 ± 0.09	0.73 ± 0.06	0.63 ± 0.13	3.37 ± 0.07
Biostimulant	0.73 ± 0.10	1.41 ± 0.30	0.48 ± 0.13	0.74 ± 0.07	0.81 ± 0.06	4.17 ± 0.07
Significance	*	**	Ns	Ns	*	**

*Mean values plus/minus standard deviations (n = 4); Two-tailed unpaired Student's t-test, ns = not significant, *P < 0.05, and **P < 0.01.*

TABLE 2 | Effect of microbial-based biostimulant application on fruit number of greenhouse-grown peppers at different days after transplanting (DAT).

Treatment	Fruit number (n. plant^{-1})					
	139 DAT	**174 DAT**	**243 DAT**	**264 DAT**	**272 DAT**	**Total**
Control	2.35 ± 0.37	3.65 ± 0.29	2.90 ± 0.53	2.20 ± 0.10	2.09 ± 0.45	13.20 ± 0.50
Biostimulant	2.75 ± 0.22	5.56 ± 1.00	1.92 ± 0.67	1.98 ± 0.20	2.42 ± 0.11	14.62 ± 0.83
Significance	ns	**	Ns	Ns	ns	*

*Mean values plus/minus standard deviations (n = 4); Two-tailed unpaired Student's t-test, ns = not significant, *P < 0.05, and **P < 0.01.*

TABLE 3 | Effect of microbial-based biostimulant application on fruit mean weight of greenhouse-grown peppers at different days after transplanting (DAT).

Treatment	Fruit mean weight (g fruit^{-1})				
	139 DAT	**174 DAT**	**243 DAT**	**264 DAT**	**272 DAT**
Control	244.0 ± 5.8	232.4 ± 2.4	204.4 ± 27.6	335.1 ± 24.1	302.5 ± 20.3
Biostimulant	264.7 ± 7.9	254.4 ± 12.8	250.4 ± 27.5	368.3 ± 3.5	334.3 ± 15.4
Significance	**	**	Ns	*	*

*Mean values plus/minus standard deviations (n = 4); Two-tailed unpaired Student's t-test, ns = not significant, *P < 0.05, and **P < 0.01.*

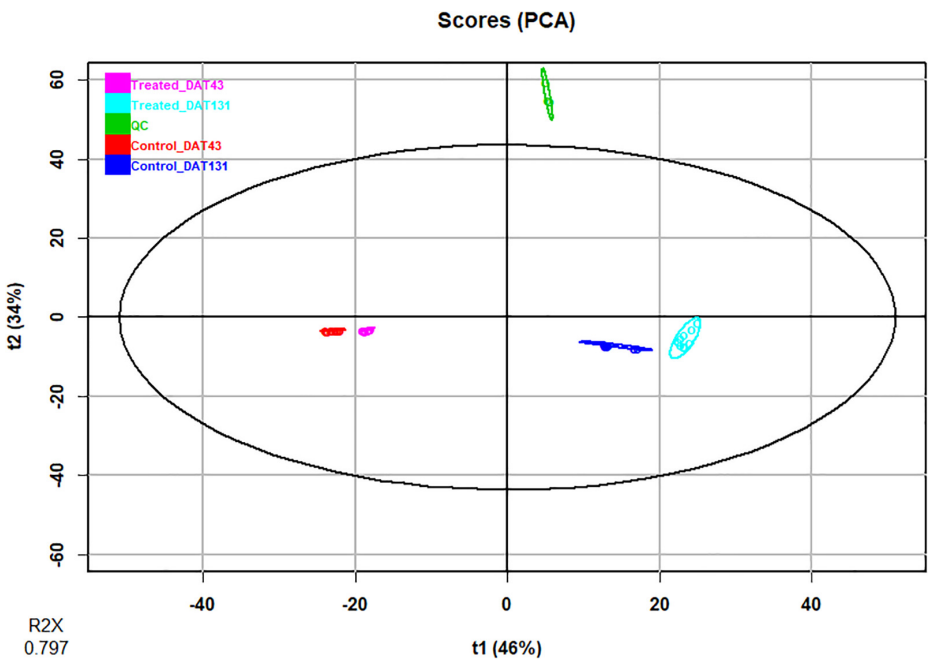

FIGURE 1 | Principal Component Analysis (PCA) of identified metabolites in pepper plants following treatment with microbial biostimulants. Compounds were profiled by untargeted metabolomics and samples harvested at two sampling dates: 43 (vegetative stage), and 131 days after transplanting (reproductive stage).

to obtain wide metabolome coverage. We applied UHPLC-QTOF-based untargeted metabolomic profiling of crude extracts to assess relative differences in the vegetative stage (43 DAT) and reproductive stage (131 DAT) leaf metabolite profiles between inoculated and uninoculated plants. A principal component analysis (PCA) explained 79% of the overall variance. The PCA score plot (**Figure 1**) showed two main clusters accounting for the vegetative and reproductive stages, respectively. Within each cluster, the metabolomic profiles of leaves from inoculated and those from the uninoculated (control) plants did not show overlapping, thus indicating distinct phytochemical signatures. Notably, considering that PCA provides unsupervised descriptions of relatedness/unrelatedness across treatments, these patterns indicate a metabolomic shift in plants following the biostimulant treatments. Thereafter, *t*-test ANOVA ($P < 0.01$) was carried out to identify differentially accumulated metabolites at each plant growth stage. This analysis disclosed > 466 annotated metabolites (Sheets 2 and 3 of **Supplementary File 1**) that had significantly changed between the vegetative and reproductive stages. Of these, 327 were common to 43 and 131 DAT sampling points (**Figure 2**). In contrast, 68 and 71 metabolites differentially accumulated during the vegetative (43 DAT) and reproductive (131 DAT) stages, respectively (**Figure 2**). The interactions between microbial

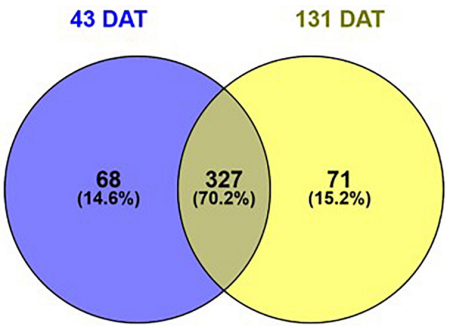

FIGURE 2 | Venn diagram of statistically different metabolites ($P < 0.05$) in pepper plants following treatment with microbial biostimulants, as a function of the sampling date. Compounds were profiled by untargeted metabolomics at two sampling dates: 43 (vegetative stage), and 131 days after transplanting (reproductive stage).

inoculants and plants are complex. Nevertheless, metabolomics effectively included the metabolic responses and mechanisms involved in the plant-microbe interactions. Considering that 327 common metabolites (i.e., 70%) out of 395 and 398 metabolites ($P < 0.05$) at 43 and 131 DAT, respectively, were shared between vegetative and reproductive phenological stages (**Figure 2**), the biostimulant-mediated metabolomic shifts we recorded represented a common signature, irrespective from the plant growth stage. On the other hand, certain stage-specific responses could be identified as well.

To clarify and visualize the variations between metabolic profiles at the vegetative and reproductive stages, we performed a chemical enrichment analysis using ChemRICH (**Figure 3** and **Tables 4**, **5**) and plotted the output by MetaMapp Cytoscape (**Figure 4**; Barupal and Fiehn, 2017). Most of the significantly upregulated and downregulated metabolites (fold-change values ≤ 0.5 and ≥ 1.5, respectively; $P \leq 0.01$) had a wide range of functions including growth stimulation, antifungal activity, pathogen resistance, energy sources, and secondary signaling cofactors.

Among other, secondary metabolites such as carotenoids and other terpenes, saponins, and phenolic compounds, were altered by the biostimulant treatment. Compared to the control, at 131 DAT, foliar vitamin A and α-carotene were 1.5 × and 8.5 × higher, respectively, following treatment. Blumenols, a class of apocarotenoids or cyclohexanone derivatives of carotenoid cleavage, also accumulated in the biostimulant-treated plants. In detail, blumenol B was 2 × and 2.5 × higher at 43 and 131 DAT, respectively, after biostimulant application. Regarding foliar saponins, their abundance was 1.5–10 × higher in plants treated with biostimulant than in the untreated control. Furthermore, irrespective of growth stage, the phenolics skullcapflavone I, pelargonidin-3-*O*-glucoside, kaempferol, genistein, apiin, and myricatomentoside I accumulated to levels 3–87 × higher in the biostimulant-treated plants than the control.

Phospholipids were also modulated by the treatment. In more detail, the accumulation of phosphatidylethanolamines [PE(P-16:0/20:5)], phosphatidic acid [PA(15:0/22:6), PA(O-18:020:3)], phosphatidylinositol [PIM4(18:1/14:0)], and phosphatidylserine [PS(P-16:013:0)] by 1.5–30 × was recorded in biostimulant-treated plants, compared to the control. Furthermore, lysophospholipids [PA(P-16:0e18:2)] increased by 6.5 × in biostimulant-treated leaves at 131 DAT sampling (reproductive stage).

Concerning hormones, the microbial-based treatment induced also the accumulation of auxins (indole-3-acetamide and indole-3-pyruvic acid increased by 1.7–7.5 × relative to the control), whereas a set of gibberellins precursors (GA81, GA36, GA37, GA12, and GA20) increased by 1.3–16 × compared to control, at both 43 and 131 DAT. Still regarding phytohormones, the biostimulant also triggered the accumulation of the cytokinin *trans*-zeatin by 2.2–5.1 × in pepper leaves, compared to control.

Purine metabolites also increased following the microbial treatments. At 43 and 131 DAT, we observed sharp increases in the guanosine (2.7 × and 8.7 ×, respectively) and N6-threonylcarbamoyladenosine (3- and 7.8-fold, respectively) levels following microbial inoculation. Similar trends could be observed for DAT, NAD, and FAD at both 43 and 131 DAT, with increases by 1.5–4.4 × in biostimulant-treated plants.

DISCUSSION

There is a growing interest in the use of beneficial microbial inoculants such as AMF, *Trichoderma* spp., and PGPR in horticulture as they have multiple beneficial effects on crops (López-Bucio et al., 2015; Rouphael et al., 2015). Similarly, to other studies (Conversa et al., 2013; Colla et al., 2015; Bakr et al., 2018), microbial inoculation of pepper plants was effective to raise significantly the mycorrhizal root colonization and the *Trichoderma* population in the soil rhizosphere.

In the present study, we observed an increase of early and total crop yield, compared to uninoculated plants. Colla et al. (2015) reported that compared with uninoculated field-grown zucchini plants, those supplied with live AMF *G. intraradices* and *T. atroviride* inocula presented with greater early and total yields. Similarly, in two field experiments, Ortas (2019) reported that mycorrhizal inoculation increased yield of the tomatoes, green peppers and eggplants and P and Zn uptake in comparison with uninoculated plants. In the current experiment the total yield increase resulting from inoculation of sweet pepper plants with AMF and *Trichoderma koningi* was higher (24%) than the value (18%) reported by Ombódi et al. (2019) using an inoculum containing six different arbuscular mycorrhizal species under unheated greenhouse conditions and the value (12.7%) recorded by Almaca et al. (2013) using an inoculum containing *Glomus mosseae* and *G. etunicatum* under field conditions. The above differences in pepper yield response could be attributed to the different mycorrhizal species used in the trials and the addition of *Trichoderma koningi* in the current experiment. Co-inoculation of *Trichoderma* spp. and AMF have been found to promote growth and plant development of several vegetable crops more than inoculation using only *Trichoderma* spp. or AMF (Colla et al., 2015). Moreover, similarly to the trial reported by Ombódi et al. (2019), we observed a better yield response of pepper to mycorrhizal inoculation (+66% in the second fruit harvest made on 9 January—174 DAT) when the microclimate conditions for plant growth were suboptimal (low light and temperature occurring during January). Finally, in the current experiment the total yield increases induced by inoculation with AMF and *Trichoderma koningii* were due to both higher fruit number and mean fruit weight whereas in the trial of Ombódi et al. (2019) the yield increases were mostly due to higher number of fruits. The above findings indicate a reduced activity of indigenous arbuscular mycorrhizal fungi and *Trichoderma* spp. in enhancing crop productivity in comparison with exogenous selected arbuscular mycorrhizal fungi and *Trichoderma* species under field conditions. Similarly, Ombódi et al. (2019) reported that inoculation of pepper plants at transplanting with a commercial product containing six different arbuscular mycorrhizal species was able to enhance mycorrhizal root colonization, leaf chlorophyll content (SPAD index) and fruit yield in comparison with naturally occurring

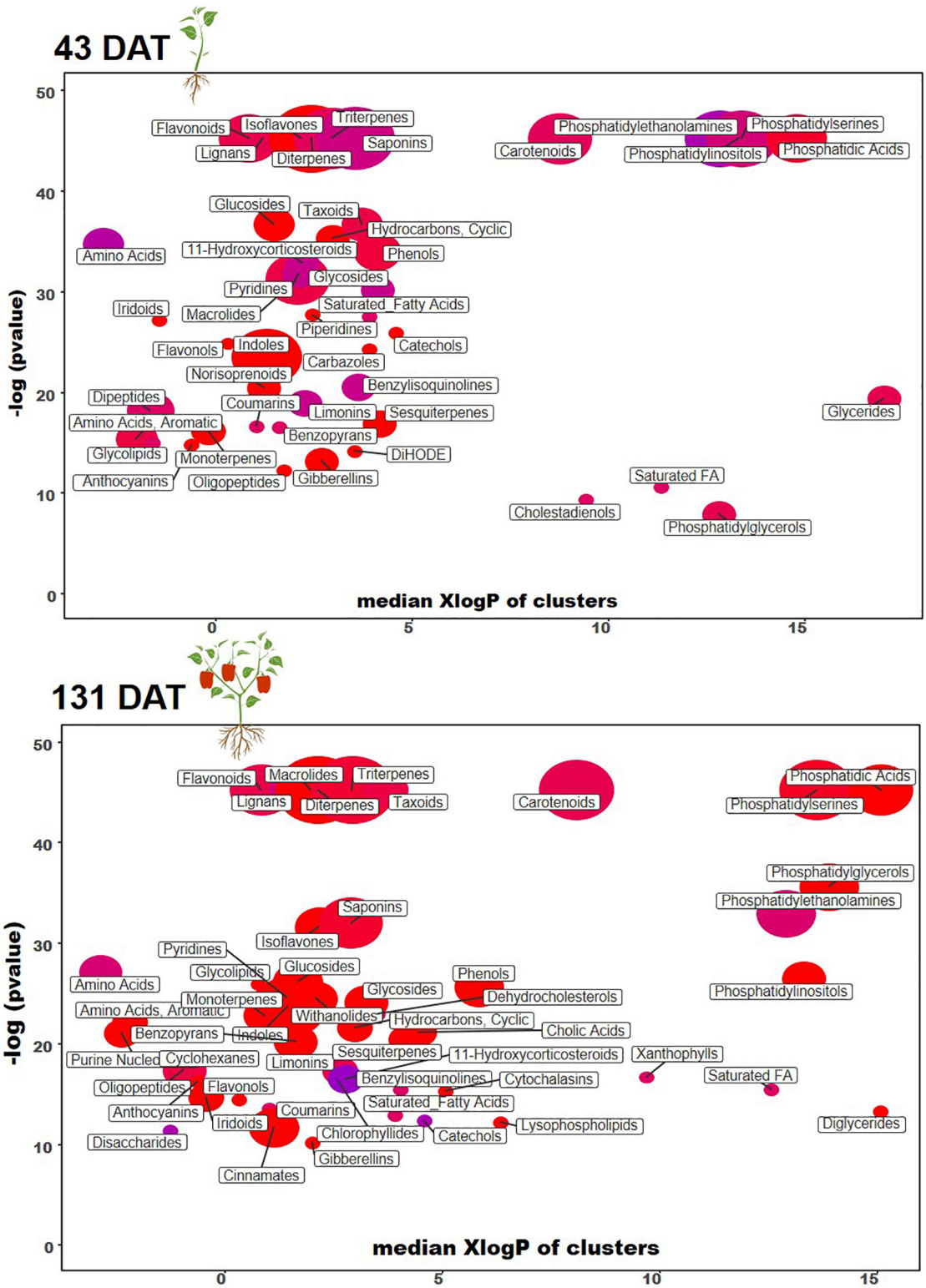

FIGURE 3 | Chemical similarity enrichment analysis (ChemRICH) of statistically different annotated metabolites in microbial-based biostimulant treated leaves compared to untreated control at 43 (vegetative stage) and 131 days after transplanting (reproductive stage). Color is according to proportion of increased or decreased compounds (red = increased, blue = decreased, pink = mixed) within each cluster.

TABLE 4 | Effect of microbial-based biostimulant application on compound chemical classes (CHEMRICH) of greenhouse-grown peppers at vegetative stage (43 DAT).

Cluster name	Cluster size	*p*-values	FDR	Key compound	Increased	Decreased
Carotenoids	10	2.2E-20	9.2E-20	Fucoxanthinol, Vit A, Alpha Carotene	7	3
Diterpenes	17	2.2E-20	9.2E-20	NCGC00385284-01_C32H54O13	17	0
Flavonoids	9	2.2E-20	9.2E-20	Skullcapflavone I 2′-(2″-E-cinnamoylglucoside)	7	2
Isoflavones	6	2.2E-20	9.2E-20	Genistein	6	0
Lignans	4	2.2E-20	9.2E-20	Myricatomentoside I	3	1
Phosphatidic Acids	9	2.2E-20	9.2E-20	PA(18:0/18:2)	8	1
Phosphatidylethanolamines	12	2.2E-20	9.2E-20	PE(P-16:0/20:5)	4	8
Phosphatidylinositols	5	2.2E-20	9.2E-20	PIM4(18:1/14:0)	5	0
Phosphatidylserines	12	2.2E-20	9.2E-20	PS(P-16:0/13:0)	7	5
Saponins	15	2.2E-20	9.2E-20	Borassoside A	8	7
Triterpenes	14	2.2E-20	9.2E-20	Cussoracoside F	10	4
Glucosides	5	1.1E-16	3.9E-16	Luteolin-4′-O-glucoside	5	0
Amino Acids	5	7.8E-16	2.2E-15	Arginine	2	3
Phenols	6	1.7E-15	4.5E-15	Gibbilimbol B	5	1
Glycosides	4	7.7E-14	1.7E-13	Melissoidesin D	2	2
Macrolides	10	2.6E-14	5.9E-14	Capsianoside	8	2
Piperidines	3	9.1E-13	1.9E-12	Andrachcinidine	3	0
Iridoids	3	1.5E-12	3E-12	NCGC00168877-02_C15H20O8	3	0
Catechols	3	5.4E-12	9.9E-12	(S)-[8]-Gingerol	3	0
Flavonols	3	1.6E-11	2.7E-11	Kaempferol	3	0
Auxins	12	6E-11	9.8E-11	Indole-3-acetamide	12	0
Glycerides	4	3.7E-09	5.4E-09	DG(19:1(9Z)/22:4(7Z,10Z,13Z,16Z)/0:0)[iso2]	3	1
Limonins	4	5.9E-09	8.4E-09	11beta-Acetoxydihydrocedrelone	2	2
Dipeptides	6	1.2E-08	1.7E-08	Ala-Phe	4	2
Sesquiterpenes	4	4.5E-08	6.1E-08	Leucascandrolide A	4	0
Coumarins	3	5.8E-08	7.6E-08	Coumarin	2	1
Monoterpenes	4	9.6E-08	1.2E-07	NCGC00384740-01_C21H34O9	4	0
Amino Acids, Aromatic	5	0.0000002	2.5E-07	Tryptophan	4	1
Glycolipids	3	3.1E-07	3.6E-07	Lyciumoside IV	2	1
Anthocyanins	3	3.7E-07	4.3E-07	Cyanidine-3-O-sambubioside	3	0
DiHODE	3	6.8E-07	7.6E-07	8(R)-Hydroperoxylinoleic acid	3	0
Gibberellins	4	0.0000019	0.0000021	Gibberellin A20	4	0
Oligopeptides	3	0.0000047	0.000005	Indole-3-acetyl-L-isoleucine	3	0
Saturated FA	3	0.000024	0.000025	Capric acid	2	1
Phosphatidylglycerols	4	0.00037	0.00037	PG(18:2/13:0)	3	1

mycorrhizal fungi in untreated control. The above findings may be explained by the depression of native mycorrhizal fungi in horticultural production systems caused by the frequent soil tillage and the overuse of chemical inputs. Under these conditions, AMF inoculation may compensate for the loss of indigenous microbial communities to support plant growth (Yu et al., 2020). The results of the current experiment proved that exogenously-applied beneficial fungi such as AMF and *Trichoderma koningi* act as phytostimulation agents and improve plant nutrient uptake. The phytostimulation efficacy of beneficial fungi is explained by complex signal exchange and crosstalk between the host plants and the microorganisms affecting phytohormone balance and plant metabolism (Sbrana et al., 2017). Metabolomics helps elucidate the metabolic pathways and processes involved in plant-microbe interactions. Growth stage has a hierarchically strong effect on the leaf metabolome. Nevertheless, microbial biostimulants significantly alter the metabolome such that it is readily distinguishable from the control. The microbial treatments elicited several processes related to plant secondary metabolism. Microbial-based biostimulants promote the accumulation of different classes of secondary metabolites and phospholipids.

Plant responses to microbial-based biostimulants involved the modulation of phytohormone network. Treatments with beneficial fungi alter auxins, cytokinins, and gibberellins. Modification of the hormone profile may be associated to the yield increases we observed. Several studies demonstrated that microbial biostimulants promote yield by changing the phytohormone balance, increasing nutrient availability and uptake, and enhancing abiotic stress tolerance (Rouphael et al., 2015; Saia et al., 2020). Certain putative mechanisms for the biostimulant activity of microbial-based inoculant (AMF + *Trichoderma*) in pepper have been proposed. Microbial-based inoculants promote root biomass, length, density, and

TABLE 5 | Effect of microbial-based biostimulant application on compound chemical classes (CHEMRICH) of greenhouse-grown peppers at reproductive stage (131 DAT).

Cluster name	Cluster size	*p*-values	FDR	Key compound	Increased	Decreased
Carotenoids	12	2.2E-20	1.3E-19	Fucoxanthinol, Vit A, Alpha Carotene	9	3
Diterpenes	15	2.2E-20	1.3E-19	Traversianal	15	0
Flavonoids	9	2.2E-20	1.3E-19	Skullcapflavone I 2′-(2″-E-cinnamoylglucoside)	7	2
Lignans	5	2.2E-20	1.3E-19	Myricatomentoside I	3	2
Macrolides	9	2.2E-20	1.3E-19	Capsianoside	8	1
Phosphatidic Acids	9	2.2E-20	1.3E-19	PA(O-18:020:3(8Z11Z14Z))	9	0
Phosphatidylserines	12	2.2E-20	1.3E-19	PS(P-16:013:0)	11	1
Triterpenes	15	2.2E-20	1.3E-19	Tricalysioside T	13	2
Phosphatidylglycerols	8	3.3E-16	1.7E-15	PG(P-18:017:2(9Z12Z))	8	0
Phosphatidylethanolamines	8	4.9E-15	2.1E-14	PE(P-16:020:5(5Z8Z11Z14Z17Z))	5	3
Saponins	9	1.2E-14	4.9E-14	Namonin E	8	1
Isoflavones	6	1.8E-14	6.8E-14	Genistein	6	0
Amino Acids	5	1.6E-12	5.4E-12	L-Valine	3	2
Phosphatidylinositols	5	3.1E-12	1E-11	PIM4(18:1(9Z)14:0)	5	0
Glucosides	6	4.3E-12	1.3E-11	Daedaleaside D	6	0
Glycolipids	3	5.3E-12	1.5E-11	Capsoside A	3	0
Phenols	6	7E-12	1.9E-11	Gibbilimbol B	6	0
Glycosides	5	3.2E-11	7.6E-11	Cyclopassifloside VII	5	0
Auxins	12	5.1E-11	1.2E-10	INDOLE-3-PYRUVIC ACID	12	0
Monoterpenes	5	1.2E-10	2.5E-10	beta-Thujaplicin	5	0
Amino Acids, Aromatic	4	2.3E-10	4.6E-10	34-Dihydroxy-L-phenylalanine	4	0
Purine Nucleosides	4	6.9E-10	1.2E-09	Adenosine	4	0
Sesquiterpenes	4	1.4E-09	2.4E-09	(+)-vulgraon B	4	0
Oligopeptides	5	2.7E-08	4.3E-08	Indole-3-acetyl-L-isoleucine	4	1
Limonins	4	2.9E-08	4.4E-08	Toonaciliatin D	3	1
Xanthophylls	3	5.6E-08	8.3E-08	Spirilloxanthin	2	1
Chlorophyllides	3	8.2E-08	1.2E-07	chlorophyllide a	3	0
Anthocyanins	3	8.4E-08	1.2E-07	Delphinidin-3-O-sambubioside	3	0
Saturated FA	3	1.8E-07	2.5E-07	Petroformyne 1	2	1
Iridoids	4	4.1E-07	5.1E-07	Eleganoside B	4	0
Flavonols	3	5E-07	6.1E-07	Kaempferol	3	0
Coumarins	3	1.3E-06	1.5E-06	Coumarin	2	1
Diglycerides	3	1.7E-06	0.000002	DG(15:1(9Z)22:6(4Z7Z10Z13Z16Z19Z)0:0)iso2	3	0
Saturated_Fatty Acids	3	2.5E-06	2.8E-06	Capric acid	2	1
Catechols	3	4.3E-06	4.8E-06	33′44′-Tetrahydroxy-55′-diisopropyl-22′-dimethylbiphenyl	1	2
Lysophospholipids	3	4.9E-06	5.2E-06	PC(O-17:00:0)	3	0
Cinnamates	6	8.2E-06	8.5E-06	Sinapine	6	0
Disaccharides	3	0.000011	0.000011	Melibiose	1	2
Gibberellins	3	0.000036	0.000036	Gibberellin A20	3	0

branching, in turn increasing macronutrient and micronutrient uptake and boosting crop productivity. They also regulate key phytohormones such as gibberellins, cytokinins, and auxins (López-Bucio et al., 2015; Rouphael et al., 2015).

Gibberellins are diterpenoid phytohormones that regulate plant development, flowering, and senescence (Shu et al., 2018). In response to microbial-based inoculant treatment, gibberellins precursors increased. Although the precursor gibberellin A20 was recently linked to increased yields in maize (Tucker et al., 2019), the concurrent increase in auxins we observed (i.e., hormones upregulating the genes encoding 2-oxidases) suggests the promotion of gibberellins catabolism (Frigerio et al., 2006). Indeed, the coordination between gibberellins biosynthesis (mediated by 20- and 3-oxidases) and their 2-oxidases inactivation affects pollination and fruit set in tomato (Serrani et al., 2007). On the other hand, auxins and gibberellins overlap in terms of root growth and fruit set regulation (Bermejo et al., 2018). The microbial-based biostimulant also increased the accumulation of *trans*-zeatin; cytokinins interact with auxins to fine-tune root and shoot development. *Trans*-zeatin modulates meristem activity and mediates plant responses to variable extrinsic factors such as abiotic stress (Werner and Schmülling, 2009).

The modulation of plant signaling compounds in response to the microbial-based biostimulant treatment also involved membrane lipids. Phospholipids are plasma membrane

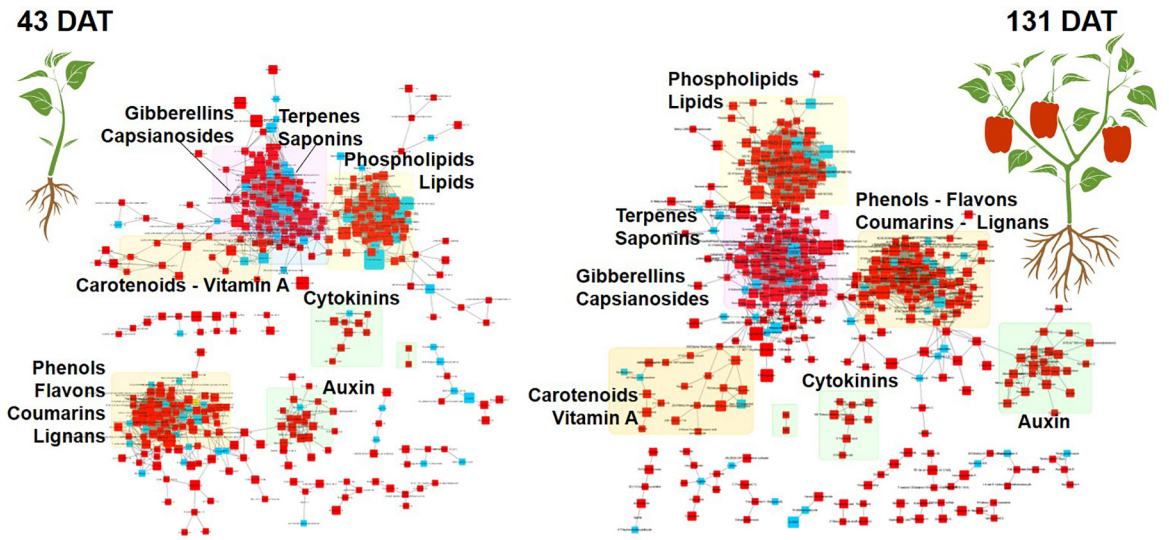

FIGURE 4 | MetaMapp Metabolomic network maps of pepper leaves at 43 (vegetative stage) and 131 days after transplanting (reproductive stage). Microbial-based biostimulant treated plants were compared to control ones. The red squares are compounds with an increase in fold change, while the blue ones represent compounds with a decrease in fold changes. Chemical similarity and KEGG reaction were utilized to draw the clusters and nodes.

components that play important roles in cell signaling, membrane trafficking, and apoptosis (Xue et al., 2009). The microbial-based biostimulant treatment changed the phospholipids profile. It altered 20 foliar metabolites at 43 DAT (vegetative stage) and 31 foliar metabolites at 131 DAT (reproductive stage). Lysophospholipids release calcium from the endoplasmic reticulum, promote cell division and inhibit apoptosis (Ye, 2008; Hou et al., 2016).

The microbial treatment also modulated secondary metabolism, i.e., a set of processes often altered in response to plant interactions with the environment, including agronomic practices and plant-microbe interactions (Yang et al., 2018). In our experiments, plant responses to microbial biostimulants entail the coordinated modulation of several unrelated pathways.

The carotenoids vitamin A and α-carotene increased following the microbial treatment. Carotenoids absorb light energy, participate in photosynthesis, protect plants against oxidative damage, and are precursors of visual pigment chromophores and volatile apocarotenoids that attract pollinators (Heath et al., 2013; Sun et al., 2018). Moreover, they are involved in plant responses to abiotic stresses and plant-microbe interactions (Felemban et al., 2019). Among carotenoids, blumenols also accumulated in the biostimulant-treated plants. Noteworthy, they are reported to accumulate in roots and shoots of mycorrhized plants and have been proposed as markers of arbuscular mycorrhizal fungi colonization (Wang et al., 2018). However, their functions in processes other than allelopathy are still unknown. Their levels are strongly correlated with the degree of mycorrhization (Fester et al., 2002). Concerning saponins, they are constitutively produced in plants and comprise part of plant defense, having both antifungal and antifeedant activity. Though they are generally associated with pathogenesis, it was reported that saponins may participate in mutualistic relationships among plants, rhizobacteria, and mycorrhizae (Szakiel et al., 2011). Despite not focusing on root metabolome (where such mutualistic associations take place), our results indicate that saponins may also be involved in aboveground response to microbial inoculation with the biostimulants.

Compared to control, plants subjected to the microbial treatments presented higher levels of phenolic compounds. Phenolic metabolites are essential for lignin and pigment biosynthesis and participate in plant responses to pathogens and external stimuli (Bhattacharya et al., 2010). Mycorrhizae elicit phenolic biosynthesis in other plant species (Baslam and Goicoechea, 2012; Jugran et al., 2015). They also trigger plant defense against abiotic and biotic stresses and improve nutrient availability and use efficiency (Sharma and Sharma, 2017). Phenolics are associated with plant defense mechanisms. Flavones may protect plants from both biotic and abiotic stress (Martinez et al., 2016). Lignans have high antioxidant activity (Hu et al., 2007; Durazzo et al., 2013). Compared with the uninoculated, the gibbilimbol B level was 1.5 × and 4.2 × higher at 43 and 131 DAT sampling dates, respectively, in the inoculated plants. Gibbilimbol B was reported to have fungicidal activity against *Fusarium oxysporum* f. sp. *dianthi*. Coumarin upregulation is related to iron nutrition (Curie and Mari, 2017), allelochemistry (Niro et al., 2016), and abiotic stress tolerance (Saleh and Madany, 2015) in plants. Plant coumarins may influence the shape of the root microbiome (Voges et al., 2019).

Relative to the control, the levels of several purines were altered in the plants treated with the microbial biostimulant here. Several studies have focused on the effects of increased levels of adenosine and purines. These compounds are recycled by the so-called "salvage pathway" (Ashihara et al., 2018). Nicotinamide adenine dinucleotide (NAD) and flavin adenine dinucleotide

(FAD) are reducing equivalent exchange cofactors that participate in several redox reactions.

Overall, our metabolomics study revealed that microbial biostimulant treatment had two major effects on pepper. First, the biostimulant modulated the phytohormone profile and phospholipid signaling in the plants. Next, it altered various secondary metabolic processes involving saponins, blumenols, carotenoids, and phenolic compounds. Phytohormones and biochemical messengers are associated with various metabolic processes (Ashihara et al., 2018) and might account for the observed biostimulant-mediated increases in crop productivity. Although it is difficult to ascribe the increased yield to few/some specific compounds, we can postulate that the altered balance of hormone profile may have played a pivotal role in fruit setting and development. Indeed, it is well recognized that yields are tightly connected to hormones profile, with an important role actually played by auxins (that increased in our experiments) (An et al., 2020). On the other hand, the involvement of phytohormones in the connection between beneficial microbes and plant productivity has already been postulated (Bhattacharyya and Jha, 2012). Comparatively, much less is known to date regarding the signaling related to membrane lipids, and future research is advisable on this topic.

The secondary metabolites modulated by biostimulant treatment have numerous positive influences on plant productivity, such as the enhancement of nutrient uptake and assimilation and biotic and abiotic stress tolerance. The elicitation of secondary metabolism by plant beneficial microbes deserves further investigation in terms of abiotic stress tolerance and induced systemic response (ISR) induction. Noteworthy, looking at food nutritional traits, carotenoids and phenolics improve quality and promote health in many fruits, including pepper. Thus, the microbial biostimulant treatments applied here could have nutritional implications as well.

CONCLUSION

Recent scientific investigations have focused on improving sustainable farming practices that stabilize yield under optimal and suboptimal conditions and comply with changing legislation regarding the application of low-input agrochemicals. Microbial-based biostimulants (for example, AMF and/or *Trichoderma*) may sustainably enhance crop productivity. Our greenhouse experiment on pepper confirmed that inoculation with a combination of AMF and *Trichoderma koningii* TK7 increased marketable fruit yield by 23.7% relative to that of the untreated control. Metabolomics analysis revealed that the biostimulant treatment reprogrammed the leaf metabolome at the vegetative and reproductive stages. Likely, several biochemical processes underly the observed increase in fruit yield. Here, we showed that the biostimulant modulated the phytohormone profile and elicited secondary metabolism. Specifically, the microbial-based biostimulant upregulated compounds such as carotenoids, saponins, and phenolics that participate in plant nutrition, defense, and stress response. The results of the present study confirm that biostimulant amendments improved the plant health status since the vegetative stage, favoring stable increases in fruit yield. This leads the way toward future investigations into their effects on plants under challenging conditions such as abiotic and biotic stress, environmental perturbations, and physicochemical imbalances.

DATA AVAILABILITY STATEMENT

The original contributions presented in the study are included in the article/**Supplementary Material**, further inquiries can be directed to the corresponding author.

AUTHOR CONTRIBUTIONS

PB, GC, YR, VC, MC, and LL designed the experiment. GC, MC, YR, and GE measured and made the interpretation of agronomical data. PB and BL acquired the metabolomics and qPCR data. PB, BM-M, and LL analyzed the metabolomics data. All authors discussed the results and contributed to the final manuscript.

ACKNOWLEDGMENTS

We thank Tobias Kind from UC Davis, Davis, CA, United States for his assistance with manuscript revision. We also thank prof. Maurizio Ruzzi for the qPCR data revision.

SUPPLEMENTARY MATERIAL

The Supplementary Material for this article can be found online at: https://www.frontiersin.org/articles/10.3389/fpls.2020.567388/full#supplementary-material

REFERENCES

Almaca, A., Almaca, N. D., Söylemez, S., and Ortaş, I. (2013). The effects of mycorrhizal species and different doses of phosphorus on pepper (*Capsicum annuum* L.) yield and development under field conditions. *J. Food Agric. Environ.* 11, 647–651.

An, J., Almasaud, R. A., Bouzayen, M., Zouine, M., and Chervin, C. (2020). Auxin and ethylene regulation of fruit set. *Plant Sci.* 292:110381. doi: 10.1016/j.plantsci.2019.110381

Ashihara, H., Stasolla, C., Fujimura, T., and Crozier, A. (2018). Purine salvage in plants. *Phytochemistry* 147, 89–124. doi: 10.1016/j.phytochem.2017.12.008

Bakr, J., Pék, Z., Helyes, L., and Posta, K. (2018). Mycorrhizal inoculation alleviates water deficit impact on field-grown processing tomato. *Pol. J. Environ. Stud.* 27, 1949–1958. doi: 10.15244/pjoes/78624

Barupal, D. K., and Fiehn, O. (2017). Chemical similarity enrichment analysis (ChemRICH) as alternative to biochemical pathway mapping for metabolomic datasets. *Sci. Rep.* 7:14567. doi: 10.1038/s41598-017-15231-w

Barupal, D. K., Haldiya, P. K., Wohlgemuth, G., Kind, T., Kothari, S. L., Pinkerton, K. E., et al. (2012). MetaMapp: mapping and visualizing metabolomic data by

integrating information from biochemical pathways and chemical and mass spectral similarity. *BMC Bioinform.* 13:99. doi: 10.1186/1471-2105-13-99

Baslam, M., and Goicoechea, N. (2012). Water deficit improved the capacity of arbuscular mycorrhizal fungi (AMF) for inducing the accumulation of antioxidant compounds in lettuce leaves. *Mycorrhiza* 22, 347–359. doi: 10.1007/s00572-011-0408-9

Bermejo, A., Granero, B., Mesejo, C., Reig, C., Tejedo, V., Agustí, M., et al. (2018). Auxin and gibberellin interact in citrus fruit set. *J. Plant Growth Regul.* 37, 491–501. doi: 10.1007/s00344-017-9748-9

Bhattacharya, A., Sood, P., and Citovsky, V. (2010). The roles of plant phenolics in defence and communication during Agrobacterium and Rhizobium infection. *Mol. Plant Pathol.* 11, 705–719. doi: 10.1111/j.1364-3703.2010.00625.x

Bhattacharyya, P. N., and Jha, D. K. (2012). Plant growth-promoting rhizobacteria (PGPR): emergence in agriculture. *World J. Microbiol. Biotechnol.* 28, 1327–1350. doi: 10.1007/s11274-011-0979-9

Bitterlich, M., Rouphael, Y., Graefe, J., and Franken, P. (2018). Arbuscular mycorrhizas: a promising component of plant production systems provided favorable conditions to their growth. *Fron. Plant Sci.* 9:1329. doi: 10.3389/fpls.2018.01329

Blaženović, I., Kind, T., Sa, M. R., Ji, J., Vaniya, A., Wancewicz, B., et al. (2019). Structure annotation of all mass spectra in untargeted metabolomics. *Anal. Chem.* 91, 2155–2162.

Bonini, P., Kind, T., Tsugawa, H., Barupal, D. K., and Fiehn, O. (2020). Retip: retention time prediction for compound annotation in untargeted metabolomics. *Anal. Chem.* 92, 7515–7522. doi: 10.1021/acs.analchem.9b05765

Colla, G., Rouphael, Y., Cardarelli, M., Tullio, M., Rivera, C. M., and Rea, E. (2008). Alleviation of salt stress by arbuscular mycorrhizal in zucchini plants grown at low and high phosphorus concentration. *Biol. Fertil. Soils* 44, 501–509. doi: 10.1007/s00374-007-0232-8

Colla, G., Rouphael, Y., Di Mattia, E., El-Nakhel, C., and Cardarelli, M. (2015). Co-inoculation of *Glomus intraradices* and *Trichoderma atroviride* acts as a biostimulant to promote growth, yield and nutrient uptake of vegetable crops. *J. Sci. Food Agric.* 95, 1706–1715. doi: 10.1002/jsfa.6875

Conversa, G., Lazzizera, C., Bonasia, A., and Elia, A. (2013). Yield and phosphorus uptake of a processing tomato crop grown at different phosphorus levels in a calcareous soil as affected by mycorrhizal inoculation under field conditions. *Biol. Fertil. Soils* 49, 691–703. doi: 10.1007/s00374-012-0757-3

Curie, C., and Mari, S. (2017). New routes for plant iron mining. *New Phytol.* 214, 521–525. doi: 10.1111/nph.14364

De Felice, B. C., Mehta, S. S., Samra, S., Čajka, T., Wancewicz, B., Fahrmann, J. F., et al. (2017). Mass spectral feature list optimizer (MS-FLO): a tool to minimize false positive peak reports in untargeted liquid chromatography–mass spectroscopy (LC-MS) data processing. *Anal. Chem.* 89, 3250–3255. doi: 10.1021/acs.analchem.6b04372

Durazzo, A., Turfani, V., Azzini, E., Maiani, G., and Carcea, M. (2013). Phenols, lignans and antioxidant properties of legume and sweet chestnut flours. *Food Chem.* 140, 666–671. doi: 10.1016/j.foodchem.2012.09.062

Ertani, A., Pizzeghello, D., Francioso, O., Sambo, P., Sanchez-Cortes, S., and Nardi, S. (2014). *Capsicum chinensis* L. growth and nutraceutical properties are enhanced by biostimulants in a long-term period: chemical and metabolomic approaches. *Front. Plant Sci.* 5:375. doi: 10.3389/fpls.2014.00375

Felemban, A., Braguy, J., Zurbriggen, M. D., and Al-Babili, S. (2019). Apocarotenoids involved in plant development and stress response. *Front. Plant Sci.* 10:1168. doi: 10.3389/fpls.2019.01168

Fester, T., Hause, B., Schmidt, D., Halfmann, K., Schmidt, J., Wray, V., et al. (2002). Occurrence and localization of apocarotenoids in arbuscular mycorrhizal plant roots. *Plant Cell Physiol.* 43, 256–265. doi: 10.1093/pcp/pcf029

Frigerio, M., Alabadí, D., Pérez-Gómez, J., García-Cárcel, L., Phillips, A. L., Hedden, P., et al. (2006). Transcriptional regulation of gibberellin metabolism genes by auxin signaling in *Arabidopsis*. *Plant Physiol.* 142, 553–563. doi: 10.1104/pp.106.084871

Giovannetti, M., and Mosse, B. (1980). An evaluation of techniques for measuring vesicular arbuscular mycorrhizal infection in roots. *New Phytol.* 84, 489–500. doi: 10.1111/j.1469-8137.1980.tb04556.x

Heath, J., Cipollini, D., and Stireman, J. (2013). The role of carotenoids and their derivatives in mediating interactions between insects and their environment. *Arthropod-Plant Interact.* 7, 1–20. doi: 10.1007/s11829-012-9239-7

Hou, Q., Ufer, G., and Bartels, D. (2016). Lipid signalling in plant responses to abiotic stress. *Plant Cell Environ.* 39, 1029–1048. doi: 10.1111/pce.12666

Hu, C., Yuan, Y. V., and Kitts, D. D. (2007). Antioxidant activities of the flaxseed lignan secoisolariciresinol diglucoside, its aglycone secoisolariciresinol and the mammalian lignans enterodiol and enterolactone in vitro. *Food Chem. Toxicol.* 45, 2219–2227. doi: 10.1016/j.fct.2007.05.017

Jugran, A. K., Bahukhandi, A., Dhyani, P., Bhatt, I. D., Rawal, R. S., Nandi, S. K., et al. (2015). The effect of inoculation with mycorrhiza: AM on growth, phenolics, tannins, phenolic composition and antioxidant activity in *Valeriana Jatamansi Jones*. *J. Soil Sci. Plant Nutr.* 15, 1036–1049. doi: 10.4067/S0718-95162015005000072

López-Bucio, J., Pelagio-Flores, R., and Herrera-Estrella, A. (2015). *Trichoderma* as biostimulant: exploiting the multilevel properties of a plant beneficial fungus. *Sci. Hortic.* 196, 109–123. doi: 10.1016/j.scienta.2015.08.043

Martinez, V., Mestre, T. C., Rubio, F., Girones-Vilaplana, A., Moreno, D. A., Mittler, R., et al. (2016). Accumulation of flavonols over hydroxycinnamic acids favors oxidative damage protection under abiotic stress. *Front. Plant Sci.* 7:838. doi: 10.3389/fpls.2016.00838

Niro, E., Marzaioli, R., De Crescenzo, S., D'Abrosca, B., Castaldi, S., Esposito, A., et al. (2016). Effects of the allelochemical coumarin on plants and soil microbial community. *Soil Biol. Biochem.* 95, 30–39. doi: 10.1016/j.soilbio.2015.11.028

Ombódi, A., Csorbainé Gógán, A., Birkás, Z., Kappel, N., Morikawa, C. K., Koczka, N., et al. (2019). Effects of mycorrhiza inoculation and grafting for sweet pepper (*Capsicum annuum* L.) crop under low-tech greenhouse conditions. *Not. Bot. Horti. Agrobo.* 47, 1238–1245. doi: 10.15835/nbha47411641

Ortas, I. (2019). Under filed conditions, mycorrhizal inoculum effectiveness depends on plant species and phosphorus nutrition. *J. Plant Nutr.* 42, 2349–2362. doi: 10.1080/01904167.2019.1659336

Paul, K., Sorrentino, M., Lucini, L., Rouphael, Y., Cardarelli, M., Bonini, P., et al. (2019). A combined phenotypic and metabolomic approach for elucidating the biostimulant action of a plant-derived protein hydrolysate on tomato grown under limited water availability. *Front. Plant Sci.* 10:493. doi: 10.3389/fpls.2019.00493

Pereira, J. A. P., Vieira, I. J. C., Freitas, M. S. M., Prins, C. L., Martins, M. A., and Rodrigues, R. (2016). Effects of arbuscular mycorrhizal fungi on *Capsicum* spp. *J. Agr. Sci.* 154, 828–849. doi: 10.1017/S0021859615000714

Rouphael, Y., and Colla, G. (2018). Synergistic biostimulatory action: designing the next generation of plant biostimulants for sustainable agriculture. *Front. Plant Sci.* 9, 1–7. doi: 10.3389/fpls.2018.01655

Rouphael, Y., and Colla, G. (2020). Editorial: biostimulants in agriculture. *Front. Plant Sci.* 11:40. doi: 10.3389/fpls.2020.00040

Rouphael, Y., Franken, P., Schneider, C., Schwarz, D., Giovannetti, M., Agnolucci, M., et al. (2015). Arbuscular mycorrhizal fungi act as biostimulants in horticultural crops. *Sci. Hortic.* 196, 91–108. doi: 10.1016/j.scienta.2015.09.002

Rouphael, Y., Lucini, L., Miras-Moreno, B., Colla, G., Bonini, P., and Cardarelli, M. (2020b). Metabolomic responses of maize shoots and roots elicited by combinatorial seed treatments with microbial and non-microbial biostimulants. *Front. Microbiol.* 11:664. doi: 10.3389/fmicb.2020.00664

Rouphael, Y., Carillo, P., Colla, G., Fiorentino, N., Sabatino, L., El-Nakhel, C., et al. (2020a). Appraisal of combined applications of *Trichoderma virens* and a biopolymer-based biostimulant on lettuce agronomical, physiological, and qualitative properties under variable N regimes. *Agronomy* 10:196. doi: 10.3390/agronomy10020196

Saia, S., Aissa, E., Luziatelli, F., Ruzzi, M., Colla, G., Fica, A. G., et al. (2020). Growth-promoting bacteria and arbuscular mycorrhizal fungi differentially benefit tomato and corn depending upon the supplied form of phosphorus. *Mycorrhiza* 30, 133–147. doi: 10.1007/s00572-019-00927-w

Saito, R., Smoot, M. E., Ono, K., Ruscheinski, J., Wang, P. L., Lotia, S., et al. (2012). A travel guide to Cytoscape plugins. *Nat. Methods* 9, 1069–1076. doi: 10.1038/nmeth.2212

Saleh, A. M., and Madany, M. M. Y. (2015). Coumarin pretreatment alleviates salinity stress in wheat seedlings. *Plant Physiol. Biochem.* 88, 27–35. doi: 10.1016/j.plaphy.2015.01.005

Sbrana, C., Turrini, A., and Giovannetti, M. (2017). "The Crosstalk between plants and their arbuscular mycorrhizal symbionts: a mycocentric view: sign-mediated interactions between cells and organisms," in *Biocommunication Sign-Mediated Interactions between Cells and Organisms*, eds R. Gordon and J.

Seckbach (Singapore: Scientific Publishing Co Pte Ltd), 285–308. doi: 10.1142/9781786340450_0011

Searchinger, T., Waite, R., Hanson, C., Ranganathan, J., and Dumas, P. (2018). *World Resources Report: Creating a Sustainable Food Future*, ed. E. Matthews (Washington, DC: World Resources Institute), 1–97.

Serrani, J. C., Sanjuán, R., Ruiz-Rivero, O., Fos, M., and García-Martínez, J. L. (2007). Gibberellin regulation of fruit set and growth in tomato. *Plant Physiol.* 145, 246–257. doi: 10.1104/pp.107.098335

Sharma, P. I., and Sharma, A. K. (2017). Co-inoculation of tomato with an arbuscular mycorrhizal fungus improves plant immunity and reduces root-knot nematode infection. *Rhizosphere* 4, 25–28. doi: 10.1016/j.rhisph.2017.05.008

Shu, K., Zhou, W., Chen, F., Luo, X., and Yang, W. (2018). Abscisic acid and gibberellins antagonistically mediate plant development and abiotic stress responses. *Front. Plant Sci.* 9:416. doi: 10.3389/fpls.2018.00416

Spatafora, J. W., Chang, Y., Benny, G. L., Lazarus, K., Smith, M. E., Berbee, M. L., et al. (2016). A phylum-level phylogenetic classification of zygomycete fungi based on genome-scale data. *Mycology* 108, 1028–1046. doi: 10.3852/16-042

Sun, T., Yuan, H., Cao, H., Yazdani, M., Tadmor, Y., and Li, L. (2018). Carotenoid metabolism in plants: the role of plastids. *Mol. Plant* 11, 58–74. doi: 10.1016/j.molp.2017.09.010

Szakiel, A., Pączkowski, C., and Henry, M. (2011). Influence of environmental biotic factors on the content of saponins in plants. *Phytochem. Rev.* 10, 493–502. doi: 10.1007/s11101-010-9164-2

Thompson, R. B., Gallardo, M., Valdez, L. C., and Fernandez, M. D. (2007). Using plant water status to define threshold values for irrigation management of vegetable crops using soil moisture sensors. *Agric. Water Manag.* 88, 147–158. doi: 10.1016/j.agwat.2006.10.007

Tsugawa, H., Cajka, T., Kind, T., Ma, Y., Higgins, B., Iked, K., et al. (2015). MS-DIAL: data-independent MS/MS deconvolution for comprehensive metabolome analysis. *Nat. Methods* 12, 523–526. doi: 10.1038/nmeth.3393

Tsugawa, H., Nakabayashi, R., Mori, T., Yamada, Y., Takahashi, M., Rai, A., et al. (2019). A cheminformatics approach to characterize metabolomes in stable-isotope-labeled organisms. *Nat. Methods* 16:446. doi: 10.1038/s41592-019-0423-x

Tucker, S. L., Dohleman, F. G., Grapov, D., Flagel, L., Yang, S., Wegener, K. M., et al. (2019). Evaluating maize phenotypic variance, heritability, and yield relationships at multiple biological scales across agronomically relevant environments. *Plant Cell Environ.* 43, 880–902. doi: 10.1111/pce.13681

Voges, M. J. E. E. E., Bai, Y., Schulze-Lefert, P., and Sattely, E. S. (2019). Plant-derived coumarins shape the composition of an *Arabidopsis* synthetic root microbiome. *Proc. Natl. Acad. Sci. U.S.A.* 116, 12558–12565. doi: 10.1073/pnas.1820691116

Wang, M., Schäfer, M., Li, D., Halitschke, R., Dong, C., McGale, E., et al. (2018). Blumenols as shoot markers of root symbiosis with arbuscular mycorrhizal fungi. *eLife* 7:e37093. doi: 10.7554/elife.37093

Werner, T., and Schmülling, T. (2009). Cytokinin action in plant development. *Curr. Opin. Plant Biol.* 12, 527–538. doi: 10.1016/j.pbi.2009.07.002

Xue, H. W., Chen, X., and Mei, Y. (2009). Function and regulation of phospholipid signalling in plants. *Biochem. J.* 421, 145–156. doi: 10.1042/bj20090300

Yakhin, O. I., Lubyanov, A. A., Yakhin, I. A., and Brown, P. H. (2017). Biostimulants in plant science: a global perspective. *Front. Plant Sci.* 7:2049. doi: 10.3389/fpls.2016.02049

Yang, L., Wen, K. S., Ruan, X., Zhao, Y. X., Wei, F., and Wang, Q. (2018). Response of plant secondary metabolites to environmental factors. *Molecules* 23:762. doi: 10.3390/molecules23040762

Ye, X. (2008). Lysophospholipid signaling in the function and pathology of the reproductive system. *Hum. Reprod.* 14, 519–536. doi: 10.1093/humupd/dmn023

Yu, M., Xie, W., Zhang, X., Zhang, S., Wang, Y., Hao, Z., et al. (2020). *Arbuscular mycorrhizal* fungi can compensate for the loss of indigenous microbial communities to support the growth of liquorice (*Glycyrrhiza uralensis* Fisch.). *Plants* 9:7. doi: 10.3390/plants9010007

Conflict of Interest: VC and GE were employed by the company Atens SL. BL and PB were employed by the laboratory NGAlab.

The remaining authors declare that the research was conducted in the absence of any commercial or financial relationships that could be construed as a potential conflict of interest.

frontiers in Plant Science

ORIGINAL RESEARCH
published: 05 November 2020
doi: 10.3389/fpls.2020.520834

In-Depth Observation on the Microbial and Fungal Community Structure of Four Contrasting Tomato Cultivation Systems in Soil Based and Soilless Culture Systems

Oliver Grunert[1,2†], Emma Hernandez-Sanabria[3†], Saskia Buysens[4], Stefaan De Neve[5], Marie-Christine Van Labeke[6], Dirk Reheul[6] and Nico Boon[1*]*

[1] Greenyard, Skaldenstraat 7a, Desteldonk, Belgium, [2] Agaris, Desteldonk, Belgium, [3] VIB – KU Leuven Center for Microbiology, Laboratory of Molecular Bacteriology, Rega Institute Herestraat, Leuven, Belgium, [4] PCG – Vegetable Research Centre, Kruishoutem, Belgium, [5] Department of Environment, Faculty of Bioscience Engineering, Ghent University, Ghent, Belgium, [6] Department of Plants and Crops, Faculty of Bioscience Engineering, Ghent University, Ghent, Belgium

OPEN ACCESS

Edited by:
Sheridan Lois Woo,
University of Naples Federico II, Italy

Reviewed by:
Francesco Di Gioia,
Pennsylvania State University (PSU), United States
Santiago Gutierrez,
Universidad de León, Spain

***Correspondence:**
Nico Boon
Nico.Boon@UGent.be
Oliver Grunert
oliver.grunert@telenet.be

† These authors have contributed equally to this work

Specialty section:
This article was submitted to Plant Pathogen Interactions, a section of the journal Frontiers in Plant Science

Received: 16 December 2019
Accepted: 06 October 2020
Published: 05 November 2020

Citation:
Grunert O, Hernandez-Sanabria E, Buysens S, De Neve S, Van Labeke M-C, Reheul D and Boon N (2020) In-Depth Observation on the Microbial and Fungal Community Structure of Four Contrasting Tomato Cultivation Systems in Soil Based and Soilless Culture Systems. Front. Plant Sci. 11:520834. doi: 10.3389/fpls.2020.520834

As soil and soilless culture systems are highly dynamic environments, the structure of rhizosphere microbial communities is consistently adapting. There is a knowledge gap between the microbial community structure of soil based and soilless culture systems and thus we aimed at surveying their impact on diversity and composition of bacterial communities across a 10-month period in a tomato cultivation system. We compared community metrics between an soil based culture system fertilized with malt sprouts and blood meal, known for its slow and high mineralization rate, respectively and a soilless culture system fertilized with fish effluent or supplemented with an liquid organic fertilizer. Bacterial and fungal community composition was followed over time using two complementary techniques, phospholipid fatty acid analysis and 16S rRNA amplicon sequencing. Nitrogen dynamics and plant performance were assessed to provide insight on how bacterial diversity of soil and soilless microbial communities ultimately impacts productivity. Similar plant performance was observed in soilless culture systems and soil based system and yield was the highest with the aquaponics-derived fertilizer. Soil and soilless cultivating systems supplemented with different nitrogen-rich fertilizers differed on its characteristics throughout the experimental period. Fast-paced fluctuations in pH(H_2O) and nutrient cycling processes were observed in growing medium. Physicochemical characteristics changed over time and interacted with bacterial community metrics. Multivariate analysis showed that plant length, pH, *Flavisolibacter*, phosphorus, chloride, ammonium, potassium, calcium, magnesium, sodium, electrical conductivity, nitrate, sulfate, and the bacterial genera *Desulfotomaculum*, *Solirubrobacter*, *Dehalococcoides*, *Bythopirellula*, *Steroidobacter*, *Litorilinea*, *Nonomuraea* were the most significant factors discriminating between natural

soils supplemented with animal and plant by-products. Long-term fertilizer regimes significantly changed the PLFA fingerprints in both the soilless culture and soil based culture system. The use of these by-products in the soil was positively associated with arbuscular mycorrhizal fungi (AMF), which may influence rhizosphere communities through root exudates and C translocation. Community structure was distinct and consistently different over time, despite the fertilizer supplementation. The fungal microbial community composition was less affected by pH, while the composition of the bacterial communities (Actinomycetes, Gram-negative bacteria, and Gram-positive bacteria) was closely defined by soil pH, demonstrating the significance of pH as driver of bacterial community composition. Fertilizer application may be responsible for variations over time in the ecosystem. Knowledge about the microbial interactions in tomato cultivating systems opens a window of opportunity for designing targeted fertilizers supporting sustainable crop production.

Keywords: tomato, soilless culture systems, growing medium, soil, microbial community, malt sprouts, aquaponics, organic fertilizer

INTRODUCTION

Over the past century, incredible advancement has been achieved worldwide in increasing global agricultural production (Ramankutty et al., 2018) The production has more than tripled between 1960 and 2015, owing predominantly to the Green Revolution technologies and a significant enlargement in the use of land, water and other natural resources for agricultural purposes (FAO, 2016; Ramankutty et al., 2018). In order to meet the agricultural demand in 2050 we will need to produce 50% more food (Alexandratos, 2009; Foley, 2011; McKenzie and Williams, 2015). This expansive food production comes at a hefty cost to the natural environment (Notarnicola et al., 2017). The urgent need for more sustainability prompted a renewed attention in the biology-based elements of soil and soilless culture crop production systems, including interest in the development of agricultural and horticultural biological solutions. The time has come for another look at using the tools of nature to enhance the intrinsically plant biological systems. This doesn't implicit an anti-chemical approach: rather, make agricultural practices both more productive and more sustainable by incorporating the next generation of biologically sourced tools into existing practices.

The use of fertilizers facilitated largely the increases in agricultural production over the last decennia. Before the 1950s, farmers used natural fertilizers such as manure (Gellings and Parmenter, 2016) and there was very limited use of chemical fertilizers. Nitrogen (N), phosphorus (P), and potassium (K) are essential for plant growth, and potassium and phosphorus are found in mineral deposits (Roberts and Stewart, 2002; Gross, 2012). A nitrogen revolution was generated by the introduction of the Haber-Bosch process: the industrial scale production of ammonia from natural gas (Smil, 1999). Today, the total fertilizer nutrient demand is more than 190 million tons (∼120 tons N, ∼46 tons P, ∼37 tons K) with an average annual growth of 1.9 percent expected over the following years next to other measures (Heffer and Prud'homme, 2016; FAO, 2017). These inorganic nutrients are instantly usable and the leftover either rises up in the soil, disappeared as run-off into the surface water or drains into the groundwater (Steiner et al., 2007). Avoiding reduction of soil organic carbon (SOC) and too expeditious availability, one can go for organic fertilizers (Diacono and Montemurro, 2011) typically produced from plant, or animal-derived materials (Dion et al., 2020) and even microbes can be used (Verstraete et al., 2016; Pikaar et al., 2017; Sakarika et al., 2019; Spanoghe et al., 2020). Blood meal has been reported to provide a fast and high-percentage N mineralization (Agehara and Warncke, 2005; Hammermeister et al., 2006; Hartz and Johnstone, 2006; Gaskell and Smith, 2007; Sullivan et al., 2010). Plant based materials are reported to be slow-release N fertilizer (Agehara and Warncke, 2005; Hammermeister et al., 2006; Sullivan et al., 2010), which is consistent with its higher C/N ratio. These organic fertilizers are mixed in the growing medium or soil and the breakdown and subsequent rate of nutrient delivery in soil and soilless culture systems largely depends on the physical, chemical and biological characteristics of the soil or soilless culture system (Schmilewski, 2008; Sonneveld and Voogt, 2009; Grunert et al., 2016a).

Besides fertilizers, the fast development in soilless production systems caused a considerable switch away from the use of soil to soilless culture systems and consequently pushed the increase in food production (Raviv et al., 2019). Soilless plant culture is any mechanism of growing plants without the benefit of soil as rooting medium (Schmilewski, 2007; Savvas et al., 2013; Raviv et al., 2019) and they play a pivotal role in horticulture and agriculture (Barrett et al., 2016). The enduring transfer from soil to soilless culture systems is also advanced by a good management of various essential factors, partly responsible for enhanced plant performance (Barrett et al., 2016). Soilless horticultural systems have benefits over soil based systems in that the nutrients (Dubik et al., 1990), oxygen and water required for a healthy plant growth are controlled (Barrett et al., 2016) and that soil-borne pathogens can be avoided (Runia, 1993; Postma, 2009). Soil-based organic culture systems are typified by a combination of low external input methods. It gives next to other measures preference to improving the soil with compost additions and animal and

plant derived green manures (Reganold and Wachter, 2016). In addition, organic soil management is inherently dependent on an active bacterial, saprotrophic and fungal community (Reganold and Wachter, 2016; Martínez-García et al., 2018) and has an increased microbial diversity (Francioli et al., 2016). However, resource efficiency and production yields in these soil based organic culture systems are relatively low (Rahmann et al., 2009).

Soil-based and soilless culture systems rely upon physicochemical features, which are distinct for each culture system. Soil and soilless culture systems have diverse physical and hydraulic characteristics (Raviv and Lieth, 2007). Soil-grown plants are encountered with relatively high water availability shortly after fertigation (Bunt, 1988). Another basic trait of soilless cultivation over soil-based cultivation is the boundless root volume, while in soilless culture the root volume is containerized (Raviv et al., 2019). Nutrients, pH and the electrical conductivity (EC) are influential chemical properties (Lauber et al., 2008, 2009, 2013; Raviv et al., 2019) and can be easily regulated in soilless culture systems to demanded nutrient, pH and EC levels. It was demonstrated, that soilless organic growing media have particular niches for diverse bacterial communities with temporal functional stability (Grunert et al., 2016a). New or sterilized growing media usually experience the absence of a diverse and competitive microbiome (Raviv and Lieth, 2007; Postma, 2009; Grunert et al., 2016a), while the soil generally holds up to 10^7 –10^9 colony-forming units (CFU) of bacteria and 10^4 –10^6 culturable fungal propagules per gram of soil (Alexander, 1977). It is postulated that organic peat based growing media used in tomato cultivation systems are mainly colonized by fungi, actinomycetes and *Trichoderma* spp. (Khalil and Alsanius, 2001; Koohakan et al., 2004), while mineral growing media are mainly colonized by bacteria (Vallance et al., 2010). In addition, changes in the soil water content as a result of fertigation activities greatly impacts microbial activity and community structure (Fierer et al., 2003). Engineering the microbial community of soilless culture systems might help to work out approaches to progress toward a more sustainable horticulture with increased productivity, quality and sustainability. However, little comparative research has been performed on the bacterial and fungal composition and development during crop growth in soil and soilless culture systems supplemented with organic and chemical fertilizers. Thus, improved understanding of the variability over time in soil and soilless microbial communities amended with organic and chemical fertilizers will provide insight into the factors influencing the overall diversity and might help developing advanced soil and soilless culture systems.

The present study used a multidisciplinary approach to study tomato cultivation systems and the overall objective of the research was to carry out an in-depth observation of four contrasting tomato cultivation systems during one growing season on the composition of the bacterial and the fungal microbiome. The objectives of the experiment were twofold. First, the effect of four different tomato cultivation systems on plant performance was studied and second changes in microbial community composition during 321 days after sowing were assessed. Assuming that each of the four contrasting tomato cultivation systems and different nutrient management have an influence on physico-chemical characteristics, we hypothesized that (i) the soil and soilless culture based edaphic properties, which are strongly altered during one tomato growing season, consecutively affect the bacterial and fungal microbial community structure. Moreover, we hypothesized that (ii) the community changes caused by four contrasting fertilization strategies included shifts in the abundance of various plant-beneficial soil- and soilless culture based microorganisms, thus influencing plant performance.

MATERIALS AND METHODS

Experimental Setup for Soil-Based and Soilless Culture System

Four Contrasting Tomato Cultivation Systems

Four contrasting tomato cultivation systems were used, i.e., two soilless grow bag (GB) based and two soil-based culture systems (SOIL). The GB were filled with an organic growing medium made of 40% v/v sod peat, 40% v/v Irish peat and 20% v/v coconut fiber. The compartment for the soilless culture system was split in two sections. In the first section liquid organic fertilizer solutions (GBOF) through the fertigation systems, while in the second section plants were fertilized with fish effluent supplemented with mineral fertilizer (GBFISH). The soil (SOIL) used for the two soil-based tomato cultivating systems at the experimental site (PCG Kruishoutem, Belgium) is an organically managed soil according to the EU Council Regulation 834/2007. For most of the European countries and for all member states of the European Union (EU), organic farming is strictly defined by the European Commission (EC) and these rules were followed for the soil based system. The soil had a loamy sand texture (Haplic Podzol: 85% sand, 11% silt, and 4% clay). For the organic soil two different kinds of fertilizers were used: plant-derived malt sprouts (3-0-0) (Orgamé, Belgium) material (SOIL-PLANT) and animal-derived blood meal (14-0-0) (Orgamé, Belgium) material (SOIL-ANIMAL). The malt sprouts and the blood meal were blended in the soil on 19/3/2015, 2/7/2015 and 22/7/2015 and 28/8/2015.

Experimental Setup of the Four Tomato Cultivation Systems

The growth tests for the two soilless culture systems (GBOF and GBFISH) were performed in the same compartment (S91), while the soil-based tomato cultivation system were performed in two different compartments (S92 and S93). For the soilless culture system, GBs or slabs were placed in gutters (or gullies) to collect the efflux solution typically called 'drain,' which was discharged. Forty one-headed tomato plants per treatment were used (GBOF, GBFISH, SOILPLANT, and SOILANIMAL) and each tomato cultivation systems had an effective experimental surface of 15.1 m^2 per treatment out of the available 80 m^2 per compartment. Slabs for the soilless culture system were placed in gutters and each gutter contained 6 slabs. Slabs of GB had the following dimensions: 1.0 m × 0.2 m × 0.085 m. The mature plants (5 plants per slab) with a visible first truss were placed on the slabs in the soilless culture system and

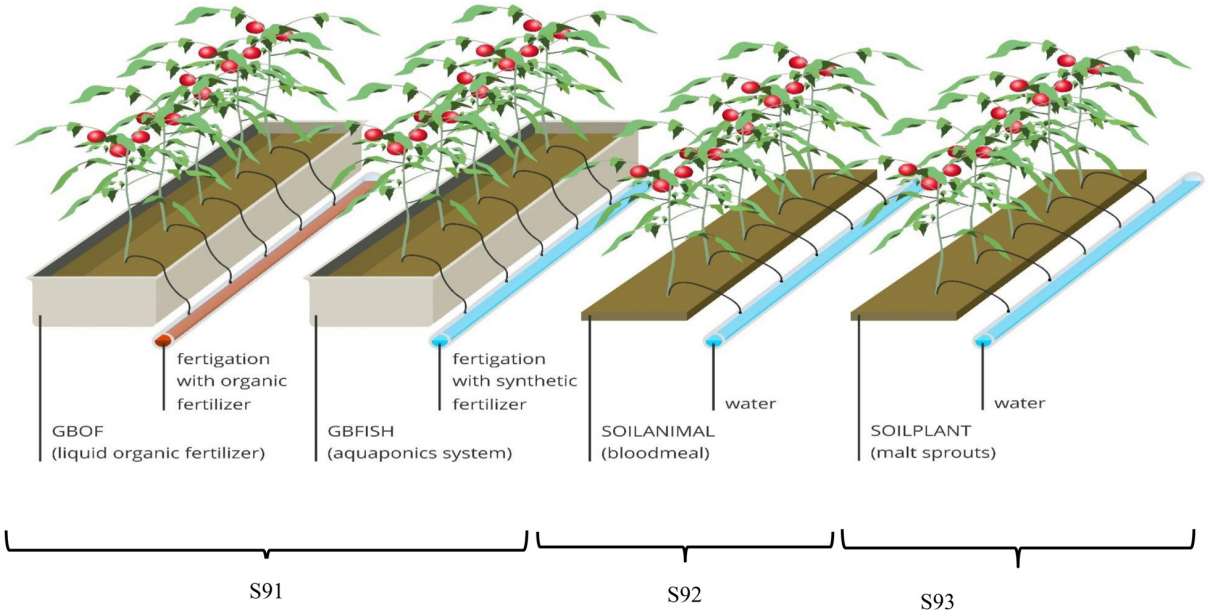

FIGURE 1 | Overview of the experimental set-up showing one experimental unit per treatment. The glass house was divided into three compartments (S91, S92, and S93) with a surface of 80 m^2 for each compartment. The compartment for the soilless culture system (S91) was subdivided into two part. i.e., GBOF and GBFISH; S92 was organic soil fertilized with animal (blood meal) derived material and S92 was the organic soil fertilized with plant-derived material (malt sprouts). In S92 and S93 the previous cultures were tomato in 2014, pepper in 2013 and cucumber in 2012. Plant density was the same for all the treatment 2.65 plants m^{-2}. For the soilless culture system and soil-based system five experimental units were randomly selected from the different compartments.

directly on the soil in the soil based system (**Figure 1**). This was done on the same date (55 DAS). Plant density was 2.65 plants m^{-2} (i.e. 1 plant per 0.47 m × 0.8 m) and was equal among treatments. The high-wire system was used for the tomato cultivation. In this system the growing tip remained at the top of the canopy and the stem was lowered allowing maximum light interception of the head of the plant. The plants grown in the organically managed soil had about 113 L soil plant $^{-1}$ at their disposal, assuming that the plants used between 0 and 30 cm of the top layer for rooting, while the plants in the soilless culture system had about 3.4 L growing medium $plant^{-1}$ at their disposal. For sampling only the inner plants were used to avoid border effects. The first harvest started on 138 DAS and ended on 321 DAS. Water gift was registerend for all the tomato cultivating systems (**Supplementary Figure S2**). All guidelines according to organic greenhouse tomato production, with respect to organic fertilizers and pesticides use, were followed. Side shoots developed from every axil and these side shoots were removed on a weekly basis leaving only one main stem as a growing point. Uniform fruit size was maintained by fruit pruning and thereby controlling the number of fruits left on the truss, i.e. 5 fruits per truss.

Tomato Plants and Transplant Production

Tomato plants (*Solanum lycopersicum* cultivar RZ 72-704, Rijk Zwaan, Fijnaart, Netherlands) was grafted on *Solanum lycopersicum* L. x *Solanum habrochaites* Maxifort (Monsanto Vegetable Seeds, Bergschenhoek, Netherlands). Tomatoes were sown on 18/12/2014 (0 DAS) and transplant production of grafted plants required up to 6 weeks. Transplant production was done in blocking compost made of white and black peat according to EU Council Regulation 834/2007. The blocking compost had the following dimensions:0.1 m × 0.1 m × 0.06 m. The tomato plants were grown until mature plants (5 plants per slab) with a visible first truss and which was as wide as it was tall.

Experimental Location

The plant experiment was established in the experimental glasshouse of the Vegetable Research Centre in Kruishoutem (longitude = 3°31′E and latitude = 50°56′N and 10 meters above sea level). The glasshouse was divided into three compartments (S91, S92, and S93) and every compartment had a surface of 80 m^2 with equal climatic conditions. Compartment S91 was used for both soilless culture systems and S92 and S93 was used for the soil based tomato cultivation system. An overview of the experimental set-up can be found in **Figure 1**. The glasshouse experiment started on the 11th of February 2015 and ended on the 4th of November 2015. *Macrolophus pygmaeus* was used to protect the plants against all kind of insects, Enermix (*Encarsia formosa* + *Eretmocerus eremicus*) was used against white flies. *Trichoderma harzanium* (Koppert, Netherlands) is a biolgical fungicide and used to protect the plants against soil borne diseases, such as *Pythium* spp., *Rhizoctonia* spp., *Fusarium* spp., *Sclerotinia* and the root mat syndrome caused by *Agrobacterium rhizogenes*. Serenade (*Bacillus amyloliquefaciens*) from Bayer Crop Science (Germany) and magnesium sulfate were used to protect the plants against *Oidium lycopersici*.

Irrigation and Nutrient Management of the Four Different Tomato Cultivating Systems

Irrigation of tomatoes was based on solar irradiation and considered amount of drained water. Irrigation varied between 3 mL J^{-1} and 4 mL J^{-1} at higher temperatures resulting in a peak water supply between 8 and 10 L m^{-2} d^{-1} in summer. For the soilless culture system (GBOF and GBFISH) the efflux solution or drain was discharged. It was estimated at the start of the experiment that about 1300 L m^{-2} water was needed for the cultivation of tomatoes during a whole season (February until November). For the four contrasting tomato cultivation systems drip irrigation was used and the nutrients were injected into the irrigation water from concentrated solutions in stock tanks (Sonneveld and Voogt, 2009). For the soil-based tomato cultivation systems (SOILANIMAL and SOILPLANT) no nutrients were infused into the irrigation water as they were blended in the soil, meaning that pure rain water was used (**Figure 1**). For the soilless culture system slabs may be watered up to 6 times per hour in peak radiation, and up to 30 times per day under summer conditions.

Nutrient Management for the Soilless Culture System (GBOF and GBFISH)

The compartment for the soilless culture system was split in two parts. One part was fertilized with a liquid organic fertilizer solution (GBOF) and another part was fertilized with fish effluent supplemented with mineral fertilizer (GBFISH). Four different organic fertilizers (ANTYS MgS, Biosyr, Nutrikali, and SP; Frayssinet, France) were used for GBOF. Detailed information about the type, composition and the amount of fertilizer used can be found in **Supplementary Table S4**.

They were combined with each other aiming at a balanced nutrient solution suitable for the cultivation of tomatoes. Moreover, a N:P:K ratio of 1:0.2:1.6 was respected throughout the whole experimental period for the soilless culture system. Nutrient solution for GBOF was supplemented with extra calcium chloride ($CaCl_2$) and Libremix (3.2% Fe-EDTA, 1.5% Mn-EDTA, 1.6% Cu-EDTA, 0.6% Zn-EDTA, 0.8% B and 2.5% Mo; Brinkman, Netherlands) if needed, such as increased incidence of blossom end rot (BER). The nitrogen dose of the nutrient solution was increased or decreased according to the growth of the plants and/or the presence or absence of deficiency symptoms.

For GBFISH the fish effluent coming from the aquaponics system was supplemented with mineral fertilizer (GBFISH). Ammonia is the main excretion product of the fish. The excreted ammonium was converted into nitrate and was used as the primary inorganic nitrogen source for the tomato plants. The fertigation solution coming from the aquaponic system was amended with the necessary nutrients and corrected when needed aiming at a final composition of 0.7 mmol NH_4^+ L^{-1}, 18.4 mmol NO_3^- L^{-1}, 10.9 mmol K L^{-1}, and 6.2 mmol Ca L^{-1}, 2.8 mmol Mg L^{-1}, 0.7 mmol Cl L^{-1}, 5.1 mmol SO_4^{2-} L^{-1} and 1.7 mmol $H_2PO_4^-$ L^{-1}.

Nitrogen supply rate per square meter increased steadily from 1.3 g N m^{-2} d^{-1} to 112.6 g N m^{-2} d^{-1} between days 78 and 161 for GBOF. Nitrogen load was decreased to 20 g N m^{-2} d^{-1} in the following next 27 days as a result of increased blossom end rot (BER) incidence, development of smaller leaves, reduced plant growth, and leaf chlorosis. Nitrogen supply rate was increased again up to 164 g N m^{-2} d^{-1} after the above mentioned period.

Nutrient management for the soil-based culture system SOILANIMAL treatment received 252 kg N ha^{-1} coming from blood meal with a total nitrogen content of 14% and 1630 kg ha^{-1} of patentkali (30% K_2O, 10% MgO, and 42% SO_3). The SOILPLANT treatment received 300 kg N ha^{-1} coming from malt sprouts (7% of nitrogen) and 1630 kg ha^{-1} of patentkali (30% K_2O, 10% MgO and 42% SO_3) at the start of the experiment. Chemical composition of the organic soil (SOILPLANT and SOILANIMAL) and the soilless culture system can be found in **Table 1**. Detailed information about the type, composition and the amount of fertilizer used can be found in **Supplementary Tables S2, S3**.

Sample Collection

For the experiment three compartments were used. The compartment for the soilless culture system was split in two parts each consisting of 6 gutters/rows. For an overview of the sampling procedure please check **Supplementary Figure S1**. For the soil based system two different compartments were used. Slabs for the soilless culture system were placed in gutters, each gutter contained 6 slabs and each slab 5 plants. The two outer rows and outer slabs of each block were not selected, because of possible interactions with the adjacent rows and to avoid side effects. One slab with 5 consecutive plants in the soilless culture system and 5 consecutive plants in the soil based system were considered as an experimental unit. Among all treatments the tomato plants were placed consecutively with an interspacing of 0.47 m and an in row interspacing of 0.8 m. For the soilless culture system and soil-based system five experimental units were randomly selected from the different compartments. Samples of the different experimental units were collected at different time points during the growing season and at the start of the experiment. Ten subsamples from each experimental unit were collected, pooled, homogenized and treated as a single sample. At each time point, samples were taken from 5 fixed experimental units of each GBOF, GBFISH, SOILANIMAL, and SOILPLANT, including root material. Samples from the soil were taken with an auger in the 0–10 soil profile and from each experimental subunit 10 subsamples were taken. Each sample contained 200 g soil or growing medium and was divided into homogenous subsamples: one subsample was used for chemical analyses (100 g) and water content (50 g), one subsample was immediately after sampling stored on dry ice, preserved at −80°C and used for molecular microbial community analysis (50 g). The ammonium and the nitrogen content, the pH and the electrical conductivity (EC) in the 0–10 cm organic soil layer and in the growing medium were taken at the start 55 DAS(T0), 68 DAS (T1), 83 DAS (T2), 113 DAS (T3), 146 DAS (T4), 172 DAS (T5), 221 DAS (T6), and 321 DAS (T7). Samples for microbial community analysis were taken at 8 different timepoints, i.e., 55 DAS, 68 DAS, 83 DAS, 113 DAS,

146 DAS, 172 DAS, 221 DAS, and 321 DAS. Samples for PLFA analyses were collected at four different time points, i.e., 55 DAS, 83 DAS, 221 DAS, and 321 DAS. Briefly, for the PLFA analyses the soil and growing media were freeze-dried using a modified technique (Bligh and Dyer, 1959). Whole plants were harvested, chopped and samples from stem and leaves without tomatoes were collected for analysis at 221 DAS and 321 DAS.

Nitrogen Determination in the Soil, Soilless Culture System and Plant

Physicochemical characteristics of the soil and soilless culture systems were determined at the start and throughout the whole experimental period. Potassium, phosphorus, calcium, magnesium, iron and manganese were extracted in ammonium acetate and measured with ICP. The electrical conductivity (EC), pH(H_2O), ammonium (NH_4^+), nitrate (NO_3^-), sulfate (SO_4^{2-}) and sodium (Na^+) were measured in a water extract according to EN 13038, EN 13037 and EN 13652, respectively. Nitrate was measured with an Dionex DX-3000 IC ion chromatograph (Dionex, Sunnyvale, CA, United States). Ammonium was measured by steam distillation (Bremner and Keeney, 1965). The elements were measured by a ICP-OES (VISTA-PRO, Varian, Palo Alto, CA, United States). The total nitrogen content of the plants sampled was determined according to Dumas (British Standards Institute Staff, 2001).

Estimation of the Nitrogen Dynamics in Soil and Soilless Culture Systems

The ammonium and the nitrogen concentration in the soil at the start 55 DAS – time point 1, 221 DAS – time point 2 and 321 DAS – time point 3) were calculated based on the ammonium, the nitrate and the estimated soil dry bulk density (1.25 kg L^{-1}) of the 0–10 cm soil layer. Fertilizers were applied in the top layer of the organic soil (0–10 cm) and soil water content was controlled in the 0–10 cm layer. The ammonium and the nitrogen concentration of GBOF and GBFISH were also determined and were recalculated based on the amount of growing medium needed per ha, i.e., 90 m^3 ha^{-1}. At time point 2 and 3 the dry matter and N content of whole plant samples were determined for calculation of dry biomass and total N uptake at time point 2 and 3. Samples were taken from shredded tomato plants ($n = 4$). Samples were dehydrated in an oven at 70°C for 48 h. N content was determined on chopped dehydrated plant material (Kjeldahl method, ISO 5983-2).

Plant Performance

The length of the plant was measured on a weekly basis with a measuring tape. Both the fresh and dry weight of the plants and nitrogen content were determined at the start (55 DAS), the middle 221 DAS and at the end 321 DAS of the experiment. Tomatoes were harvested on a weekly basis or whenever necessary and cumulative yield (fresh weight) was determined.

DNA Extraction

Total DNA was extracted using physical disruption with the bead beating method from Hernandez-Sanabria et al. (2020) and Grunert et al. (2016a). Cells were lysed in a FastPrep-96 homogenizer (MP Biomedicals, Illkirch, France) and DNA was precipitated with cold ethanol and resuspended in 30 µl of TE buffer (10 mM Tris-HCl, 1 mM EDTA [pH 8.0]). Concentration and quality of DNA were measured based on the absorbance at 260 and 280 nm in a Nanodrop ND 1000 spectrophotometer (NanoDrop Technologies, Wilmington, DE, United States).

Total Biomass and Overall Fingerprint of the Viable Fungal and Bacterial Communities

Microbial community composition was determined by phospholipid fatty acid analysis (PLFA). Briefly, PLFAs were obtained from freeze-dried soil and growing media using a modified technique (Bligh and Dyer, 1959) The PLFAs were determined using a procedure modified from Balser (2001) and Moeskops et al. (2010). To identify Gram-positive bacteria, the sum of i14:0, i15:0, a15:0, i16:0, a16:0, i17:0, and a17:0 was computed. The fatty acids cy17:0, cy17:0new, cy19:0 and cy19:0 new were considered to be representative for Gram-negative bacteria. The sum of 10Me16:0, 10Me17:0 and 10Me18:0 were an indicator for the Actinomycetes. The fatty acid 18:2ω6c was used as fatty acid for fungi, and two alternative signature fatty acids for fungi were considered as well, i.e., 18:1ω9 and 18:3 ω3. The fatty acid 16:1ω5c was an indicator for AMF. Bacteria: fungi (B:F) ratios were calculated by dividing the sum of markers for Gram-positive, Gram-negative bacteria, 15:0 and 17:0 by the fungal marker 18:2ω6c.

Bacterial Community Structure and Composition

Total DNA was extracted from the growing medium samples using the Power Soil® DNA Isolation Kit (MoBio Laboratories Inc., Carlsbad, CA, United States). Five hundred milligrams were used from the bulk as previously described (Grunert et al., 2019). High-throughput amplicon sequencing of the V3 – V4 hypervariable region (Klindworth et al., 2012) was performed with the Illumina MiSeq platform (LGC Genomics GmbH, Berlin, Germany) and the following primers were used 338f and the 518 r (Øvreås et al., 1997). Bioinformatics and data pre-processing followed a protocol developed in-house (El Hage et al., 2019; Grunert et al., 2019; Hernandez-Sanabria et al., 2020). A generalized linear mixed model was employed to compute the effect of tomato cultivating system and time and the interactions between "tomato cultivating system" and time on each individual genus (El Hage et al., 2019; Grunert et al., 2019; Hernandez-Sanabria et al., 2020). Differences among library size sample were accounted for with the offset option in proc GLIMMIX in SAS (Paschold et al., 2012; El Hage et al., 2019). P values for each comparison were converted to q-values that were then used to identify

differences in relative abundances of bacterial genera while controlling the false discovery rate (FDR) at the 5% level (Storey, 2015).

Evaluating Relationships Between Microbial Community Characteristics and Culturing System Features

Variations in tomato cultivation systems and nitrogen dynamics were computed using a repeated measures mixed in SAS (version 9.4, SAS Institute, Cary, United States). *P*-values for Pearson correlation coefficients and regression coefficients were used to determine significant relations with a significance level of $P < 0.05$ (Grunert et al., 2019). Multiple Factor Analysis (MFA) was employed to detect how the microbial community composition based on a PLFA analysis and bacterial abundance contributed to the differences between the four different tomato cultivating systems across time points. In addition, MFA was applied to assess the correlations between the chemical and microbiological variables based on the PLFA analysis and bacterial abundance detected in the four tomato cultivating systems. R was used (Grunert et al., 2019; Hernandez-Sanabria et al., 2020) to compute the function MFA from the FactoMineR package (Lê et al., 2008).

Richness, Fishers diversity, Shannon, Simpson and inverse Simpson indices were used to calculate the alpha diversity within each sample. Pielou was used as an index of evenness in the community. Variations in alpha diversity and evenness indexes between treatments were statistically analyzed using a repeated measures mixed model in SAS (version 9.4, SAS Institute, Cary, United States) with the four tomato cultivating systems as a fixed effect and time. This method allowed us to attribute the differences in the diversity measures to time or tomato cultivating system or to the interaction of the two factors.

Chao and Bray–Curtis indices were used to check dissimilarity and find out the impact of experimental factors on microbial community composition. Principal Coordinate Analysis (PCoA) visualized the differences between samples, using the vegan package in R (Oksanen et al., 2007), and stratified permutational multivariate analysis of variance (PERMANOVA) with 999 permutations were run to display the significance of each covariate on the microbial community of the bulk soil (Grunert et al., 2019). ANOVA was applied to reveal whether the distribution of the genera was different between treatments (Oksanen et al., 2007).

Statistical Analysis

The data about the fresh plant weight, cumulative yield, the amount of red tomatoes, the percentage of green tomatoes and percentage of blossom end rot were not statistically analyzed. The length of the plant was measured on a weekly basis for the 5 experimental units and for the 5 plants per experimental unit with a measuring tape and a 95% confidence interval was plotted for the different treatments for the first 120 days (55 DAS till 175 DAS).

RESULTS

Similar Plant Performance Was Observed in Soilless Culture Systems and Soil Based System and Yield Was the Highest With the Aquaponics-Derived Fertilizer

Plant length was followed during the whole experimental period (55 DAS till 321 DAS). **Figure 2** shows the evolution of the plants length from 55 DAS till 175 DAS. The final plant length for GBOF, GBFISH, SOILANIMAL, and SOILPLANT was 6.96 ± 0.06 m, 6.74 ± 0.07 m, 7.04 ± 0.03 m, and 7.04 ± 0.04 m, respectively. The average fresh plant weight follows a similar trend as the plant length (**Figure 2**). The average fresh plant weight showed significant differences ($P < 0.05$) for GBOF> <0.05) for GBOF, GBFISH, SOILANIMAL and SOILPLANT was 4.081^{a} ± 0.901 kg.m^{-2}, 3.074 ± 0.557^{b} kg.m^{-2}, 4.081 ± 1.034^{a} kg.m^{-2} and 4.691 ± 0.477^{a} kg.m^{-2}, respectively. The dry matter content of the plants was 0.481 ± 0.051 kg.m^{-2}, 0.31 ± 0.054 kg.m^{-2}, 0.44 ± 0.080 kg.m^{-2}, and 0.49 ± 0.089 kg.m^{-2}, respectively. **Table 1** shows that the cumulative yield of the system with soilless organic growing medium plus inorganic fertilizer (GBFISH) resulted in higher tomato yield (kg of tomatoes) in comparison with the three other cultivation systems. After 117 days since plantation, the cumulative yield dropped and followed the same trend as that observed in the soil supplied with either fertilizer.

Fast-Paced Fluctuations in pH(H_2O) and Nutrient Cycling Processes Were Observed in Growing Medium

Evolution of the electrical conductivity, pH(H_2O) and nitrate and ammonium concentration (**Figure 3**) was followed over time. Electrical conductivity, nitrate, ammonium, phosphorus, potassium, sodium and chloride differed among the four different tomato cultivating systems ($P < 0.001$) and time was a factor significantly influencing these traits ($P < 0.001$, **Table 2**). Soil fertilized with animal-derived material (243 ± 111 µS.cm^{-1}) or plant-derived material (344 ± 192 µS.cm^{-1}) showed the lowest average electrical conductivity, which decreased over time. On the contrary, the soilless culture system showed increasingly higher values (**Figure 3**) (GBOF = 551 ± 323 µS cm^{-1} and GBFISH = 905 ± 614 µS cm^{-1}). The pH(H_2O) of the soil increased over time for SOILANIMAL from 6.3 to 7.3 and SOILPLANT from 6.6 to 6.9, while the pH(H_2O) in the organic growing medium was very dynamic and fluctuated over time (**Figure 3**). The pH(H_2O) of GBFISH dropped between days 13 and 91 from 5.7 to 4.6 indicating increased uptake of cations, such as potassium and ammonium. Indeed, we found an increased amount of ammonium in GBFISH until days 69. GBOF, however, showed the highest ammonium concentration (41.2 ± 39.1 mg NH_4^+-N L^{-1}), while nitrate was significantly higher for GBFISH ($P < 0.05$, **Figure 3**) and decreased over time in soil supplemented with either fertilizer.

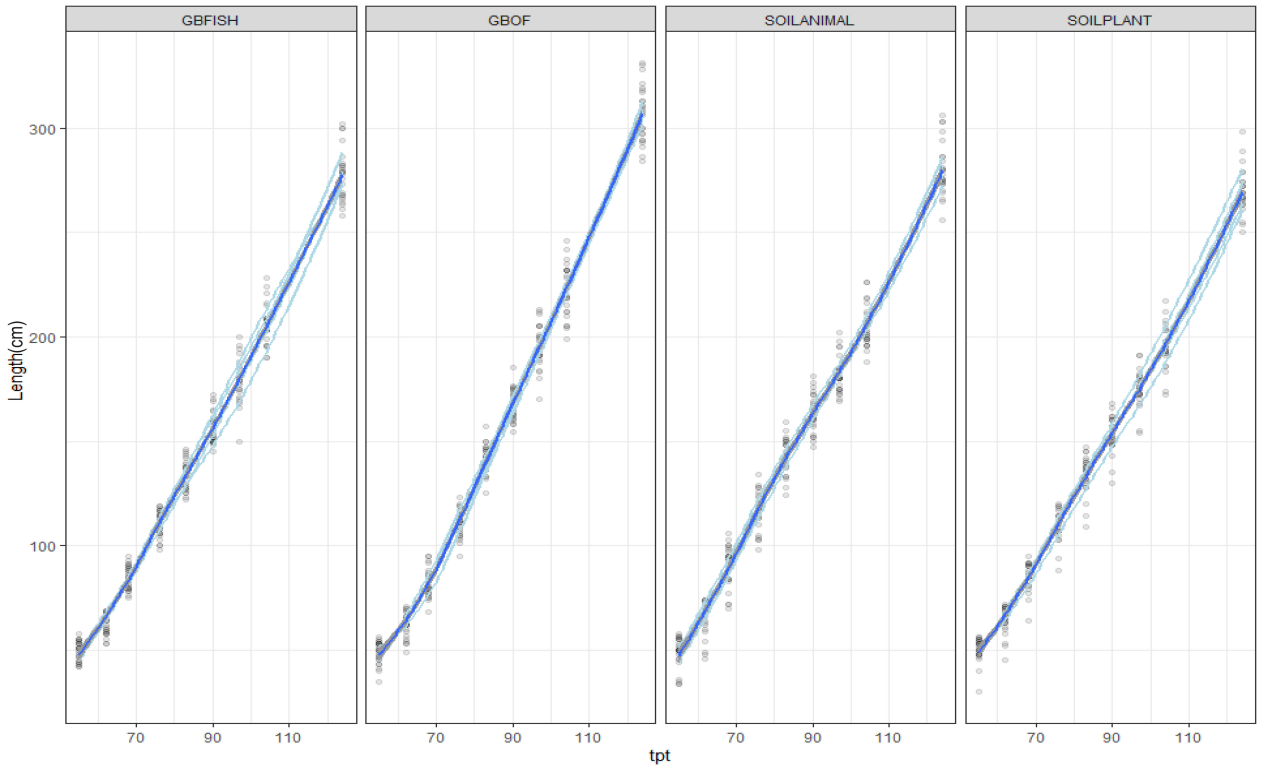

FIGURE 2 | Evolution of the plant length (cm) from 55 DAS till 125 DAS in the growing medium. i.e., GBOF and GBFISH and the organic soil. i.e., SOILANIMAL and SOILPLANT. The graph shows the 95% confidence interval, which was plotted around the dark blue line. The light blue lines are the values of the different experimental units.

Physicochemical Characteristics Changed Over Time and Interacted With Bacterial Community Metrics

Cultivation system ($P < 0.01$), time ($P < 0.01$) and the interaction between tomato cultivation system and time ($P < 0.01$) significantly influenced species richness, diversity and evenness (Pielou's index) (**Table 3**). Alpha diversity (**Figure 4**) oscillated in the soil, while remaining consistent on the soilless system throughout time. On the contrary, evenness (**Figure 5**) was persistently high in soil but not in growing medium and significantly decreased at the final harvest in soilless culture supplemented with fish fertilizer (GBFISH). Richness (**Figure 6**) followed the same trend observed for alpha diversity and shifted toward a decrease with plant-derived fertilizer but not when blood meal was added. These results indicate that soil is a highly dynamic environment, where bacterial communities are rapidly adapting, while community characteristics of bacteria inhabiting growing medium stay uniform over time despite fertilizer application.

Treatment ($P < 0.001$), time ($P < 0.001$) and the interaction between treatment and time ($P < 0.001$) had a significant effect on the relative abundances of the bacterial genera. PERMANOVA showed that communities in soil remained similar throughout the trial ($P < 0.001$), while those in the growing medium were significantly different at the beginning and converged over time. **Figures 7**, **8** show the beta diversity of bacterial communities in the soil harboring tomato plants and supplemented with different fertilizers. "Substrate" indicates whether the culture system contributed to the variance among bacterial communities. PERMANOVA results indicate that substrate (soil or growing medium) is the factor explaining the highest percentage of the variance among communities in the rhizosphere in both culture systems and PERMANOVA results indicate that communities inhabiting growing medium were significantly different from those in soil, even if they hosted the same cultivar.

Community composition on soil plus either fertilizer remained unaltered over time (**Figure 9A**), excepting on the first time point of soil supplemented with plant-derived fertilizer, when the relative abundance of *Mycoplasma* was significantly increased. Unclassified bacteria and *Clostridium* were taxa exclusively present when soil was amended with animal manure, while the relative abundance of *Bacillus* increased when plant-derived fertilizer was added. On the contrary, community composition of soilless systems (**Figure 9B**) was impacted by fertilizer and *Mycoplasma*, *Rhizomicrobium*, *Nocardioides* and *Devosia* were only detected in the aquaponics, while *Pseudomonas*, *Dyella,* and *Flavobacterium* increased relative abundance in soilless systems with organic fertilizer. Thus, differences in the rhizosphere bacterial community composition

TABLE 1 | Overview of the yield [short culture from May till November, tomatoes with blossom end rot (BER)], the total number tomatoes and the distribution in percentage between loose and tomatoes per vine for four different tomato cultivating systems (GBOF, GBFISH, SOILANIMAL, and SOILPLANT).

Object	Total yield (kg m^{-2})	BER	Tomatoes (number of tomatoes m^{-2})	Loose tomatoes	2 tomatoes per vine	3 tomatoes per vine	4 tomatoes per vine	5 tomatoes per vine	6 tomatoes per vine	7 tomatoes per vine
		%		%	%	%	%	%	%	%
GBOF	22.378	2.8	239	2.1	6.4	17.0	34.0	27.7	8.2	4.6
GBFISH	27.840	0.9	274	0.8	5.2	12.5	22.7	35.8	15.2	7.8
SOILANIMAL	22.501	0	226	3.3	7.2	12.7	24.7	35.0	12.7	4.4
SOILPLANT	24.127	0	224	4.4	5.0	15.6	22.4	37.2	11.9	3.6

were mainly impacted by fertilizer within soilless systems, while the opposite occurred in soil.

Multiple Factor Analysis showed that the environment in the soil (**Figures 10A–C**) at the start of the cropping (T0) was significantly different and the variance (given by the size of the confidence ellipse) reduced over time. The opposite happened in the soilless culture system (**Figures 10A–C**) and bacterial relative abundances were similar at the beginning, but variance increased over time and GBOF and GBFISH become differentiated as a result of the fertilizer used. Multiple factor analyses (**Figures 10A–C**) of the soil showed that plant length, pH, *Flavisolibacter*, phosphorus, chloride, ammonium, potassium, calcium, magnesium, sodium, electrical conductivity, nitrate, sulfate, *Desulfotomaculum*, *Solirubrobacter*, *Dehalococcoides*, *Bythopirellula*, *Steroidobacter*, *Litorilinea*, *Nonomuraea* were the variables significantly discriminating between SOILANIMAL and SOILPLANT. The first dimension (33.9% of variance) of the soil was positively correlated with T0 ($P < 0.001$), and T1 ($P < 0.05$) and negatively correlated with T6 ($P = 0.006$) and T7 ($P = 0.0003$), whereas the second dimension (14.1% of variance) was positively correlated with SOILANIMAL ($P < 0.03$), and T4 ($P = 0.03$) and negatively correlated with T6 ($P = 0.03$), SOILPLANT ($P = 0.003$) and T7 ($P = 0.001$). In contrast, nitrate, *Acidobacteria Gp 14*, *Rhizomicrobium*, *Unclassified bacteria*, *Verrucomicrobia SD3*, magnesium, electrical conductivity, *Parcubacteria*, sulfate, sodium, potassium, phosphorus, plant length, calcium, chloride, *Amaricoccus*, *Gemmobacter*, ammonium, *Brevundimonas*, pH were the variables discriminating between GBOF and GBFISH (**Figures 10A–C**). The first dimension (29.9% of variance) of the soilless culture system was positively correlated with GBFISH ($P = 0.001$), T5 ($P = 0.001$), T7 ($P = 0.005$) and negatively correlated with T2 ($P = 0.02$), T1 ($P = 0.001$), T0 ($P = 0.002$) and GBOF ($P < 0.001$), whereas the second dimension (14.7% of variance) was positively correlated with GBOF ($P < 0.001$), T6 ($P = 0.004$), and T7 ($P = 0.002$) and negatively correlated with T0 ($P = 0.009$) and GBFISH ($P < 0.001$).

Long-Term Fertilizer Regimes Significantly Changed the PLFA Fingerprints in Both the Soilless Culture and Soil Based Culture System

Combinations of organic soil with plant and animal-derived material and organic growing medium with fish effluent and organic fertilizer differed in its characteristics throughout the experimental period. Eleven soil and growing media characteristics and eight microbial characteristics (gram-positive, gram-negative bacteria, 18:1, 18:2, and 18:3 fungi, actinomycetes, arbuscular mycorrhizal fungi and protozoa) were analyzed together in a MFA (**Figure 11**). Overall, long-term fertilizer regimes significantly alternated the PLFA marks in both the soilless culture and soil based culture system.

Regarding to the four different tomato cultivation systems, the first two dimensions (**Supplementary Table S5**) accounted for 60.3% of the total variance, indicating a good reproducibility

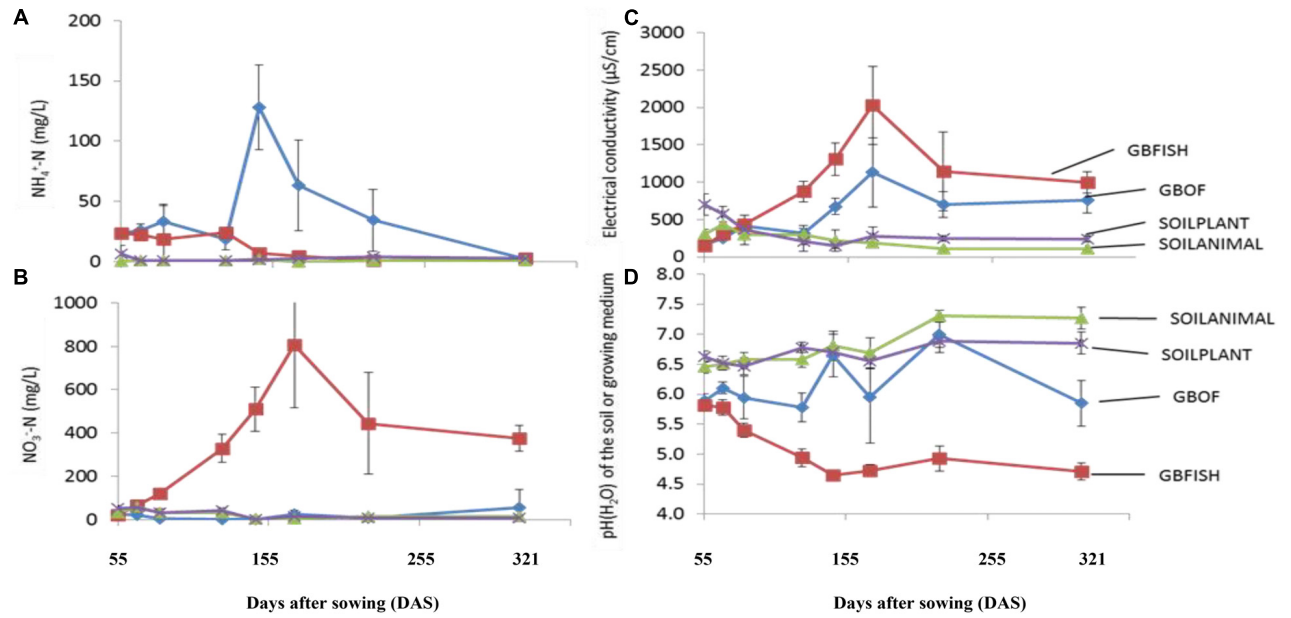

FIGURE 3 | Evolution of the ammonium concentration **(A)**. Nitrate concentration **(B)**. The electrical conductivity **(C)** and pH(H_2O) **(D)** in the growing medium. i.e., GBOF and GBFISH and the organic soil. i.e., SOILANIMAL and SOILPLANT during the whole experimental period which lasted 321 days. The ammonium and the nitrogen content, the pH and the electrical conductivity (EC) in the 0–10 cm organic soil layer and in the growing medium were taken at the start 55 DAS (T0), 68 DAS (T1), 83 DAS (T2), 113 DAS (T3), 146 DAS (T4), 172 DAS (T5), 221 DAS (T6), and 321 DAS (T7).

TABLE 2 | Average values of 11 different variables throughout the whole experimental period with standard error.

Variable	Treatment (trt)				*p*-value (trt)	*p*-value (time)
	GBOF	GBFISH	SOILANIMAL	SOILPLANT		
pH(H_2O)	6.1 ± 0.04^{b}	5.1 ± 0.04^{a}	6.8 ± 0.05^{c}	6.6 ± 0.05^{c}	<0.001	<0.001
EC (µS cm^{-1})	596 ± 34^{c}	883 ± 34^{d}	243 ± 37^{a}	364 ± 40^{b}	<0.001	<0.001
NO_3^--N (mg L^{-1}*)	14 ± 12^{a}	332 ± 12^{c}	23 ± 13^{b}	25 ± 14^{b}	<0.001	<0.001
NH_4^+-N (mg L^{-1})	40 ± 2^{c}	12 ± 2^{b}	1 ± 2^{a}	3 ± 2^{a}	<0.001	<0.001
NO_3^--N/NH_4^+-N ratio	0.35	27	23	8		
P (mg L^{-1})	218 ± 14^{b}	216 ± 14^{b}	37 ± 15^{a}	35 ± 16^{a}	<0.001	<0.001
K^+ (mg L^{-1})	382 ± 12^{c}	423 ± 12^{d}	58 ± 13^{a}	88 ± 15^{b}	<0.001	<0.001
Ca^{2+} (mg L^{-1})	1234 ± 33^{b}	1173 ± 34^{b}	937 ± 36^{a}	1103 ± 38^{b}	<0.001	<0.001
Mg^{2+} (mg L^{-1})	254 ± 9^{c}	286 ± 9^{d}	138 ± 10^{a}	182 ± 10^{b}	<0.001	<0.001
SO_4^{2-} (mg L^{-1})	740 ± 40^{c}	708 ± 40^{b}	448 ± 44^{a}	799 ± 4^{c}	<0.001	<0.001
Na^+ (mg L^{-1})	118 ± 4^{c}	97 ± 6^{b}	33 ± 7^{a}	42 ± 7^{a}	<0.001	<0.001
Cl^- (mg L^{-1})	340 ± 20^{c}	43 ± 20^{b}	18 ± 22^{a}	18 ± 24^{a}	<0.001	<0.001

n = 5. Differences in variables among treatments were compared using a repeated measures mixed model in SAS. For each column, different superscripts indicate significantly different means according to Duncan's multiple range test (P < 0.05).

of the data of the 5 experimental units per treatment. The first dimension is positively correlated with GBOF ($P < 0.05$) and GBFISH ($P < 0.05$) and negatively correlated with SOILANIMAL and SOILPLANT (**Supplementary Table S5**), whereas the second dimension 2 is positively correlated with SOILPLANT ($P < 0.05$) and time point 4 ($P = 0.014$) and negatively correlated with GBFISH and timepoint 1. Dimension 3 is positively correlated with GBOF ($P < 0.001$) and negatively correlated with GBFISH. Dimension 4 is negatively correlated with SOILANIMAL ($P < 0.05$).

The soilless culture systems GBOF and GBFISH, showed a positive correlation (dimension 1) with potassium, protozoa, electrical conductivity, the fungal FAME marker 18:3, sodium, total biomass, calcium, phosphorous, nitrate, fungal FAME marker 18:2, chloride, magnesium and sulfate, while the soil based system is positively correlated with actinomycetes, pH, the bacteria to fungi ratio and the gram-positive bacteria. GBOF showed a positive correlation (dimension 3) with ammonium, the total biomass, chloride, pH, magnesium and phosphorous, while GBFISH was positively

TABLE 3 | Effect of tomato cultivation system (GBOF, GBFISH, SOILANIMAL, and SOILPLANT) on species richness (total species), diversity (Shannon, Fisher's alpha, Simpson and Inverse Simpson indices), and evenness (Pielou's index) for all the 8 time points (n = 3).

Index	Time	Tomato cultivation system (treatment)				SEM	Effect		
		GBOF	GBFISH	SOILANIMAL	SOILPLANT		Treatment	Time	Treatment* time interaction
Total species	0	124.3^{a}	98.8^{a}	332.8^{b}	336.8^{b}	37.3	<0.0001	<0.0001	<0.0001
	1	84.5^{ab}	52.8^{a}	413.5^{c}	116.0^{b}				
	2	100.5^{a}	143.0^{b}	394.3^{c}	437.3^{d}				
	3	295.0^{a}	205.3^{b}	412.0^{c}	413.5^{c}				
	4	281.5^{a}	203.5^{b}	406.5^{c}	403.3^{c}				
	5	265.5^{b}	105.5^{a}	321.5^{c}	382.3^{d}				
	6	339.5^{b}	145.3^{a}	385.8^{c}	403.0^{c}				
	7	179.8^{a}	223.3^{b}	151.0^{a}	409.0^{c}				
Pielou	0	0.625^{a}	0.595^{a}	0.783^{b}	0.793^{b}	0.024	<0.0001	<0.0001	<0.0001
	1	0.647^{a}	0.706^{a}	0.777^{b}	0.792^{b}				
	2	0.810^{a}	0.713^{c}	0.772^{b}	0.760^{b}				
	3	0.708^{a}	0.758^{a}	0.784^{b}	0.775^{b}				
	4	0.750	0.760	0.768	0.772				
	5	0.753	0.795	0.785	0.781				
	6	0.736	0.726	0.785	0.776				
	7	0.714^{a}	0.687^{b}	0.700^{c}	0.767^{a}				
Shannon	0	2.778^{a}	2.563^{a}	4.544^{b}	4.609^{b}	0.211	<0.0001	<0.0001	<0.0001
	1	2.709^{a}	2.794^{a}	4.678^{b}	3.764^{c}				
	2	3.568^{a}	3.293^{a}	4.616^{b}	4.618^{b}				
	3	4.022^{a}	3.952^{a}	4.718^{b}	4.665^{b}				
	4	4.211^{a}	3.912^{a}	4.613^{b}	4.626^{b}				
	5	4.062^{a}	3.631^{a}	4.484^{b}	4.640^{b}				
	6	4.288^{a}	3.256^{b}	4.672^{c}	4.651^{c}				
	7	3.602^{a}	3.647^{a}	3.302^{b}	4.613^{c}				
Simpson	0	0.862^{a}	0.812^{a}	0.973	0.977	0.028	<0.0001	<0.0001	<0.0001
	1	0.790^{a}	0.816^{a}	0.979	0.921				
	2	0.935^{a}	0.891^{a}	0.978^{b}	0.979^{b}				
	3	0.964	0.960	0.982	0.980				
	4	0.969	0.928	0.976	0.976				
	5	0.955	0.936	0.974	0.980				
	6	0.963^{a}	0.858^{b}	0.979^{c}	0.979^{c}				
	7	0.934	0.899	0.858	0.974				
Inverse Simpson	0	7.427^{a}	6.049^{a}	38.127^{b}	44.223^{c}	4.884	<0.0001	<0.0001	<0.0001
	1	7.891^{a}	6.564^{a}	48.304^{b}	14.460^{c}				
	2	19.618^{a}	13.168^{a}	46.218^{b}	47.679^{b}				
	3	27.817^{a}	26.136^{a}	55.706^{b}	49.539^{c}				
	4	33.674^{a}	32.469^{a}	41.571^{b}	42.066^{b}				
	5	33.669^{a}	21.518^{a}	41.184^{b}	50.692^{c}				
	6	37.159^{a}	18.664^{b}	47.643^{b}	48.561^{c}				
	7	16.600^{a}	19.257^{a}	15.655^{b}	38.384^{c}				
Fisher's	0	26.966^{a}	22.582^{a}	63.810^{b}	63.979^{b}	4.640	<0.0001	<0.0001	<0.0001
	1	23.416^{a}	22.138^{a}	68.101^{b}	51.262^{c}				
	2	34.273^{a}	35.035^{a}	65.298^{b}	69.475^{b}				
	3	47.982^{a}	48.614^{a}	68.776^{b}	66.327^{b}				
	4	48.196^{a}	49.268^{a}	67.699^{b}	66.150^{b}				
	5	50.323^{a}	37.039^{b}	62.389^{c}	67.027^{c}				
	6	55.162^{a}	36.092^{b}	69.952^{b}	68.985^{b}				
	7	37.651^{a}	45.136^{a}	35.967^{b}	67.726^{c}				

GBOF, organic growing medium with organic fertilizer; GBFISH, organic growing medium with fish effluent; SOILANIMAL, organic soil with animal derived material as fertilizer (blood meal); and SOILPLANT, organic soil with plant derived material as fertilizer (malt sprouts). NS, not significant effect. For each column, different superscripts indicate significantly different means according to Duncan's multiple range test ($P < 0.05$). SEM, standard error of the mean.

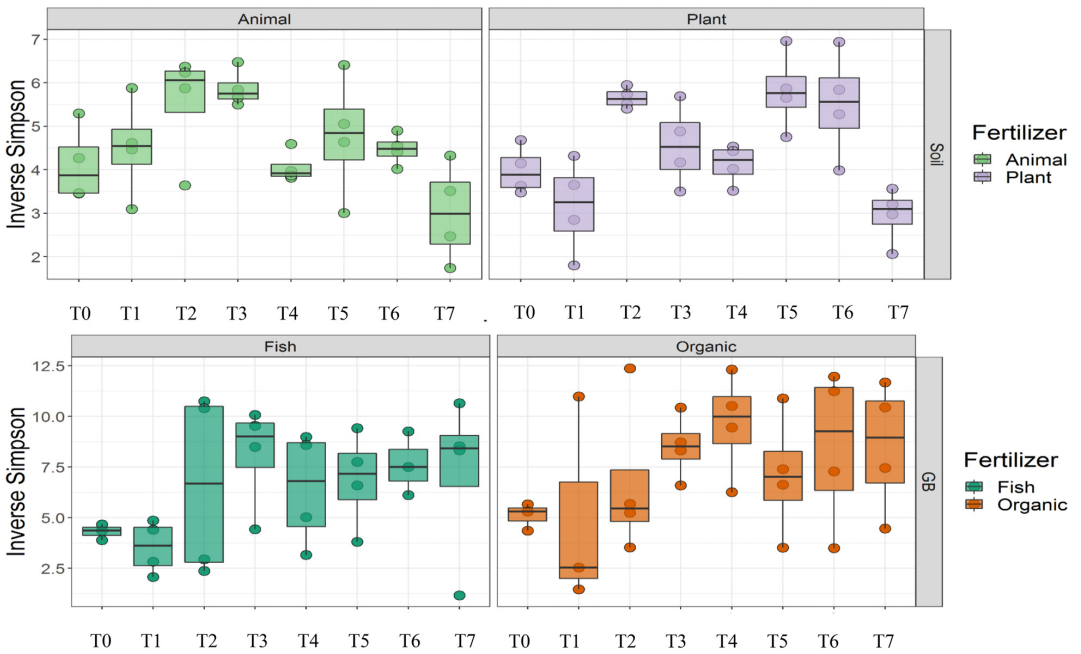

FIGURE 4 | Culture system impacted bacterial community characteristics and showed opposite trends. Alpha diversity was lower and oscillated over time in soil **(upper panel)**, while it steadily increased in soilless systems and remained high at the end of the experiment **(lower panel)**. Samples for microbial community analysis were taken at 8 different timepoints, i.e., 55 DAS (T0), 68 DAS (T1), 83 DAS (T2), 113 DAS (T3), 146 DAS (T4), 172 DAS (T5), 221 DAS (T6), and 321 DAS (T7).

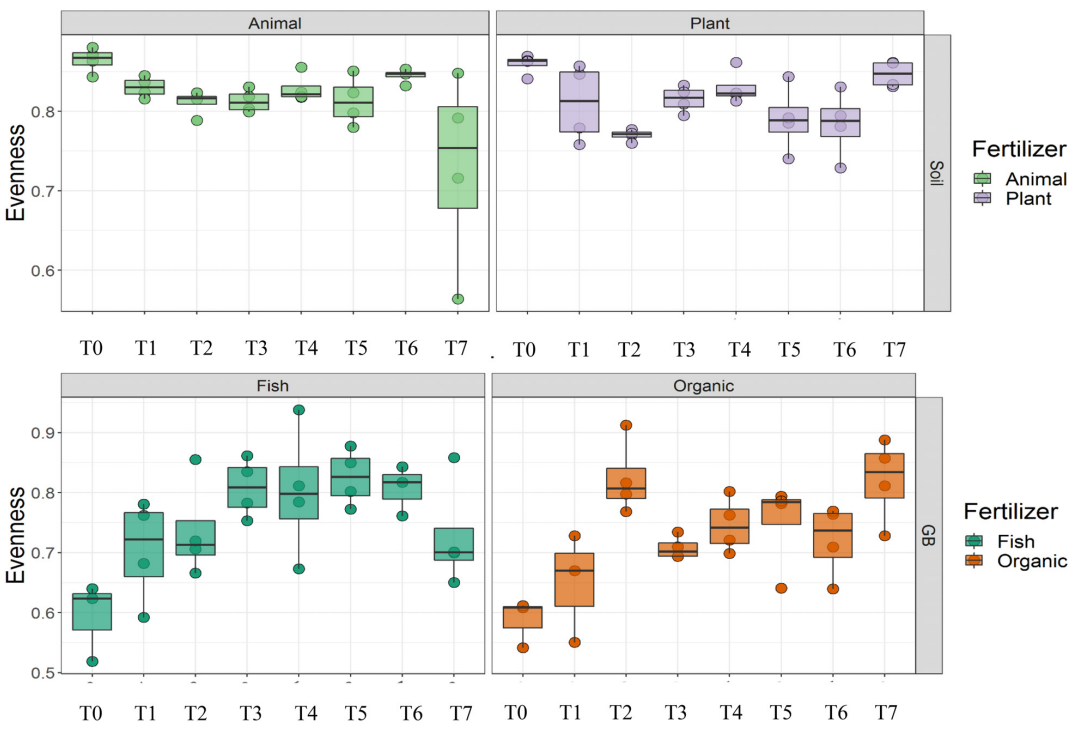

FIGURE 5 | Culture system impacted bacterial community characteristics and showed opposite trends. On the contrary, evenness was consistently higher in soil **(upper panel)**, while it tend to decrease in the aquaponics soilless system. **(lower panel left)** Samples for microbial community analysis were taken at 8 different timepoints, i.e., 55 DAS (T0), 68 DAS (T1), 83 DAS (T2), 113 DAS (T3), 146 DAS (T4), 172 DAS (T5), 221 DAS (T6), and 321 DAS (T7).

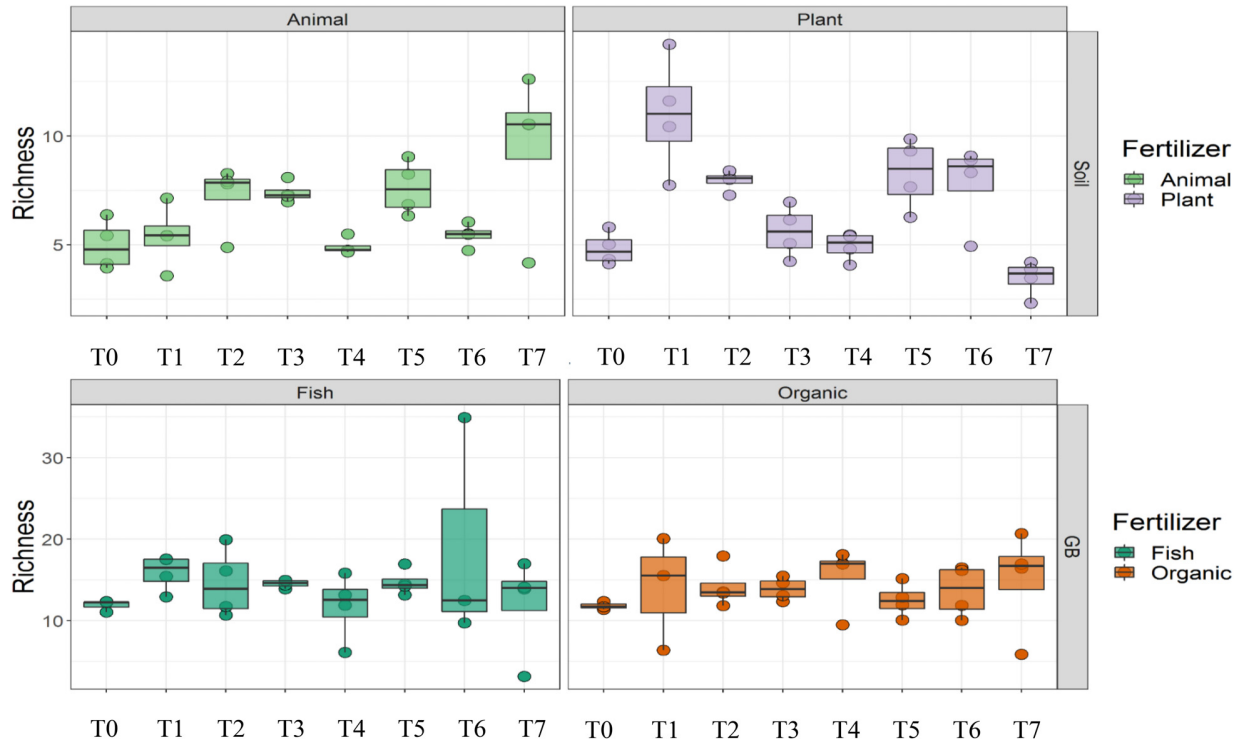

FIGURE 6 | Culture system impacted bacterial community characteristics and showed opposite trends. Richness followed the oscillatory trend in soil **(upper panel)** but not in growing medium **(lower panel)**. Samples for microbial community analysis were taken at 8 different timepoints, i.e., 55 DAS (T0), 68 DAS (T1), 83 DAS (T2), 113 DAS (T3), 146 DAS (T4), 172 DAS (T5), 221 DAS (T6), and 321 DAS (T7).

correlated with fungal FAME marker 18:2 and fungal FAME marker 18:3 and nitrate. SOILPLANT, SOILANIMAL and timepoint 4 were positively correlated with AMF (arbuscular mycorrhizal fungi), gram-negative bacteria, the bacteria to fungi ratio, calcium, sulfate, phosphorous, gram-positive bacteria, pH, sodium and chloride, while GBFISH was correlated with the fungal FAME marker 18:3, ammonium, actinomycetes, the fungal FAME marker 18:2 and the fungal FAME marker 18:1.

DISCUSSION

Healthy soils are decisive to biodiversity and play a paramount role in fighting climate change. Soils are a non-renewable resource on which 95% of our food supply depends. Organic agriculture is a production system that nurses the health of soils, ecosystems and people. It builds on ecological processes, biodiversity, instead of using resources with inimical effects. Soilless culture systems and consequently growing media are also an fundamental sector of the food supply chain. Growing media facilitates sustainable horticulture and protected culture systems are vital for producing fruits and vegetables. Both (organic) soil based and soilless culture systems are principal members in the transition toward a more sustainable food production. It has been shown that it is possible to grow tomatoes in soilless culture systems in combination with inorganic and organic fertilizers (Heeb et al., 2005b; Zhai et al., 2009; Gravel et al., 2010a; Grunert et al., 2016a), in aquaponic systems (Suhl et al., 2016) and in organic soil based systems (Bélair and Tremblay, 1995; Gravel et al., 2010b). Moreover, it was demonstrated that soil and soilless culture systems and soil amendments and fertilizers can have a clear impact on plant growth, tomato fruit quality and on the suppression of plant diseases (Cotxarrera et al., 2002; Gruda, 2008; Zhai et al., 2009; Coppens et al., 2015; Sakarika et al., 2019; Dion et al., 2020). Several research papers have associated these favorable effects on the microbiome of the soil and the rhizosphere of the plant (Tu et al., 2006; El-Yazeid and Abou-Aly, 2011; Bona et al., 2018; Sellitto et al., 2019). In addition, it has been proven that temporal, biotic and abiotic components have considerable influence on the bulk microbiome and the rhizosphere of tomatoes (Maloney et al., 1997; Grunert et al., 2016a; Grunert et al., 2019). In the presented study, we cultivated tomato plants grown in soil based and soilless culture systems. We hypothesized that (i) the soil and soilless culture based edaphic properties, which are strongly altered during one tomato growing season, consecutively affect the bacterial and fungal microbial structure. Moreover, we hypothesized that (ii) the community changes caused by four contrasting fertilization strategies included shifts in the abundance of various plant-beneficial soil- and soilless culture based microorganisms, thus influencing plant performance.

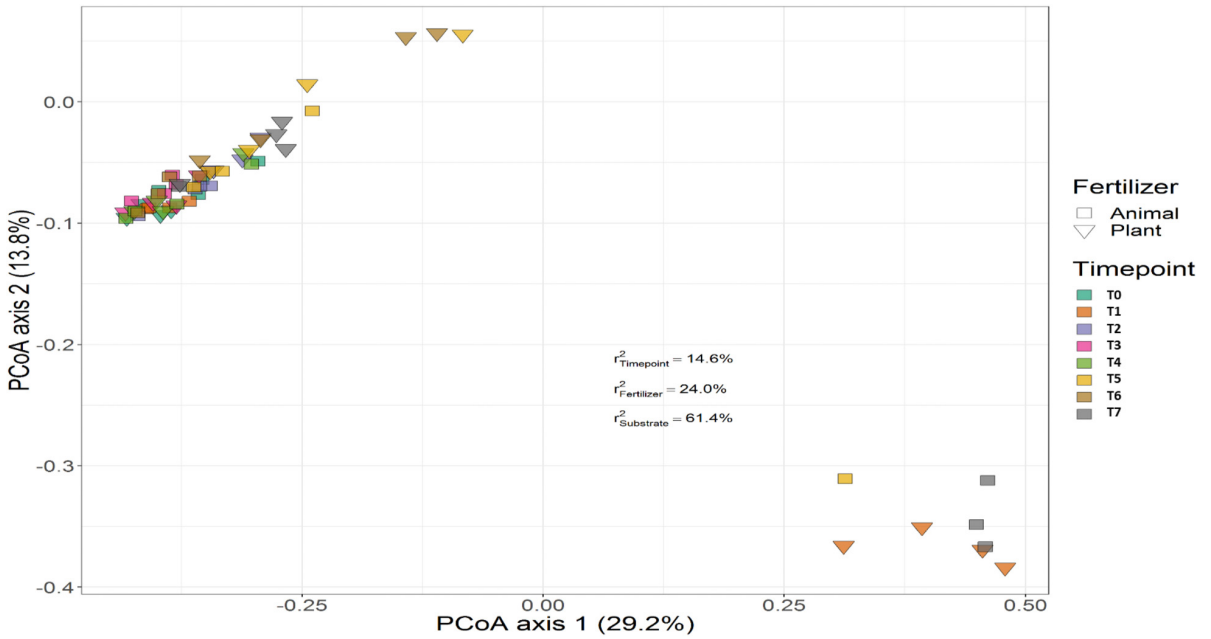

FIGURE 7 | Beta diversity of bacterial communities in soil harboring tomato plants and supplemented with different fertilizers. Squares indicate communities from soil fertilized with animal-origin fertilizer and inverted triangles show communities supplemented with plant-derived fertilizer. Samples of soil were followed over time to observe the bacterial community development. A color code on the right indicates the community sampled at different time points (time point 0-time point 8). "Substrate" indicates whether culture system contributed to the variance among bacterial communities. PERMANOVA results indicate that substrate (soil or growing medium) is the factor explaining the highest percentage of the variance among communities in the rhizosphere in both culture systems.

A total of 11 chemical variables were monitored for the four different tomato cultivating systems. No major plant growth anomalies were found, except for GBOF with the highest nitrogen supply rate. We found a significant effect tomato cultivating system and time on species richness. Our MFA analysis based on the PLFA results (**Figure 11**) and based on high throughput sequencing of the 16S rRNA gene and chemical factors, indicate that the dispersion of the genera among treatments is significantly different. Long-term fertilizer regimes significantly changed the PLFA fingerprints in both the soilless culture and soil based culture system. Indeed, the diversity of microbial communities associated with the soil or soilless culture system are directly influenced by the physical and chemical properties of the soil. It must be considered that four different tomato cultivating systems supplemented with different fertilizers were compared with each other, making it impossible to estimate the separate effect of soil type or growing medium or fertilizer used on the microbial community composition. However, SOILANIMAL and SOILPLANT displayed similar microbial community composition, i.e., richness, evenness and GBOF and GBFISH also revealed a more similar microbial community composition indicating a potential soil or growing medium effect. On the other hand, within the organic soil and soilless culture system the microbial community composition seemed to be different depending on the fertilizer used (animal or plant based nutrients or organic versus inorganic). Alpha diversity (**Figure 4**) oscillated in the soil, while remaining consistent in the soilless system throughout time. On the contrary, evenness (**Figure 6**) was persistently high in soil but not in growing medium and significantly decreased at the final harvest in soilless culture supplemented with fish fertilizer (GBFISH). Richness (**Figure 5**) followed the same trend observed for alpha diversity (**Figure 4**) and shifted toward a decrease with plant-derived fertilizer but not when blood meal was added. In many cases, alterations in evenness crop up with little or no changes in species richness, and this illustrates the pertinence of evenness as a component of diversity (Wilsey and Potvin, 2000). As stated by Wittebolle (2009) unevenness could block the rapid response of a community to a particular stress if the dominant species are not resistant to this stress. It is reported that even communities can recover their function more easily, provided with sufficient time (Wittebolle, 2009). The higher similarity in soil properties of the organic soil and the organic growing medium may also explain that no major differences in bacterial community structure were found between SOILANIMAL and SOILPLANT and GBOF and GBFISH, respectively, indicating that soil or growing medium are major discriminants of the microbial community composition. Amplicon sequencing showed that differences in the rhizosphere bacterial community composition were mainly impacted by fertilizer within soilless systems, while the opposite occurred in soil. PLFA results showed GBOF showed a positive correlation with ammonium, the total biomass, chloride, pH, magnesium and phosphorous, while GBFISH was positively correlated with fungal FAME marker 18:2 and fungal FAME marker 18:3 and nitrate. SOILPLANT, SOILANIMAL were positively correlated with AMF (arbuscular mycorrhizal fungi),

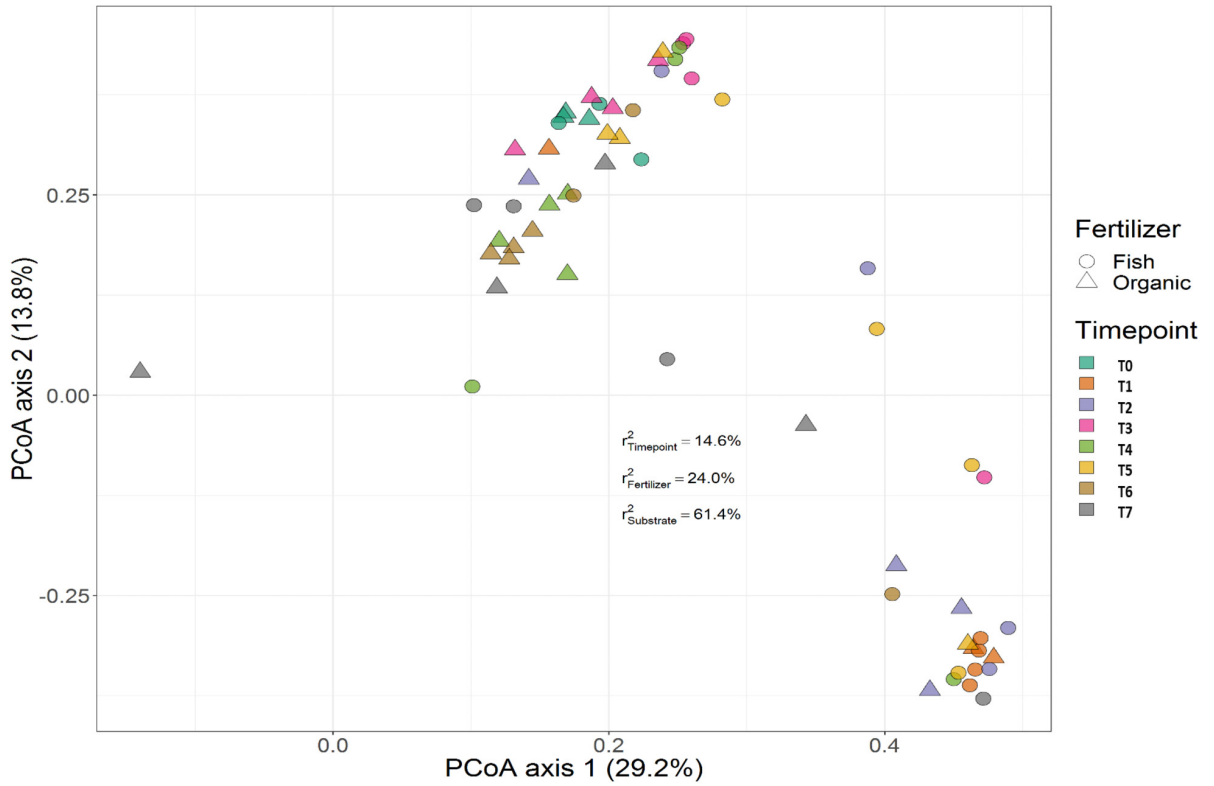

FIGURE 8 | Beta diversity of rhizosphere bacterial communities in growing media harboring tomato plants and supplemented with different fertilizers. Circles indicate communities supplemented with GBFISH. and triangles show bacterial communities amended with organic fertilizer (GBOF). Samples of growing media were followed over time to observe the bacterial community development. A color code on the right indicates the community sampled at different time points (time point 0-time point 8). "Substrate" indicates whether culture system contributed to the variance among bacterial communities. PERMANOVA results indicate that communities inhabiting growing medium were significantly different from those in soil, even if they hosted the same cultivar.

gram-negative bacteria, the bacteria to fungi ratio, calcium, sulfate, phosphorous, gram-positive bacteria, pH, sodium, and chloride. The soilless culture systems GBOF and GBFISH, however, showed a positive correlation with protozoa and the fungal fatty acid methyl esters (FAME) marker 18:2 and 18:3 and it was negatively correlated with the Gram-positive bacteria and the Actinomycetes. The use of blood meal and malt sprouts in the organic soil was positively correlated to AMF, Gram-negative and Gram-positive bacteria. Fungal FAME marker 18:1, 18:2, and 18:3 was negatively influenced by the application of blood meal and malt sprouts. These results indicated that fertilizer incorporation increased disturbance in fungal communities in both cultivation systems. Overall the soil culture system seems to be positively correlated with Gram negative, Gram positive bacteria and AMF. Arbuscular mycorrhizal fungi (AMF) are ubiquitous organism that influence soil fertility through the enhancement of chemical, biological and physical content. Actinomycetes are an important class of soil microorganisms that are known to decompose complex polymers and cycle more recalcitrant soil organic matter. These results indicate that soil is a highly dynamic environment, where bacterial communities are rapidly adapting, while community characteristics of bacteria inhabiting growing medium stay uniform over time despite fertilizer application.

The four tomato cultivation systems were managed independently from each other and we demonstrated that it is possible to grow tomatoes in soilless culture and in soil based systems. Similar plant performance was observed in soilless culture systems and soil based system and yield was the highest with the aquaponics-derived fertilizer, but showed on the contrary the lowest average fresh and dry plant weight. This is in agreement with the study of Heeb (2005); Heeb et al. (2005a), and Heuvelink (2018). The yield per surface unit for GBOF and SOILANIMAL and SOILPLANT was quite similar for the three treatments. However, when yield is calculated per unit of available root volume, we found final cumulative yield of 3.1 kg tomatoes L^{-1} of growing medium and 2.8 kg tomatoes L^{-1} of growing medium for GBFISH and GBOF, respectively, while the soil based system produced approximately 0.5 kg tomatoes L^{-1} soil. Soilless culture systems possess a finite root volume, but they give complete control over water and the fertigation solution with a more precise composition and ratio of nutrients resulting in higher yields (Gruda, 2008). However, unbalanced water supply and high organic nitrogen supply rates will easily result in nutrient imbalance and further induce blossom end-rot (BER) of glasshouse tomatoes, which was reflected in the

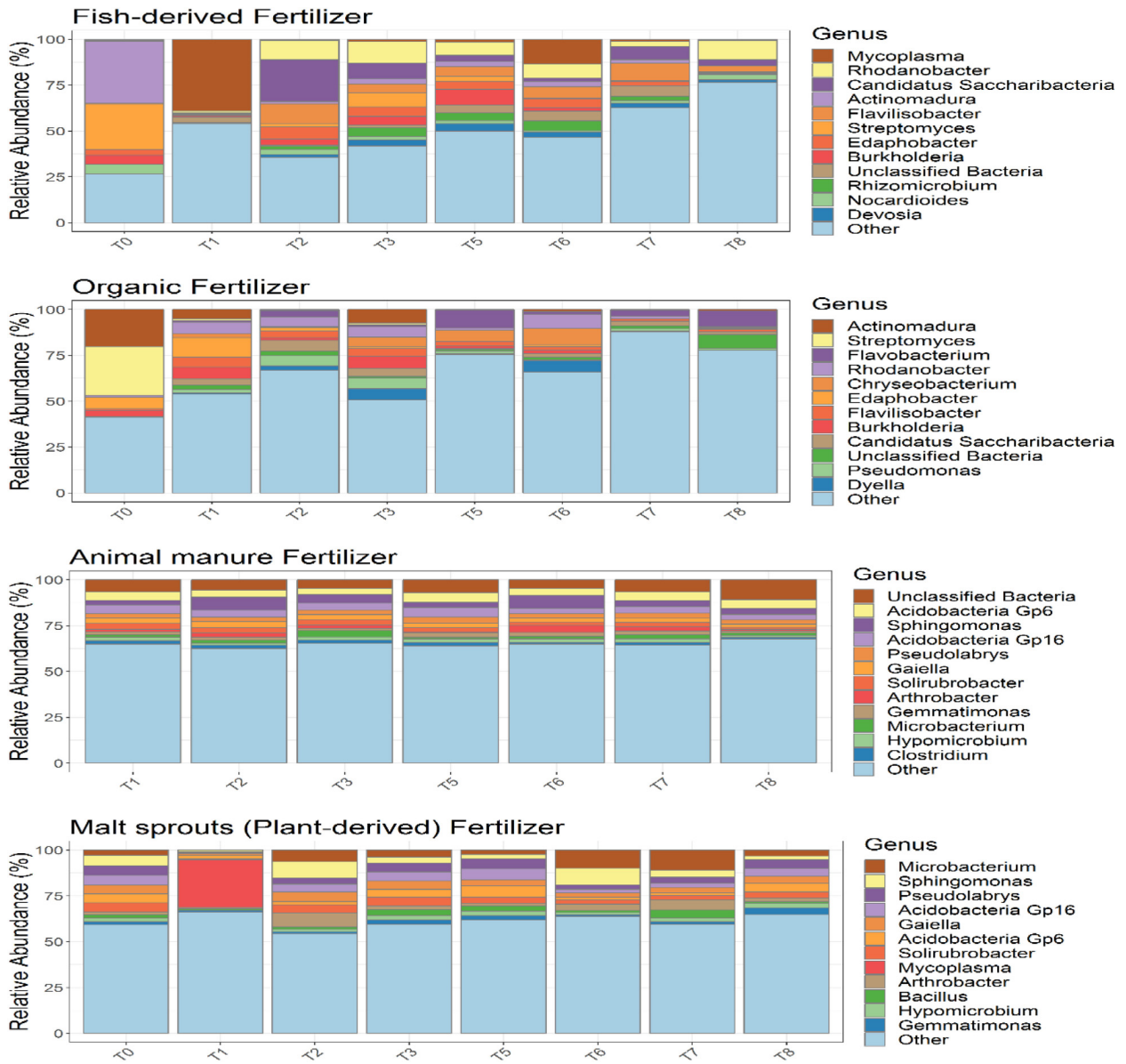

FIGURE 9 | Analysis of the bacterial composition of the different tomato cultivation systems: GBOF (organic fertilizer), GBFISH (fish derived fertilizer), SOILANIMAL (animal based fertilizer) and SOILPLANT (plant derived fertilizer). Relative abundance (percentages) of the different bacterial phyla (16S V3–V4 region) in the tomato bulk soil. Phyla representing less than 1% of the total community are bundled in the group "other", as their taxonomic composition may be uncertain.

highest percentage of BER, i.e., 2.8% in the soilless culture system (Britto and Kronzucker, 2002; Heeb, 2005). Evolution of plant length (**Figure 2**) was quite similar between the four contrasting tomato cultivation systems, except for GBOF where plants were longer. From the experimental setup it is clear that we have different forms (organic nitrogen, ammonium and nitrate – nitrite is not considered) and concentrations of nitrogen in the four tomato cultivating systems. Plants can assimilate these different kind of nitrogen forms (Näsholm et al., 2009; Marschner, 2011). Mineralization rates are not equal for the different organic fertilizers, such as the blood meal, malt sprouts and the organic fertilizers used in combination with GBOF (Stadler et al., 2006; Dion et al., 2020). In addition, mineralization first releases ammonium, that is then converted in nitrate during nitrification, so the concentration of nitrate depends on both the concentration of ammonium and the ammonia and nitrite oxidation rate (Boudsocq et al., 2012). Our results show a higher ammonium concentration in combination with GBOF, indicating a higher ammonification rate or a lower nitrification rate. Ammonium uptake and assimilation are less energy demanding than nitrate uptake and assimilation, indicating a competitive advantage for plants with a high ammonium absorption capacity. High ammonium concentrations, however, can also cause severe

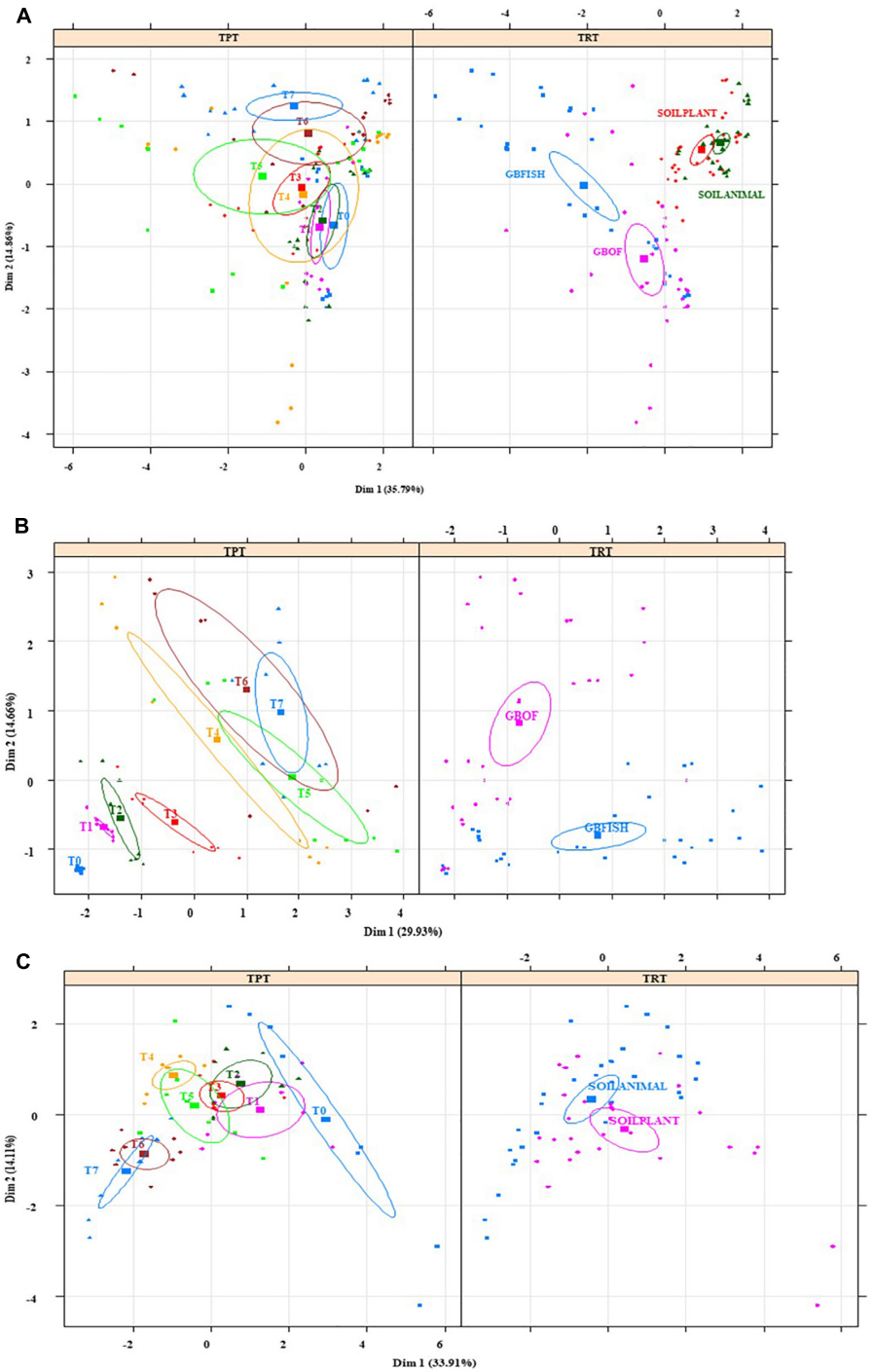

FIGURE 10 | Multiple factor analysis in which 20 of the most significant factors were taken into account for the four contrasting culture systems **(A)**, organic soil **(B),** and for the soilless culture system **(C)**. TRT indicates the tomato cultivating system (GBOF, organic growing medium with organic fertilizers; GBFISH, organic growing medium with fish effluent; SOILANIMAL, organic soil that was fertilizer with animal-derived material; and SOILPLANT, soil that was fertilized with plant-derived material). TRT, time point. Samples for microbial community analysis were taken at 8 different timepoints, i.e., 55 DAS (T0), 68 DAS (T1), 83 DAS (T2), 113 DAS (T3), 146 DAS (T4), 172 DAS (T5), 221 DAS (T6), and 321 DAS (T7). Circles indicate the 95% confidence interval.

toxicity symptoms (Britto and Kronzucker, 2002). This ammonium toxicity may jeopardize the energetic advantage of taking up ammonium rather than nitrate. Furthermore, ammonium is known for its abiotic immobilization, while nitrate is highly mobile and can lead to leaching losses. These physical limitations, energetic costs and competition with the

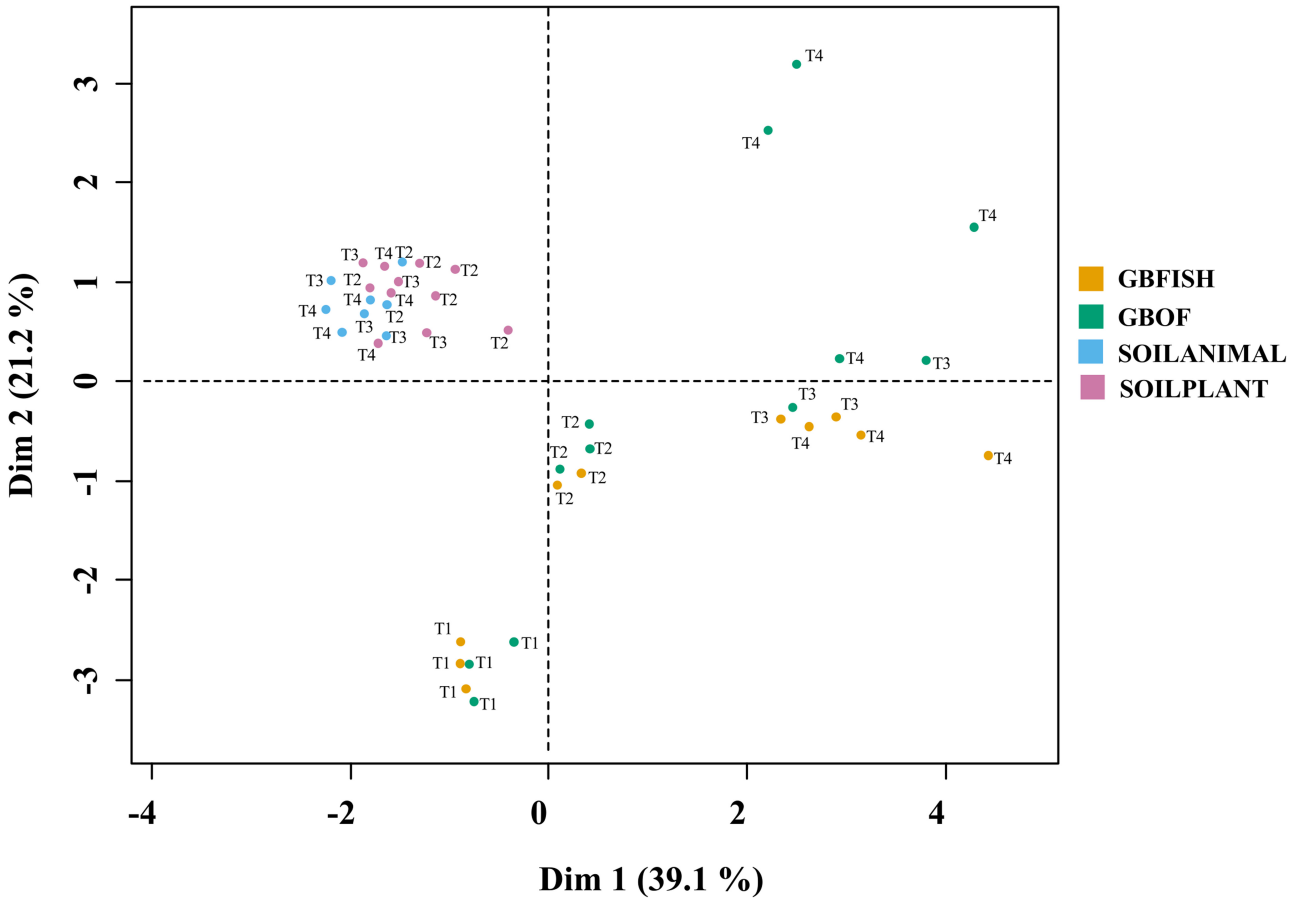

FIGURE 11 | Multiple factor analysis in which 11 chemical soil and growing medium characteristics [pH(H_2O)]. EC (nitrate, ammonium, phosphorus, potassium, calcium, magnesium, sulfate, sodium, and chloride) and eight microbial characteristics [Gram-positive, Gram-negative bacteria, fungi 18:1, fungi 18:2, fungi 18:3, Actinomycetes, arbuscular mycorrhizal fungi (AMF), and protozoa] were used to discriminate between the different tomato cultivation systems. GBOF, organic growing medium with organic fertilizers. GBFISH, organic growing medium with fish effluent. SOILANIMAL, organic soil that was fertilizer with animal-derived material; and SOILPLANT, soil that was fertilized with plant-derived material. Samples for PLFA analyses were collected at four different time points, i.e. 55 DAS (T1), 83 DAS (T2), 221 DAS (T6) and 321 DAS (T7).

soil microorganisms make these systems highly dynamic and almost unpredictable.

Our study highlights some limitations of previous studies and enlarges our awareness about the impact of soilless culture and soil based culture systems and different fertilizers on the below ground microbiology in tomato cultivation systems, because (1) soil and soilless culture systems were assessed at the same time, (2) amplicon sequencing and PLFA were similarly used as supplementary techniques to allow quantification of microbial biomass and (3) nutrient and N dynamics and (4) plant performance was followed and assessed over time. Community composition in soil plus either fertilizer remained unaltered over time, excepting on the first time point of soil supplemented with plant-derived fertilizer, when the relative abundance of *Mycoplasma* was significantly increased. Unclassified bacteria and *Clostridium* were taxa exclusively present when soil was amended with animal manure, while the relative abundance of *Bacillus* increased when plant-derived fertilizer was added. On the contrary, community composition of soilless systems was impacted by fertilizer and *Mycoplasma*, *Rhizomicrobium*, *Nocardioides* and *Devosia* were only detected in the aquaponics, while *Pseudomonas*, *Dyella* and *Flavobacterium* increased relative abundance in soilless systems with organic fertilizer. Thus, differences in the rhizosphere bacterial community composition were mainly impacted by fertilizer within soilless systems, while the opposite occurred in soil.

To the best of our knowledge, the presented study is the first study that carried out an in-depth observation of four contrasting tomato cultivation systems during one growing season on the composition of the bacterial and the fungal microbiome by using amplicon sequencing and PLFA. At the start of a soilless culture, which is considered as a microbial vacuum (Postma et al., 2000) and in contrast to an organic soil based systems, a microbial community promptly occupies the growing medium (Grunert et al., 2016a), the fertigation solutions and the rhizosphere of the cultivated plants (Grunert et al., 2016b, 2019). The microbial community composition is affected by the type of growing medium (Grunert et al., 2016a), the fertilizer used

(Grunert et al., 2019) and plant species (Vallance et al., 2010). For the soil and growing media sampling soil was taken close to the rootstock. As these zones were fully colonized it might be the case that the "bulk" soil samples for the microbial community analysis can be considered as rhizosphere soil samples. Due to this experimental restriction and differences in root density between the four contrasting tomato cultivation systems, this might impact the microbiome present. Cultural methods have been used to characterize this microbial community, but molecular based techniques such as amplicon sequencing is known to give solid data on microbial taxonomy, species richness, evenness and diversity, while PLFA analysis add completing information on total biomass, and biomass per specific group.

CONCLUSION

In the current study, we demonstrated and confirmed that it is possible to grow tomatoes in soilless culture systems in combination with organic fertilizers or in an aquaponics systems and in an organic soil fertilized with plant, i.e., malt sprouts or animal derived, i.e., blood meal during a whole season (321 DAS). We compared the bacterial and fungal community structure of soil and soilless culture systems for the cultivation of tomatoes with two complementary molecular techniques. We showed that the culture system impacted bacterial community characteristics and showed opposite trends. The individual observations are not new and confirm the results of earlier studies, however, this is the first study to show that bacterial and fungal diversity under long term fertilization with malt sprouts and blood meal show a similar behavior in soil, while soilless culture systems show higher responsiveness to fertigation management. This work contributes to a better understanding of the general principles governing fungal and bacterial community structure and adaptation in soil and soilless culture systems, and is widely applicable to sustainable agriculture and horticulture. This work also addresses a knowledge gap between soil based and soilless culture systems.

DATA AVAILABILITY STATEMENT

The sequencing data generated for this study can be found in NCBI using accession number PRJNA574435 (https://www.ncbi.nlm.nih.gov/bioproject/PRJNA574435).

AUTHOR CONTRIBUTIONS

OG, EH-S, SB, and NB conceived and designed the experiments. OG performed the experiments. EH-S processed the Illumina libraries, performed the data mining, statistical analysis, interpretation, and figure and table preparation of the 16S rRNA amplicon sequencing results. OG completed the statistical data processing of the physicochemical variables measured. NB and SD contributed with the reagents, materials, analysis tools, and revisions of the manuscript. Contributed equally co-authors contributed equally to revisions of the manuscript. All the authors contributed to the article and approved the submitted version.

FUNDING

OG was supported by the project grant IWT Baekeland mandate 120200. EH-S is a postdoctoral fellow supported by Flanders Innovation and Entrepreneurship (Agentschap Innoveren & Ondernemen) grant TRAIN 179PO8916W.

ACKNOWLEDGMENTS

The authors acknowledge Catherine De Moor, Barbara Ottevaere, and Christel Moerenhout for their technical support and the department of soil management at UGent for the great assistance with the PLFA analyses.

SUPPLEMENTARY MATERIAL

The Supplementary Material for this article can be found online at: https://www.frontiersin.org/articles/10.3389/fpls.2020.520834/full#supplementary-material

Supplementary Figure 1 | (A) Sample collection and analysis procedure. Slabs for the soilless culture system were placed in gutters, each gutter contained 6 slabs and each slab 5 plants. The two outer rows and outer slabs of each block were not selected, because of possible interactions with the adjacent rows and to avoid side effects. One slab with 5 consecutive plants in the soilless culture system and 5 consecutive plants in the soil based system were considered as an experimental unit. Among all treatments the tomato plants were placed consecutively with an interspacing of 0.47 m and an in row interspacing of 0.8 m. For the soilless culture system and soil-based system five experimental units were randomly selected from the different compartments. Samples of the different experimental units were collected at different time points during the growing season and at the start of the experiment. Ten subsamples from each experimental unit were collected, pooled, homogenized and treated as a single sample. **(B)** At each time point, samples were taken from 5 fixed experimental units of each GBOF, GBFISH, SOILANIMAL and SOILPLANT, including root material. Samples from the soil were taken with an auger in the 0–10 soil profile and from each experimental subunit 10 subsamples were taken. Each sample contained 200 *g* soil or growing medium and was divided into homogenous subsamples: one subsample was used for chemical analyses (100 g) and water content (50 g), one subsample was immediately after sampling stored on dry ice, preserved at −80°C and used for molecular microbial community analysis (50 g). The ammonium and the nitrogen content, the pH and the electrical conductivity (EC) in the 0–10 cm organic soil layer and in the growing medium were taken at the start 55 DAS(T0), 68 DAS (T1), 83 DAS (T2), 113 DAS (T3), 146 DAS (T4), 172 DAS (T5), 221 DAS (T6), and 321 DAS (T7). Samples for microbial community analysis were taken at 8 different timepoints, i.e., 55 DAS, 68 DAS, 83 DAS, 113 DAS, 146 DAS, 172 DAS, 221 DAS, and 321 DAS. Samples for PLFA analyses were collected at 4 different time points, i.e., 55 DAS, 83 DAS, 221 DAS and 321 DAS. Briefly, for the PLFA analyses the soil and growing media were freeze-dried using a modified technique (Bligh and Dyer, 1959). Whole plants were harvested, chopped and samples from stem and leaves without tomatoes were collected for analysis at 221 DAS and 321 DAS.

Supplementary Figure 2 | Overview of the cumulative water dosage (L per m^2) for the different tomato cultivating systems.

Supplementary Table 1 | Overview of the chemical composition of SOILPLANT and SOILANIMAL before the start of the experiment (8/1/2015) and throughout the whole experimental period. $n = 1$. As bulk density 1.25 t ha^{-1} (Vlaamse zandstreek; Arthur et al., 2011) was chosen for the 0.3 m top soil layer.

Supplementary Table 2 | Overview of the chemical composition of the different fertilizers used. "–" means that the elements was not analyzed or specified. "*" means according to the specifications of the supplier. "**" means that the chemical composition was actually analyzed.

Supplementary Table 3 | Overview of the fertilizers used and the total amount used for the different treatments. GBOF, soilless culture system with organic growing medium and organic fertilizer. GBFISH, soilless culture system with organic growing medium and fish. SOILANIMAL, organic soil with animal-derived material as fertilizer; and SOILPLANT, organic soil with plant-derived material as fertilizer.

Supplementary Table 4 | Overview of the chemical composition of the four different organic fertilizers (Nutrikali, ANTYS MgS, Biosyr and SP). "–": means that this element was not determined in the fertilizer.

Supplementary Table 5 | Correlations between microbial community composition and chemical characteristics in four different tomato cultivating systems across time points. indicated by the Multiple Factor Analysis. Dimensions of the MFA can be described by the categorical variables included in the analysis. For each categorical variable (growing medium and time point). *A* one-way analysis of variance was performed with the coordinates of the samples on the axis. explained by the time point or growing medium type. Then, for each level of the category (i.e., time point 1. time point 2 or time point 3 or growing medium GB). *A* Hotelling T^2-test was used to compare the average of the category with the general average (using the constraint $P\ i\ \alpha i = 0$. $\alpha i = 0$). For instance. the coordinates of the relative abundance of family "x" at GB at time point 1 were compared with the average coordinates of the relative abundance of family "x" in GB. The P-value associated to this test is transformed to a normal quantile to assess whether the mean of the category is significantly less or greater than 0. Negative values indicate negative correlations.

REFERENCES

Agehara, S., and Warncke, D. D. (2005). Soil moisture and temperature effects on nitrogen release from organic nitrogen sources. *Soil Sci. Soc. Am. J.* 69, 1844–1855. doi: 10.2136/sssaj2004.0361

Alexander, M. (1977). *Introduction to Soil Microbiology*. Hoboken, NJ: John Wiley & Sons.

Alexandratos, N. (2009). *World Food and Agriculture to 2030/50. Highlights and Views from MID-2009: Paper for the Expert Meeting on "How to Feed the World in 2050, 24-26 June 2009*. Rome: FAO.

Arthur, E., Cornelis, W., Vermang, J., and De Rocker, E. (2011). Amending a loamy sand with three compost types: impact on soil quality. *Soil Use Manage.* 27, 116–123. doi: 10.1111/j.1475-2743.2010.00319.x

Balser, T. C. (2001). The impact of long-term nitrogen addition on microbial community composition in three Hawaiian forest soils. *Sci. World J.* 1, 500–504. doi: 10.1100/tsw.2001.450

Barrett, G., Alexander, P., Robinson, J., and Bragg, N. (2016). Achieving environmentally sustainable growing media for soilless plant cultivation systems–a review. *Sci. Horticult.* 212, 220–234. doi: 10.1016/j.scienta.2016.09.030

Bélair, G., and Tremblay, N. (1995). The influence of chitin-urea amendments applied to an organic soil on a Meloidogyne hapla population and on the growth of greenhouse tomato. *Phytoprotection* 76, 75–80. doi: 10.7202/706087ar

Bligh, E. G., and Dyer, W. J. (1959). A rapid method of total lipid extraction and purification. *Can. J. Biochem. Physiol.* 37, 911–917. doi: 10.1139/o59-099

Bona, E., Todeschini, V., Cantamessa, S., Cesaro, P., Copetta, A., Lingua, G., et al. (2018). Combined bacterial and mycorrhizal inocula improve tomato quality at reduced fertilization. *Sci. Horticult.* 234, 160–165. doi: 10.1016/j.scienta.2018.02.026

Boudsocq, S., Niboyet, A., Lata, J. C., Raynaud, X., Loeuille, N., Mathieu, J., et al. (2012). Plant preference for ammonium versus nitrate: a neglected determinant of ecosystem functioning? *Am. Nat.* 180, 60–69. doi: 10.1086/665997

Bremner, J., and Keeney, D. R. (1965). Steam distillation methods for determination of ammonium, nitrate and nitrite. *Anal. Chim. Acta* 32, 485–495. doi: 10.1016/S0003-2670(00)88973-4

British Standards Institute Staff (2001). *Soil Improvers and Growing Media. Determination of Nitrogen (Dumas method). Equivalent to ISO 5725: 1994*. London: The British Standards Institution.

Britto, D. T., and Kronzucker, H. J. (2002). NH4+ toxicity in higher plants: a critical review. *J. Plant Physiol.* 159, 567–584. doi: 10.1078/0176-1617-0774

Bunt, A. (1988). *Media and Mixes for Container Grown Plants: a Manual on the Preparation and Use of Growing Media for Growing Pot Plants*. London: Springer Science & Business Media. doi: 10.1007/978-94-011-7904-1

Coppens, J., Grunert, O., Van Den Hende, S., Vanhoutte, I., Boon, N., Haesaert, G., et al. (2015). The use of microalgae as a high-value organic slow-release fertilizer results in tomatoes with increased carotenoid and sugar levels. *J. Appl. Phycol.* 28, 2367–2377. doi: 10.1007/s10811-015-0775-2

Cotxarrera, L., Trillas-Gay, M., Steinberg, C., and Alabouvette, C. (2002). Use of sewage sludge compost and *Trichoderma asperellum* isolates to suppress Fusarium wilt of tomato. *Soil Biol. Biochem.* 34, 467–476. doi: 10.1016/S0038-0717(01)00205-X

Diacono, M., and Montemurro, F. (2011). Long-term effects of organic amendments on soil fertility. *Sustain. Agric.* 2, 761–786. doi: 10.1007/978-94-007-0394-0_34

Dion, P.-P., Jeanne, T., Thériault, M., Hogue, R., Pepin, S., and Dorais, M. (2020). Nitrogen release from five organic fertilizers commonly used in greenhouse organic horticulture with contrasting effects on bacterial communities. *Can. J. Soil Sci.* 100, 1–16. doi: 10.1139/cjss-2019-0056

Dubik, S. P., Krizek, D. T., and Stimart, D. P. (1990). Influence of root zone restriction on mineral element concentration, water potential, chlorophyll concentration, and partitioning of assimilate in spreading euonymus (E. Kiautschovica Loes.'Sieboldiana'). *J. Plant Nutr.* 13, 677–699. doi: 10.1080/01904169009364109

El Hage, R., Hernandez-Sanabria, E., Calatayud Arroyo, M., Props, R., and Van de Wiele, T. (2019). Propionate-producing consortium restores antibiotic-induced dysbiosis in a dynamic in vitro model of the human intestinal microbial ecosystem. *Front. Microbiol.* 10:1206. doi: 10.3389/fmicb.2019.01206

El-Yazeid, A., and Abou-Aly, H. (2011). Enhancing growth, productivity and quality of tomato plants using phosphate solubilizing microorganisms. *Aust. J. Basic Appl. Sci.* 5, 371–379.

FAO (2016). *World Fertilizer Trends and Outlook to 2019 [Online]*. Rome: FAO.

FAO (2017). *World fertilizer Trends and Outlook to 2020*. Rome: Food and Agriculture Organanization United Nations.

Fierer, N., Schimel, J., and Holden, P. (2003). Influence of drying–rewetting frequency on soil bacterial community structure. *Microb. Ecol.* 45, 63–71. doi: 10.1007/s00248-002-1007-2

Foley, J. A. (2011). CAN WE FEED THE WORLD SUSTAIN THE PLANET? *Sci. Am.* 305, 60–65. doi: 10.1038/scientificamerican1111-60

Francioli, D., Schulz, E., Lentendu, G., Wubet, T., Buscot, F., and Reitz, T. (2016). Mineral vs. organic amendments: microbial community structure, activity and abundance of agriculturally relevant microbes are driven by long-term fertilization strategies. *Front. Microbiol.* 7:1446. doi: 10.3389/fmicb.2016.01446

Gaskell, M., and Smith, R. (2007). Nitrogen sources for organic vegetable crops. *HortTechnology* 17, 431–441. doi: 10.21273/HORTTECH.17.4.431

Gellings, C. W., and Parmenter, K. E. (2016). "Energy efficiency in fertilizer production and use. Efficient Use and Conservation of Energy," in *Encyclopedia of Life Support Systems*, ed. C. W. Gellings (Oxford: Eolss Publishers), 123–136.

Gravel, V., Blok, W., Hallmann, E., Carmona-Torres, C., Wang, H., Van De Peppel, A., et al. (2010a). Differences in N uptake and fruit quality between organically and conventionally grown greenhouse tomatoes. *Agron. Sustain. Dev.* 30, 797–806. doi: 10.1051/agro/2010025

Gravel, V., Ménard, C., Dorais, M., and Pepin, S. (2010b). "Greenhouse tomato plant development under organic growing conditions: a case study of six organic soils," in *I International Conference on Organic Greenhouse Horticulture 915*, Bleiswijk, 83–89. doi: 10.17660/ActaHortic.2011.915.10

Gross, M. (2012). *We Need to Talk about Nitrogen*. Amsterdam: Elsevier. doi: 10.1016/j.cub.2011.12.033

Gruda, N. (2008). Do soilless culture systems have an influence on product quality of vegetables? *J. Appl. Bot. Food Quality* 82, 141–147.

Grunert, O., Hernandez-Sanabria, E., Vilchez-Vargas, R., Jauregui, R., Pieper, D. H., Perneel, M., et al. (2016a). Mineral and organic growing media have distinct

community structure, stability and functionality in soilless culture systems. *Sci. Rep.* 6:18837. doi: 10.1038/srep18837

Grunert, O., Reheul, D., Van Labeke, M. C., Perneel, M., Hernandez-Sanabria, E., Vlaeminck, S. E., et al. (2016b). Growing media constituents determine the microbial nitrogen conversions in organic growing media for horticulture. *Microb. Biotechnol.* 9, 389–399. doi: 10.1111/1751-7915.12354

Grunert, O., Robles-Aguilar, A. A., Hernandez-Sanabria, E., Schrey, S. D., Reheul, D., Van Labeke, M.-C., et al. (2019). Tomato plants rather than fertilizers drive microbial community structure in horticultural growing media. *Sci. Rep.* 9:9561. doi: 10.1038/s41598-019-45290-0

Hammermeister, A. M., Astatkie, T., Jeliazkova, E. A., Warman, P. R., and Martin, R. C. (2006). Nutrient supply from organic amendments applied to unvegetated soil, lettuce and orchardgrass. *Can. J. Soil Sci.* 86, 21–33. doi: 10.4141/S05-021

Hartz, T. K., and Johnstone, P. R. (2006). Nitrogen availability from high-nitrogen-containing organic fertilizers. *HortTechnology* 16, 39–42. doi: 10.21273/HORTTECH.16.1.0039

Heeb, A. (2005). *Organic or Mineral Fertilization: Effects on Tomato Plant Growth and Fruit Quality. 2005*. Uppsala: Swedish University of Agricultural Sciences.

Heeb, A., Lundegårdh, B., Ericsson, T., and Savage, G. P. (2005a). Effects of nitrate-, ammonium-, and organic-nitrogen-based fertilizers on growth and yield of tomatoes. *J. Plant Nutr. Soil Sci.* 168, 123–129. doi: 10.1002/jpln.200420420

Heeb, A., Lundegårdh, B., Ericsson, T., and Savage, G. P. (2005b). Nitrogen form affects yield and taste of tomatoes. *J. Sci. Food Agric.* 85, 1405–1414. doi: 10.1002/jsfa.2127

Heffer, P., and Prud'homme, M. (2016). "Global nitrogen fertilizer demand and supply: trend, current level and outlook," in *Proceedings of the International Nitrogen Initiative Conference*, Melbourne.

Hernandez-Sanabria, E., Heiremans, E., Arroyo, M. C., Props, R., Leclercq, L., Snoeys, J., et al. (2020). Short-term supplementation of celecoxib-shifted butyrate production on a simulated model of the gut microbial ecosystem and ameliorated *in vitro* inflammation. *NPJ Biofilms Microbiomes* 6, 1–12. doi: 10.1038/s41522-020-0119-0

Heuvelink, E. (2018). *Tomatoes*. Wallingford: CABI. doi: 10.1079/9781780641935.0000

Khalil, S., and Alsanius, B. W. (2001). Dynamics of the indigenous microflora inhabiting the root zone and the nutrient solution of tomato in a commercial closed greenhouse system. *Gartenbauwissenschaft* 66, 188–198.

Klindworth, A., Pruesse, E., Schweer, T., Peplies, J., Quast, C., Horn, M., et al. (2012). Evaluation of general 16S ribosomal RNA gene PCR primers for classical and next-generation sequencing-based diversity studies. *Nucleic Acids Res.* 41:e1. doi: 10.1093/nar/gks808

Koohakan, P., Ikeda, H., Jeanaksorn, T., Tojo, M., Kusakari, S.-I., Okada, K., et al. (2004). Evaluation of the indigenous microorganisms in soilless culture: occurrence and quantitative characteristics in the different growing systems. *Sci. Horticult.* 101, 179–188. doi: 10.1016/j.scienta.2003.09.012

Lauber, C. L., Hamady, M., Knight, R., and Fierer, N. (2009). Pyrosequencing-based assessment of soil pH as a predictor of soil bacterial community structure at the continental scale. *Appl. Environ. Microbiol.* 75, 5111–5120. doi: 10.1128/AEM.00335-09

Lauber, C. L., Ramirez, K. S., Aanderud, Z., Lennon, J., and Fierer, N. (2013). Temporal variability in soil microbial communities across land-use types. *ISME J.* 7, 1641–1650. doi: 10.1038/ismej.2013.50

Lauber, C. L., Strickland, M. S., Bradford, M. A., and Fierer, N. (2008). The influence of soil properties on the structure of bacterial and fungal communities across land-use types. *Soil Biol. Biochem.* 40, 2407–2415. doi: 10.1016/j.soilbio.2008.05.021

Lê, S., Josse, J., and Husson, F. (2008). FactoMineR: an R package for multivariate analysis. *J. Stat. Softw.* 25, 1–18. doi: 10.18637/jss.v025.i01

Maloney, P., Van Bruggen, A., and Hu, S. (1997). Bacterial community structure in relation to the carbon environments in lettuce and tomato rhizospheres and in bulk soil. *Microb. Ecol.* 34, 109–117. doi: 10.1007/s002489900040

Marschner, H. (2011). *Marschner's Mineral Nutrition of Higher Plants*. London: Academic press.

Martínez-García, L. B., Korthals, G., Brussaard, L., Jørgensen, H. B., and De Deyn, G. B. (2018). Organic management and cover crop species steer soil microbial community structure and functionality along with soil organic matter properties. *Agricult. Ecosyst. Environ.* 263, 7–17. doi: 10.1016/j.agee.2018.04.018

McKenzie, F. C., and Williams, J. (2015). Sustainable food production: constraints, challenges and choices by 2050. *Food Security* 7, 221–233. doi: 10.1007/s12571-015-0441-1

Moeskops, B., Buchan, D., Sleutel, S., Herawaty, L., Husen, E., Saraswati, R., et al. (2010). Soil microbial communities and activities under intensive organic and conventional vegetable farming in West Java, Indonesia. *Appl. Soil Ecol.* 45, 112–120. doi: 10.1016/j.apsoil.2010.03.005

Näsholm, T., Kielland, K., and Ganeteg, U. (2009). Uptake of organic nitrogen by plants. *New Phytol.* 182, 31–48. doi: 10.1111/j.1469-8137.2008.02751.x

Notarnicola, B., Tassielli, G., Renzulli, P. A., Castellani, V., and Sala, S. (2017). Environmental impacts of food consumption in Europe. *J. Cleaner Prod.* 140, 753–765. doi: 10.1016/j.jclepro.2016.06.080

Oksanen, J., Kindt, R., Legendre, P., O'Hara, B., Stevens, M. H. H., Oksanen, M. J., et al. (2007). The vegan package. *Commun. Ecol. Package* 10, 631–637.

Øvreås, L., Forney, L., Daae, F. L., and Torsvik, V. (1997). Distribution of bacterioplankton in meromictic Lake Saelenvannet, as determined by denaturing gradient gel electrophoresis of PCR-amplified gene fragments coding for 16S rRNA. *Appl. Environ. Microbiol.* 63, 3367–3373. doi: 10.1128/AEM.63.9.3367-3373.1997

Paschold, A., Jia, Y., Marcon, C., Lund, S., Larson, N. B., Yeh, C.-T., et al. (2012). Complementation contributes to transcriptome complexity in maize (*Zea mays* L.) hybrids relative to their inbred parents. *Genome Res.* 22, 2445–2454. doi: 10.1101/gr.138461.112

Pikaar, I., Matassa, S., Rabaey, K., Bodirsky, B. L., Popp, A., Herrero, M., et al. (2017). Microbes and the next Nitrogen revolution. *Environ. Sci. Technol.* 51, 7297–7303. doi: 10.1021/acs.est.7b00916

Postma, J. (2009). "The status of biological control of plant diseases in soilless cultivation," in *Recent Developments in Management of Plant Diseases*, ed. M. L. Gullino (Cham: Springer), 133–146. doi: 10.1007/978-1-4020-8804-9_11

Postma, J., Willemsen-de Klein, M. J., and van Elsas, J. D. (2000). Effect of the indigenous microflora on the development of root and crown rot caused by *Pythium aphanidermatum* in cucumber grown on rockwool. *Phytopathology* 90, 125–133. doi: 10.1094/PHYTO.2000.90.2.125

Rahmann, G., Oppermann, R., Paulsen, H. M., and Weißmann, F. (2009). Good, but not good enough? Research and development needs in Organic Farming. *Landbauforschung Völkenrode* 59, 29–40.

Ramankutty, N., Mehrabi, Z., Waha, K., Jarvis, L., Kremen, C., Herrero, M., et al. (2018). Trends in global agricultural land use: implications for environmental health and food security. *Annu. Rev. Plant Biol.* 69, 789–815. doi: 10.1146/annurev-arplant-042817-040256

Raviv, M., and Lieth, J. H. (2007). *Soilless Culture: Theory and Practice*. Amsterdam: Elsevier.

Raviv, M., Lieth, J. H., and Bar-Tal, A. (2019). *Soilless Culture: Theory and Practice: Theory and Practice*. Amsterdam: Elsevier.

Reganold, J. P., and Wachter, J. M. (2016). Organic agriculture in the twenty-first century. *Nat. Plants* 2:15221. doi: 10.1038/nplants.2015.221

Roberts, T., and Stewart, W. (2002). Inorganic phosphorus and potassium production and reserves. *Better Crops* 86, 6–7.

Runia, W. T. (1993). "A review of possibilities for disinfection of recirculation water from soilless cultures," in *Proceedings of the IV International Symposium on Soil and Substrate Infestation and Disinfestation*, Leuven, 221–229. doi: 10.17660/ActaHortic.1995.382.25

Sakarika, M., Spanoghe, J., Sui, Y., Wambacq, E., Grunert, O., Haesaert, G., et al. (2019). Purple non−sulphur bacteria and plant production: benefits for fertilization, stress resistance and the environment. *Microb. Biotechnol.* 13, 1336–1365. doi: 10.1111/1751-7915.13474

Savvas, D., Gianquinto, G., Tuzel, Y., and Gruda, N. (2013). *Soilless Culture. FAO Plant Production and Protection Paper No. 217. Good Agricultural Practices for Greenhouse Vegetable Crops. Principles for Mediterranean Climate Areas*. Rome: FAO, 303–354.

Schmilewski, G. (2007). "Growing medium constituents used in the EU," in *Proceedings of the International Symposium on Growing Media 2007 819*, eds W. R. Carlile and A. Coules (Nottingham: ActaHort), 33–46.

Schmilewski, G. (2008). The role of peat in assuring the quality of growing media. *Mires Peat* 3, 1–8.

Sellitto, V. M., Golubkina, N. A., Pietrantonio, L., Cozzolino, E., Cuciniello, A., Cenvinzo, V., et al. (2019). Tomato yield, quality, mineral composition and antioxidants as affected by beneficial microorganisms under soil salinity induced by balanced nutrient solutions. *Agriculture* 9:110. doi: 10.3390/agriculture9050110

Smil, V. (1999). Detonator of the population explosion. *Nature* 400, 415–415. doi: 10.1038/22672

Sonneveld, C., and Voogt, W. (2009). *Plant Nutrition of Greenhouse Crops*. London: Springer. doi: 10.1007/978-90-481-2532-6

Spanoghe, J., Grunert, O., Wambacq, E., Sakarika, M., Papini, G., Alloul, A., et al. (2020). Storage, fertilization and cost properties highlight the potential of dried microbial biomass as organic fertilizer. *Microb. Biotechnol.* 13, 1377–1389. doi: 10.1111/1751-7915.13554

Stadler, C., Von Tucher, S., Schmidhalter, U., Gutser, R., and Heuwinkel, H. (2006). Nitrogen release from plant−derived and industrially processed organic fertilizers used in organic horticulture. *J. Plant Nutr. Soil Sci.* 169, 549–556. doi: 10.1002/jpln.200520579

Steiner, C., Teixeira, W. G., Lehmann, J., Nehls, T., de Macêdo, J. L. V., Blum, W. E., et al. (2007). Long term effects of manure, charcoal and mineral fertilization on crop production and fertility on a highly weathered Central Amazonian upland soil. *Plant Soil* 291, 275–290. doi: 10.1007/s11104-007-9193-9

Storey, J. (2015). qvalue: Q-value Estimation for False Discovery Rate Control. R Package Version 2.0.0. Available online at: www.github.com/jdstorey/qvalue (accessed April 14, 2017).

Suhl, J., Dannehl, D., Kloas, W., Baganz, D., Jobs, S., Scheibe, G., et al. (2016). Advanced aquaponics: evaluation of intensive tomato production in aquaponics vs. conventional hydroponics. *Agric. Water Manage.* 178, 335–344. doi: 10.1016/j.agwat.2016.10.013

Sullivan, D. M., Andrews, N. A., Luna, J. M., McQueen, J. P. G., and Gilkes, R. (2010). "Estimating N contribution from organic fertilizers and cover crop residues using online calculators," in *Proceedings of the 19th World Congress of Soil Science*, Brisbane, QLD.

Tu, C., Ristaino, J. B., and Hu, S. (2006). Soil microbial biomass and activity in organic tomato farming systems: effects of organic inputs and straw mulching. *Soil Biol. Biochem.* 38, 247–255. doi: 10.1016/j.soilbio.2005.05.002

Vallance, J., Déniel, F., Le Floch, G., Guérin-Dubrana, L., Blancard, D., and Rey, P. (2010). Pathogenic and beneficial microorganisms in soilless cultures. *Agron. Sustain. Dev.* 31:191. doi: 10.1051/agro/2010018

Verstraete, W., Clauwaert, P., and Vlaeminck, S. E. (2016). Used water and nutrients: recovery perspectives in a 'panta rhei'context. *Bioresource Technol.* 215, 199–208. doi: 10.1016/j.biortech.2016.04.094

Wilsey, B. J., and Potvin, C. (2000). Biodiversity and ecosystem functioning: importance of species evenness in an old field. *Ecology* 81, 887–892. doi: 10.1890/0012-9658(2000)081[0887:BAEFIO]2.0.CO;2

Wittebolle, L. (2009). *Diversity, Stability and Functionality of Bacterial Communities in the Nitrogen Cycle*. Doctoral Ph.D. Ghent University, Ghent.

Zhai, Z., Ehret, D. L., Forge, T., Helmer, T., Lin, W., Dorais, M., et al. (2009). Organic fertilizers for greenhouse tomatoes: productivity and substrate microbiology. *HortScience* 44, 800–809. doi: 10.21273/HORTSCI.44.3.800

Conflict of Interest: OG was employed by the company Greenyard Horticulture Belgium at the time this research was carried out, and is now employed by Aphea.bio.

The remaining authors declare that the research was conducted in the absence of any commercial or financial relationships that could be construed as a potential conflict of interest.

Advantages of publishing in Frontiers

OPEN ACCESS
Articles are free to read for greatest visibility and readership

FAST PUBLICATION
Around 90 days from submission to decision

HIGH QUALITY PEER-REVIEW
Rigorous, collaborative, and constructive peer-review

TRANSPARENT PEER-REVIEW
Editors and reviewers acknowledged by name on published articles

Frontiers
Avenue du Tribunal-Fédéral 34
1005 Lausanne | Switzerland

Visit us: www.frontiersin.org
Contact us: frontiersin.org/about/contact

REPRODUCIBILITY OF RESEARCH
Support open data and methods to enhance research reproducibility

DIGITAL PUBLISHING
Articles designed for optimal readership across devices

FOLLOW US
@frontiersin

IMPACT METRICS
Advanced article metrics track visibility across digital media

EXTENSIVE PROMOTION
Marketing and promotion of impactful research

LOOP RESEARCH NETWORK
Our network increases your article's readership